Ψηφιακή συλλογή
Βιβλιοθήκη
"ΘΕΟΦΡΑΣΤΟΣ"
Τμήμα Γεωλογίας
Α.Π.Θ

ARISTOTLE UNIVERSITY OF THESSALONIKI
FACULTY OF SCIENCES
SCHOOL OF GEOLOGY

CHRISTOS ALEXANDROS PLASTIRAS
MSc Geologist

ECOLOGICAL DIVERSITY OF PLIOCENE TO PLEISTOCENE PALEARCTIC CERCOPITHECIDS (PRIMATES, MAMMALIA); EVIDENCE FROM THE DENTAL TISSUE

DISSERTATION THESIS

This research is co-financed by Greece and the European Union (European Social Fund – ESF) through the Operational Programme «Human Resources Development, Education and Lifelong Learning» in the context of the project "Strengthening Human Resources Research Potential via Doctorate Research" (MIS-5000432-2nd cycle), implemented by the State Scholarships Foundation (IKY).

THESSALONIKI
2021

Ψηφιακή βιβλιοθήκη Θεόφραστος – Τμήμα Γεωλογίας – Αριστοτέλειο Πανεπιστήμιο Θεσσαλονίκης

Ψηφιακή συλλογή
Βιβλιοθήκη
"ΘΕΟΦΡΑΣΤΟΣ"
Τμήμα Γεωλογίας
Α.Π.Θ

Ψηφιακή βιβλιοθήκη Θεόφραστος – Τμήμα Γεωλογίας – Αριστοτέλειο Πανεπιστήμιο Θεσσαλονίκης

Ψηφιακή συλλογή
Βιβλιοθήκη
"ΘΕΟΦΡΑΣΤΟΣ"
Τμήμα Γεωλογίας
Α.Π.Θ

ΑΡΙΣΤΟΤΕΛΕΙΟ ΠΑΝΕΠΙΣΤΗΜΙΟ ΘΕΣΣΑΛΟΝΙΚΗΣ
ΣΧΟΛΗ ΘΕΤΙΚΩΝ ΕΠΙΣΤΗΜΩΝ
ΤΜΗΜΑ ΓΕΩΛΟΓΙΑΣ

ΧΡΗΣΤΟΣ ΑΛΕΞΑΝΔΡΟΣ ΠΛΑΣΤΗΡΑΣ
MSc Γεωλόγος

ΟΙΚΟΛΟΓΙΚΗ ΔΙΑΦΟΡΟΠΟΙΗΣΗ ΠΛΕΙΟΚΑΙΝΙΚΩΝ ΕΩΣ ΠΛΕΙΣΤΟΚΑΙΝΙΚΩΝ ΠΑΛΑΙΑΡΚΤΙΚΩΝ ΚΕΡΚΟΠΙΘΗΚΩΝ; ΤΕΚΜΗΡΙΑ ΑΠΟ ΟΔΟΝΤΙΚΟΥΣ ΙΣΤΟΥΣ

ΔΙΔΑΚΤΟΡΙΚΗ ΔΙΑΤΡΙΒΗ

Το έργο συχρηματοδοτείται από την Ελλάδα και την Ευρωπαϊκή Ένωση (Ευρωπαϊκό Κοινωνικό Ταμείο) μέσω του Επιχειρησιακού Προγράμματος «Ανάπτυξη Ανθρώπινου Δυναμικού, Εκπαίδευση και Διά Βίου Μάθηση», στο πλαίσιο της Πράξης «Ενίσχυση του ανθρώπινου ερευνητικού δυναμικού μέσω της υλοποίησης διδακτορικής έρευνας» (MIS-5000432-2ος κύκλος), που υλοποιεί το Ίδρυμα Κρατικών Υποτροφιών (ΙΚΥ).

European Union
European Social Fund

Operational Programme
Human Resources Development,
Education and Lifelong Learning
Co-financed by Greece and the European Union

ΕΣΠΑ 2014-2020
ανάπτυξη - εργασία - αλληλεγγύη

ΘΕΣΣΑΛΟΝΙΚΗ
2021

Ψηφιακή βιβλιοθήκη Θεόφραστος – Τμήμα Γεωλογίας – Αριστοτέλειο Πανεπιστήμιο Θεσσαλονίκης

Ψηφιακή συλλογή
Βιβλιοθήκη
"ΘΕΟΦΡΑΣΤΟΣ"
Τμήμα Γεωλογίας
Α.Π.Θ

Ψηφιακή βιβλιοθήκη Θεόφραστος – Τμήμα Γεωλογίας – Αριστοτέλειο Πανεπιστήμιο Θεσσαλονίκης

Ψηφιακή συλλογή
Βιβλιοθήκη
"ΘΕΟΦΡΑΣΤΟΣ"
Τμήμα Γεωλογίας
Α.Π.Θ

ΧΡΗΣΤΟΣ ΑΛΕΞΑΝΔΡΟΣ ΠΛΑΣΤΗΡΑΣ
MSc Γεωλόγος

ΟΙΚΟΛΟΓΙΚΗ ΔΙΑΦΟΡΟΠΟΙΗΣΗ ΠΛΕΙΟΚΑΙΝΙΚΩΝ ΕΩΣ ΠΛΕΙΣΤΟΚΑΙΝΙΚΩΝ ΠΑΛΑΙΑΡΚΤΙΚΩΝ ΚΕΡΚΟΠΙΘΗΚΩΝ; ΤΕΚΜΗΡΙΑ ΑΠΟ ΟΔΟΝΤΙΚΟΥΣ ΙΣΤΟΥΣ

Εκπονήθηκε στον Τομέα Γεωλογίας και Στρωματογραφίας του Τμήματος Γεωλογίας Α.Π.Θ.
Υποβλήθηκε στο Τμήμα Γεωλογίας Α.Π.Θ. τον Νοέμβριο του 2021

Ημερομηνία Προφορικής Εξέτασης: 08/11/2021

Αριθμός Παραρτήματος Επιστημονικής Επετηρίδας Τμήματος Γεωλογίας N°: 221

Συμβουλευτική Επιτροπή

Καθηγητής Κωστόπουλος Δ. Σ, Επιβλέπων
Καθηγητής Merceron G., Συνεπιβλέπων
Ερευνητής Α' Alba D.M., Μέλος Τριμελούς Συμβουλευτικής Επιτροπής

Εξεταστική Επιτροπή

Ερευνητής Α' Guy F.
Καθηγητής Γιουλάτος Δ.
Αν. Καθηγητής Ηλιόπουλος Γ.
Επ. Καθηγητής Ρουσιάκης Σ.

Ψηφιακή βιβλιοθήκη Θεόφραστος – Τμήμα Γεωλογίας – Αριστοτέλειο Πανεπιστήμιο Θεσσαλονίκης

Ψηφιακή συλλογή
Βιβλιοθήκη
"ΘΕΟΦΡΑΣΤΟΣ"
Τμήμα Γεωλογίας
Α.Π.Θ

CHRISTOS ALEXANDROS PLASTIRAS
MSc Geologist

ECOLOGICAL DIVERSITY OF PLIOCENE TO PLEISTOCENE PALAEARCTIC CERCOPITHECIDS (PRIMATES, MAMMALIA); EVIDENCE FROM THE DENTAL TISSUE

Prepared at the Department of Geology of the School of Geology of A.U.Th.
Submitted at the School of Geology of A.U.Th. on November 2021

Date of Oral Examination: 08/11/2021

Annex Number of the Scientific Annals of the School of Geology A.U.Th. N°: 221

Three-Member Advisory Committee

Professor Kostopoulos Dimitrios S., Supervisor.
CNRS Senior Researcher, Dr Merceron G. Co-supervisor.
Director of ICP, Dr Alba D. M. Member.

Εξεταστική Επιτροπή

CNRS Senior Researcher, Dr Guy F.
Professor Youlatos D.
Associate Professor Iliopoulos G.
Assistant Professor Roussiakis S.

Ψηφιακή βιβλιοθήκη Θεόφραστος – Τμήμα Γεωλογίας – Αριστοτέλειο Πανεπιστήμιο Θεσσαλονίκης

Ψηφιακή συλλογή
Βιβλιοθήκη
"ΘΕΟΦΡΑΣΤΟΣ"
Τμήμα Γεωλογίας

© Chris Alexander Plastiras, PhD Geologist, 2021
All rights reserved.

ECOLOGICAL DIVERSITY OF PLIOCENE TO PLEISTOCENE PALAEARCTIC CERCOPITHECIDS (PRIMATES, MAMMALIA); EVIDENCE FROM THE DENTAL TISSUE. – *Ph.D. Thesis*

ΟΙΚΟΛΟΓΙΚΗ ΔΙΑΦΟΡΟΠΟΙΗΣΗ ΠΛΕΙΟΚΑΙΝΙΚΩΝ ΕΩΣ ΠΛΕΙΣΤΟΚΑΙΝΙΚΩΝ ΠΑΛΑΙΑΡΚΤΙΚΩΝ ΚΕΡΚΟΠΙΘΗΚΩΝ; ΤΕΚΜΗΡΙΑ ΑΠΟ ΟΔΟΝΤΙΚΟΥΣ ΙΣΤΟΥΣ. – *Διδακτορική Διατριβή*

Citation:
Plastiras C. A., 2021 – Ecological diversity of Pliocene to Pleistocene Palaearctic cercopithecids (Primates, Mammalia); evidence from dental tissue. Ph.D. Thesis, School of Geology, Aristotle University of Thessaloniki, Annex Number of Scientific Annals of the School of Geology No ???, 228 pp.
Πλαστήρας Χ. Α., 2021 – Οικολογική διαφοροποίηση Πλειοκαινικών έως Πλειστοκαινικών Παλαιαρκτικών κερκοπιθήκων; τεκμήρια από οδοντικούς ιστούς. Διδακτορική Διατριβή, Τμήμα Γεωλογίας Α.Π.Θ., Αριθμός Παραρτήματος Επιστημονικής Επετηρίδας Τμ. Γεωλογίας Νο ???, 228 σελ.

It is forbidden to copy, store and distribute this work, in whole or in part, for commercial purposes. It is permissible to reprint, store and distribute for non–profit, educational or research purposes, provided that the source is mentioned and the present message is maintained. Questions concerning the use of the work for profit should be addressed to the author.

The views and conclusions contained in this document express the author and it should not be construed that they express the official positions of the AUTh.
Cover picture:

Ψηφιακή βιβλιοθήκη Θεόφραστος – Τμήμα Γεωλογίας – Αριστοτέλειο Πανεπιστήμιο Θεσσαλονίκης

Ψηφιακή συλλογή
Βιβλιοθήκη
"ΘΕΟΦΡΑΣΤΟΣ"
Τμήμα Γεωλογίας

PREFACE

The aim of the present work is to explore the ecological diversity of the Plio-Pleistocene cercopithecids of Europe, by analyzing their dietary ecology, which will contribute to the knowledge of the evolution of Cercopithecidae in the area of European region during the studied time period.

This was achieved by using the combined application of two methodologies: dental topographic - enamel thickness analysis and dental microwear texture analysis. The study is focused on four fossil taxa, *Mesopithecus monspessulanus*, *Dolichopithecus*, *Paradolichopithecus* and *Macaca*, and the studied fossil material derives from several institutional and museum collections across Europe. The results of this work are expected to increase the overall amount of information regarding the ecological background of the fossil Cercopithecidae from Europe, and further contribute to the better understanding of how ecological processes such as interspecific competition for space and resources may have influenced the evolution of this primate family in this geographic region. All these are expected to fuel more researchers to investigate the potential effects of these ecological interactions in past and present day primate habitats.

ACKNOWLEDGEMENTS

First of all, I would like to express my sincere gratitude to the Laboratory of Geology and Paleontology of the University of Thessaloniki (LGPUT) and the Laboratory Paleontology Evolution Paleoecosystems Paleoprimatology (PALEVOPRIM) for giving me the opportunity to work on this project.

This work would not have been possible without the everlasting support of my supervisor Kostopoulos D.S. throughout my studies. He was always there for me, and he shaped me into being a paleontologist. I am eternally grateful to him for believing in my potential, for recognizing from the first moment my passion for paleontology and for his priceless teachings and mentorship in both academic and field parts. I would also like to express my sincere gratitude to my co-supervisor Merceron G., whose contribution on this project was immense. Many thanks for entrusting me with this important work, for his hospitality during the time I spent in France, and for his constant help and support when I was abroad. Furthermore, many thanks to Alba D.M., member of my three-member committee, for his contribution on this project, for his rapid response and help with several things needed along the way for the purposes of this thesis, as well as his invaluable and constructive comments on the manuscript which contributed significantly for the improvement and clarity of this scientific work.

Moreover, sincere thanks to Guy F., for his invaluable contribution on this project. Many thanks for entrusting me with this job, for the time spent to show me several technical details regarding μ-CT scanning when I was in PALEVOPRIM, his rapid response in order to assist me with any techical issue that I had along the way, his constructive comments on the manuscript, as well as for the fruitful discussions about Cercopithecidae, dental topography and enamel thickness. Furthemore, many thanks to Youlatos D., Iliopoulos G., and Roussiakis S., members of the examining committee, for their constructive comments which improved significantly the final version of the manuscript, as well as for their inspiring comments during the PhD defense.

Ψηφιακή βιβλιοθήκη Θεόφραστος – Τμήμα Γεωλογίας – Αριστοτέλειο Πανεπιστήμιο Θεσσαλονίκης

Ψηφιακή συλλογή
Βιβλιοθήκη
"ΘΕΟΦΡΑΣΤΟΣ"
Τμήμα Γεωλογίας
Α.Π.Θ.

I am also greatly indebted to Koufos G.D., for contributing fossil material for this project and also for his constant support throughout the years of my studies. Sincere thanks for believing in my potential and my passion for paleontology. The fruitful discussions, advices, lessons and teachings all these years, both in the university and in the field, will stay with me for the rest of my life.

Many thanks also to Tsoukala E., for giving me the opportunity to join her in the field and other projects, for always believing in me, and for the many fruitful discussions regarding paleontology and several other topics that helped me along the way.

Moreover, many thanks to all the people who helped and contributed with fossil or extant material in this work, as well as their host institutions: Spassov N., (Natural History Museum of Sofia), Surault J., (PALEVOPRIM), Mille A. and Didier M. (Muséum d'Histoire Naturelle de Perpignan), Didier B. (Musée des Confluences – Lyon), Robert E. (Université de Lyon), Costeru L. (Natural History Museum Basel), Popescu A. (Muzeul Olteniei Craiova), Petculescu A. ("Emil Racoviță" Institute of Speleology, Bucharest), Tibuleac P. and Haiduc B. and Ratoi B. (University Alexandru Ioan Cuza of Iasi), Lyras G. (Museum of Palaeontology and Geology of the University of Athens), Galindo J. (Institut Català de Paleontologia Miquel Crusafont, Universitat Autònoma de Barcelona), Marivaux L. (Institute of Science De L'évolution De Montpellier), Thiery G., Lazzari V., Boisserie J. R., Daver G. (PALEVOPRIM), Nishimura T. and Takai M. (Kyoto University Primate Research Institute, Inuyama), and Taru H. (Kanagawa Prefectural Museum of Natural History, Odawara). Also, many thanks to several people I had the opportunity to work with in the field, and also to people who worked hard in the field in the past to unearth these rare fossils in order for future researchers to work with.

Furthermore, sincere thanks to the following institutions for contributing with extant material: American Museum of Natural History (AMNH), Authority for Research and Conservation of Cultural Heritage in Addis Ababa (ARRCH), Academy of Sciences Moldova, Chișinău (ASM), Muséum National d'Histoire Naturelle de Paris (MNHN), Museum of Natural History of Vienna (NHMW), Royal Museum of Central Africa, Tervuren (RMCA), Senckenberg Museum of Frankfurt (SMF), Zoologische Staatssammlung München (ZSM), including Morphosource digital database.

I would also like to thank the National Foundation of Greece (IKY) for funding this thesis, as well as sincere thanks to the Eiffel Excellence Programme promoted by Campus France (EIFFEL-DOCTORAT 2018 / n°P729158B), for providing the necessary funds during my stay in France at the second year of the thesis (2018-2019), and the Diet Scratches Project (ANR – 17CE27-0002; PI: Merceron G.).

Moreover, I would like to express my sincere love and gratitude to my friends in Greece for their compassion and support, for the wonderful memories we created together all these years, and for always believing in me. Among my precious friends, I have two honorable mentions, my dear friend and roommate Pagonis D. who stood by my side and endured me these last two difficult years his help has been immense, and my friend and colleague Gkeme A. for always being there for me to discuss several difficulties along the way.

Last but not least, sincere love and thanks to my family, most notably to my father, mother and brother for their love and support all these years. and for always showing me how to be a good and ethical person.

Ψηφιακή βιβλιοθήκη Θεόφραστος – Τμήμα Γεωλογίας – Αριστοτέλειο Πανεπιστήμιο Θεσσαλονίκης

Ψηφιακή συλλογή
Βιβλιοθήκη
"ΘΕΟΦΡΑΣΤΟΣ"
Τμήμα Γεωλογίας
Α.Π.Θ

Table of Contents

Ψηφιακή βιβλιοθήκη Θεόφραστος – Τμήμα Γεωλογίας – Αριστοτέλειο Πανεπιστήμιο Θεσσαλονίκης

Ψηφιακή συλλογή
Βιβλιοθήκη
"ΘΕΟΦΡΑΣΤΟΣ"
Τμήμα Γεωλογίας

Ψηφιακή βιβλιοθήκη Θεόφραστος – Τμήμα Γεωλογίας – Αριστοτέλειο Πανεπιστήμιο Θεσσαλονίκης

Ψηφιακή συλλογή
Βιβλιοθήκη
"ΘΕΟΦΡΑΣΤΟΣ"
Τμήμα Γεωλογίας

Ψηφιακή βιβλιοθήκη Θεόφραστος – Τμήμα Γεωλογίας – Αριστοτέλειο Πανεπιστήμιο Θεσσαλονίκης

Ψηφιακή συλλογή
Βιβλιοθήκη
"ΘΕΟΦΡΑΣΤΟΣ"
Τμήμα Γεωλογίας

Ψηφιακή βιβλιοθήκη Θεόφραστος – Τμήμα Γεωλογίας – Αριστοτέλειο Πανεπιστήμιο Θεσσαλονίκης

Ψηφιακή συλλογή
Βιβλιοθήκη
"ΘΕΟΦΡΑΣΤΟΣ"
Τμήμα Γεωλογίας

List of Institutional Abbreviations

AMNH – American Museum of Natural History.

AMPG – Museum of Palaeontology and Geology of the University of Athens.

ARRCH – Authority for Research and Conservation of Cultural Heritage in Addis Ababa, Ethiopia.

ASM – Academy of Sciences Moldova (Chișinău).

ERIS – "Emil Racoviță" Institute of Speleology, Bucharest (Romania).

ISEM – Institute of Science De L'évolution De Montpellier (France).

LGPUT – Museum of Geology–Paleontology–Paleoanthropology of University of Thessaloniki (Greece).

MNHL – Musée des Confluences – Lyon (France).

MNHN – Muséum National d'Histoire Naturelle de Paris (France).

MNHP – Muséum d'Histoire Naturelle de Perpignan (France).

MOC – Muzeul Olteniei, Craiova (Romania).

NHMB – Basel Natural History Museum (Switzerland).

NHMW – Museum of Natural History of Vienna (Austria).

NHMS – Natural History Museum of Sofia (Bulgaria).

KPMNHO – Kanagawa Prefectural Museum of Natural History, Odawara (Japan).

PALEVOPRIM – Laboratoire Paléontologie Evolution Paléoécosystèmes Paléoprimatologie, Poitiers (France).

RMCA – Royal Museum of Central Africa, Tervuren (Belgium).

SMF – Senckenberg Museum of Frankfurt (Germany).

ICP – Institut Català de Paleontologia Miquel Crusafont (Spain), Universitat Autònoma de Barcelona

UAIC – University Alexandru Ioan Cuza of Iași (Romania).

UCBL–1 – Université de Lyon (France).

KUPRI – Kyoto University Primate Research Institute, Inuyama (Japan).

ZSM – Zoologische Staatssammlung München (Germany)

Ψηφιακή βιβλιοθήκη Θεόφραστος – Τμήμα Γεωλογίας – Αριστοτέλειο Πανεπιστήμιο Θεσσαλονίκης

Ψηφιακή συλλογή
Βιβλιοθήκη
"ΘΕΟΦΡΑΣΤΟΣ"
Τμήμα Γεωλογίας
Α.Π.Θ

Chapter 1. Introduction

1.1 Diet and dentition: Implications for dietary reconstruction on fossil forms

Two basic biological demands presumed to be of key importance in the course of evolution of every species are sexual reproduction and diet, both necessary for life continuity. Nevertheless, the importance of diet is beyond question, as it is a daily need in the life of every living organism in order to survive. Mammalian diets overall exhibit three basic categories: carnivorous, herbivorous and omnivorous. These mostly depend on the mammalian group of study. However, it can be rather complex to explore the subtle variation of these three basic dietary categories, as several factors throughout the year may influence dietary habits. For instance, ungulates are herbivorous mammals exploiting food resources from the herbaceous layer and/or browse from trees, bushes and other types of vegetation. Variations in feeding preferences and dietary repertoire depend mostly on seasonal and spatial factors which may vary even between populations of the same species. In the case of primates dietary characterizations can be more complex. In general, primates are considered as omnivorous organisms (Harding, 1981), however, this dietary characterization usually refers to primates which habitually consume meat along with other vegetal resources (e.g. Watts, 2020). In this sense, only humans may be considered as truly omnivorous, as meat is an almost indispensable dietary component in their diet. The diets of most non-human primates are very diverse being primarily constituted by‘plant-source foods’ (PSFs; cf. Milton, 2003a, b), with some species also including animal-source foods (ASFs; cf. Milton, 2003a,b). Primate species exhibit a wide variation of dietary preferences and foraging strategies (e.g. Garber, 1987), they will exploit food resources available on the terrestrial substrate if possible, also in the canopy (Milton, 1993). Furthremore, some primate species occasionally will resort to object manipulation, or even devise tools to acquire and efficiently process targeted food resources (Hernandez–Aguilar et al., 2007; Falótico and Ottoni, 2016). Several researchers throughout the years dedicated their lives studying and recording the dietary ecology of primate species.

To depict the dietary ecology of a primate species, first information is extracted from field studies. The most usual approaches on recording the diet of free-ranging primate populations are time sampling methods. The feeding behavior, the dietary intake and composition, as well as the specific amount of time it required to consume/process it, is recorded for specific periods of time. Alternative feeding methods are also used in some circumstances such as analysis of stomach content, fecal analysis, and identification of food remains (see National Research Council, 2003 for more details). The amount of time spent resting is also informative. In addition, all these require to be observed on several populations of the same species, in the different habitats of its geographical distribution, and on different periods of time throughout the year if possible. In addition to these, one important aspect that should also be considered in investigations of dietary ecology, is the niche partitioning with other primates species that occur in the same habitat and their direct interactions. Lastly, the anthropogenic effects on primate habitats should also be considered.

If it can be so complex to determine the dietary ecology of extant primates, how can we infer diet for extinct primate species? This still troubles paleontologists even today, while we need to further accept that there is probably a limit in the information that can be extracted from fossils, as potentially important behavioral aspects of dietary ecology cannot be directly observed. Lastly, some important anatomical and physiological features related to diet (e.g. digestive system) do not generally fossilize. Despite these facts, direct observations of modern primate species and comparisons with the fossil record, enable us to better understand primate diets and their importance in primate evolution. In paleontological studies, the most widely used anatomical trait in dietary investigations is the dentition.

Ψηφιακή βιβλιοθήκη Θεόφραστος – Τμήμα Γεωλογίας – Αριστοτέλειο Πανεπιστήμιο Θεσσαλονίκης

Ψηφιακή συλλογή
Βιβλιοθήκη
"ΘΕΟΦΡΑΣΤΟΣ"

Studies of fossil dental remains in mammalian paleontology and paleoprimatology have always been the center of attention. The major interest derives from the fact that teeth retain phylogenetic information and therefore are useful for taxonomic and systematic purposes, while dietary information can be crucial for interpreting their way of life. Also, compared to other anatomical parts teeth are more frequently preserved in the fossil record mostly due to the physical properties of enamel tissue. Thus, studies of tooth form and function are necessary to decipher the dietary ecology of extant and extinct primates. Morphological comparisons of dental characters in extant species, such as relief, presence/absence of shearing crests, enamel thickness and its distribution along the tooth crown, along with available recorded dietary information from observational studies, enable us to depict the dietary ecology of extinct forms. Nevertheless, this comparative approach does carry some potential problems that must be resolved before we try to reach a reliable conclusion about dietary adaptations. First, the potential dietary adaptation must be generally observed. For example, if most insectivorous primates have molars with sharp cusps, high relief and long shearing crests, while frugivorous/hard object feeders do not, this observation provides additional support to the argument. But still we have to consider the possibility of an extinct primate with similarly observed morphology occupying a specific ecological niche not analogous to some modern relative.

Secondly, the adaptive hypotheses based on comparison are subject to the problem of confounding variables (Clutton-Brock and Harvey, 1979). A similar morphology may evolve under different selection regimes and vice versa (Kay and Covert, 1984). Folivorous primate molar structure possesses a set of characteristics that favor the exploitations of plant-fiber, while a similar set of characteristics is present also in insectivorous primate molars. In this case, to generally distinguish between folivorous and insectivorous species we will need additional information as for instance about body mass, since insectivorous primates are overall smaller compared to folivorous.

Thirdly, the morphological expression of a particular adaptive character may constrain the form of others. Kay and Covert (1984) quoted sloths as one striking example of constraints in adaptive pathways. Having greatly reduced their cheeck teeth early in their evolutionary history, they lack most of the cutting/shearing systems observed in most herbivores. However, they possess particularly enlarged stomachs, which greatly slows food passage time combined with a slow metabolic rate; these can be considered as alternative adaptive changes to more efficiently handle a leafy diet. Something similar is observed in colobine monkeys, which exhibit differences in forestomatch anatomy most likely reflecting adaptations to different dietary niches (Matsuda et al., 2019).

Intepretations of extinct species adaptations must take all the above into account, as well as keeping in mind that we cannot observe any of these behaviors. Moreover, another important issue is also fallback foods which may be critical to the survival of the studied species, but are seldom traced in morphological characters. This is also influenced by the fact that fossil remains are generally fragmentary and sparse, making investigations more difficult. To conclude, the interpretation of extinct species adaptive morphologies related to diet, are possible only by means of analogy and comparisons with living animals, but still we need to be cautious and conservative.

1.2 Primate dental form and function

Primate dentition can be characterized as a synthesis of effective dental structures, shaped throughout the complicated evolution of this order. Primate teeth are multifunctional tools that play an important role in food item processing and breakdown (Berthaume et al., 2020). Nevertheless, not all tooth loci are solely dedicated to dietary functions. For instance,

Ψηφιακή βιβλιοθήκη Θεόφραστος – Τμήμα Γεωλογίας – Αριστοτέλειο Πανεπιστήμιο Θεσσαλονίκης

Ψηφιακή συλλογή
Βιβλιοθήκη
"ΘΕΟΦΡΑΣΤΟΣ"

most Hominoids possess size dimorphic canines with only few exceptions (e.g. hylobatids) and this is related to sociosexual behavior (e.g. Plavcan and van Schaik, 1992; Plavcan, 2012). Moreover, female and male langurs grind their teeth to produce certain sounds that are probably associated with intra-group competition for reproduction and/or food resources (Hrdy, 1974; Ahsan and Khan, 2006). Furthermore, the relationship between diet and incisor size has been emphasized by some researchers (Anthony & Kay, 1993; Eaglen, 1984; Goldstein et al., 1978; Hylander, 1975; Jolly 1970a; b; Kay and Hylander 1978; Kinzey 1974). Posterior dentition or cheeck teeth (i.e premolars and molars) are considered to be the primary food processing tools of the oral cavity, yet primates also use their hands which may be considered as the first step of ingestion (Nishida, 1976; Milton, 1993). Be that as it may, the relation of posterior dentition and diet is more well understood compared to hands for now, with dietary investigations being primarily focused on molars and premolars (Scott et al., 2018; Thiery and Sha, 2020 and references therein).

One of the first efforts to quantify primate molar shape in respect to dietary behavior is a measure of molar shearing capability correlated with chewing efficiency named shearing quotient (SQ; e.g., Sheine and Kay, 1977; Kay and Sheine, 1979). In these pioneer studies, they found that insectivores, which possessed relatively longer molar shearing crests, showed higher chewing efficiency than frugivores with relatively shorter molar shearing crests. The SQ is determined by regressing shearing crest length against tooth length (the sum of a set of linear distances between discrete, homologous, anatomical landmarks on the occlusal surface). Later, it was shown that folivores also possess relatively long shearing crests, associated with a diet with high fiber content (Boyer et al., 2015; Kay, 1981; Ungar & Kay, 1995; Winchester et al., 2014). These studies showed marked differences among insectivores and folivores comparing to primates that rely on harder food resources, such as fruits and seeds. This indicates that the same adaptive response (e.g. higher shearing capability through crest development) can be useful in different diets (e.g. insectivorous and folivorous), whereas a different adaptive response is manifested in order to sustain high biting forces related to the exploitation of mechanically challenging food items. Even if these estimates produced reasonable results, subsequent works indicated their somehow limited efficiency and disadvantages, especially when it comes to worn dentition (Winchester et al., 2014; Boyer et al., 2015). In addition, studies of dental wear may be particularly important in dietary investigations, and consequently how primate dental form and function evolved throughout time (Yamashita, 1998; King et al., 2005; Cuozzo and Sauther, 2006; Marshall and Wrangham, 2007; Dominy et al., 2008; Berthaume, 2016a). To address all these complicated issues, new methods needed to be developed.

One challenging problem was how to digitally capture the whole tooth shape. Eventually laser and micro-computed tomographic scanners (μ-CT) were chosen as effective ways to digitally represent teeth (Ungar & Williamson, 2000). The application of geographic information system software (GIS) enabled the representation of the whole tooth morphology as a topographic landscape and consequently more detailed investigation of dental morphological aspects (Jernvall & Selänne, 1999; Ungar & Williamson, 2000; Zuccotti et al., 1998). Maybe the most important advantage of dental topographic analysis, is the fact that it is a landmark-free approach to quantify and represent tooth shape with a single metric (Berthaume, 2016a). Although several methodological protocols have been suggested, all topographic studies follow the same steps: tooth digitization, processing/editing of tooth surface and finally tooth shape quantification. In addition to dietary inferences (Ledogar et al., 2013; Allen et al., 2015; Berthaume et al., 2018; Ungar et al., 2018), dental topography has been used to investigate evolutionary pressures, such as niche partitioning (Godfrey et al., 2012; Berthaume and Schroer, 2017), to predict enamel surface morphology from the shape of the enamel-dentine junction surface (Skinner et al., 2010; Guy et al., 2015), describe a new fossil plesiadapid (Boyer et al., 2012), as well as to explore the relationship between tooth shape and food breakdown (Berthaume, 2016b, 2016a; Thiery et al., 2017a,b). Today, new non-GIS

Ψηφιακή βιβλιοθήκη Θεόφραστος – Τμήμα Γεωλογίας – Αριστοτέλειο Πανεπιστήμιο Θεσσαλονίκης

Ψηφιακή συλλογή
Βιβλιοθήκη
"ΘΕΟΦΡΑΣΤΟΣ"

software and techniques have been used and dental topographic studies have developed several metrics to characterize aspects of tooth morphology such as complexity, curvature and sharpness, dental relief, and tooth wear (M'Kirera and Ungar, 2003; Evans et al., 2007; Boyer, 2008; Evans and Jernvall, 2009; Klukkert et al., 2012b; Guy et al., 2013, 2017; Allen et al., 2015; Pampush et al., 2016; Berthaume et al., 2019a).

Even though dental topographic analysis has proven to be a useful method to characterize tooth morphology, it has certain limitations that should be considered (see Berthaume et al., 2020 for a detailed review). One of the most important is the sensitivity of dental topographic metrics to data acquisition and processing. The total number of triangles in 3D meshes as well as the effect of smoothing and cropping methods may influence topographic estimates (Berthaume et al., 2019b). Sensitivity studies usually investigate the effect of such methodological parameters; while some metrics remain unaffected, others are more significantly influenced (Berthaume et al., 2018, 2019; Eronen et al., 2017; Spradley et al., 2017).

Another important condition that must be considered is the comparability between topographic metrics. For instance, there are different measures of sharpness suggested, all of them basically quantifying the same morphological aspect (Ungar and Williamson, 2000; Bunn et al., 2011; Guy et al., 2017; Shan et al., 2019). Yet, the underlying differences in the mathematic computations for each metric do not enable direct comparisons. As a result, this emphasizes the problem of choice of the most suitable metric for analyses. However, this also depends on the question being asked, and on the tooth being investigated. All the above make it harder to directly compare results between dental topographic studies. Furthermore dental topographic metrics are usually correlated with each other (Winchester et al., 2014; Thiery et al., 2017a). These correlations are usually related to parameters such as dietary variability, phylogenetic context, as well as the method of data acquisition. This implies that potential correlation between metrics should also be investigated (see Berthaume et al., 2020 for a detailed discussion). Lastly, the incorporation of several metrics together in studies is suggested, as investigations of multiple aspects of tooth shape may increase the confidence of results, while also providing useful information for future investigations.

1.3 Analyzing wear on teeth

Studies of tooth wear use data from worn tooth surfaces as proxies for recording the dietary ecology of extant and extinct mammals. Wear gradients (Meikle, 1977), unusual patterns of wear (Kilgore, 1989), as well as the inclination of worn areas on the occlusal surface (Butler, 1952, 1973), have been used to assess potential diets and further interpret their paleoecology. These areas are usually referred as dental wear facets. The development of such facets may be a result of abrasion (i.e. tooth wear caused by interactions between a tooth and exogenous particles of food and/or grit) or attrition (i.e. when opposable teeth contact each other). These processes can contribute to the excessive wear of the molar and incisal occlusal surfaces. Yet, evidence suggests that other tooth wear mechanisms might also contribute to the whole tooth wear pattern (see Ch.3 in Lussi & Jaeggi, 2006, for a detailed discussion). Moreover, dental wear is also related to the aging process, as older individuals usually exhibit advanced degree of wear. However, tooth wear may sculpt occlusal morphology to maintain and/or improve functional efficiency throughout lifetime (Ungar, 2015). Notwithstanding the above, abrasion seems to play the most significant role in the dental wear process. A commonly employed method for quantifying wear in some mammalian clades is mesowear analysis.

The term mesowear was initially conceived by Fortelius and Solounias (2000) as "*the average diet of an individual or a particular species from a particular location in space and time*" and it refers to the intermediate time scale at which this type of wear is formed, slower

Ψηφιακή βιβλιοθήκη Θεόφραστος – Τμήμα Γεωλογίας – Αριστοτέλειο Πανεπιστήμιο Θεσσαλονίκης

Ψηφιακή συλλογή
Βιβλιοθήκη
"ΘΕΟΦΡΑΣΤΟΣ"

than microwear but more rapid than evolutionary changes in overall tooth structure, which occur at a geological time scale. It is the macroscopic tooth wear that is visible to the naked eye as a smooth flattened area of enamel on the occlusal surface, and is developed over the course of an animal's lifetime. In herbivorous mammals that consume mostly relatively soft or tough food objects, such as leaves of dicotyledonous plants, twigs, flowers and some fruits (i.e. browsers), attrition is the primary cause of tooth wear. Attrition creates sharp enamel edges with well-developed facets. In herbivorous mammals that mostly graze on the terrestrial substrate and consume grasses and other low–growing vegetation (i.e. grazers), the food consumed causes most of the tooth wear instead of teeth. This process tends to create round off enamel edges with not so clearly defined wear facets. One important advantage of this methodology is the generally quick and easy acquisition of data, making it a suitable technique to explore large samples (Mihlbachler et al., 2011). However, since mesowear was initially developed for some ungulates extending the method to other groups with other teeth types and/or mastication styles required the development of different scoring techniques, thus making it difficult to directly compare results. Nevertheless, this method has been extended to other groups as well (see Green and Croft, 2018; Ackermans, 2020 for extended discussions).

One important dental wear proxy with wide application on several mammalian groups that has been proven to be one of the most efficient in characterizing dietary habits is dental microwear analysis (see Calandra & Merceron, 2016). Unlike mesowear, microwear analyses, focus on the microscopic wear features on the occlusal surface, produced by food abrasion during mastication. Dental microwear data provide direct evidence of food consumption on tooth surfaces, if care is taken with specimen preparation and selection (Gordon, 1982; Ungar et al., 2007). Microscopic wear features (e.g. microwear) are not a cumulative record of chewing, in contrast with macroscopic methods (e.g. mesowear), instead its a continuous record that gets erased with subsequent feeding events within days or even weeks (Teaford and Oyen, 1989). Thus, it is a record of what the studied organism consumed several days prior to its death, a characteristic usually referred as "Last Supper" effect (Grine, 1986; Winkler et al., 2020). The turnover rates of microwear textures have been recorded in most vertebrates, ranging from days even to weeks (Baines et al., 2014; Hoffman et al., 2015; Teaford & Oyen, 1989). The first microwear studies using optical light microscopy looked for evidence on teeth as a proxy to identify the direction of jaw movement during chewing (Butler, 1952; Mills, 1963, 1967). Such studies though, focused more on jaw movements and the mechanics of chewing instead on the direct associations between foods eaten and the resulting patterns of microscopic dental wear. The initial work that tried to associate microscopic wear features on nonhuman primate teeth with diet can be credited to Walker (1976). In his work he examined the incisors in a series of living Old World monkeys using light microscopy, and he suggested texture differences between terrestrial and arboreal monkeys. Walker (1976) attributed these differences to feeding substrate, siliceous material in food eaten and the mechanical demands of food breakdown. He further noticed diet–related differences, such as that folivores had more laterally oriented striated incisal surfaces than frugivores, possibly related to the lateral stripping of leaves across incisors.

Later research has shown that optical light microscopy had significant restrictions for dental microwear research as it limited depth of field and low resolving power (Ungar et al., 2008), which turned out to be problematic when analyzing curved microwear surfaces. Consequently, researchers abandoned light microscopy and by the late 1970's, several workers had already adopted scanning electron microscopy (SEM) as the most suitable instrument for microwear analysis (Rensberger, 1978; Ryan, 1979; Walker et al., 1978). The higher resolving power, maximal resolution, working distance and depth of field at a given magnification, gave SEM a significant advantage over conventional light microscopy. The latter methodology (i.e. SEM) allowed researchers to view and identify smaller microwear features, having whole fields of view focused, even on curved surfaces. Hence, in order to exploit the full potential of SEM for identifying dietary differences, soon after started the quantification of microwear patterns.

Ψηφιακή βιβλιοθήκη Θεόφραστος – Τμήμα Γεωλογίας – Αριστοτέλειο Πανεπιστήμιο Θεσσαλονίκης

Ψηφιακή συλλογή
Βιβλιοθήκη
"ΘΕΟΦΡΑΣΤΟΣ"

This early phase of research was focused on primates, and it demonstrated similar microwear patterns within the same species (Gordon, 1982), and distinct microwear among species with contrasting diets (Teaford and Walker, 1984). However, the ability of microwear as a tool for reconstructing diet was questioned (Covert and Kay, 1981). Soon it became clear that standardization of SEM instrumental parameters and magnification was a necessity, along with control of tooth position and dental wear facet types between analyses (Gordon, 1984). Eventually, the quantification of microwear features enabled statistical testing, which lead to a more advanced understanding of the relationship between microwear and dietary ecology (Teaford & Walker, 1984; Ungar & Spencer, 1999).

During the late 1980's and early 1990's, microwear research focused on how to more accurately quantify microwear using a variety of approaches (Grine, 1986; Maas, 1991; Ungar & Kay, 1995), and variables (e.g. pit: striation ratios, feature length/breadth, orientation). By the early 2000's, it was recognized that there was inconsistency among observers on the recognition and measurement of microwear features on SEM images which limited interpretations (Grine et al., 2002). Furthermore, it was argued that SEM analysis was expensive and very time–consuming (Solounias and Semprebon, 2002). To avoid this, it was further suggested to return to low–magnification light microscopy (LM), which at least was inexpensive in time and cost. Indeed, for a brief period of time the interest in LM reignited, while at the same time there was an increase in the diversity of non–primate mammal analyzed (Green & Croft, 2018 and references therein). Regardless, as with SEM methods, LM also demonstrated problems of observer consistency (Ungar et al., 2008). Even though earlier studies suggested that inter/intra observer error was not significant (Semprebon et al., 2004), later studies questioned this opinion (Mihlbachler et al., 2012; Mihlbachler & Beatty, 2012).

All the aforementioned problems lead to the development of new automated three–dimensional techniques for analyzing surface textures. The first automated technique was developed by Scott et al. (2005, 2006) named dental microwear texture analysis (DMTA). This method uses confocal microscopy and computes five basic parameters that characterize surface textures (since it is one of the methods used in this study, it will be discussed in the next chapter). To this day it is the most widely used technique and it has been applied to primates (El-Zaatari et al., 2005; Merceron et al., 2006, 2009b; Krueger et al., 2008; Scott et al., 2012; Williams and Holmes, 2012; Williams and Geissler, 2014; Martin et al., 2018; Ungar et al., 2020), ungulates (Merceron et al., 2010, 2016; Scott, 2012; Ungar et al., 2007), marsupials (Prideaux et al., 2009), proboscideans (Zhang et al., 2017), chiroptera (Purnell et al., 2013), suids (Souron et al., 2015; Lazagabaster, 2019), bears (Donohue, 2013; Peigné and Merceron, 2019), micromammals (Hopley et al., 2006; Calandra et al., 2016) as well as carnivorans (Schubert et al., 2010; DeSantis et al., 2012). The majority of microwear studies is focused on the microwear present on the occlusal enamel surface while few analyses have used non-occlusal molar facets and wear facets of incisors (Ungar, 1994; Estebaranz et al., 2009; Martínez et al., 2016, 2020).

More recently a new three-dimensional automated technique was developed, termed dental areal surface texture analysis (DASTA). This technique is based on standardized industrial surface texture parameters (ISO). Therefore, these parameters can be readily compared throughout studies and they can be quantified by various 3D acquisition and processing softwares (Calandra et al., 2012). Both DMTA and DASTA have proven to be useful in distinguishing diet, but so far DMTA has a better and more clear baseline for comparisons between mammalian groups. Nevertheless, both methods are very promising for the future of this field (Calandra & Merceron, 2016; see also Francisco et al., 2018). Until today, microwear researchers still use all three types of microscopy (light, scanning electron, confocal microscopy) while modifications for each method are still being proposed (LM, Hoffman et al.,

Ψηφιακή βιβλιοθήκη Θεόφραστος – Τμήμα Γεωλογίας – Αριστοτέλειο Πανεπιστήμιο Θεσσαλονίκης

Ψηφιακή συλλογή
Βιβλιοθήκη
"ΘΕΟΦΡΑΣΤΟΣ"
Τμήμα Γεωλογίας
Α.Π.Θ

2015; SEM, Green & Kalthoff, 2015; Green & Resar, 2012; DMTA, Gill et al., 2014; Purnell et al., 2012).

Besides extensive application to mammalian ecology and paleoecology, dietary proxies such as microwear analyses, have their own limitations, which should be taken into account before inferring diet and deriving conclusions regarding palaeohabitats. The temporal scale of any dietary proxy must be considered when attempting to reconstruct the feeding ecology of mammals. More specifically, microwear is an accumulations of wear features produced in weeks or even some months prior to animal's death.This can be useful in detecting seasonal and/or temporal variations in diet (Martin et al., 2018), dietary differences among extinct and extant populations (Merceron et al., 2010, 2020; Rivals et al., 2015), and also investigating intra and interspecific ecology among sympatric species (Calandra and Merceron, 2016). But what if the animal dies at a time period where resources were scarce or during fallback episodes (e.g. McGraw et al., 2012; Lambert and Rothman, 2015), thus providing only a glimpse of the diet of the species. Furthermore, if the sample size is also low it may not be sufficient enough to extract clear conclusions and therefore intepretations should be treated with caution (Kay & Covert, 1983).

A thorough review of the theoretical limits of dental microwear is provided by Teaford (2007), briefly summarized below. Post-mortem processes can potentially alter or even destroy the microwear signal. Consequently, if all known specimens from a fossil species have been altered, the feeding ecology of this animal must be determined using other dietary proxies beside microwear. Furthermore, it has been suggested that the consumption of food resources with mechanical properties softer than enamel may not produce sufficient microwear signal (e.g. Lucas et al., 2013). Nevertheless, more recent experimental studies have shown that even materials softer than enamel may abrade enamel (e.g. Xia et al., 2015; Daegling et al., 2016). Another factor that should be taken into account is that modern habitats may not share the same ecological conditions with habitats in the past. So it is impossible to know the imprint of these conditions in microwear textures.

All microwear studies rely on microwear patterns among extant animals with available dietary information to infer about paleodiet of extinct organisms (Teaford & Glander, 1991). Most of the time, microwear studies rely on specimens belonging to museum collections, in which the absence of useful information, such as specific age, diet, geographic location, and season of death is common. However, in vivo experiments show great potential and are one of the most important directions in microwear analysis. Their application to animal populations with all previously mentioned information available, will improve our understanding of how microwear textures are produced, as well as the possible significant or trivial effects of other factors as well (Merceron et al., 2016, 2017; Ackermans et al., 2020). The lack of associated environmental parameters and climatic factors may also potentially affect negatively interpretations (Teaford, 2007). Moreover, many mammals especially primates are opportunistic with significant dietary variations between seasons and geographic populations. Thus, simply mixing individuals of a single species from different regions could provide a skewed microwear signal (Rivals and Semprebon, 2010), especially if the sample size is low. Indeed, substantial sample size can be necessary to identify significant differences (Gordon 1988). However, low sample size is a common problem in fossil primate analyses, so there is a general consensus accepting this fact. Regardless, interpretations should be treated conservatively.

1.4 Primate diets

Even if generally primates are generally considered omnivorous organisms (e.g. Harding, 1981), many researchers have dedicated their lives to characterize the dietary habits

Ψηφιακή βιβλιοθήκη Θεόφραστος – Τμήμα Γεωλογίας – Αριστοτέλειο Πανεπιστήμιο Θεσσαλονίκης

Ψηφιακή συλλογή
Βιβλιοθήκη
"ΘΕΟΦΡΑΣΤΟΣ"
Τμήμα Γεωλογίας

of primate species in order to make inferences on the fossil record, and consequently better understand primate evolution. Usually four basic dietary categories for primates are most commonly employed in the literature by behaviorists and anatomists (Clutton-Brock & Harvey, 1977; Kay, 1975; Kay & Hylander, 1975), folivory, frugivory, omnivory and insectivory.

The distinction of frugivorous, folivorous and insectivorous primates is based on the type of food item they primarily consumed. A frugivore consumes a high percentage of fruits (ripe or unripe), nuts, seeds and other plant products. A folivore primarily relies on leaves (young or mature), shoots, stems or buds throughout the year. Insectivorous primates mostly rely on insects as a primary food resource. In addition, there are also some food resources that require certain types of anatomical and/or physiological modifications for the acquisition, consumption and digestion. That is why some researchers recognize additional minoritary dietary categories (gummivory, granivory, nectivory, e.g., Fleagle, 2013). A common example, a special case in extant primate dietary ecology, is *Theropithecus gelada* which feeds almost exclusively on grassland products, like tough grasses, sedges and grass seeds (Jarvey et al., 2018; but see Fashing et al., 2014). Grass leaves are an important resource of structural carbohydrates, as tree leaves; however, high in silica content. The high consumption of vegetal resources with high silica content, can eventually abrade teeth to a degree not observed in a diet focused on tree leaves (Walker et al. 1978). Thus, potentially promoting certain dental morphological adaptations, as suggested in the case of *Theropithecus* (Iwamoto, 1979). Omnivory is a wide dietary category and it can be rather complex to define. Omnivorous primates exploit a wide array of vegetal resources including invertebrates, but this dietary characterization usually refers to primates that also consume various amounts of vertebrate flesh (Watts, 2020). In order to specify this detail, sometimes the term mixed-feeder is used depending on the taxon of study and the researcher (e.g. Teaford et al., 1996; Cerling et al., 2004). The dietary preferences of omnivorous and mixed-feeding primates are somehow opportunistic as they mostly rely on the food resources available on their surrounding habitat. For instance, representatives of the genus *Pan* are commonly referred as frugivores (e.g., Hladik, 1977; Tutin et al., 1991), yet their diet varies depending on habitat and season (Yamagiwa and Basabose, 2006; Hernandez-Aguilar et al., 2007; McGrew, 2007; Hockings et al., 2010; Matthews et al., 2019), whereas the consumption of other smaller vertebrates has been observed as well (McGrew, 1983; Teelen, 2007; Surbeck et al., 2009; Watts, 2020). Similar behaviors have been observed in representatives of the genus *Papio* and to a lesser extent *Mandrillus* (Hoshino, 1985; Rhine et al., 1986, 1989; Norton et al., 1987; Hill and Dunbar, 2002; Newton-Fisher and Okecha, 2006). Notwithstanding the above, it is commonly accepted that these dietary categories are somehow oversimplified (Chapman and Chapman, 1990), as primate species placed into one dietary category may show significant overlap with other species included in other dietary categories (Davies et al., 1999; Vogel et al., 2009; Randimbiharinirina et al., 2018), meaning that different dietary behaviors can coexist at different frequencies in different taxa.

Primate feeding behavior is associated with certain rules that govern the dietary ecology of primates. These rules are related to a series of biotic and abiotic factors, that may influence the spatial availability of food resources. Some food resources are chosen more often than others given their spatiotemporal abundance in a habitat, and provide plentiful source of easily consumed calories (e.g. preferred food resources). On the other hand, some food resources are non-preferred but highly important seasonally, when preferred foods are absent/scarce (e.g. fall back food resources). These resources are typically abundant but are harder to process and less nutritious, and may require specializations to access, ingest masticate or digest (Rosenberger, 2013). Resource utilization is related to body size, metabolic rates and nutritional requirements of individual species, as well as scale factors associated with gut size, food passage rate, home range area and the cost of locomotion and foraging (Garber, 1987 and references therein). Notwithstanding the above, the most important factor that affects the availability of food resources and consequently primate diets through time is climatic

Ψηφιακή βιβλιοθήκη Θεόφραστος – Τμήμα Γεωλογίας – Αριστοτέλειο Πανεπιστήμιο Θεσσαλονίκης

Ψηφιακή συλλογή
Βιβλιοθήκη
"ΘΕΟΦΡΑΣΤΟΣ"
Τμήμα Γεωλογίας

variations. Nevertheless, most primates manage somehow to cope with climatic fluctuations, habitat and resource availability, and various dietary strategies have evolved depending on the species of interest. Two options are the most commonly observed: either expanding their home range which in time may drive a species to move into distinct micro-habitats, and/or expand their dietary spectrum (see Garber, 1987; Milton, 1993 for more detailed discussion). This can be rather challenging for some primates, especially in cases of species that may have adapted to distinct ecological conditions (e.g., specialists), compared to others (e.g., generalists). Nevertheless, some primate families may exhibit higher adaptability than others. One example of high adaptability and ecological flexibility in non-human primates is the family of Cercopithecidae.

1.5 Cercopithecidae: Origin, evolution and ecology

The current state of knowledge on the Cercopithecidae or Old World monkeys (OWM), recognizes them as one of the most diverse group of primates (Fleagle, 2013 and references therein), living in an array of different habitats in Africa and Asia. This is evidenced in their extensive and often well dated fossil record from Late Miocene and onwards, especially in Africa (Jablonski and Frost, 2010; Frost, 2017). The family appeared as a part of major radiation of catarrhines in Africa, and diverged from other catarrhines between 35.0–25.0 Ma (Kumar and Hedges, 1998; Steiper et al., 2004; Raaum et al., 2005). They originated from an extinct group, the family Victoriapithecidae, which are found in fossiliferous localities in northern and eastern Africa dated around 19.0–12.5 Ma (Harrison, 1989; Benefit, 1994; Benefit and McCrossin, 1997; Hill et al., 2002; Miller et al., 2009), but possibly as early as 25.0–22.0 Ma (Stevens et al., 2013; Rasmussen et al., 2019). The Cercpopithecidae or Old World monkeys include two subfamilies, Cercopithecinae and Colobinae. The divergence of the subfamilies is thought to be at least in progress by the middle Miocene (17.9–14.4 Ma) (Delson, 1975; Raaum et al., 2005).

Until 10.0–9.0 Ma, all cercopithecids were restricted to Africa. In that early time of their evolutionary history, cercopithecids are quite rare compared to other known catarrhines. An interesting fact is, that all early cercopithecids belong to Colobinae (Benefit and Pickford, 1986; Hlusko, 2007; Nakatsukasa et al., 2010; Rossie et al., 2013). However, the group's earliest evolution remains enigmatic because of the sparse fossil evidence (Pilbeam and Walker, 1968; Stevens et al., 2013; Rasmussen et al., 2019). Around 8.0 to 7.0 Ma, cercopithecids became much more common elements of the African fauna and they became more ecologically diverse. Cercopithecids gradually replaced apes as the predominant non-human primates of the Old World, but it is still unclear if this replacement was caused by climatic and associated vegetation changes (Elton, 2006; Frost, 2016 and references therein). This time period also marks the first members of the subfamily Cercopithecinae, being present in both North and Eastern Africa. After that time the cercopithecids underwent major adaptive radiations in Africa and Eurasia, which canalized future evolutionary changes and affected significantly their past and present day distribution.

1.5.1 Africa

The earliest occurrence of the Cercopithecidae comes from Tugen Hills, with two fossil teeth identified as belonging to early colobine monkeys, dated around 12.5 Ma (Rossie et al., 2013). Previously, the earliest record of colobines consisted of the type specimen *Microcolobus tugenensis* (10 Ma e.g., Benefit and Pickford, 1986), which is similar in size to the smallest extant colobine *Procolobus verus* (Delson et al., 2000), but lacks some derived characteristics of later and present day colobines. Like most of the living colobines, it was primarily arboreal, but it seems likely that it preferred to feed on fruits, seeds and other hard food objects, unlike most of the living forms which usually show advanced folivorous habits. Colobines are also

Ψηφιακή βιβλιοθήκη Θεόφραστος – Τμήμα Γεωλογίας – Αριστοτέλειο Πανεπιστήμιο Θεσσαλονίκης

Ψηφιακή συλλογή
Βιβλιοθήκη
"ΘΕΟΦΡΑΣΤΟΣ"
Τμήμα Γεωλογίας

known from the roughly contemporaneous site of Nakali in Kenya (9.9-9.8 Ma), where they appear to be represented by the same genus (Nakatsukasa et al., 2010). Between latest Miocene to Plio-Pleistocene times, there are at least five extinct genera representing colobine monkeys in Africa (Jablonski and Frost, 2010; Frost, 2017), with a noticeable general mass increase (Delson et al., 2000). These Plio-Pleistocene colobine forms were more ecologically diverse compared to the extant representatives.

There are three large colobine genera known from the Pliocene of eastern Africa, *Rhinocolobus*, *Cercopithecoides* and *Paracolobus* (Leakey, 1982). The genus *Cercopithecoides* is present in eastern, central and southern Africa with two different species known, *Cercopithecoides williamsi* and *Cercopithecoides kimeui* (Frost et al., 2003, 2015; Pallas et al., 2019). The genus included large bodied colobines ranging from ~20 kg, similar to some extant forms such as *Colobus*, but presumably reaching up to 50 kg in some cases (see Delson et al., 2000 for more extended discussion). These large colobines show postcranial adaptations that suggest they spend significant amount of time on the ground (Birchette, 1981; Leakey, 1982; Pallas et al., 2019). Moreover, *Cercopithecoides williamsi* was associated with more savanna-like environments with its wear pattern also suggesting a very abrasive diet (El-Zaatari et al., 2005; Williams and Geissler, 2014). *Paracolobus* is mostly known from two species, *Paracolobus chemeroni* and *Paracolobus mutiwa*, while more recently another new species was described, increasing significantly the chronostratigraphic range of this genus (Hlusko, 2007). This large colobine also exhibits postcranial adaptations towards terrestriality, while it also presents varying degrees of sexual dimorphism, in some cases resembling the high degree observed in *Nasalis larvatus*, or the largest *Papio* species (Delson et al., 2000). *Rhinocolobus* differs from the other Plio-Pleistocene colobine genera in some craniofacial characters, such as an elongate face with very short retracted nasal bones, while it exhibits adaptations for arboreal locomotion (Leakey, 1982; Delson et al., 2000; Frost, 2017; Laird et al., 2018). Another contemporaneous genus, *Kuseracolobus*, is also present in fossiliferous localities of eastern Africa. Two species are recognized: *Kuseracolobus aramisi* was similar to the extant proboscis monkey in terms of size, while *Kuseracolobus hafu* was considerably larger (Frost, 2001; Frost et al., 2020). Similarly to the genus *Rhinocolobus*, *Kuseracolobus* species appear to have been arboreal folivorous monkeys. Lastly, the genus *Libypithecus* is known only from Wadi Natrum fossil site in northern Africa, being of similar size to extant African colobines (Stromer, 1913; Meikle, 1987; Jablonski, 2002).

Cercopithecines appear later on the fossil record than colobines, although today they represent the most diverse and successful living non-human primate group. The subfamily consists of two tribes, Cercopithecini and Papionini, with molecular studies suggesting a possible divergence in the two tribes around 11.5 - 10.0 Ma (Tosi et al., 2005). The tribe Cercopithecini includes the African guenons and is comprised by six genera: *Allenopithecus*, *Erythrocebus*, *Chlorocebus*, *Cercopithecus*, *Allochrocebus*, *Miopithecus*. Guenons are very rare on the fossil record, and until recently, the sparse fossil evidence suggested that they never left the African continent. It is possible that the evolutionary history of this group occurred in regions where few fossils have been discovered, especially the forests of central Africa (Frost, 2017). Nevertheless, two dental specimens from the Late Miocene of Abu Dhabi (~8.0-6.5 Ma), extended significantly the biogeographic distribution of this tribe (see Gilbert et al., 2014).

The tribe Papionini today includes the genus *Macaca*, which is the only extant cercopithecine found outside Africa, and six more genera are found only in Africa, *Lophocebus*, *Rungwecebus*, *Theropithecus*, *Mandrillus*, *Cercocebus* and *Papio*, with the latter genus being present also in Arabia (Kopp et al., 2014). There are contrasting views regarding the phylogenetic relationships among papionin genera according to morphology-based cladistics and molecular evidence (Page et al., 1999; Pugh and Gilbert, 2018). It seems that the intergeneric and interspecies relationships among the members of this tribe are particularly

Ψηφιακή βιβλιοθήκη Θεόφραστος – Τμήμα Γεωλογίας – Αριστοτέλειο Πανεπιστήμιο Θεσσαλονίκης

Ψηφιακή συλλογή
Βιβλιοθήκη
"ΘΕΟΦΡΑΣΤΟΣ"

complex, possibly affected by hybridization events. In contrast to the extremely rare fossil guenons (Plavcan et al., 2019), papionins dominate the fossil record in Africa after 4.5 Ma. The oldest unambiguous papionin occurences are ?*Macaca* sp. from Menacer (formerly Marceau), Algeria (~7.0-5.8 Ma; Szalay and Delson, 1979; Geraads, 1987; Werdelin, 2010), *Macaca libyca* from Wadi Natrun, Egypt and possibly As Sahabi, Libya (6.2-5.0 and 6.3-5.3 Ma respectively, Szalay and Delson, 1979; Benefit, 2008; Werdelin, 2010), and "*Parapapio*" *lothagamensis* from Lothagam (~7.4-5.0 Ma; Leakey et al., 2003; Jablonski and Frost, 2010). After 2.0 Ma, *Parapapio* got gradually replaced from early members of the extant genus *Papio*, which became the predominant monkey genus of southern Africa. Despite the extensive distribution of extant representatives of the genus *Papio* in Africa today, and its relative abundance in the Pleistocene of southern Africa, it can be relatively sparse in the eastern African fossil record. Instead, the large terrestrial baboon-like *Theropithecus* dominated the Pleistocene fossil record of eastern Africa. Currently, there are three fossil species recognized, *Theropithecus brumpti*, *Theropithecus darti*, and *Theropithecus oswaldi*, while today it is only represented by a single species *Theropithecus gelada*, found only in the mountainous regions of Ethiopia. Unlike its present day distribution, fossil representatives of this genus were widely distributed in Africa during Plio-Pleistocene (Delson, 1993; Geraads and de Bonis, 2020). *Theropithecus oswaldi* was one of the most abundant and widely distributed monkey species in the Plio-Pleistocene of Africa, while available fossil evidence from Europe records the presence of this genus in Cueva Victoria fossil site in Spain (Gibert et al., 1995a; Ferràndez-Cañadell et al., 2014; Marigó et al., 2014). Moreover, the presence of the genus *Theropithecus* has been suggested in Pirro Nord in Italy based on a fossil cervical vertebrae (Lorenzo Rook et al., 2004; Rook and Martínez-Navarro, 2013), yet it is now clear that the fossil vertebrae does not correspond to a fossil primate (Alba et al., 2014). Additional fossil remains of *Theropithecus* has been found in Pleistocene fossil sites of Israel and India as well (Gupta and Sahni, 1981; Delson, 1993; Belmaker, 2010). It is worth mentioning that, fossil populations of *Theropithecus oswaldi* show a trend towards size increase throughout the Pleistocene, to the point that they were the largest monkeys ever recorded and among the largest known primates (Delson et al., 2000). The underlying reasons behind the size increase, as well as for the relatively rapid downfall of this once very successful primate genus still remain a mystery (see Jablonski, 2005 for extended discussion).

1.5.2 Eurasia

The first cercopithecid outside Africa is recorded in the Late Miocene (de Bonis et al., 1990), with the fossil colobine *Mesopithecus* being the sole representative across western Europe (Alba et al., 2015a) to Pakistan (Khan et al., 2020), Iran (Ataabadi et al., 2016; Suwa et al., 2016), Afghanistan (Heintz et al., 1981), and China (Jablonski et al., 2020). The genus *Mesopithecus* is best known from its rich fossil material from the type locality of Pikermi near Athens (Greece), attributed to several intermediate forms or time-succesive chronospecies, which span the whole Turolian (Koufos, 2009a). The genus included medium to large sized colobine monkeys, with evidence suggesting a semi-terrestrial lifestyle (Youlatos, 2003; Youlatos et al., 2012; but see also Escarguel, 2005), with a more opportunistic dietary behavior (Merceron et al., 2009a,b; Clavel et al., 2012). This ecological profile is in contrast with most of its extant African and Asian colobine relatives, which are usually considered as arboreal monkeys, with anatomical and physiological adaptations towards leaf consumption (Chivers, 1994; Matsuda et al., 2019). There are three species formally recognized from the area of Europe, *Mesopithecus delsoni*, *Mesopithecus pentelicus*, and *Mesopithecus monspessulanus* (Fig. 1.1), with the latest biochronological evidence suggesting the possible temporal coexistence of the latter two fossil species (Koufos, 2019). In addition, *Mesopithecus pentelicus* was found in sympatry with early European *Macaca* (Alba et al., 2014), while the smaller species *Mesopithecus monspessulanus* is found in sympatry with another large fossil colobine *Dolichopithecus ruscinensis*, and also *Macaca* (see Eronen and Rook, 2004 and references therein). This possibly reflects the new environmental conditions in the Early Pliocene and their

Ψηφιακή βιβλιοθήκη Θεόφραστος – Τμήμα Γεωλογίας – Αριστοτέλειο Πανεπιστήμιο Θεσσαλονίκης

Ψηφιακή συλλογή
Βιβλιοθήκη
"ΘΕΟΦΡΑΣΤΟΣ"
Τμήμα Γεωλογίας
Α.Π.Θ.

effects on the European habitats (Delson, 1994), which favored in cases the presence of more diverse primate communities. Nevertheless, the possible ecological terms of coexistence of cercopithecids within the same community are so far unknown.

Fig. 1.1 Geographic distribution of *Mesopithecus monspessulanus* in Europe (modified after Koufos, 2019).

Fig. 1.2 Geographic distribution of the genus *Dolichopithecus* in Europe (modified after Ardito & Mottura, 1987.

The genus *Dolichopithecus* included large-sized extinct colobine monkeys found in Pliocene localities in the area of Europe (Ardito & Mottura, 1987; Koufos et al., 1991). It is mostly represented by a single species. *Dolichopithecus ruscinensis* (Delson, 1994; Delson et al., 2000, 2005; Spassov & Geraads, 2007; but see Maschenko, 1991), while most of the known material derives from the type locality Serrat d'en Vaquer-Perpignan (France). Studies on available postcranial remains suggested semi or even fully terrestrial locomotor adaptations (Gabis, 1961; Jolly, 1967; Strasser and Delson, 1987; Delson et al., 2000; Ingicco, 2008). The biochronological range of this genus spans from the early Ruscinian to the early Villfranchian.

Ψηφιακή βιβλιοθήκη Θεόφραστος – Τμήμα Γεωλογίας – Αριστοτέλειο Πανεπιστήμιο Θεσσαλονίκης

Ψηφιακή συλλογή
Βιβλιοθήκη
"ΘΕΟΦΡΑΣΤΟΣ"

It is also hypothesized that *Dolichopithecus ruscinensis* derived from a marginal population of *Mesopithecus*, and later on became the dominant colobine in Europe for a brief time (Delson, 1973, 1975). However, this hypothesis was based on an ulnar specimen from Pestszentlőrinc in Hungary, initially considered of Late Miocene age, but later shown to be earlier Pliocene which somehow disproves this hypothesis for now (see Delson, 1994). Nevertheless, its phylogenetic relationships and taxonomic affiliations either to Colobini or Presbytini remain unclear. The earliest expansion of Cercopithecines out of Africa is dated around 8.0–6.5 Ma as evidenced by two dental specimens discovered in the Baynunah Formation in Abu Dhabi, United Arab Emirates (Gilbert et al., 2014). However, there is no record of cercopithecini beyond Afro-Arabia. The first record of papionins in Eurasia is later than the colobines, probably between 6.0–5.0 Ma (Fa, 1989; Maschenko and Baryshnikov, 2002; Alba et al., 2015a; Christian Roos et al., 2019). Around that time, all cercopithecines outside of Africa were most likely early members of the genus *Macaca* (Roos et al., 2019), with the European representatives of this genus probably being related to the sole extant macaque of Africa, *Macaca sylvanus* (e.g. Delson, 1980). The oldest member of the European fossil macaques is *Macaca sylvanus prisca*, recorded in some fossiliferous localities in southern Europe dated from the Ruscinian (5.0–4.0 Ma), and perhaps early Villfaranchian (4.0–3.0 Ma; Delson, 1980). The type locality of *Macaca sylvanus prisca* is Montpellier (France), associated with the large colobine *Dolichopithecus ruscinensis*, as well as the smaller more arboreal species of *Mesopithecus monspessulanus* (Delson, 1980; Eronen and Rook, 2004 and references therein). A very interesting case is a roughly contemporaneous but morphologically distinct population known from the Capo Figari fossil site in Sardinia, while later it was recorded also in other contemporaneous fossil sites of the island (Gentili et al., 1998; Rook & O'Higgins, 2005; Zoboli et al., 2016). This endemic form was described by Azzaroli (1946), as a 'dwarf' species namely *Macaca majori*, after Forsyth Major which discovered the fossil primate remains during the early 19th century (see Rook & Alba, 2012). Preliminary comparisons of dental material suggested 10–15% differences in size from the living *Macaca sylvanus* populations (Delson, 1980). Moreover, there is a number of sites yielding fossil macaque remains in the Iberian Peninsula (Alba et al., 2011; Castaños et al., 2011; Alba et al., 2014) and Italy (Eronen & Rook, 2004; Rook et al., 2001, 2013), usually referrable as *Macaca sylvanus florentina*. There are also later occurences of macaques all the way to the North Sea and England, extending significantly the biogeographical range of this genus (Singer et al., 1982; Schreiber and Löscher, 2011; Reumer et al., 2018; Schreiber, 2020). Over a dozen other localities of Late Pleistocene age have produced specimens indicating a range across Europe to Caucasus and Israel (Delson, 1980), being correlated with warm interglacial phases, possibly dated around the Last Eemian Interglacial (175.0–12.0 Kya). The local conditions of these ecosystems may have been more favorable for macaques, thus working as refugial biomes to withstand the harsher conditions during colder glacial intervals (see Fig. 2, 3 in Elton and O'Regan, 2014 for distribution of the genus *Macaca* in Europe).

In Asia the cercopithecid fossil record is even less complete than the European one. As in Europe, the oldest known cercopithecid is the colobine *Mesopithecus* (Jablonski et al., 2020; Ji et al., 2020), with the oldest fossil remains occurring in the latest Miocene (7.9–7.1 Ma) of Pakistan (Khan et al., 2020). Setting the genus *Mesopithecus* aside, there are three additional fossil colobine genera present in Eurasia during Late Miocene to Late Pliocene; the genus *Myanmarcolobus* from the Late Miocene/Early Pliocene of Myanmar (Takai et al., 2015), *Parapresbytis* from the Middle to Late Pliocene of Siberia and Mongolia (Egi et al., 2007; Takai and Maschenko, 2009), and *Kanagawapithecus* from the Late Pliocene of Japan (Iwamoto et al., 2005; Nishimura et al., 2012). Still, there are much to be known regarding the phylogenetic relationships of these Asian genera with *Mesopithecus* and *Dolichopithecus*. Furthermore, during Pleistocen times the fossil record of Asia evidence the presence of several colobines many of which are most likely related to the extant some extant Asian genera (e.g. Takai et al., 2014). The oldest Asian papionin in Eurasia was reported by Delson (1996), which suggested the presence of cf. *Macaca* sp. in China (~5.5 Ma), but this has been subsequently revised to

Ψηφιακή βιβλιοθήκη Θεόφραστος – Τμήμα Γεωλογίας – Αριστοτέλειο Πανεπιστήμιο Θεσσαλονίκης

Ψηφιακή συλλογή
Βιβλιοθήκη
"ΘΕΟΦΡΑΣΤΟΣ"
Τμήμα Γεωλογίας

indicate that the fossil material most likely comes from Pliocene deposits (Alba et al., 2014), thus the presence of the genus *Macaca* in Asia before the early Pliocene remains to be demonstrated (Roos et al., 2019). Fossil macaques have been reported from the Pleistocene fossil record of China (Schlosser, 1924), from Mianchi in Henan Province (2.5–1.0 Ma; Schlosser, 1924; Szalay and Delson, 1979), from Zhoukoudian locality 1 in the vicinity of Beijing (800–400 Ka; Young, 1934; Shen et al., 2009), and several fossil macaque remains recovered from a series of 14 fossil sites in the Chongzuo region in Guangxi Province (2.2 Ma and 5 Ka; Takai et al., 2014; see Roos et al., 2019 for extended discussion). Setting the macaques aside, two larger papionins are known from Eurasia, *Paradolichopithecus* and *Procynocephalus*, with uncertainty regarding their taxonomic and phylogenetic relationship.

Fig. 1.3 Geographic distribution of the genus *Paradolichopithecus* in Europe (modified after Ardito & Mottura, 1987).

The genus *Procynocephalus* was the first primate fossil formally described (Baker and Durand, 1836), alas, the information about this taxon is limited mostly due to the scarcity of available fossl material. *Procynocephalus* was widely distributed in eastern Eurasia in Late Pliocene and Early Pleistocene sites such as Xin'an (Henan Province), Gudi of Jingxing (Hebei Province), Locality 12 of Zhoukoudian, Renzidong of Fangchang (Anhui Province), and Zhongdian (Yunnan Province) (see Takai et al., 2014 and references therein). The type species *Procynocephalus wimani* is recorded in China, whereas specimens found in India and Pakistan are formally assigned to other species, *Procynocephalus subhimalayanus* or *Procynocephalus pinjorii* (Verma, 1969). *Paradolichopithecus* was a large cercopithecine mostly known from Pliocene to Early Pleistocene faunas of Europe (Delson and Nicolaescu–Plopsor, 1975a; de Vos et al., 2002; Takai et al., 2008; Kostopoulos et al., 2018; Radović et al., 2019). It is presumed that it exhibits postcranial adaptations more similar to the degree seen in *Papio* species, whereas some craniofacial features are more similar to macaques (Szalay and Delson, 1979). The specimens found in fossiliferous localities of Europe, are usually assigned to either *Paradolichopithecus arvernensis* (Depéret, 1929) or *Paradolichopithecus geticus* (Necrasov, 1961). Besides the European occurrences of the genus, there are two other species known: *Paradolichopithecus sushkini* (Trofimov, 1977) from Kuruksay, Tadjikistan, and *Paradolichopithecus gasuensis* (Qiu, 2004) from Longdan-Gansu, China. The limited fossil material available from the latter two fossil Plio–Pleistocene cercopithecine genera from Europe and Asia, makes their phylogenetic and taxonomic relationships debatable (Kostopoulos et al., 2018).

Ψηφιακή βιβλιοθήκη Θεόφραστος – Τμήμα Γεωλογίας – Αριστοτέλειο Πανεπιστήμιο Θεσσαλονίκης

Ψηφιακή συλλογή
Βιβλιοθήκη
"ΘΕΟΦΡΑΣΤΟΣ"
Τμήμα Γεωλογίας
Α.Π.Θ.

1.6 Main research questions and objectives

The environment has always been a key factor for understanding evolution, as it determines selection pressures that affect the way of life of every organism. Furthermore, environment include also surrounding organisms, for which competition for resources may occur. Hence, accurate and precise reconstructions of paleoenvironments play a crucial role in interpreting evolutionary scenarios. Diet is one of the most important aspects in the life of an organism while it is also associated with its surrounding environment. As a result, detailed understanding of evolution requires further information regarding the relationship between diet and environment. Thus, to understand the evolution and present day distribution of cercopithecids, it is necessary to decipher these key elements of their way of life now and also in the past. Several researchers have focused on the early cercopithecid fossil record (Delson, 1973; Szalay and Delson, 1979; Benefit and McCrossin, 1997; Frost, 2001; Rossie et al., 2013). This consequently led to a more detailed view of the evolutionary path of cercopithecids in respect to local and/or global environmental changes, but still there is much to be known.

Perhaps the most characteristic or hallmark feature of the dentition of Old World monkeys is their bilophodont upper and lower molars. The evolution of bilophodonty as a dental trait and the reasons behind it, still troubles paleontologists and people that study tooth wear until today. The molars of Cercopithecidae consist of a crown with four marginal cusps linked by transverse crests, with the exception of the lower third molar (M_3) which possesses an additional cusp (i.e., hypoconulid). Three dental cavities are formed by the two ridges: the mesial and distal foveas and the central basin . In occlusion, the transverse crests on the lower teeth fit into corresponding embrasures on the upper teeth and vice versa (Delson, 1973). Hence, shearing and crushing actions are performed every time molars come into occlusion (Swindler, 2002). The molars possess long shearing crests with various degree of expression depending on the species, the tooth position and the individual, and large crushing facets relative to body size (Kay, 1975). These observations suggest that bilophodonty may have been an adaptive response to increased consumption of leaves (Kay, 1978), while later Happel (1988) suggested that the bilophodont molars may reflect an original adaptation to increased reliance on seeds (e.g., Benefit, 2000). Furthermore, other primates that consume large quantities of leaves (i.e. *Propithecus* and *Allouatta*) exhibit bilophodont conditions as well (Swindler, 2002), while Gregory (1922) observed the parallel development of bilophodont molars in other leaf-eating mammals, like tapirs and kangaroos. Notwithstanding the above, more recently the description of a primitive monkey from Kenya that dates from ~22 Ma ago, which presumably exhibited dental adaptations for frugivory and perhaps hard object feeding, suggests that full bilophodont conditions in cercopithecid check teeth may have evolved later, likely in response to the inclusion of leaves in the diet (e.g., Rasmussen et al., 2019).

It has been hypothesized that leaf consumption would have been an adaptive response to selective pressures associated with scarcity of food resources and/or interspecific competition (Napier, 1970). In this sense, leaves are used as a fallback resource when needed, rather as a preferred food resource. This raises further questions regarding the importance of fallback foods in the evolution of cercopithecid dietary ecology, the association of such fallback resources with the effects of other selective pressures in the evolution of Colobinae and Cercopithecinae, such as niche partitioning, as well as their ecological diversity. To address these questions, some tried to decipher the ecological profile of the ancestral cercopithecid group Victoriapithecidae (Harrison, 1989; Benefit and McCrossin, 1997; Benefit, 1999; Dean and Leakey, 2004). Even though the molars of the latter group do not exhibit full bilophodont conditions, victoriapithecid molar morphology resembles more closely the cercopithecines instead of colobines, suggesting early adaptations towards frugivory and/or seed consumption (Benefit, 1993). This further supports a previous hypothesis that the evolution of colobines may have been related to natural selective forces for seed predation, and further proposes that folivory might have evolved independently in colobines (e.g. Happel, 1988; Chivers, 1994).

Ψηφιακή βιβλιοθήκη Θεόφραστος – Τμήμα Γεωλογίας – Αριστοτέλειο Πανεπιστήμιο Θεσσαλονίκης

Ψηφιακή συλλογή
Βιβλιοθήκη
"ΘΕΟΦΡΑΣΤΟΣ"

Many researchers have tried to characterize the diet of fossil cercopithecids via comparison with the modern analogues using a wide range of proxies. Studies of dental microwear (El–Zaatari et al., 2005; Merceron et al., 2009b, 2021; Williams and Holmes, 2011; Scott et al., 2012; Geissler, 2013; Engle et al., 2014; Martin et al., 2018), isotopic analysis (Pochron, 2000; Codron et al., 2005; Chenery et al., 2008; O'Regan et al., 2008; Crowley, 2012; Cerling et al., 2013; Macharia et al., 2014; Levina et al., 2015), dental morphology (Kay, 1977; Kay and Sheine, 1979; Kirk and Simons, 2001; Singleton, 2003), enamel thickness (Lambert et al., 2004; McGraw et al., 2012, 2014; Kato et al., 2014; Beaudet et al., 2016; Thiery et al., 2017a), and dental topographic analyses (Lazzari et al., 2008a; Bunn et al., 2011; Klukkert et al., 2012b; Guy et al., 2013, 2015; Winchester, 2016; Thiery et al., 2017b; 2019; Berthaume et al., 2020), have been applied on fossil and extant cercopithecids demonstrating the usefulness of these methods on extracting dietary information. However most of the studies have focused on the African cercopithecid fossil record, being more abundant, and more abundant and diverse. Even though we have a fairly detailed picture of the African Plio–Pleistocene cercopithecids, this is not the case concerning the early forms of Europe.

Available information considering the palaeoecology of European cercopithecids are very limited, based mainly on indirect evidence from the associated fauna (Jolly, 1967, 1972; Strasser, 1988; Szalay & Delson, 1979). The main reasons behind this are the scarcity of the available material and the limited technological means until the early 80's. Now, new discoveries of fossil material and newly advanced technological tools can add novel information regarding the ecological profile of these extinct forms. The primary goal of this thesis is to characterize the dietary habits and preferences of the Pliocene to Pleistocene cercopithecids that inhabited the Palearctic region, mostly focused on the western part (i.e. Europe). To achieve that, the present study aims to use the combination of two methodologies: dental topographic analysis and dental microwear texture analysis (DMTA).

Dental topographic and enamel thickness analysis (3D relative enamel thickness and distribution), are used as a proxy to explore potential adaptive morphologies in cercopithecid dentition associated with selective pressures related to diet. Dental microwear texture analysis is applied to investigate their feeding behavior prior to death. The combined application of these two distinct methodologies hopefully will provide a more detailed picture regarding the dietary ecology of Plio–Pleistocene Eurasian cercopithecids. This will enable to address questions such as, **a)** if, how and to what extent, the global and/or local climatic events during Plio–Pleistocene are associated with the phylogenetic radiation of cercopithecids in the Palearctic, **b)** in which way did cercopithecids respond to possible selective pressures in Europe, **c)** what was the ecological context that possibly led to their coexistence within the same community. Lastly, **d)** the very wide geographical distribution of some Eurasian taxa, such as the Early Pleistocene *Paradolichopithecus* (which ranged from Spain all the way to China), is yet to be investigated under a paleoecological perspective. Taking under consideration the co-occurence of cercopithecids with hominoids in the same geographic regions (e.g. Africa and Eurasia), making accurate interpretations of the Palearctic environments during Plio–Pleistocene is critically important for understanding the evolution of *Homo* as well.

Ψηφιακή βιβλιοθήκη Θεόφραστος – Τμήμα Γεωλογίας – Αριστοτέλειο Πανεπιστήμιο Θεσσαλονίκης

Ψηφιακή συλλογή
Βιβλιοθήκη
"ΘΕΟΦΡΑΣΤΟΣ"
Τμήμα Γεωλογίας
Α.Π.Θ

Chapter 2. Material and methods

2.1 Material

2.1.1 Fossil species

This work is focused on the Plio-Pleistocene fossil cercopithecids found in the western Palearctic (i.e. Europe), as there was no available fossil material from the eastern Palearctic. The only available specimen for this study from the eastern part of the Palearctic derives from Late Pliocene Kosawa fossil site in Aikawa-cho, Aikou-gun, Kanagawa Prefecture, Japan, namely *Kanagawapithecus leptopostorbitalis* (Iwamoto et al., 2005). The μ-CT scan of its upper molars was kindly provided by T. D. Nishimura and M. Takai from the Primate Research Institute of the University of Kyoto, Japan (KUPRI), while the dental molds were made during my visit in the Kanagawa Prefectural Museum of Natural History. However, the advanced dental wear of the specimen, due to the old age of the individual and possibly taphonomic processes, did not permit a detailed investigation of its dental tissue. However, the specimen retained microwear signal. Nevertheless, since the fossil material for this taxon consists only of the holotype specimen from Nakatsu, and it was not possible to apply both methodologies used here, it was finally decided to exclude it from the present work pending future analyses. It may be useful to explore the type of wear of this fossil colobine from Japan and compare it with other Eurasian fossil colobines, such as *Dolichopithecus* and *Parapresbytis*, but this is beyond the scope of this work. In the western Palearctic (i.e. Europe), cercopithecids are mostly represented by four fossil genera: *Mesopithecus*, *Dolichopithecus*, *Macaca*, and *Paradolichopithecus*.

All analyses are focused on molar teeth, because these teeth are commonly used in most of the dietary investigations (see Ungar, 2019 and references therein). The total fossil sample used for dental topographic and enamel thickness analyses is shown in Table 2.2, while all measurements are summarized in the respective appendix of each chapter. All μ-CT scanned fossil specimens investigated, were also used for dental microwear texture analysis.

Table 2.1 Fossil sample for each fossil species included for dental topographic and enamel thickness analysis with the respective host institutions.

Taxon	ID	Locality	Tooth	Institutions
D. ruscinensis	MEV−1	Megalo Emvolon (Greece)	M_3 dex	LGPUT
D. ruscinensis	MHNPn−PR39	Perpignan (France)	M_2 sin	MHNP
D. ruscinensis	MHNPn−PR01	Perpignan (France)	M^1 dex	MHNP
Me. monspessulanus	DKV480	Dorkovo (Bulgaria)	M^3 sin	NHMS
Me. monspessulanus	UM4043	Montpellier (France)	M_1 dex	ISEM
Me. monspessulanus	UM4043	Montpellier (France)	M_2 sin	ISEM
Me. monspessulanus	UM4043	Montpellier (France)	M_3 sin	ISEM
P. arvernensis	DFN3−150	Dafnero (Greece)	M^2 sin	LGPUT
P. arvernensis	DFN3−150	Dafnero (Greece)	M^3 sin	LGPUT
M. majori	Ty5203	Capo Figari, Sicily (Italy)	M^2 dex	NHMB
M. majori	Ty5203	Capo Figari, Sicily (Italy)	M^3 dex	NHMB
M. majori	Ty5199	Capo Figari, Sicily (Italy)	M^2 sin	NHMB
M. majori	Ty5199	Capo Figari, Sicily (Italy)	M^3 sin	NHMB

The fossil material used for dental microwear texture analysis is summarized in Table 2.1, whereas all raw data are given in the supplementary material of each respective chapter. A total of 17 Plio-Pleistocene European fossiliferous localities are included (Fig. 2.1), with biochronological range of the relevant faunas spannning from MN13-MNQ18 (5.3–1.0 Ma) (Table 2.1). The majority of these localities have yielded either isolated or a couple of dental remains, which makes it difficult to explore dietary variations between different geographic locations; thus, interpretations should be treated with caution. Be that as it may, and even if diet

Ψηφιακή βιβλιοθήκη Θεόφραστος – Τμήμα Γεωλογίας – Αριστοτέλειο Πανεπιστήμιο Θεσσαλονίκης

Ψηφιακή συλλογή
Βιβλιοθήκη
"ΘΕΟΦΡΑΣΤΟΣ"

may vary between members of the same species in different geographic locations, the total number of individuals for each fossil taxon included in the dental microwear sample is sufficient to provide useful information regarding their dietary behavior.

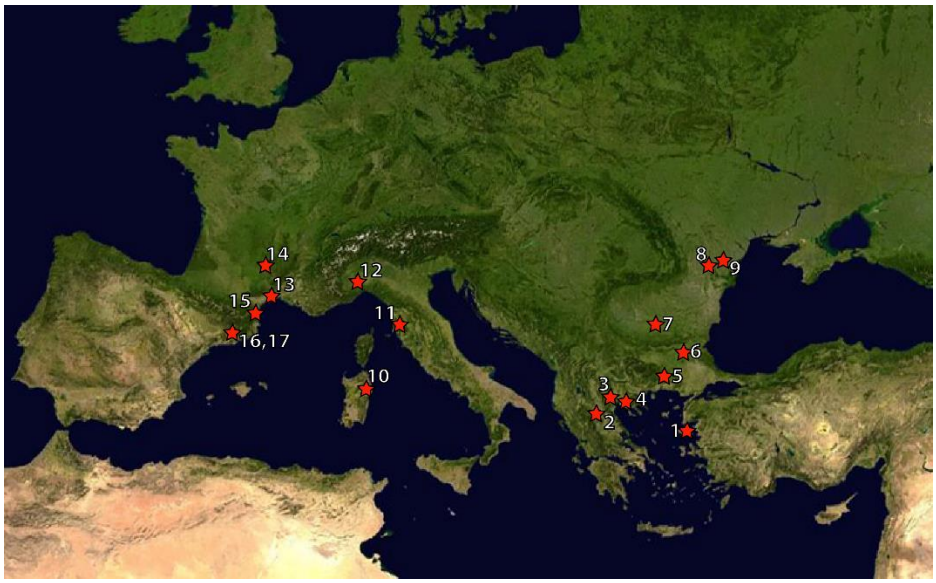

Fig. 2.1 The fossiliferous localities included in this study for dental microwear texture analysis. **1**: Vatera, Lesvos Island (Greece); **2**: Dafnero, Kozani (Greece); **3**: Dytiko, Axios Valley (Greece); **4**: Megalo Emvolon, Agelochori–Cape Megalo Emvolon (Greece); **5**: Dorkovo (Bulgaria); **6**: Tenevo (Bulgaria); **7**: Valea Graunceanului (Romania); **8**: Măluşteni (Romania); **9**: Taraclia (Moldova); **10**: Capo Figari (Sardinia); **11**: Upper Valdarno (Italy); **12**: Villafranca d'Asti (Italy); **13**: Montpellier (France); **14**: Senèze (France); **15**: Perpignan (France); **16**, **17**: Cal Guardiola, Vallparadís, Terrassa (Spain).

Table 2.2. Fossil sample for each species included for dental microwear texture analysis with number of specimens per fossiliferous locality, age with references.

Taxon	**Locality**	**Age[a]**	**n[b]**	**References**
D. ruscinensis	Perpignan	MN15 (4.2 – 3.4 Ma)	32	Depéret, 1889
D. ruscinensis	Megalo Emvolon	MN15 (4.2 – 3.4 Ma)	1	Koufos et al., 1991
D. ruscinensis	Dorkovo	MN14 (5.3 – 4.2 Ma)	3	Delson et al., 2005
D. ruscinensis	Măluşteni	MN15 (4.2 – 3.4 Ma)	1	Petculescu et al., 2003
D. balcanicus sp.	Tenevo	MN15 (4.2 – 3.4 Ma)	1	Spassov and Geraads, 2007
D. ruscinensis	Taraclia	MN15? (4.2 – 3.4 Ma)	1	–
Me. monspessulanus	Montpellier	MN14 (5.3 – 4.2 Ma)	6	Mauche 1906
Me. monspessulanus	Dytiko 2	MN13 (7.0 – 6.0 Ma)	1	de Bonis et al., 1990; Koufos, 2019
Me. monspessulanus	Dorkovo	MN14 (5.3 – 4.2 Ma)	1	Delson et al., 2005
Me. monspessulanus	Măluşteni	MN15 (4.2 – 3.4 Ma)	1	Simionescu, 1930
Me. monspessulanus	Villafranca D' Asti RDB	MN16 (3.4 – 2.6 Ma)	2	Pradella and Rook, 2007
P. geticus	Valea Graunceanului	MN17 (2.4 – 2.2 Ma)	3	Petculescu et al., 2003
P. arvernensis	Vatera	MN17 (2.5 – 1.9 Ma)	2	Van der Geer and Sondaar, 2002
P. arvernensis	Senèze	MN17 (2.5 – 1.9 Ma)	1	Depéret, 1929
P. arvernensis	Dafnero–3	MN17 (2.4 – 2.3 Ma)	1	Kostopoulos et al., 2018
M. majori	Capo Figari	MN 16 – 17 (3.55 – 1.9 Ma)	30	Zoboli et al., 2016
M. s. prisca	Villafranca d'Asti RDB	MN16 (3.4 – 2.6 Ma)	1	Rook et al., 2001
M. s. cf. *fiorentina*	Upper Valdarno	MN16 – 17 (3.6 – 2.58 Ma)	5	Rook et al., 2013
M. s. cf. *fiorentina*	Cal Guardiola	MN18 (~1.0 Ma)	2	Alba et al., 2008
M. s. cf. *fiorentina*	Vallparadís	MN18 (~1.0 Ma)	1	Alba et al., 2008

Ψηφιακή βιβλιοθήκη Θεόφραστος – Τμήμα Γεωλογίας – Αριστοτέλειο Πανεπιστήμιο Θεσσαλονίκης

Ψηφιακή συλλογή Βιβλιοθήκη "ΘΕΟΦΡΑΣΤΟΣ" Τμήμα Γεωλογίας Α.Π.Θ

[a] The ages of the localities are taken from NOW (2019) except for: Dytiko (Koufos & Vasileiadou, 2015); Cal Guardiola and Vallparadís (Alba et al., 2008); Dafnero (Benammi et al., 2020); Valea Graunceanului (Petculescu et al., 2003);[b] n: number of possible individuals.

2.1.2 Extant species

This study includes a total of 30 extant species of cercopithecids, ensuring that these species encompass a wide range of dietary habits and behaviors usually shown by modern members of this group. The aim was to include as many extant species as possible, with available both μ-CT scans and dental microwear texture data. However, this was not possible in all cases (see Table 2.3).

The molar sample of extant cercopithecid species used for dental topographic and enamel thickness analyses, consists of a total of 65 molars (M^2, n = 48; M^3, n = 4; M_2, n = 9; M_3, n = 4) from 26 extant species from Africa and Asia, while a total of 14 extant species are used for dental microwear texture analysis (see Table 2.3). The exact number of specimens from each species analyzed using either methodology is summarized in the respective appendix of each chapter.

All extant specimens belong to collections from the following institutions: Royal Museum of Central Africa (RMCA) Tervuren, Belgium; Seckenberg Museum of Frankfurt (SMF), Germany; Muséum National d'Histoire Naturelle (MNHN), Paris, France; Laboratoire Paléontologie, Evolution Paléoécosystèmes, Paléoprimatologie (PALEVOPRIM), Université de Poitiers, France; Primate Research Institute of Kyoto University (KUPRI) Inuyama, Japan; and American Museum of Natural History (AMNH), New York, United States, Authority for Reasearch and Conservation of Cultural Heritage in Addis Ababa (AARCH), Ethiopia; Museum of Natural history of Vienna (NHMW), Austria; Bavarian State Collection of Zoology, Munich (ZSM), Germany. Some additional raw microwear data were available from previous analyses (e.g. Percher et al., 2018).

Table 2.3 Modern species used in this study with dietary references.

Taxon	Methodologies[a]	References
Cercocebus galeritus	Dental topographic, enamel thickness analysis	Homewood, 1978; Wahungu, 1998; Wieczkowski, 2004, 2009
Cercocebus sp	Dental topographic, enamel thickness analysis	Fleagle and McGraw, 2002; Daegling et al., 2011; McGraw et al., 2012
Cercocebus torquatus	Dental topographic, enamel thickness analysis	Cashner, 1972; Mitani, 1989; Daegling et al., 2011; Cooke, 2012
Chlorocebus aethiops	Dental topographic, enamel thickness analysis	Kavanagh, 1978; Whitten, 1983; Pruetz and Isbell, 2000a; Nakagawa, 2003a; Barrett, 2005
	DMTA	
Cercopithecus cephus	Dental topographic, enamel thickness analysis	Gautier-Hion, 1980; Tutin et al., 1997a; Chapman et al., 2005
Cercopithecus campbelli	Dental topographic, enamel thickness analysis	Buzzard, 2006
Cercopithecus diana	Dental topographic, enamel thickness analysis	Buzzard, 2010; Curtin, 2005; Kane & McGraw, 2018; Oates & Whitesides, 1990; Rowe et al., 1996
Cercopithecus nictitans	Dental topographic, enamel thickness analysis	Brugiere et al., 2002
Cercopithecus pogonias	Dental topographic, enamel thickness analysis	Brugiere et al., 2002
Erythrocebus patas	Dental topographic, enamel thickness analysis	Hall, 1966; Isbell, 1998; Isbell & Young, 2007; Nakagawa, 2000a, 2000b, 2003
	DMTA	
Lophocebus albigena	Dental topographic, enamel thickness analysis	Olupot, 1988; Poulsen et al., 2001; Chapman et al., 2005; McGraw et al., 2012; McGraw, 2017
	DMTA	
Lophocebus atterimus	Dental topographic, enamel thickness analysis	Cashner, 1972; Horn, 1987; McGraw et al., 2012

Ψηφιακή βιβλιοθήκη Θεόφραστος – Τμήμα Γεωλογίας – Αριστοτέλειο Πανεπιστήμιο Θεσσαλονίκης

Ψηφιακή συλλογή Βιβλιοθήκη "ΘΕΟΦΡΑΣΤΟΣ" Τμήμα Γεωλογίας ΑΠΘ

Mandrillus leucophaeus	Dental topographic, enamel thickness analysis	Lahm, 1986; Norris, 1988; Astaras et al., 2008; 2011; Owens et al., 2015; Nsi Akoue et al., 2017
Mandrillus sphinx	DMTA	Hoshino, 1985; Lahm, 1986; Norris, 1988; Rowe et al., 1996; Tutin et al., 1997a; Peignot et al., 2008; Percher et al., 2018
Papio anubis	Dental topographic, enamel thickness analysis	Hill and Dunbar, 2002; Newton-Fisher and Okecha, 2006; Akosim, et al., 2010; Johnson et al., 2012
Papio cynocephalus	Dental topographic, enamel thickness analysis	Rhine et al., 1986, 1989; Norton et al., 1987; Whiten et al., 1991; Hill et al., 2003; Bentley-Condit, 2009
Papio hamadryas	Dental topographic, enamel thickness analysis	Pochron, 2000; Swedell et al., 2008; Henzi et al., 2011
	DMTA	
Theropithecus gelada	Dental topographic, enamel thickness analysis	Fashing et al., 2014; Abu, 2018; Jarvey et al., 2018
	DMTA	
Macaca sylvanus	Dental topographic, enamel thickness analysis	Ménard and Vallet, 1997; Ménard, 2002; El Alami et al., 2012; Maibeche et al., 2015
	DMTA	
Macaca fuscata	DMTA	Maruhashi, 1980; Iguchi and Izawa, 1990; Agetsuma, 1995; Hill, 1997; Tsuji et al., 2015
Macaca nemestrina	DMTA	Bernstein, 1967
Macaca tonkeana	Dental topographic, enamel thickness analysis	Riley, 2008; Riley et al., 2013; Riptianingsih et al., 2015
Colobus satanas	Dental topographic, enamel thickness analysis	McKey et al., 1981; Kelley, 1990; Tutin et al., 1997a; Brugiere et al., 2002
Piliocolobus badius	Dental topographic, enamel thickness analysis	Daegling & Mcgraw, 2001; Dasilva, 1994; Davies et al., 1999; Kibaja, 2014; Marsh, 1981; Mowry et al., 1996; Shimizu, 2002
	DMTA	
Colobus guereza	Dental topographic, enamel thickness analysis	Fashing, 2001; Harris, 2010; Harris & Chapman, 2007; Oates, 1978; Oates et al., 1977
	DMTA	
Colobus polykomos	Dental topographic, enamel thickness analysis	Daegling & Mcgraw, 2001; Dasilva, 1994; Davies et al., 1999; McGraw et al., 2016
Nasalis larvatus	Dental topographic, enamel thickness analysis	Bennett & Sebastian, 1988; Boonratana, 1993; Matsuda et al., 2009; 2017; Salter et al., 1985; Yeager, 1989
	DMTA	
Procolobus verus	Dental topographic, enamel thickness analysis	Daegling & McGraw, 2001; Davies et al., 1999; Oates & Whitesides, 1990
Semnopithecus entellus	Dental topographic, enamel thickness analysis	Newton, 1992; Rowe et al., 1996; Punekar, 2002; Dela, 2007; Sayers and Norconk, 2008; Vandercone et al., 2012
	DMTA	
Trachypithecus cristatus	Dental topographic, enamel thickness analysis	Kool, 1992, 1993; Caton, 1999; Wright et al., 2008
Presbytis melalophos	DMTA	Davies et al., 1988; Rodman, 1991; Rowe et al., 1996

2.2 METHODS

2.2.1 Dental microwear texture analysis (DMTA)

The need for a new instrument for microwear analysis was first emphasized by Boyde and Fortelius (1991) who suggested that confocal microscopy, with its capability of collecting 3D surface data, might be an answer. In the upcoming years, confocal microscopy was brought together with scale–sensitive fractal analysis (SSFA) (Ungar et al., 2003). This offered a more practical approach to characterize microwear surface textures, now known as dental microwear texture analysis (DMTA) (Scott et al., 2005, 2006).

SSFA was developed for a broad spectrum of industrial applications (Kennedy et al., 1999; Pedreschi et al., 2000; Brown and Siegmann, 2001; Zhang et al., 2002) and it is based on the principle of fractal geometry that a surface can look different at different scales. Thus, surface textures that appear smooth at coarse scales can be demonstrably rough at finer scales.

Ψηφιακή βιβλιοθήκη Θεόφραστος – Τμήμα Γεωλογίας – Αριστοτέλειο Πανεπιστήμιο Θεσσαλονίκης

Ψηφιακή συλλογή
Βιβλιοθήκη
"ΘΕΟΦΡΑΣΤΟΣ"

SSFA can be applied to length profiles or to three–dimensional surfaces and it calculates five basic textures parameters: area-scale fractal complexity (Asfc), exact proportion length-scale anisotropy of relief (epLsar), scale of maximal complexity (Smc), textural fill volume (Tfv) and heterogeneity of complexity (Hasfc). Combined they provide a far more detailed characterization of dental microwear surface textures than any other traditional measurement applied in previous methods (e.g measurements of striations/scratches and pits).

A surface microwear texture is characterized as 'anisotropic' when the texture features share similar orientations (e.g many parallel striations; Fig. 2.2a), whereas 'complex' textures possess microwear features such as pits and scratches of different sizes overlaying each other with no particular orientation (Fig. 2.2b). Furthermore, 'homogeneous' microwear textures will exhibit similar microwear features from place to place across a surface, in contrast to 'heterogeneous' microwear textures (Fig. 2.2c). The specific algorithms used to calculate all parameters considered here are mentioned in detail by Scott et al., (2006).

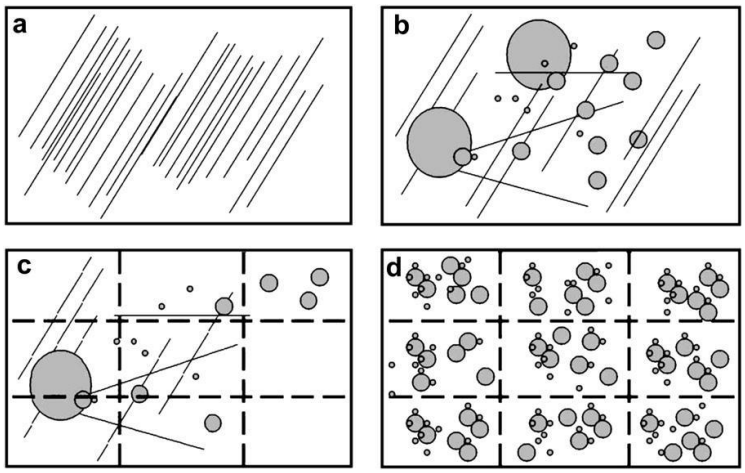

Fig. 2.2 Example of schematic microwear surfaces showing anisotropic texture (a), complex texture (b) and heterogenous (c) and homogenous (d) textures (taken from Scott et al. 2006).

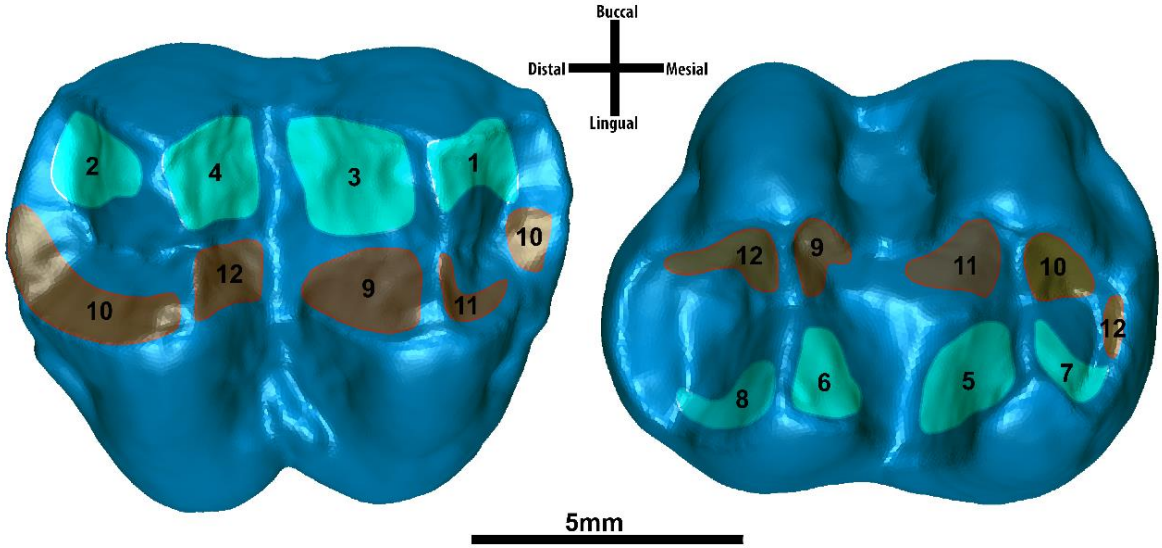

Fig. 2.3 Illustration of microwear facets on digitally reconstructed molar specimens of *Dolichopithecus ruscinensis* **left**) M^1, MHNPn–PR01, **right**) M_2, MHNPn–PR39 (**Brown**: Phase II; **Green**: Phase I).

Ψηφιακή βιβλιοθήκη Θεόφραστος – Τμήμα Γεωλογίας – Αριστοτέλειο Πανεπιστήμιο Θεσσαλονίκης

Ψηφιακή συλλογή
Βιβλιοθήκη
"ΘΕΟΦΡΑΣΤΟΣ"
Τμήμα Γεωλογίας
Α.Π.Θ.

Technical implementations and surface data collection

The mastication process is divided in two intervals: 'Phase I' and 'Phase II'. The former precedes centric occlusion and the latter follows it. The wear facets in which wear features are produced by the shearing action of the tooth are attributed to Phase I, while wear facets produced to the surface of the cusp where food is crushed are attributed to Phase II (Krueger et al., 2008). Data collection was performed on both Phase I and II dental facets (Maier, 1977; Fig**.** 2.3). All analyses were preferentially done on second upper and lower molars but first or third molars were also investigated to complement the fossil sample in cases of postmortem alterations or very early wear stages of the second molars. Moreover, since the occluding facets do not significantly differ from each other (Teaford & Walker, 1984), data from homologous facets of upper and lower molars were both considered for this study. Experimental works have shown no significant variations along the upper and lower molar rows (Ramdarshan et al., 2017).

Following standard protocols (e.g. Merceron et al., 2016), teeth were cleaned two times (up to three in some case) with cotton swabs using either aceton or highly concentrated (> 90%) alcohol. After cleaning and drying from the alcohol/acetone, each specimen was molded (2–3 molds per specimen) with a silicone dental molding material (polyvinyl siloxane Coltene Whaledent, President Regular Body). All dental facets were scanned with 'TRIDENT', a confocal DCM8 Leica Microsystems surface profilometer housed at the PALEVOPRIM lab at the University of Poitiers using a 100× lens (Merceron et al., 2016). The scanned surfaces were mirrored and automatically freed from any abnormal peaks, and a 200 × 200 μm area was extracted and saved as a digital elevation model to be used for DMTA. The resulting data were analyzed in Toothfrax (v 1.0) and Sfrax (v 1.11.882) (Surfract, www.surfract.com). Five variables were used to characterize microwear surface textures: complexity (Asfc; no unit), scale of maximum complexity (Smc in μm^2), heterogeneity (Hasfc with 9, 36, 81 cells; no units), anisotropy (epLsar at 1.8 μm; no unit) and textural fill volume (Tfv at the scale of 2.0 μm^3).

Area–scale fractal complexity (Asfc)

Complexity is a measure of changes in surface roughness at different scales. Changes in relative area with scale can then be used to characterize the complexity of the surface roughness. *Asfc* is the slope of the steepest part of the curve, fit to a log–log plot over the range of scales at which those measurements are made (Fig. 2.4). The steeper the slope is, the more complex surface. Complexity has been shown that is a good metric to distinguish primates that eat harder, more brittle foods from those that consume tougher foods (Ragni et al., 2017; Scott et al., 2012). For each scan examined here, the relative areas were calculated for scales ranging from 7200 mm^2 to 0.02 mm^2 using Toothfrax software. In order to calculate complexity, during the scanning procedure the surface is separated into four adjoining scans, of which the median Asfc's are used to calculate the single value for this parameter. The scale range over which Asfc is calculated (steepest part of the rel. area vs. scale curve) may also be informative and is summarized here by the Scale of maximum complexity (Smc) (Scott et al., 2006).

Ψηφιακή βιβλιοθήκη Θεόφραστος – Τμήμα Γεωλογίας – Αριστοτέλειο Πανεπιστήμιο Θεσσαλονίκης

Ψηφιακή συλλογή
Βιβλιοθήκη
"ΘΕΟΦΡΑΣΤΟΣ"
Τμήμα

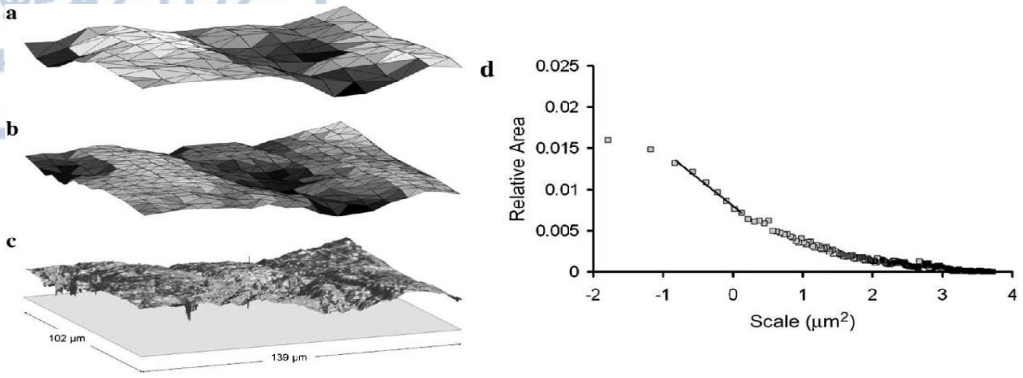

Fig. 2.4 Area scale analysis. A virtual tiling algorithm using triangles of different sizes can be used to measure surface roughness (compare **a**, **b** and **c**). Complexity is represented by the steepest part of a curve fitted to the plot of relative area over scale (**d**) (modified from Scott et al., 2006).

Exact proportion length–scale anisotropy of relief (epLsar)

Anisotropy is a measure of directionality, orientation of the surface relief. Relative lengths of depth profiles are different from orientation when the surface roughness is anisotropic (Fig. 2.5). Relative lengths with specific orientation can be defined as vectors. The vectors calculated are at 5º intervals for a total of 36 measures, and normalized using the exact proportion method to determine a mean vector length. Normalized relative length vectors can be displayed graphically in a rosette diagram (Fig. 2.5b) The length of the mean vector is a measure of anisotropy called exact proportion Length–scale anisotropy of relief, or epLsar (Merceron et al., 2009). It was calculated for each scan using Toothfrax (Surfract, www.surfract.com) at a 1.8 μm scale of observation. A surface which is dominated with scratches, linear striations following the same direction would present high value of epLsar (Ungar et al., 2008).

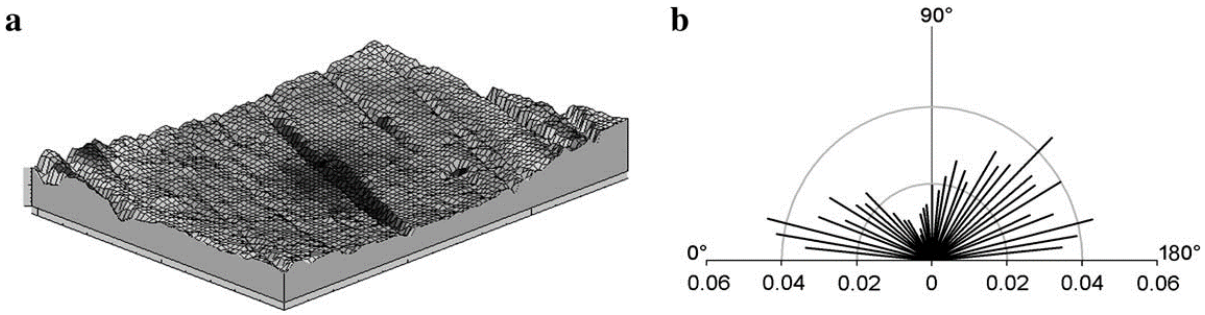

Fig. 2.5 Three–dimensional rendering of striated surface (a) and the corresponding rosette plot of relative lengths taken at 36 different orientations (b) (taken from Scott et al. 2006).

Heterogeneity of complexity (Hasfc)

While complexity and anisotropy provide us with useful characterization of the surface texture, their variation across the surface may be also important. For instance, two scans across a surface, focusing on different parts of the surface, can yield different values for Asfc or epLsar (Fig. 2.2c, d). Heterogeneity of area–scale fractal complexity (Hasfc) can be calculated by splitting individual scanned areas into smaller subdivisions with equal number of rows and columns (4 cells, 9 cells, 16 cells, 25 cells … 121 cells) using Toothfrax software (Scott et al., 2006).

Ψηφιακή βιβλιοθήκη Θεόφραστος – Τμήμα Γεωλογίας – Αριστοτέλειο Πανεπιστήμιο Θεσσαλονίκης

Ψηφιακή συλλογή
Βιβλιοθήκη
"ΘΕΟΦΡΑΣΤΟΣ"
Τμήμα Γεωλογίας
Α.Π.Θ.

Textural fill volume (Tfv)

This measure examines the summed volumes of square cuboids that fill the surface at a given scale. The total volume filled is a function of two components: a) the shape of the surface, and b) the texture of the surface. A planar surface would have lesser total fill volume than a concave or convex surface even if the two textures are identical (Scott et al., 2006). Essentially, textural fill volume is computed as the difference in summed volumes of very fine cuboids and larger ones (2 μm and 10 μm on a side) (Fig. 2.5). This procedure removes the structure of the overall surface and enables the characterization only of the microwear features. A surface dominated with more features in the mid-scale range would present high values of Tfv (Ungar et al., 2008).

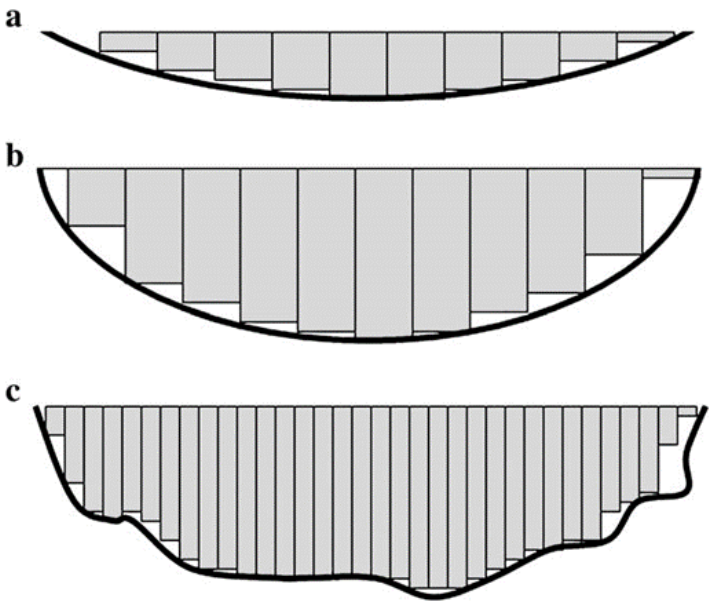

Fig. 2.6 Drawing comparing surfaces with (**a**) lower and (**b**) higher structural fill volumes. Finer scale prisms (**c**) yield structural and textural fill volumes. Textural fill volumes by subtracting (**b**) from (**c**). (taken from Scott et al. 2006).

2.2.2 Dental topographic and enamel thickness analyses

Throughout the years, several noninvasive techniques have been developed in order to capture the three–dimensional form of objects (Cnudde and Boone, 2013; Sutton et al., 2016; Berthaume et al., 2020). Microtomographic systems (μ-CT) have proven to be a powerful and efficient tool to retrieve detailed aspects of dental morphology, isolate and extract specific dental components (e.g occlusal enamel surface and enamel-dentine junction surface, henceforth referred as OES and EDJ respectively). X-ray microtomography has been used thoroughly in dental topographic and enamel thickness analyses of extant and extinct primates (Kono, 2004; Tafforeau et al., 2006; Lazzari et al., 2008b). Here, the standard protocol for topographical quantification of Guy et al., (2013, 2015) is followed, which will be explained in detail next.

Data acquisition and surface processing

Only unworn or minimally worn molars were selected ensuring that no macro-elements were altered by wear following previous standard approaches (e.g. King et al., 2005; Olejniczak et al., 2008 among others). All fossil molars were previously scanned using EasyTom XL duo μ-CT (Plateforme PLATINA, IC2MP, University of Poitiers, France), with voxel size ranging from 9.0 to 40.0 μm. Most of the extant molar specimens were scanned using the latter micro-

Ψηφιακή βιβλιοθήκη Θεόφραστος – Τμήμα Γεωλογίας – Αριστοτέλειο Πανεπιστήμιο Θεσσαλονίκης

Ψηφιακή συλλογή
Βιβλιοθήκη
"ΘΕΟΦΡΑΣΤΟΣ"

tomographic system, and with the same scanning resolution (Chapters 3, 5 and 6). However, a number of extant specimens were downloaded from MorphoSource.org digital repository to expand the comparative sample of upper and lower molars. These specimens were scanned using GE phoenix v tome xs240 housed in the American Museum of Natural History (AMNH), with voxel size ranging from 50.0 to 120.0 μm (Chapter 4).

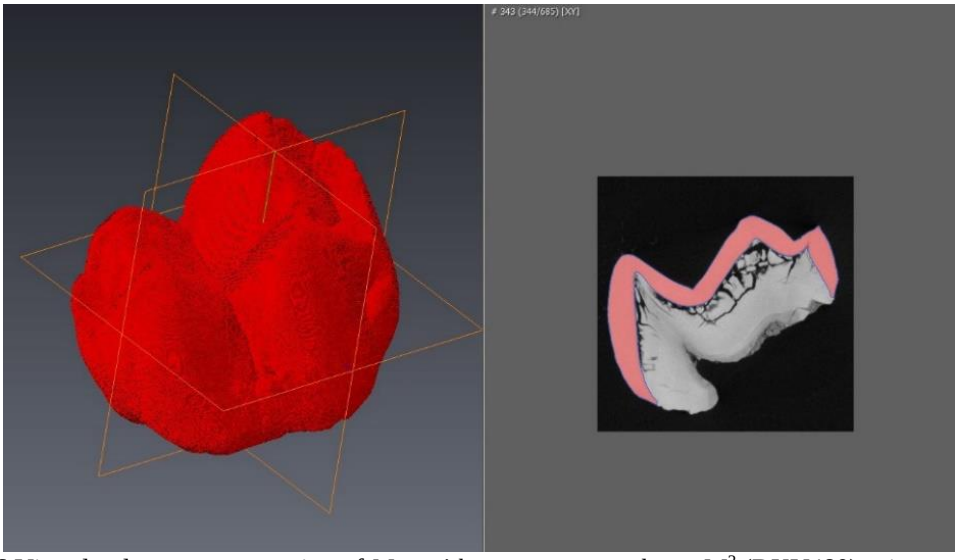

Fig. 2.6 Virtual volume reconstruction of *Mesopithecus monspessulanus* M^3 (DKV480) using automatic segmentation tools with ©Avizo v. 7.0.

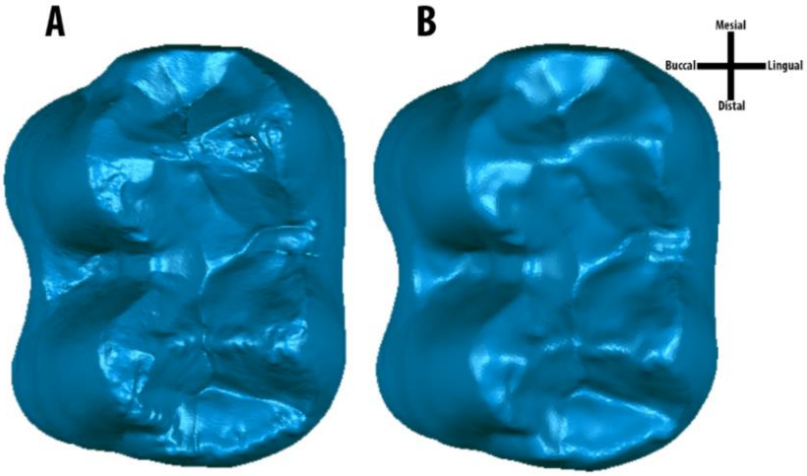

Fig. 2.7 The effect of decimation process proposed by Guy et al., (2013) in the molar morphology, example on fossil M_2 of *Macaca sylvanus cf. florentina* (Va1088), **A**) virtual enamel volume reconstruction before decimation procedure (~2.940k polygons), **B**) after decimation procedure and corrections (~110k polygons).

In order to isolate the enamel cap, the virtual volumes were reconstructed and processed from micro-tomographic images using automatic segmentation tools with manual corrections using Avizo v. 7.0 commercial software (Visualization Sciences Group, 2011) (Fig. 2.6). Each enamel cap was isolated from the other dental parts (e.g. dentine and pulp canals) using automatic segmentation tools and then was smoothed using 'smoothing labels' command (size= 3, 3D volume). Then the volume of the enamel was converted to a polygonal surface (3D triangular mesh), using 'generate surface' module with unconstrained smoothing type (smoothing extent = 3).

Ψηφιακή βιβλιοθήκη Θεόφραστος – Τμήμα Γεωλογίας – Αριστοτέλειο Πανεπιστήμιο Θεσσαλονίκης

Ψηφιακή συλλογή
Βιβλιοθήκη
"ΘΕΟΦΡΑΣΤΟΣ"

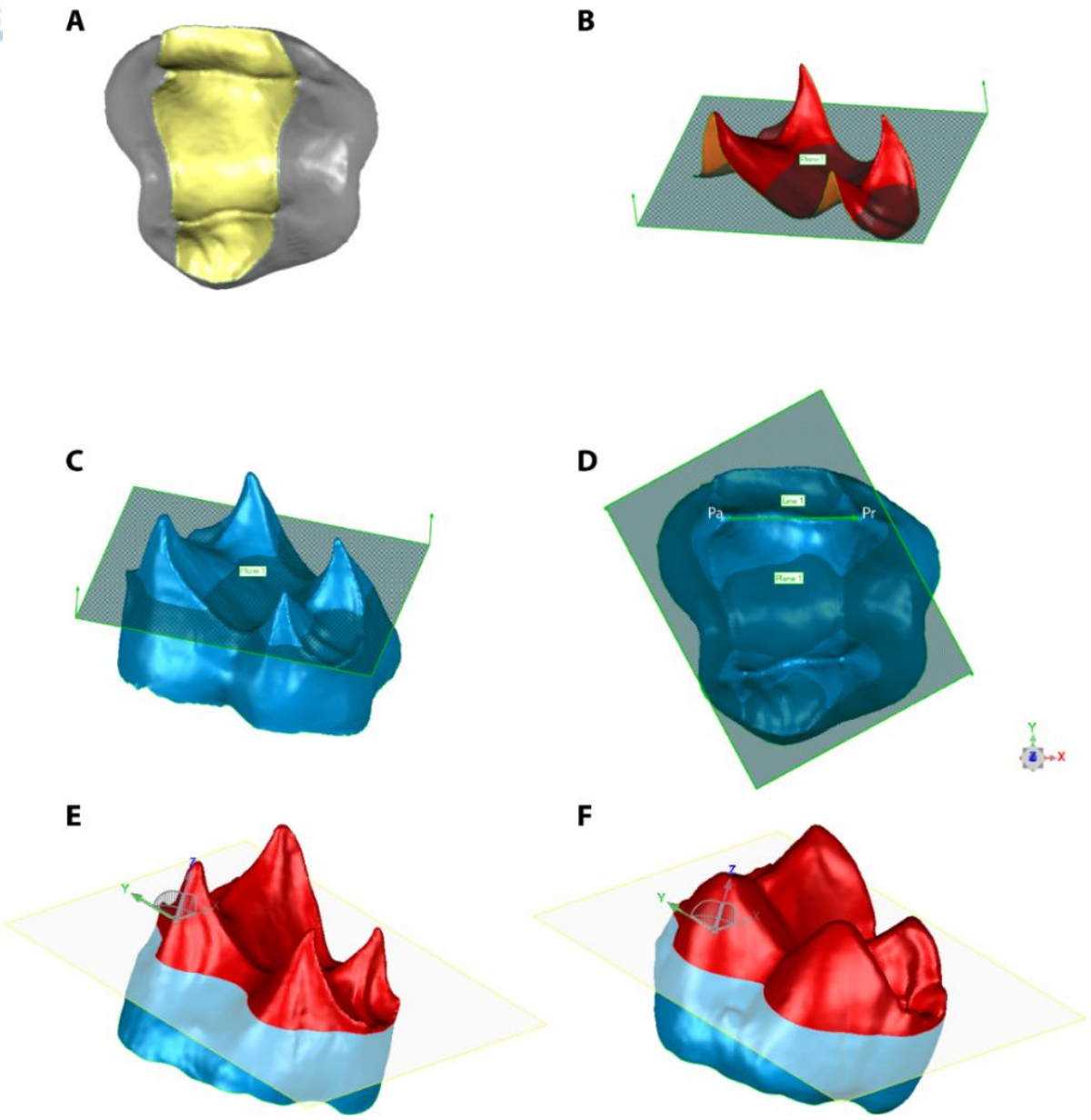

Fig. 2.8 Molar orientation protocol schematic representation after Guy et al., (2015) on *Me. monspessulanus* M^3 (DKV480), (**A**) isolation of occlusal dentine basin, (**B**) reference plane created by Best Fit (least square) procedure, **C**) un-oriented EDJ with reference plane, (**D**) EDJ surfaces are re–aligned to 3D virtual space with plane parallel to (xy) and (Pa–Pr) axis parallel to x and pointing toward x positive with the lowermost point of the occlusal basin is set to z = 0. The OES and EDJ subsampled surfaces correspond to the regions above a plane parallel to the (xy) reference plane (colored in red) and passing respectively by the lowermost point of the EDJ (**E**) and OES (**F**).

The next step was to segregate the OES and EDJ into different components using Geomagic studio 2013 software. To do that, the selection of triangles composing the cervix of the tooth was first outlined, expanded two times, and then the selected material was deleted. If parts of the dentine were exposed in the occlusal surface, they were outlined using the same way as the cervix, the selected material deleted and the resulting open hole filled. Then, and if there was no further connection between the OES and EDJ surfaces, they were separated into two components, which can be done either manually or with automatic tools of Geomagic studio 2013 software. Once the two components were cleaned from potential artifacts of the scanning procedure, the pointed fetures of each surface were reduced by 50%, and then,to

Ψηφιακή βιβλιοθήκη Θεόφραστος – Τμήμα Γεωλογίας – Αριστοτέλειο Πανεπιστήμιο Θεσσαλονίκης

Ψηφιακή συλλογή
Βιβλιοθήκη
"ΘΕΟΦΡΑΣΤΟΣ"

minimize the computational load for analytical purposes, each surface (i.e. OES and EDJ) was set to an equivalent amount of of 50–55k polygons by a re-tessellation of the original polyhedral surface. More clearly, the initial surface (i.e. the virtual volume after the segmentation process with Avizo) was constituted by a certain large amount of polygons (Fig. 2.7A), which needs to be reduced to approximately 55–50k polygons (Lazzari & Guy, 2014). This was achieved by changing the dimensions of the triangles that constitute each surface; a decrease in triangle dimensions increases the amount of polygons, while an increase triangle dimensions will reduce the total amount of polygons. This process did not significantly alter tooth morphology (Fig. 2.7 B).

In order to standardize the surfaces, each OES/EDJ pair needed to be oriented in 3D virtual space using a common reference plane and axis. In the first step, the occlusal dentine basin was isolated (Fig. 2.8A). Then a geometrically constructed reference plane was created by the best fit plane procedure applied on the occlusal basin of EDJ surface, which represents the virtual space xy axis **(**Fig. 2.8B). Then the reference plane was copied on EDJ surface (Fig. 2.8C) and the x-axis was aligned with an axis formed by connecting the dentine horn tips of paracone and protocone (Pa and Pr respectively; Fig. 8D), to have the occlusal surface parallel to the viewer plane (Guy et al. 2013; Benazzi et al. 2009). Lastly, the lowermost point of each molar cervix was set to (x, y, 0) so that the crown height is measured on a z-positive scale. Then, each OES and EDJ surface for every specimen underwent a subsampling procedure (Guy et al., 2013; Thiery et al., 2017; Ulhaas et al., 2004), to retain only the regions above a plane parallel to xy reference plane passing through the lowermost point of the occlusal basin for both EDJ and OES surfaces (Fig. 2.8E, F). This subsampling procedure has been suggested in previous works (Allen et al., 2015), as it reduces the influence of non-directly functional tooth elements of the enamel cap which actually do not participate actively in food comminution (Thiery et al., 2017).

Variable computations were mostly performed on these subsampled surfaces (i.e. Chapter 3, 5 and 6). However, some computations were perforfmed on the whole molar crown (i.e. Chapter 4), as some comparisons included data previously published in the literature where computations were performed on the whole molar crown (e.g. Beaudet et al., 2016).

Enamel thickness and tooth crown strength

In this study, the relationship of enamel thickness and diet is investigated in a broad sample of cercopithecoids taking available dietary information from the literature. Three measures that characterize enamel thickness and tooth crown strength are used: the "volumetric" approach of characterizing 3D relative enamel thickness ($3DRET_{vol}$) following Kono (2004), the "geometric" approach ($3DRET_{geo}$) following Guy et al. (2013, 2015), and the newly devised 2D measure absolute crown strength (ACS) by Schwartz et al. (2020).

First the three-dimensional average enamel thickness ($3DAET_{vol}$) is computed which corresponds to the ratio between the volume of the enamel cap and the enamel-dentine junction surface. The three-dimensional relative enamel thickness corresponds to the ratio between the three-dimensional average enamel thickness and the cubic root of the volume of the coronal dentine (e.g. the total volume of dentine included in the molar crown). Both average and relative enamel thickness have been measured using analytical tools of Geomagic studio 2013 software, according to the following formulas:

$$\mathbf{3DAETvol} = \frac{Enamel\ Cap\ Volume}{Enamel{-}Dentine\ junction\ surface} \qquad \mathbf{3DRETvol} = \frac{3DAETvol}{\sqrt[3]{Volume\ of\ coronal\ dentine}}$$

Ψηφιακή βιβλιοθήκη Θεόφραστος – Τμήμα Γεωλογίας – Αριστοτέλειο Πανεπιστήμιο Θεσσαλονίκης

Ψηφιακή συλλογή
Βιβλιοθήκη
"ΘΕΟΦΡΑΣΤΟΣ"

The $3DRET_{geo}$ is calculated as the minimum Euclidean distance between the centroid of each triangle of the OES and the centroid of the triangle closest to EDJ (Guy et al., 2013, 2015). The $3DAET_{geo}$ corresponds to the average distance among the triangles that constitute the surface:

$$\mathbf{3DAETgeo} = \frac{\sum \text{distances (OES–EDJ)}}{Number\ of\ triangles} \qquad \mathbf{3DRETgeo} = \frac{\text{3DAETgeo}}{\sqrt[3]{Volume\ of\ coronal\ dentine}}$$

The ACS is measured on the 2D mesial cusps and corresponds to the square root of the product of 2D AET (i.e. the area of the enamel cap divided by the length of the enamel-dentine junction surface) and coronal dentine radius, which is the bi-cervical diameter (BCD) divided by two (i.e BCD/2; Fig. 2.10) or:

$$\boldsymbol{ACS} = \sqrt{(\boldsymbol{AET} \times \left(\frac{\boldsymbol{BCD}}{\boldsymbol{2}}\right))}$$

Both $3DRET_{geo}$ and ACS have been calculated using a package in R v. 3.6 (Team, 2013) namely 'Doolkit' (Thiery et al. in press.). It is important to note that in the work of Schwartz et al., (2020), ACS was measured on the whole tooth crown, whereas here this metric is measured on subsampled surface (Fig. 2.10). Some differences can be expected in cases, yet this notion needs further investigation.

The functional significance of enamel was first discussed by Molnar and Gantt (1977) who investigated enamel thickness among humans and apes; they proposed that thick enamel in humans, together with low cusp morphology, was an adaptation for a crushing-grinding function. Kay (1981) measured enamel thickness on a wide range of primate taxa and noticed that enamel tends to be thicker among frugivorous taxa, whereas folivorous taxa tend to have thinner enamel. Even if the adaptive function of thick molar enamel is still being discussed (Molnar and Gantt, 1977; Kay, 1981; Lambert et al., 2004; King et al., 2005; Lucas et al., 2008; Vogel et al., 2008; Rabenold and Pearson, 2011; Constantino et al., 2012; Kato et al., 2014), enamel is relatively thicker in primates that consume harder food resources (Kay, 1981; Dumont, 1995; Shellis et al., 1998; Martin et al., 2003; Lambert et al., 2004), and it is expected to increase tooth resistance to high stress (Lucas et al., 2008). As a result, most of the research has been focused on the adaptive function of thick enamel in the context of hard object feeding rather than exploring other hypotheses (see Pampush et al., 2013).

Martin (1983) devised a scale-free metric namely "relative enamel thickness" (RET) as a means to compare enamel thickness between taxa with different tooth size. This metric was adopted by several researchers in the subsequent years to describe enamel thickness and investigate tooth functional, taxonomic and ecological scenarios (Macho, 1994; Dumont, 1995; Shellis et al., 1998 and references therein), creating a good background for comparative purposes. However, these early studies measured RET using histological sections of molars on molar cusps (e.g. Macho, 1994; Schwartz et al., 1998), which restricted samples available and made it inviable to compute three-dimensional aspects of the enamel. Lastly, relative enamel thickness measured on 2D ignores the topographic variation of enamel thickness throughout the enamel cap which can be important in function-related scenarios (e.g. Pampush et al., 2013). Nevertheless, even after the introduction of three-dimensional approaches several more recent works continued to explore 2D RET because of the overall large comparative sample (Kato et al., 2014; Smith et al., 2019).

Ψηφιακή βιβλιοθήκη Θεόφραστος – Τμήμα Γεωλογίας – Αριστοτέλειο Πανεπιστήμιο Θεσσαλονίκης

Ψηφιακή συλλογή
Βιβλιοθήκη
"ΘΕΟΦΡΑΣΤΟΣ"

The introduction of computed tomography as a non-destructive method of measuring enamel thickness opened new pathways of investigation (Schwartz, 1997). Kono (2004) devised a method to estimate 3D average enamel thickness (3D AET), which is the quotient of the enamel cap volume over the 3D area of dentine surface, which is widely used until today often referred as the 'volumetric' approach (e.g. Thiery et al., 2017c). Additionally, the distribution of enamel thickness along the molar crown was measured (Kono and Suwa, 2008; Zanolli et al., 2010; Guy et al., 2013; Thiery et al., 2017a,c; Thiery et al., 2019; Fortuny et al., 2021). This 'geometric' approach (e.g. Thiery et al., 2017c) relies on 3D polygonal meshes of the OES and EDJ, measured as the distance of each OES triangle with its respective EDJ triangle, and it can be used to depict the 3D spatial distribution of enamel along the molar crown. It has been suggested that the 'volumetric' approach better characterizes the raw amount of enamel and can be used to assess rate and speed of enamel secretion, whereas the geometric approach better characterizes resistance to loading, as it measures local thickness and better suits biomechanical models (Thiery et al., 2017c).

More recently, a new linear measure of enamel thickness has been devised namely absolute crown strength (ACS; Schwartz et al., 2020). This metric measures the average thickness of the enamel on a tooth modelled as a hemisphere assuming uniform distribution (for further details regarding computations see SOM Schwartz et al., 2020). In the work of Schwartz et al. (2020), they quantify the resistance of a tooth (e.g. tooth strength) against radial-median and margin fracture (e.g. P_{RF} and P_{MF} respectively; see Lawn and Lee, 2009) and they found that there is a higher correlation between ACS and these estimates of tooth strength (e.g. P_{RF} and P_{MF}), which further suggests that it might be a more accurate predictor of tooth strength compared to other traditional metrics (e.g. relative enamel thickness). This might be related to the fact that RET is directionally proportional to enamel thickness but it does not consider the overall tooth size, unlike ACS. These investigation suggest that it may be useful to explore ACS along with RET, as they might reveal some hidden aspects of the feeding biology (e.g. Schwarrtz et al., 2020). Nevertheless, this requires further investigation in abroad spectrum of primate families.

Relief estimates

Dental relief corresponds to the variation of elevation across a tooth crown surface (Thiery et al., 2019). Topographic estimates of dental relief are commonly employed metrics and have been used extensively in the literature to characterize the overall relief of the molar crown of both extant and extinct organisms (Ungar and Williamson, 2000; M'Kirera and Ungar, 2003; Merceron et al., 2006; Boyer, 2008; Boyer et al., 2010, 2012; Guy et al., 2013; Prufrock et al., 2016; Ungar et al., 2017). Several metrics have been proposed throughout the years, while the names and definitions can vary from one author to another (see Thiery et al., 2019 for extended discussion). Here two estimates of relief are used, inclination (λ; Guy et al. 2013), and the relief index (LRFI; sensu Boyer, 2008) computed on subsampled occlusal surfaces (e.g. Ulhaas et al., 2004; Guy et al., 2015) both calculated using 'Doolkit'(Thiery et al., 2021).

Inclination (λ) is a estimate of relief that quantifies in more detail the variation of relief across a tooth's surface, and can be defined as the average change in elevation across a given surface (Guy et al., 2013). Slope was initially estimated with geographic information system (GIS) software and it was commonly used in early analyses (Zuccotti et al., 1998; Ungar and Williamson, 2000; Merceron et al., 2006). Slope is measured as the tangent of the angle (θ) between a surface and the horizontal plane and it is expressed between 0 and 90°. However, the slope of triangles that are not facing the occlusal surface, for example because the enamel forms folds, does not exceed 90°. To confront this, Guy et al., (2013, 2015) proposed inclination (λ), which corresponds to the angle between the vector normal to the triangle in the – z direction

Ψηφιακή βιβλιοθήκη Θεόφραστος – Τμήμα Γεωλογίας – Αριστοτέλειο Πανεπιστήμιο Θεσσαλονίκης

Ψηφιακή συλλογή
Βιβλιοθήκη
"ΘΕΟΦΡΑΣΤΟΣ"
Α.Π.Θ

and the horizontal xy plane, and it is coded on 180°, from 180° for horizontal polygons to 90° for vertical polygons (Guy et al., 2013, 2015).

In primate molars, the average slope seems to carry a signal related to diet. It has been shown that the values of average slope of molars are higher in folivorous than in frugivorous primates (M'Kirera and Ungar, 2003; Bunn and Ungar, 2009). This probably relates to the fact that tough fibrous material, such as grasses and leaves, are broken down more efficiently by teeth with adaptive morphologies towards shearing (e.g. long and well pronounced shearing crests; Kay and Hiimae, 1974; Kay, 1977). Furthermore, differences in the overall dental relief and slope values have been observed among different populations of *Lemur cattta* (Yamashita et al., 2016). These differences have been interpreted as differences in the frequency of consumption of mechanically challenging food resources, in that particular case the fruit *Tamarinus indica* trees (Yamashita et al., 2012). Therefore, variations in slope values may be informative of hard food consumption.

In order to provide a more global estimate of relief, Ungar and Williamson (2000) proposed a relief index computed as the quotient of tooth crown 3D area divided by the two-dimensional projection of the area on the horizontal plane. However, the distribution of this relief index is exponential, making it difficult to map (Thiery et al., 2019). To avoid this issue, an alternative calculation was proposed by Boyer (2008) that corresponds to the natural log of the ratio of the square roots of the surface area of the enamel crown and the surface area crown's projection into an occlusal plane (LRFI). Relief indices have proven to be suitable estimates of dietary behaviors. Primates whose diets are primarily focused on insects and leaves tend to possess tooth crowns with higher slopes and LRFI values than primates that tend to consume primarily fruits (M'Kirera and Ungar, 2003; Ulhaas et al., 2004; Boyer, 2008; Bunn and Ungar, 2009; Bunn et al., 2011; Klukkert et al., 2012a). Moreover, primates that consume large amounts of mechanically challenging food resources (i.e. seeds, bark etc.), are characterized by lower slopes and LRFI values (Ledogar et al., 2013; Winchester et al., 2014).

Curvature estimates

The variation and the magnitude of curvature (alternatively sharpness) of the occlusal dental features can be crucial in understanding dental functions, and may be decisive in interpreting dietary adaptations through primate evolutionary history (Guy et al., 2017). In general, plant and animal-based structural fibers require large amounts of energy to cut and usually primates with diets high in fiber content tend to have sharper teeth (Bunn et al., 2011; Winchester et al., 2014). Comparative work on great apes and insectivorous primates support this interpretation (Kay and Sheine, 1979; Berthaume and Schroer, 2017). Thus, curvature/sharpness is an important morphological aspect associated with dietary adaptations. In order to quantify this aspect of dental morphology, two metrics were computed on subsampled occlusal surfaces (e.g. Ulhaas et al., 2004; Guy et al, 2015): Dirichlet normal energy (DNE; see Bunn et al., 2011) and area-relative curvature (ARC; Guy et al., 2017). Both curvature metrics were calculated with 'Doolkit' (Thiery et al., 2021) in R v. 3.6 (Team, 2013).

Dirichlet normal energy (DNE) of the normal map of a tooth surface quantifies tooth sharpness independent of position, orientation, scale and landmarks. DNE actually measures the deviation of a surface from being planar using the mathematical concept of Dirichlet energy (see Pinkall and Polthier, 1993 for further details). Essentially it measures how much the tooth's surface bends at different points in the surface, with areas that bend more being overall sharper (Berthaume et al., 2020). Hence, teeth with higher DNE values, possess curvier or more variable surfaces. Within primates, teeth with curvy surfaces (e.g crests and crenulations) are in general sharper (Bunn et al., 2011), and primates with relatively taller, sharp cusps and crenulations

Ψηφιακή βιβλιοθήκη Θεόφραστος – Τμήμα Γεωλογίας – Αριστοτέλειο Πανεπιστήμιο Θεσσαλονίκης

Ψηφιακή συλλογή
Βιβλιοθήκη
"ΘΕΟΦΡΑΣΤΟΣ"

tend to have higher DNE compared to those with relatively shorter and blunt cusps (Guy et al., 2015; Berthaume and Schroer, 2017; Berthaume et al., 2018). One problem regarding DNE is that every study utilizing DNE has used slightly different protocol to produce and analyze 3D meshes, which raises concerns about the comparabilty and repeatability of results (Pampush et al., 2016). Different computational algorithms have been proposed (Pampush et al., 2016; Winchester, 2016; Shan et al., 2019), which have different protocols for excluding triangles at the edge of the surface. Still, excluding a variable number of triangles can be questionable, as DNE is sensitive to triangle count as well as different cropping and smoothing methods (Spradley et al., 2017; Berthaume et al., 2019b).

Mean curvature is the mean value of two principal curvatures, the minimum and maximum normal curvatures (Klette and Rosenfeld, 2004; Rugis and Klette, 2006). These two quantities measure the deviation of tooth surface from flatness. Mean curvature (φ) vary from negative values in strictly concave regions to positive values in strictly convex (Guy et al., 2013). By this way, (φ) also provides a quantitative assessment of the convexity/concavity profile (slightly concave or smooth convex regions like basins and cusps have low (φ) values, whereas highly concave or sharp convex regions like grooves, dentine horn apex and crests, show high values of (φ)). Additionally, flat regions where positive and negative principal curvatures "cancel" each other, present (φ) values equal or close to zero (Guy et al., 2013). Area-relative curvature (ARC) is a normalized version of the mean curvature (φ) (Guy et al., 2013, 2017). It actually corresponds to the mean curvature (φ) normalized by the size of the tooth using a theoretical linear model. This metric offers the opportunity to interpret dental patterns in terms of functions potentially related to different types of diet (Guy et al., 2017).

Dental complexity

Another important aspect of tooth morphology is dental complexity, which may be considered as the number of locations on tooth's surface where food can be fractured and is correlated with the number of dental elements (i.e crenulations, cusps, crests) on the occlusal surface (Berthaume et al. 2020). In this study, dental complexity is assessed using OPCR (Evans and Janis, 2014) computed on subsampled occlusal surfaces (e.g. Ulhaas et al., 2004; Guy et al., 2015), and calculated using 'Doolkit'(Thiery et al., 2021) in R v. 3.6 (Team, 2013).

In general, it has been shown that the cheek teeth of herbivores have higher complexity than those of carnivores (Evans et al., 2007). Indeed, some correlations between complexity and diet seem to exist at higher taxonomic levels. However, in primates so far complexity is a relatively poor indicator of diet, showing large overlap among species (Guy et al., 2013; Winchester et al., 2014; Berthaume et al., 2018; Ungar et al., 2018). Further investigation is needed to understand the association between dental complexity and diet in the primate dentition.

The first metric used for investigating dental complexity is orientation patch count (OPC), being introduced by Evans et al. (2007), with later works suggesting equivalent metrics that mostly differ on the computation algorithm (orientation e.g., Guy et al., 2013).This metric quantifies the orientation of each polygon on the digital tooth surface and counts the number of "patches" present on tooth surface (i.e a predetermined number of adjacent polygons with the same orientation). In this case, the spectrum of possible orientations is divided in eight increments of 45°. The patches formed by a certain number of triangles, usually three or five, belonging to the same orientation are counted. The total number of patches depends on the tooth structure and scanning resolution (Evans et al., 2007; Guy et al., 2015).

Ψηφιακή βιβλιοθήκη Θεόφραστος – Τμήμα Γεωλογίας – Αριστοτέλειο Πανεπιστήμιο Θεσσαλονίκης

Ψηφιακή συλλογή
Βιβλιοθήκη
"ΘΕΟΦΡΑΣΤΟΣ"

A similar metric and derivative of occlusal patch count is orientation patch count rotated (OPCR) introduced by Evans and Janis (2014). This metric was devised in order to minimize the effects of manual orientation of the tooth surface in the occlusal plane. It uses the same principles as OPC, but OPCR is measured for eight different orientations, all offset by 45/8 = 5.625°. The OPCR is then obtained by taking the average of these eight orientations (Thiery, 2016). Results on this metric seem not to be significantly different from those obtained with OPC (Evans and Jernvall, 2009); however, OPCR is preferred by several authors (Monteiro, 2013; Winchester et al., 2014; Pampush et al., 2016). Regardless, as in DNE, these metrics are sensitive to triangle count, thus also to different cropping, smoothing protocols, and resolution, making it difficult to compare results among different studies (Berthaume et al., 2019b).

Ψηφιακή βιβλιοθήκη Θεόφραστος – Τμήμα Γεωλογίας – Αριστοτέλειο Πανεπιστήμιο Θεσσαλονίκης

Ψηφιακή συλλογή
Βιβλιοθήκη
"ΘΕΟΦΡΑΣΤΟΣ"
Τμήμα Γεωλογίας
Α.Π.Θ.

Chapter 3. Deciphering the dietary ecology of *Dolichopithecus ruscinensis*

3.1 Introduction

3.1.1 Colobinae evolution and paleoecology

The subfamily Colobinae includes highly folivorous monkeys with their anatomy and physiology adapted for the consumption of high amounts of leafy material (Davies, 1994 and references therein). They possess a multi-chambered stomach with an enlarged forestomach adapted to microbial food fermentation, and also robust jaws along with bilophodont molars that enable them to process tough and fibrous material as leaves (Chivers, 1994; Ravosa, 1996; Lambert, 1998; Matsuda et al., 2019). Moreover, most of the extant species exhibit locomotor behaviors associated with an arboreal lifestyle, except *Semnopithecus entellus* which spends significant amounts of time on terrestrial substrates (Sayers and Norconk, 2008).

The first evidence of the Colobinae dates back to the middle Miocene of Kenya (12.5–10.0 Ma; Rossie et al., 2013), while during the late Miocene colobines dispersed into Eurasia with *Mesopithecus*, whose earliest occurrence most likely dates to the early Turolian (8.7–8.2 Ma) faunas of northern Greece (Koufos, 2009a, 2019). During the Pliocene, the European fossil record shows the presence of two colobine genera, *Mesopithecus* and *Dolichopithecus*, coexisting temporally and occurring sympatrically in Early Pliocene fossil sites of France (Montpeller, Perpignan), Bulgaria (Dorkovo), and Romania (Măluşteni) (Eronen and Rook, 2004; Delson et al., 2005). From the Middle to Late Pleistocene onwards, colobines disappeared from Europe, whereas some extinct Asian species may have led to the living representatives in Asia (Andrews et al., 1996; Jablonski, 1998; Frost et al., 2015).While the phylogenetic relationships of *Mesopithecus* and *Dolichopithecus* with modern Asian Colobinae remain unclear, the numerous extant representatives of this group combined with fossil evidence from Africa and Eurasia support the evolutionary success of this family.

Unlike most extant African and Asian colobines, which exhibit physiological and morphological adaptations to folivory and arboreality (Davies, 1994; Rowe et al., 1996), evidence suggests that it was not the same in the past (Leakey, 1982). African Plio-Pleistocene colobines were represented by at least five genera (e.g., *Cercopithecoides*, *Libypithecus*, *Rhinocolobus*, *Paracolobus*, *Kuseracolobus*), which were considerably more diverse in terms of ecological adaptations (Frost, 2017). Furthermore, there are contrasting opinions concerning the type of locomotor adaptations of early colobines, with some authors stating that modern colobine arboreal adaptations are a recent development (Andrews, 1982; Benefit, 1999; Leakey et al., 2003), while others suggest that early colobines in Africa were mainly arboreal and that the semi-terrestrial locomotion in some late Miocene and Plio-Pleistocene colobine taxa (e.g. *Cercopithecoides williamsi*, *Cercopithecoides kimeui*, *Cercopithecoides bruneti*, *Paracolobus mutiwa*, *Paracolobus chemeroni*), is a secondary derived state (Hlusko, 2006; Gilbert et al., 2010; Nakatsukasa et al., 2010).

The controversies surrounding the evolution of locomotor adaptations in colobines lead to the question of the role of dietary specialization of early colobine taxa in their out-of-Africa dispersal. Were early colobines that first migrated into Eurasia steno- or eurytopic? There is evidence concerning the earliest Eurasia colobine, *Mesopithecus pentelicus*, which would exclude specialization for folivory (Merceron et al., 2009b, 2009a; Thiery et al., 2017a). Instead, available evidence suggests seed consumption and more opportunistic feeding habits, consistent with semi-terrestrial locomotion (Youlatos, 2003; Youlatos and Koufos, 2010; Ji et

Ψηφιακή βιβλιοθήκη Θεόφραστος – Τμήμα Γεωλογίας – Αριστοτέλειο Πανεπιστήμιο Θεσσαλονίκης

Ψηφιακή συλλογή
Βιβλιοθήκη
"ΘΕΟΦΡΑΣΤΟΣ"
Τμήμα Γεωλογίας
Α.Π.Θ.

al., 2020). Available dietary information for the rest of the Eurasian fossil cercopithecid taxa is however very limited precluding broader conclusions. *Dolichopithecus* is a suitable taxon to address this question, especially as it shows a wide geographic distribution and also co-occurred sometimes with *Mesopithecus*. Exploring the dietary ecology of early colobine taxa, such *Dolichopithecus ruscinensis*, is of high interest for understanding the evolution and diversification of Colobinae.

3.1.2 *Dolichopithecus* fossil record and palaeoecology

Dolichopithecus is a large-bodied extinct colobine genus (Delson et al., 2000), that inhabited Europe between Pliocene and Pleistocene, being recorded at several sites in France, Greece, Ukraine and Spain (Koufos et al., 1991; Eronen and Rook, 2004; Marigó et al., 2014). In Europe, the taxon is mostly represented by a single species *Dolichopithecus ruscinensis*, without apparent diffences in morphology across geography and time (Maschenko, 1991; Delson et al., 2005). Two additional species have been described, *Dolichopithecus balcanicus* sp. and *Dolichopithecus hypsilophus*, yet the limited material of these two taxa does not allow to conclusively support their distinct species status (Gremiatskiy, 1958; Maschenko, 2005; Spassov and Geraads, 2007). Most of the fossil European specimens of *Dolichopithecus ruscinensis* belong to the type locality of Serrat d'en Vaquer-Perpignan (France). The biochronological range of this fossil species spans from 5.3 to 1.0 Ma while it is also considered to be closely related to *Kanagawapithecus leptopostorbitalis* from the late Pliocene of Japan (Delson, 1994; Iwamoto et al., 2005; Nishimura et al., 2012), as well as *Parapresbytis eohanuman* from the late Pliocene of Udunga and Shamar in Transbaikal area, Siberia (Kalmykov, 1992; Jablonski, 2002). Still, the phylogenetic relationships between the Western Eurasian species of *Dolichopithecus*, these Asian fossil taxa, or the extant taxa remain under discussion (Delson, 1994; Egi et al., 2007).

Available paleoecological inferences for *Dolichopithecus ruscinensis* mostly derives from analyses of postcranial morphology (Depéret, 1890; Gabis, 1961; Jolly, 1967, 1970; Szalay and Delson, 1979; Ingicco, 2008). The earliest view suggested semi–terrestrial locomotor adaptations more similar to those of macaques (Depéret, 1890; Jolly, 1967). Other studies considered even fully terrestrial adaptations, similar to those of living savannah baboons (Gabis, 1960, 1961). Be that as it may, the degree of terrestrial adaptations seen in *Dolichopithecus ruscinensis* was considered higher than in any living colobine (except maybe *Semnopithecus entellus*), being more similar to *Mandrillus sphinx* and *Macaca sylvanus*. The environment inhabited by *Dolichopithecus ruscinensis* has been briefly discussed by some researchers (Tobien, 1970; Delson, 1994), but a detailed investigation is still pending. The appearance of *Dolichopithecus ruscinensis* in Europe postdates the refilling of the desiccated Mediterranean Basin, which is considered to have probably led to the development of widespread woodland and humid forests across southern Europe (Delson, 1994; Popescu, 2002; Kovar-Eder et al., 2006; Jiménez-Moreno et al., 2010, 2013). This study aims to investigate the dietary ecology of the last fossil European colobine, *Dolichopithecus ruscinensis* by combining information from different dental proxies.

3.2 Material

3.2.1 Dental topographic and enamel thickness analyses

Dental topographic and enamel thickness analyses are applied on a M^1 from a palate of a juvenile individual (MHNPn–PR01; Fig. 3.1A1–A4) found in Serrat d'en Vaquer-Perpignan (France). The analyzed molar is fully erupted (Fig. 3.1B1–B5), retains minimal wear, and shows basal flaring on the lingual part, a typical feature on cercopithecid cheek teeth (Delson,

Ψηφιακή βιβλιοθήκη Θεόφραστος – Τμήμα Γεωλογίας – Αριστοτέλειο Πανεπιστήμιο Θεσσαλονίκης

Ψηφιακή συλλογή
Βιβλιοθήκη
"ΘΕΟΦΡΑΣΤΟΣ"

1973; Swindler, 2002). The molar possesses well-defined mesio-distal shearing crests and both distal and mesial margins. The distal fovea is wider than the mesial, both mesial and distal lingual clefts are well pronounced and the central basin (trigon) is deep. This fossil specimen collected by Albert Donnezan along with other mammalian fossil remains is dated around 3.4 to 2.8 Ma, and it was found in concreted marls (Philippe and Bourgat, 1985). The fossil primate material was later described by Depéret (1889). The specimen is stored in the Museum d'Histoire Naturelle Perpignan, France. Our comparative sample consists of 39 M^2 belonging to 20 extant cercopithecid species (Table 3.1), because the available M^1 material of modern species showed advanced wear which prohibited morphological comparisons.

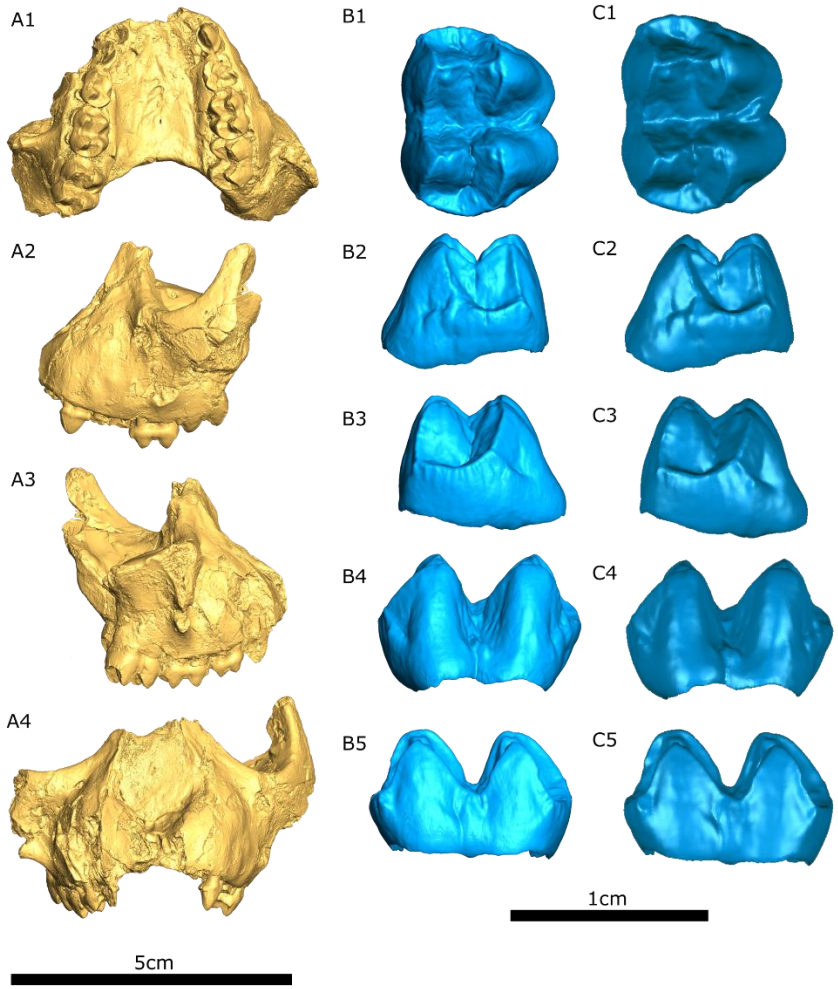

Fig. 3.1 Virtual reconstruction of *Dolichopithecus ruscinensis* (MHNPn–PR01) palate specimen in (A1) occlusal, (A2) lateral right, (A3) lateral left, (A4) facial; right M1 virtual reconstruction before (B) and after (C) processing in (B1, C1) occlusal, (B2, C2) mesial, (B3, C3) distal, (B4, C4) lingual, (B5, C5) buccal. A total of eight variables were measured on each virtually reconstructed subsampled molar surface (Fig. 3.2 B). Calculations for Dirichlet normal energy (DNE), relief index (LRFI), area–relative curvature (ARC), orientation patch count rotated (OPCR), absolute crown strength (ACS), 3D relative geometric enamel thickness ($3DRET_{geo}$), and inclination were performed using 'Doolkit' package (Thiery et al., 2021) in R v. 3.6 (R Core Team, 2013). The 3D relative volumetric enamel thickness ($3DRET_{vol}$) was calculated using Geomagic studio 2013 (3D Systems Inc., 2013). Also, the 2D projection (OES 2D) and the 3D area of the outer enamel surface were quantified as measures of tooth size. The values of all metrics are given in Table S1 Appendix 3.7.

Ψηφιακή βιβλιοθήκη Θεόφραστος – Τμήμα Γεωλογίας – Αριστοτέλειο Πανεπιστήμιο Θεσσαλονίκης

Ψηφιακή συλλογή
Βιβλιοθήκη
"ΘΕΟΦΡΑΣΤΟΣ"
Τμήμα Γεωλογίας
Α.Π.Θ.

Dietary categorization

All extant species used in the comparative sample for dental topographic analysis in this chapter were assigned to one of three general dietary categories: folivory, mixed-feeding, and fruit/seed consumption. This division is based on dietary information from previously published studies on wild populations (see Table 2.3). Even though these categories are relatively broad it is expected to encompass the basic differences and/or similarities in dental morphology between primates with contrasting diets (e.g. folivorous vs fruit/seed-eaters), but also intermediate morphologies as a result of an overall more mixed diet (e.g. mixed feeders). For instance, folivorous species are usually expected to possess higher crowned teeth with sharper features and thinner enamel overall, compared with fruit/seed eaters, which usually exhibit lower overall relief, less sharp surfaces, and thicker enamel. However, it must be noted that most cercopithecid species do not fit neatly into these categories. Most of the extant colobines are considered primarily folivorous, but some species eat also fruits when available, while others fall back on seeds when other preferred food resources are absent (Rowe et al., 1996). These fallback behaviors are hypothesized to exert strong selective pressure on dental morphology and can be expected to entail particular dental morphological adaptations (e.g. Lambert et al., 2004; Marshall and Wrangham, 2007; Lambert, 2009; Wright and Willis, 2012).

Hence, 'folivory' as defined here includes species that primarily rely on foliage throughout the year (leaf and flower consumption > 50% of their annual diet), even if in most cases the consumption of fruits, seeds, and other plant resources are also expected, such as in African and Asian colobines (Table 3.1). 'Fruit/seed' consumption includes cercopithecids, that primarily exploit fruits and seeds throughout the year (fruits and seeds > 50% of their annual diet), such as *Lophocebus albigena*, *Cercocebus torquatus*, and *Cercopithecus diana*, even if they also occasionally consume leaves and animal matter (Mitani, 1989; Ham, 1994; Poulsen et al., 2001; Curtin, 2004; Buzzard, 2006; McGraw et al., 2012). 'Mixed-feeding' includes a total of six species (e.g. *Papio anubis*, *Papio hamadryas*, *Mandrillus leucophaeus*, *Cercopithecus campbelli*, *Chlorocebus aethiops*, *Erythrocebus patas*) that tend to show more opportunistic dietary behaviors and usually consume a wider array of food resources in various amounts throughout the year such as leaves, fruits, seeds, tree exudates (gum), grass, shoots, roots and tubers, bark, while some also consume animal matter (Table 2.3). Hence, in terms of dietary composition this dietary category can be considered somewhat heterogeneous. For instance, cercopithecid representatives like *Papio*, are considered dietary generalists including a wide array of plant parts, from leaves to fruits, stems seedlings, roots, bark, seeds, as well as underground storage organs and vertebrate flesh (Whiten et al., 1991; Byrne et al., 1993; Newton-Fisher and Okecha, 2006). *Mandrillus* seems to follow the same dietary pattern but the importance of seeds in its diet has been emphasized (Hoshino, 1985; Astaras et al., 2008; Owens et al., 2015; Percher et al., 2017). On the other hand, species such as *Cercopithecus campbelli*, may primarily feed on fruits, but include significant portions of animal matter (e.g. invertebrates and arthropods) depending on seasonal variation (Buzzard, 2006). Similarly, *Erythrocebus patas* diet consists of fruits, seeds, animal matter (mostly arthropods), but also includes gum from Acacia trees, whereas similar dietary preferences have been suggested for *Chlorocebus aethiops* depending on habitat and food resource availability (Happel, 1988; Isbell, 1998a; Barrett, 2005). In addition, differences in dietary choices between *Erythrocebus patas* and *Chlorocebus aethiops* might be also influenced by the more terrestrial behavior of the former compared with the latter (Rowell, 1966; Isbell, 1998b; Nakagawa, 2000a, 2003b; Pruetz and Isbell, 2000; Barrett, 2005). Hence, the latter category encompasses a wide range of dietary preferences and dietary behaviors.

Table 3.1 Extant cercopithecid sample used for dental topographic analysis along with dietary assignments.

Subfamily	Taxa	*n*	ID number	Institution[a]	Diet
Papionini	*Lophocebus albigena*	4	83–006–M–276, 90–042–M–301, 90–042–M–301, Cb4	RMCA, PALEVOPRIM	Fruit/seed eater

Ψηφιακή βιβλιοθήκη Θεόφραστος – Τμήμα Γεωλογίας – Αριστοτέλειο Πανεπιστήμιο Θεσσαλονίκης

Ψηφιακή συλλογή Βιβλιοθήκη "ΘΕΟΦΡΑΣΤΟΣ" Τμήμα Γεωλογίας Α.Π.Θ.

	Lophocebus aterrimus	1	14113	RMCA	Fruit/seed eater
	Cercocebus torquatus	1	81–07–M–44	RMCA	Fruit/seed eater
	Mandrillus leucophaeus	2	1893–269, 2002–105	PALEVOPRIM	Mixed feeder
	Papio anubis	3	MRAC–80–044–M101, C2, MRAC–90042–M226	PALEVOPRIM	Mixed feeder
	Papio hamadryas	1	MRAC–97–020–M004	RMCA	Mixed feeder
Cercopithecini	*Cercopithecus diana*	2	Cc1, Cc2	PALEVOPRIM	Fruit/seed eater
	Cercopithecus nictitans	1	15650	RMCA	Fruit/seed eater
	Cercopithecus pogonias	2	15595, 18273	RMCA	Fruit/seed eater
	Cercopithecus campbelli	2	36280, 80–028–M–24	RMCA	Mixed feeder
	Chlorocebus aethiops	2	1972–302, 1972–328	MNHN	Mixed feeder
	Erythrocebus patas	1	8629	RMCA	Mixed feeder
Colobinae (African)	*Colobus guereza*	2	1216, 3800	RMCA	Folivore
	Colobus polykomos	5	38158, 81–07–M174, 10602, 10548, 10307	RMCA	Folivore
	Colobus satanas	1	33512	RMCA	Folivore
	Piliocolobus badius	3	83–042–M77, 91–060–M57, 91–060–M76	RMCA	Folivore
	Procolobus verus	3	86–002–M–34, 86–002–M–48, 86–002–M–50	RMCA	Folivore
Colobinae (Asian)	*Nasalis larvatus*	1	5042	SMF	Folivore
	Semnopithecus entellus	1	1964–1615	MNHN	Folivore
	Trachypithecus cristatus	1	1085	SMF	Folivore

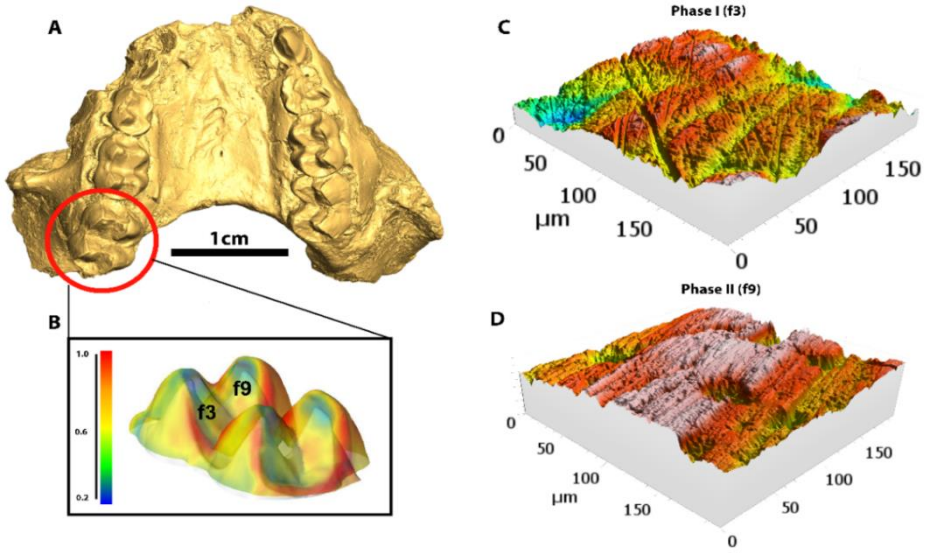

Fig. 3.2 *Dolichopithecus ruscinensis* (MHNPn–PR01) palate (A), the subsampled occlusal enamel surface and enamel dentine junction surface of the right M^1 with the localtion of dental wear facets (B), and their respective 3D surface representation (C, D).

3.2.1 Dental microwear texture analysis

The fossil material investigated by the means of dental microwear texture analysis consists of a total of 30 specimens of *Dolichopithecus* (Table 3.2; Table S2 Appendix 3.7). All fossil samples belong to *Dolichopithecus ruscinensis*, except the specimen from Tenevo (Bulgaria), which was assigned to *Dolichopithecus balcanicus* (Spassov and Geraads, 2007). Here DMTA is discussed at the genus level only as the sample composition does not allow investigation among fossil species of *Dolichopithecus* or fossil sites. The fossil material was collected from the fossiliferous localities of Serrat d'en Vaquer-Perpignan (France, *n* = 23), Dorkovo (Bulgaria, *n* = 3), Tenevo (Bulgaria, *n* = 1) and Vorog (Bulgaria, *n* = 1), Megalo Emvolon (Greece, *n* = 1) and Măluşteni (Romania, *n* = 1), and is housed in the Museum d'Histoire Naturelle Perpignan (France Măluşteni), Musée des Confluences and Université de

Ψηφιακή βιβλιοθήκη Θεόφραστος – Τμήμα Γεωλογίας – Αριστοτέλειο Πανεπιστήμιο Θεσσαλονίκης

Ψηφιακή συλλογή
Βιβλιοθήκη
"ΘΕΟΦΡΑΣΤΟΣ"

Lyon (France), Natural History Museum of Sofia (Bulgaria), Museum of Geology-Paleontology-Paleoanthropology of Aristotle University of Thessaloniki (Greece), and Department of Geology of Alexandru Ioan Cuza University of Iasi (Romania). Both Phase I and II facets are investigated (Fig. 2C, D), as they bear complementary signals (Merceron et al., 2021). Data for these fossil specimens are compared with eight cercopithecid species (Table 3.2), including five colobines (*Colobus guereza*, *n* = 22; *Piliocolobus badius*, *n* = 12; *Nasalis larvatus*, *n* = 7; *Semnopithecus entellus*, *n* = 8; *Presbytis melalophos*, *n* = 13) and three cercopithecines (*Lophocebus albigena*, *n* = 15; *Erythrocebus patas*, *n* = 13; *Chlorocebus aethiops*, *n* = 37).

3.3 Statistical analysis

3.3.1 Dental topographic and enamel thickness analysis

Topographical estimates, enamel thickness and crown strength metrics are often correlated, while the presence and the strength of such correlations could be affected by parameters such as dietary variability and the degree of the phylogenetic relatedness (Berthaume et al., 2020). Closely related species are assumed to have similar traits because of their shared ancestry and thus produce more similar residuals from the least squares regression line (Symonds and Blomberg, 2014)(Symonds and Blomberg, 2014). Hence, the relationships between all enamel thickness, tooth strength, and topographic variables were assessed using phylogenetic generalized least squares (PGLS) regression analysis, in which the potential effect of phylogeny on the distribution of data is considered (Thiery, et al., 2017; Winchester et al., 2014). The effect of phylogeny is measured using Pagel's Lambda, (henceforth referred to as λ) which is a measure of phylogenetic signal with values ranging from 0 to 1 (0 representing no phylogenetic structuring, 1 representing a perfect fit between data and a Brownian motion model of change in values through evolution). A phylogeny for the 20 cercopithecids species included in this study was generated using a consensus tree (100 iterations) downloaded from the 10k Trees Project website v. 3 (Arnold et al., 2010). We included the 2D projection of occlusal enamel surface (OES 2D) in our PGLS regression analysis to investigate the effect of size on the distribution of data. To perform the PGLS we used 'caper' v. 1.0.1 in R v. 3.6 (R Core Team, 2013).

In order to identify morphological differences between the proposed dietary categories the variables (i.e. 3DRETvol, 3DRETgeo, ACS, LRFI, inclination, OPCR, DNE, and ARC) were compared between the dietary categories in SPSS v. 22.0 (Corp, 2013) using the Kruskal-Wallis test with Mann-Whitney U pairwise tests with Bonferroni adjustment, with a significance level set to 0.05. Furthermore, a set of linear discriminant analyses (LDA) was performed using several variable combinations, to determine which combination/s provides the most successful classification of individuals in the proposed dietary categories. In each variable combination, we only incorporated variables that were not correlated in the PGLS, including jack-knife resampling method. Lastly, in each variable combination, we included the 3D occlusal enamel surface (OES 3D), as it has been shown to improve the success rate of classification (Allen et al., 2015). Computations and visualizations were performed using PAST v. 3.22 (Hammer et al., 2001).

3.3.2 Dental microwear texture analysis

Before the analysis, all texture variables were box-cox transformed to avoid normality assumption violations in parametric tests (Conover and Iman, 1981). To identify microwear texture differences related to diet in both dental facet types, two-way analyses of variance (ANOVAs) were performed on modern species and *Dolichopithecus* to target which variables

Ψηφιακή βιβλιοθήκη Θεόφραστος – Τμήμα Γεωλογίας – Αριστοτέλειο Πανεπιστήμιο Θεσσαλονίκης

Ψηφιακή συλλογή
Βιβλιοθήκη
"ΘΕΟΦΡΑΣΤΟΣ"

significantly vary depending on species, dental facets, and interactions. Then, pairwise comparisons between species including both types of facets were performed using Tukey's Honest Significant Differences (HSD) and the less conservative test Fisher's Least Significant Differences (LSD) following Scott et al., (2012). Comparisons in which Tukey's HSD was significant are interpreted as grounds to reject the null hypothesis, whereas comparisons where Fisher's LSD was not significant, are interpreted as grounds to not reject the null hypothesis (Cook and Farewell, 1996). More clearly, the use of both Tukey's HSD and Fisher's LSD tests allows us to partition comparisons into significant, not significant, and suggestive of significance (Scott et al., 2012). To enhance the robustness of the model, every analysis included bootstrap resampling (n = 1000) and computations were performed using SPSS v. 22.0 (Corp, 2013). Lastly, to observe the variations of dental microwear textures across dental facet types, we compared the values of complexity (Asfc) and anisotropy (epLsar) between facet type from one species to another.

3.4 Results

3.4.1. Dental topographic and enamel thickness analyses

The PGLS analysis reveals significant correlations between variable pairs with some containing significant phylogenetic signal (Table S3 Appendix 3.6). The 3D relative volumetric and geometric enamel thickness (i.e. 3DRETvol and 3DRETgeo) are significantly correlated ($p < 0.05$), consistent with previous results (Thiery et al., 2017c). Furthermore, both 3DRETvol and 3DRETgeo are strongly and positively correlated with inclination and inversely correlated with the LRFI with a null Lambda ($\lambda = 0$). LRFI is strongly correlated with inclination ($p < 0.05$), ARC and DNE ($p < 0.05$). ARC is significantly positively correlated with LRFI, inclination, and DNE, but negatively correlated with 3DRETvol, 3DRETgeo. ACS is significantly correlated with DNE, OPCR, 3DRETvol, the latter correlation suggesting a strong phylogenetic relationship, and DNE is also significantly correlated with OPCR. In addition, size has a significant influence on some variables in our sample as the largest species (i.e. *Papio anubis, Papio hamadryas, Mandrillus leucophaeus*) are separated from the rest of the sample (see specimens labeled 1 and 2 in the blue box in Figs. S1-S4 Appendix 3.6). The projected two-dimensional area of the occlusal enamel surface (OES 2D) is significantly correlated with 3DRETvol, and ACS, with a strong phylogenetic signal (Figs. S1, S2 Appendix 3.6). Lastly, OPCR and DNE are also influenced by size as shown by the significant correlations with OES 2D (Figs. S3, S4), however with a null lambda (Table S3 Appendix 3.6).

The Kruskal-Wallis test detected significant ($p < 0.05$) differences among dietary categories in 3DRETvol and 3DRETgeo, LRFI, inclination, and ARC (Table 3.3). The species classified as folivores have significantly lower values of 3DRETvol, 3DRETgeo, and inclination (Table 3.4; Fig. 3.3A, B; Fig. 3.5B), and significantly higher values of LRFI and ARC (Table 3.4; Fig. 3.5A, 3.6B) compared to species classified as fruit/seed consumers. The mixed feeders possess significantly lower 3DRETvol, 3DRETgeo (Fig. 3.3A, B), and significantly higher ARC compared to fruit/seed-eaters (Table 3.4; Fig. 3.6B), whereas they differ from folivorous cercopithecids in having significantly higher 3DRETgeo (Table 3.4; Fig. 3.3B) and lower LRFI and ARC (Table 3.4; Fig. 3.5A, 3.B).

Table 3.2 Kruskal-Wallis on enamel thickness, tooth crown strength and dental topographic variables between the dietary categories proposed[a,b].

Kruskal–Wallis			
Variables[a]	df[b]	χ^2	*p*–value
$3DRET_{vol}$	2	21.887	< **0.05**
$3DRET_{geo}$	2	24.879	< **0.05**
LRFI	2	16.606	< **0.05**

Ψηφιακή βιβλιοθήκη Θεόφραστος – Τμήμα Γεωλογίας – Αριστοτέλειο Πανεπιστήμιο Θεσσαλονίκης

Ψηφιακή συλλογή
Βιβλιοθήκη
"ΘΕΟΦΡΑΣΤΟΣ"
Τμήμα Γεωλογίας
Α.Π.Θ

DNE	2	4.372	0.112
OPCR	2	4.629	0.098
ACS	2	4.978	0.082
Inclination	2	17.634	< **0.05**
ARC	2	26.377	< **0.05**

[a]$3DRET_{vol}$ = 3D volumetric relative enamel thickness; $3DRET_{geo}$ = 3D geometric relative enamel thickness; ACS = absolute crown strength; LRFI = relief index; ARC = area–relative curvature; DNE = Dirichlet normal energy; OPCR = orientation patch–count rotated; OES 3D = 3D occlusal enamel surface; OES 2D = 2D occlusal enamel surface; [b]df = degrees of freedom; χ^2 = Chi square.

Table 3.3 Kruskal-Wallis pairwise comparisons of enamel thickness, tooth crown strength and dental topographic variables between the dietary categories proposed with Bonferroni adjustment[a].

Dietary category	Fruit/seed–eaters	Folivores	Mixed-feeders
Fruit/seed-eaters		$3DRET_{vol}$(–), $3DRET_{geo}$(–), Inclination(–), LRFI(+), ARC(+)	$3DRET_{vol}$(–), $3DRET_{geo}$(–), ARC(+)
Folivores	$3DRET_{vol}$(+), $3DRET_{geo}$(+), Inclination(+), LRFI(–), ARC(–)		$3DRET_{geo}$(+), LRFI(–), ARC(–)
Mixed-feeders	$3DRET_{vol}$(+), $3DRET_{geo}$(+), ARC(–)		

[a] (–) and (+) indicate values that are either lower or higher, respectively, for species in column compared to the one in the row.

While seed specialists such as *L. albigena*, *L. aterrimus* and *Cercocebus torquatus* possess the highest values of 3DRETvol and 3DRETgeo (Fig. 3.7A, B), the highest values of ACS in our sample are shown by *Papio* (*P. hamadryas* then *P. anubis*) followed by *Mandrillus*, which all possess moderate values of 3DRETvol and 3DRETgeo (Fig. 3.7 A, B). The folivorous cercopithecids exhibit the lowest values of ACS (Fig. 3.4A).The LRFI value of MHNPn-PR01 places the fossil molar closer to folivorous species (Fig. 4A), such as *Co. satanas*, *Pi. badius*, and *Pr. verus*, while it also falls within the range of *M. leucophaeus* and *Chlorocebus aethiops* (Fig. 3.9A). The inclination value of MHNPn-PR01 places it within the range of folivorous species, such as *Co. satanas*, *Pi. badius*, and *Pr. verus* (Fig. 3.9B). The DNE value of MHNPn-PR01 places it closer to *Pi. badius*, *P. anubis* and *Mandrillus* (Fig. 3.10A). The ARC value of MHNPn-PR01 places the fossil molar within the range of *Pi. badius*, *N. larvatus*, and *Pr. verus*. In terms of OPCR, MHNPn-PR01 is placed closer to folivorous representatives such as *Co. polykomo*s, *Co. guereza*, *Pr. verus*, and Pi. badius, however, it also falls within the range of *Cercopithecus pogonias* (Fig. 3.8B).

Ψηφιακή βιβλιοθήκη Θεόφραστος – Τμήμα Γεωλογίας – Αριστοτέλειο Πανεπιστήμιο Θεσσαλονίκης

Ψηφιακή συλλογή
Βιβλιοθήκη
"ΘΕΟΦΡΑΣΤΟΣ"
Τμήμα Γ
Α.Π.Θ.

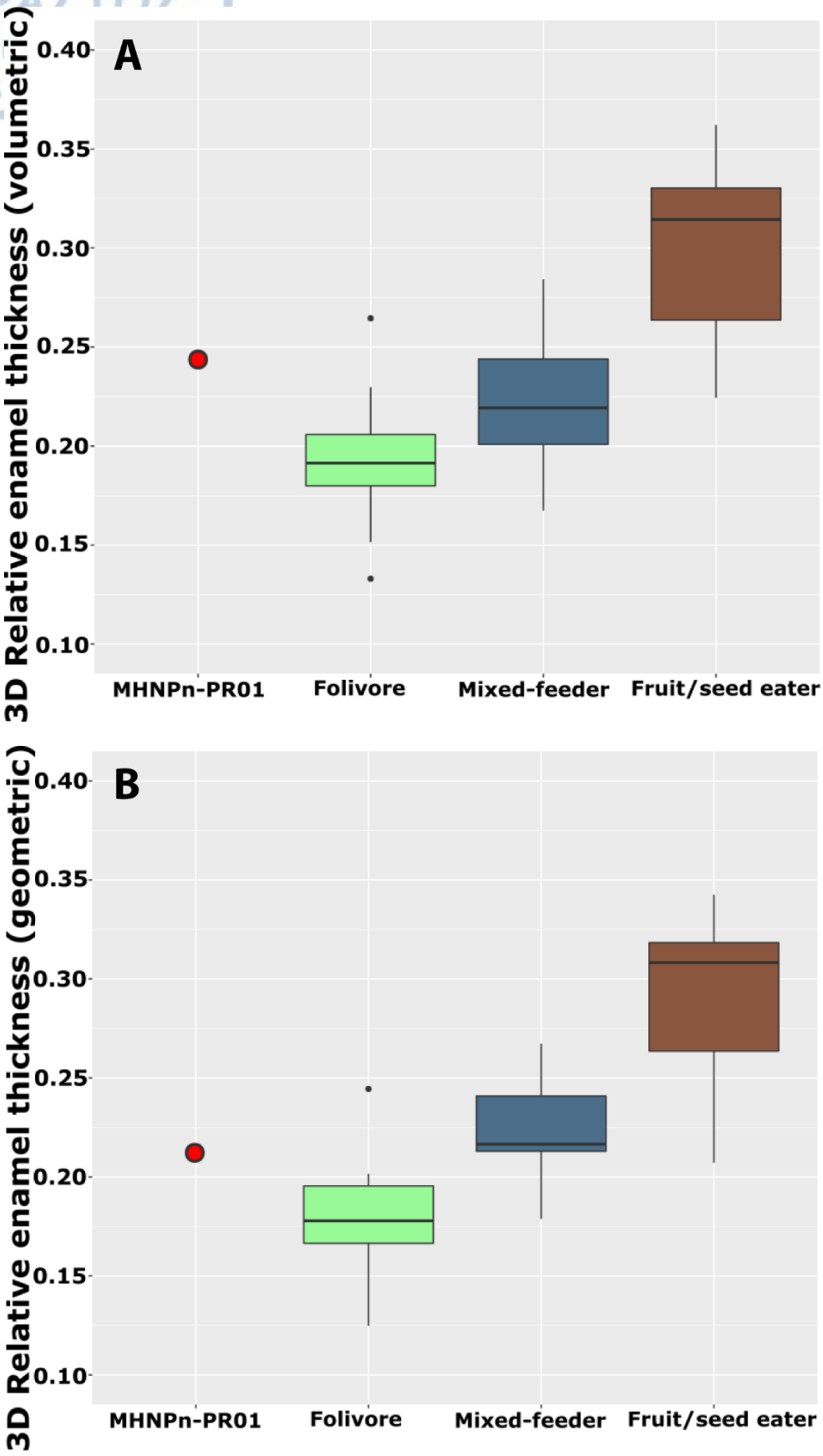

Fig. 3.3 Boxplots comparisons of 3D relative (volumetric and geometric) enamel thickness (A, B), between the dietary categories and *Dolichopithecus ruscinensis* (MHNPn–PR01). The fossil M^1 exhibits tooth strength, enamel thickness and distribution similar to mixed feeding cercopithecids.

Ψηφιακή βιβλιοθήκη Θεόφραστος – Τμήμα Γεωλογίας – Αριστοτέλειο Πανεπιστήμιο Θεσσαλονίκης

Ψηφιακή συλλογή
Βιβλιοθήκη
"ΘΕΟΦΡΑΣΤΟΣ"
Τμήμα
Α.

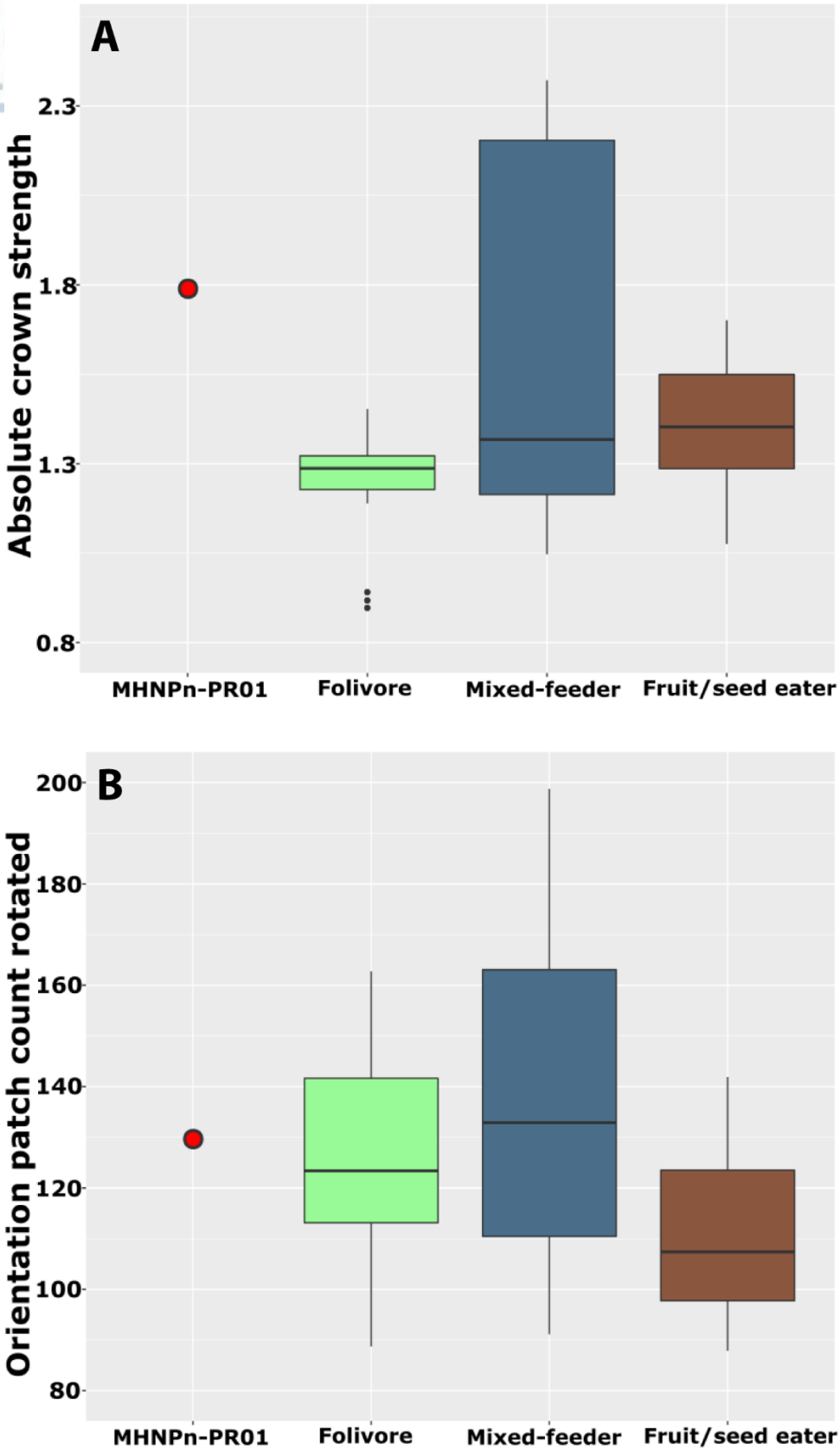

Fig. 3.4 Boxplot comparisons of the absolute crown strength (A), orientation patch count rotated (B), between the dietary categories and *Dolichopithecus ruscinensis* (MHNPn–PR01). The fossil M^1 exhibits tooth strength, more closely resembling mixed feeding cercopithecids, while complexity (based on OPCR) shows high overlap between dietary categories.

Ψηφιακή βιβλιοθήκη Θεόφραστος – Τμήμα Γεωλογίας – Αριστοτέλειο Πανεπιστήμιο Θεσσαλονίκης

Ψηφιακή συλλογή
Βιβλιοθήκη
"ΘΕΟΦΡΑΣΤΟΣ"
Τμήμα
Α

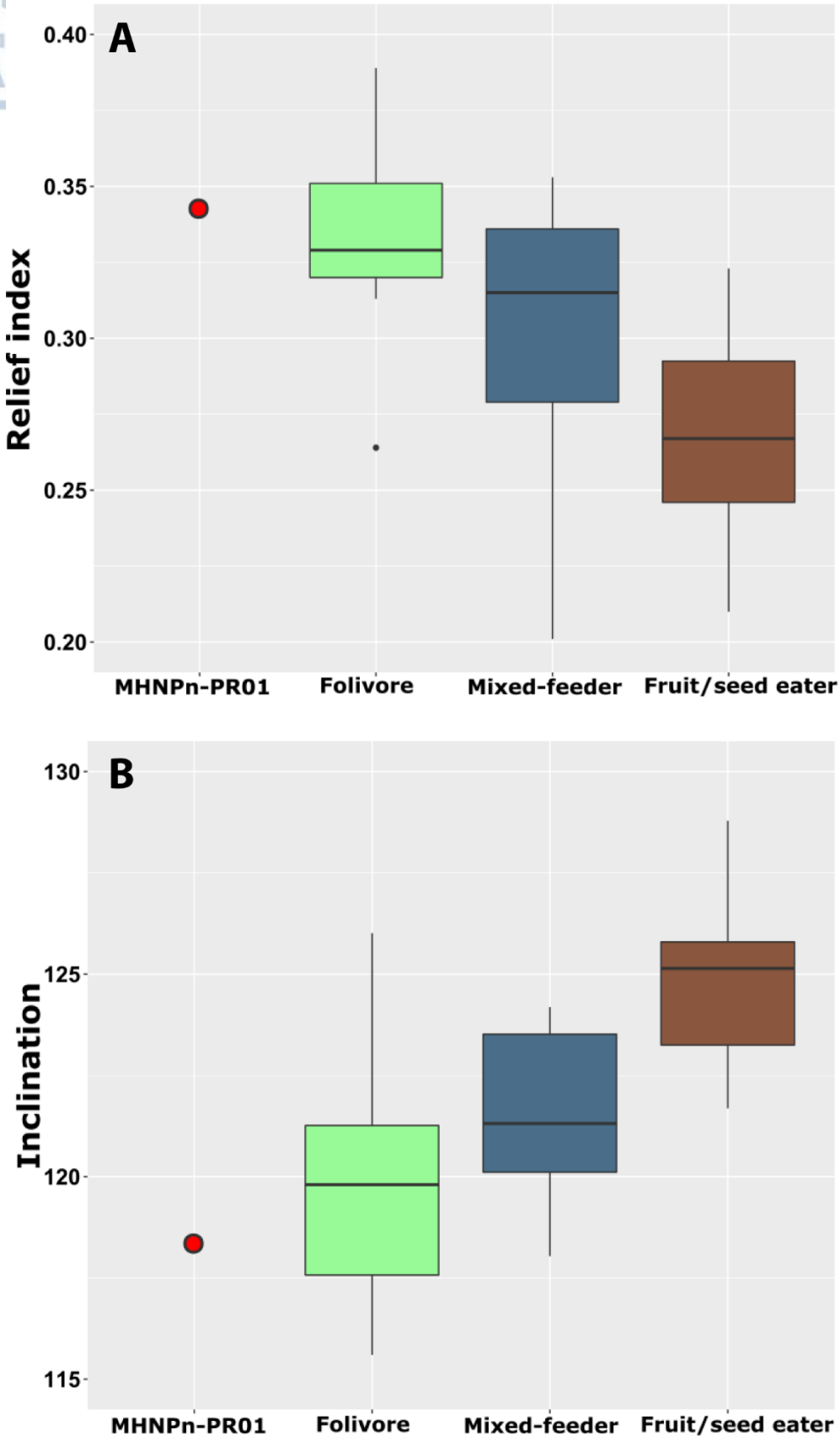

Fig. 3.5 Boxplot comparisons of the relief index (A), inclination (B), between the dietary categories and *Dolichopithecus ruscinensis* (MHNPn–PR01). The fossil M^1 exhibits occlusal relief similar to folivorous cercopithecids.

Ψηφιακή βιβλιοθήκη Θεόφραστος – Τμήμα Γεωλογίας – Αριστοτέλειο Πανεπιστήμιο Θεσσαλονίκης

Ψηφιακή συλλογή
Βιβλιοθήκη
"ΘΕΟΦΡΑΣΤΟΣ"
Τμήμα

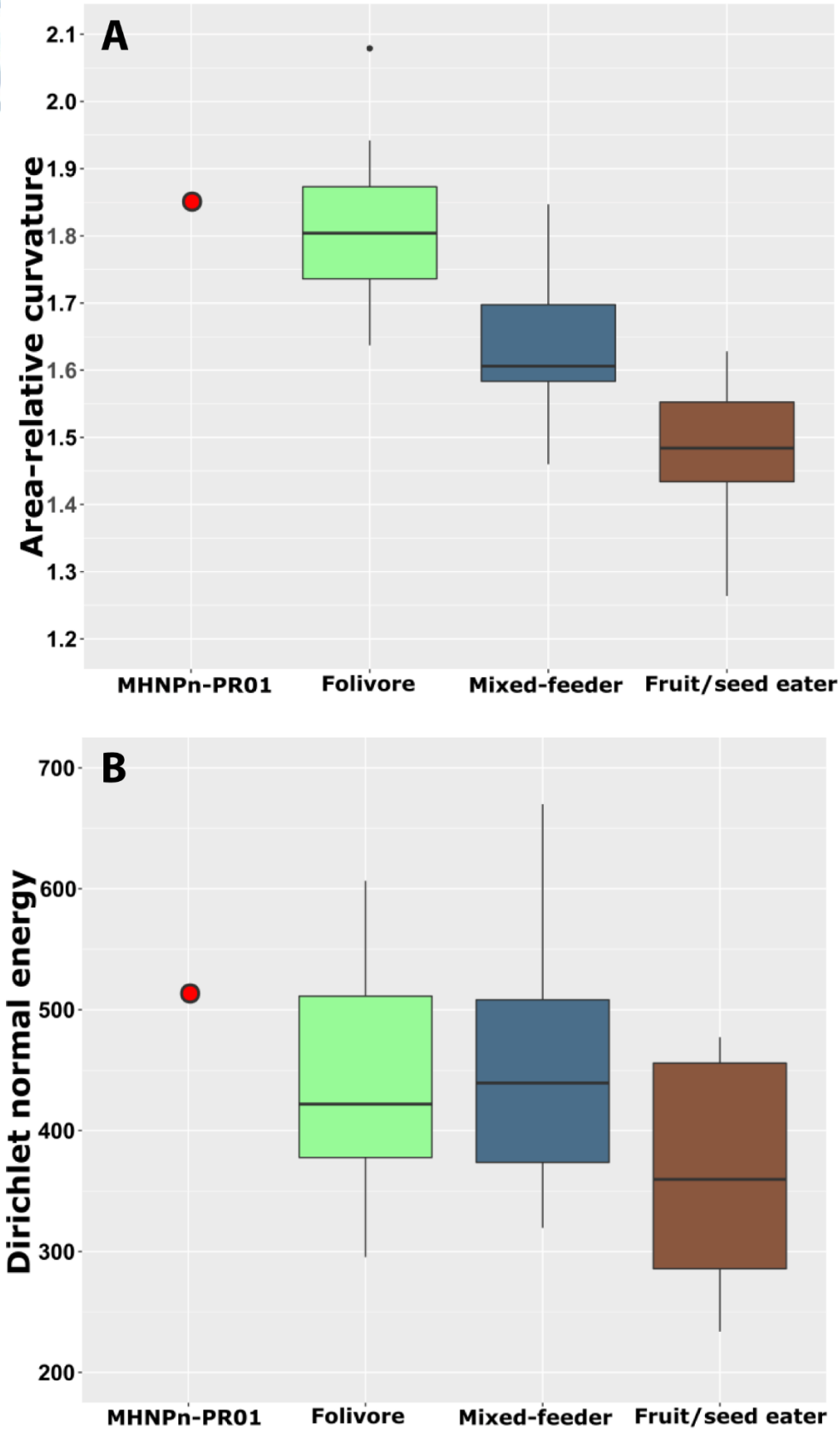

Fig. 3.6 Boxplot comparisons of the Dirichlet normal energy (A), area–relative curvature (B), between the dietary categories and *Dolichopithecus ruscinensis* (MHNPn–PR01). The fossil M^1 exhibits ARC and DNE similar to folivorous cercopithecids, yet DNE shows considerable overable among dietary categories.

Ψηφιακή βιβλιοθήκη Θεόφραστος – Τμήμα Γεωλογίας – Αριστοτέλειο Πανεπιστήμιο Θεσσαλονίκης

Ψηφιακή συλλογή
Βιβλιοθήκη
"ΘΕΟΦΡΑΣΤΟΣ"
Τμήμα Γε
Α.Π

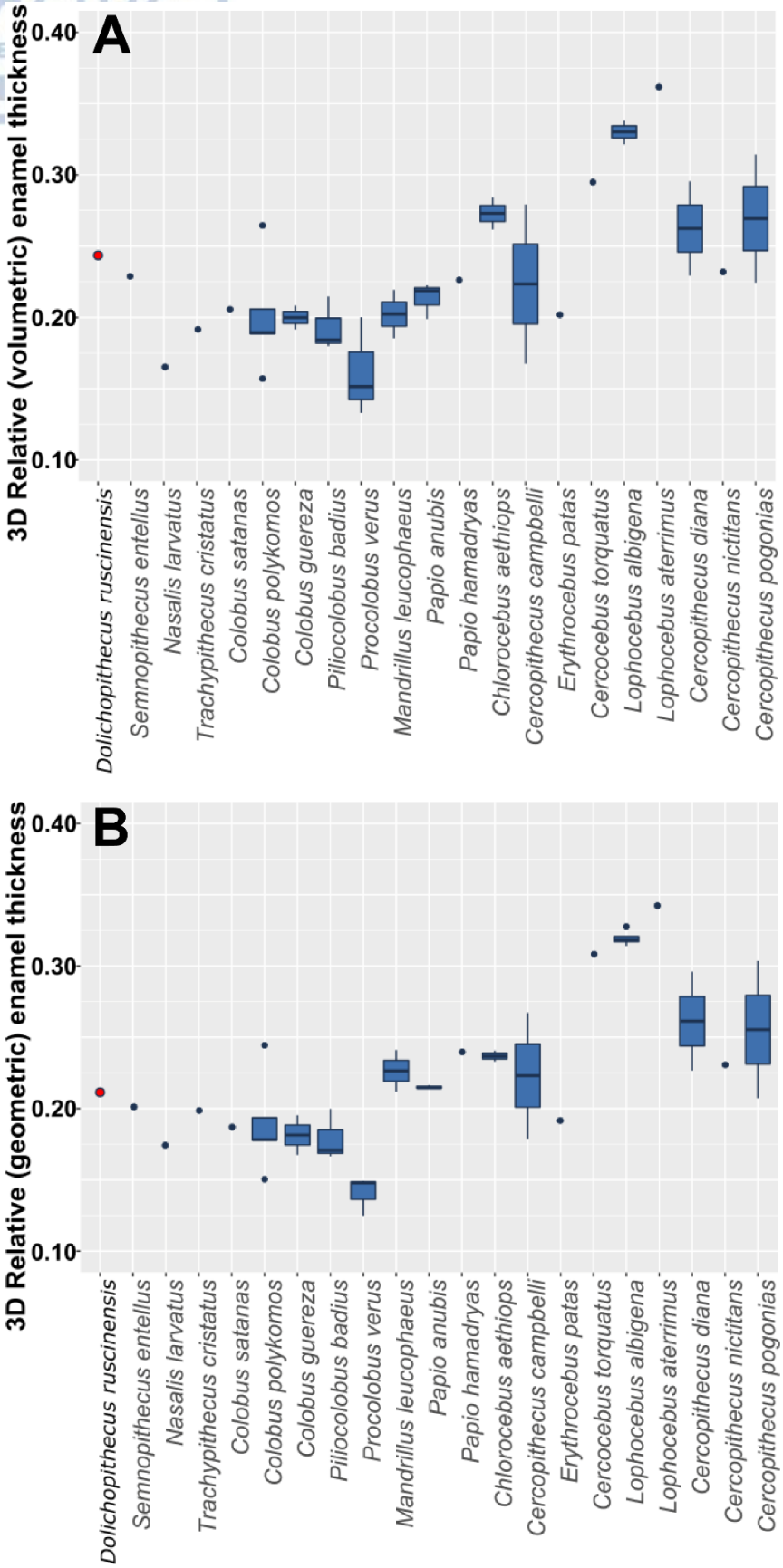

Fig. 3.7 Boxplot comparisons of A) 3D relative volumetric enamel thickness B) 3D relative geometric enamel thickness, between modern species and *Dolichopithecus ruscinensis* M^1; MHNPn–PR01 exhibits similar or slightly higher relative enamel thickness value than most extant folivorous cercopithecids in the comparative sample.

Ψηφιακή βιβλιοθήκη Θεόφραστος – Τμήμα Γεωλογίας – Αριστοτέλειο Πανεπιστήμιο Θεσσαλονίκης

Ψηφιακή συλλογή
Βιβλιοθήκη
"ΘΕΟΦΡΑΣΤΟΣ"
Τμήμα Γε
Α.Π

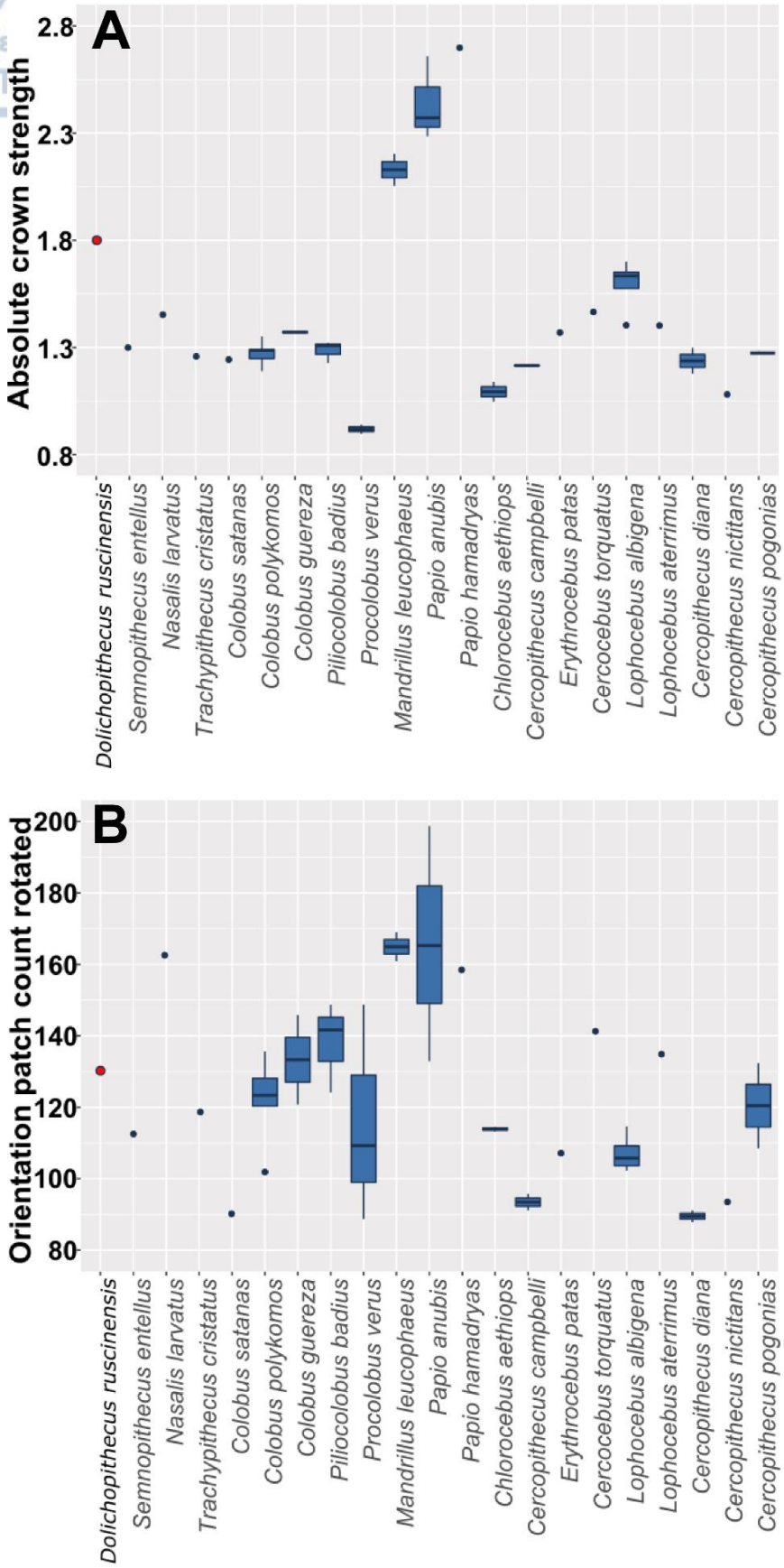

Fig. 3.8 Boxplot comparisons of A) absolute crown strength B) orientation patch count rotated, between modern species and *Dolichopithecus ruscinensis* M^1; MHNPn–PR01 exhibits higher ACS compared with the folivorous and fruit/seed eating cercopithecids in the comparative sample.

Ψηφιακή βιβλιοθήκη Θεόφραστος – Τμήμα Γεωλογίας – Αριστοτέλειο Πανεπιστήμιο Θεσσαλονίκης

Ψηφιακή συλλογή
Βιβλιοθήκη
"ΘΕΟΦΡΑΣΤΟΣ"
Τμήμα Γε
Α.Π

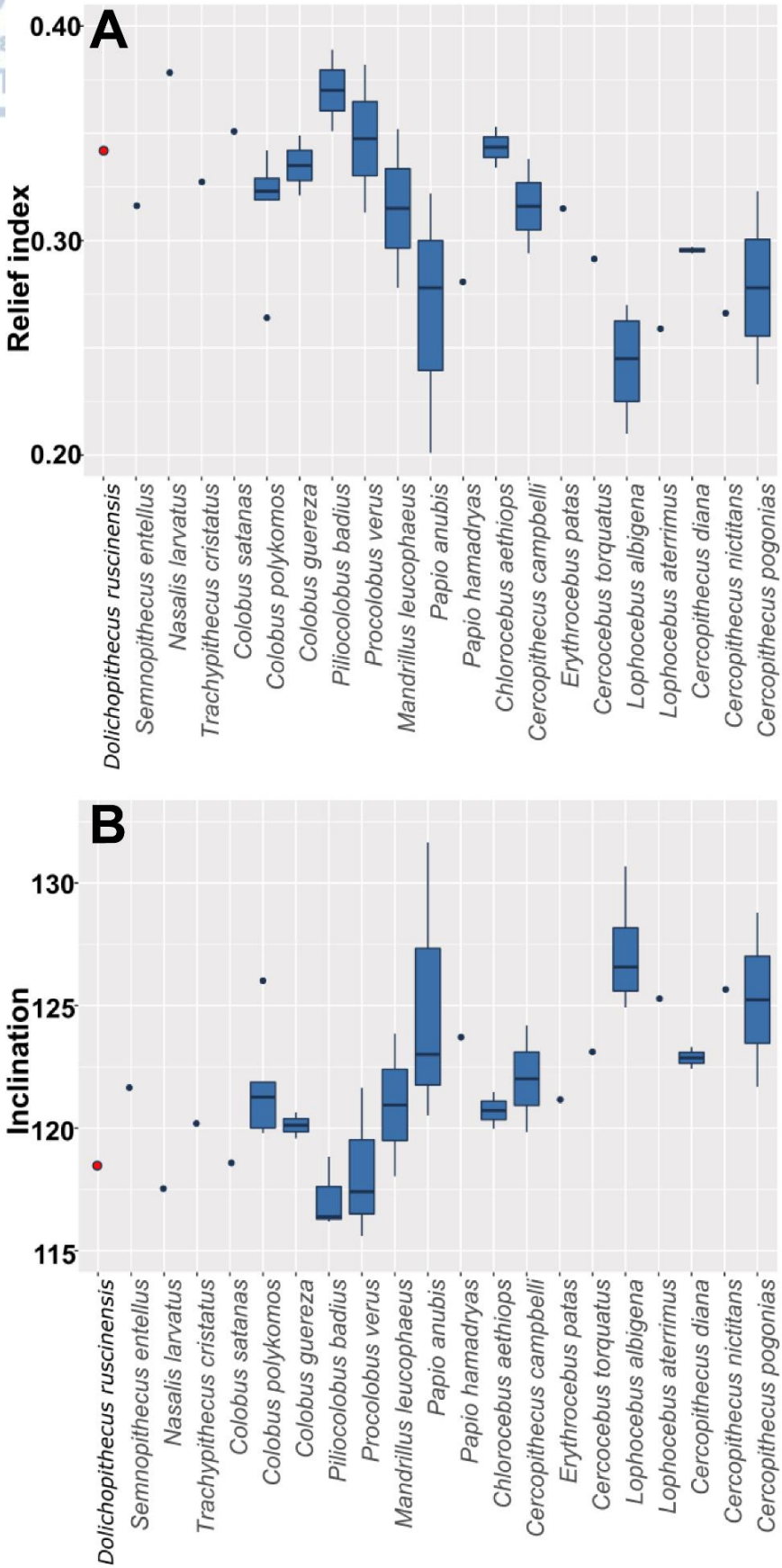

Fig. 3.9 Boxplot comparisons of A) relief index B) inclination, between modern species and *Dolichopithecus ruscinensis* M^1; MHNPn–PR01 exhibits occlusal relief similar to most folivorous cercopithecids in the comparative sample.

Ψηφιακή βιβλιοθήκη Θεόφραστος – Τμήμα Γεωλογίας – Αριστοτέλειο Πανεπιστήμιο Θεσσαλονίκης

Ψηφιακή συλλογή
Βιβλιοθήκη
"ΘΕΟΦΡΑΣΤΟΣ"
Τμήμα Γε
Α.Π

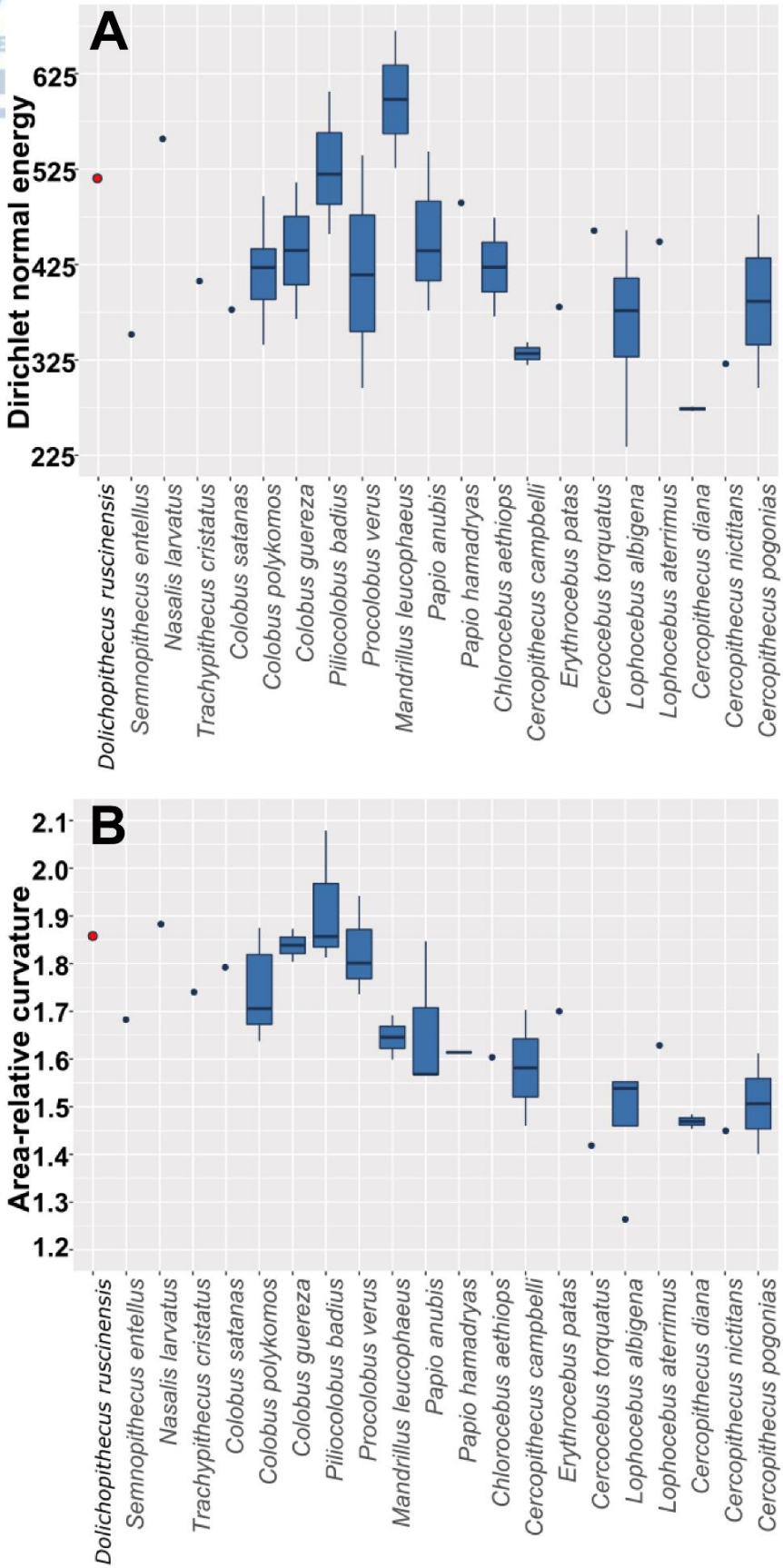

Fig. 3.10 Boxplot comparisons of A) Dirichlet normal energy B) area—relative curvature, between modern species and *Dolichopithecus ruscinensis* M^1; MHNPn—PR01 exhibits similar DNE and ARC values with the folivorous cercopithecids in the comparative sample, yet DNE shows high overlap among species and it is significantly influenced by size.

Ψηφιακή βιβλιοθήκη Θεόφραστος – Τμήμα Γεωλογίας – Αριστοτέλειο Πανεπιστήμιο Θεσσαλονίκης

Ψηφιακή συλλογή Βιβλιοθήκη "ΘΕΟΦΡΑΣΤΟΣ" Τμήμα Γεωλογίας

The results of the linear discriminant analyses are presented in Table 3.4. The combination of ACS, ARC, and OES 3D presents the highest rate of classification. ARC (-0.098) explains the most variance along axis 1, followed by ACS (0.078) and OES 3D (0.053),although all with low effects. However, OES 3D (42.185) contributes the most to the second axis, followed by ACS (0.346) then ARC (0.015) with the latter two having a much lower effect. This implies that the second axis is heavily influenced by tooth size, most likely related to species size. Indeed, the largest representatives in our sample (e.g., *Papio* and *Mandrillus*) are separated from the rest of the cercopithecids (see specimens labeled 1 and 2 in the blue box in Fig. 3.11). The fossil M^1 (MHNPn-PR01) is placed out of the range of the dietary categories, in a space between mixed feeding and folivorous cercopithecids (Fig. 3.11).

Table 3.4 Combination of topographic enamel thickness and tooth crown strength variables and probabilities of successful classification for LDAs using the proposed dietary categories as factor; best set of variables and their success rate indicated in bold[a].

Variables			**(%) Variance explained**		**(%) Correctly classified**	
			Axis 1	Axis 2	Normal	Resampling
RET_{vol}	DNE	OES 3D	74.44	24.44	72.5	67.5
RET_{vol}	OPCR	OES 3D	74.70	25.22	70	65
RET_{geo}	ACS	OES 3D	8.87	19.04	70	62.5
RET_{geo}	OPCR	OES 3D	81.77	18.09	77.5	62.5
LRFI	ACS	OES 3D	63.55	35.32	67.5	60
LRFI	OPCR	OES 3D	63.57	35.79	67.5	62.5
DNE	λ	OES 3D	62.35	37.51	70	60
λ	OPCR	OES 3D	61.42	37.72	67.5	62.5
λ	ACS	OES 3D	62.35	34.84	72.5	65
ARC	OPCR	OES 3D	8.88	18.6	77.5	70
ARC	ACS	OES 3D	8.29	18.79	**77.5**	**72.5**

[a] $3DRET_{vol}$ = 3D volumetric relative enamel thickness; $3DRET_{geo}$ = 3D geometric relative enamel thickness; ACS = absolute crown strength; LRFI = relief index; ARC = area-relative curvature; DNE = Dirichlet normal energy; OPCR = orientation patch-count rotated; OES 3D = 3D occlusal enamel surface.

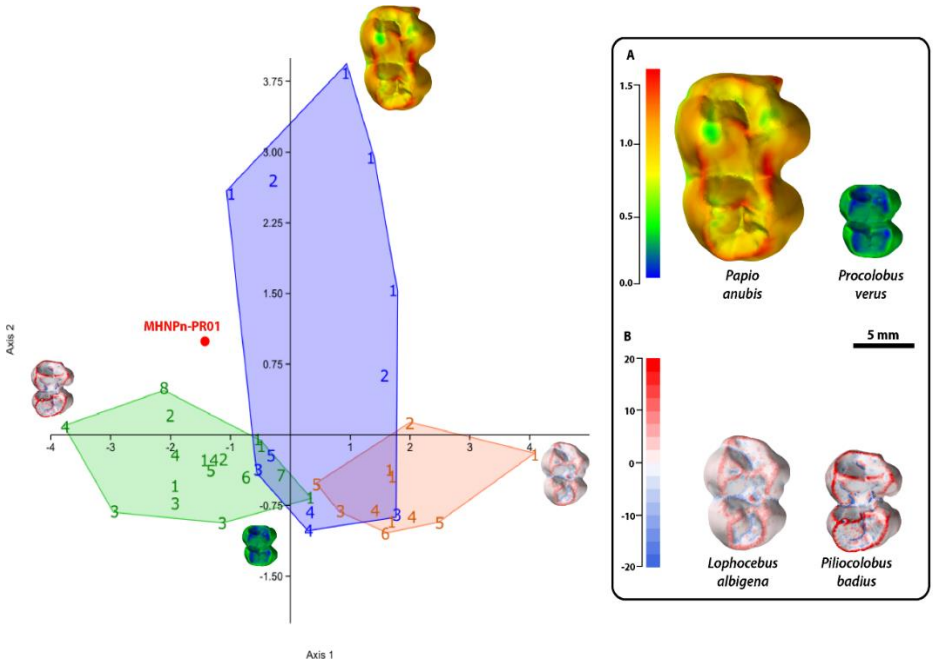

Fig. 3.11 Linear discriminant analysis (LDA) with the best rate of classification for inferring diet on the proposed categories with absolute crown strength (ACS), area-relative curvature (ARC) and the three-dimensional area of occlusal surface (OES 3D) including *Dolichopithecus* ruscinensis M^1 (MHNPn–PR01, red dot); enamel distribution maps retaining original size (**A**), area-relative

Ψηφιακή βιβλιοθήκη Θεόφραστος – Τμήμα Γεωλογίας – Αριστοτέλειο Πανεπιστήμιο Θεσσαλονίκης

Ψηφιακή συλλογή Βιβλιοθήκη "ΘΕΟΦΡΑΣΤΟΣ" Τμήμα Γεωλογίας

visualization based on the lowest (*Lophocebus albigena*) and the highest value in our sample (**B**); **Blue** = Mixed-feeders (1: *Papio*, 2: *Mandrillus leucophaeus*; 3: *Cercopithecus campbelli*, 4: *Chlorocebus aethiops*, 5: *Erythrocebus patas*), **Orange** = Fruit/seed eaters (1: *Lophocebus albigena*, 2: *Cercocebus torquatus*, 3: *Lophocebus aterrimus*; 4: *Cercopithecus diana*, 5: *Cercopithecus pogonias*, 6: *Cercopithecus nictitans*, **Green** = Folivores (1: *Colobus polykomos*, 2: *Colobus guereza*, 3: *Procolobus verus*, 4: *Piliocolobus badius*, 5: *Colobus satanas*; 6: *Trachypithecus cristatus*, 7: *Semnopithecus entellus*, 8: *Nasalis larvatus.*

3.4.2. Dental microwear texture analysis

The two-way ANOVAs showed significant variations in complexity (Asfc; $p < 0.05$), anisotropy (epLsar; $p < 0.05$) and scale of maximal complexity (Smc; $p < 0.05$) between species and in complexity (Asfc; $p < 0.05$) between facets as well. There are no interaction effects between factors (Table 3.5). The pairwise comparisons indicate the differences between species and facet types (Table 3.7). Concerning Phase II facets, the African colobines *Colobus guereza* and *Piliocolobus badius* have lower values of complexity than *Lophocebus albigena*, *Chlorocebus aethiops*, and *Erythrocebus patas*, while the African colobines also differ from the latter two in having higher anisotropy values (Fig. 3.12). *Presbytis melalophos* differs from *Erythrocebus patas* having lower values of complexity and higher anisotropy (Table 3.7).

Table 3.5 Results of two-way analyses of variance (ANOVA) between the extant species and *Dolichopithecus* on both Phase I and II facets with species and facet as factors[a].

		Two–way ANOVA				
Factors	Variable	df	SS	MS	F	*p*–value
Species	*Asfc*	8.00	4.382	0.548	10.834	**< 0.05**
	Smc	8.00	59.957	7.495	46.790	**< 0.05**
	epLsar	8.00	1.291	0.161	3.205	**< 0.05**
	Tfv	8.00	1.111	0.139	1.833	0.070
	$Hasfc_{9}$	8.00	0.136	0.017	0.999	0.437
	$Hasfc_{36}$	8.00	0.221	0.028	1.634	0.114
	$Hasfc_{81}$	8.00	0.197	0.025	1.216	0.289
Facet	*Asfc*	1.00	1.771	1.771	35.023	**< 0.05**
	Smc	1.00	0.249	0.249	1.553	0.214
	epLsar	1.00	0.107	0.107	2.133	0.145
	Tfv	1.00	0.059	0.059	0.783	0.377
	$Hasfc_{9}$	1.00	0.015	0.009	0.881	0.349
	$Hasfc_{36}$	1.00	0.006	0.006	0.327	0.568
	$Hasfc_{81}$	1.00	0.004	0.004	0.201	0.654
Interaction	*Asfc*	8.00	0.116	0.014	0.286	0.970
	Smc	8.00	1.781	0.223	1.390	0.200
	epLsar	8.00	0.428	0.054	1.063	0.389
	Tfv	8.00	0.574	0.072	0.947	0.478
	$Hasfc_{9}$	8.00	0.071	0.009	0.523	0.839
	$Hasfc_{36}$	8.00	0.051	0.006	0.374	0.934
	$Hasfc_{81}$	8.00	0.050	0.006	0.306	0.963

[a] SS = sum of squares; df = degrees of freedom; MS = mean square, F = *F*-test; Asfc = area-scale fractal complexity; epLsar = exact-proportion length-scale anisotropy of relief; Smc = scale of maximal complexity, $Hasfc_{9,36,81}$ = heterogeneity of area-scale fractal complexity on 9, 36 and 81 cell.

The dental microwear texture sample of *Dolichopithecus* differs from *Colobus guereza*, *Piliocolobus badius*, and *Presbytis melalophos* (Fig. 3.12), having lower anisotropy values, while it differs from all modern species compared in having higher values of scale of maximal complexity (Table 3.5, 3.7). Concerning Phase I facets, *Colobus guereza*, and *Piliocolobus badius* differ from *Lophocebus albigena*, *Chlorocebus aethiops*, and *Erythrocebus patas* in

Ψηφιακή βιβλιοθήκη Θεόφραστος – Τμήμα Γεωλογίας – Αριστοτέλειο Πανεπιστήμιο Θεσσαλονίκης

Ψηφιακή συλλογή Βιβλιοθήκη "ΘΕΟΦΡΑΣΤΟΣ" Τμήμα Γεωλογίας Α.Π.Θ

Table 3.6 Microwear texture variables descriptive statistics on Phase I and II dental wear facets of *Dolichopithecus* and modern sample[a].

Taxa		***n***	**Phase I**							***n***	**Phase II**						
Dolichopithecus			Asfc	epLsar ($\times 10^3$)	Smc (μm^2)	Tfv (μm^3)	$Hasfc_9$	$Hasfc_{36}$	$Hasfc_{81}$		Asfc	epLsar ($\times 10^3$)	Smc (μm^2)	Tfv (μm^3)	$Hasfc_9$	$Hasfc_{36}$	$Hasfc_{81}$
	Mean	25		1.36	3.32	68.04	35528.40	0.351	0.473	0.616	27	1.777	2.638	74.516	37661.75	0.305	0.418
	sd			0.859	1.735	54.637	11478.50	0.347	0.401	0.618		0.855	1.247	62.127	14167.91	0.175	0.166
	sem			0.172	0.347	10.927	2295.70	0.069	0.080	0.124		0.164	0.240	11.956	2726.61	0.034	0.032
Nasalis larvatus	Mean	7		1.505	3.531	0.346	25575.18	0.351	0.526	0.758	7	2.260	2.744	0.277	36665.23	0.308	0.450
	sd			1.551	1.797	0.196	10141.31	0.221	0.300	0.598		1.972	1.479	0.144	15936.64	0.178	0.220
	sem			0.586	0.679	0.074	3833.05	0.083	0.113	0.226		0.745	0.559	0.054	6023.48	0.067	0.083
Semnopithecus entellus	Mean	8		0.934	5.319	1.266	36114.45	0.390	0.580	0.743	8	1.497	4.131	22.733	34105.96	0.530	0.621
	sd			0.711	2.392	2.175	8126.46	0.195	0.254	0.374		0.679	2.076	38.339	12535.85	0.442	0.292
	sem			0.251	0.846	0.769	2873.13	0.069	0.090	0.132		0.240	0.734	13.555	4432.09	0.156	0.103
Presbytis melalophos	Mean	17		1.149	3.974	0.604	25434.82	0.280	0.406	0.538	19	1.632	4.411	21.362	35671.93	0.354	0.517
	sd			0.670	1.248	0.465	19868.65	0.151	0.198	0.253		0.832	2.048	86.470	16422.18	0.225	0.337
	sem			0.163	0.303	0.113	4818.85	0.037	0.048	0.061		0.202	0.497	20.972	3982.96	0.055	0.082
Colobus guereza	Mean	21		0.749	4.053	31.277	29588.78	0.268	0.391	0.506	25	1.128	4.495	0.370	30196.70	0.298	0.415
	sd			0.369	2.387	138.871	10703.93	0.164	0.174	0.213		0.467	1.755	0.154	9873.72	0.148	0.134
	sem			0.081	0.521	30.304	2335.79	0.036	0.038	0.047		0.093	0.351	0.031	1974.74	0.030	0.027
Piliocolobus badius	Mean	12		0.706	3.639	0.674	34306.51	0.374	0.512	0.597	17	1.191	4.690	60.011	37329.29	0.349	0.479
	sd			0.614	2.207	1.630	13649.04	0.321	0.362	0.380		0.825	2.540	170.449	17626.00	0.192	0.216
	sem			0.177	0.637	0.470	3940.13	0.093	0.105	0.110		0.200	0.616	41.340	4274.93	0.047	0.052
Erythrocebus patas	Mean	13		1.619	3.703	29.923	41234.20	0.307	0.484	0.580	16	3.116	2.565	0.397	41359.01	0.370	0.511
	sd			0.885	2.510	102.391	7138.79	0.136	0.261	0.263		1.466	1.237	0.228	9775.96	0.172	0.213
	sem			0.245	0.696	28.398	1979.94	0.038	0.072	0.073		0.366	0.309	0.057	2443.99	0.043	0.053
Chlorocebus aethiops	Mean	37		1.710	3.682	0.266	34543.57	0.374	0.510	0.674	37	2.586	2.975	10.359	35382.82	0.320	0.477
	sd			1.525	1.891	0.159	9862.58	0.443	0.499	0.611		1.764	1.615	60.013	14750.39	0.328	0.455
	sem			0.251	0.311	0.026	1621.44	0.073	0.082	0.100		0.290	0.265	9.866	2424.94	0.054	0.075
Lophocebus albigena	Mean	15		1.895	3.229	3.558	36235.56	0.319	0.507	0.659	15	2.608	3.011	25.450	45004.68	0.400	0.586
	sd			1.046	1.366	8.045	13290.69	0.124	0.175	0.255		1.246	1.763	92.205	10906.67	0.184	0.194
	sem			0.270	0.353	2.077	3431.64	0.032	0.045	0.066		0.322	0.455	23.807	2816.09	0.047	0.050

[a] sd = standard deviation; sem = std. error of the mean; Asfc = Area-scale fractal complexity; epLsar = exact proportion length-scale anisotropy of relief; $Hasfc_{81}$ = Heterogeneity of area-scale fractal complexity on 81 cells; Tfv = Textural fill volume at the scale of 2 μm; in μm^3 (see Scott et al., 2006 for details).

Ψηφιακή βιβλιοθήκη Θεόφραστος – Τμήμα Γεωλογίας – Αριστοτέλειο Πανεπιστήμιο Θεσσαλονίκης

Ψηφιακή συλλογή
Βιβλιοθήκη
"ΘΕΟΦΡΑΣΤΟΣ"
Τμήμα Γεωλογίας
Α.Π.Θ

Table 3.7 Pairwise comparisons of *Dolichopithecus* and extant cercopithecids with both Phase I and II facets. Differences indicated by Tukey's HSD and Fisher's LSD are above and below the black diagonal, respectively[a].

Species	*Dolichopithecus*		*Colobus guereza*		*Piliocolobus badius*		*Semnopithecus entellus*		*Nasalis larvatus*		*Presbytis melalophos*		*Lophocebus albigena*		*Chlorocebus aethiops*		*Erythrocebus patas*	
Facet	II	I	II	I	II	I	II	I	II	I	II	I	II	I	II	I	II	I
Dolichopithecus			epLsar(+) Smc(–)	Smc(–)	epLsar(+) Smc(–)	Smc(–)	Smc(–)	Smc(–)	Smc(–)	Smc(–)	epLsar(+) Smc(–)	Smc(–)	Smc(–)	Smc(–)	Smc(–)	Smc(–)	Smc(–)	Smc(–)
Colobus guereza	Asfc(+) Smc(+) epLsar(–)	Asfc(+) Smc(+)											Asfc(+)	Asfc(+)	Asfc(+) epLsar(–)	Asfc(+)	Asfc(+) epLsar (–)	Asfc(+)
Piliocolobus badius	Asfc(+) Smc(+) epLsar(–)	Asfc(+) Smc(+)											Asfc(+)	Asfc(+)	Asfc(+) epLsar(–)	Asfc(+)	Asfc(+) epLsar(–)	Asfc(+)
Semnopithecus entellus	Smc(+) epLsar(–)	Smc(+)	Smc(–)															
Nasalis larvatus	Smc(+)	Smc(+)	epLsar(+)				Smc(+)											
Presbytis melalophos	Smc(+) epLsar(–)	Smc(+)	Smc(–)			Asfc(–)			epLsar(–)								Asfc(+) epLsar(–)	
Lophocebus albigena	Asfc(–) Smc(+)	Smc(+)	Asfc(–) epLsar(+)	Asfc(–) Smc(+)	Asfc(–) epLsar(+)	Asfc(–) Smc(+)	Asfc(–)	Asfc(–)			Asfc(–) epLsar(+)	Asfc(–)				Smc(–)		
Chlorocebus aethiops	Asfc(–) Smc(+)	Smc(+)	Asfc(–) epLsar(+)	Asfc(–)	Asfc(+) epLsar(+)	Asfc(–)					Asfc(–) Smc(+) epLsar(+)			Smc(+)				
Erythrocebus patas	Asfc(–) Smc(+)	Smc(+)	Asfc(–) epLsar(+)	Asfc(–)	Asfc(–) epLsar(+)	Asfc(–)	Asfc(–) Smc(+) epLsar(+)	Asfc(–) epLsar(+)	Asfc(+)		Asfc(–) Smc(+) epLsar(+)							

[a](–) and (+) indicate values that are either lower or higher, respectively, for species in column compared to the one in the row.

Ψηφιακή βιβλιοθήκη Θεόφραστος – Τμήμα Γεωλογίας – Αριστοτέλειο Πανεπιστήμιο Θεσσαλονίκης

Ψηφιακή συλλογή
Βιβλιοθήκη
"ΘΕΟΦΡΑΣΤΟΣ"

having lower complexity (Asfc) values (Fig. 3.12). *Dolichopithecus* has higher values of scale of maximal complexity (Smc) than all extant taxa compared here (Table 3.7).

The comparisons of complexity (Asfc) between species and dental facet types show that all extant taxa and *Dolichopithecus* have higher values on Phase II facets (Fig. S5A Appendix 3.7), in support of previous works that incorporated both facet types (Krueger et al., 2008). This is not the same regarding anisotropy (epLsar). All taxa have higher values of anisotropy in Phase I facets except *Colobus guereza*, *Piliocolobus badius*, and *Presbytis melalophos* (Fig. S5B Appendix 3.7), which reflects that the slicing movement is important during the two masticatory phases for leaf-eating monkeys (Walker and Murray, 2011).

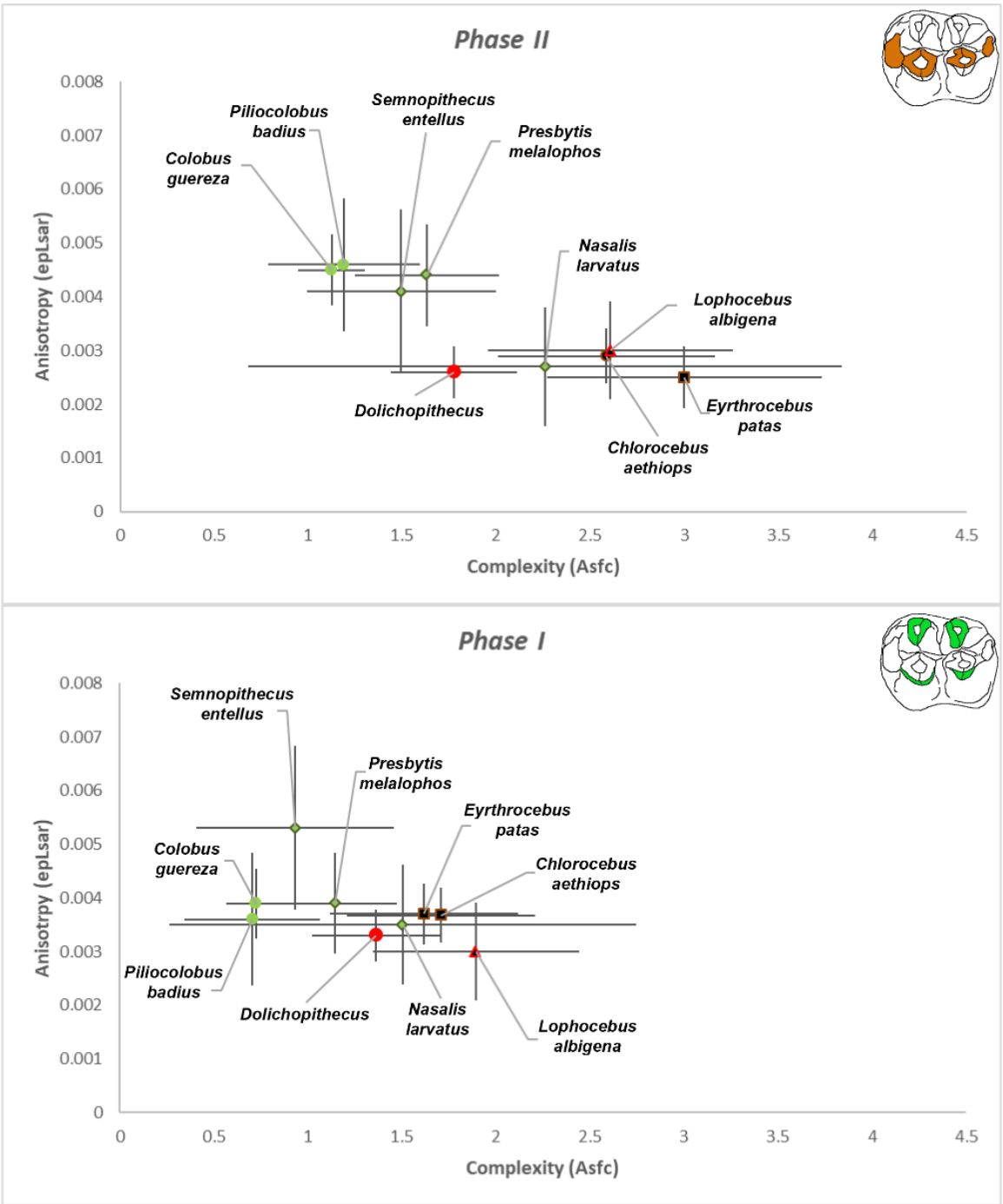

Fig. 3.12 Bivariate plots (means with 95% conf. interval) of complexity (Asfc) and anisotropy (epLsar) on Phase I and II (green circles = African colobines; green diamonds = Asian colobines; squares = Cercopithecines; triangles = Papionins). *Dolichopithecus* (red dot) is placed in an intermediate space between highly folivorous species and more durophagous cercopithecids.

Ψηφιακή βιβλιοθήκη Θεόφραστος – Τμήμα Γεωλογίας – Αριστοτέλειο Πανεπιστήμιο Θεσσαλονίκης

Ψηφιακή συλλογή
Βιβλιοθήκη
"ΘΕΟΦΡΑΣΤΟΣ"
Τμήμα Γεωλογίας

When looking at the two dental facet types, *Dolichopithecus* differs from both specialized folivores and hard object feeders. This result is consistent on both facet types, although Phase II seems to better discriminate dietary differences (Fig. 3.12), in support of previous works (Krueger et al., 2008). The analysis revealed differences in complexity between facet types (Table 3.5). As probably expected, the higher values are observed in Phase II facets (Fig. S5 Appendix 3.7). Be that as it may, in our case here the majority of the fossil sample involved in dental microwear texture analysis derives from the locality of Serrat d'en Vaquer-Perpignan (France). Earlier studies have shown that diet can vary between groups of the same species in different habitats at one time, thus not being representative of the species as a whole (Chapman et al., 2002; Ganas et al., 2004; Vandercone et al., 2012). The variations of complexity (Asfc) and anisotropy (epLsar) between fossiliferous localities can be informative on this subject (Fig. 3.13).

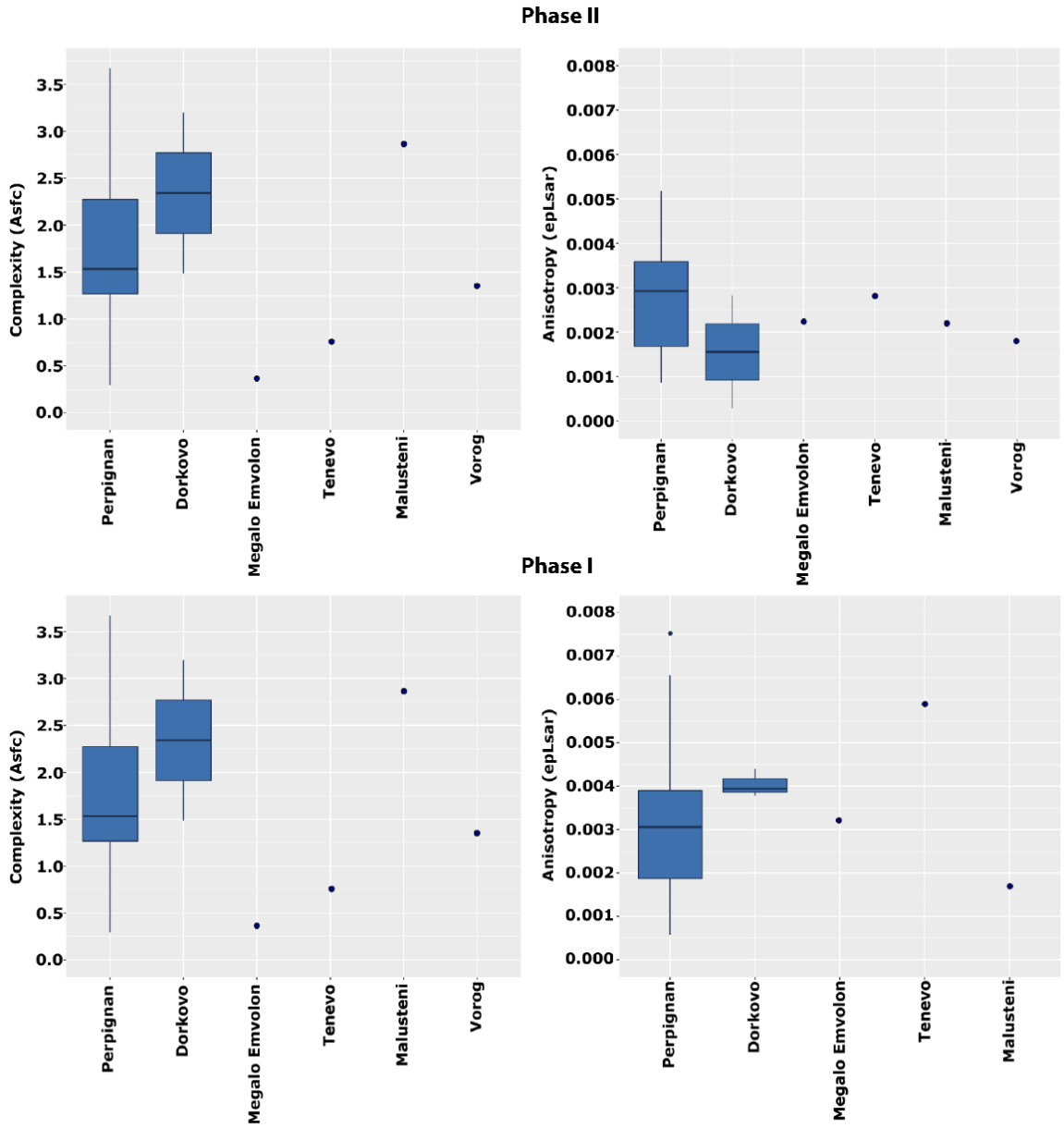

Fig. 3.13 Variations of complexity (Asfc) and anisotropy (epLsar) within the fossil sample of *Dolichopithecus* between fossiliferous localities included here on Phase I and II dental wear facets. Individuals from some localities fall near the extreme limits of the sample from Perpignan, suggesting that diet can vary between geography and time.

Ψηφιακή βιβλιοθήκη Θεόφραστος – Τμήμα Γεωλογίας – Αριστοτέλειο Πανεπιστήμιο Θεσσαλονίκης

Ψηφιακή συλλογή
Βιβλιοθήκη
"ΘΕΟΦΡΑΣΤΟΣ"
Τμήμα Γεωλογίας

Regarding Phase II facets, for both complexity (Asfc) and anisotropy (epLsar) all individuals from the rest of the fossiliferous localities (e.g Dorkovo, Megalo Emvolon, Tenevo, Malusteni, and Vorog), fall within the range of the confidence interval of the fossil sample from Serrat d'en Vaquer-Perpignan. The same applies to Phase I facets, although in this case complexity (Asfc) values of two individuals, one from Dorkovo and one from Megalo Emvolon, marginally fall out of the range of the lower limit of the confidence interval of the Perpignan's sample. Hence, these individuals most likely included softer/tougher food objects in their diet before death. Nonetheless, such differences could be explained by regional, geochronological, or even seasonal factors. Hopefully, additional fossil findings of *Dolichopithecus* in other Pliocene fossil sites of Europe will enable future investigation.

3.5 Discussion

3.5.1. What can teeth break down

The analyses reported here reveal differences between the dietary groups of cercopithecids, supporting the efficiency of dental topographic analyses to investigate aspects of dental morphology associated with diet.

The fruit/seed eaters are separated from folivores, whereas the mixed feeders are intermediately placed between the latter two categories. This could be suggestive of omnivores lacking specialized features related to consumption of certain food resources, unlike folivores or fruit/seed eaters. However, it could also mean that omnivores possess all the features necessary to process a wide range of food items. The wider distribution of values of each variable used here for the omnivore group more likely suggests the latter (Fig. 3.3, 3.4, 3.5, 3.6). Yet, the mixed feeding category here includes also large bodied representatives, such the *Papio* species, and larger primates may be able to process a wider range of food items, regardless of the dental tools they possess. The involvement of other factors, such as muscle recruitment and anatomy, bite force, relative dental size and food item size, enable larger primates to expand their dietary repertoire when needed.

The overall results of the dental topographic analysis suggest that the MHNPn–PR01 fossil molar displays a morphology that can efficiently process tough fibrous material like leaves, as observed in modern colobines, but it could also exploit a wide range of food resources if needed. The high relief of MHNPn–PR01 fossil M^1 suggests that it would be able to process and consume large quantities of young or mature leaves and other tough food resources. This is evidenced by the comparisons of the relief index (LRFI) and inclination (λ) (Fig. 3.5), but also by the high area-relative curvature (ARC) which places the fossil molar closer to folivorous cercopithecids (Fig, 3.6B).

The value of 3D relative enamel thickness (both $3DRET_{vol}$ and $3DRET_{geo}$) for the fossil M^1 suggests similarities with both folivorous and omnivorous cercopithecids (Fig. 3.7), while the comparisons of absolute crown strength (ACS) separate the MHNPn–PR01 fossil M^1 from folivorous cercopithecids (Fig. 3.4A, 3.8A). Previous comparisons of relative enamel thickness and absolute crown strength between extant hominoids were not in total agreement with each other (e.g. Schwartz et al., 2020). For instance, the relatively thin enamel of *Gorilla* compared to *Pongo* was traditionally viewed as evidence of adaptations towards a diet composed mostly of tough foliage for the former and hard–object feeding for the latter (Martin, 1985). However, *Gorilla* exhibited higher ACS than *Pongo*, suggesting an ability to exploit mechanically challenging food resources and/or to withstand higher bite force, even though such resources are representing only a low portion of its diet (Tutin et al., 1997b; Rogers et al., 2004; Constantino et al., 2012; Scott et al., 2012). On the other hand, a group of western gorillas in Loango National Park (Gabon) were found to seasonally exploit seeds of *Coula edulis* fruit (van Casteren et al., 2019), a mechanically challenging resource that requires high tooth strength to process. However, *Pongo* may also exploit seeds, and its occlusal molar surface exhibits many

Ψηφιακή βιβλιοθήκη Θεόφραστος – Τμήμα Γεωλογίας – Αριστοτέλειο Πανεπιστήμιο Θεσσαλονίκης

Ψηφιακή συλλογή
Βιβλιοθήκη
"ΘΕΟΦΡΑΣΤΟΣ"
Τμήμα Γεωλογίας
Α.Π.Θ.

crenulations/wrinkling, which could be adaptations to hard object feeding (e.g. stabilizing the food items) and/or additional tools to process tough and fibrous food resources. Yet, *Gorilla* also displays crenulated/wrinkled cusps, which could be adaptations towards the increased consumption of foliage. That being said, ACS is affected by allometry (Schwartz et al., 2020), as evidenced also by its high correlation with 2D OES surface (Table S4, Fig. S2 Appendix 3.7). In the analysis here, ACS suggests differences of MHNPn–PR01 fossil molar with extant folivorous cercopithecids, which can be suggestive of consumption of mechanically challenging food resources, at least seasonally. On the other hand, it could also just reflect a difference in size, as *Dolichopithecus ruscinensis* is possibly the largest colobine in this study (22 kg average and 14 kg average for males and females respectively based on postcrania; 28 kg average and 17 kg average for males and females respectively based on dentition [taken from Delson et al., (2000)]), followed by *Semnopithecus entellus* (20kg average and 15 kg average for males and females respectively) and *Nasalis larvatus* (19kg average and 9.5kg average for males and females respectively)(Body mass data were taken from Delson et al. 2000). These observations further support previous notions that size can be an important factor in feeding biology (Kay, 1975; Gingerich, 1977; Wood, 1979; Gingerich et al., 1982), possibly by contributing to absolute crown strength.

The results presented here are consistent with previous suggestions that the use of both 3D relative enamel thickness ($3DRET_{vol}$ and $3DRET_{geo}$) and absolute crown strength (ACS) can potentially be used together profitably to understand the evolution of tooth form (Schwartz et al., 2020). Nonetheless, this requires more investigation in other primate families as well. The comparisons of metrics of curvature/sharpness (i.e ARC and DNE) are somewhat ambiguous (Fig. 3.6, 3.10). While DNE seems not to be able to distinguish clearly among dietary groups, ARC does so. It has been suggested that more folivorous taxa should have higher values of curvature than frugivorous taxa (Ungar and M'Kirera, 2003; Bunn et al., 2011). While this is observed in both curvature estimates, DNE cannot clearly distinguish folivores from omnivores (Fig. 3.6A). In this sense, ARC seems to be more efficient at discriminating diet as it distinguishes all three dietary categories (Fig. 3.6B). One basic difference between DNE and ARC is that the latter metric differentiates between convexities and concavities (i.e., positive and negative curvatures), which might be important when investigating curvature/sharpness in respect to diet, at least in cercopithecids. Hence, ARC seems to be quite promising and requires more investigation in future dental topographic analyses. Results of complexity (OPCR) are more difficult to interpret, as they indicate a high overlap between dietary categories. The OPCR value of MHNPn–PR01 fossil molar falls within the range of all dietary categories, but more closely to folivorous species (Fig. 3.4B, Fig. 3.8B).

The linear discriminant analyses seem to satisfactorily separate the dietary categories although some overlap exists. The MHNPn–PR01 fossil M^1 is placed out of the range of all categories, being clearly separated from fruit/seed-eaters and placed between folivores and omnivores, but relatively closer to the latter (Fig. 3.11). Yet, size highly influences the distribution of our comparative sample. This may suggest a molar morphology different from any modern colobine species investigated here, and may be indicative of distinct/different dietary niche. Alternatively, it could suggest that the model here is not complete and that it needs further investigation with the addition of other extant cercopithecids, additional fossil molars of *Dolichopithecus ruscinensis*, and if possible other fossil colobine species as well. Regardless, a previous study has shown that *Mesopithecus pentelicus* was also classified outside of the range of extant cercopithecids to which it was compared (Fig. IV and Fig. III in Thiery et al., 2017a, b respectively), suggesting that extinct colobine monkeys might have distinct dental topographic features, possibly related to an ecological niche not found among cercopithecids today. Nevertheless, it could also mean that *Dolichopithecus ruscinensis* might not yet have acquired the adaptations or full specializations seen in extant colobine species.

Notwithstanding all the above observations, there are few caveats to be aware of. First, the present study focuses on upper molars, while it has been shown that lower molars can be informative about diet in other primate groups (Boyer, 2008). Therefore, to assess the dental

Ψηφιακή βιβλιοθήκη Θεόφραστος – Τμήμα Γεωλογίας – Αριστοτέλειο Πανεπιστήμιο Θεσσαλονίκης

Ψηφιακή συλλογή
Βιβλιοθήκη
"ΘΕΟΦΡΑΣΤΟΣ"
Τμήμα Γεωλογίας
Α.Π.Θ.

adaptations of *Dolichopithecus* in respect to diet, lower molars, should also be investigated in the future if possible. Posterior dentition aside, anterior teeth (e.g. incisors), and possibly hands, are important during food processing (Hylander, 1975; Kupczik and Chattah, 2014). Moreover, the masticatory movements and chewing behavior along with bite force seem to be significant during food comminution, as bite force may vary during chewing cycles, which depends also on the mechanical resistance of the food item and so may affect how food is processed (Daegling and Mcgraw, 2001; Berthaume, 2016a; Dunham and Lambert, 2016).

Second, the chewing mechanics/feeding action involved in processing specific mechanically challenging food resources seem to be important as well (Thiery et al., 2017b). For instance, some fallback resources, especially the staple ones, can play a major role in tooth adaptation (Marshall and Wrangham, 2007; Constantino and Wright, 2009; Lambert, 2009). Therefore, it is possible to detect dental morphologies that are not adaptive responses to the main feeding preferences, which further emphasizes the importance of food mechanical properties as a factor of investigation. However, most studies on colobines do not report food mechanical properties (Wright et al., 2008; Susan Coiner-Collier et al., 2016), assuming that there is no difference between present and past.

Third, the fossil sample consists of an M^1 whereas the modern sample consists of M^2s. Nevertheless, in most cases cercopithecid first and second molars are not distinguishable from each other when the same species is considered, as the only obvious difference between them is in terms of size with no major differences in occlusal shape. This implies that even if differences may occur between tooth positions in some variables considered here, it is more likely to influence variables already affected by size. Even if that were the case, it is assumed that differences would be expected to be minor as size variation. Previous research by Bunn and Ungar (2009) has shown that different tooth types should not be directly compared, at least in cercopithecoids, as the values of some topographic metrics may vary between M^1 and M^2. In the latter study, variably worn M^1 and M^2 were considered and it was shown that wear can significantly affect the values of some topographic estimates but not others. It is also shown that variation in topography between taxa or between wear stages are not the same for M^1s as they are for M^2s. However, when the low wear stage is considered the values between M^1 and M^2 show no significant variation, at least in the investigated colobine taxa (Bunn and Ungar, 2009). In our case, only unworn to minimally worn upper molar specimens were considered, thus removing the potential effect of wear on the analyzed variables. As previously explained, some differences between M^1 and M^2 can be expected in estimates already influenced by size (e.g., DNE, OPCR, ACS, $3DRET_{vol}$, Fig. S1–4 Appendix 3.7), yet these differences are probably subtle, and not significant at the (taxonomical) scale of our study. This is further supported by preliminary comparisons between first and second lower molars of *Dolichopithecus ruscinensis* from Serrat d'en Vaquer-Perpignan, which suggests no significant variation when no and/or minimal wear is considered (C.A Plastiras personal data). Notwithstanding the above, these observations do not affect our interpretations, as all the affected metrics will probably have slightly higher values in the M^2, as shown by the positive correlations with tooth size, except $3DRET_{vol}$, which shows a negative correlation (Table S4 Appendix 3.7). Still, even if the values of $3DRET_{vol}$ are expected to be slightly lower on the respective M^2 of *Dolichopithecus ruscinensis*, it will fall between the range of both folivorous and omnivorous categories here. Nevertheless, previous research have shown that the relative enamel thickness may vary even within the same tooth locus (Macho, 1994; Shellis et al., 1998; Schwartz, 2000; Kono, 2004; Smith et al., 2005, 2012; Olejniczak et al., 2008). Hence, interpretations of relative enamel thickness should be treated with caution.

3.5.2. What did teeth break down

Early works in dental microwear texture analysis have shown that primates having different feeding habits differ also in several texture parameters on Phase II crushing facets (Scott et al., 2005, 2006). Indeed, species involved in folivory have lower complexity (Asfc) and higher anisotropy (epLsar) than primates foraging on fruits and seeds. Furthermore, the

Ψηφιακή βιβλιοθήκη Θεόφραστος – Τμήμα Γεωλογίας – Αριστοτέλειο Πανεπιστήμιο Θεσσαλονίκης

Ψηφιακή συλλογή
Βιβλιοθήκη
"ΘΕΟΦΡΑΣΤΟΣ"

occurrence of outliers with high complexity among a population betrays a higher frequency of hard food resources (Merceron et al., 2009; Scott et al., 2012). Alternatively, some studies have challenged this view in arguing that food material properties are not hard enough to abrade enamel surface (Lucas et al., 2013; Ackermans et al., 2020; van Casteren et al., 2020). These authors instead suggest the ingestion of exogenous silica particles ('grit') as the main driver of tooth wear (Madden, 2014). Other authors fed the debate by confirming (using in vitro testing) that food objects, although softer than enamel, generate different wear traces (Xia et al., 2018). Although exogenous particles impact the enamel surface depending on their nature, density, and shape (Schulz-Kornas et al., 2020), controlled food testing has shown that there is no need to invoke dust to generate differences in tooth wear. When dust is considered, it does not overwhelm the biotic signal, at least considering wild mammal's foraging on pasture having known dust deposit similar to the Harmattan windblown in Western Africa (Merceron et al., 2016; Sanson et al., 2017). Besides, when focusing on the present datasets, several pieces of evidence support that dental microwear reflects dietary habits rather than morphology or amount of exogenous particles. For instance, among colobine monkeys, the most distinct microwear texture differences are not between arboreal and semi-terrestrial species, such as *Colobus guereza* and *Semnopithecus entellus*, but between *Colobus guereza* and *Nasalis larvatus*, the latter including a significantly higher amount of seeds and fruits than the former (Kool, 1993; Bennett, 1994; Yeager and Kool, 1994). The same tendency can be seen among cercopithecines, with *Lophocebus albigena*, which feeds mostly on fruits and seeds having similar dental microwear textures on both dental wear facets types, whereas the semi-terrestrial and overall more omnivorous *Chlorocebus aethiops* showing higher microwear texture variation between dental wear facet types (Fig. 3.12). When considering the inter-population scale with a large dataset of wild trapped *Mandrillus sphinx*, it has been shown that dental microwear texture on both shearing and crushing molar facets reflect variations in diet between seasons, age classes, and sex (Percher et al., 2017). There is no doubt that the processes behind dental microwear formation are complex and need further work to be fully understood; however, most datasets issued from wild populations as well as in vitro and in vivo experiments support the relation between texture and proportion of hard items in the dietary habits.

3.5.3. The dietary ecology of *Dolichopithecus*

Our results suggest that *Dolichopithecus ruscinensis* fossil M^1 (MNHPn–PR01) displays morphology which suggests a masticatory capability that enables the processing of abrasive food items, tough fibrous material, which usually require longer time to process and efficiently breakdown (i.e., ARC, λ, LRFI, OPCR, DNE, $3DRET_{vol}$ and $3DRET_{geo}$). Furthermore, its molar morphology suggest that it could withstand resistance to high stresses related to ingestion of more mechanically challenging food resources (ACS, $3DRET_{vol}$ and $3DRET_{geo}$). Moreover, the dental microwear textures of *Dolichopithecus* individuals from sites in France, Bulgaria, Greece, and Romania and notably complexity (Asfc) and anisotropy (epLsar), also indicates that *Dolichopithecus* occupied an intermediate ecospace between highly specialized folivorous colobines and durophagous cercopithecines.

The intermediate pattern in both molar topography and dental microwear texture suggests that *Dolichopithecus ruscinensis* could potentially enlarge its dietary niche by incorporating other food resources other than the preferred ones when needed. Combining these data with available evidence from postcranial morphology, which indicates semi-terrestrial locomotor adaptations (robust and long bones, short phalanges, and several aspects of the elbow joint; [see Delson 1973 for further details]), suggests that this extinct species was able to exploit both arboreal and terrestrial substrates as well as transit from one micro-habitat to another. This may have influenced its ranging patterns and its biogeographic distribution. While leaf consumption was presumably an integral part of *Dolichopithecus* dietary repertoire between seasons, other food resources may have complemented its diet from a wide array of foods

Ψηφιακή βιβλιοθήκη Θεόφραστος – Τμήμα Γεωλογίας – Αριστοτέλειο Πανεπιστήμιο Θεσσαλονίκης

Ψηφιακή συλλογή
Βιβλιοθήκη
"ΘΕΟΦΡΑΣΤΟΣ"
Τμήμα Γεωλογίας
Α.Π.Θ

available in the arboreal and terrestrial substrates of each habitat. This picture seems not to be a novelty in colobine ecology (Benefit, 2000; Reitz and Benefit, 2001; Jablonski et al., 2020).

Earlier Eurasian and African fossil colobine (i.e. *Mesopithecus pentelicus* and *Cercopithecoides williamsi* respectively) representatives are also depicted as monkeys with mixed arboreal-terrestrial locomotor behavior (Youlatos and Koufos, 2010; Youlatos et al., 2012; Frost et al., 2015) and opportunistic dietary habits (Codron et al., 2005; Fourie et al., 2008; Merceron et al., 2009b; Williams and Geissler, 2014), which further suggests that early colobine ecology was more diverse in terms of locomotor and dietary behavior than most extant African and Asian representatives (Leakey, 1982; El-Zaatari et al., 2005; Hlusko, 2006; Merceron et al., 2009b; Nakatsukasa et al., 2010; Youlatos et al., 2012; Geissler, 2013; Engle et al., 2014; Frost et al., 2015; Pallas et al., 2019; Ji et al., 2020). Thus, early colobine taxa were probably able to inhabit various micro-habitats in both Africa and Eurasia, by exploiting a wide array of food resources and/or by targeting food resources that are not primarily preferred by other sympatric primate species, such as leaves. Leaves, young and/or mature, are usually abundant in most habitats with tree cover and most of the time throughout the year. Hence, it is plausible that folivory may have represented an adaptive advantage to withstand selective ecological pressures, such as scarcity of preferred resources, large or small scale environmental changes and also interspecific competition.

Interspecific and resource competition between colobines and cercopithecines has been reported, particularly during some periods throughout the year when preferred food resources are abundant (Yeager, 1989; Singh et al., 2011; Sterck and Steenbeek, 2012; Ruslin et al., 2019). In order to coexist and reduce/avoid interspecific competition, sympatric primates must find ways to partition the niche they occupy (MacKinnon and MacKinnon, 1980; Garber, 1987; Ungar, 1995; Grueter et al., 2010; Astaras et al., 2011; Hadi et al., 2012). Perhaps interspecific competition and the terms of coexistence with other sympatric primates (Teelen, 2007), influenced the colobine evolutionary history more than previously thought. Colobines might have coexisted with the latest hominoids for a short period of time in eastern Europe (Spassov et al., 2012; Böhme et al., 2017), although there is no co-occurrence of Miocene hominoids and cercopithecids in Eurasia, except Shuitangba (China) and Maragheh (Iran) fossil sites, where *Mesopithecus* were likely sympatric with *Lufengpithecus* and *Sivapithecus* respectively (Ataabadi et al., 2016; Suwa et al., 2016; Jablonski et al., 2020). Regardless, colobines have co-existed with cercopithecines (i.e., the genus *Macaca*) in Europe. The earliest European occurrence of both *Macaca* and *Mesopithecus* is in the latest Miocene site of Moncucco Torinese (Alba et al., 2014), but they are more commonly associated in several Pliocene localities of Europe (Eronen and Rook, 2004).

Usually, the underlying causes of the Plio-Pleistocene phylogenetic radiation of cercopithecids, their biogeographical expansion, and ecological diversity, are attributed to global climatic variations that took place at latest Miocene/early Pliocene to Pleistocene (Cerling et al., 1993, 1998; Vrba, 1993; Frost, 2002; Jablonski, 2002; Bobe and Behrensmeyer, 2004). However, the cumulative effects of resource variations impacted by global climate changes but amplified or tempered by local and/or regional geomorphological context and interspecific competition when several species exploit the same habitat (Elton, 2007; Macho, 2016), need to be considered more thoroughly.

Ψηφιακή βιβλιοθήκη Θεόφραστος – Τμήμα Γεωλογίας – Αριστοτέλειο Πανεπιστήμιο Θεσσαλονίκης

Ψηφιακή συλλογή
Βιβλιοθήκη
"ΘΕΟΦΡΑΣΤΟΣ"
Τμήμα Γεωλογίας
Α.Π.Θ

3.6 Appendix

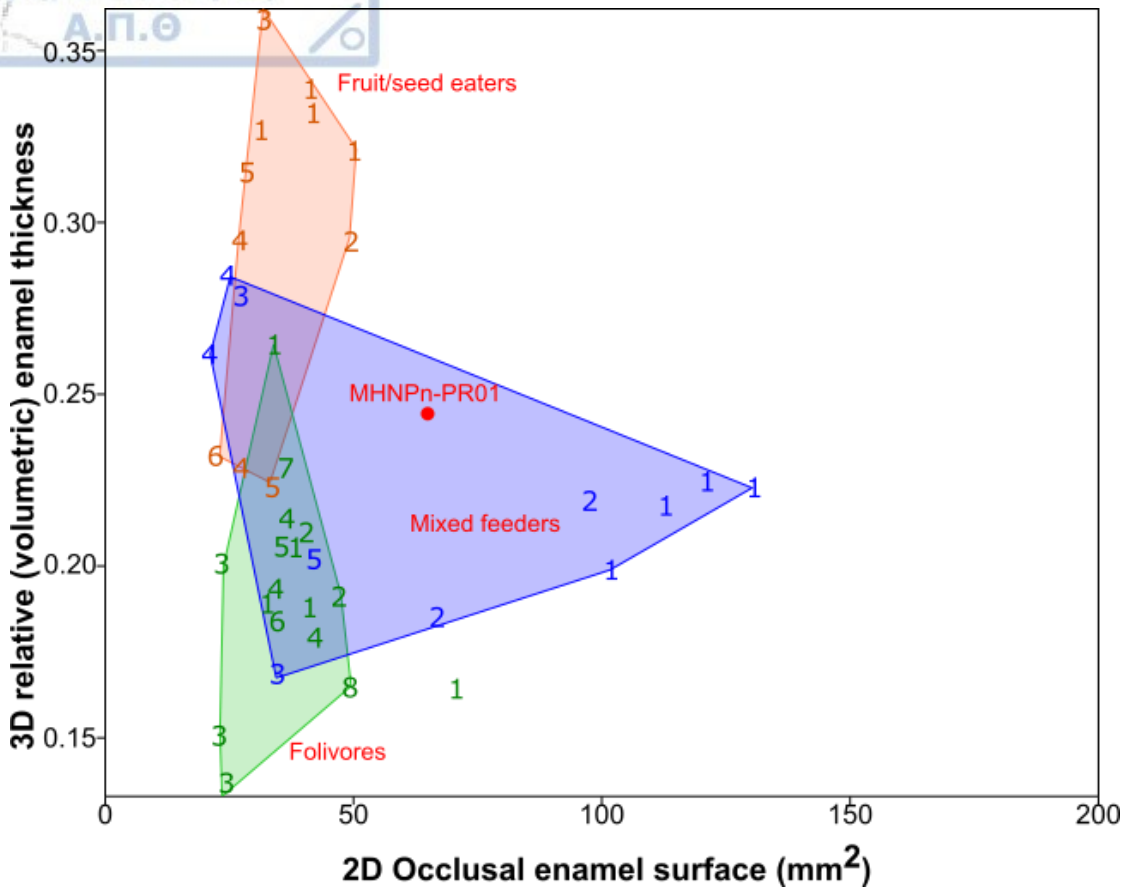

Fig. S1 Bivariate plot of 2D occlusal enamel surface (OES 2D) on 3D relative volumetric enamel thickness (3DRETvol) between dietary categories including MHNPn–PR01 fossil M^1, **Blue** = Mixed feeders (1: *Papio*, 2: *Mandrillus*; 3: *Cercopithecus campbelli*, 4: *Chlorocebus aethiops*, 5: *Erythrocebus patas*), **Orange** = Fruit/seed eaters (1; *Lophocebus albigena*, 2: *Cercocebus torquatus*, 3: *Lophocebus aterrimus*; 4: *Cercopithecus diana*, 5: *Cercopithecus pogonias*, 6: *Cercopithecus nictitans*, **Green** = Folivores (1: *Colobus polykomos*, 2: *Colobus guereza*, 3: *Procolobus verus*, 4: *Piliocolobus badius*, 5: *Colobus satanas*; 6: *Trachypithecus cristatus*, 7: *Semnopithecus entellus*, 8: *Nasalis larvatus*; ACS is heavily influenced by size. MHNPn–PR01 is situated closer to omnivores and fruit/seed eaters, suggesting higher tooth strength than most extant colobines.

Ψηφιακή βιβλιοθήκη Θεόφραστος – Τμήμα Γεωλογίας – Αριστοτέλειο Πανεπιστήμιο Θεσσαλονίκης

Ψηφιακή συλλογή
Βιβλιοθήκη
"ΘΕΟΦΡΑΣΤΟΣ"
Τμήμα Γεωλογίας
Α.Π.Θ

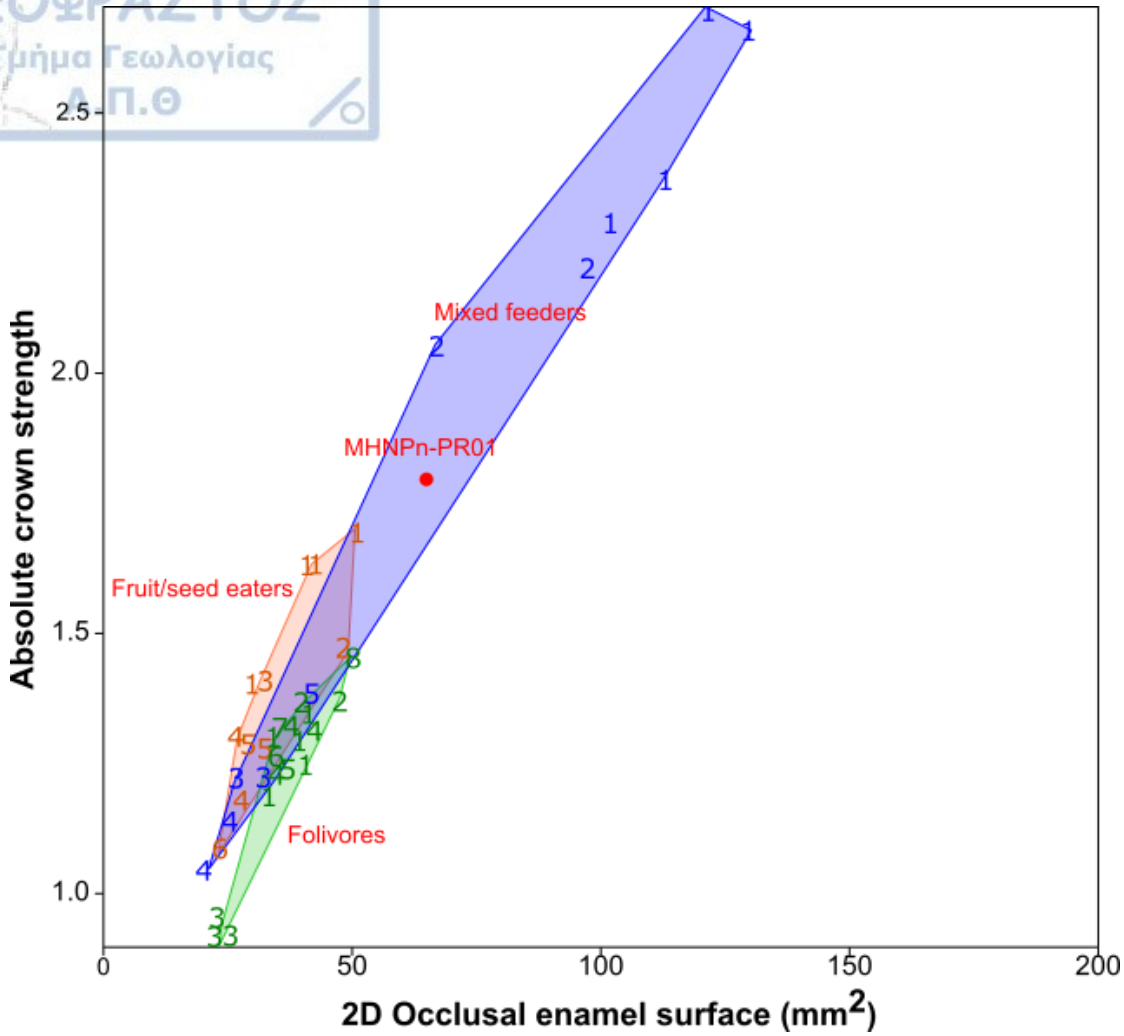

Fig. S2 Bivariate plot of 2D occlusal enamel surface (OES 2D) on absolute crown strength (ACS) between dietary categories including MHNPn–PR01 fossil M^1, **Blue** = Omnivores (1: *Papio*, 2: *Mandrillus*; 3: *Cercopithecus campbelli*, 4: *Chlorocebus aethiops*, 5: *Erythrocebus patas*), **Orange** = Fruit/seed eaters (1; *Lophocebus albigena*, 2: *Cercocebus torquatus*, 3: *Lophocebus aterrimus*; 4: *Cercopithecus diana*, 5: *Cercopithecus pogonias*, 6: *Cercopithecus nictitans*, **Green** = Folivores (1: *Colobus polykomos*, 2: *Colobus guereza*, 3: *Procolobus verus*, 4: *Piliocolobus badius*, 5: *Colobus satanas*; 6: *Trachypithecus cristatus*, 7: *Semnopithecus entellus*, 8: *Nasalis larvatus*; ACS is heavily influenced by size. MHNPn–PR01 is situated closer to omnivores and fruit/seed eaters, suggesting higher tooth strength than most extant colobines.

Ψηφιακή βιβλιοθήκη Θεόφραστος – Τμήμα Γεωλογίας – Αριστοτέλειο Πανεπιστήμιο Θεσσαλονίκης

Ψηφιακή συλλογή
Βιβλιοθήκη
"ΘΕΟΦΡΑΣΤΟΣ"
Τμήμα Γεωλογίας
Α.Π.Θ

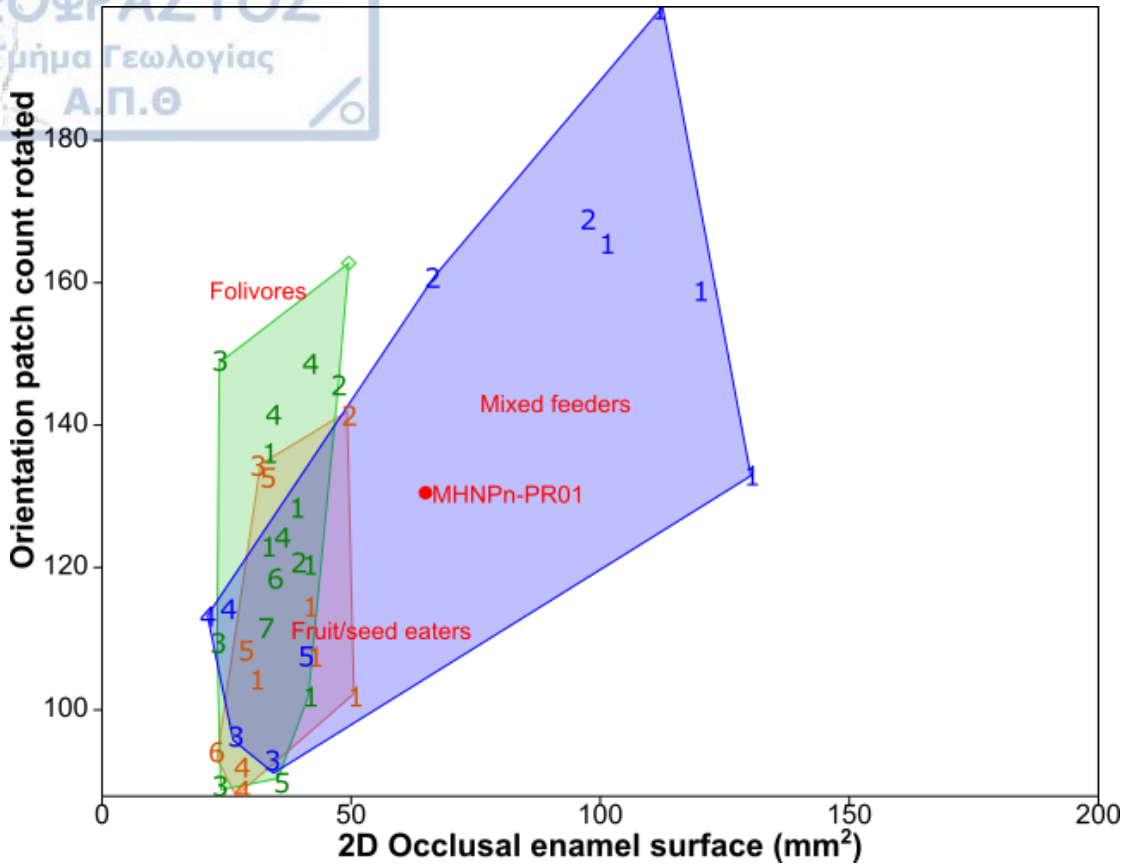

Fig. S3 Bivariate plot of 2D occlusal enamel surface (OES 2D) on orientation patch count rotated (OPCR) between dietary categories including MHNPn–PR01 fossil M^1, **Blue** = Omnivores (1: *Papio*, 2: *Mandrillus*; 3: *Cercopithecus campbelli*, 4: *Chlorocebus aethiops*, 5: *Erythrocebus patas*), **Orange** = Fruit/seed eaters (1; *Lophocebus albigena*, 2: *Cercocebus torquatus*, 3: *Lophocebus aterrimus*; 4: *Cercopithecus diana*, 5: *Cercopithecus pogonias*, 6: *Cercopithecus nictitans*, **Green** = Folivores (1: *Colobus polykomos*, 2: *Colobus guereza*, 3: *Procolobus verus*, 4: *Piliocolobus badius*, 5: *Colobus satanas*; 6: *Trachypithecus cristatus*, 7: *Semnopithecus entellus*, 8: *Nasalis larvatus*; OPCR exhibits high overlap between dietary categories suggesting low efficiency in discriminating diet in our sample. MHNPn–PR01 exhibits similar values with folivores and fruit/seed eaters but is situated within omnivores based on his size.

Ψηφιακή βιβλιοθήκη Θεόφραστος – Τμήμα Γεωλογίας – Αριστοτέλειο Πανεπιστήμιο Θεσσαλονίκης

Ψηφιακή συλλογή
Βιβλιοθήκη
"ΘΕΟΦΡΑΣΤΟΣ"
Τμήμα Γεωλογίας
Α.Π.Θ

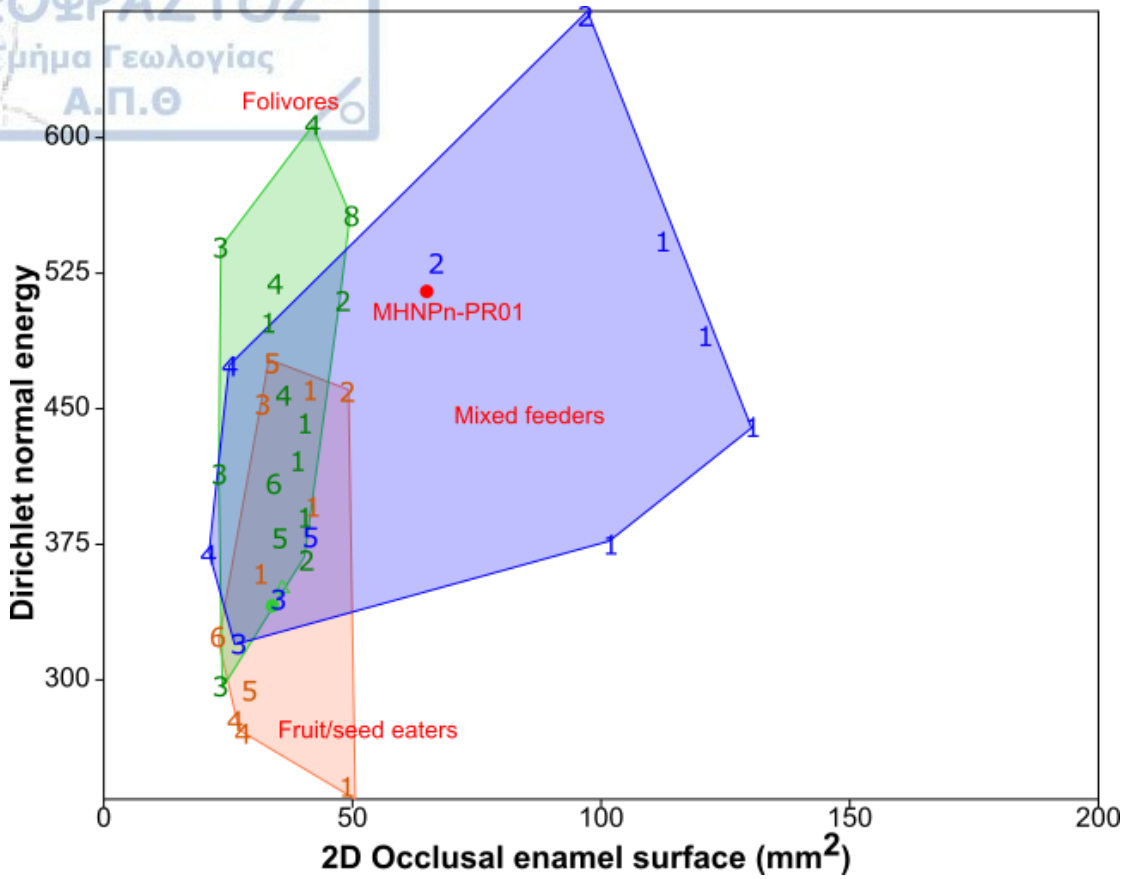

Fig. S4 Bivariate plot of 2D occlusal enamel surface (OES 2D) on Dirichlet normal energy (DNE) between dietary categories including MHNPn–PR01 fossil M^1, **Blue** = Omnivores (1: *Papio*, 2: *Mandrillus*; 3: *Cercopithecus campbelli*, 4: *Chlorocebus aethiops*, 5: *Erythrocebus patas*), **Orange** = Fruit/seed eaters (1; *Lophocebus albigena*, 2: *Cercocebus torquatus*, 3: *Lophocebus aterrimus*; 4: *Cercopithecus diana*, 5: *Cercopithecus pogonias*, 6: *Cercopithecus nictitans*, **Green** = Folivores (1: *Colobus polykomos*, 2: *Colobus guereza*, 3: *Procolobus verus*, 4: *Piliocolobus badius*, 5: *Colobus satanas*; 6: *Trachypithecus cristatus*, 7: *Semnopithecus entellus*, 8: *Nasalis larvatus*; DNE exhibits high overlap between dietary categories and it separates the largest omnivorous cercopithecids (*Papio* and *Mandrillus*) from the rest of our sample. MHNPn–PR01 is exhibits similar values with folivores but it placed within omnivores based on its size.

Ψηφιακή βιβλιοθήκη Θεόφραστος – Τμήμα Γεωλογίας – Αριστοτέλειο Πανεπιστήμιο Θεσσαλονίκης

Ψηφιακή συλλογή
Βιβλιοθήκη
"ΘΕΟΦΡΑΣΤΟΣ"
Τμήμα
Α

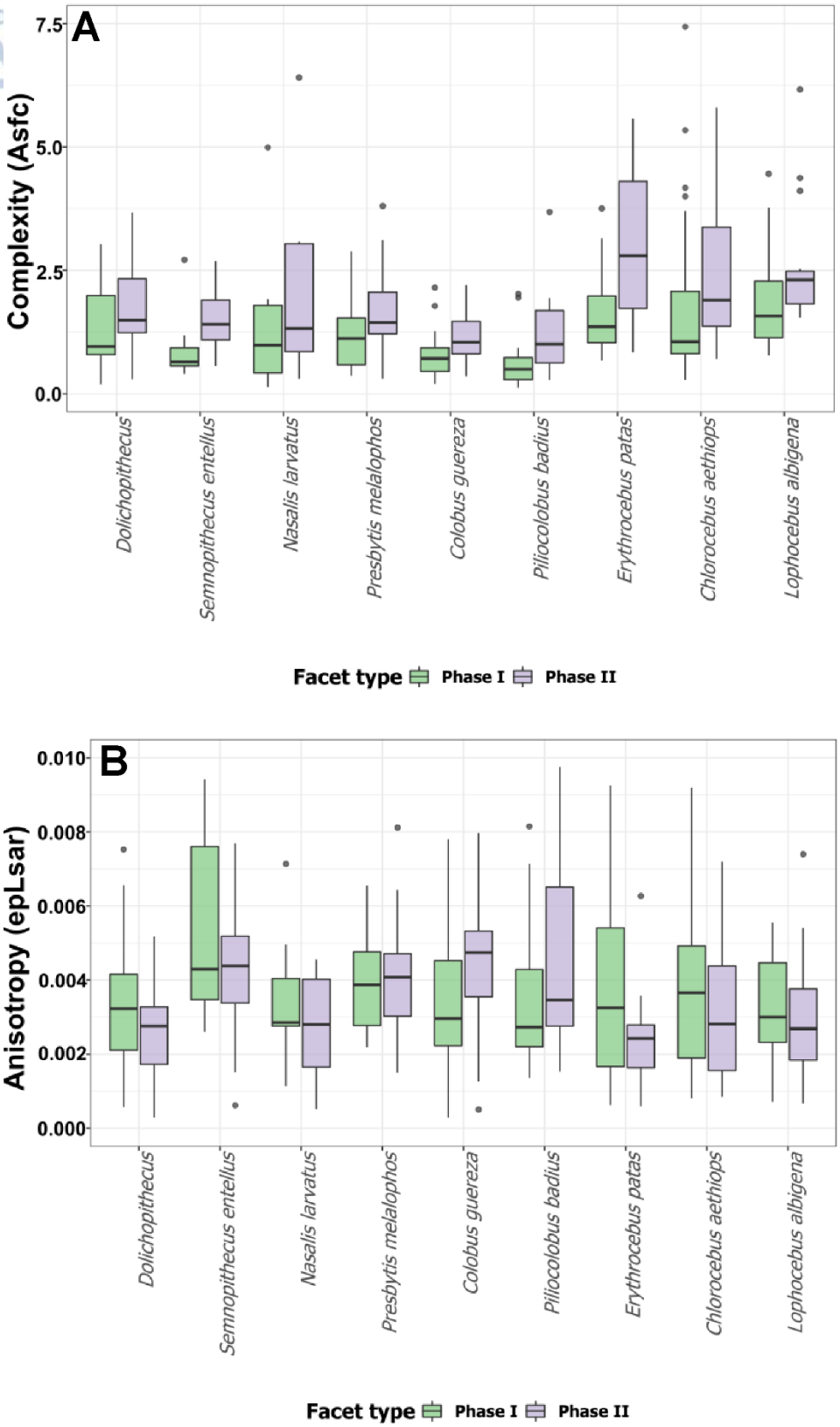

Fig. S5 Variation in (**A**) complexity (Asfc) and (**B**) anisotropy (epLsar) between facet types and species. The higher values of complexity are shown by Phase II facets, but anisotropy is always higher in Phase I dental facets in some species, while others not.

Ψηφιακή βιβλιοθήκη Θεόφραστος – Τμήμα Γεωλογίας – Αριστοτέλειο Πανεπιστήμιο Θεσσαλονίκης

Ψηφιακή συλλογή
Βιβλιοθήκη
"ΘΕΟΦΡΑΣΤΟΣ"
Τμήμα Γεωλογίας
Α.Π.Θ

Table S1 Enamel thickness, crown strength and dental topographic variables[a] raw data for modern sample of upper second molars and *Dolichopithecus* upper first molar[a].

Species	ID	Institution	$3DRET_{vol}$	$3DRET_{geo}$	ACS	LRFI	λ	ARC	DNE	OPCR	OES 3D	OES 2D
Cercocebus torquatus	81–07–M–44	RMCA	0.295	0.308	1.466	0.291	123.232	1.417	460.573	141.875	88.059	49.206
Cercopithecus diana	Cc1	PALEVOPRIM	0.229	0.227	1.177	0.294	123.306	1.484	271.495	91.125	49.801	27.672
Cercopithecus diana	Cc2	PALEVOPRIM	0.295	0.296	1.298	0.297	122.427	1.454	275.994	87.875	48.705	26.884
Colobus guereza	1216	RMCA	0.192	0.167	1.375	0.349	119.584	1.873	511.233	145.875	95.35	47.476
Colobus guereza	3800	RMCA	0.208	0.195	1.368	0.321	120.654	1.804	368.015	12.75	76.618	4.332
Colobus polykomos	10307	RMCA	0.265	0.244	1.287	0.264	126.014	1.637	340.975	123.375	57.542	33.908
Colobus polykomos	10548	RMCA	0.206	0.194	1.291	0.319	121.873	1.819	421.911	128.125	74.443	39.346
Colobus polykomos	10602	RMCA	0.157	0.150	1.248	0.342	119.803	1.673	441.497	12.375	80.684	4.709
Colobus polykomos	8107–M174	RMCA	0.189	0.178	1.352	0.329	120.004	1.706	388.484	101.875	79.992	41.396
Colobus polykomos	38158	RMCA	0.189	0.178	1.189	0.323	121.263	1.875	496.536	135.625	63.084	33.096
Lophocebus albigena	*83006–M276*	RMCA	0.327	0.318	1.404	0.23	127.332	1.525	359.662	104.125	49.526	31.274
Lophocebus albigena	90042–M–301	RMCA	0.338	0.318	1.633	0.27	124.923	1.552	461.065	114.625	71.77	41.831
Lophocebus albigena	90042–M–301	RMCA	0.333	0.314	1.634	0.26	125.815	1.553	393.931	107.375	70.98	42.236
Lophocebus albigena	Cb4	PALEVOPRIM	0.321	0.328	1.701	0.21	130.679	1.264	233.94	102.25	76.931	50.561
Lophocebus aterrimus	14113	RMCA	0.362	0.343	1.403	0.259	125.357	1.628	451.067	134.5	53.429	31.798
Nasalis larvatus	5042	SMF	0.165	0.174	1.453	0.378	117.571	1.885	557.442	162.75	105.409	49.522
Procolobus verus	86–002–M48	RMCA	0.133	0.149	0.918	0.382	117.408	1.942	539.493	148.75	50.566	23.536
Procolobus verus	86–002–M34	RMCA	0.151	0.125	0.897	0.41	115.602	1.801	414.207	109.25	52.508	23.115
Procolobus verus	86–002–M50	RMCA	0.200	0.148	0.941	0.313	121.642	1.736	295.388	88.75	44.555	23.815
Semnopithecus entellus	1964–1615	MNHN	0.230	0.202	1.317	0.317	121.695	1.685	351.854	113.125	67.651	35.906
Chlorocebus aethiops	1972–302	MNHN	0.262	0.233	1.047	0.334	121.473	1.602	370.557	113.25	41.298	21.155

Ψηφιακή βιβλιοθήκη Θεόφραστος – Τμήμα Γεωλογίας – Αριστοτέλειο Πανεπιστήμιο Θεσσαλονίκης

Ψηφιακή συλλογή
Βιβλιοθήκη
"ΘΕΟΦΡΑΣΤΟΣ"
Τμήμα Γεωλογίας
Α.Π.Θ

Chlorocebus aethiops	1972–328	MNHN	0.284	0.241	1.14	0.353	119.975	1.606	474.058	114.5	51.036	25.186
Colobus satanas	33512	RMCA	0.206	0.186	1.246	0.351	118.648	1.798	377.846	90.375	71.253	35.309
Erythrocebus patas	8629	RMCA	0.203	0.191	1.368	0.315	121.152	1.703	381.657	107.625	77.38	41.189
Papio anubis	80–44–M–101	RMCA	0.223	0.214	2.659	0.322	120.52	1.568	439.389	132.875	247.963	130.242
Papio anubis	C2	PALEVOPRIM	0.219	0.217	2.372	0.278	123.007	1.847	543.391	198.75	196.231	112.51
Papio anubis	90–042–M226	RMCA	0.199	0.215	2.285	0.201	131.65	1.567	376.859	165.25	152.096	101.673
Papio hamadryas	97–020–M004	RMCA	0.226	0.241	2.704	0.28	123.688	1.614	489.983	158.625	211.835	121.057
Trachypithecus cristatus	1085	SMF	0.191	0.199	1.259	0.328	120.159	1.741	408.08	118.875	66.377	34.462
Cercopithecus campbelli	80–028–M–24	RMCA	0.167	0.179	1.218	0.338	119.841	1.703	343.609	91.125	67.647	34.43
Cercopithecus campbelli	36280	RMCA	0.279	0.267	1.214	0.294	124.186	1.46	319.583	95.75	47.334	26.315
Cercopithecus nictitans	15650	RMCA	0.232	0.231	1.076	0.267	125.737	1.451	321.576	93.25	39.336	23.062
Cercopithecus pogonias	15595	RMCA	0.224	0.207	1.284	0.323	121.687	1.612	477.263	132.375	63.344	33.187
Cercopithecus pogonias	18273	RMCA	0.314	0.304	1.289	0.233	128.787	1.401	295.574	108.5	45.548	28.607
Piliocolobus badius	91–060–M57	RMCA	0.184	0.171	1.228	0.403	116.188	1.857	519.659	141.625	76.394	34.096
Piliocolobus badius	91–060–M76	RMCA	0.180	0.166	1.309	0.389	116.396	2.079	606.586	148.75	91.462	41.971
Piliocolobus badius	83–042–M77	RMCA	0.215	0.200	1.322	0.351	118.836	1.813	456.921	124.125	73.75	36.564
Mandrillus leucophaeus	2002–105	RMCA	0.219	0.212	2.204	0.352	118.038	1.692	669.965	169.0	196.586	97.255
Mandrillus leucophaeus	1893–269	RMCA	0.185	0.241	2.055	0.278	123.855	1.599	526.326	160.875	116.258	66.709
Dolichopithecus ruscinensis	MNHPn–PR01	MHNPn	0.244	0.212	1.796	0.343	118.547	1.859	514.918	130.5	128.975	64.931

[a] $3DRET_{vol}$ = 3D volumetric relative enamel thickness; $3DRET_{geo}$ = 3D geometric relative enamel thickness; ACS = absolute crown strength; LRFI = relief index; ARC = area–relative curvature; DNE = Dirichlet normal energy; OPCR = orientation patch–count rotated; OES 3D = 3D occlusal enamel surface; OES 2D = 2D occlusal enamel surface.

Ψηφιακή βιβλιοθήκη Θεόφραστος – Τμήμα Γεωλογίας – Αριστοτέλειο Πανεπιστήμιο Θεσσαλονίκης

Ψηφιακή συλλογή
Βιβλιοθήκη
"ΘΕΟΦΡΑΣΤΟΣ"
Τμήμα Γεωλογίας
Α.Π.Θ

Table S2 Raw microwear data for *Dolichopithecus* and modern species[a].

Filename	Species	Institution	Locality	Asfc	epLsar ($x10^3$)	Tfv	$HAsfc_9$	$HAsfc_{36}$	$HAsfc_{81}$	Smc
DORKOVO–DKV483–UM3–dex–f4	*D. ruscinensis*	NHMS	Dorkovo	1.97	4.40	30697.4	0.11	0.23	0.31	25.11
DORKOVO–DKV483–UM3–dex–f9	*D. ruscinensis*	NHMS	Dorkovo	1.48	0.30	27009.8	0.14	0.14	0.21	58.43
DORKOVO–DKV78–lm3–dex–f5	*D. ruscinensis*	NHMS	Dorkovo	85.00	3.90	28886.8	0.49	0.60	0.68	15.50
DORKOVO–DKV78–lm3–dex–f9	*D. ruscinensis*	NHMS	Dorkovo	3.20	2.80	51084.1	0.40	0.85	0.98	48.25
DORKOVO–DKV82–lm1–sin–f5	*D. ruscinensis*	NHMS	Tenevo	0.20	3.80	26378.9	0.06	0.18	0.27	136.18
TENEVO–FM1739–lm2–dex–f6	*D. balcanicus sp.*	NHMS	Tenevo	0.31	3.20	41782.6	0.16	0.20	0.30	6.01
TENEVO–FM1739–lm2–dex–f9	*D. balcanicus sp.*	NHMS	Tenevo	0.38	2.20	57537.7	0.16	0.22	0.32	144.63
Dolicho–Vorog1968–M2s–g–f9bis.sur	*D. ruscinensis*	–	Vorog	1.36	1.80	53271.7	0.20	0.36	0.42	0.53
LGPUT–MEV1–lm2–sin–f5	*D. ruscinensis*	LGPUT	Megalo Emvolo	0.61	5.90	2430.3	0.37	0.45	0.50	57.65
LGPUT–MEV1–lm2–sin–f11	*D. ruscinensis*	LGPUT	Megalo Emvolo	0.76	2.80	0	0.29	0.36	0.48	179.50
Malushteni–723–SM1–lm1s–f11	*D. ruscinensis*	UAIC	Măluşteni	2.89	2.20	49882.9	0.21	0.34	0.51	0.42
Malushteni–723–SM1–lm1s–f6	*D. ruscinensis*	UAIC	Măluşteni	2.15	1.70	27499.8	0.44	0.58	0.75	0.42
PERPIGNAN–FSL40992–lm1–dex–f11	*D. ruscinensis*	UCBL-1	Perpignan	1.42	4.40	21452.1	0.34	0.61	0.67	1.77
PERPIGNAN–FSL40992–lm1–dex–f6	*D. ruscinensis*	UCBL-1	Perpignan	2.72	3.10	21055.5	0.32	0.51	0.62	9.72
PERPIGNAN–FSL41045–lm2–sin–f5	*D. ruscinensis*	UCBL-1	Perpignan	2.05	3.10	4960.0	0.79	0.89	0.98	141.58
PERPIGNAN–FSL41045–lm2–sin–f9	*D. ruscinensis*	UCBL-1	Perpignan	1.37	5.00	38004.3	0.40	0.50	0.63	142.50
PERPIGNAN–FSL41288–lm2–sin–f6	*D. ruscinensis*	UCBL-1	Perpignan	0.44	7.50	23537.6	1.70	2.17	3.46	89.31
PERPIGNAN–FSL41288–lm2–sin–f9	*D. ruscinensis*	UCBL-1	Perpignan	1.14	3.00	56432.2	0.27	0.40	0.49	39.03
PERPIGNAN–FSL49993–UM2–sin–f4	*D. ruscinensis*	UCBL-1	Perpignan	0.66	0.90	34642.6	0.17	0.28	0.34	71.13
PERPIGNAN–FSL49993–UM2–sin–f9	*D. ruscinensis*	UCBL-1	Perpignan	1.49	1.80	49484.8	0.25	0.37	0.41	53.53
PERPIGNAN–FSL49994–UM3–sin–f4	*D. ruscinensis*	UCBL-1	Perpignan	2.56	2.20	15724.3	0.10	0.23	0.39	73.16
PERPIGNAN–FSL49994–UM3–sin–f9	*D. ruscinensis*	UCBL-1	Perpignan	2.63	2.70	46246.9	0.30	0.38	0.49	33.88
PERPIGNAN–FSL49998–lm3–sin–f6	*D. ruscinensis*	UCBL-1	Perpignan	2.56	1.80	48299.6	0.36	0.48	0.59	15.03
PERPIGNAN–FSL49998–lm3–sin–f9	*D. ruscinensis*	UCBL-1	Perpignan	3.44	1.00	43279.8	1.00	0.83	1.20	63.74

Ψηφιακή βιβλιοθήκη Θεόφραστος – Τμήμα Γεωλογίας – Αριστοτέλειο Πανεπιστήμιο Θεσσαλονίκης

Ψηφιακή συλλογή
Βιβλιοθήκη
"ΘΕΟΦΡΑΣΤΟΣ"
Τμήμα Γεωλογίας
Α.Π.Θ

PERPIGNAN–Pp1–lm2–dex–f5	*D. ruscinensis*	MNHL	Perpignan	0.84	4.20	37159.1	0.19	0.29	0.38	55.87
PERPIGNAN–Pp1–lm2–dex–f9	*D. ruscinensis*	MNHL	Perpignan	1.98	2.80	25581.2	0.59	0.65	0.86	175.92
PERPIGNAN–Pp10–lm3–dex–f6	*D. ruscinensis*	MNHL	Perpignan	1.40	2.60	47675.9	0.20	0.27	0.00	88.29
PERPIGNAN–Pp11–lm2–dex–f6	*D. ruscinensis*	MNHL	Perpignan	1.02	1.10	47333.9	0.14	0.25	0.38	142.88
PERPIGNAN–Pp11–lm2–dex–f9	*D. ruscinensis*	MNHL	Perpignan	3.67	2.60	18972.7	0.43	0.50	0.63	146.29
PERPIGNAN–Pp13–UM3–sin–f3	*D. ruscinensis*	MNHL	Perpignan	1.35	3.30	23556.0	0.35	0.48	0.63	166.55
PERPIGNAN–Pp13–UM3–sin–f9	*D. ruscinensis*	MNHL	Perpignan	1.21	3.10	54552.1	0.26	0.45	0.63	164.98
PERPIGNAN–Pp28–lm3–sin–f6	*D. ruscinensis*	MNHL	Perpignan	0.91	1.50	24406.4	0.32	0.33	0.35	10.24
PERPIGNAN–Pp28–lm3–sin–f9	*D. ruscinensis*	MNHL	Perpignan	2.38	0.90	39959.6	0.45	0.54	0.58	44.14
PERPIGNAN–Pp29–lm3–sin–f5	*D. ruscinensis*	MNHL	Perpignan	0.99	0.60	49989.9	0.28	0.40	0.51	123.13
PERPIGNAN–Pp29–lm3–sin–f9	*D. ruscinensis*	MNHL	Perpignan	1.53	4.30	31201.4	0.15	0.23	0.37	67.48
PERPIGNAN–Pp3–lm3–sin–f5	*D. ruscinensis*	MNHL	Perpignan	1.45	2.90	24621.9	0.32	0.39	0.58	155.82
PERPIGNAN–Pp4–UM2–sin–f3	*D. ruscinensis*	MNHL	Perpignan	0.84	1.90	44694.4	0.12	0.20	0.26	10.00
PERPIGNAN–Pp4–UM2–sin–f9	*D. ruscinensis*	MNHL	Perpignan	0.79	1.70	30787.5	0.20	0.28	0.42	121.47
PERPIGNAN–Pp5–lm1–sin–f5	*D. ruscinensis*	MNHL	Perpignan	2.98	3.70	38184.7	0.28	0.47	0.72	147.48
PERPIGNAN–Pp5–lm1–sin–f9	*D. ruscinensis*	MNHL	Perpignan	1.03	5.20	8207.3	0.33	0.51	0.89	16.59
PERPIGNAN–PR34–UM2–dex–f3	*D. ruscinensis*	MNHP	Perpignan	0.46	4.10	44407.1	0.10	0.26	0.32	25.25
PERPIGNAN–PR34–UM2–dex–f9	*D. ruscinensis*	MNHP	Perpignan	0.30	3.60	20464.9	0.27	0.32	0.38	109.72
PERPIGNAN–PR36–UM3–sin–f4	*D. ruscinensis*	MNHP	Perpignan	0.87	6.60	31863.8	0.23	0.40	0.44	56.27
PERPIGNAN–PR36–UM3–sin–f9	*D. ruscinensis*	MNHP	Perpignan	1.27	4.30	35829.2	0.20	0.29	0.39	175.51
PERPIGNAN–PR39–lm2–sin–f6	*D. ruscinensis*	MNHP	Perpignan	0.93	3.20	39516.2	0.15	0.28	0.33	33.37
PERPIGNAN–PR39–lm2–sin–f9	*D. ruscinensis*	MNHP	Perpignan	1.89	1.10	41208.8	0.21	0.42	0.54	122.92
Dolicho–C4–nn1–M2–cfbis	*D. ruscinensis*	MNHP	Perpignan	1.43	3.00	45745.0	0.15	0.27	0.44	0.30
Dolicho–MNHN–843V–M2i–f12	*D. ruscinensis*	MNHN	Perpignan	1.87	3.50	40841.9	0.47	0.52	0.94	0.21
Dolicho–Perpignan–PR38–lm2–f11	*D. ruscinensis*	MNHP	Perpignan	2.21	2.90	45139.9	0.25	0.38	0.43	0.13
Dolicho–Pp31bisb–M2s–cfbis	*D. ruscinensis*	MNHL	Perpignan	2.27	1.40	46270.6	0.13	0.24	0.31	0.53

Ψηφιακή βιβλιοθήκη Θεόφραστος – Τμήμα Γεωλογίας – Αριστοτέλειο Πανεπιστήμιο Θεσσαλονίκης

Ψηφιακή συλλογή
Βιβλιοθήκη
"ΘΕΟΦΡΑΣΤΟΣ"
Τμήμα Γεωλογίας
Α.Π.Θ

Dolicho–C3–Pp11–M2–f9	*D. ruscinensis*	MNHL	Perpignan	2.63	1.00	38417.9	0.19	0.33	0.43	0.53
Dolicho–C3–Pp11–M2–sf	*D. ruscinensis*	MNHL	Perpignan	3.03	5.90	62394.7	1.01	1.03	1.07	0.13

[a] Asfc = Area-scale fractal complexity; epLsar = exact proportion length-scale anisotropy of relief; Smc = scale of maximal complexity, $Hasfc_{9,36,81}$ = heterogeneity of area-scale fractal complexity on 9, 36 and 81 cell.

Ψηφιακή βιβλιοθήκη Θεόφραστος – Τμήμα Γεωλογίας – Αριστοτέλειο Πανεπιστήμιο Θεσσαλονίκης

Ψηφιακή συλλογή
Βιβλιοθήκη
"ΘΕΟΦΡΑΣΤΟΣ"
Τμήμα Γεωλογίας
Α.Π.Θ

Table S3 Phylogenetic generalized least squares (PGLS) correlations between dental topographic, enamel thickness and tooth crown strength variables, pairs of variables that are significantly correlated are in bold, $\alpha = 0.05$ [a].

Variables	Lambda	*p–value*	Slope	Std.er.	*t*–value	AIC	logL	BIC	Multiple R^2	Adjusted R^2
RET_{geo}–Inclination	0	**< 0.05**	7.490	1.371	5.46	–19.900	11.950	–17.909	0.623	0.602
RET_{vol}–Inclination	0	**< 0.05**	6.829	1.399	4.878	–19.093	11.546	–17.101	0.569	0.545
LRFI–Inclination	0.391	**< 0.05**	–5.271	0.268	–19.64	–92.688	48.344	–90.697	0.955	0.952
ARC–Inclination	0.499	**< 0.05**	–2.568	0.647	–3.967	–58.445	31.222	–56.453	0.466	0.436
OES 2D–ACS	1	**< 0.05**	1.981	0.167	11.856	–15.104	9.552	–13.113	0.886	0.880
OES 2D–OPCR	0	**< 0.05**	1.945	0.375	5.185	14.152	–5.076	16.143	0.599	0.576
OES 2D–DNE	0.083	**< 0.05**	1.772	0.463	3.825	20.093	–8.046	22.084	0.448	0.417
OES 2D–RET_{vol}	1	**< 0.05**	–1.408	0.473	–2.977	20.399	–8.199	22.391	0.330	0.292
RET_{geo}–LRFI	0	**< 0.05**	–1.388	0.244	–5.67	–20.856	12.428	–18.865	0.641	0.621
RET_{vol}–LRFI	0	**< 0.05**	–1.228	0.261	–4.701	–18.264	11.132	–16.273	0.551	0.526
RET_{vol}–RET_{geo}	0.95	**< 0.05**	1.036	0.09	11.416	–49.848	26.924	–47.857	0.878	0.871
DNE–OPCR	0.127	**< 0.05**	0.846	0.101	8.334	–38.742	21.371	–36.70	0.794	0.782
OPCR–ACS	0.102	**< 0.05**	0.525	0.135	3.879	–17.084	10.542	–15.092	0.455	0.421
ARC–RFI	0.611	**< 0.05**	0.490	0.122	3.989	–58.800	31.400	–56.809	0.469	0.439
RETvol–ACS	1	**< 0.05**	–0.401	0.178	–2.248	–12.415	8.207	–10.423	0.219	0.175
DNE–ACS	0.493	**< 0.05**	0.366	0.163	2.237	–13.135	8.567	–11.144	0.217	0.174
ARC–RET_{geo}	0.161	**< 0.05**	–0.281	0.062	–4.501	–57.963	30.981	–55.971	0.529	0.503
LRFI–DNE	1	**< 0.05**	0.239	0.093	2.551	–39.511	21.755	–37.520	0.265	0.224
ARC–RET_{vol}	0.376	**< 0.05**	–0.221	0.072	–3.046	–53.555	28.777	–51.563	0.340	0.303
ARC–DNE	0.796	**< 0.05**	0.216	0.077	2.794	–52.946	28.473	–50.955	0.302	0.263
OES 2D–RET_{geo}	0.992	0.068	–1.126	0.58	–1.94	24.478	–10.239	26.469	0.172	0.127
OES 2D–Inclination	0.948	0.356	–5.346	5.653	–0.945	27.358	–11.679	29.350	0.047	-0.005
DNE–Inclination	0.706	0.063	–4.173	2.112	–1.975	–12.401	8.200	–10.410	0.178	0.132
OPCR–Inclination	0.663	0.455	–1.833	2.402	–0.763	–7.064	5.532	–5.072	0.031	-0.022
OES 2D–ARC	0.938	0.525	0.905	1.399	0.646	27.934	–11.967	29.925	0.022	-0.031

Ψηφιακή βιβλιοθήκη Θεόφραστος – Τμήμα Γεωλογίας – Αριστοτέλειο Πανεπιστήμιο Θεσσαλονίκης

Ψηφιακή συλλογή
Βιβλιοθήκη
"ΘΕΟΦΡΑΣΤΟΣ"
Τμήμα Γεωλογίας
Α.Π.Θ

OES 2D–LRFI	0.961	0.493	0.779	1.115	0.698	27.723	–11.816	29.715	0.026	-0.027
ACS–Inclination	0.963	0.789	–0.734	2.704	–0.271	–1.798	2.899	0.193	0.004	-0.051
RET_{vol}–DNE	0.685	0.18	–0.321	0.23	–1.395	–9.351	6.675	–7.359	0.097	0.047
RET_{vol}–OPCR	0.719	0.241	–0.268	0.221	–1.211	–8.909	6.454	–6.917	0.075	0.023
RET_{geo}–ACS	0.980	0.221	–0.222	0.175	–1.264	–13.388	8.694	–11.396	0.081	0.030
RET_{geo}–DNE	0.899	0.447	–0.163	0.21	–0.776	–12.193	8.096	–10.201	0.032	-0.021
ARC–OPCR	0.766	0.076	0.150	0.08	1.877	–49.470	26.735	–47.478	-	-
RET_{geo}–OPCR	0.925	0.545	–0.121	0.197	–0.615	–12.053	8.026	–10.061	0.020	-0.033
LRFI–OPCR	0.934	0.369	0.100	0.109	0.919	–35.538	19.769	–33.547	0.044	-0.008
ARC–ACS	0.676	0.569	0.042	0.073	0.579	–46.503	25.251	–44.512	0.018	-0.036
LRFI–ACS	0.916	0.977	0.003	0.102	0.029	–34.644	19.322	–32.652	0.0000476	-0.055

[a] Pagel's Lambda = is a measure of phylogenetic signal; Slope = an estimate that relates the two variables being regressed, values above 1.0 indicate that assumptions of Brownian motion are incorrect; std.er = standard error; AIC = Akaike information criterion; LogL = Log likelihood; BIC = Bayesian information criterion; R^2 = Determination coefficient (higher values of R^2 indicate stronger correlation, i.e. less dispersion of values).

Ψηφιακή βιβλιοθήκη Θεόφραστος – Τμήμα Γεωλογίας – Αριστοτέλειο Πανεπιστήμιο Θεσσαλονίκης

Ψηφιακή συλλογή
Βιβλιοθήκη
"ΘΕΟΦΡΑΣΤΟΣ"
Τμήμα Γεωλογίας
Α.Π.Θ

Chapter 4. Investigating the niche partitioning among European Pliocene colobines

4.1 Introduction

Mesopithecus is the earliest of at least four genera of cercopithecoids in Europe (e.g. *Mesopithecus, Dolichopithecus, Paradolichopithecus, Macaca*) ranging from the late Miocene until earliest Pleistocene times (Andrews et al., 1996). *Mesopithecus* is a widely distributed and well–studied medium sized colobine monkey genus that inhabited Eurasia, with its oldest occurrence traced back to early Turolian of Greece (Koufos, 2009, 2016). An older occurrence is documented (based on an isolated premolar) in the Vallesian locality of Wissberg (Germany), but its origin has been questioned (Andrews et al., 1996). It is best known from the large collection of Pikermi fossil assemblage (Athens, Greece), but has also been recognized in many Late Miocene and Pliocene sites throughout Europe and southwestern Asia (Alba et al., 2015; de Bonis et al., 1990; Heintz et al., 1981; Jablonski et al., 2020; Khan et al., 2020; Koufos et al., 2003).

The genus *Mesopithecus* includes at least four species: *Mesopithecus pentelicus*, *Mesopithecus monspessulanus*, *Mesopithecus sivalensis*, and *Mesopithecus delsoni* (Koufos, 2019). However, there is a disagreement regarding the taxonomic status of the latter fossil species (e.g. Andrews et al., 1996; Delson, 1994; Rook, 1999; Szalay & Delson, 1979; Zapfe, 1991), with some supporting the specific distinction for this somewhat larger species (e.g. Koufos et al., 2003), while others provisionally distinguish it as a subspecies (e.g. *Mesopithecus pentelicus delsoni*; Alba et al., 2015), at least until a thorough revision of the genus is undertaken. Furthermore, various intermediate forms have been recognized (Szalay and Delson, 1979; Ardito and Mottura, 1987; Gentili et al., 1998; Koufos, 2019 and references therein), while often considered as successive chrono-species of a single phyletic lineage (Delson et al., 2005; Koufos, 2009a). Based on palaeobiogeographical criteria, closer relationships of *Mesopithecus* with the Asian colobines have been suggested (Delson, 1973; Szalay and Delson, 1979), whereas later cladistics analyses imply however, close relationships with the Asian odd-nosed monkeys, especially *Pygathrix* (Jablonski, 1998, 2002). Nevertheless, there is still uncertainty regarding the phylogenetic position of the genus *Mesopithecus*, as the most recent available evidence is consistent with *Mesopithecus* being a stem colobine (Frost et al., 2015; Alba et al., 2015b).

The genus *Mesopithecus* appeared during a period of warm and dry climate conditions in the Mediterranean area. Its presumed semi–terrestrial habits promoted their dispersion in Eurasia, and facilitated its survival in the more open and/or mixed habitats of that period (Szalay and Delson, 1979; Youlatos et al., 2012). *Mesopithecus monspessulanus* is the youngest species of this genus in Europe first discovered in the Lower Pliocene (MN 14, 5.3–4.2 Ma) fossiliferous locality of Montpelllier (France), and later recognized in some other localities of Europe (see Fig. IX in Koufos, 2019). This species was originally assigned to the genus *Semnopithecus* (e.g. *Semnopithecus monspessulanus*), but now it is widely accepted that shows sufficient similarity with *Mesopithecus pentelicus* to be considered congeneric (Szalay and Delson, 1979). Unlike *Mesopithecus pentelicus*, the overall fossil material for this overall smaller species is very limited (Delson, 1973; Delson et al., 2005; Koufos, 2019; Pradella & Rook, 2007; Rook, 1999). Its earliest known occurrence is recorded in the fossiliferous locality of Dytiko (Axios Valley, northwestern Macedonia, Greece) dated around latest Miocene (7.0–6.0 Ma), along with other intermediate forms between *Mesopithecus pentelicus* and *Mesopithecus monspessulanus* (de Bonis et al., 1990; Koufos, 2009a). This observation along with most recent pieces of evidence (Koufos, 2019), strengthen the hypothesis that these two species briefly coexisted (e.g. Delson et al., 2005). The last known occurrence of *Mesopithecus*

Ψηφιακή βιβλιοθήκη Θεόφραστος – Τμήμα Γεωλογίας – Αριστοτέλειο Πανεπιστήμιο Θεσσαλονίκης

Ψηφιακή συλλογή
Βιβλιοθήκη
"ΘΕΟΦΡΑΣΤΟΣ"
Τμήμα Γεωλογίας

monspessulanus in Europe comes from the Early Villafranchian (MN 17), based on an isolated M^3 crown from Red Crag site in England. Nevertheless, the possibility of sampling bias of the specimen with the Red Crag fossil assemblage cannot be rejected (Delson, 1973). Thus, for the time being it is safer to assume that the latest occurrence of this species is documented in the early Villafranchian faunal assemblage of Villafranca d'Asti Fornace (RDB) in northwestern Italy (Gentili et al., 1998; Rook, 1999).

The limited ecological information for *Mesopithecus monspessulanus* derives from analysis of postcranial morphology, and has been briefly discussed by some researchers (Ciochon, 1993; Delson, 1994; Szalay & Delson, 1979; see also Youlatos & Koufos, 2010). These interpretations depict a small-sized gracile cercopithecid, with some postcranial features indicating less terrestrial locomotor habits than its predecessor *Mesopithecus pentelicus*, presumably associated with a more arboreal niche (Delson, 1994). In addition, *Mesopithecus monspessulanus* is sometimes found associated with other cercopithecid remains, belonging either to the genus *Macaca* and/or *Dolichopithecus*, thus not excluding the possibility of living in the same place and time as they surely overlapped in geographic distribution and chronostratigraphic range (see Table I in Eronen & Rook, 2004). In order to coexist and/or to avoid competition, primate species can undergo behavioral but also anatomical changes (Macho, 2016). Competition for space and resources can influence the behavior and ecology of organisms in a wide range of ecological communities (Vandercone, 2011). Still, the broader effect/role of interspecific competition in primate communities is relatively unclear. In any case, little is known about Eurasian fossil primate paleoecology (but see Eronen and Rook, 2004; Sukselainen et al., 2015; DeMiguel et al., 2021) and the role of intespecific competition as it is difficult to evaluate even in extant primate communities, not to mention the fossil record. This is mostly due to the scarcity of fossil material, commonly distributed in several institutions throughout Europe that makes it difficult to study.

To extend our understanding of Eurasian fossil primate paleoecology, the present chapter aims to a) explore the dietary ecology of *Mesopithecus monspessulanus*, and b) investigate the potential effects of niche partitioning with its contemporary and sometimes sympatric European fossil colobine *Dolichopithecus ruscinensis*, by quantifying its enamel thickness analogies and dental microwear texture patterns. Two approaches have been followed for enamel thickness investigations, a) upper molar comparisons focusing on a fossil M^3 (DKV480) assigned to *Mesopithecus monspessulanus* from the fossil site of Dorkovo (Bulgaria), including also available data for modern taxa found in the literature; b) lower molar comparisons between modern and fossil taxa using available fossil lower molar material of *Mesopithecus monspessulanus* and *Dolichopithecus ruscinensis*, followed by a qualitative assessment of enamel distribution on lower molars (e.g. M_2 and M_3) between the two fossil taxa. Lastly, dental microwear texture analysis is used as a proxy to make inferences about the feeding behavior of *Mesopithecus monspessulanus* and *Dolichopithecus ruscinensis*.

4.2 Material

4.2.1. Enamel thickness

The fossil upper molar material of *Mesopithecus monspessulanus* consists of an M^3 (DKV480) from the locality of Dorkovo in Bulgaria (Delson et al., 2005) and it is housed in Natural History Museum of Sofia (Table 4.1). The modern comparative material consists of eight cercopithecid genera from published data found in the literature (see Table II in Beaudet et al., 2016), and specimens archived in MorphoSource.org digital drepository (see Table 4.2 and Table S1 Appendix 4.7 for details). The fossil lower molar material for *Mesopithecus monspessulanus* consists of an M_2 and M_3 from a mandibular specimen (UM 4043 here, given as UM 4001 in Delson, 1973) from the fossil site of Montpellier-Celleneuve (France), and it is

Ψηφιακή βιβλιοθήκη Θεόφραστος – Τμήμα Γεωλογίας – Αριστοτέλειο Πανεπιστήμιο Θεσσαλονίκης

Ψηφιακή συλλογή Βιβλιοθήκη "ΘΕΟΦΡΑΣΤΟΣ" Τμήμα Γεωλογίας. Α.Π.Θ.

housed in the Institute of Science de l'évolution de Montpellier (ISEM). The fossil specimen is in good condition, and it belongs to a female juvenile individual with an erupted M_3 on the left side; the right M_3, both rami as well as the incisors and canines are missing (Delson, 1973).

The fossil lower molar material of *Dolichopithecus* consists of an isolated M_2 found in the fossiliferous locality of Serrat d'en Vaquer-Perpignan (France), and a M_3 from the mandibular specimen found in Megalo Emvolon (Greece). The specimens are housed in the Museum d'Histoire Naturelle Perpignan (France) and Museum of Geology-Paleontology-Paleoanthropology of Aristotle University of Thessaloniki (Greece) respectively. The modern comparative material consists of a total of 13 molars (nine M_2 and four M_3) from six extant cercopithecid genera and are housed in the Laboratory Paleontology Evolution Paleoecosystems Paleoprimatology, University of Poitiers (PALEVOPRIM, France), Muséum National d'Histoire Naturelle, Paris (France) and the American Museum of Natural History, New York (United States of America) (Table 4,2 4.3). All fossil and extant material used in this chapter is summarized in Table S1 Appendix 4.7.

Table 4.1 Description and linear measurements of the fossil material.

Taxon	**Locality**	**ID**	**Tooth**	**Wear grade[a]**	**Linear measurements**		
					AW (mm)	L (mm)	AW/L
Me. monspessulanus	Dorkovo	DKV480	M^3 sin	1B	7.271	7.583	0.958
Me. monspessulanus	Montpellier	UM4043	M_2 sin	1B	5.607	7.143	0.784
		UM4043	M_3 sin	0	5.692	8.887	0.640
D. ruscinensis	Perpignan	MHNPn–PR39	M_2 sin	4B	7.796	11.005	0.708
D. ruscinensis	Megalo Emvolon	MEV–1	M_3 dex	1B	8.128	11.612	0.699

[a]Wear grades following the scoring system of Delson (1973).

Table 4.2 Three dimensional average and relative enamel thickness for *Mesopithecus monspessulanus* (DKV480) and modern sample of M^3.

Fossil taxa	**Specimen**		**3DAET$_{vol}$ (mm)**	**3DRET$_{vol}$**	**Source**
Me. monspessulanus	DKV480	mean	0.7	16.52	This study
		range	–	–	
Extant taxa[a]					
Papio (*n* = 4)		mean	1.1	18.2	Beaudet et al. 2016
		range	1.0–1.2	17.3–18.8	
Lophocebus (*n* = 3)		mean	0.69	18.7	Beaudet et al. 2016
		range	0.68–0.7	18.3–19.3	
Mandrillus (*n* = 1)		mean	0.8	13.4	Beaudet et al. 2016
		range	–	–	
Macaca (*n* = 2)		mean	0.75	15.8	Beaudet et al. 2016
		range	0.7–0.8	15–16.7	
Chlorocebus (*n* = 4)		mean	0.5	14.3	Beaudet et al. 2016
		range	0.4–0.6	11.5–16	
Colobus (*n* = 2)		mean	0.65	16	Beaudet et al. 2016
		range	0.6–0.7	14.3–17.7	
Cercocebus (*n* = 3)		mean	0.8	17.4	Beaudet et al. 2016
		range	0.7–0.9	15.9–19.1	
Nasalis (*n* = 2)	AMNH:M:103458 AMNH:M:103468	mean	0.65	15.88	MorphoSource.org
		range	0.61–0.69	13.9–17.8	
Cercocebus (*n* = 1)	AMNH:M:70063	mean	1.05	20.62	MorphoSource.org

[a]Values for all extant taxa, except the ones downloaded from MorphoSource.org, are taken from Table II in Beaudet et al. (2016).

Ψηφιακή βιβλιοθήκη Θεόφραστος – Τμήμα Γεωλογίας – Αριστοτέλειο Πανεπιστήμιο Θεσσαλονίκης

Ψηφιακή συλλογή Βιβλιοθήκη "ΘΕΟΦΡΑΣΤΟΣ" Τμήμα Γεωλογίας ΑΠΘ

Table 4.3 3D average and relative enamel thickness for fossil and extant sample of lower molars[a,b].

Fossil taxa	ID	Tooth	Wear grade[b]	3DAET$_{vol}$(mm)	3DRET$_{vol}$
Me. monspessulanus	UM4043	M_2	1B	0.60	14.54
	UM4043	M_3	0	0.64	15.66
D. ruscinensis	MHNPn–PR39	M_2	4B	0.64	10.99
	MEV–1	M_3	0	0.94	17.28
Extant taxa					
Lophocebus (*n* = 2)	AMNH:M:52613 AMNH:M:52607	M_2	1B	0.80–0.81	22.35–21.94
		M_3	1B	0.88–0.89	24.67–23.01
Cercocebus (*n* = 1)	AMNH:M:70063	M_2	0	1.05	21.09
		M_3	0	1.11	20.30
Mandrillus (*n* = 2)	2002–105 1893–269	M_2	2B	0.89–0.91	12.26–15.03
Chlorocebus (*n* = 2)	1972–302 1972–328	M_2	2B	0.45–0.52	15.32–15.89
Colobus (*n* = 1)	1969–388	M_2	0	0.56	12.86
Semnopithecus (*n* = 1)	AMNH:M:90328	M_2	3B	0.39	13.47
		M_3	0	0.40	14.33

[a]3DAET$_{vol}$ = 3D volumetric average enamel thickness; 3DRET$_{vol}$ = 3D volumetric relative enamel thickness; [b]Wear grades following the scoring system of Delson (1973).

4.2.1. Dental microwear texture analysis

The fossil material used for dental microwear texture analysis consists of a total of 10 specimens for *Mesopithecus monspessulanus* and 22 of *Dolichopithecus*. All fossil dental material for the *Dolichopithecus* (see previous chapter for material and fossil sites or Table S2 Appendix 3.7, 4.7). The fossil material of *Mesopithecus monspessulanus* was found in the fossiliferous localities of Montpellier (France, *n* = 6), Villafranca d'Asti (Italy, *n* = 2), Dorkovo (Bulgaria, *n* = 1), Dytiko-2 (Greece, *n* = 1). The hosting institutions of the fossil material are given in Table 4.4. The modern comparative material used for the analysis here consists of the same species and inviduals used in the previous chapter (see section 3.2.1 and Table S2 Appendix 3.7).

Table 4.4 Dental microwear fossil sample and the respective fossiliferous localities and host institutions[a].

Taxon	Locality	Epoch	*n*[a]	References	Institutions
Me. monspessulanus	Montpellier	E. Pliocene	6	Eronen and Rook, 2004	ISEM, UCBL–1
Me. monspessulanus	Villafranca d'Asti	L. Pliocene	2	Pradella and Rook, 2007	NHMB
Me. monspessulanus	Dorkovo	E. Pliocene	1	Delson et al., 2005	NHMS
Me. monspessulanus	Dytiko	latest Miocene	1	de Bonis et al., 1990; Koufos, 2009b, 2009a	LGPUT
D. ruscinensis	Serrat d'en Vaquer–Perpignan	E. Pliocene	16	Depéret, 1889; Eronen and Rook, 2004	MHNP, UCBL–1, MNHL
D. ruscinensis	Dorkovo	E. Pliocene	3	Delson et al., 2005	NHMS
D. ruscinensis	Megalo Emvolon	E. Pliocene	1	Koufos et al., 1991	LGPUT
D. ruscinensis	Măluşteni	E. Pliocene	1	Eronen and Rook, 2004	UAIC
D. ruscinensis	Taraclia	L. Pliocene	1	–	ASM
D. balcanicus	Tenevo	E. Pliocene	1	Spassov and Geraads, 2007	NHMS

[a]*n* = number of individuals.

Ψηφιακή βιβλιοθήκη Θεόφραστος – Τμήμα Γεωλογίας – Αριστοτέλειο Πανεπιστήμιο Θεσσαλονίκης

Ψηφιακή συλλογή
Βιβλιοθήκη
"ΘΕΟΦΡΑΣΤΟΣ"
Τμήμα Γεωλογίας

4.3 Data acquisition and statistical analysis

4.3.1. Enamel thickness

In this chapter, μ-CT scan specimens with various scan resolutions were included to expand the comparative modern sample of M^3, M_2 and M_3, as most of the available comparative sample consisted of M^2 (see section 2.1.2). The fossil molars from Dorkovo (DKV480), Serrat d'en Vaquer-Perpignan (MHNPn–PR39), and Megalo Emvolon (MEV–1), along with the lower molars from *Mandrillus*, *Chlorocebus* and *Colobus*, were scanned using EasyTom XL duo μ-CT (Plateforme PLATINA, PALEVOPRIM) in the University of Poitiers (France), with voxel size ranging between 9.2 to 40.1 μm. The fossil specimen from Montpellier (UM 4043) is housed in the University of Montpellier and was scanned using the same μ-CT system as the rest of the fossil specimens with a resolution of 26.16 μm. The μ-CT scan file was kindly provided by the Institut des Sciences de l'Évolution de Montpellier (ISEM) for the purposes of this dissertation. Technical details concerning each specimen taken from the literature, were not available (but see Table I in Beaudet et al., 2016). The modern specimens downloaded from MorphoSource.org digital repository were scanned using using GE phoenix v tome xs240 housed in the American Museum of Natural History (AMNH), with voxel size ranging between 52.2 to 117.9 μm (see Table S1 Appendix 4.7 for details).

Three variables were measured in each molar specimen for the overall crown portion: volume of the enamel cap (EVOL, mm^3), volume of the coronal dentine that includes the coronal aspect of the pulp chamber (VCDP, mm^3), and the surface of the enamel–dentine junction (EDJS, mm^2). Then, two indices of enamel thickness were computed: 3D average enamel thickness ($3DAET_{vol}$, mm) calculated as the ratio between the enamel volume and enamel–dentine junction surface area (EVOL/EDJS), and 3D relative enamel thickness ($3DRET_{vol}$) obtained through the ratio of 3D average enamel thickness and the cubic root of the volume of coronal dentine multiplied by one hundred ($3DAET_{vol}/((VCDP)^{(1/3)})*100$), allowing direct and scale–free comparisons (Kono, 2004; Olejniczak et al., 2008). Previously published studies have shown that intra/inter–observer tests for measurement accuracy run by more than one observer using a similar analytical protocol revealed differences less than 5% (Bondioli et al., 2010; Zanolli et al., 2014). Furthermore, the 3D enamel distribution across fossil M_2s and M_3s of *Mesopithecus monspessulanus* and *Dolichopithecus ruscinensis* was illustrated for qualitative assessment. This was achieved by computing the distances between the occlusal and the enamel–dentine junction surfaces using available tools ("Distance module") on Avizo v. 7.0. In order to qualitatively characterize the overall differences in enamel distribution, all fossil molar specimens retained their actual size, with a scale ranging from zero to maximal values of enamel given independently for each specimen. The values of each variable measured for each specimen analyzed are summarized in Table S1 Appendix 4.7.

4.3.2. Dental microwear texture analysis

The dental microwear texture analysis in this chapter includes the same sample of modern species given on the previous chapter (i.e. Chapter 3). However, here only individuals were chosen with both dental facet types available (i.e. Phase I and II), whereas the fossil sample of *Dolichopithecus ruscinensis* and *Mesopithecus monspessulanus* also includes individuals with a single dental facet type available to expand the fossil sample size. Nevertheless, the variation in the mean values of the microwear texture parameters analyzed here may be considered non-significant (see Table 3.2 and Table 4.6). All dental facets were scanned with 'TRIDENT' Leica Microsystems DCM8 with a 100× objective housed in PALEVOPRIM, University of Poitiers (France). Four variables are used here to characterize microwear surface textures (Scott et al., 2006): complexity (Asfc; no unit), heterogeneity (Hasfc

Ψηφιακή βιβλιοθήκη Θεόφραστος – Τμήμα Γεωλογίας – Αριστοτέλειο Πανεπιστήμιο Θεσσαλονίκης

Ψηφιακή συλλογή
Βιβλιοθήκη
"ΘΕΟΦΡΑΣΤΟΣ"
Τμήμα Γεωλογίας
Α.Π.Θ.

with 81 cells; no unit), anisotropy (epLsar at 1.8 μm; no unit) and textural fill volume (Tfv at the scale of 2 μm; in μm^3).

Prior to the analysis, all texture variables were box-cox transformed to avoid normality assumption violations in parametric tests (Conover and Iman, 1981). To explore variations of microwear variables, two Kruskal-Wallis tests were performed, one for each dental wear facet type, with species as factor followed by pairwise comparisons with Bonferroni adjustment. Computations were carried out using SPSS v. 22 (IBM Corp, 2013) and R v. 3.6 (Team, 2013).

4.4 Results

4.4.1. Enamel thickness

Estimates of the whole crown enamel tissue proportions for the upper third and lower molar comparisons among fossil and extant taxa are shown in Table 4.2 and Table 4.3 while values of all variables measured are given in Table S1 Appendix 4.7. The value of 3D average (volumetric) enamel thickness ($3DAET_{vol}$) places DKV480 closer to colobines (e.g. *Nasalis* and *Colobus*), but also near to *Macaca* and the lower extreme of *Cercocebus* range (Fig. 4.1A). The scale-free 3D relative (volumetric) enamel thickness ($3DRET_{vol}$) value places DKV480 within the range of values of *Nasalis*, *Colobus* and *Macaca*, being also near to the lower and higher extreme of values for *Cercocebus* and *Chlorocebus* respectively (Fig. 4.1B).

Concerning lower molars, $3DAET_{vol}$ of M_2s shows that both *Mesopithecus monspessulanus* and *Dolichopithecus ruscinensis* molar specimens (UM 4043 and MHNPn–PR39 respectively) have similar values (Fig. 4.2A), although *Dolichopithecus ruscinensis* appears to display slightly higher values. Both fossil taxa have higher values than *Semnopithecus*, *Colobus*, *Chlorocebus* and lower than *Lophocebus*, *Cercocebus* and *Mandrillus* (Fig. 4.2A). The M_3s of all fossil and extant taxa have higher $3DAET_{vol}$ than their respective M_2s (Fig. 4.2A). The comparisons of $3DRET_{vol}$ reveal that the M_2 of UM 4043 exhibits slightly higher value than the extant extant colobine taxa (e.g. *Semnopithecus* and *Colobus*), whereas MHNPn–PR39 exhibits the lowest value in our sample (Fig. 4.2B). The comparisons of $3DRET_{vol}$ of the available M_3s among fossil and extant taxa show a similar pattern with $3DAET_{vol}$, with the exception of *Cercocebus* M_3 which shows lower $3DRET_{vol}$ than its respective M_2.

The enamel distribution maps of fossil lower molars of *Mesopithecus monspessulanus* and *Dolichopithecus ruscinensis* are shown in Fig. 4.3. The comparisons indicate that in both molar types the two fossil taxa exhibit differences in their enamel distribution patterns. *Mesopithecus monspessulanus* fossil M_2 (UM 4043) exhibits more unevenly distributed enamel with the thickest parts (red values) being located on the buccal side of the molar, on mesial and distal shelves and along the transverse and longitudinal shearing crests, whereas it exhibits intermediate values of (yellow to green values) enamel across the mesial, trigon and distal foveas. The enamel distribution pattern of *Dolichopithecus ruscinensis* fossil M^2 (MHNPn–PR39) indicates more evenly distributed enamel with the thickest parts being on the molar cusps, more specifically on the hypoconid and entoconid, and along the transverse and longitudinal shearing crests which are very well defined. Moreover, it exhibits thin values of enamel across the mesial and distal foveas (green to blue values). Concerning lower third molars, *Mesopithecus monspessulanus* fossil molar (UM 4043) exhibits overall the same pattern as seen in its respective M_2, yet in this case thick values are distributed on the hypoconulid. Likewise, the fossil M_3 of *Dolichopithecus ruscinensis* (MEV–1) follows similar pattern of enamel distribution as seen in the fossil M_2 (MHNPn–PR39), yet in this case thick values are distributed on the hypoconulid.

Ψηφιακή βιβλιοθήκη Θεόφραστος – Τμήμα Γεωλογίας – Αριστοτέλειο Πανεπιστήμιο Θεσσαλονίκης

Ψηφιακή συλλογή
Βιβλιοθήκη
"ΘΕΟΦΡΑΣΤΟΣ"

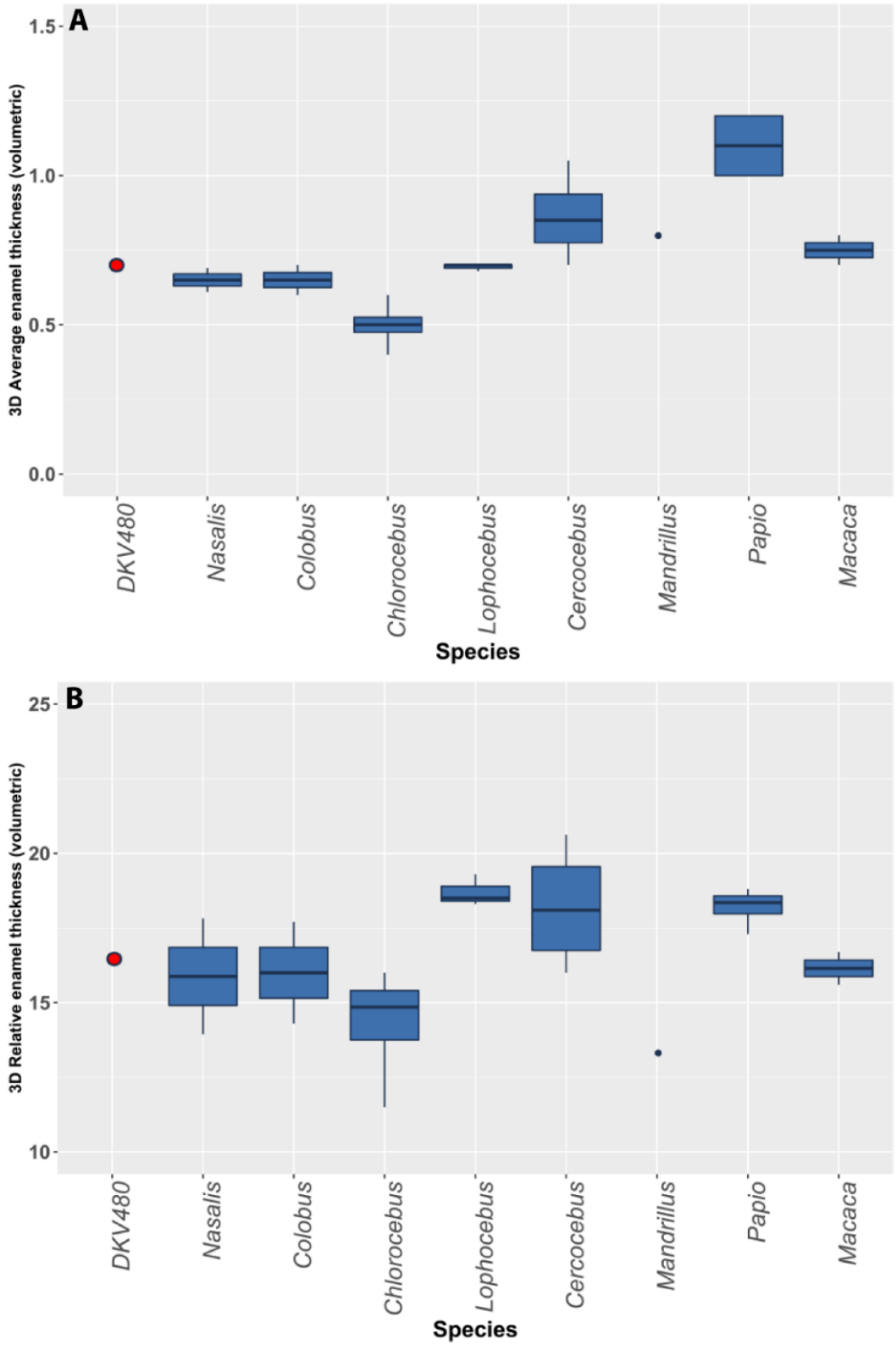

Fig. 4.1 Boxplot comparisons of 3D average (**A**) and relative enamel thickness (**B**) on M^3 between modern genera and *Mesopithecus monspessulanus* (DKV480). All data except the fossil specimen, one specimen of *Cercocebus* and two *Nasalis* specimens are taken from **Table II** in Beaudet et al., (2016).

Ψηφιακή βιβλιοθήκη Θεόφραστος – Τμήμα Γεωλογίας – Αριστοτέλειο Πανεπιστήμιο Θεσσαλονίκης

Ψηφιακή συλλογή
Βιβλιοθήκη
"ΘΕΟΦΡΑΣΤΟΣ"

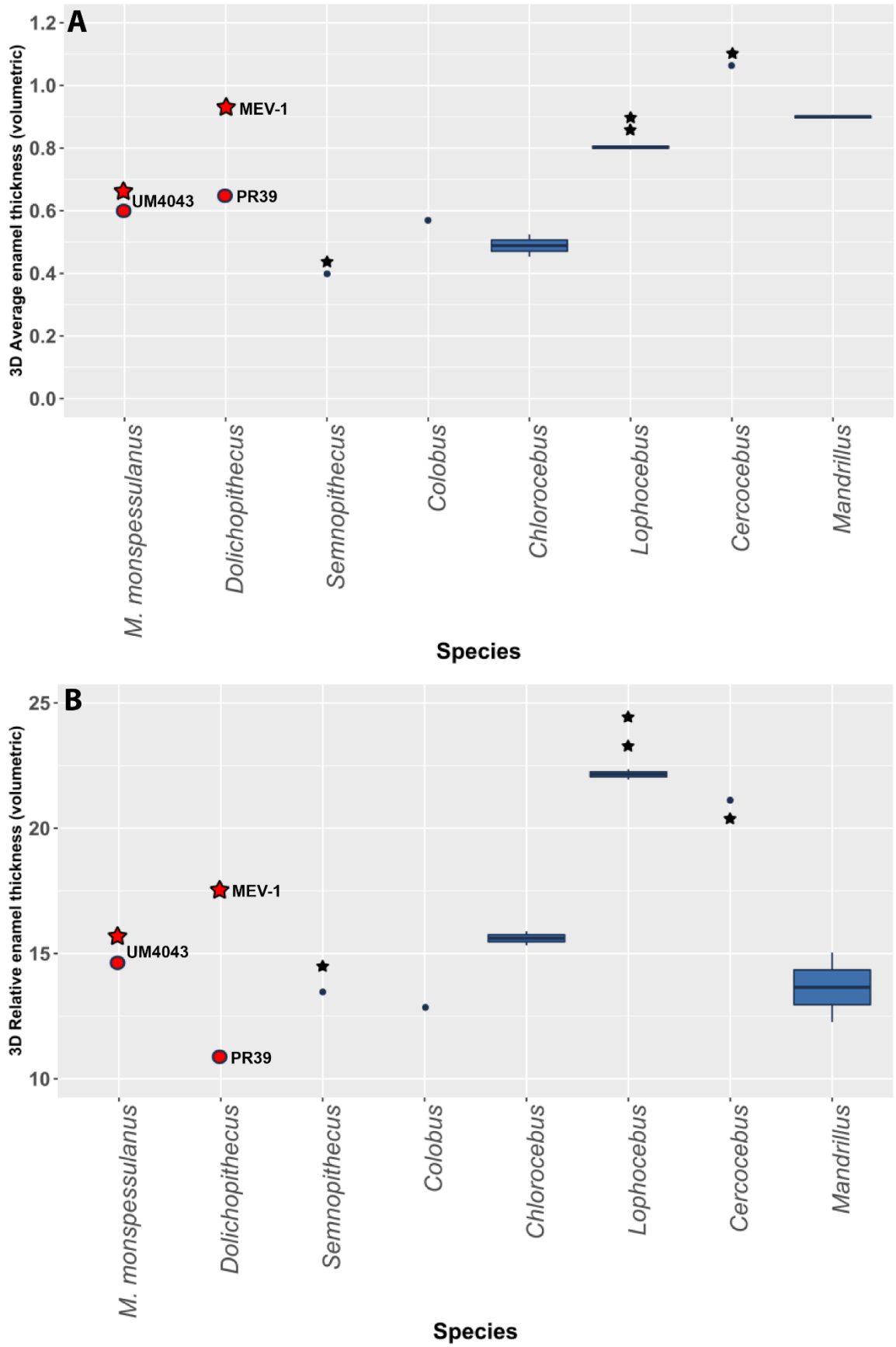

Fig. 4.2 Boxplot comparisons of 3D average (**A**) and relative enamel thicness (**B**) on M_2 (circles) and M_3 (stars) between modern genera, *Dolichopithecus ruscinensis* and *Mesopithecus monspessulanus*.

Ψηφιακή βιβλιοθήκη Θεόφραστος – Τμήμα Γεωλογίας – Αριστοτέλειο Πανεπιστήμιο Θεσσαλονίκης

Ψηφιακή συλλογή
Βιβλιοθήκη
"ΘΕΟΦΡΑΣΤΟΣ"
Τμήμα
Α.

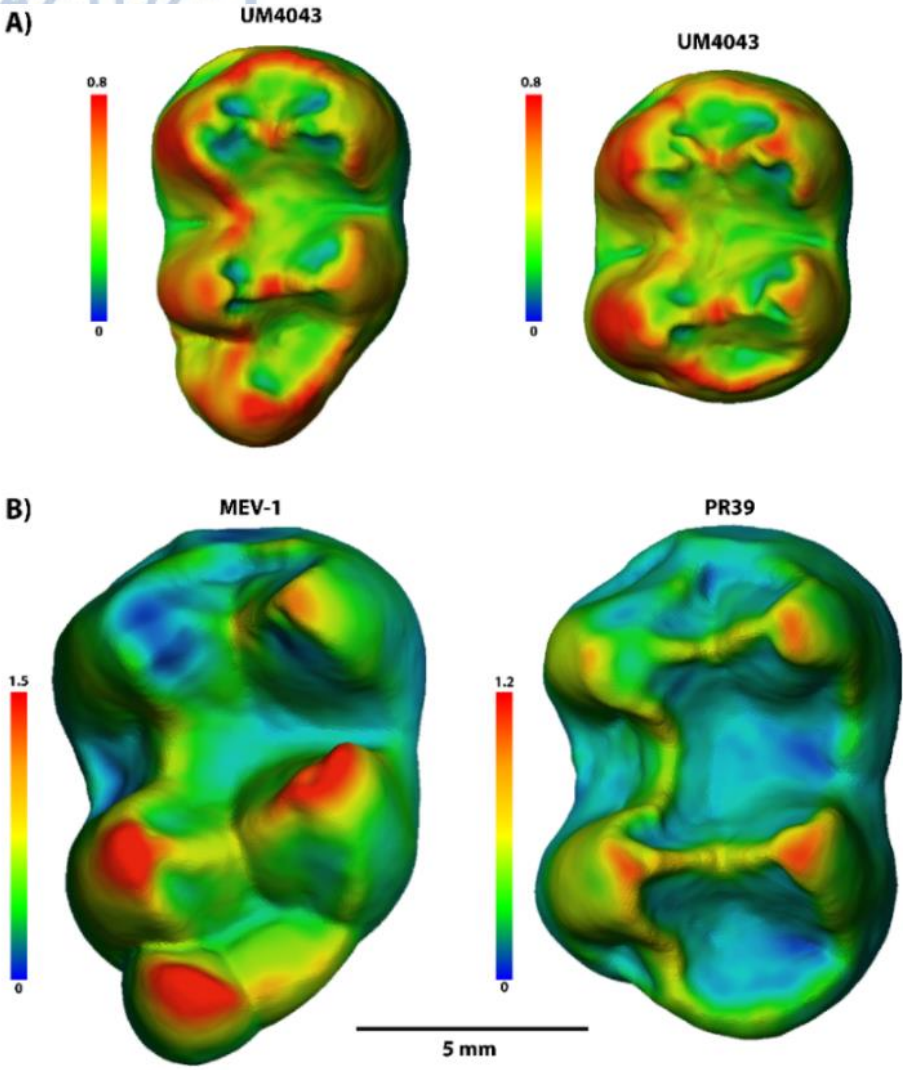

Fig. 4.3 Enamel distribution maps in occlusal view of M_2 and M_3 of **A**) *Mesopithecus monspessulanus* specimen from Montpellier and **B**) *Dolichopithecus ruscinensis* specimens from Megalo Emvolon and Perpignan. Topographic thickness variation is rendered by a color scale ranging from thinner dark–blue to thicker red and for convenience purposes all molars were oriented the same way. Because of variation in enamel thickness values between fossil species, a specific color scale is attributed to each specimen (values in mm).

4.4.2. Dental microwear texture analysis

The Kruskal-Wallis test detected significant differences in texture variables between species in both dental facet types (Table 4.5). There are marked differences in microwear textures between colobines and cercopithecines in both dental facet types indicating their overall differences in dietary preferences (Table 4.6, 4.7).

Concenring Phase II dental facets, significant differences are revealed in the values of complexity (Asfc) and anisotropy (epLsar), whereas in Phase I by complexity (Asfc) and textural fill volume (Tfv). In Phase II dental facets *Mesopithecus monspessulanus* possess lower values of complexity (Asfc) than *Nasalis larvatus*, *Chlorocebus aethiops*, *Erythrocebus patas*, *Lophocebus albigena*, and lower values of textural fill volume than *Piliocolobus badius*, *Erythrocebus patas* and *Lophocebus albigena* (Table 4.6, 4.7). In Phase I dental facets, *Mesopithecus monspessulanus* shows lower values of complexity (Asfc) than *Chlorocebus aethiops*, *Erythrocebus patas* and *Lophocebus albigena*, having also significantly lower values

Ψηφιακή βιβλιοθήκη Θεόφραστος – Τμήμα Γεωλογίας – Αριστοτέλειο Πανεπιστήμιο Θεσσαλονίκης

Ψηφιακή συλλογή Βιβλιοθήκη "ΘΕΟΦΡΑΣΤΟΣ" Τμήμα Γεωλογίας ΑΠΘ

of textural fill volume than the latter two (Table 4.6, 4.7). There are no microwear texture differences revealed between *Mesopithecus monspessulanus* and *Dolichopithecus* (Table 4.7).

Table 4.5 Kruskal-Walis test performed on dental microwear texture variables between fossil and extant taxa; significant differences are shown in bold[a].

	Phase II			**Phase I**		
Variable	df	χ^2	*p*	df	χ^2	*p*
Asfc	9	39.038	**< 0.05**	9	33.489	**< 0.05**
epLsar	9	2.910	**< 0.05**	9	18.795	0.290
$Hasfc_{81}$	9	13.293	0.149	9	11.237	0.259
Tfv	9	19.930	**< 0.05**	9	18.436	**< 0.05**

[a] df: degrees of freedom; χ^2: Chi squared; F: F–statistic; *p* value: significance value.

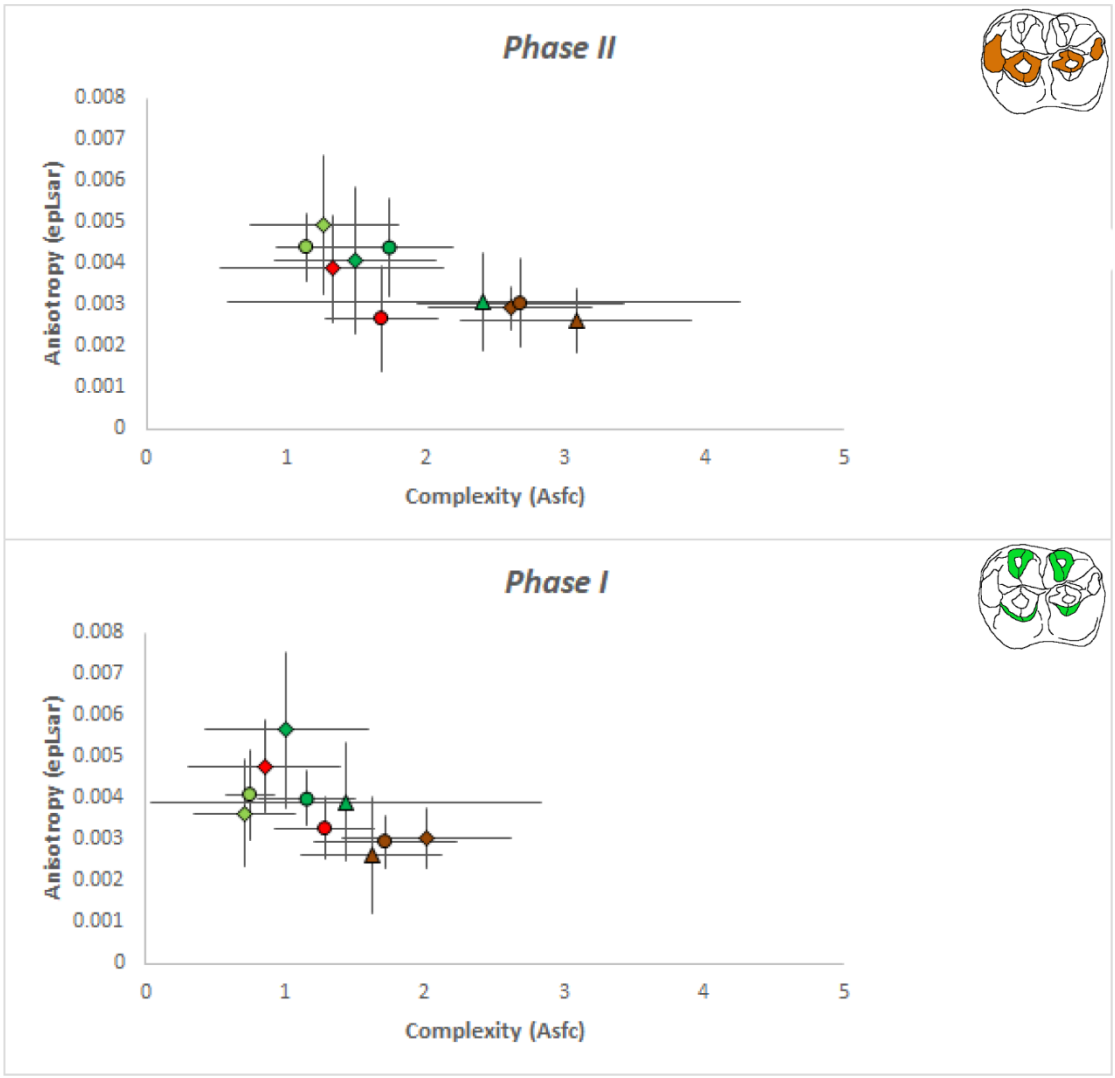

Fig. 4.4 Bivariate plots (means with 95% conf. interval) using complexity (Asfc) and anisotropy (epLsar) between modern and fossil sample on Phase II and I dental wear facets. **Brown**: Cercopithecines (circle: *Lophocebus albigena*, triangle: *Erythrocebus patas*, diamond: *Chlorocebus aethiops*), **Light Green**: African colobines (circle: *Colobus guereza*, diamond: *Piliocolobus badius*), **Green**: Asian colobines (circle: *Presbytis melalophos*, triangle: *Nasalis larvatus*, diamond: *Semnopithecus entellus*).

Ψηφιακή βιβλιοθήκη Θεόφραστος – Τμήμα Γεωλογίας – Αριστοτέλειο Πανεπιστήμιο Θεσσαλονίκης

Ψηφιακή συλλογή
Βιβλιοθήκη
"ΘΕΟΦΡΑΣΤΟΣ"
Τμήμα Γεωλογίας
Α.Π.Θ

Table 4.6 Microwear texture variables descriptive statistics on Phase I, II facets of *Mesopithecus monspessulanus, Dolichopithecus* and modern sample[a].

Taxa	**facet**	***n*[b]**	**Asfc**				**epLsar(x10^3)**				**Hasfc$_{81}$**				**Tfv** (μm^3)			
Extinct			**Mean**	sd	sem	C.I	**Mean**	sd	sem	C.I	**Mean**	sd	sem	C.I	**Mean**	sd	sem	C.I
Mesopithecus monspessulanus	*Ph. II*	10	**1.331**	1.297	0.410	0.803	**3.880**	2.080	0.657	1.289	**0.639**	0.208	0.065	0.128	**27956**	20929.53	6618.5	12972.3
	Ph. I	9	**0.853**	0.829	0.276	0.541	**4.780**	1.690	0.563	1.104	**0.626**	0.327	0.109	0.213	**25969**	12679.9	4226.63	8284.2
Dolichopithecus	*Ph. II*	22	**1.683**	0.968	0.206	0.404	**2.670**	1.300	0.277	0.543	**0.569**	0.234	0.049	0.097	**35341**	12854.35	2740.56	5371.49
	Ph. I	22	**1.284**	0.859	0.183	0.358	**3.264**	1.796	0.383	0.750	**0.613**	0.662	0.141	0.276	**34251**	10396.15	2216.47	4344.27
Modern																		
Colobus guereza	*Ph. II*	20	**1.146**	0.484	0.108	0.212	**4.410**	1.870	0.418	0.819	**0.560**	0.147	0.032	0.064	**30720**	9841.72	2200.68	4313.32
	Ph. I	20	**0.750**	0.387	0.086	0.169	**4.080**	2.500	0.559	1.095	**0.511**	0.222	0.049	0.097	**29841**	11190.15	2502.19	4904.30
Piliocolobus badius	*Ph. II*	12	**1.275**	0.937	0.270	0.530	**4.950**	2.960	0.854	1.674	**0.573**	0.255	0.073	0.144	**43220**	15797.27	4560.28	8938.15
	Ph. I	12	**0.705**	0.641	0.185	0.362	**3.639**	2.305	0.665	1.304	**0.597**	0.396	0.114	0.224	**34307**	14255.96	4115.34	8066.07
Presbytis melalophos	*Ph. II*	15	**1.744**	0.901	0.232	0.455	**4.400**	2.370	0.611	1.199	**0.648**	0.420	0.108	0.212	**39369**	14201.62	3620.37	7095.92
	Ph. I	15	**1.148**	0.690	0.178	0.349	**4.000**	1.286	0.332	0.650	**0.539**	0.270	0.069	0.135	**28826**	19354.96	4997.43	9794.96
Semnopithecus entellus	*Ph. II*	7	**1.502**	0.783	0.295	0.580	**4.080**	2.390	0.903	1.770	**0.763**	0.341	0.129	0.252	**38018**	8162.31	3085.07	6046.73
	Ph. I	7	**1.007**	0.790	0.298	0.585	**5.650**	2.560	0.967	1.896	**0.788**	0.409	0.154	0.303	**36431**	9333.68	3527.80	6914.49
Nasalis larvatus	*Ph. II*	6	**2.416**	2.289	0.934	1.831	**3.080**	1.470	0.600	1.176	**0.602**	0.258	0.105	0.207	**42776**	6472.08	2642.22	5178.75
	Ph. I	6	**1.436**	1.824	0.744	1.400	**3.920**	1.780	0.726	1.424	**0.538**	0.315	0.128	0.252	**25200**	11949.91	4878.53	9561.91
Chlorocebus aethiops	*Ph. II*	36	**2.607**	1.808	0.301	0.590	**2.937**	1.600	0.267	0.522	**0.651**	0.734	0.122	0.239	**36366**	13901.2	2316.87	4541.06
	Ph. I	36	**1.721**	1.566	0.261	0.511	**3.720**	1.920	0.320	0.627	**0.672**	0.627	0.104	0.204	**34858**	9954.06	1659.01	3251.66
Erythrocebus patas	*Ph. II*	13	**3.081**	1.518	0.421	0.825	**2.630**	1.390	0.385	0.755	**0.594**	0.224	0.062	0.121	**42422**	9649.83	2676.38	5245.71
	Ph. I	13	**1.619**	0.920	0.255	0.500	**3.703**	2.613	0.724	1.420	**0.579**	0.273	0.075	0.148	**41234**	7430.29	2060.79	4039.15
Lophocebus albigena	*Ph. II*	13	**2.682**	1.367	0.379	0.743	**3.050**	1.960	0.543	1.065	**0.764**	0.262	0.072	0.142	**45872**	11958.8	3316.77	6500.88
	Ph. I	13	**2.010**	1.112	0.308	0.604	**3.120**	1.330	0.368	0.723	**0.686**	0.273	0.075	0.148	**38994**	10293.11	3029.53	5937.87

[a] sd = standard deviation; sem = std. error of the mean; 95% C.I = Confidence interval on 5% threshold; Asfc = Area-scale fractal complexity; epLsar = exact proportion length-scale anisotropy of relief; Hasfc$_{81}$ = Heterogeneity of area-scale fractal complexity on 81 cells; Tfv = Textural fill volume at the scale of 2 μm; in μm^3 (see Scott et al., 2006 for details); [b] n = number of possible individuals.

Ψηφιακή βιβλιοθήκη Θεόφραστος – Τμήμα Γεωλογίας – Αριστοτέλειο Πανεπιστήμιο Θεσσαλονίκης

Ψηφιακή συλλογή Βιβλιοθήκη "ΘΕΟΦΡΑΣΤΟΣ" Τμήμα Γεωλογίας Α.Π.Θ

Table 4.7 Pairwise comparisons on dental microwear texture variables between genus; variables in bold indicate differences highlighted with Bonferroni adjustment[a].

	Mesopithecus monspessulanus		*Dolichopithecus ruscinensis*		*Colobus guereza*		*Piliocolobus badius*		*Presbytis melalophos*		*Semnopithecus entellus*		*Nasalis larvatus*		*Chlorocebus aethiops*		*Erythrocebus patas*		*Lophocebus albigena*	
Facet	*II*	*I*	*II*	*I*	*II*	*I*	*II*	*I*	*II*	*I*	*II*	*I*	*II*	*I*	*II*	*I*	*II*	*I*	*II*	*I*
Mesopithecus monspessulanus							Tfv(+)						Asfc(+)		Asfc(+)	Asfc(+)	Asfc(+) Tfv(+)	Asfc(+) Tfv(+)	Asfc(+) Tfv(+)	**Asfc**(+) Tfv(+)
Dolichopithecus ruscinensis					epLsar (+)	Asfc(–)	epLsar (+)	Asfc(–)	epLsar(+)						Asfc(+)		Asfc(+) epLsar(–)		Asfc(+) Tfv(+)	Asfc(+)
Colobus guereza			epLsar(–)	Asfc(+)						Asfc(+)					**Asfc**(+) epLsar(–)	Asfc(+)	**Asfc**(+)	Asfc(+) Tfv(+)	**Asfc**(+) epLsar(–)	**Asfc**(+) Tfv(+)
Piliocolobus badius	Tfv(–)		epLsar(–)	Asfc(+)											Asfc(+) epLsar(–)	Asfc(+)	**Asfc**(+) epLsar(–)	**Asfc**(+)	**Asfc**(+)	**Asfc**(+)
Presbytis melalophos			epLsar(–)			Asfc(–)									epLsar(–)		Asfc(+) epLsar(–)	Tfv(+)		
Semnopithecus entellus																	Asfc(+)			Asfc(+)
Nasalis larvatus	Asfc(–)																	Tfv(+)		Asfc(+) Tfv(+)
Chlorocebus aethiops	Asfc(–)	Asfc(–)	Asfc(–)		**Asfc**(–) epLsar(+)	Asfc(–)	**Asfc**(–) epLsar(+)	Asfc(–)	epLsar(+)											
Erythrocebus patas	Asfc(–) Tfv(–)	Asfc(–) Tfv(–)	Asfc(–) epLsar(+)		**Asfc**(–)	Asfc(–) Tfv(–)	**Asfc**(–)	**Asfc**(–)	Asfc(–) epLsar(+)	Tfv(–)	Asfc(–)			Tfv(–)						
Lophocebus albigena	Asfc(–) Tfv(–)	**Asfc**(–) Tfv(–)	Asfc(–) Tfv(–)	Asfc(–)	**Asfc**(–) epLsar(+)	**Asfc**(–) Tfv(–)	**Asfc**(–)	**Asfc**(–)						Asfc(–) Tfv(–)						

[a] (–) and (+) indicate values that are either lower or higher respectively for species in column compared to the one in row.

Ψηφιακή βιβλιοθήκη Θεόφραστος – Τμήμα Γεωλογίας – Αριστοτέλειο Πανεπιστήμιο Θεσσαλονίκης

Ψηφιακή συλλογή
Βιβλιοθήκη
"ΘΕΟΦΡΑΣΤΟΣ"
Τμήμα Γεωλογίας
Α.Π.Θ.

4.5 Discussion

The results suggest that the *Mesopithecus monspessulanus* molar specimens here analyzed possessed similar or slightly thicker enamel than the extant colobine species compared. This is consistent for both upper and lower molar comparisons. However, the range of values of the extant taxa seem to be biased by the low sample size, thus making the comparisons of relative enamel thickness somehow ambiguous. Furthermore, the fossil sample is very limited not enabling detailed statistical analysis. This makes it difficult to extract reliable conclusions, as enamel thickness shows a wide range of interspecific and intrageneric variation (Macho, 1994; Shellis et al., 1998; Schwartz, 2000; Kono, 2004; Smith et al., 2005, 2012; Olejniczak et al., 2008), even within the same tooth locus. Moreover, enamel thickness has also been demonstrated to be an evolutionary plastic trait, capable of rapid adaptation in response to functional dietary requirements (Hlusko et al., 2004; Kelley and Swanson, 2008; Pampush et al., 2013; Kato et al., 2014). Thus, caution is required when interpreting these results given the small samples analyzed for both extinct and extant taxa, which also preclude analyzing sexes or dental loci separately, and the effects of both sexual dimorphism (Alba et al., 2010; Fortuny et al., 2021). Future investigations with additional fossil and extant sample size and with comparisons on the species level if possible, will enable more safe conclusions regarding the potential adaptive function of the molar enamel thickness of both *Mesopithecus monspessulanus* and *Dolichopithecus ruscinensis*.

The two basic competing arguments regarding the adaptive function of thick enamel are: a) thick enamel helps to resist tooth crown failure in durophagous species that might result in the subsequent loss of the whole teeth (e.g. Kay, 1981; Lambert et al., 2004), b) thick enamel helps resist wear and abrasion in order to maintain masticatory competence over the lifespan of the animal (Molnar and Gantt, 1977; King et al., 2005). The fossil M^3 from Dorkovo (DKV480) exhibits similar values of $3DRET_{vol}$ with the modern colobines, being also within the range of *Macaca* and slightly higher value than *Chlorocebus*. This observation might suggest slightly more durophagous dietary preferences compared to its modern colobine relatives compared, which usually exhibit folivorous dietary habits (Rowe et al., 1996). However, evidence suggest that colobines consume various amounts of seeds and other mechanically challenging food resources throughout the year depending on factors such as seasonal and spatial availability of preferred food resources, as well as niche partitioning with other primate species (Davies et al., 1999; Tutin et al., 1997; Yeager, 1989). Nevertheless, this does not seem to be a newly derived ecological profile, as early colobine taxa in Africa exhibit anatomical modifications associated with arboreal and semi-terrestrial locomotion (Leakey, 1982; Hlusko, 2006, 2007; Nakatsukasa et al., 2010; Frost et al., 2015), also possibly influencing the dietary ecology of some taxa (Geissler, 2013; Williams and Geissler, 2014). This is also consistent with previous investigations on the Late Miocene European *Mesopithecus pentelicus*, which unlike most extant colobine taxa exhibited semi-terrestrial locomotion (Youlatos and Koufos, 2010; Youlatos et al., 2012), with a more opportunistic dietary behavior and dental morphology capable of processing a wide array of food resources (Merceron et al., 2009b; Thiery et al., 2017a, 2021).

The comparisons of enamel distribution between lower molar types revealed that *Mesopithecus monspessulanus* fossil molars analyzed here possess overall thicker enamel compared to *Dolichopithecus ruscinensis*. Setting dietary assessments aside, molar enamel thickness and distribution has been used for taxonomic and phylogenetic inferences (Kay, 1981; Gantt, 1982; Martin, 1985; Grine et al., 2005; Olejniczak et al., 2008; Zanolli et al., 2020). Hence, it is also possible that the observed differences in the overall distribution of enamel on the fossil molars could highlight phylogenetic differences instead of dietary adaptations. Alternatively, the thick overall enamel analogies of *Mesopithecus monspessulanus* along with its narrower molars compared to *Mesopithecus pentelicus* (e.g. Szalay & Delson, 1979), could

Ψηφιακή βιβλιοθήκη Θεόφραστος – Τμήμα Γεωλογίας – Αριστοτέλειο Πανεπιστήμιο Θεσσαλονίκης

Ψηφιακή συλλογή
Βιβλιοθήκη
"ΘΕΟΦΡΑΣΤΟΣ"
Τμήμα Γεωλογίας
Α.Π.Θ.

be a consequence of its overall smaller size. Be that as it may, both hypotheses need further investigation, and there is scarce information regarding the variation of enamel thickness within both fossil genera.

Notwithstanding the above, the thicker overall molar enamel in *Mesopithecus monspessulanus* might be suggestive of a more abrasive diet or a diet including more frequently hard food resources compared to *Dolichopithecus ruscinensis*. Still, based on evidence about their dietary behavior before death, as interpreted by dental microwear texture analysis, this seems not to be the case. As a matter of fact, the dietary behavior of *Mesopithecus monspessulanus* as inferred from microwear texture analysis resembles more closely modern colobine species, such as *Colobus guereza* and *Piliocolobus badius*, which primarily feed on leaves (Fig. 4.4), whereas *Dolichopithecus* shows a more mixed feeding behavior, ranging from folivorous habits to consumption of hard food objects. This suggests relatively different dietary niches for the two fossil colobines, with *Mesopithecus mospessulanus* foraging mainly on vegetation available in arboreal strata, supporting previous suggestions regarding the locomotor and positional behavior for this fossil species (Delson, 1973; Koufos, 2009b; Szalay & Delson, 1979 and references therein). It has been suggested that throughout the Turolian (9.0-5.3 Ma) there was a trend towards size decrease in *Mesopithecus,* consequently resulting in the overall smaller form of *Mesopithecus monspessulanus* (de Bonis et al., 1990; Koufos, 2009a, 2019). Thus, the available evidence so far and the results presented here, towards the end of Miocene and the beginning of Pliocene there is a selection towards smaller dimensions in the genus *Mesopithecus*, consequently evolving to the smaller form *Mesopithecus monspessulanus*, which may have affected its dietary ecology. However, it is also possible that selection could acted simultaneously in size and diet, or even diet could have been the primary aspect being selected and size following as a consequence. Therefore, it is possible that the morphological and dietary changes suggested for *Mesopithecus monspessulanus* might reflect an ecological shift towards a more arboreal niche, consistent with its inferred locomotor adaptations. To better understand the possible reasons behind this ecological shift, we need to further examine the available ecological information about the genus *Mesopithecus*, as well as available information regarding the primate communities of Europe from Late Miocene to Pliocene times.

The genus *Mesopithecus* appeared in Europe as early as the Late Miocene persisting throughout Pliocene and going extinct around Early Pleistocene (Koufos, 2009a, 2019). The latest Miocene and Early Pliocene were periods of significant changes in climate and geography in the Mediterranean area that affected significantly the existing ecosystems of southern Europe. While the latest Miocene marks a period of more arid conditions in Southern Europe as a result of the Mediterranean sea level drop due to major tectonic events (e.g. Hsü et al., 1973), the Early Pliocene marks a time period with more humid and warm conditions which led to the renewal of forested habitats (Koufos & Vasileiadou, 2015). Therefore, it is suggested that the appearance of *Mesopithecus monspessulanus* in the earliest Pliocene, most likely reflects adaptations to cope with the new environmental conditions of European environments (Koufos, 2019; Pradella & Rook, 2007). This is consistent with the results presented here and available evidence regarding its locomotor and positional behavior (Ciochon, 1993; Youlatos and Koufos, 2010). However, the most recent available evidence for *Mesopithecus monspessulanus* (Koufos, 2019), supports previous hypotheses that might have briefly coexisted with *Mesopithecus pentelicus* (e.g. Delson et al., 2005). This might be suggestive of a higher diversity of available ecological niches around 7.0–6.0 Ma and/or a more gradual transition in the new environmental conditions of the Early Pliocene. Nevertheless, it might be related to other ecological factors such as the effect of niche partitioning for space and resources within the primate communities of Europe in the latest Turolian.

Ψηφιακή βιβλιοθήκη Θεόφραστος – Τμήμα Γεωλογίας – Αριστοτέλειο Πανεπιστήμιο Θεσσαλονίκης

Ψηφιακή συλλογή
Βιβλιοθήκη
"ΘΕΟΦΡΑΣΤΟΣ"
Τμήμα Γεωλογίας
Α.Π.Θ

4.6 Appendix

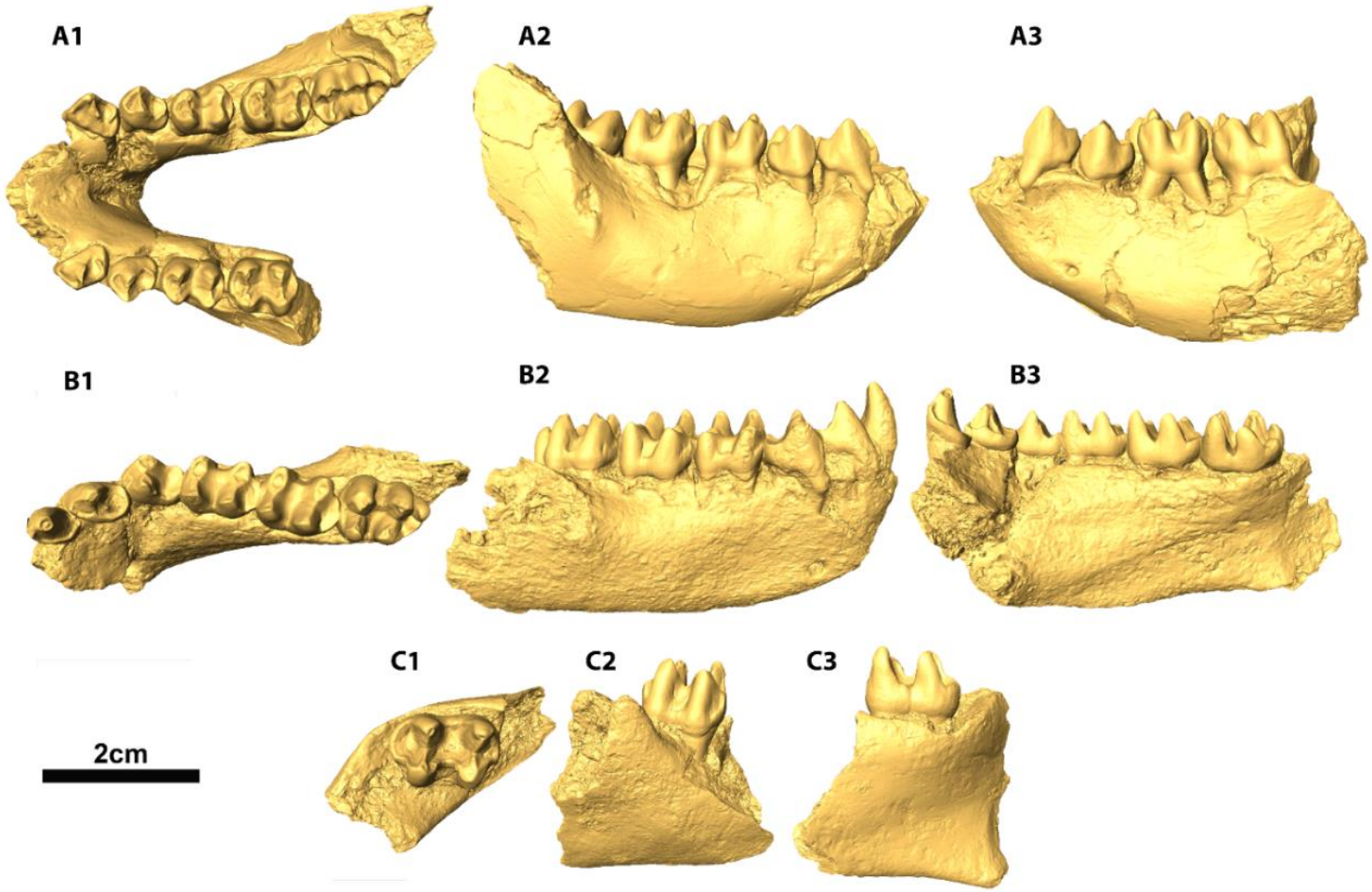

Fig. S1 The fossil specimens of *Mesopithecus monspessulanus* (A) and *Dolichopithecus ruscinensis* (B, C) used in this chapter. UM4043 in occlusal (A1), lateral dex (A2), lateral sin (A3), MEV–1 and MHNPn–PR39 in occlusal (B1, C1), buccal (B2, C2) and lingual (B3, C3).

Ψηφιακή βιβλιοθήκη Θεόφραστος – Τμήμα Γεωλογίας – Αριστοτέλειο Πανεπιστήμιο Θεσσαλονίκης

Ψηφιακή συλλογή
Βιβλιοθήκη
"ΘΕΟΦΡΑΣΤΟΣ"
Τμήμα Γεωλογίας
Α.Π.Θ

Table S1 Enamel thickness measurements and variables used for the analysis[a].

ID	Taxon	Tooth	Wear grade[b]	EVOL (mm^3)	EDJS (mm^2)	VCDP (mm^3)	$3DAET_{vol}$ (mm)	$3DRET_{vol}$	Institutions	Voxel size (µm)
DKV480	*M. monspessulanus*	M^3	1B	62.10	88.76	75.97	0.70	16.52	NHMS	11.33
AMNH:M:103458	*N.larvatus*	M^3	4B	54.09	78.68	57.39	0.68	17.82	AMNH	54.71
AMNH:M:103468	*N.larvatus*	M^3	4B	63.23	103.52	84.22	0.61	13.93	AMNH	62.61
AMNH:M:70063	*Ce. torquatus*	M^3	0	116.06	11.67	131.64	1.05	20.61	AMNH	117.96
UM 4043	*Me. monspessulanus*	M_2	1B	47.97	79.86	70.41	0.60	14.55	ISEM	26.16
UM 4043	*Me. monspessulanus*	M_3	0	54.36	85.12	67.72	0.64	15.67	ISEM	26.16
MHNPn–PR39	*D. ruscinensis*	M_2	4B	119.01	184.18	203.00	0.65	10.99	MNHNP	9.24
MEV–1	*D. ruscinensis*	M_3	0	154.79	164.19	162.33	0.94	17.28	LGPUT	40.10
AMNH:M:90328	*S. entellus*	M_2	3B	17.76	45.06	25.02	0.39	13.47	AMNH	52.20
AMNH:M:90328	*S. entellus*	M_3	0	19.01	47.48	21.80	0.40	14.33	AMNH	52.20
AMNH:M:52607	*L. albigena*	M_2	1B	47.05	59.14	45.09	0.80	22.35	AMNH	91.92
AMNH:M:52607	*L. albigena*	M_3	1B	52.49	59.40	45.93	0.88	24.67	AMNH	91.92
AMNH:M:52613	*L. albigena*	M_2	1B	51.00	63.08	50.00	0.81	21.94	AMNH	93.16
AMNH:M:52613	*L. albigena*	M_3	1B	52.94	59.79	56.92	0.89	23.01	AMNH	93.16
AMNH:M:70063	*Ce. torquatus*	M_2	0	126.36	119.66	125.54	1.06	21.08	AMNH	117.96
AMNH:M:70063	*Ce. torquatus*	M_3	0	146.01	13.96	165.53	1.12	20.30	AMNH	117.96
1972–302	*Ce. torquatus*	M_2	2B	2.08	44.28	25.91	0.45	15.32	MNHN	N/A
1972–328	*Ce. torquatus*	M_2	2B	29.48	56.23	35.90	0.52	15.89	MNHN	N/A
2002–105	*M. leucophaeus*	M_2	2B	171.98	19.10	217.71	0.91	15.03	PALEVOPRIM	N/A
1893–269	*M. leucophaeus*	M_2	2B	262.35	293.35	387.48	0.89	12.26	PALEVOPRIM	N/A
1969–388	*Co. guereza*	M_2	0	54.91	96.81	85.76	0.57	12.86	MNHN	N/A

[a]EVOL = Volume of the enamel cap; EDJS = Enamel–dentine junction surface; VCDP = Volume of the coronal dentine; $3DAET_{vol}$ = 3D volumetric average enamel thickness; $3DRET_{vol}$ = 3D volumetric relative enamel thickness; [b]Wear grades following the scoring system of Delson (1973).

Ψηφιακή βιβλιοθήκη Θεόφραστος – Τμήμα Γεωλογίας – Αριστοτέλειο Πανεπιστήμιο Θεσσαλονίκης

Ψηφιακή συλλογή Βιβλιοθήκη "ΘΕΟΦΡΑΣΤΟΣ" Τμήμα Γεωλογίας

Table S2 Raw dental microwear texture data for *Mesopithecus monspessulanus* and *Dolichopithecus*[a].

Filename	Taxon	Locality	Asfc	epLsar(x10^3)	HAsfc$_{81}$	Tfv
DKV483–UM3–dex–f4	*D. ruscinensis*	Dorkovo	1.974	4.41	0.304	30697.4
DKV483–UM3–dex–f9	*D. ruscinensis*	Dorkovo	1.484	3.94	0.209	27009.8
DKV078–lm3–dex–f5	*D. ruscinensis*	Dorkovo	0.853	2.80	0.682	28886.8
DKV078–lm3–dex–f9	*D. ruscinensis*	Dorkovo	3.199	4.36	0.976	51084.1
MEV1–lm2–sin–f11	*D. ruscinensis*	Megalo Emvolo	0.755	3.05	0.481	30804.0
MEV1–lm2–sin–f5	*D. ruscinensis*	Megalo Emvolo	0.613	7.52	0.504	24300.3
FSL40992–lm1–dex–f11	*D. ruscinensis*	Perpignan	1.419	0.92	0.673	21452.1
FSL40992–lm1–dex–f6	*D. ruscinensis*	Perpignan	2.723	2.17	0.615	21055.5
FSL41045–lm2–sin–f5	*D. ruscinensis*	Perpignan	2.049	1.83	0.975	49600.0
FSL41045–lm2–sin–f9	*D. ruscinensis*	Perpignan	1.365	4.22	0.628	38004.3
FSL41288–lm2–sin–f6	*D. ruscinensis*	Perpignan	0.444	1.08	3.459	23537.6
FSL41288–lm2–sin–f9	*D. ruscinensis*	Perpignan	1.138	3.26	0.491	56432.2
FSL49993–UM2–sin–f4	*D. ruscinensis*	Perpignan	0.663	1.53	0.340	34642.6
FSL49993–UM2–sin–f9	*D. ruscinensis*	Perpignan	1.489	0.56	0.414	49484.8
FSL49994–UM3–sin–f4	*D. ruscinensis*	Perpignan	2.555	1.90	0.392	15724.3
FSL49994–UM3–sin–f9	*D. ruscinensis*	Perpignan	2.626	3.66	0.492	46246.9
FSL49998–lm3–sin–f6	*D. ruscinensis*	Perpignan	2.555	4.13	0.589	48299.6
FSL49998–lm3–sin–f9	*D. ruscinensis*	Perpignan	3.436	6.56	1.199	43279.8
Pp1–lm2–dex–f5	*D. ruscinensis*	Perpignan	0.838	3.24	0.381	37159.1
Pp1–lm2–dex–f9	*D. ruscinensis*	Perpignan	1.978	1.74	0.858	25581.2
Pp11–lm2–dex–f6	*D. ruscinensis*	Perpignan	1.016	3.77	0.375	47333.9
Pp11–lm2–dex–f9	*D. ruscinensis*	Perpignan	3.670	3.20	0.625	18972.7
Pp13–UM3–sin–f3	*D. ruscinensis*	Perpignan	1.351	1.89	0.629	23556.0
Pp13–UM3–sin–f9	*D. ruscinensis*	Perpignan	1.204	2.01	0.626	54552.1
Pp28–lm3–sin–f6	*D. ruscinensis*	Perpignan	0.911	2.33	0.354	24406.4
Pp28–lm3–sin–f9	*D. ruscinensis*	Perpignan	2.381	2.21	0.580	39959.6
Pp29–lm3–sin–f5	*D. ruscinensis*	Perpignan	0.987	3.29	0.508	49989.9
Pp29–lm3–sin–f9	*D. ruscinensis*	Perpignan	1.532	7.44	0.366	31201.4
Pp4–UM2–sin–f3	*D. ruscinensis*	Perpignan	0.838	5.63	0.257	44694.4
Pp4–UM2–sin–f9	*D. ruscinensis*	Perpignan	0.785	1.06	0.415	30787.5
Pp5–lm1–sin–f5	*D. ruscinensis*	Perpignan	2.977	6.14	0.717	38184.7
Pp5–lm1–sin–f9	*D. ruscinensis*	Perpignan	1.027	4.40	0.891	8207.3
PR34–UM2–dex–f3	*D. ruscinensis*	Perpignan	0.456	3.94	0.322	44407.1
PR34–UM2–dex–f9	*D. ruscinensis*	Perpignan	0.295	2.80	0.383	20464.9
PR36–UM3–sin–f4	*D. ruscinensis*	Perpignan	0.868	4.36	0.436	31863.8
PR36–UM3–sin–f9	*D. ruscinensis*	Perpignan	1.265	3.05	0.386	35829.2
PR39–lm2–sin–f6	*D. ruscinensis*	Perpignan	0.928	7.52	0.330	39516.2
PR39–lm2–sin–f9	*D. ruscinensis*	Perpignan	1.885	0.92	0.534	41208.8
723–SM1–lm1s–f11	*D. ruscinensis*	Măluşteni	2.885	2.17	0.506	49882.9
723–SM1–lm1s–f6	*D. ruscinensis*	Măluşteni	2.152	1.83	0.754	27499.8
Taraclia–lm2d–f9	*D. ruscinensis*	Taraclia	0.834	4.22	0.475	25589.4
DKV82–lm1–sin–f5	*D. ruscinensis*	Dorkovo	0.195	1.08	0.266	26378.9
FM1739–lm2–dex–f6	*D. balcanicus*	Tenevo	0.312	3.26	0.301	41782.6
FM1739–lm2–dex–f9	*D. balcanicus*	Tenevo	0.377	1.53	0.316	31463.6
DKV480–UM3–sin–f3	*M. monspessulanus*	Dorkovo	0.346	0.56	1.448	3624.0
DKV480–UM3–sin–f9	*M. monspessulanus*	Dorkovo	0.230	1.90	0.247	0
Vj130–lm2–dex–f6	*M. monspessulanus*	Villafranca d"Asti	3.022	3.66	0.531	21887.2
Vj130–lm2–dex–f9	*M. monspessulanus*	Villafranca d"Asti	4.609	4.13	0.525	38644.0
Vj87–lm2–dex–f6	*M. monspessulanus*	Villafranca d"Asti	0.681	6.56	0.390	18226.6
Vj87–lm2–dex–f9	*M. monspessulanus*	Villafranca d"Asti	0.723	3.24	0.916	23991.9
UM4017–lm2–dex–f6b	*M. monspessulanus*	Montpellier	0.368	1.74	0.610	26114.1
UM4017–lm2–dex–f9b	*M. monspessulanus*	Montpellier	0.199	3.77	0.598	4156.9
UM4018–lm3–dex–f5	*M. monspessulanus*	Montpellier	0.601	3.20	0.545	18467.2
UM4018–lm3–dex–f9	*M. monspessulanus*	Montpellier	0.978	1.89	0.843	31976.5
UM4019–lm2–sin–f6	*M. monspessulanus*	Montpellier	0.679	2.01	0.749	25577.0
UM4019–lm2–sinvf9	*M. monspessulanus*	Montpellier	0.700	2.33	0.478	746.1
UM4043–lm2–sin–f11	*M. monspessulanus*	Montpellier	1.998	2.21	0.776	27574.7
UM4043–lm2–sin–f6	*M. monspessulanus*	Montpellier	0.442	3.29	0.518	43759.1
DIT22–lm2–sin–f5	*M. monspessulanus*	Dytiko	0.725	7.44	0.401	42848.5
DIT22–lm2–sin–f9	*M. monspessulanus*	Dytiko	1.344	5.63	0.478	48528.7
FSL49990–lm3–dex–f5	*M. monspessulanus*	Montpellier	0.815	1.06	0.444	33213.0
FSL49990–lm3–dex–f9	*M. monspessulanus*	Montpellier	0.738	6.14	0.766	43865.5
MP88i–lm1–dex–f9	*M. monspessulanus*	Montpellier	1.788	4.40	0.765	60072.8

[a] Asfc = area scale fractal complexity; epLsar = exact proportion length–scale anisotropy of relief; Smc = scale of maximal complexity, Hasfc$_{9,36,81}$ = heterogeneity of area–scale fractal complexity on 9, 36 and 81 cell.

Ψηφιακή βιβλιοθήκη Θεόφραστος – Τμήμα Γεωλογίας – Αριστοτέλειο Πανεπιστήμιο Θεσσαλονίκης

Ψηφιακή συλλογή
Βιβλιοθήκη
"ΘΕΟΦΡΑΣΤΟΣ"
Τμήμα Γεωλογίας
Α.Π.Θ.

Chapter 5. Dietary reconstruction of Plio-Pleistocene European *Paradolichopithecus* using dental topographic and dental microwear texture analysis

5.1 Introduction

Papionins have a long fossil record in the Palearctic (e.g. Eurasia), extending from the late Miocene up to the Late Pleistocene (Szalay and Delson, 1979; Ardito and Mottura, 1987; Elton and O'Regan, 2014). They are mainly represented by the genus *Macaca* and it is presumed that all fossil European macaques are closely related to the living Barbary macaque (e.g. *Macaca sylvanus*) (Alba et al., 2008; Delson, 1980; Szalay & Delson, 1979; but see Rook & O'Higgins, 2005; Zoboli et al., 2016). Besides the genus *Macaca*, two more cercopithecine genera occurred in Eurasia from the Middle Pliocene to the Early Pleistocene (i.e., the time period referred to as Villafranchian Land Mammal Age in the European literature): *Paradolichopithecus* and *Procynocephalus* (Szalay and Delson, 1979; Takai et al., 2008).

Paradolichopithecus represents one of the largest fossil cercopithecines recorded in Eurasia (24.0 to 44.0kg for males and 19.0 to 39.0kg depending on the fossil species, for more details see Delson et al., 2000). Still it remains sparsely documented mostly due to the limited published material. To date, four species are recognized: *Paradolichopithecus arvernensis*, from Sèneze, France (Depéret, 1929), also found in Vialette, France (Delson, 1973), La Puebla de Valverde, Spain (Aguirre and Soto, 1978) and Vatera, Greece (de Vos et al., 2002); *Paradolichopithecus geticus* from Valea Graunceanului, Romania (Necrasov et al., 1961; Terhune et al., 2020); *Paradolichopithecus sushkini* (Trofimov, 1977) from Kuruksay, Tadjikistan, and the more recently assigned *Paradolichopithecus gansuensis* from Longdan, Gansu, China (Qiu et al., 2004). Additional material attributed to this genus comes from Măluşteni, Romania (Delson, 1973), Almenara-Casablanca 1, Canal Negre I, Moreda 1 and Cova Bonica, Spain (Delson et al., 2014; Marigó et al., 2014) and more recently from Dafnero-3, Greece (Kostopoulos et al., 2018) and Ridjake, Serbia (Radović et al., 2019). The oldest occurences are from Romania, Spain and possibly France, dated around 3.2 Ma (Eronen and Rook, 2004). Delson and Nicolaescu-Plopsor (1975), and Szalay and Delson (1979) suggested synonymizing the French and Romanian species, while Jablonski (2002) synonymized the species from Tadjikistan with *Paradolichopithecus arvernensis*. More recently it was suggested that *Paradolichopithecus* from Cova Bonica and Moreda may represent an earlier smaller variety (e.g. *Paradolichopithecus sp.*), potentially distinct from other European species (Delson et al., 2014; Marigó et al., 2014).

Procynocephalus represents another large cercopithecine genus from the Plio-Pleistocene of Asia. Two species are formally distinguished, *Procynocephalus wimani* Schlosser, 1924 from China and *Procynocephalus subhimalayanus* von Meyer, 1848 from India and Pakistan. Although the species from India is barely known (Verma, 1969; Williams and Holmes, 2012), more recent data from China enriched the available information (Takai et al., 2014). Jolly (1967) and Simons (1970) argued that *Paradolichopithecus* showed minor differences in dental morphology and size from *Procynocephalus*, suggesting that the former was a junior synonym for the latter. Conversely, Trofimov (1977) classified them as two different genera based on differences in some dental features. Still, the available fossil material is too limited for *Procynocephalus* (Szalay and Delson, 1979; Takai et al., 2008), prolonging the debate (e.g., Kostopoulos et al., 2018).

The phylogenetic relationships of both *Paradolichopithecus* and *Procynocephalus* are also controversial. The best known *Paradolichopithecus* is presumed as displaying a

Ψηφιακή βιβλιοθήκη Θεόφραστος – Τμήμα Γεωλογίας – Αριστοτέλειο Πανεπιστήμιο Θεσσαλονίκης

Ψηφιακή συλλογή
Βιβλιοθήκη
"ΘΕΟΦΡΑΣΤΟΣ"
Τμήμα Γεωλογίας

combination of cranio–dental characters more similar to macaques (Szalay & Delson, 1979; but see also Kostopoulos et al., 2018), whereas postcranial long bones suggest baboon–like features, reflecting its terrestrial locomotor habits (Frost et al., 2005; Jablonski, 2002; Szalay & Delson, 1979; but see also Sondaar, 2006; Van der Geer & Sondaar, 2002). Others examined the presence and development of paranasal sinuses, as among Old World monkeys, macaques are the only species that possess such features (Nishimura et al., 2007, 2010, 2014; Takai et al., 2008). However, evidence also suggest that paranasal pneumatization might have independently evolved a minimum of two and possibly three times in cercopithecoids (e.g. Rae, 2008). Be that as it may, the discussion still continues.

All Asian records of *Paradolichopithecus* appear to be Early Pleistocene in age (i.e. ~2.6 Ma) (Takai et al., 2008). Around that time period, *Paradolichopithecus* was widely distributed across Eurasia. However, around 2.5 Ma the global climate started to shift towards more open, cooler and drier conditions (Bibi et al., 2013; Jablonski, 1993; Kostopoulos et al., 2007; Lawrence et al., 2010; McLaren & Wallace, 2010), which promoted the expansion of grasslands and prairies across Eurasian mid–latitudes (Agustí & Antón, 2002). In the increasingly challenging environments of the Plio–Pleistocene *Paradolichopithecus* was widely distributed from western Europe to Tadjikistan to China, further demonstrating the ability of Old World monkeys to exploit various and diverse habitats (Elton, 2007). It is speculated that the replacement of forests by open grasslands and prairies, possibly facilitated the rapid expansion and wide distribution of *Paradolichopithecus* throughout Eurasia during Early Pleistocene (MN17) (Williams & Holmes, 2011; Kostopoulos et al., 2018). Nevertheless, around ~1.6 Ma both *Paradolichopithecus* (along with *Procynocephalus*) went extinct. The relatively sudden disappearance of *Paradolichopithecus* still remains unresolved, as it seems that it is not associated with any major environmental change or faunal turnover (Kostopoulos et al., 2018), and raises further questions regarding its ecological profile. The limited available information depicts a large cercopithecine mainly terrestrial (Szalay and Delson, 1979; Frost et al., 2005; Sondaar, 2006), which probably possessed a wide dietary repertoire (Plastiras et al., 2019; Williams & Holmes, 2011). However, detailed investigation regarding the latter ecological aspect of *Paradolichopithecus* is still pending.

The present chapter aims to explore the feeding ecology of *Paradolichopithecus*, by applying dental topographic and dental microwear texture analyses (DMTA). Dental topographic analysis is used to explore the potential dental adaptations of *Paradolichopithecus* associated with diet, by characterizing morphological aspects of its molars (e.g. relief, sharpness, complexity). Dental microwear texture analysis is used as a proxy to identify the dietary habits of *Paradolichopithecus* over a period of time prior to its death. Commonly, microwear analyses on primates are performed on dental facets resulting from Phase II stroke of mastication instead of Phase I, as it was suggested that they better discriminate primates with differing diets (Krueger et al., 2008). In this analysis we include both Phase I and II facets as they bear complementary signals (Merceron et al., 2021).

5.2 Material

5.2.1. Dental topographic and enamel thickness analysis

The analysis is focused on a left M^2 of *Paradolichopithecus*, deriving from the fossil cranium of a subadult female individual which lacks canines and incisors but possess all posterior dentition. The molar specimen retains minimal wear, corresponding to wear grade 2B (Delson, 1973). It was discovered in the Lower Pleistocene fossil site of Dafnero-3 (DFN3–150) in Northern Greece (see Kostopoulos et al., 2018 for detailed description), dated to 2.3 Ma (Benammi et al., 2020), and it is housed in the Museum of Geology-Palaeontology-Palaeoanthropology, University of Thessaloniki (LGPUT). The comparative sample consists of

Ψηφιακή βιβλιοθήκη Θεόφραστος – Τμήμα Γεωλογίας – Αριστοτέλειο Πανεπιστήμιο Θεσσαλονίκης

Ψηφιακή συλλογή
Βιβλιοθήκη
"ΘΕΟΦΡΑΣΤΟΣ"

a total of 20 M^2s (Table S1 Appendix 5.7), from six extant papionin genera: *Papio* (*Papio anubis*, *n* = 4; *Papio cynocephalus*, *n* = 1; *Papio hamadryas*, *n* = 1), *Macaca* (*Macaca sylvanus*, *n* = 2), *Mandrillus* (*Mandrillus leucophaeus*, *n* = 2), *Theropithecus* (*Theropithecus gelada*, *n* = 2), *Lophocebus* (*Lophocebus albigena*, *n* = 4; *Lophocebus atterimus*, *n* = 1) and *Cercocebus* (*Cercocebus torquatus*, *n* = 1; *Cercocebus sp.*, *n* = 1; *Cercocebus galeritus*, *n* = 1). The specimens are housed in the osteological collection of Royal Museum of Central Africa Tervuren (Belgium), Muséum National d'Histoire Naturelle Paris (France), and Laboratoire Paléontologie, Evolution Paléoécosystèmes, Paléoprimatologie (PALEVOPRIM) CNRS-Université de Poitiers (France) (Table 5.1).

Table 5.1 Modern sample used for dental topography with respective host institutions.

Taxa	*n*	ID	Institution
Lophocebus albigena	4	83_006_M_276, 90_042_M_301, 90_042_M_301, Cb4	RMCA, PALEVOPRIM
Lophocebus aterrimus	1	14113	RMCA
Cercocebus torquatus	1	81_07_M_44	RMCA
Cercocebus sp.	1	Cb2	PALEVOPRIM
Cercocebus galeritus	1	14486	RMCA
Macaca sylvanus	2	T150kV	MNHN
Theropithecus gelada	2	1969_449, 1969_450	MNHN
Mandrillus leucophaeus	2	1893_269, 2002_105	PALEVOPRIM
Papio anubis	4	MRAC_80_044_M101, C2, MRAC_90042_M226	RMCA, PALEVOPRIM
Papio hamadryas	1	MRAC_97_020_M004	RMCA

5.2.2. Dental microwear texture analysis

The fossil material used for dental microwear texture analysis consists of a total of seven *Paradolichopithecus* individuals (Table 5.2), derived from a total of four fossiliferous sites. The specimens from Senèze (FSL-41366, *n* = 1), Vatera in Lesvos island (PO-170, PO-114, *n* = 2), and Dafnero-3 (DFN3-150, *n* = 1), are assigned to *Paradolichopithecus arvernensis*. The fossil specimens from Romania derive from the sedimentary sequence of the Lower Pleistocene deposits Tetoiu–Bugiulesti in the middle valley of the Oltet river, which contains several fossiliferous horizons (see Radulescu et al., 2003; Terhune et al., 2020). In this sedimentary sequence, the fossil locality of Valea Graunceanului have yielded the fossil material of *Paradolichopithecus* (VGr/345, VGr/346, MO 20069, *n* = 3), which are tentatively assigned to *Paradolichopithecus geticus*. However, given the low total number of individuals for each fossil species, here the analysis is focused at the genus level. The fossil material is housed in Université de Lyon (France), Athens Museum of Palaeontology and Geology (Greece), Museum of Geology-Paleontology-Paleoanthropology of Aristotle University of Thessaloniki (Greece), Institute of Speleology "Emil Racovita" of Bucharest (Romania), and Olteniei Museum-Department of Natural Sciences of Craiova (Romania).

For the comparisons we use wild shot specimens from five species belonging to the five extant papionin genera: *Macaca fuscata (n* = 27), *Papio hamadryas* (*n* = 39), *Theropithecus gelada (n* = 20), *Mandrillus sphinx* (*n* = 33), and *Lophocebus albigena* (*n* = 14) (see Tables 5.2 and S2 Appendix 5.7). The sample of *Papio*, *Theropithecus* and *Lophocebus* derive from skeletal specimens housed in the Authority for Research and Conservation of Cultural Heritage in Addis Ababa (Ethiopia), Musée des Confluences in Lyon (France), Muséum National d'Histoire Naturelle de Paris (France), and Basel Natural History Museum (Switzerland). The sample of *Macaca* belongs to the collection of the Primate Research Institute of the University of Kyoto in Inuyama (Japan). These skeletal remains derived from three free-ranging populations found in different latitudes in Japan: 11 individuals from the northern population situated Aomori Prefecture (Tōhoku region), 12 from the central population situated in Nagano Prefecture (Chūbu region), and 4 from the southern population situated in the island of Yakushi-

Ψηφιακή βιβλιοθήκη Θεόφραστος – Τμήμα Γεωλογίας – Αριστοτέλειο Πανεπιστήμιο Θεσσαλονίκης

Ψηφιακή συλλογή Βιβλιοθήκη "ΘΕΟΦΡΑΣΤΟΣ" Τμήμα Γεωλογίας Α.Π.Θ

Table 5.2 Microwear texture variables descriptive statistics on Phase I, II facets of *Paradolichopithecus* and modern sample[a].

Taxa	**facet**	***n***	**Asfc**				**epLsar (x10^3)**				**Hasfc$_{81}$**				**Tfv**			
Extinct			Mean	stdev	sem	95% C.I	Mean	stdev	sem	95% C.I	Mean	stdev	sem	95% C.I	Mean	stdev	sem	95% C.I
Paradolichopithecus	*Phase II*	7	**1.443**	0.518	0.196	0.480	**3.417**	1.311	0.187	0.367	**0.627**	0.278	0.105	0.158	**41632.2**	9584.1	3622.4	8864.0
	Phase I	6	**2.080**	3.116	1.272	3.270	**3.935**	1.849	0.092	0.018	**0.520**	0.172	0.070	0.181	**16677.1**	14295.1	6093.1	15662.0
Modern																		
Theropithecus gelada	*Phase II*	20	**1.181**	0.731	0.163	0.343	**4.240**	1.903	0.095	0.186	**0.424**	0.135	0.030	0.059	**41824.8**	8776.7	1962.5	4108.0
	Phase I	20	**0.836**	0.407	0.091	0.191	**3.160**	1.383	0.069	0.135	**0.428**	0.145	0.032	0.063	**34655.6**	11756.3	2628.7	5502.0
Papio hamadryas	*Phase II*	39	**1.708**	1.055	0.166	0.338	**2.878**	1.494	0.038	0.075	**0.564**	0.201	0.031	0.062	**34123.7**	13846.7	2189.3	4429.0
	Phase I	39	**1.251**	0.702	0.111	0.225	**3.333**	1.674	0.083	0.164	**0.481**	0.142	0.022	0.044	**34409.1**	13449.1	2126.4	4301.0
Macaca fuscata	*Phase II*	28	**2.418**	1.285	0.242	0.499	**3.320**	1.374	0.050	0.099	**0.484**	0.319	0.060	0.118	**32974.2**	13201.2	2494.7	5119.0
	Phase I	28	**1.609**	0.764	0.144	0.296	**3.767**	2.096	0.104	0.205	**0.433**	0.176	0.033	0.065	**36870.4**	924.7	1746.3	3582.0
Lophocebus albigena	*Phase II*	14	**2.613**	1.290	0.345	0.676	**3.033**	1.822	0.130	0.255	**0.735**	0.263	0.070	0.138	**45212.5**	1126.7	3009.6	5898.74
	Phase I	14	**1.974**	1.038	0.277	0.544	**3.297**	1.440	0.072	0.141	**0.670**	0.260	0.069	0.136	**28618.3**	10203.0	2726.9	5344.7
Mandrillus sphinx	*Phase II*	33	**1.810**	0.773	0.206	0.405	**4.205**	1.729	0.052	0.102	**0.559**	0.350	0.093	0.119	**47838.5**	10924.5	2919.7	5722.6
	Phase I	33	**1.536**	0.843	0.147	0.287	**3.609**	1.940	0.097	0.190	**0.511**	0.191	0.033	0.065	**46883.1**	8436.8	1468.7	2878.6

[a] sd = standard deviation; sem = std. error of the mean; 95% C.I = Confidence interval on 5% threshold; Asfc = Area-scale fractal complexity; epLsar = exact proportion length-scale anisotropy of relief; Hasfc$_{81}$ = Heterogeneity of area-scale fractal complexity on 81 cells, Tfv = Textural fill volume at the scale of 2 μm; in μm^3 (see Scott et al., 2006 for details).

Ψηφιακή βιβλιοθήκη Θεόφραστος – Τμήμα Γεωλογίας – Αριστοτέλειο Πανεπιστήμιο Θεσσαλονίκης

Ψηφιακή συλλογή
Βιβλιοθήκη
"ΘΕΟΦΡΑΣΤΟΣ"
Τμήμα Γεωλογίας
Α.Π.Θ.

ma which is one of the Ōsumi Islands in Kagoshima Prefecture. The sample of *Mandrillus sphinx* derives from a free-ranging population living in Lékédi Park and surrounding areas, in southern Gabon (e.g. Percher et al., 2018).

5.3 Statistical analysis

5.3.1. Dental topographic and enamel thickness analysis

The relationships among variables (3DRETvol, 3DRETgeo, ACS, OPCR, Inclination, LRFI, DNE, ARC) in the modern sample were evaluated using Pearson's correlation test including also bootstrap resampling (n = 1000). Variable differences between modern genera were assessed using a Kruskal-Wallis test with the significance level set at 0.05 followed by pairwise comparisons with Bonferroni adjustment to take into account possible biases due to multiple testing. All computations were performed using SPSS v. 22 (IBM Corp, 2013.) and '*stats'* package of R v. 3.6 (R Core Team, 2013).

5.3.2. Dental microwear texture analysis

The dispersion of each texture variable for each species was calculated for both dental facet types using Ln-Levine's test (Plavcan & Cope 2001). Specifically, it was computed by applying the Ln-Levine's test on the raw texture variable data of each individual (X'=|ln(X)-median(ln(X))|, where X represents the value of the texture variable and X' the new resulting value; e.g, Asfc'=|ln(Asfc)-median(ln(Asfc))|, see Box 2 in Plavcan and Cope, 2001 for more details). Then, all microwear texture variables were box-cox transformed to avoid normality assumption violations in parametric tests (Conover and Iman, 1981).

Texture variable differences among genera were assessed using two Kruskal-Wallis tests (one for each dental facet type) with the significance level set at 0.05 including pairwise comparisons with Bonferroni adjustment. Similarly, variable dispersion differences among genera were assessed using two Kruskal-Wallis tests (one for each dental wear facet type) with the significance level set at 0.05 including pairwise comparisons with Bonferroni adjustment. Lastly, given the number of texture variables considered here and the fact that some are likely correlated (Ungar et al., 2019), two principal component analyses were performed (one for each facet type) using the texture variable data (i.e. Asfc, epLsar, Tfv, $Hasfc_{81}$) to reduce the number of dimensions considered. The resulting principal component scores (i.e. PC1, PC2, PC3, PC4) were box-cox transformed and used to perform two single analyses of variance (ANOVAs) (one for each dental wear facet type), followed by pairwise comparisons using the combination of Tukey's Honest Significant Difference (HSD) and the less conservative Fisher's Least Significant Difference (LSD) following Scott et al., (2012). Computations were performed using SPSS v. 22 (IBM Corp , 2013.) and PAST v. 3.22 (Hammer et al., 2001).

5.4 Results

5.4.1. Dental topographic and enamel thickness analysis

The Pearson's test revealed that significant correlations exist between variables in the extant comparative sample of papionins (Table 5.3). Inclination (λ) is significantly correlated with the relief index (LRFI), area-relative curvature (ARC), Dirichlet normal energy (DNE) and 3D relative geometric enamel thickness ($3DRET_{geo}$). The relief index (LRFI) is also correlated with area–relative curvature (ARC), Dirichlet normal energy (DNE) and 3D relative enamel thickness (both $3DRET_{vol}$ and $3DRET_{geo}$). Additionally, area-relative curvature (ARC) is correlated with Dirichlet normal energy (DNE), orientation patch count rotated (OPCR), 3D

Ψηφιακή βιβλιοθήκη Θεόφραστος – Τμήμα Γεωλογίας – Αριστοτέλειο Πανεπιστήμιο Θεσσαλονίκης

Ψηφιακή συλλογή Βιβλιοθήκη "ΘΕΟΦΡΑΣΤΟΣ" Τμήμα Γεωλογίας

relative geometric enamel thickness ($3DRET_{geo}$) and absolute crown strength (ACS). Moreover, orientation patch count rotated (OPCR) is correlated with Dirichlet normal energy (DNE), 3D relative enamel thickness ($3DRET_{vol}$ and $3DRET_{geo}$) and absolute crown strength (ACS). Lastly, the 3D relative enamel thickness ($3DRET_{vol}$ and $3DRET_{geo}$) is correlated with absolute crown strength (ACS).

The Kruskal-Wallis analysis of variance revealed significant differences in 3DRETvol, 3DRETgeo, OPCR, ACS and ARC (Table 5.4). *Papio* differs significantly from *Macaca* having higher ARC and OPCR (Table 5.4). Moreover, *Papio* possess higher ARC and ACS comparedto *Cercocebus,* and higher OPCR, ACS, and lower $3DRET_{vol}$, $3DRET_{geo}$ than *Lophocebus* (Table 5.4). *Mandrillus* has significantly higher values of ARC and OPCR compared to *Macaca,* and higher ARC and lower 3DRETvol than *Cercocebus* (Table 5.4).

Table 5.3 Pearson's correlation test on enamel thickness and topographic variables. Pairs of variables that are significantly correlated are shown in bold.

		λ	**LRFI**	**ARC**	**DNE**	**OPCR**	**$3DRET_{vol}$**	**$3DRET_{geo}$**	**ACS**
λ	corr.		–0.986[b]	–0.552[a]	–0.662[b]	–0.360	–0.425	0.571[b]	–0.408
	sig.		**< 0.05**	**< 0.05**	**< 0.05**	0.119	0.062	**< 0.05**	0.074
LRFI	corr.	–0.986		0.469[a]	0.599[b]	0.325	–0.452	–0.601[b]	0.389
	sig.	**< 0.05**		**< 0.05**	**< 0.05**	0.162	**< 0.05**	**< 0.05**	0.090
ARC	corr.	–0.552[a]	0.469[a]		0.784[b]	0.722	–0.415	–0.505[a]	0.455[a]
	sig.	**< 0.05**	**< 0.05**		**< 0.05**	**< 0.05**	0.069	**< 0.05**	**< 0.05**
DNE	corr.	–0.662[b]	0.599[b]	0.784[b]		0.771[b]	–00.347	–0.423	0.331
	sig.	**< 0.05**	**< 0.05**	**< 0.05**		**< 0.05**	.133	0.063	0.155
OPCR	corr.	–0.360	0.325	0.722[b]	0.771[b]		–0.489[a]	–0.542[a]	0.459[a]
	sig.	0.119	0.162	**< 0.05**	**< 0.05**		**< 0.05**	**< 0.05**	**< 0.05**
$3DRET_{vol}$	corr.	0.425	–0.452[a]	–0.415	–0.347	–0.489[a]		0.953[b]	–0.700[b]
	sig.	0.062	**p<0.05**	0.069	0.133	**< 0.05**		**< 0.05**	**< 0.05**
$3DRET_{geo}$	corr.	0.571[b]	–0.601[b]	–0.505[a]	–0.423	–0.542[a]	0.953[b]		–0.744[b]
	sig.	**< 0.05**	**< 0.05**	**< 0.05**	0.063	**< 0.05**	**< 0.05**		**< 0.05**
ACS	corr.	–0.408	0.389	0.455[a]	0.331	0.459[a]	–0.700[b]	–0.744[b]	
	sig.	0.074	0.090	**< 0.05**	0.155	**< 0.05**	**< 0.05**	**< 0.05**	

[a]Correlation is significant at the .05 level (2-tailed); [b]Correlation is significant at the .01 level (2-tailed).

Table 5.4 Pairwise comparisons of enamel thickness and dental topographic variables among genera. Variables in bold signify differences highlighted with Bonferroni adjustment[a].

Genus	*Papio*	*Mandrillus*	*Theropithecus*	*Macaca*	*Cercocebus*	*Lophocebus*
Papio				ARC(–), OPCR(–)	ARC(–), **ACS**(–)	OPCR(–), **ACS**(–), RET_{vol}(+), **RET_{geo}**(+)
Mandrillus				ARC(–), OPCR(–)	ARC(–), RET_{vol}(+)	OPCR(–), RET_{vol}(+), RET_{geo}(+)
Theropithecus					RET_{vol}(+), RET_{geo}(+)	RET_{vol}(+), RET_{geo}(+)
Macaca	ARC(+), OPCR(+)	ARC(+), OPCR(+)				
Cercocebus	ARC(+), **ACS**(+)	ARC(+), RET_{vol}(–)	RET_{vol}(–), RET_{geo}(–)			
Lophocebus	OPCR(+), **ACS**(+), RET_{vol}(–), **RET_{geo}**(–)	OPCR(+), RET_{vol}(–), RET_{geo}(–)	RET_{vol}(–), **RET_{geo}**(–)			

[a](–) and (+) indicate values that are either lower or higher respectively for species in column compared to the one in row.

Ψηφιακή βιβλιοθήκη Θεόφραστος – Τμήμα Γεωλογίας – Αριστοτέλειο Πανεπιστήμιο Θεσσαλονίκης

Ψηφιακή συλλογή
Βιβλιοθήκη
"ΘΕΟΦΡΑΣΤΟΣ"

The value of 3DRETvol places the *Paradolichopithecus* molar from Dafnero-3 (DFN3–150) within the range of *Papio*, while it is also placed close to the lower limit of the *Macaca* molar sample. Similarly, the value of $3DRET_{geo}$ places DFN3–150 fossil M^2 closer to *Papio*, yet in this case the fossil M^2 is also close to the upper limit of the *Mandrillus* molar sample (Fig. 5.1A, B). The values of ACS and OPCR places the DFN3–150 fossil M^2 within the range of the *Papio* molar sample, however, the value of the former metric shows considerable overlap among genera (Fig. 5.1C, D). The values of LRFI and λ place DFN3–150 fossil M^2 within the range of *Papio* and *Mandrillus* molar samples (Fig. 5.2A, B). The value of DNE places DFN3–150 fossil M^2 within the range of *Papio*, *Cercocebus* and *Lophocebus* molar samples, but this variable also shows high overlap between extant genera (Fig. 5.2C). Lastly, DFN3–150 fossil M^2 exhibits the highest ARC value of our molar sample, being close only to one *Papio* individual (Fig. 5.2D).

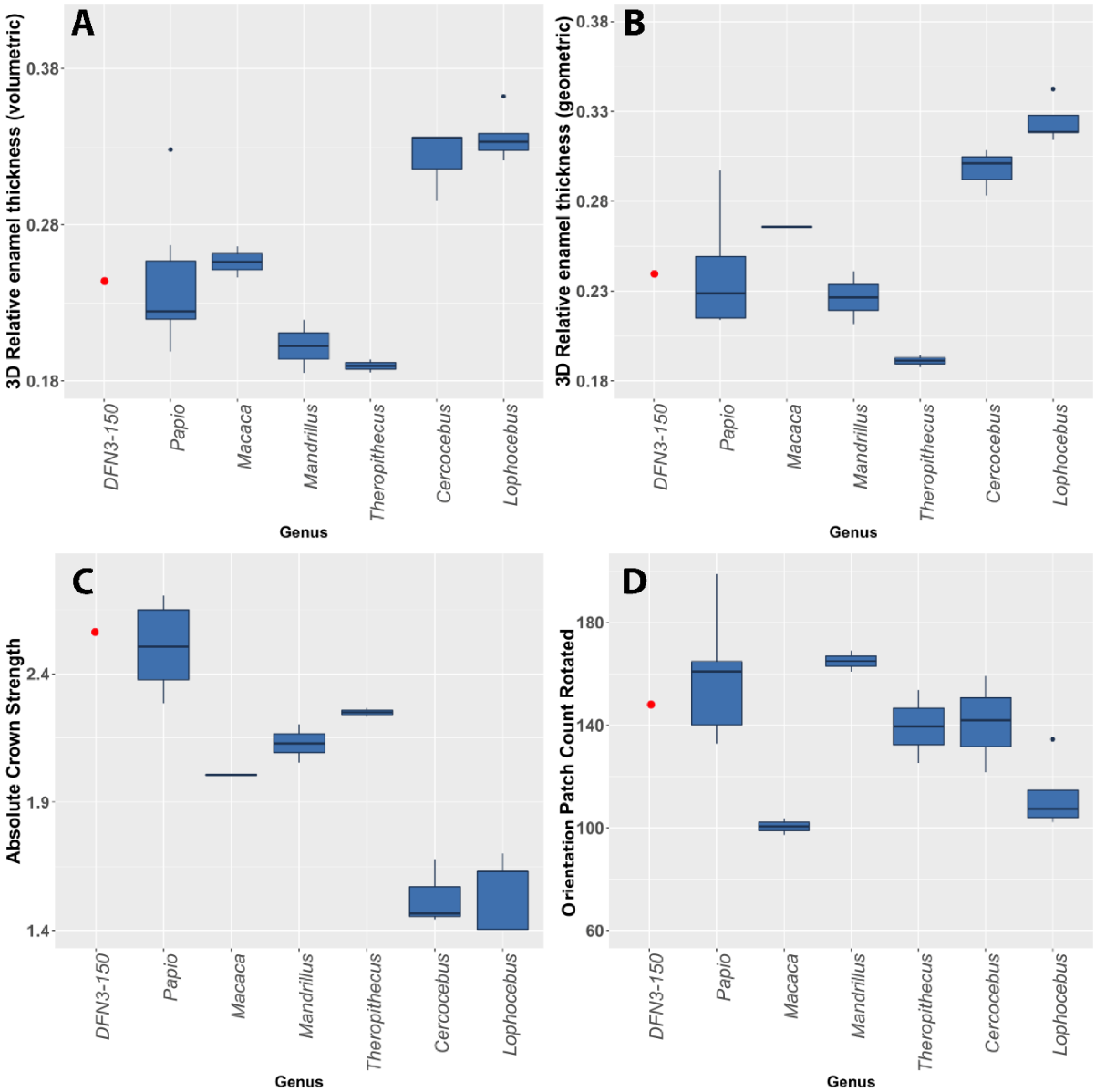

Fig. 5.1 Boxplots comparisons of 3D relative volumetric enamel thickness (**A**), 3D relative geometric enamel thickness (**B**), absolute crown strength (**C**), and orientation patch count rotated (**D**) between extant genera and *Paradolichopithecus* M^2 (DFN3–150).

Ψηφιακή βιβλιοθήκη Θεόφραστος – Τμήμα Γεωλογίας – Αριστοτέλειο Πανεπιστήμιο Θεσσαλονίκης

Ψηφιακή συλλογή
Βιβλιοθήκη
"ΘΕΟΦΡΑΣΤΟΣ"

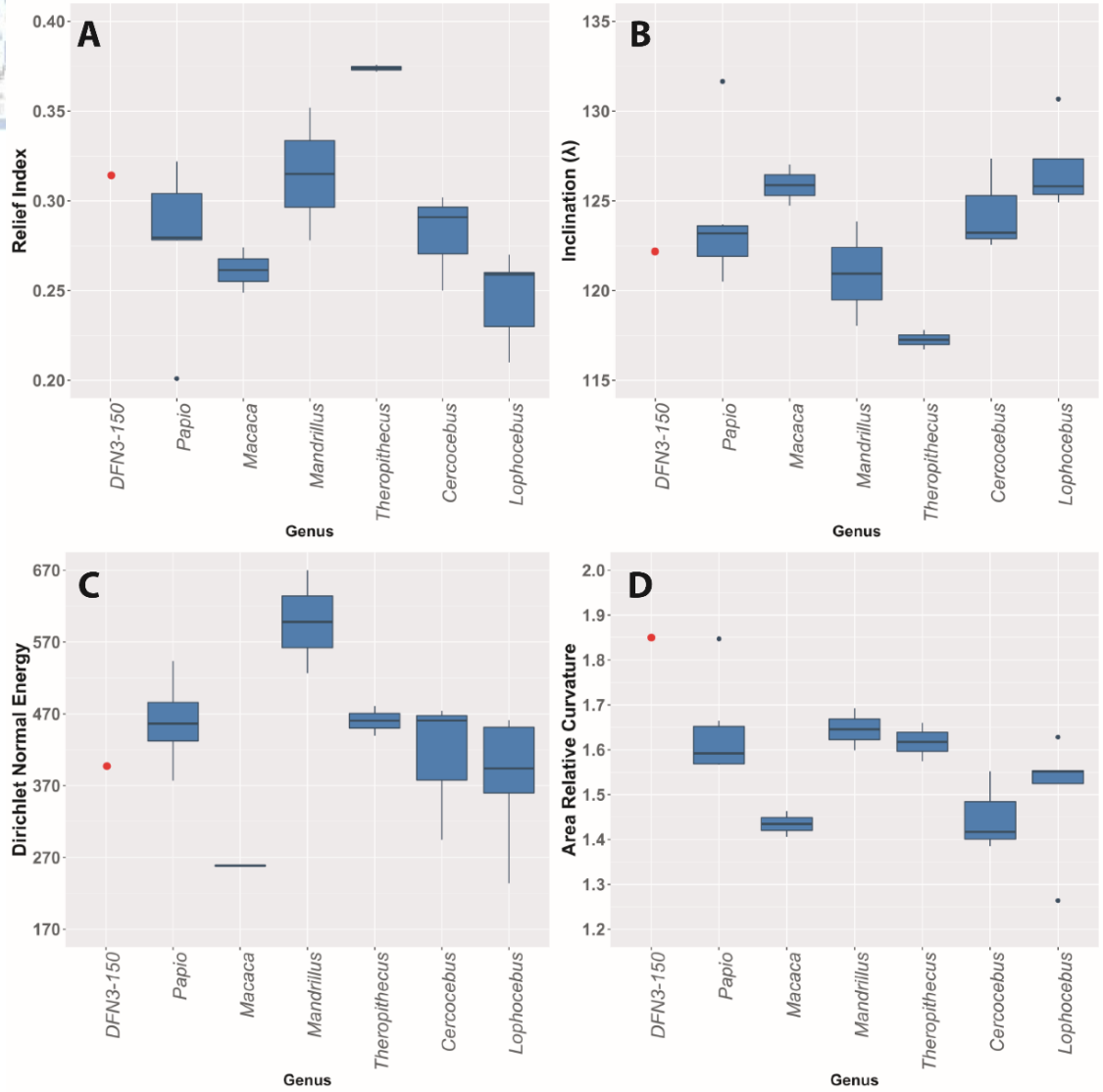

Fig. 5.2 Boxplots comparisons of relief index (**A**), inclination (**B**), Dirichlet normal energy (**C**) and area–relative curvature (**D**) between extant genera and *Paradolichopithecus* M^2 (DFN3–150).

5.4.2. Dental microwear texture analysis

The Kruskal-Wallis test on Phase II facets revealed significant variation in complexity (Asfc), anisotropy (epLsar), heterogeneity ($Hasfc_{81}$) and textural fill volume (Tfv) while on Phase I facets in complexity (Asfc), heterogeneity ($Hasfc_{81}$) and textural fill volume (Tfv) (Table S5 Appendix 5.7).

In Phase II facets, *Lophocebus*, *Macaca*, *Mandrillus* and *Papio* possess significantly higher mean values of complexity (Asfc) than *Theropithecus*, whereas *Macaca* exhibits higher values than *Papio* and *Lophocebus* than *Mandrillus* (Table 5.5). Furthermore, *Lophocebus* has significantly higher values of heterogeneity ($Hasfc_{81}$) than *Theropithecus* and *Mandrillus*, and higher than *Macaca* (Table 5.5). The values of anisotropy (epLsar) suggest significant differences only between *Papio* and *Mandrillus* with the latter showing higher mean values. In terms of textural fill volume, *Papio* exhibits higher values than *Theropithecus* and *Macaca* and significantly lower than *Mandrillus*. Moreover, *Macaca* possess significantly lower textural fill volume (Tfv) than *Mandrillus*, lower than *Lophocebus*, and significantly higher values than

Ψηφιακή βιβλιοθήκη Θεόφραστος – Τμήμα Γεωλογίας – Αριστοτέλειο Πανεπιστήμιο Θεσσαλονίκης

Ψηφιακή συλλογή
Βιβλιοθήκη
"ΘΕΟΦΡΑΣΤΟΣ"
Α.Π.Θ

Theropithecus. *Paradolichopithecus* differs from *Macaca* and *Lophocebus* having overall lower mean complexity (Table 5.5).

In Phase I facets, *Lophocebus*, *Macaca* and *Mandrillus* exhibit significantly higher complexity (Asfc) than *Theropithecus*, whereas *Papio* also exhibits higher values of complexity (Asfc) than *Theropithecus*. Moreover, *Lophocebus* possess more complex and significantly more heterogeneous textures than *Macaca*, while the *Cercocebus* also differs from *Papio*, *Theropithecus* and *Mandrillus* in having higher heterogeneity ($Hasfc_{81}$). In terms of textural fill volume (Tfv), *Mandrillus* possess significantly higher values than *Papio*, *Theropithecus*, *Macaca* and higher than *Lophocebus*. The fossil papionin *Paradolichopithecus* differs from all extant representatives studied here in having significantly lower values of textural fill volume (Table 5.5).

In Phase II dental facets, there is significant variation in the dispersion of heterogeneity (Disp–$Hasfc_{81}$), with *Lophocebus* and *Mandrillus* exhibiting higher dispersion of values than *Theropithecus* and *Paradolichopithecus* (Table 5.5). In Phase I dental facets, the analysis revealed significant differences in the dispersion of textural fill volume (Disp–Tfv), with *Mandrillus* having lower dispersion than *Papio* and *Theropithecus*. The fossil papionin *Paradolichopithecus* shows significantly higher dispersion than *Mandrillus* and *Lophocebus* and higher than *Theropithecus* and *Macaca* (Table 5.5).

The analyses of variance on the coordinates obtained from principal component analysis (PCA) including the microwear texture variables (e.g. Asfc, epLsar, $Hasfc_{81}$, Tfv) from Phase II and I dental facets, revealed significant differences among genera in PC1, PC2, PC3 and PC2, PC3, PC4 respectively. However, PC4 of Phase I dental facets explain only a minor amount of the total variance (Table S6 Appendix 5.7).

Concerning Phase II facets, PC1 accounts for 54.89% of the total variance, and it is mainly explained by anisotropy (epLsar, 56.37%), followed by complexity (Asfc, 36.14%), heterogeneity ($Hasfc_{81}$, 7.22%), and textural fill volume with a minor effect (Tfv, 0.26%), with only anisotropy showing positive correlation. Therefore, an increase in the values of PC1 can be interpreted as a slight increase in anisotropy along with a mild decrease in complexity and heterogeneity. The pairwise comparisons suggest that *Theropithecus* differs from *Papio*, *Macaca* and *Lophocebus*, with the latter also showing differences in the values of PC1 with *Mandrillus* (Fig. 5.3). PC2 accounts for 31.38% of the total variance and it is primarily explained by complexity (Asfc, 56.16%) followed by anisotropy (epLsar, 36.78%), heterogeneity ($Hasfc_{81}$, 5.98%) and textural fill volume again with a low effect (Tfv, 1.06%), with all variables showing positive correlation with PC2. Thus, an increase in the values of PC2 can be seen as an increase in complexity along with a lower increase in anisotropy, and a slighter increase in heterogeneity and textural fill volume. The pairwise comparisons indicate that *Theropithecus* differs from *Mandrillus*, *Macaca* and *Lophocebus*. *Paradolichopithecus* differs from *Macaca* having lower PC2 values as evidenced by Fishers LSD (Table S7 Appendix 5.7).

Concerning Phase I dental facets, PC2 accounts for 38.27% of the total variance and it is primarily explained by complexity (Asfc, 74.25%) followed by heterogeneity ($Hasfc_{81}$, 13.47%), anisotropy (epLsar, 11.00%) and textural fill volume (Tfv, 1.30%), with all variables showing positive correlation. Thus, an increase in the values of PC2 can be interpreted as an increase in complexity, followed by a lower increase of both heterogeneity and anisotropy, with

Ψηφιακή βιβλιοθήκη Θεόφραστος – Τμήμα Γεωλογίας – Αριστοτέλειο Πανεπιστήμιο Θεσσαλονίκης

Ψηφιακή συλλογή
Βιβλιοθήκη
"ΘΕΟΦΡΑΣΤΟΣ"
Τμήμα Γεωλογίας
Α.Π.Θ

Table 5.5 Pairwise comparisons of dental microwear texture variables between genus. Variables in bold signify differences highlighted with Bonferroni adjustment[a].

Species	*Paradolichopithecus*		*Papio*		*Theropithecus*		*Mandrillus*		*Macaca*		*Lophocebus*	
Facet	*II*	*I*	*II*	*I*	*II*	*I*	*II*	*I*	*II*	*I*	*II*	*I*
Paradolichopithecus				Disp–Tfv(–) Tfv(+)		Disp–Tfv(–) Tfv(+)	Disp–Hasfc$_{81}$(+)	**Disp–Tfv**(–) **Tfv**(+)	Asfc(+)	Disp–Tfv(–) Tfv(+)	Disp–Hasfc$_{81}$(+) Asfc(+)	**Disp–Tfv**(–) Asfc(+) Tfv(+)
Papio		Disp–Tfv(+) Tfv(–)			Asfc(–) Hasfc$_{81}$(–) Tfv(–) epLsar(+)	Asfc(–)	**epLsar**(+) **Tfv**(+)	Disp–Tfv(–) **Tfv**(+)	Asfc(+) Hasfc$_{81}$(+) Tfv(+)		Asfc(+)	Hasfc$_{81}$(+)
Theropithecus		Disp–Tfv(+) Tfv(–)	Asfc(+) Hasfc$_{81}$(+) Tfv(+) epLsar(–)	Asfc(+)			Disp–Hasfc$_{81}$(+) **Asfc**(+)	Disp–Tfv(–) **Asfc** **Tfv**(+)	**Asfc**(+) **Tfv**(+)	**Asfc**(+)	Disp–Hasfc$_{81}$(+) **Asfc**(+) **Hasfc$_{81}$**(+) epLsar(–)	**Asfc**(+) **Hasfc$_{81}$**(+)
Mandrillus	Disp–Hasfc$_{81}$(–)	**Disp–Tfv**(+) **Tfv**(–)	**epLsar**(–) **Tfv**(–)	Disp–Tfv(+) **Tfv**(–)					**Tfv**(–)	**Tfv**(–)	Asfc(+) Hasfc$_{81}$(+) epLsar(–)	Hasfc$_{81}$(+) Tfv(–)
Macaca	Asfc(–)	Disp–Tfv(+) Tfv(–)	Asfc(–) Hasfc$_{81}$(–) Tfv(–)		**Asfc**(–) **Tfv**(–)	**Asfc**(–)	**Tfv**(+)	**Tfv**(+)			Tfv(+) **Hasfc$_{81}$**(+)	Asfc(+) **Hasfc$_{81}$**(+)
Lophocebus	Disp–Hasfc$_{81}$ Asfc(–)	Disp–Tfv(+) Asfc(–) Tfv(–)	Asfc(–)	Hasfc$_{81}$(–)	**Asfc**(–) **Hasfc$_{81}$**(–) epLsar(+)	**Asfc**(–) Hasfc$_{81}$(–)	Asfc(–) Hasfc$_{81}$(–) epLsar(+)	Hasfc$_{81}$(–) Tfv(+)	Tfv(–) **Hasfc$_{81}$**(–)	Asfc(–) **Hasfc$_{81}$**(–)		

[a](–) and (+) indicate values that are either lower or higher respectively for species in column compared to the one in row.

Ψηφιακή βιβλιοθήκη Θεόφραστος – Τμήμα Γεωλογίας – Αριστοτέλειο Πανεπιστήμιο Θεσσαλονίκης

Ψηφιακή συλλογή
Βιβλιοθήκη
"ΘΕΟΦΡΑΣΤΟΣ"

just a minor increase in textural fill volume (Fig. 5.3). *Theropithecus* has significantly lower PC2 values than *Mandrillus*, *Macaca* and *Lophocebus*, while *Cercocebus* shows higher values than *Papio*. PC3 accounts for 6.09% of the total variance and it is mostly explained by heterogeneity ($Hasfc_{81}$, 81.66%), followed by complexity (Asfc, 14.34%), anisotropy (epLsar, 3.31%), and lastly textural fill volume (Tfv, 0.74%). Heterogeneity and textural fill volume show positive correlation with the axis while complexity and anisotropy negative. So, an increase in the values of PC3 can be seen as an increase in heterogeneity and just a minimal increase in textural fill volume, along with a decrease in complexity and anisotropy (Fig. 5.3).

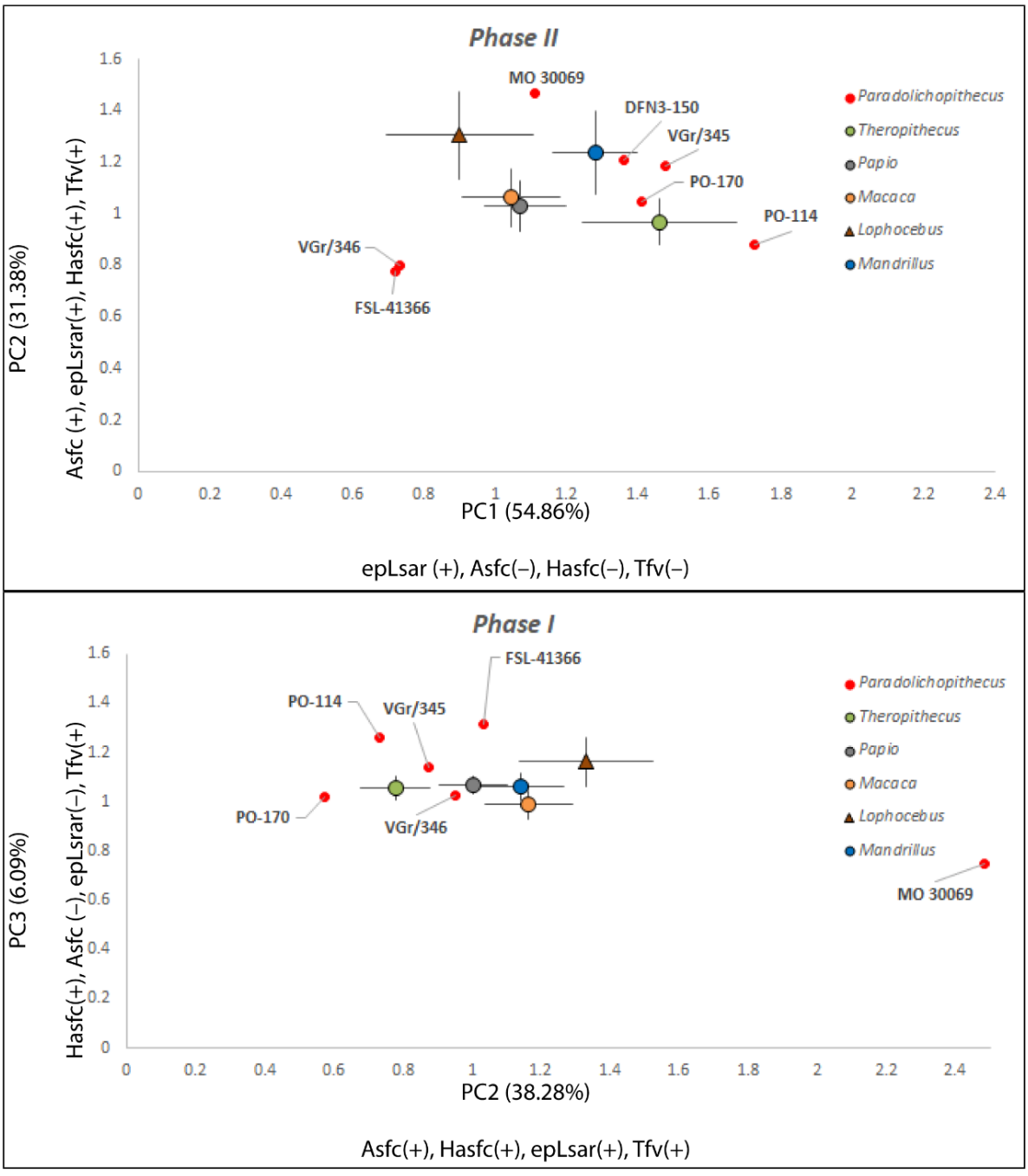

Fig. 5.3 Bivariate plots (means with 95% conf. interval) of PC1–PC2 from Phase II and PC2–PC3 from Phase I dental facets between extant papionin genera and *Paradolichopithecus* dental microwear sample, including the total amount of variance explained by each principal component and the effect (positive or negative) of each microwear texture variable. The texture variables are placed in order (from left to right) based on their effect on the principal component (see text for details).

Ψηφιακή βιβλιοθήκη Θεόφραστος – Τμήμα Γεωλογίας – Αριστοτέλειο Πανεπιστήμιο Θεσσαλονίκης

Ψηφιακή συλλογή
Βιβλιοθήκη
"ΘΕΟΦΡΑΣΤΟΣ"
Τμήμα Γεωλογίας

5.5 Discussion

5.5.1. Dental topographic and enamel thickness analysis

The analysis reveals differences in some aspects of dental morphology among modern papionin genera, which may be suggestive of distinct adaptive morphologies potentially associated with different ecological niches. The overall results of dental topographic and enamel thickness analyses suggest that DFN3–150 second upper molar could efficiently process a wide array of food resources from tough and fibrous material to more mechanically challenging food objects.

The values of 3D relative enamel thickness (both $3DRET_{vol}$ and $3DRET_{geo}$) and absolute crown strength (ACS) of DFN3–150 are similar to *Papio* (Fig. 5.2), which is suggestive of similar dietary preferences in terms of food resource mechanical properties. *Papio* is customarily depicted as opportunistic mixed feeders (Harding, 10981; Newton-Fisher & Okecha, 2006; Rhine et al., 1986, 1989), while they exhibit significant differences in dietary composition and foraging behavior among populations and across geography (Whiten et al., 1991; Codron et al., 2005). Baboon diets mainly consist of fruits and seeds, grasses and sedges, flowers, bark, roots, and animal matter (Hill & Dunbar, 2002; Katsvanga et al., 2009; Newton–Fisher & Okecha, 2006; Pochron, 2000; Whiten et al., 1991). In addition, members of the genus *Papio* also consume more mechanically challenging resources, such as underground storage organs (USOs), roots, tubers/rhizomes in resource limited habitats (Jolly, 1970; Akosim et al., 2010; Dominy et al., 2008; Landen & Wrangham, 2005; Wrangham et al., 2009). Underground plant products can be a targeted food resource for baboons in resource limited environments or during seasonal variation of resources (Dominy et al., 2008; van Doorn et al., 2010; Coiner–Collier et al., 2016).

The estimates of relief (i.e. LRFI and λ) suggest that DFN3–150 M^2 could effectively process tough and fibrous material, in a manner similar to *Papio* and *Mandrillus* (Astaras & Waltert, 2010; Astaras et al., 2011; Byrne et al., 1993; Hoshino, 1985; Newton–Fisher & Okecha, 2006; Percher et al., 2017; Swedell et al., 2008; Tutin et al., 1997; van Doorn et al., 2010; Whiten et al., 1991). The comparisons of curvature/sharpness (i.e. DNE and ARC) and complexity (i.e. OPCR) are more difficult to interpret. On one hand, Dirichlet normal energy (DNE) shows significant overlap between genera, placing *Paradolichopithecus* within the range of values of *Papio*, *Cercocebus* and *Lophocebus*. On the other hand, ARC shows less overlap and separates *Paradolichopithecus* from the rest of the taxa, while both *Macaca* and *Cercocebus* show significant lower values than *Papio* and *Mandrillus*. *Mandrillus* and *Cercocebus* are usually described as frugivorous seed–predators foraging on the forest floor (Astaras & Waltert, 2010; Cooke, 2012; Lahm, 1986), while anatomical (e.g. enlarged forelimb muscles) and dental evidence (e.g. enlarged premolars) are consistent with this notion (Fleagle & McGraw, 1999; Fleagle & McGraw, 2002). However, *Mandrillus* is more specialized in terrestrial locomotor behavior compared to *Cercocebus* (Cooke, 2012). The locomotor behavior of *Cercocebus* varies between species (McGraw et al., 2011), seasons (Shan, 2003), and when in sympatry with *Mandrillus* (Astaras et al., 2011). These shifts from terrestrial to arboreal substrates and vice versa, presumably reflect an evolved strategy to reduce potential competition for resources when they are ecologically associated (Astaras et al., 2011). The comparisons of ARC indicate blunter occlusal surfaces for *Cercocebus*, suggesting dental adaptations driven by the more increased reliance on mechanically challenging food resources such as some hard fruits (McGraw et al., 2012; Susan Coiner-Collier et al., 2016). A similar picture is illustrated by *Papio* and *Macaca*, because both display overall opportunistic dietary habits, however, in general *Macaca* species tend to rely more on fruits than *Papio* species (Post, 1982; Rhine et al., 1986; Richard et al., 1989; Goldstein and Richard, 1989; Ungar, 1995; Daegling and Grine, 1999; Ménard, 2002; Newton-Fisher and Okecha, 2006; Kunz and

Ψηφιακή βιβλιοθήκη Θεόφραστος – Τμήμα Γεωλογίας – Αριστοτέλειο Πανεπιστήμιο Θεσσαλονίκης

Ψηφιακή συλλογή
Βιβλιοθήκη
"ΘΕΟΦΡΑΣΤΟΣ"

Linsenmair, 2007, 2010; V. K. Bentley-Condit, 2009; Hanya et al., 2011; Feeroz, 2012). Regardless, there are considerable differences in the dietary breadth and composition between *Papio* and *Macaca*, and even between species within the same genus, which are probably related to habitat differences (Elton & O'Regan, 2014; Hill & Dunbar, 2002; Ménard & Vallet, 1997; Norton et al., 1987; O'Regan et al., 2008).

Results on complexity (OPCR) are difficult to interpret, with the overall comparisons showing high overlap between *Papio*, *Mandrillus*, *Theropithecus* and *Cercocebus*, whereas the fossil DFN3–150 falls within the range of *Papio*, *Theropithecus* and *Cercocebus*. Complexity quantifies the number of locations on the tooth's surface where foods are likely to fracture, and is presumably associated with the number of occlusal features (Berthaume et a., 2020). Furthremore, higher values of complexity have been linked with herbivory in some mammalian clades (Evans et al., 2007). The highlighted significant differences in OPCR values (i.e. both *Papio* and *Mandrillus* differ from *Macaca* and *Lophocebus*; Table 5.3), might reflect the overall more variable dietary behavior of *Papio* and *Mandrillus* compared to *Macaca* and *Lophocebus* (Lahm, 1986; Hill and Dunbar, 2002; Akosim et al., 2010; McGraw et al., 2012; Owens et al., 2015). Notwithstanding the above, previous studies have suggested that complexity can be a poor indicator of diet among primates (Berthaume et al., 2020 and references therein). The overlap between *Theropithecus* and *Cercocebus* in the comparisons here, which are considered as the only grazing primate species and a dedicated seed-eater respectively, is consistent with the latter claim. Lastly, the presence of features such as accessory cusps and crenulations may also influence OPCR values. This suggests that every specimen must be treated with caution and the presence of such features must be accounted in comparisons.

5.5.2. Dental microwear texture analysis

Most of the earlier works in dental microwear texture analysis were primarily focused on Phase II dental facets, as it was suggested that they better discern dietary differences among primates with contrasting dietary habits (e.g. folivorous vs frugivorous) (King et al., 1999; Krueger et al., 2008). Texture parameters, such as complexity (Asfc) and anisotropy (epLsar), provided meaningful results (Ragni et al., 2017; Scott et al., 2006, 2012). For instance *Theropithecus* (whose diet is almost exclusively composed of tough herbaceous vegetation) usually possesses less complex and more anisotropic dental microwear textures compared with dedicated seed specialists like *Lophocebus* species (Scott et al., 2012). Indeed, in the present study the observed differences in Phase II dental facets among cercopithecid genera are mostly explained by differences in the values of anisotropy (epLsar) followed by complexity (Asfc) along PC1, while the reverse applies for PC2 (Fig. 5.3). However, in Phase I facets anisotropy (epLsar) shows no significant variation. This is not surprising considering that Phase I and II dental facets involve different kinds of masticatory movements (Kay, 1975; Kay & Hiiemae, 1974), thus potentially carrying different dietary signals (Krueger et al., 2008). Anisotropy (epLsar) has been linked to food toughness, and higher values of this variable are found in surfaces that are dominated by parallel striations (Scott et al., 2012). These striations result from the shearing actions that take place on the occlusal surface during processing of tough and fibrous material. Since Phase I facets are also associated with shearing actions (Kay & Hiiemae, 1974), it is possible that differences in anisotropy (epLsar) can be minor and cannot be detected due to the biomechanic nature of these dental wear facets. However, this observation could also be affected by the general trend seen in cercopithecid diets towards leaf consumption (Hladik, 1978). Even dedicated hard object foragers, such as species of the genus *Cercocebus*, tend to consume varying amounts of tough vegetation throughout the year depending on seasonal and spatial availability of preferred food resources (McGraw et al., 2011). Setting complexity (Asfc) and anisotropy (epLsar) aside, other texture parameters such as heterogeneity of complexity (Hasfc) and textural fill volume (Tfv) may also provide complementary and useful information.

Ψηφιακή βιβλιοθήκη Θεόφραστος – Τμήμα Γεωλογίας – Αριστοτέλειο Πανεπιστήμιο Θεσσαλονίκης

Ψηφιακή συλλογή
Βιβλιοθήκη
"ΘΕΟΦΡΑΣΤΟΣ"

Heterogeneity (Hasfc) has been linked with size and variability of wear–inducing particles, with higher values indicating a broader diet in terms of fracture properties (Scott et al., 2012). Indeed, results of previous analyses suggest differences between more durophagous primate species and tough foliage consumers, as a result of more heterogeneous diet of the former compared to the latter, in terms of wear particle size and food composition (Krueger et al., 2008; Ragni et al., 2017; Scott et al., 2012). The observed variations in heterogeneity in the analysis performed here are consistent with this notion, as the overall more durophagous *Lophocebus* exhibits higher values of heterogeneity compared to *Theropithecus* in both dental facet types. This suggests a more restricted dietary spectrum for *Theropithecus* compared with *Cercocebus*, along with low spatial heterogeneity of resources. This can be expected, as there is considerably lower diversity of food resources in the high altitude habitats of Ethiopia where *Theropithecus* is mostly found today, compared to the habitats usually inhabited by *Cercocebus* usually inhabit (Fashing et al., 2014; Abu, 2018; Souron, 2018). Moreover, the results revealed differences in the values of heterogeneity between *Lophocebus* and *Papio*, *Macaca*, and *Mandrillus*. To better understand these variations requires a closer inspections of the comparative dataset here.

The microwear sample of *Macaca* consists of one species (e.g. *Macaca fuscata*), which derives from three free-ranging populations from Japan (see section 5.2.2). Macaques are routinely considered primarily frugivorous, yet their diet is opportunistic and mostly dependent on habitat, as macaque species found in tropical forests of southeast Asia feed primarily on fruits mostly available throughout the year (O'Brien and Kinnaird, 1997; Drapier et al., 2002; Zhou et al., 2011; Albert et al., 2013b), whereas species found in more temperate habitats exhibit marked seasonal variation in their diets (Hill, 1997; Tsuji et al., 2013). The Japanese macaques are one of the most well studied primate species, and their distribution throughout a wide array of habitats across latitudes in Japan makes them a very interesting primate species to address diet-related questions. In Japan, the diversity of vegetation types decreases towards the northern parts. In order to secure a diverse diet, which requires a staple quantity and quality of food resources, Japanese macaque troops may range over larger areas, thereby expanding their home range (Maruhashi, 1980). Thus, on one hand the differences between *Lophocebus* and *Macaca* might reflect the low diversity of vegetal resources available for Japanese macaques compared to *Lophocebus*. On the other hand, leaves can be an important dietary component of the diet of Japanese macaques (Hanya et al., 2004; Kato et al., 2014 and references therein), which suggests that the highlighted differences in heterogeneity ($Hasfc_{81}$) reflect the overall higher preference of the Japanese macaques for leaves compared to *Lophocebus*. Similarly, the higher values of heterogeneity ($Hasfc_{81}$) of *Lophocebus* compared with *Mandrillus* and *Papio* may suggest a more mechanically diverse spectrum of foods and/or lower overall amounts of fibrous food resources consumed by the former taxon compared to the latter two. Likewise, the observed differences in the values of heterogeneity ($Hasfc_{81}$) between *Macaca* and *Papio* may reflect the overall more frugivorous dietary tendencies of *Macaca* species compared with *Papio* species. Nevertheless, these hypotheses require additional investigation in the future.

The variations of textural fill volume are more difficult to interpret. This variable is associated with the number, size and depth of wear features across a microwear surface. So, a surface showing large and deep features is expected to have high values. Scott et al. (2006) reported positive correlation between complexity (Asfc) and textural fill volume (Tfv), while follow-up investigation suggested the use of this variable as a complement to complexity (Asfc) (Scott et al., 2012). However, other studies on ungulates have yielded contrasting results about this parameter (Scott et al., 2012; Merceron et al., 2016;). In the present study, the variations of textural fill volume (Tfv) might be associated with hard object feeding, with higher values indicating more frequent consumption of mechanically challenging food resources. This is consistent with the higher values of textural fill volume (Tfv) and complexity (Asfc) of *Papio* compared to *Theropithecus*, and the lower textural fill volume (Tfv) of *Papio* compared to

Ψηφιακή βιβλιοθήκη Θεόφραστος – Τμήμα Γεωλογίας – Αριστοτέλειο Πανεπιστήμιο Θεσσαλονίκης

Ψηφιακή συλλογή
Βιβλιοθήκη
"ΘΕΟΦΡΑΣΤΟΣ"
Α.Π.Θ

Mandrillus and *Macaca* (Table 5.5). However, since the dietary meaning of this variable has so far proven somewhat ambiguous, interpretations should be treated with caution.

The microwear sample of *Paradolichopithecus* exhibits texture variable differences from all genera: with *Lophocebus*, *Macaca* and *Mandrillus* in both Phase II and I dental facets, and with *Papio* and *Theropithecus* only in Phase I (Table 5.5). The significantly lower values of complexity (Asfc) of *Paradolichopithecus* in both dental facet types (i.e. Phase II and I) compared to *Lophocebus* suggest less durophagous dietary habits for the fossil papionin, as further supported by the significantly lower values of textural fill volume in Phase I dental wear facets. The same is inferred from comparisons between *Paradolichopithecus* and *Macaca*. The texture differences between *Paradolichopithecus* and *Mandrillus* may also suggest slightly different dietary habits, which may indicate a wider dietary spectrum in terms of food mechanical properties for the latter. Alternatively, such differences may reflect a distinct vegetal composition of their respective habitats. The significantly lower values of textural fill volume (Tfv) of *Paradolichopithecus* compared to *Papio* and *Theropithecus*, might be suggestive of a more constrained spectrum of available vegetal resources for the fossil papionin. All these observations may suggest that *Paradolichopithecus* had slightly different dietary habits compared to modern papionins, while displaying an opportunistic strategy as observed in modern *Papio* and *Mandrillus* species (see Table 5.1 and references therein). Yet, they may also suggest a more tough and fibrous vegetal component in its dietary repertoire, but probably to a lesser extent than in extant geladas. Be that as it may, individuals such as MO 30069 from the Romanian site of Valea Graunceanului (Fig. 5.3), denote a durophagous dietary behavior days or even weeks prior to death. The oldest occurrence of *Paradolichopithecus* in our fossil sample for microwear analysis derives from Dafnero–3 in northern Greece (2.4–2.3 Ma, Benammi et al., 2020), followed by Senèze in southern France (2.21–2.09 Ma, Pastre et al., 2015), and then Vatera in Greece (~2.0 Ma, de Vos et al., 2002). Moreover, the latter fossil site from Greece is roughly contemporary with the fossil sites from the area of Valea Graunceanului in Romania (~2.2–1.9 Ma, Radulescu et al., 2003; Terhune et al., 2020; Curran et al., 2021), with the latter sites from Romania probably being slightly younger (Spassov, 2000). Available evidence suggests that the environmental context of these fossil sites was most likely mixed/mosaic habitats and open landscapes with temperate climate (de Vos et al., 2002; Delson et al., 2006; Lyras and Van Der Geer, 2007; Terhune et al., 2013; Berlioz et al., 2018; Hermier et al., 2020; Curran et al., 2021 and references therein). The results of dental microwear texture analysis are consistent with such interpretations as the microwear textures of *Paradolichopithecus* individuals indicate a more mixed and opportunistic dietary behavior, yet with a more tough vegetal component and/or a more abrasive diet. This dietary behavior might be related with the expansion of more open and dry condition in European environments, promoting the expansion of grasslands and prairies (Agusti and Antón, 2002). However, this observation can also be a seasonal bias in the fossil record, where more specimens likely died at a given season than at another one. Hence, it requires caution when interpreting these results, especially when the fossil sample size is considerably lower compared to the extant taxa such as in the case here.

5.5.3. The dietary ecology of *Paradolichopithecus* and implications for its extinction from Eurasia

Until today the large Eurasian papionin is enigmatic, mostly due to the scarcity of available published material. Owing to its suggested importance in biochronology (e.g. Delson & Nicolaescu-Plopsor, 1975), previous research has focused on understanding its taxonomy and phylogenetic relationships rather its ecological profile (Aguirre & Soto, 1978; Delson, 1975; Delson et al., 2014; Kostopoulos et al., 2018; Moyà Solà et al., 1990; Nishimura & Takai, 2010; Nishimura et al., 2007, 2014; O'Shea et al., 2016; Takai et al., 2008). However, to better

Ψηφιακή βιβλιοθήκη Θεόφραστος – Τμήμα Γεωλογίας – Αριστοτέλειο Πανεπιστήμιο Θεσσαλονίκης

Ψηφιακή συλλογή
Βιβλιοθήκη
"ΘΕΟΦΡΑΣΤΟΣ"
Α.Π.Θ

comprehend its evolutionary history, it is also necessary to understand the paleoecological context that influenced the origin and subsequent evolution of this taxon.

A few early studies tried to decipher the ecological profile of *Paradolichopithecus*, mostly focusing on its locomotor behavior. These studies suggested that it possessed baboon-like terrestrial features (Jolly, 1967; Simons, 1970), further supported by later research (Delson, 1975; Delson & Frost, 2004; Frost et al., 2005; Groves, 2000, 2001; Jablonski et al., 2002; Sondaar, 2006; Szalay & Delson, 1979; Van der Geer & Sondaar, 2002). Besides postcranial evidence, there is some limited information based on dental tissues. Williams and Holmes (2011) investigated the dietary profiles of Pliocene Eurasian papionins using low-magnification stereomicroscopy. They concluded that *Paradolichopithecus*, along with the rest of Eurasian papionins studied (*Procynocephalus subhimalayanus* from Upper Siwaliks and *Macaca sp*. from Yushe) showed features indicative of hard-object foraging and suggested a more abrasive diet with limited grasses and possible exploitation of underground plant parts (e.g. USOs), such as roots, corms, bulbs and plant stem bases, in resource limited environments. The results of the dental topographic and enamel thickness analysis are consistent with the latter hypothesis, as the investigated specimen from Dafnero-3 (DFN3–150) exhibits an upper molar morphology capable to withstand high biting forces potentially related to consumption of mechanically challenging food objects, while also being able to consume abrasive vegetation, as well as underground plant parts. This is also consistent with the results of dental microwear texture analysis, which show similarities with the sample of extant *Papio hamadryas* and *Mandrillus sphinx*. However, the results of the analysis also suggest similarities with *Theropithecus*, implying that *Paradolichopithecus* probably consumed tough herbaceous terrestrial vegetation prior to death. *Papio hamadryas* exhibits high ecological plasticity and is usually associated with more open and dry environments (Pochron, 2000; Zinner et al., 2001; Swedell et al., 2008), whereas *Theropithecus gelada* is mostly restricted to high altitude habitats of Ethiopia, feeding mainly on grass blades (Iwamoto, 1993; but see also Fashing et al., 2014; Abu et al., 2018). On the other hand, *Mandrillus sphinx* is found in coastal tropical forests in central Africa where resource production varies seasonally, and exhibits opportunistic but eclectic feeding behavior with a high preference for seeds found on the forest floor (Hoshino, 1985; Lahm, 1986; White, 1994; Tutin et al., 1997a; Newbery et al., 1998; Owens et al., 2015). These evidences further imply that *Paradolichopithecus* was probably able to exploit various habitats, in agreement with its extensive biogeographic distribution and previous interpretations regarding its locomotor behavior (Frost et al., 2005). Moreover, *Mandrillus sphinx*, *Papio hamadryas* and *Theropithecus gelada* have been observed to exploit subterranean plant products when needed, depending on seasonal variation and habitat (Pochron, 2000; Jarvey et al., 2018; Percher et al., 2018). Based on the above and the results presented here, it is plausible that *Paradolichopithecus* followed a similar dietary strategy in resource limited environments.

Seasonal shifts in resource availability that prompt primates to choose less preferred foods, including fallback foods, are frequently viewed as being adaptively significant (Marshall and Wrangham, 2007; Rosenberger, 2013). It is assumed that such resources might have played a prominent role in hominin evolution (Landen and Wrangham, 2005; Wrangham et al., 2009; Singels, 2013) as they gradually colonized the more seasonal and dry environments of Africa during the Plio-Pleistocene (Bobe et al., 2002; Bobe & Behrensmeyer, 2004; deMenocal, 2004; Hernández Fernández & Vrba, 2006; Reed, 1997; but see also Cerling et al., 1998). Indeed, several primate species today, including cercopithecines (Altmann, 1998; Fashing et al., 2014; Jarvey, 2016; Maibeche et al., 2015; Percher et al., 2018; Pochron, 2000; Whiten et al., 1991; Wrangham et al., 2009), chmpanzees (Kortlandt and Holzhaus, 1987; Lanjouw, 2002; Hernandez-Aguilar et al., 2007; McGrew, 2007), as well as members of Cebidae (Moura and Lee, 2004; Falótico and Ottoni, 2016; Truppa et al., 2019) have been observed to exploit underground plant parts as fallback resources, while in some cases anthropogenic disturbances seem to influence this feeding behavior (e.g. Hockings et al., 2010; Jarvey et al., 2018). Aside from their usually mechanically challenging nature (Dominy et al., 2008), harvesting and

Ψηφιακή βιβλιοθήκη Θεόφραστος – Τμήμα Γεωλογίας – Αριστοτέλειο Πανεπιστήμιο Θεσσαλονίκης

Ψηφιακή συλλογή
Βιβλιοθήκη
"ΘΕΟΦΡΑΣΤΟΣ"

processing can be rather time consuming (Alatmann, 1998; Lanjouw, 2002). This implies higher energy costs for acquisition compared to other more easily accessible resources, as well as increased predation risk (e.g. Krebs & Davies, 2009). Therefore, it is suggested that the consumption of such food resources may potentially drive morphological and/or behavioral adaptations (enamel thickness, mandibular robusticity, ranging behavior and gut physiology; e.g., Lambert et al., 2004; Lucas et al., 2008; Rosenberger & Kinzey, 1976). Be that as it may, the limited fossil sample analyzed (for both dental microwear and dental topography) does not enable any clear conclusions regarding potential dental adaptive traits or consumption of specific food resources (e.g. USOs); although, it suggests opportunistic tendencies for *Paradolichopithecus*. Such feeding strategies (i.e. generalist and opportunistic) are more likely to succeed in a wide range of habitats.

Accumulated evidence suggests that, around the Pliocene/Pleistocene boundary (~2.6 Ma), global climate started to get progressively colder and drier, which profoundly affected existing ecosystems of both Africa and Asia (Bibi et al., 2013; Bobe & Behrensmeyer, 2004; Cai et al., 2012; Cerling et al., 2013; Hernández Fernández & Vrba, 2006; Wu et al., 2007, 2011). Around this time permanent ice sheets began to form in the Northern Hemisphere (Bartoli et al., 2005), gradually leading also to the expansion of xerophytic flora in Eurasian mid-latitudes (Agusti and Antón, 2002; Hoyle et al., 2020). As a result, Eurasian primate faunas would have been forced to adapt to increasingly colder and seasonal habitats and/or retreat to regions that acted as climatic refugia, or else become extinct (Bobe et al., 2002; Bobe & Behrensmeyer, 2004; Jablonski, 1998). Even if cercopithecids were influenced by the challenging environmental conditions of the Pleistocene, which probably significantly affected food resource availability, it was probably to a lesser extent compared to other primate families, due to their ecological plasticity, compared to the overall more stenotopic Great apes (Jablonski et al., 2000).

Cercopithecid life history traits, such as shorter gestation times, shorter weaning periods and interbirth intervals, as well as the ability to survive on a wider variety of vegetation in seasonal habitats, are considered to be key elements for their survival in the increasingly more seasonal environments of Africa and Eurasia during Plio-Pleistocene (Jablonski, 1993; Jablonski et al., 2000). In these challenging environmental conditions, *Paradolichopithecus* expanded rapidly throughout Eurasia, which further suggests an eurytopic dietary profile. Nevertheless, the relatively sudden absence of *Paradolichopithecus* from the latest Early Pleistocene fossil record onwards, however, has led to various hypotheses. Setting aside the effects of resource variation in the dietary ecology of *Paradolichopithecus* impacted by global and regional climatic events as a factor that might have contributed in the decline of this fossil genus from Europe, it is also speculated that the invasion of the potentially competitive African *Theropithecus* into Eurasia may explain its relatively fast extinction (Delson, 1993; Jablonski et al., 2002). However, this seems unlikely as all Eurasian *Theropithecus* records significantly post-date the last occurrence of *Paradolichopithecus* (Delson, 1993; Gibert et al., 1995b; Roberts et al., 2016), even though this could also be a sampling bias. Moreover, the genus *Theropithecus* expanded in Eurasia only for a relatively brief amount of time, which further refutes the possibility that it ecologically outcompeted *Paradolichopithecus*, a fossil taxon that possibly evolved and thrived there for some time. It is however possible that *Theropithecus* may have occupied for a brief period of time the empty niche left by *Paradolichopithecus*.

Another possible cause that might have contributed in the extinction of *Paradolichopithecus* from Eurasia is the effect of predation pressures. Many primatologists assumed that predation was responsible for many behavioral and anatomical features of the species they studied, and emphasized its importance as a driving factor in primate evolution (see Anderson, 1986 and references therein). Anderson (1981a,b) observed behavioral differences in different baboon populations in South and East Africa that were best explained

Ψηφιακή βιβλιοθήκη Θεόφραστος – Τμήμα Γεωλογίας – Αριστοτέλειο Πανεπιστήμιο Θεσσαλονίκης

Ψηφιακή συλλογή
Βιβλιοθήκη
"ΘΕΟΦΡΑΣΤΟΣ"

by the absence of predators at one site compared to the other, with later works on desert baboons confirming this notion (Cowlishaw, 1997). Furthermore, it has been shown that large birds of prey have been the main accumulating agents in some fossil faunas in southern Africa (Berger and Clarke, 1995; Gilbert et al., 2009), further suggesting that raptor predation might have been a strong and underappreciated selective force in the course of primate evolution. As a result, primate species display various antipredator behavior/strategies (Buzzard, 2006; Hill & Dunbar, 1998; Stanford, 2002), which might have also affected their socioecological behavior. Be that as it may, it seems unlikely that raptors could exert strong predation pressures to *Paradolichopithecus*, as the genus included large species with mostly terrestrial locomotor habits.

In most of Eurasia, the Plio-Pleistocene transition and the Early Pleistocene assemblages are characterized by the presence of the large hyaenid *Pachycrocuta brevirostris* (Martínez-Navarro, 2010), which also coincides with the appearance of large canids in Europe (e.g., Azzaroli, 1983). Additionally, large felid forms such as *Homotherium* and *Megantereon* are present in Europe at Late Pliocene to Early Pleistocene that may have posed a major threat to *Paradolichopithecus* populations. Indeed, felids can significantly affect the mortality rate of a primate population even in quite short time periods (Isbell, 1990). However, even if the previously mentioned carnivores did pose a threat to *Paradolichopithecus* populations, it seems improbable that are the primary cause of its extinction, as these large carnivores disappeared along with *Paradolichopithecus* by the earliest Middle Pleistocene (Martínez-Navarro, 2010 and references therein). The time of extinction of *Paradolichopithecus* roughly coincides with the arrival of the spotted hyena (e.g., *Crocuta crocuta*) from Africa into Europe and Asia. The more generalistic nature and social hunting and scavenging behavior was probably a key to the survival of *Crocuta crocuta* throughout the harsh climatic conditions from Middle Pleistocene and forward. Thus, it is possible that the arrival of *Crocuta crocuta* in Europe may have exerted predation pressures to *Paradolichopithecus* populations, contributing to the extinction of this large fossil papionin. Another possible factor that may have contributed to the relatively rapid extinction of *Paradolichopithecus*, could be antagonistic pressures by early *Homo*. The extinction of *Paradolichopithecus* as well as *Procynocephalus*, is dated around the same time with the first direct and indirect evidence of *Homo* in Eurasia (e.g. Jablonski, 2002; Abbate & Sagri, 2012). Human activity has been discussed as a possible factor for the decline of other fossil European and African cercopithecines (e.g., Elton & O'Regan, 2014; Hughes et al., 2008), yet this hypothesis has received little attention so far. When the genus *Homo* arrived into Eurasia, was forced to adapt in the more seasonal habitats compared to Africa, in which meat could have served as a staple food resource (Martínez-Navarro, 2010). Hence, the possibility that anthropogenic pressures might be related to *Paradolichopithecus* extinction by the latest Early Pleistocene cannot be ruled out. Nevertheless, these hypotheses remain largely speculative and cannot be tested with the present sample and it is also beyond the scope of this study. They also require further zooarcheological research including other papionins, such as the genus *Macaca,* which survived the dispersal of humans for a long time in Europe.

Ψηφιακή βιβλιοθήκη Θεόφραστος – Τμήμα Γεωλογίας – Αριστοτέλειο Πανεπιστήμιο Θεσσαλονίκης

Ψηφιακή συλλογή
Βιβλιοθήκη
"ΘΕΟΦΡΑΣΤΟΣ"
Τμήμα Γεωλογίας
Α.Π.Θ

5.6 Appendix

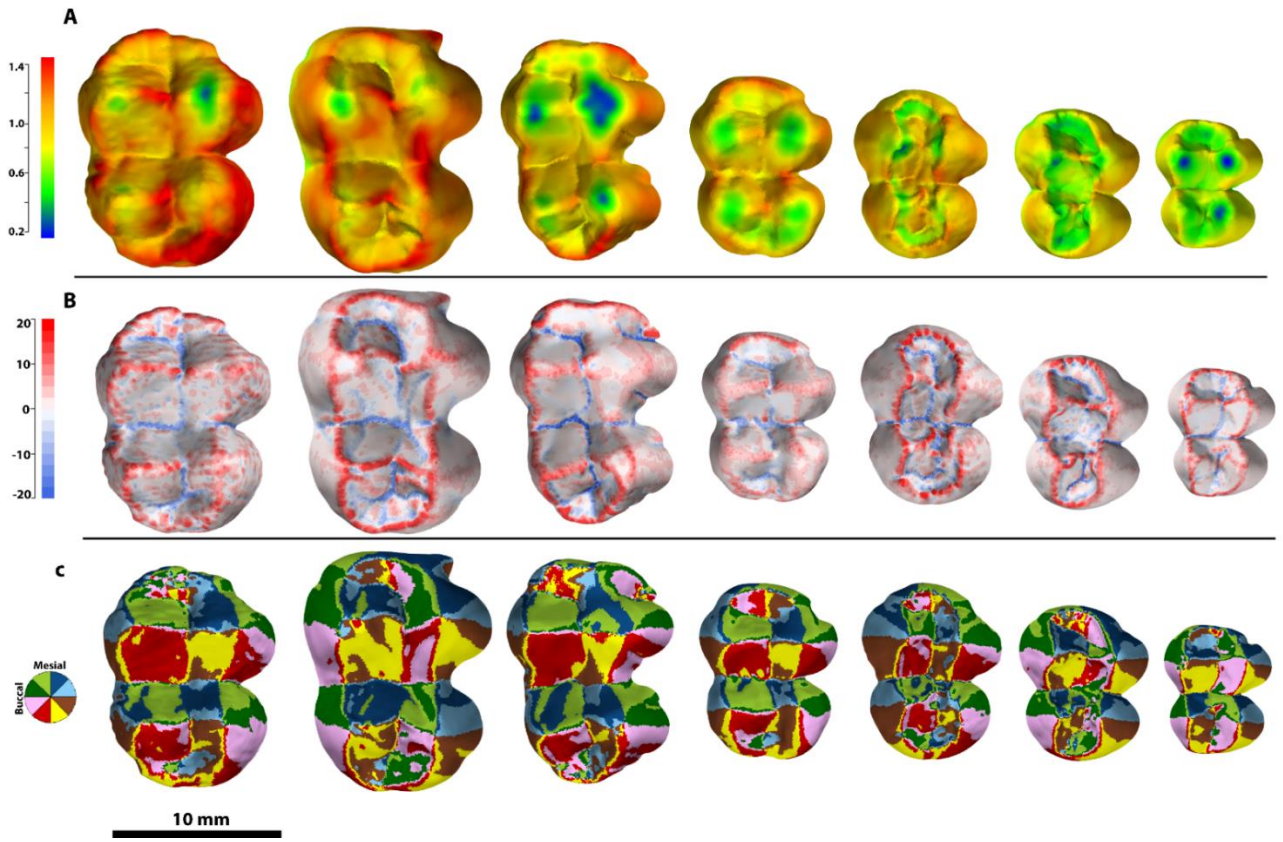

Fig. S1 Topographic maps of enamel distribution ($3DRET_{geo}$), curvature/sharpness (ARC) and complexity (OPCR) of M^2 (from left to right) of DFN3–150, *Papio anubis*, *Theropithecus gelada*, *Macaca sylvanus*, *Mandrillus leucophaeus*, *Cercocebus torquatus* and *Lophocebus albigena*: (**A**) enamel-dentine distance, (**B**) area-relative curvature and (**C**) orientation patch count rotated.(all molars were mirrored to have the same orientation for convenience purposes).

Ψηφιακή βιβλιοθήκη Θεόφραστος – Τμήμα Γεωλογίας – Αριστοτέλειο Πανεπιστήμιο Θεσσαλονίκης

Ψηφιακή συλλογή
Βιβλιοθήκη
"ΘΕΟΦΡΑΣΤΟΣ"
Τμήμα Γεωλογίας
Α.Π.Θ

Table S1 Enamel thickness and dental topographic variables raw data for modern sample and *Paradolichopithecus*[a].

Taxon	ID	Institution	λ	LRFI	ARC	DNE	OPCR	$3DRET_{vol}$	$3DRET_{geo}$	ACS
Par. arvernensis	DFN3–150	LGPUT	122.217	0.314	1.853	397.654	148.0	0.245	0.240	2.569
M. leucophaeus	2002–105	RMCA	118.038	0.352	1.692	669.965	169.0	0.219	0.212	2.204
M. leucophaeus	1893–269	RMCA	123.855	0.278	1.599	526.326	16.87	0.185	0.241	2.055
P. anubis	80–44–M–101	RMCA	120.520	0.322	1.568	439.389	132.87	0.223	0.214	2.659
P. anubis	Pp4	PALEVOPRIM	121.559	0.312	1.664	473.599	163.25	0.267	0.252	2.394
P. anubis	90–042–M226	RMCA	131.650	0.201	1.567	376.859	165.25	0.199	0.215	2.285
P. anubis	C2	PALEVOPRIM	123.007	0.278	1.847	543.391	198.75	0.219	0.217	2.372
P. cynocephalus	Pp3	PALEVOPRIM	123.383	0.279	1.57	430.042	134.0	0.328	0.297	2.616
P. hamadryas	97–020–M004	RMCA	123.688	0.280	1.614	489.983	158.62	0.226	0.241	2.704
Th. gelada	1969–449	MNHN	117.809	0.372	1.575	481.098	153.75	0.194	0.195	2.268
Th. gelada	1969–450	MNHN	116.726	0.376	1.66	439.736	125.37	0.186	0.188	2.232
Ma. sylvanus	T150kV	MNHN	124.733	0.274	1.463	257.836	97.375	0.266	0.266	2.006
Ma. sylvanus	T150kV	MNHN	127.022	0.249	1.406	259.168	103.75	0.246	0.265	2.007
Ce. torquatus	81–07–M–44	RMCA	123.232	0.291	1.417	460.573	141.875	00.295	0.283	1.677
Ce. galeritus	14486	RMCA	122.564	0.302	1.552	474.249	159.25	0.336	0.308	1.466
Ce. sp	Cb2	PALEVOPRIM	127.353	0.250	1.385	294.715	121.62	.336	0.301	1.444
Lo. albigena	83006–M276	RMCA	127.332	0.230	1.525	359.662	104.12	0.327	0.318	1.404
Lo. albigena	90042–M–301	RMCA	124.923	0.270	1.552	461.065	114.62	0.338	0.318	1.633
Lo. albigena	90042–M–301	RMCA	125.815	0.260	1.553	393.931	107.37	0.333	0.314	1.634
Lo. albigena	Cb4	PALEVOPRIM	130.679	0.210	1.264	233.94	102.25	0.321	0.328	1.701
Lo.atterimus	14113	RMCA	125.357	0.259	1.628	451.067	134.5	0.362	0.343	1.403

[a] $3DRET_{vol}$ = 3D volumetric relative enamel thickness; $3DRET_{geo}$ = 3D geometric relative enamel thickness; ACS = absolute crown strength; LRFI = relief index; ARC = area-relative curvature; DNE = Dirichlet normal energy; OPCR = orientation patch–count rotated; OES 3D = 3D occlusal enamel surface; OES 2D = 2D occlusal enamel surface.

Ψηφιακή βιβλιοθήκη Θεόφραστος – Τμήμα Γεωλογίας – Αριστοτέλειο Πανεπιστήμιο Θεσσαλονίκης

Ψηφιακή συλλογή Βιβλιοθήκη "ΘΕΟΦΡΑΣΤΟΣ" Τμήμα Γεωλογίας Α.Π.Θ.

Table S2 Raw microwear data of *Paradolichopithecus* fossil sample[a].

Filename	Taxon	Institution	Phase	Asfc	epLsar ($x10^3$)	$HAsfc_{81}$	Tfv
MO 30069-Bugiulesti-UM2s-f3	*Par. arvernensis*	MO	1	8.423	2.549	0.371	15348.74
MO 30069-Bugiulesti-UM2s-f12	*Par. arvernensis*	MO	2	2.446	4.767	0.611	39270.685
VGR0345-UM2s-f3	*Par. geticus*	ISER	1	0.903	4.336	0.535	4476.716
VGR0345-UM2s-f10-front	*Par. geticus*	ISER	2	1.338	5.634	0.606	38642.666
VGR0346-UM3d-f3	*Par. geticus*	ISER	1	1.087	3.897	0.425	24592.2
VGR0346-UM3d-f9	*Par. geticus*	ISER	2	1.523	2.415	0.511	30821.446
VATERA-PO114-lm2-sin-f6	*Par. arvernensis*	AMPG	1	0.633	5.094	0.645	42854.431
VATERA-PO114-lm2-sin-f9	*Par. arvernensis*	AMPG	2	0.721	5.71	0.426	45256.879
VATERA-PO170-lm2-dex-f6	*Par. arvernensis*	AMPG	1	0.456	5.756	0.352	5009.658
VATERA-PO170-lm2-dex-f9	*Par. arvernensis*	AMPG	2	1.206	4.872	0.484	33676.805
SENEZE-FSL41336-lm3-dex-f5	*Par. arvernensis*	UCBL-1	1	0.98	7.979	0.792	7780.959
SENEZE-FSL41336-lm3-dex-f9	*Par. arvernensis*	UCBL-1	2	1.35	2.404	1.241	60043.926
DFN3-150-UM1-f9.sur	*Par. arvernensis*	LGPUT	2	1.522	5.123	0.515	43713.142

[a] Asfc = area-scale fractal complexity; epLsar = exact proportion length-scale anisotropy of relief; Smc = scale of maximal complexity, $Hasfc_{9,36,81}$ = heterogeneity of area-scale fractal complexity on 9, 36 and 81 cell.

Table S3 Kruskal-Walis on dental topographic and enamel thickness variables with genus as a factor[a].

Kruskal–Wallis			
Variables	df	χ^2	*p*
$3DRET_{vol}$	5	14.580	< **0.05**
$3DRET_{geo}$	5	16.671	< **0.05**
LRFI	5	1.628	0.059
DNE	5	9.994	0.075
OPCR	5	13.394	< **0.05**
ACS	5	17.261	< **0.05**
λ	5	1.051	0.073
ARC	5	12.208	< **0.05**

[a] df = degrees of freedom; χ^2 = Chi squared; p value = significance value.

Table S5 Kruskal-Wallis on dental microwear texture variables and their dispersions with genus as factor[a].

Kruskal–Wallis						
	Phase I			**Phase II**		
Variables	df	χ^2	*p*	df	χ^2	*p*
Asfc	5	27.436	< **0.05**	5	30.841	< **0.05**
epLsar	5	1.653	0.895	5	15.376	< **0.05**
$Hasfc_{81}$	5	17.497	< **0.05**	5	19.360	< **0.05**
Tfv	5	32.306	< **0.05**	5	28.492	< **0.05**
Disp–Asfc	5	2.357	0.797	5	4.933	0.424
Disp–epLsar	5	1.641	0.896	5	2.881	0.718
Disp–$Hasfc_{81}$	5	2.658	0.752	5	11.144	< **0.05**
Disp–Tfv	5	19.879	< **0.05**	5	4.776	0.443

[a] df = degrees of freedom, χ^2 = Chi squared, p value = significance value.

Ψηφιακή βιβλιοθήκη Θεόφραστος – Τμήμα Γεωλογίας – Αριστοτέλειο Πανεπιστήμιο Θεσσαλονίκης

Ψηφιακή συλλογή
Βιβλιοθήκη
"ΘΕΟΦΡΑΣΤΟΣ"
Τμήμα Γεωλογίας
Α.Π.Θ

Table S6 Analyses of variance on principal components using microwear texture variables, with genus as a factor[a].

	Phase II						
Variable	Eig.	% Var.	df	SS	MS	F	*p*
PC1	0.086	54.892	5	3.931	0.786	4.767	< **0.05**
PC2	0.049	31.388	5	2.604	0.521	5.452	< **0.05**
PC3	0.018	11.64	5	0.483	0.097	2.347	< **0.05**
PC4	0.003	2.079	5	0.049	0.01	1.666	0.147
	Phase I						
Variable	Eig.	% Var.	df	SS	MS	F	*p*
PC1	0.082	55.274	5	0.161	0.032	.181	0.969
PC2	0.057	38.278	5	3.217	0.643	5.251	< **0.05**
PC3	0.009	6.090	5	0.293	0.059	2.889	< **0.05**
PC4	0.000	0.358	5	0.053	0.011	12.257	< **0.05**

[a] SS = sum of squares; df = degrees of freedom; MS = mean square, F = F–test.

Ψηφιακή βιβλιοθήκη Θεόφραστος – Τμήμα Γεωλογίας – Αριστοτέλειο Πανεπιστήμιο Θεσσαλονίκης

Ψηφιακή συλλογή
Βιβλιοθήκη
"ΘΕΟΦΡΑΣΤΟΣ"
Τμήμα Γεωλογίας
Α.Π.Θ

Table S7 Pairwise comparisons of principal components using microwear texture variables between *Paradolichopithecus* and extant papionin genera, with both Phase I and II facets. Differences indicated by Tukey's HSD and Fisher's LSD are above and below the black diagonal respectively[a].

LSD / HSD	*Paradolichopithecus*		*Papio*		*Theropithecus*		*Mandrillus*		*Macaca*		*Lophocebus*	
Facet	*II*	*I*	*II*	*I*	*II*	*I*	*II*	*I*	*II*	*I*	*II*	*I*
Paradolichopithecus				PC4(+)		PC4(+)		PC4(+)		PC4(+)		PC4(+)
Papio		PC4(–)			PC1(+)			PC4(+)				PC2(+)
Theropithecus		PC2(+), PC4(–)	PC1(–)	PC2(+)			PC2(+)	PC2(+)	PC1(–), PC2(+)	PC2(+)	PC1(–), PC2(+)	PC2(+)
Mandrillus		PC4(–)	PC1(–), PC2(–)	PC4(–)	PC2(–)	PC2(–)					PC1(–)	
Macaca	PC2(–)	PC4(–)	PC2(–), PC3(+)	PC3(+)	PC1(+), PC2(–)	PC2(–)	PC1(+)	PC3(+)			PC3(+)	PC3(+)
Lophocebus		PC4(–)	PC2(–)	PC2(–)	PC1(+), PC2(–), PC3(–)	PC2(–), PC3(–)	PC1(+)	PC3(–)	PC3(–)	PC3(–)		

[a](–) and (+) indicate values that are either lower or higher respectively for species in column compared to the one in row.

Ψηφιακή βιβλιοθήκη Θεόφραστος – Τμήμα Γεωλογίας – Αριστοτέλειο Πανεπιστήμιο Θεσσαλονίκης

Ψηφιακή συλλογή
Βιβλιοθήκη
"ΘΕΟΦΡΑΣΤΟΣ"
Τμήμα Γεωλογίας
Α.Π.Θ

Chapter 6. Investigating the dietary niches of fossil Plio–Pleistocene European macaques.

6.1 Introduction

The genus *Macaca* is the oldest cercopithecine recorded in Eurasia. It arrived probably as early as the latest Miocene, a time in which the level of the Mediterranean Sea fluctuated and eventually dried out facilitating its dispersal from North Africa where it originated (Delson, 1980). There are few macaque specimens from late Miocene sites in Europe with only two fossil finds being fully published, from Almenara-Casablanca M (Köhler et al., 2000) in Spain, and Moncucco Torinese in Italy (Alba et al., 2014). By the Early Pliocene macaques were distributed along the Southern Europe including also the modern Black sea region and southern France (Delson, 1974). During earliest Pleistocene, fossil representatives of *Macaca* were present in southern Europe but also as far as north as Tegelen in the Netherlands (van den Hoek Ostende and de Vos, 2006). Toward the end of the Early Pleistocene, macaques maintained their broad distribution around Europe, where they persisted into the Middle Pleistocene, being present in south-eastern and eastern Britain. However, by the end of Middle and beggining of Late Pleistocene macaques are found mostly in North Africa and Spain, yet Late Pleistocene macaque remains have been recovered from a wider range of European sites but with a less northerly distribution compared to Middle Pleistocene (Elton and O'Regan, 2014). Nonetheless, macaques are absent from Europe with only exception the colony in Gibraltar introduced by humans in historical times (Modolo et al., 2005).

The fossil Plio-Pleistocene European macaques have been attributed to multiple nominal species, but usually most of them considered to be closely related to the extant *Macaca. sylvanus* (Delson, 1975, 1980; Szalay and Delson, 1979; Alba et al., 2011; Roos et al., 2019). Currently, three extinct European subspecies are generally distinguished (Alba et al., 2008, 2018): *Macaca s. prisca*, from the Pliocene of Europe; *Macaca s. florentina*, from the Late Pliocene to Early Pleistocene of southern and central Europe; and *Macaca s. pliocena*, from the Middle Pleistocene of Europe including Caucasus and Israel (Alba et al., 2008). Furthermore, there is an additional fossil species found in the Early to Middle Pleistocene of Sardinia namely *Macaca majori* (Gentili et al., 1998; Zoboli et al., 2016).

Macaca s. prisca is the first macaque from Europe assigned to subspecies rank. It was originally found in the fossil site of Montpellier, in southern France, but it is common in a number of sites from southern Europe spanning from the Ruscinian to the early Villafranchian (5.0-3.0 Ma) land mammal ages (Alba et al., 2018). This subspecies is sometimes found associated with other cercopithecids, *Dolichopithecus ruscinensis* and *Mesopithecus monspessulanus*. Additional fossil remains are known from Italy, France, Hungary, Spain and Germany (Alba et al., 2018). *Macaca s. florentina* was described on the basis of a mandibular specimen (IGF10034) found in the fossiliferous assemblage of Upper Valdarno, which is still one of the most complete and well preserved specimens for this subspecies (Alba et al., 2011; Rook et al., 2013). Other samples are known mostly from isolated specimens from Spain, France, the Netherlands and Italy (Delson, 1980; Gentili et al., 1998; Marigó et al., 2014). *Macaca s. pliocena* has been found in a number of sites across Europe represented mostly by fragmentary dentognathic remains. This subspecies was originally described on the basis of a single upper molar dated from Grays Thurrock, near London. Over a dozen other localities have yielded specimens, all seemingly dated to warm interglacial phases, indicating a range from central Spain to eastern England, Italy, former Czechoslovakia, Italy, Caucasus and Israel (Delson, 1980).

Ψηφιακή βιβλιοθήκη Θεόφραστος – Τμήμα Γεωλογίας – Αριστοτέλειο Πανεπιστήμιο Θεσσαλονίκης

Ψηφιακή συλλογή
Βιβλιοθήκη
"ΘΕΟΦΡΑΣΤΟΣ"

Macaca majori was described on the basis of a relatively large fossil sample found in Capo Figari (Golfo Aranci, north-eastern Sardinia) (Forsyth Major, 1913). Based on its small size, comparable with the smallest extant macaque species of insular and peninsular areas of south-eastern Asia, and a series of distinct cranio-dental features, it is considered to represent an endemic dwarfed species in Sardinia. It still remains unknown if these anatomical traits are associated with somehow different ecological adaptations related to the Sardinian habitats (Rook & O'Higgins, 2005). Be that as it may, some authors casted doubts on the supposed insular dwarfism of the Sardinian macaque (Szalay and Delson, 1979; Delson, 1980; Jablonski, 2002). Nevertheless, on the basis of more recent evidence (e.g. Rook & O'Higgins, 2005), it seems unlikely that the fossils represent a subspecies of *Macaca sylvanus* (e.g. *Macaca sylvanus majori*), rather pointing to a distinct specific status for the Sardinian fossil macaque (Zoboli et al., 2016). Additional fossil remains were recovered from other fossil sites, such Is Oreris (Fluminimaggiore) in southwestern Sardinia, (Zoboli et al., 2016), and more recently from fissure fillings at Monte Tuttavista (Orosei, eastern Sardinia) (Abbazzi et al., 2004). It is uncertain when *Macaca majori* went extinct, due to the rather complex history of Sardinian faunal assemblages, along with the absence of certain age correlations for most of the fossil sites (Sondaar, 1987; Sondaar and Van Der Geer, 2005; Abbazzi et al., 2008b; see also Palombo and Rozzi, 2014 for extended discussion).

The chronostratigraphic range of *Macaca majori* extinction is uncertain, while the relatively complex history of Sardinian faunal assemblages, along with the absence of certain age correlations in most fossil sites recorded makes it more difficult to determine. The only available information regarding its age derives from electron spin resonance (ESR) applied to tooth enamel from a *Nesogoral* tooth which indicates an approximate age of 1.8 Ma (van der Made, 1999). While macaques were present in the Early to Middle Pleistocene of Sardinia, their absence from fossil assemblages postdating the Middle Pleistocene suggests that it became extinct then, although the causes remain unknown (Abbazzi et al., 2004).

Even though Plio-Pleistocene macaques were widely distributed in Europe, there is a general lack of dietary information about them. Macaques today occupy tropical but also more temperate habitats, and are usually regarded as opportunistic and highly eclectic feeders (Fa, 1989; Rowe et al., 1996). They primarily depend on plant matter for food, even though they may supplement their diet with faunal resources like insects, invertebrates, eggs, fish, gastropod and crustaceans (Fooden, 2000; O'Regan et al., 2008; Stewart et al., 2008; Pal et al., 2018). The presumed closest relative of fossil European macaques, the extant *Macaca sylvanus* found in North Africa, appear to prefer fruit and/or seeds such as acorns when available but has diet dominated by leaves (Ménard and Vallet, 1997; Ménard, 2002). This seems to be a common dietary strategy in macaque species found in temperate habitats, such as *Macaca fuscata* found in Japan (Hanya et al., 2011) and some *Macaca mulatta* populations found in high altitudes in China (Sengupta and Radhakrishna, 2016; Cui et al., 2019, 2020). In contrast, macaque species, such as *Macaca nemestrina* and *Macaca nigra* apparently consume more fruits than those in temperate and marginal zones (O'Brien and Kinnaird, 1997; Hanya et al., 2013; Ruppert et al., 2018). Since European Plio-Pleistocene macaques inhabited more temperate habitats, it is assumed that had similar dietary composition and strategies, as seen in extant temperate macaque species (Elton and O'Regan, 2014). However, it must not be taken into account that the behaviors seen in modern species, are equivalent to those of extinct forms, especially when considering the anthropogenic effects on the present day ecosystems.

The present chapter examines the dietary niches of fossil Plio-Pleistocene European *Macaca* representatives. To do that, the analysis is mainly focused on available fossil material of *Macaca majori*, and explores its dental adaptations using dental topographic and enamel thickness analysis on fossil upper molars found in the fossil site of Capo Figari, along with a broad sample of modern cercopithecids. Moreover, the dietary habits of fossil *Macaca* forms

Ψηφιακή βιβλιοθήκη Θεόφραστος – Τμήμα Γεωλογίας – Αριστοτέλειο Πανεπιστήμιο Θεσσαλονίκης

Ψηφιακή συλλογή
Βιβλιοθήκη
"ΘΕΟΦΡΑΣΤΟΣ"
Τμήμα Γεωλογίας
Α.Π.Θ.

(e.g. *Macaca majori* vs *Macaca s*. *florentina*) are assessed, by analyzing their dental microwear textures and compare them with a set of three extant macaque species from different eco-geographic areas: *Macaca sylvanus* from Algeria and Morocco, *Macaca nemestrina* from south-eastern Asia, and *Macaca fuscata* from Japan.

6.2 Material

6.2.1. Dental topographic and enamel thickness analysis

The analysis is focused on two M^2s of *Macaca majori* deriving from two fossil crania specimens found in the fossil site of Capo Figari (Italy, Sardinia). The fossil specimens were unearthed during systematic excavations in the early 20th century by Charles Immanuel Forsyth Major (Rook & Alba, 2012), and they are housed in the Museum of Natural History of Basel. One of the specimens (Ty5199) is a cranium of an adult male individual that preserves all posterior dentition but lacks incisors and left canine (see Rook & O'Higgins, 2005). The other specimen (Ty5203) is a partial skull belonging to a small and possibly sub-adult/juvenile individual, preserving right I^1-M^2 and left central incisor. The selected specimens were slightly worn corresponding to wear grades A to C according to Delson (1973). Additionally, the M^3s of each fossil specimen are included to explore the differences between molar types (Table 6.1). The comparative sample consists of 49 M^2s from 26 extant species of cercopithecids (Table S1 Appendix 6.7).

Table 6.1 Description and linear measurements of fossil sample used for dental topography[a,b].

Locality	Age	ID	Tooth	Wear grades	Linear measurements[b]		
					AW (mm)	L (mm)	AW/L
Capo Figari	~1.8 Ma	Ty5199	M^2 sin	C	8.368	8.466	0.988
			M^3 sin	B	7.926	8.433	0.939
Capo Figari	~1.8 Ma	Ty5203	M^2 dex	B	7.975	7.598	1.049
			M^3 dex	A	7.628	7.631	0.999

[a]Wear grades follow the classification of Delson (1973), ranging from A (no wear) to F (contact between the four dentine wells); [b]AW = Buccolingual anterior width; L = Mesiodistal length.

6.2.2. Dental microwear texture analysis

The fossil material used for dental microwear texture analysis consists of a total 30 specimens (see Table S2 Appendix 6.7) of *Macaca majori*, from the Early to Middle Pleistocene locality of Capo Figari (Italy, Sardinia), five specimens (Va1088, Va1415, Va2058, Va2075, Va352) of *Macaca s. florentina* from the Upper Valdarno fossil sites (Italy), one specimen of *Macaca s.* cf. *prisca*, from the Upper Pliocene/Lower Pleistocene locality of Villafranca d'Asti-Fornace RDB (Italy), and two and one specimens of *Macaca s.* cf. *florentina* from the late Early Pleistocene fossil sites of Cal Guardiola and Vallparadís (Spain) respectively (Alba et al., 2008). The analysis is performed at the species level, as the available sample for each subspecies is limited (Table 6.2; Table S2 Appendix 6.7).

The sample of extant macaques is composed of a total of 86 individuals belonging to three species: *Macaca sylvanus*, *Macaca nemestrina* and *Macaca fuscata*. All specimens of *Macaca fuscata* (*n* = 66) are stored at the Primate Research Institute of the University of Kyoto (KUPRI, Inuyama, Japan), whereas *Macaca sylvanus* (*n* = 9) and *Macaca nemestrina* (*n* = 11) are housed in Muséum National d'Histoire Naturelle de Paris (France). The sample of *Macaca fuscata* comes from three free–ranging populations found at different latitudes in Japan. The

Ψηφιακή βιβλιοθήκη Θεόφραστος – Τμήμα Γεωλογίας – Αριστοτέλειο Πανεπιστήμιο Θεσσαλονίκης

Ψηφιακή συλλογή Βιβλιοθήκη "ΘΕΟΦΡΑΣΤΟΣ" Τμήμα Γεωλογίας Α.Π.Θ.

northern population is situated in Aomori Prefecture in Tōhoku region, the central population in Nagano Prefecture in Chūbu region, and the southern population is situated in the island of Yakushima which is one of the Ōsumi Islands in Kagoshima Prefecture. There is no specific information regarding the specific geographic origin of *Macaca sylvanus* and *Macaca nemestrina* specimens included here.

Table 6.2 Fossiliferous sites with fossil *Macaca* used for dental microwear texture analysis[a].

Taxon	**Locality**	**Age** (Ma)	***n*[a]**	**Phase II**	**Phase I**	**References**
Macaca s. cf. *prisca*	Villafranca d'Asti (RDB)	~3.0	1	1	1	Gentili et al., 1998; Rook et al., 2001
Macaca s. fiorentina	Upper Valdarno	~ 2.7 – 2.6	5	3	5	Rook et al., 2013
Macaca s. cf. *fiorentina*	Cal Guardiola	~1.0 – 0.8	2	2	2	Alba et al., 2008; Madurell-Malapeira et al., 2010, 2014; Strani et al., 2019
Macaca s. cf. *fiorentina*	Vallparadís	~1.0 – 0.8	1	1	1	Alba et al., 2008; Madurell-Malapeira et al., 2010, 2014; Strani et al., 2019
Macaca majori	Capo Figari	~1.8	30	24	26	Abbazzi et al., 2004

[a]n = number of possible individuals.

6.3 Statistical analysis

6.3.1. Dental topographic and enamel thickness analysis

For the upper molar sample, the relationships between variables in our modern sample were evaluated using Pearson's correlation test, including bootstrap resampling (n = 1000), followed by univariate comparisons of each variable between the fossil specimens and modern comparative sample. Furthermore, in order to reduce the number of dimensions considered, after correlations test, the values of all dental topographic variables were box–cox transformed and used to generate a principal component analysis (PCA), including also the fossil specimens. All computations were performed using SPSS v. 22 (IBM Corp, 2013.), PAST v. 3.22 (Hammer et al., 2001), and R v. 3.6 (Team, 2013).

6.3.2. Dental Microwear Texture Analysis

In DMTA, every available facet was considered from both Phase I and II dental wear facets. The dispersion of each texture variable was calculated for both dental facet types using Ln-Levine's test (see section 5.3.2 for more details). Then, all raw microwear texture variable were box-cox transformed to avoid normality assumption violations in parametric tests (Conover and Iman, 1981).

The texture variable differences among populations of *M. fuscata* were assessed using two Kruskal-Wallis tests (one for each dental facet type) with the significance level set at 0.05 including pairwise comparisons with Bonferroni adjustment. Likewise, variable dispersion differences among populations of *M. fuscata* were assessed using two Kruskal-Wallis tests (one for each dental facet type) with the significance level set at 0.05 including pairwise comparisons with Bonferroni adjustment.

The texture variable differences among European fossil (i.e. *M. sylvanus* and *M. majori*) and extant *Macaca* (*M. fuscata*, *M. sylvanus* and *M. nemestrina*) were assessed using two Kruskal-Wallis tests (one for each dental facet type) with the significance level set at 0.05 including pairwise comparisons with Bonferroni adjustment. Similarly, the variable dispersion differences among European fossil and extant *Macaca* were assessed using two Kruskal-Wallis

Ψηφιακή βιβλιοθήκη Θεόφραστος – Τμήμα Γεωλογίας – Αριστοτέλειο Πανεπιστήμιο Θεσσαλονίκης

Ψηφιακή συλλογή
Βιβλιοθήκη
"ΘΕΟΦΡΑΣΤΟΣ"

tests (one for each dental facet type) with the significance level set at 0.05 including pairwise comparisons with Bonferroni adjustment. Lastly, given the number of texture variables considered here and the fact that some are likely correlated (Ungar et al., 2019), two principal component analyses were performed (one for each facet type) using the texture variable data (i.e. Asfc, epLsar, Tfv, $Hasfc_{81}$) to reduce the number of dimensions considered. The resulting principal component scores (i.e. PC1, PC2, PC3, PC4) were box-cox transformed and used to perform two single analyses of variance (ANOVAs) (one for each dental wear facet type), followed by pairwise comparisons using the combination of Tukey's Honest Significant Difference (HSD) and the less conservative Fisher's Least Significant Difference (LSD) following Scott et al., (2012). Computations were performed using SPSS v. 22 (IBM Corp , 2013.) and PAST v. 3.22 (Hammer et al., 2001).

6.4 Results

6.4.1. Dental topographic and enamel thickness analysis

The Pearson's test revealed significant correlations among dental topographic and enamel thickness variables in our sample (Table S3 Appendix 6.7). The area-relative curvature (ARC) is significantly correlated with all variables. Dirichlet normal energy (DNE) is correlated with all variables except absolute crown strength (ACS). Orientation patch count rotated (OPCR) is significantly correlated with area-relative curvature (ARC), Dirichlet normal energy (DNE) and absolute crown strength (ACS). Moreover, the 3D relative volumetric and geometric enamel thickness ($3DRET_{vol}$ and $3DRET_{geo}$) are positively associated, whereas they are significantly correlated with inclination (λ), relief index (LRFI), area-relative curvature (ARC), and Dirichlet normal energy (DNE). Lastly, absolute crown strength (ACS) is significantly correlated with the relief index (LRFI), orientation patch count rotated (OPCR) and 3D relative geometric enamel thickness ($3DRET_{geo}$).

The comparisons of fossil upper molars of *Macaca majori* with extant cercopithecids, indicate closer similarities with durophagous species, but also species with opportunistic dietary habits. The values of $3DRET_{vol}$ for both fossil M^2s of *Macaca majori* fall within the range of hard object feeders like *Lophocebus albigena*, *Lophocebus atterimus* and *Cercocebus galeritus*, whereas Ty5203 specimen possess the highest value in our sample (Fig. 6.1A). The same applies to the values of $3DRET_{geo}$, but in this case the highest values are shown by *Cercocebus galeritus* (Fig. 6.1B). The highest values of ACS are shown by *Papio* (*Papio hamadryas* then *Papio anubis* and *Papio cynocephalus*) followed by *Theropithecus*, *Mandrillus* and *Macaca sylvanus*, whereas the lowest values are shown by *Procolobus verus*. Both Ty5203 and Ty5199 show intermediate values between the extant *Macaca sylvanus*, *Lophocebus albigena* and *Cercocebus torquatus* (Fig. 6.2A). The value of OPCR for Ty5199 falls within the range of *Lophocebus albigena* and *Erythrocebus patas*, while it also falls within the range of values for *Procolobus verus*. Ty5203 exhibits the lowest value in our sample (Fig. 6.2B). The value of LRFI for Ty5203 falls within the range of *Papio anubis*, *Mandrillus leucophaeus* and *Cercopithecus pogonias*, while Ty5199 exhibits the lowest value in our sample, falling within the range of Papio but near the lowest extreme of values (Fig. 6.3A). The value of λ for Ty5203 resembles the extant *Macaca sylvanus*, *Papio anubis*, *Lophocebus albigena* and *Cercopithecus pogonias*, whereas Ty5199 exhibits the highest value in our sample (Fig. 6.3B). The value of DNE for Ty5199 resembles *Cercopithecus diana* and *Macaca sylvanus* while it also falls within the range of *Lophocebus albigena*, while Ty5203 exhibits the lowest value in our sample (Fig. 6.4A). Lastly, both Ty5199 and Ty5203 exhibit low values of ARC, with Ty5203 resembling only one specimen of *Lophocebus albigena* (Fig. 6.4B).

Ψηφιακή βιβλιοθήκη Θεόφραστος – Τμήμα Γεωλογίας – Αριστοτέλειο Πανεπιστήμιο Θεσσαλονίκης

Ψηφιακή συλλογή
Βιβλιοθήκη
"ΘΕΟΦΡΑΣΤΟΣ"
Τμήμα

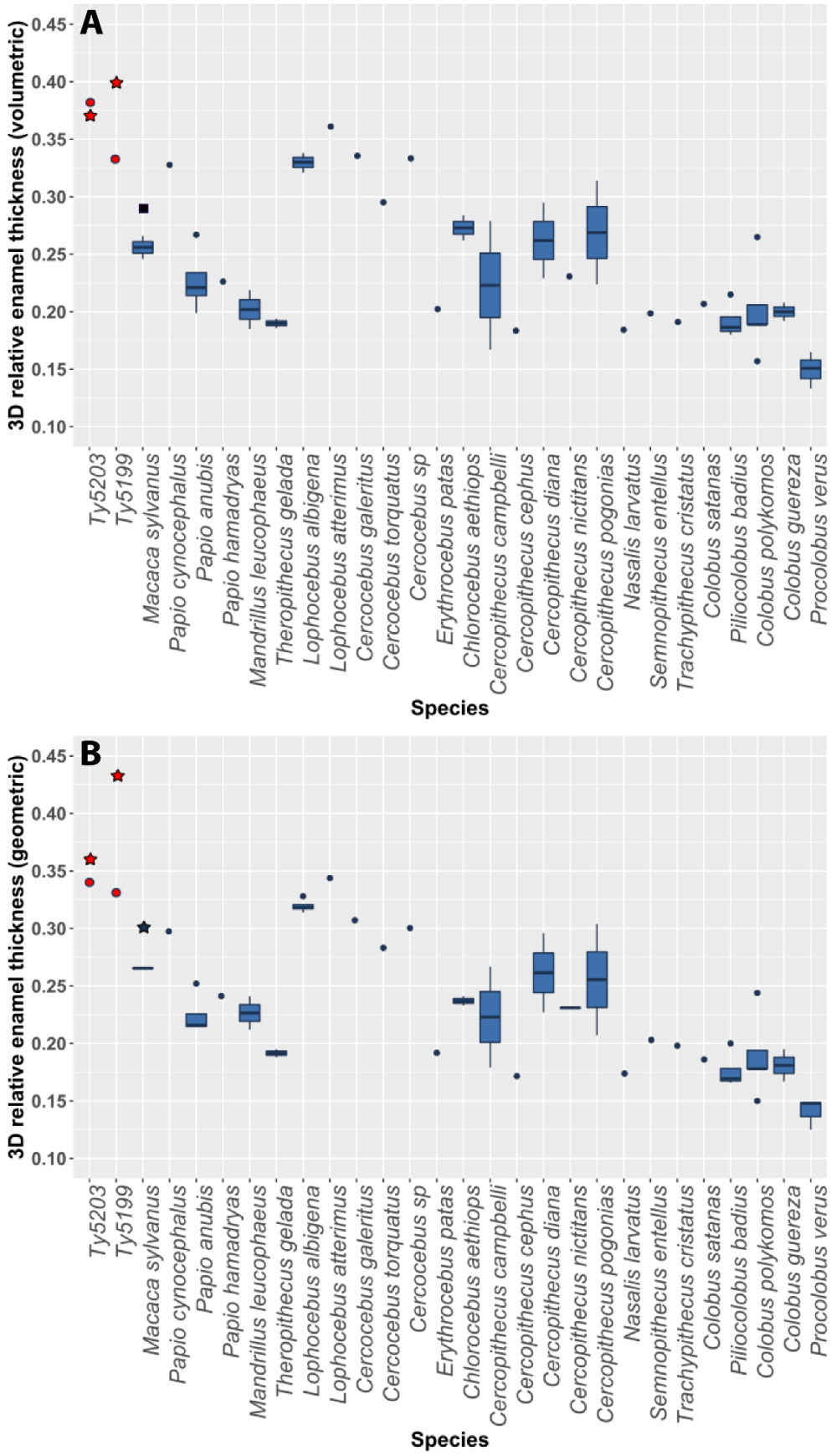

Fig. 6.1 Boxplot comparisons of 3D relative volumetric enamel thickness (**A**), 3D relative geometric enamel thickness (**B**) between extant sample of cercopithecids and fossil *Macaca majori* (Ty5199 and Ty5203). Circle = M^2, Star = M^3.

Ψηφιακή βιβλιοθήκη Θεόφραστος – Τμήμα Γεωλογίας – Αριστοτέλειο Πανεπιστήμιο Θεσσαλονίκης

Ψηφιακή συλλογή
Βιβλιοθήκη
"ΘΕΟΦΡΑΣΤΟΣ"

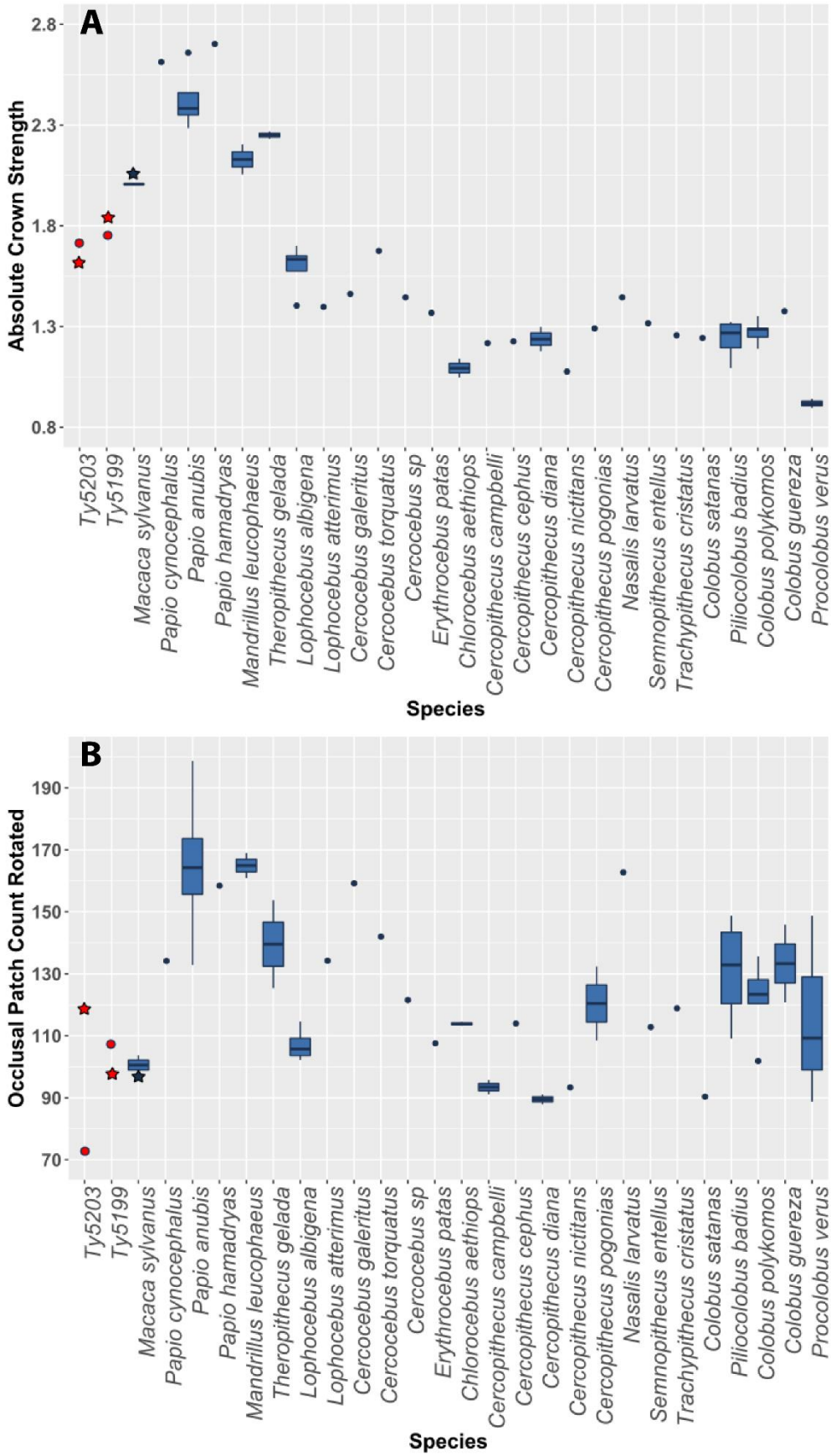

Fig. 6.2 Boxplot comparisons of absolute crown strength (**A**) and orientation patch count rotated (**B**) between extant sample of cercopithecids and fossil *Macaca majori* (Ty5199 and Ty5203). Circle = M^2, Star = M^3.

Ψηφιακή βιβλιοθήκη Θεόφραστος – Τμήμα Γεωλογίας – Αριστοτέλειο Πανεπιστήμιο Θεσσαλονίκης

Ψηφιακή συλλογή
Βιβλιοθήκη
"ΘΕΟΦΡΑΣΤΟΣ"
Τμήμα

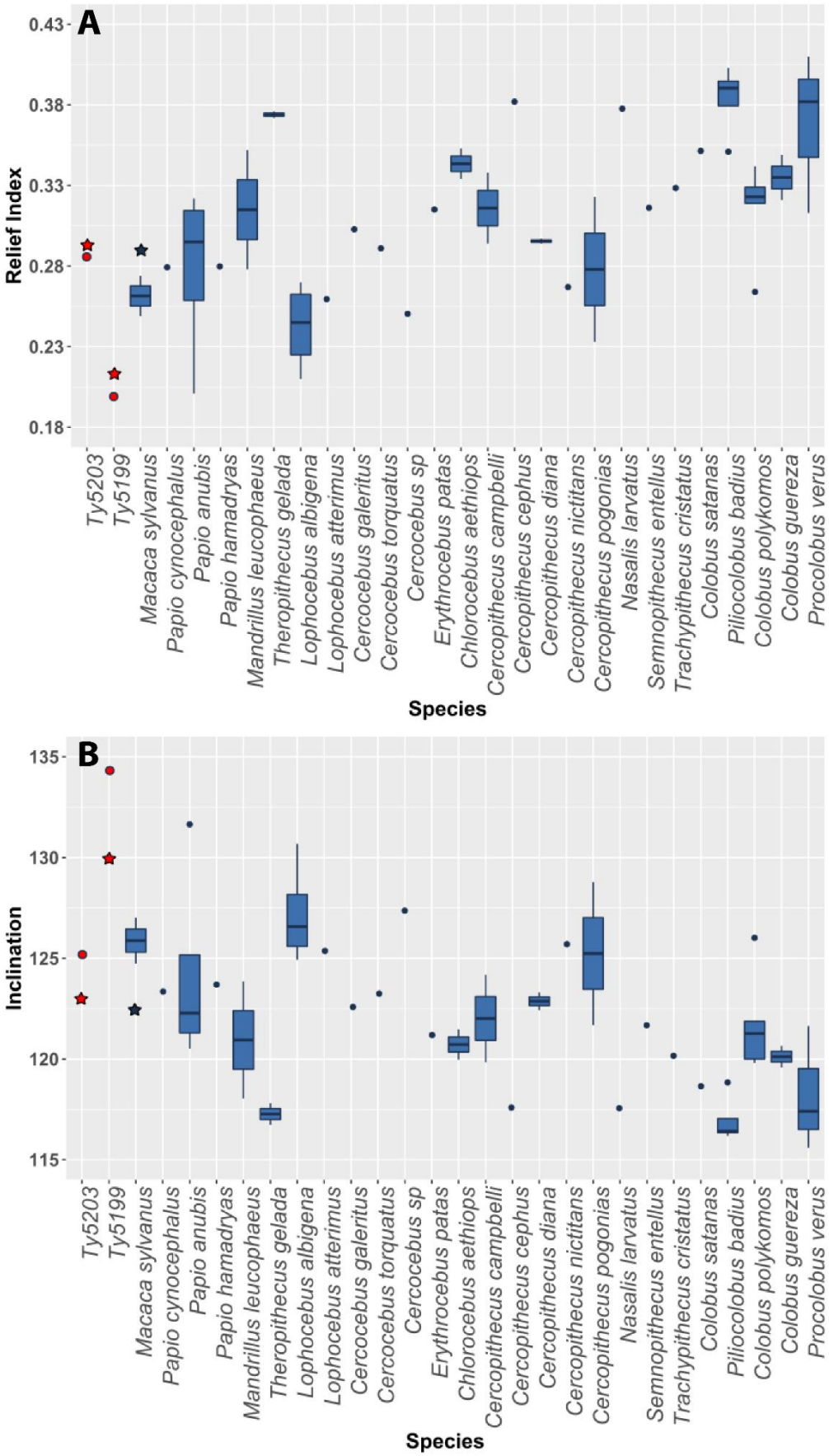

Fig. 6.3 Boxplot comparisons of the relief index (**A**) and inclination (**B**) between extant sample of cercopithecids and fossil *Macaca majori* (Ty5199 and Ty5203). Circle = M^2, Star = M^3.

Ψηφιακή βιβλιοθήκη Θεόφραστος – Τμήμα Γεωλογίας – Αριστοτέλειο Πανεπιστήμιο Θεσσαλονίκης

Ψηφιακή συλλογή
Βιβλιοθήκη
"ΘΕΟΦΡΑΣΤΟΣ"
Τμήμα

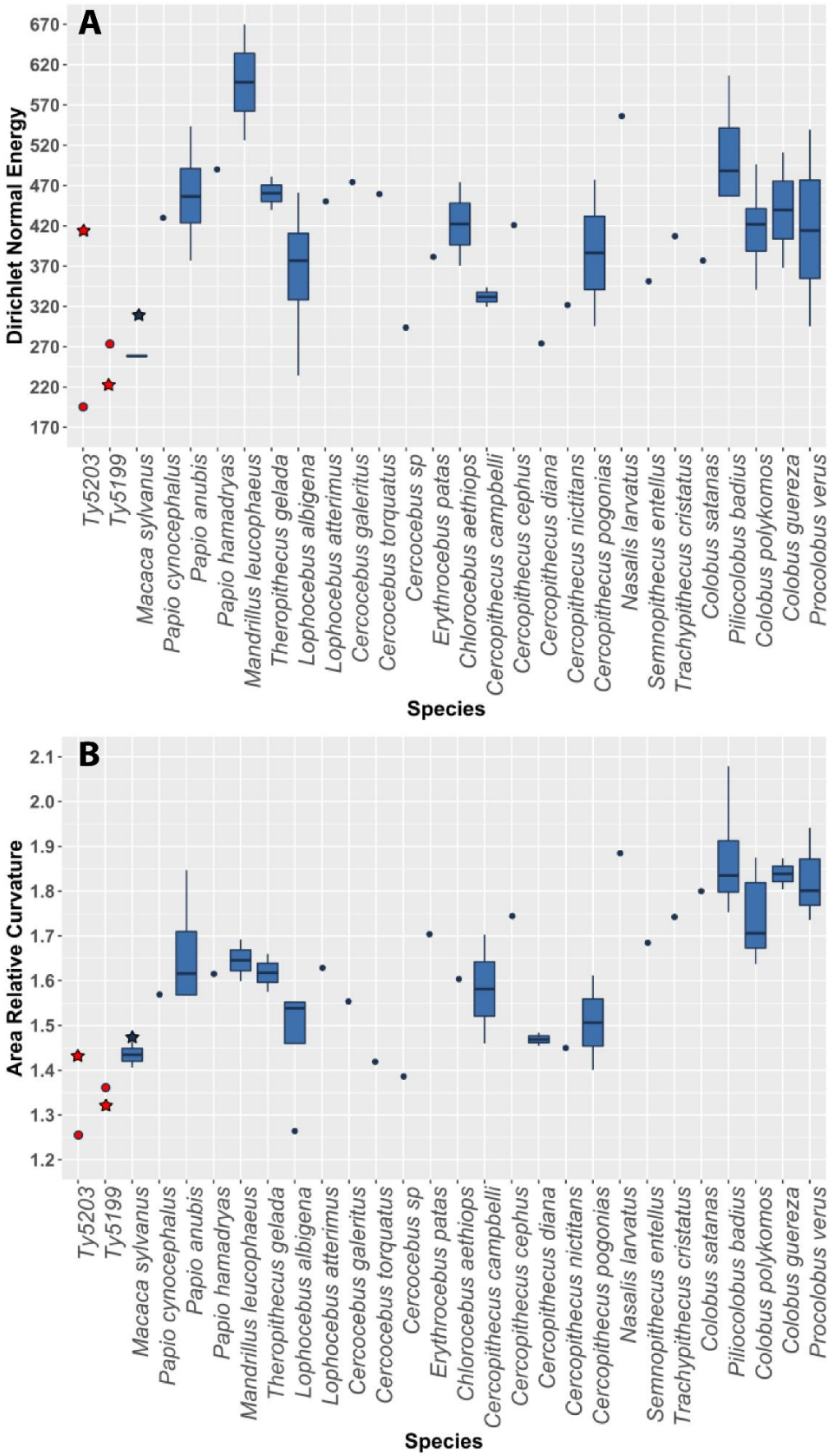

Fig. 6.4 Boxplot comparisons of Dirichlet normal energy (**A**) and area–relative curvature (**B**) between extant sample of cercopithecids and fossil *Macaca majori* (Ty5199 and Ty5203). Circle = M^2, Star = M^3.

Ψηφιακή βιβλιοθήκη Θεόφραστος – Τμήμα Γεωλογίας – Αριστοτέλειο Πανεπιστήμιο Θεσσαλονίκης

Ψηφιακή συλλογή
Βιβλιοθήκη
"ΘΕΟΦΡΑΣΤΟΣ"
Τμήμα Γεωλογίας
Α.Π.Θ

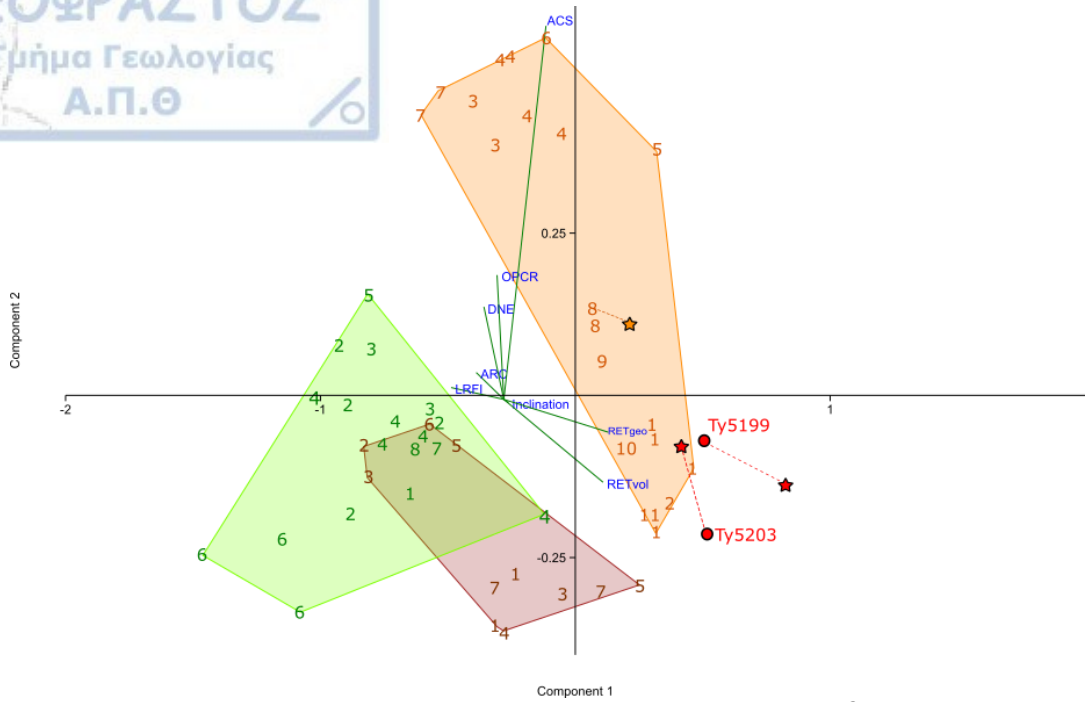

Fig. 6.5 Principal component analysis using dental topographic variables on M^2s of extant cercopithecid species including *Macaca majori* (Ty5199 and Ty5203) fossil molars (Red dots and triangles represent the M^2s and M^3s respectively). **Orange**: Papionini (1: *Lophocebus albigena*, 2*: Lophocebus atterimus*, 3: *Mandrillus leucophaeus*, 4: *Papio anubis*, 5: *Papio cynocephalus*, 6: *Papio hamadryas*; 7: *Theropithecus gelada*, 8: *Macaca sylvanus*, 9: *Cercocebus torquatus*, 10: *Cercocebus galeritus*, 11: *Cercocebus sp.*), **Brown**: Cercopithecini (1: *Chlorocebus aethiops*, 2: *Cercopithecus cephus*, 3: *Cercopithecus campbelli*, 4: *Cercopithecus nictitans*, 5: *Cercopithecus pogonias*, 6: *Erythrocebus patas*, 7: *Cercopithecus diana*), **Green**: Colobinae (1: *Colobus satanas*, 2: *Piliocolobus badius*, 3: *Colobus guereza*, 4: *Colobus polykomos*, 5: *Nasalis larvatus*, 6: *Procolobus verus*, 7: *Semnopithecus entellus*, 8*: Trachypithecus cristatus*).

Differences are observed between the values of M^2 and M^3 but this seems to vary depending on the fossil individual considered. While the M^3 of Ty5199 shows higher value of $3DRET_{vol}$ and ACS than the M^2, as seen in the extant *Macaca sylvanus*, the reverse applies for Ty5203 with the M^2 showing higher value than M^3 (Fig. 6.1A, 6.2A). In $3DRET_{geo}$, both fossil M^3s possess higher values than its respective M^2s and the same applies to the extant *Macaca sylvanus* molars (Fig. 6.1B). The OPCR value fot Ty5203 M3 is higher compared to its respective M^2 and lower in M^3 than its respective M^2 for Ty5199 (Fig. 6.2B). Both Ty5199 and Ty5203 exhibit higher values of LRFI and λ in M^3s instead of its respective M^2s (Fig. 6.3A, B). Concerning DNE and ARC, Ty5203 shows higher values in M^3 compared to its respective M^2, whereas the reverse applies for Ty5199 (Fig. 6.4A, B).

The first two principal components (e.g. PC1 and PC2) summarize 88.57% of the total variance of the sample (Table S4 Appendix 6.6). PC1 accounts for 71.11% of the total variance and it is primarily explained by $3DRET_{geo}$ (29.30%), $3DRET_{vol}$ (27.80%) and LRFI (14.76%), followed by ACS (11.80%), ARC (7.73%), DNE (5.57%), OPCR (1.90%) and λ (1.29%). $3DRET_{geo}$, $3DRET_{vol}$, ACS and λ show positive correlation with the axis, whereas LRFI, ARC, DNE and OPCR negative. PC2 accounts for 17.46% of the total variance and is mainly explained by ACS (50.00%), OPCR (16.65%) and DNE (12.40%), followed by $3DRET_{vol}$ (11.09%), $3DRET_{geo}$ (4.40%), ARC (3.60%), LRFI (1.58%) and λ (0.44%). ACS, OPCR, DNE, ARC and LRFI are positively correlated with the axis, while $3DRET_{vol,}$ $3DRET_{geo}$ and λ show negative correlation with the axis. Both fossil second upper molar specimens (Ty5199 and Ty5203) fall outside of the space occupied by the modern cercopithecids in our sample, yet close to papionins such as *Lophocebus albigena* and *Lophocebus atterimus* (Fig. 6.5).

Ψηφιακή βιβλιοθήκη Θεόφραστος – Τμήμα Γεωλογίας – Αριστοτέλειο Πανεπιστήμιο Θεσσαλονίκης

Ψηφιακή συλλογή
Βιβλιοθήκη
"ΘΕΟΦΡΑΣΤΟΣ"
Τμήμα Γεωλογίας
Α.Π.Θ

Table 6.3 Microwear texture variables descriptive statistics on Phase I, II facets of *Macaca majori*, *Macaca s. florentina* and modern sample[a,b].

Taxa	**facet**	***n***	**Asfc**					**epLsar (x10^3)**					**Hasfc$_{81}$**					**Tfv** (μm^3)				
Extinct			Mean	sd	sem	C.I	disp.	Mean	sd	sem	C.I	disp.	Mean	sd	sem	C.I	disp.	Mean	sd	sem	C.I	disp.
Macaca majori	*Ph. II*	24	**4.478**	2.494	0.509	0.997	0.335	**2.193**	1.286	0.263	0.515	0.274	**0.697**	0.230	0.047	0.097	0.100	**59797**	58453	11931	24682	0.379
	Ph. I	26	**3.595**	1.759	0.345	0.676	0.328	**2.304**	1.334	0.262	0.513	0.348	**0.785**	0.362	0.071	0.146	0.150	**45167**	23059	4522	9313	0.208
Macaca s. florentina	*Ph. II*	7	**1.987**	1.378	0.521	1.021	0.264	**3.275**	1.454	0.550	1.077	0.264	**0.531**	0.120	0.046	0.111	0.051	**37623**	10320	3900	9545	0.172
	Ph. I	9	**0.983**	0.242	0.080	0.156	0.091	**3.558**	1.207	0.402	0.789	0.208	**0.486**	0.167	0.055	0.128	0.082	**35055**	24136	8045	18553	0.450
Modern																						
Macaca fuscata	*Ph. II*	54	**2.325**	1.224	0.166	0.325	0.266	**3.364**	1.589	0.216	0.424	0.311	**0.436**	0.248	0.033	0.068	0.089	**34228**	15233	2072	4157	0.736
	Ph. I	40	**1.634**	0.788	0.124	0.243	0.197	**3.782**	2.057	0.325	0.637	0.318	**0.428**	0.180	0.028	0.057	0.075	**37793**	8724	1379	2790	0.182
(Aomori, North)	*Ph. II*	23	**1.996**	0.867	0.180	0.352	0.226	**3.317**	1.421	0.296	0.581	0.294	**0.374**	0.196	0.041	0.085	0.091	**31811**	15465	3224	6688	0.817
	Ph. I	14	**1.178**	0.524	0.140	0.274	0.128	**3.576**	2.424	0.648	1.270	0.357	**0.386**	0.195	0.052	0.112	0.075	**37797**	9849	2632	5587	0.191
(Nagano, Central)	*Ph. II*	19	**2.680**	1.394	0.319	0.625	0.309	**3.237**	1.407	0.323	0.633	0.300	**0.440**	0.137	0.031	0.066	0.071	**31445**	15501	3556	7470	0.967
	Ph. I	20	**1.835**	0.816	0.182	0.356	0.240	**4.249**	1.606	0.359	0.704	0.250	**0.453**	0.192	0.043	0.090	0.087	**36591**	9014	2015	4218	0.054
(Yakushima, South)	*Ph. II*	12	**2.395**	1.445	0.417	0.817	0.276	**3.654**	2.008	0.580	1.136	0.363	**0.548**	0.408	0.117	0.260	0.115	**43267**	11479	3313	7293	0.216
	Ph. I	6	**2.027**	0.818	0.334	0.654	0.210	**2.705**	1.788	0.730	1.431	0.452	**0.442**	0.075	0.030	0.079	0.034	**41789**	2786	1137	2924	0.054
Macaca sylvanus	*Ph. II*	9	**4.150**	2.200	0.244	0.478	0.381	**2.598**	1.332	0.444	0.870	0.302	**0.718**	0.274	0.030	0.059	0.121	**40469**	8077	897	1759	0.170
	Ph. I	6	**2.107**	1.157	0.193	0.378	0.331	**2.990**	1.012	0.413	0.810	0.143	**1.025**	0.963	0.161	0.315	0.260	**29646**	14043	2340	4587	0.461
Macaca nemestrina	*Ph. II*	11	**3.948**	2.925	0.265	0.519	0.445	**3.248**	2.809	0.847	1.660	0.459	**0.689**	0.167	0.015	0.029	0.084	**45674**	8904	809	1586	0.168
	Ph. I	11	**2.552**	1.685	0.153	0.299	0.382	**4.766**	1.479	0.446	0.874	0.217	**0.917**	0.317	0.029	0.056	0.140	**39465**	8663	787	1543	0.151

[a] sd = standard deviaton; sem =standard error of the mean; C. I = 95% confidence interval; disp. = the mean value of dispersion of the sample (see section 5.3.2 for explanations on calculations); [b]Asfc = Area-scale fractal complexity; epLsar = exact proportion length-scale anisotropy of relief; Hasfc$_{9,36,81}$ = Heterogeneity of area-scale fractal complexity on 9, 36 and 81 cells Tfv = textural fill volume.

Ψηφιακή βιβλιοθήκη Θεόφραστος – Τμήμα Γεωλογίας – Αριστοτέλειο Πανεπιστήμιο Θεσσαλονίκης

Ψηφιακή συλλογή Βιβλιοθήκη "ΘΕΟΦΡΑΣΤΟΣ" Τμήμα Γεωλογίας ΑΠΘ

6.4.2. Dental microwear texture analysis

The Kruskal-Wallis test revealed significant differences between the three populations of *Macaca fuscata* in both dental facet types (Table S5 Appendix 6.6). In Phase II dental facets, the populations from central (Nagano) and southern (Yakushima) Japan exhibit significantly higher values of heterogeneity ($Hasfc_{81}$) compared to the northern (Aomori) population. In Phase I dental facets, the northern (Aomori) population exhibits significantly lower values of complexity (Asfc) compared to southern (Yakushima) and central (Nagano) populations (Table S6 Appendix 6.6).

Significant differences in dental microwear textures are revealed between fossil and extant *Macaca* species in both Phase II and I dental facets (Table 6.3, 6.4). In Phase II dental facets, the Sardinian macaque (*Macaca majori*) possess significantly higher values of complexity (Asfc) than *Macaca fuscata* and *Macaca s. florentina* with the latter also showing significantly lower values compared to *Macaca sylvanus* and *Macaca nemestrina* (Table 6.5). Moreover, *Macaca fuscata* differs from *Macaca sylvanus* having lower values of complexity. In terms of anisotropy (epLsar), significant differences are revealed between *Macaca majori* and *Macaca fuscata* with the latter showing higher values compared to the former (Table 6.5). *Macaca majori* possess significantly higher values of heterogeneity ($Hasfc_{81}$) compared to *Macaca fuscata*, with the latter also having significantly lower values for this variable compared to *Macaca sylvanus* and *Macaca nemestrina* (Table 6.5). Lastly, textural fill volume (Tfv) is significantly higher in *Macaca majori* compared with *Macaca sylvanus* and *Macaca fuscata*, whereas the latter two possess significantly lower textural fill volume compared to *Macaca nemestrina* (Table 6.5).

Table 6.4 Kruskal-Wallis test performed on fossil and extant macaques using dental microwear texture variables and their dispersions with species as factor[a].

	Phase II			**Phase I**		
Variable	**df**	χ^2	***p***	**df**	χ^2	***p***
Asfc	4	24.24	< **0.05**	4	3.814	< **0.05**
epLsar	4	10.401	< **0.05**	4	18.603	< **0.05**
$Hasfc_{81}$	4	37.924	< **0.05**	4	32.873	< **0.05**
Tfv	4	11.157	< **0.05**	4	8.279	0.081
Disp–Asfc	4	2.548	0.636	4	11.778	< **0.05**
Disp–epLsar	4	2.804	0.591	4	5.485	0.241
Disp–$Hasfc_{81}$	4	3.865	0.424	4	13.462	< **0.05**
Disp–Tfv	4	4.859	0.302	4	5.948	0.203

[a]df = degrees of freedom; χ^2 = Chi squared; F = F-statistic; *p* value = significance value.

In Phase I dental facets, *Macaca majori* possess significantly higher values of heterogeneity ($Hasfc_{81}$), higher dispersion of complexity (Disp-Asfc) and lower anisotropy (epLsar) than *Macaca s. florentina*. *Macaca majori* also differs from *Macaca fuscata* having higher complexity (Asfc), higher heterogeneity ($Hasfc_{81}$) and lower anisotropy (epLsar) (Table 6.5). Moreover, *Macaca majori* exhibits significantly higher values of complexity (Asfc) than *Macaca sylvanus* and lower anisotropy (epLsar) compared to *Macaca nemestrina* (Table 6.5). Furthermore, *Macaca s. florentina* shows less dispersion of complexity (Disp-Asfc) than *Macaca sylvanus* and *Macaca nemestrina* (Table 6.5), with the latter also exhibiting significantly higher values of complexity (Asfc) and heterogeneity ($Hasfc_{81}$). The sample of *Macaca fuscata* possess significantly lower values of heterogeneity ($Hasfc_{81}$) compared to *Macaca sylvanus* and *Macaca nemestrina*, with the latter also exhibiting significantly higher dispersion of heterogeneity (Disp-$Hasfc_{81}$). Lastly, *Macaca sylvanus* differs from *Macaca nemestrina* having lower values of anisotropy (epLsar) (Table 6.5).

Ψηφιακή βιβλιοθήκη Θεόφραστος – Τμήμα Γεωλογίας – Αριστοτέλειο Πανεπιστήμιο Θεσσαλονίκης

Ψηφιακή συλλογή
Βιβλιοθήκη
"ΘΕΟΦΡΑΣΤΟΣ"
Τμήμα Γεωλογίας
Α.Π.Θ

Table 6.5 Pairwise comparisons dental microwear texture variables between genus. Variables in bold indicate differences highlighted with Bonferroni adjustment[a].

Species	*Macaca majori*		*Macaca s.florentina*		*Macaca fuscata*		*Macaca sylvanus*		*Macaca nemestrina*	
Facet	*Phase II*	*Phase I*	*Phase II*	*Phase I*	*Phase II*	*Phase I*	*Phase II*	*Phase I*	*Phase II*	*Phase I*
Macaca majori			**Asfc**(–)	**Asfc**(–) epLsar(+) Hasfc$_{81}$(–) Disp–Asfc(–)	**Asfc**(–) **Hasfc$_{81}$**(–) **epLsar**(+) Tfv(–)	**Asfc**(–) **epLsar**(+) **Hasfc$_{81}$**(–) **Disp**–**Hasfc$_{81}$**(–)	Tfv(–)	**Asfc**(–)		**epLsar**(+)
Macaca s.florentina	**Asfc**(+)	**Asfc**(+) epLsar(–) Hasfc$_{81}$(+) Disp–Asfc(+)					Asfc(+)	Disp– Asfc(+)	Asfc(+)	Asfc(+) Hasfc$_{81}$(+) Disp–Asfc(+)
Macaca fuscata	**Asfc**(+) **epLsar**(–) **Hasfc$_{81}$**(+) Tfv(+)	**Asfc**(+) **Hasfc$_{81}$**(+) **epLsar**(–) **Disp– Hasfc$_{81}$**(+)					Asfc(+) Hasfc$_{81}$(+)	Hasfc$_{81}$(+)	**Hasfc$_{81}$**(+) Tfv(+)	**Hasfc$_{81}$**(+) Disp– Hasfc$_{81}$(+)
Macaca sylvanus	Tfv(+)	**Asfc**(+)	Asfc(–)	Disp–Asfc(–)	Asfc(–) Hasfc$_{81}$(–)	Hasfc$_{81}$(–)			Tfv(+)	epLsar(+)
Macaca nemestrina		**epLsar**(–)	Asfc(–)	Asfc(–) Hasfc$_{81}$(–) Disp–Asfc(–)	**Hasfc$_{81}$**(–) Tfv(–)	**Hasfc$_{81}$**(–) Disp–Hasfc$_{81}$(–)	Tfv(–)	epLsar(–)		

[a](–) and (+) indicate values that are either lower or higher respectively for species in column compared to the one in row.

Ψηφιακή βιβλιοθήκη Θεόφραστος – Τμήμα Γεωλογίας – Αριστοτέλειο Πανεπιστήμιο Θεσσαλονίκης

Ψηφιακή συλλογή
Βιβλιοθήκη
"ΘΕΟΦΡΑΣΤΟΣ"
Τμήμα Γεωλογίας

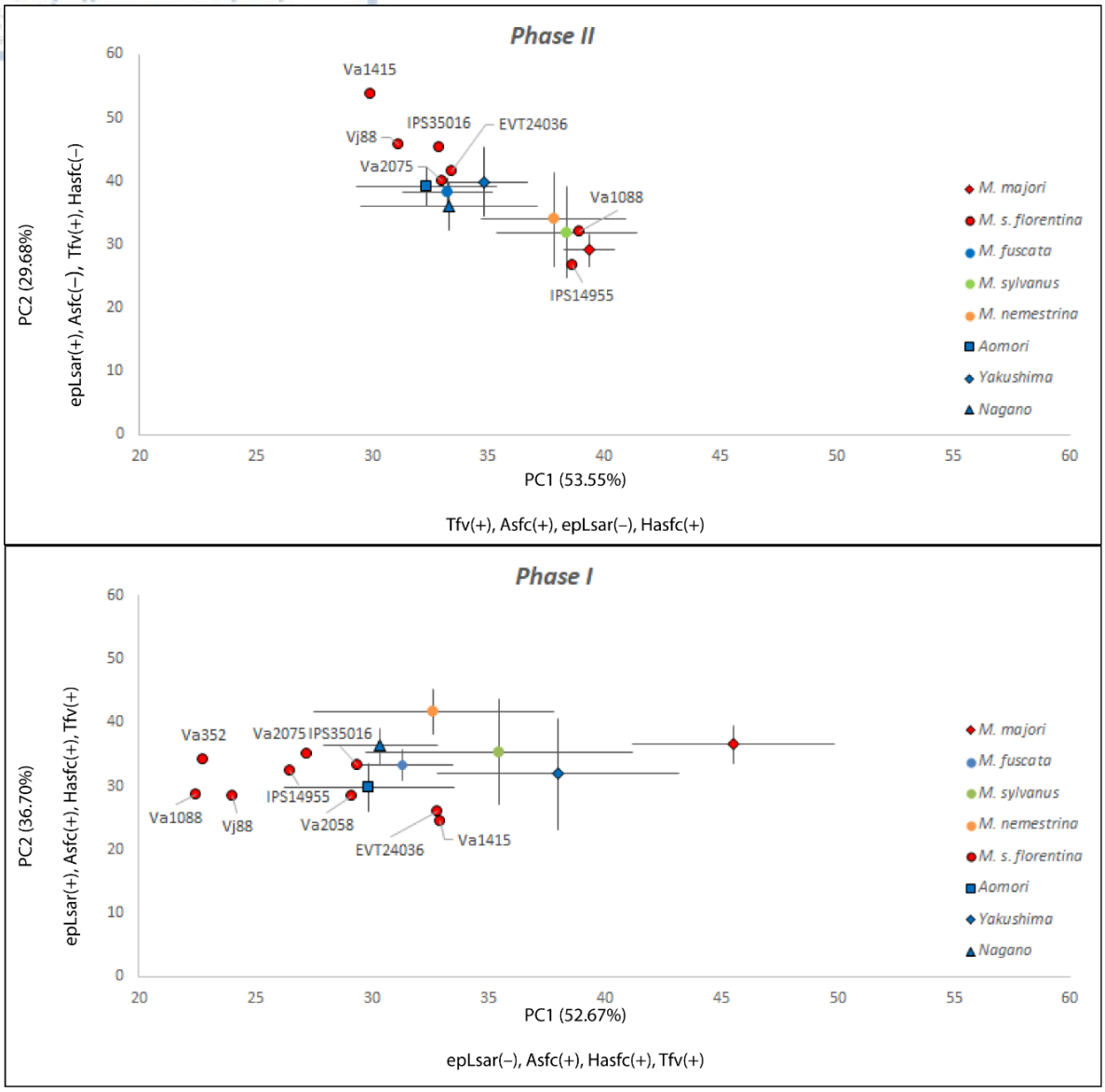

Fig. 6.6 Bivariate plots (means with 95% conf. interval) of PC1 and PC2 between fossil and extant *Macaca* species on Phase II and I dental wear facets, including the total amount of variance explained by each principal component and the effect (positive or negative) of each microwear texture variable. The texture variables are placed in order (from left to right) based on their effect on the principal component (see text for details).

The analyses of variance (ANOVA), performed on the coordinates obtained from principal component analysis (PCA) based on the microwear texture variables, on Phase II dental facets revealed that PC1, PC2 and PC4 shows significant variation, whereas on Phase I, PC1, PC2 and PC3 (Table S7 Appendix 6.7). Concerning Phase II dental facets, PC1 accounts for 53.55% of the total variance and it is primarily explained by textural fill volume (Tfv, 61.59%), complexity (Asfc, 22.16%), anisotropy (epLsar, 10.13%) and heterogeneity ($Hasfc_{81}$, 6.22%), with only anisotropy showing negative correlation with the axis. So, an increase in the values of PC1 can be interpreted as an increase in textural fill volume along with a lesser and slight increase in complexity and heterogeneity respectively, and a decrease in anisotropy (Fig. 6.6). *Macaca majori* has significantly

Ψηφιακή βιβλιοθήκη Θεόφραστος – Τμήμα Γεωλογίας – Αριστοτέλειο Πανεπιστήμιο Θεσσαλονίκης

Ψηφιακή συλλογή
Βιβλιοθήκη
"ΘΕΟΦΡΑΣΤΟΣ"

lower values of PC1 than *Macaca s. florentina* and higher than *Macaca fuscata*, whereas the latter possess significantly lower values of PC1 than both *Macaca sylvanus* and *Macaca nemestrina* (Table S8 Appendix 6.7). In addition, PC2 accounts for 29.68% of the total variance and it is primarily explained by anisotropy (epLsar, 37.95%), complexity (Asfc, 35.50%), textural fill volume (Tfv, 19.72%) and heterogeneity ($Hasfc_{81}$, 6.92%). Complexity and heterogeneity show negative correlation with the axis, while anisotropy and textural fill volume positive. So, an increase in the values of PC2 can be seen as an increase in anisotropy and textural fill volume with a concomitant decrease in complexity and a slight decrease in heterogeneity (Fig. 6.6). *Macaca majori* differs from *Macaca s. florentina* and *Macaca fuscata* having significantly lower values of PC2 (Table S8 Appendix 6.7). Concerning Phase I dental facets, PC1 accounts for 52.67% of the total variance and it is mainly explained by anisotropy (epLsar, 44.04%), complexity (Asfc, 41.67%), heterogeneity ($Hasfc_{81}$, 14.14%), and textural fill volume showing only a trivial effect (Tfv, 0.6%). Anisotropy is negatively associated with the axis whereas complexity, heterogeneity and textural fill volume positively. Thus, an increase in the values of PC1 can be seen as a decrease in anisotropy with an increase in complexity and heterogeneity values (Fig. 6.4). *Macaca majori* exhibits significantly higher values of PC1 compared to *Macaca s. florentina*, *Macaca fuscata*, *Macaca nemestrina* and *Macaca sylvanus*, with the latter showing significantly higher values than *Macaca s. florentina* (Table S8 Appendix 6.7). Furthermore, PC2 accounts for 36.70% of the total variance. It is mostly explained by anisotropy (epLsar, 43.68%), complexity (Asfc, 41.13%) and heterogeneity ($Hasfc_{81}$, 14.81%), while textural fill volume shows a minor effect on the axis, as in PC1. In this case all variables show positive association with the axis. The post hoc comparisons indicate that *Macaca nemestrina* possess significantly higher values of PC2 than both *Macaca s. florentina* and *Macaca sylvanus*, whereas *Macaca majori* has significantly higher values than *Macaca s. florentina* (Table S8 Appendix 6.7). Lastly, PC3 explains a total of 1.50% of the total variance and it is principally explained by textural fill volume (Tfv, 96.58%), whereas the rest of the variables show only a minor effect on this axis (Asfc, 1.71%; $Hasfc_{81}$, 1.64%; epLsar, 0.21%). *Macaca fuscata* has significantly lower values of PC4 than both *Macaca sylvanus* and *Macaca nemestrina* with the latter showing higher values than *Macaca majori* (Table S8 Appendix 6.7).

6.5 Discussion

6.5.1. Dental topographic and enamel thickness analysis

The dental topographic analysis revealed some differences between extant cercopithecid species, that could be used as a baseline to make inferences about the dietary adaptations of *Macaca majori* fossil individuals (Ty5203 and Ty5199). The overall results suggest an upper molar morphology more similar to cercopithecids that primarily consume mechanically challenging food resources such as some fruits, nuts and seeds (e.g. Coiner-Collier et al., 2016). This implies that *Macaca majori* could efficiently process foods with a wide spectrum of mechanical properties, similar to modern macaque species, but it primarily consumed mechanically challenging food items available in its habitat.

The enamel thickness and distribution ($3DRET_{vol}$ and $3DRET_{geo}$ respectively) of Ty5203 and Ty5199 resembles the extant mangabey species such as *Lophocebus albigena*, *Lophocebus atterimus*, *Cercocebus galeritus* and *Cercocebus* sp., which are commonly referred as durophagous species (Daegling et al., 2011; McGraw et al., 2012). It is noteworthy that both fossil specimens exhibit considerably higher values compared to the extant *Macaca sylvanus*, to which all mainland fossil Plio-Pleistocene macaques from Europe are customarily assigned (Delson, 1980; see also

Ψηφιακή βιβλιοθήκη Θεόφραστος – Τμήμα Γεωλογίας – Αριστοτέλειο Πανεπιστήμιο Θεσσαλονίκης

Ψηφιακή συλλογή
Βιβλιοθήκη
"ΘΕΟΦΡΑΣΤΟΣ"

Fooden, 2011). Enamel thickness and its distribution have been used for taxonomic and phylogenetic purposes (Martin, 1985; Thiery et al., 2019), but being subjected to natural selection, its variation patterns have been also used to infer about the ecology of our extinct relatives (Lucas et al., 2008). Factors such as food hardness (Lambert et al., 2004), abrasiveness of food particles and life expectancy (e.g. Pampush et al., 2013), as well as other ecological factors (see Kato et al., 2014), all seem to somehow influence this trait. Therefore, the observed differences in enamel thickness and distribution (e.g. $3DRET_{vol}$ and $3DRET_{geo}$) between the extant *Macaca sylvanus* and *Macaca majori* may reflect ecological differences and/or phylogenetic divergence or both (e.g. allopatric speciation) between them. *Macaca sylvanus* and *Macaca majori* probably shared a common *Macaca* ancestor, which entered Sardinia either by the latest Miocene, when the sea level dropped resulting in connection of Sardinia with mainland Europe during the Messinian Salinity Crisis, although a later arrival during low sea level phases which occurred about 3.8 or 2.9 Ma cannot be ruled out (Haq et al., 1987; van der Made, 1999). A population of this *Macaca* ancestor remained isolated in the insular environment of Sardinia, and being subjected to different selective pressures related with the new ecological conditions it evolved into the smaller form. Nevertheless, this requires further investigation with additional fossil sample from the rest of the fossil Plio-Pleistocene macaques species of Europe (Delson, 1980; Köhler et al., 2000; Alba et al., 2008, 2011, 2014, 2018; Roos et al., 2019 and references therein), and additional sample of extant *Macaca sylvanus*.

Both fossil M^2s show intermediate values of absolute crown strength (ACS) being situated in a space between the largest extant representatives in our sample (e.g. *Papio*, *Theropithecus*, *Mandrillus* and *Macaca*) and the extant *Lophocebus* species, but relatively closer to the latter. This measure (ACS) characterizes the ability of the molar crown to withstand fractures and crack propagation related to high biting forces, yet it is influenced by allometric factors (Schwartz et al., 2020). Indeed, size is a factor that influences dietary ecology (e.g. Leonard & Robertson, 1994) with large bodied primates usually having diets composed mostly of difficult to digest nutrient-poor foods, while the smallest primates tend to specialize on nutrient-high food resources (Clutton-Brock and Harvey, 1977; Gaulin and Konner, 1977; see also Coiner-Collier et al., 2016). Additionally, smaller primates have a more limited ability to forage over long distances and produce high biting forces. These observations suggest that *Macaca majori* possessed the necessary molar size to produce high biting forces for the consumption of mechanically challenging food resources and large food objects, as well as thick enamel to enhance its molars for an abrasive diet and/or avoid tooth failure.

The comparison of relief estimates (e.g. LRFI and λ) are consistent with the previous observations, but the fossil molars show differences between them (Fig. 6.3A, B). While Ty5203 exhibits LRFI values resembling modern *Papio*, *Cercocebus torquatus* and C*ercopithecus pogonias*, Ty5199 exhibits the lowest value in our sample. Moreover, Ty5203 λ values resemble *Macaca sylvanus, Papio anubis*, *Lophocebus albigena*, *Lophocebus atterimus* and *Cercopithecus pogonias*, whereas Ty5199 exhibits the highest value in our sample (Fig. 6.3B). The observed differences are more likely attributed to the different degree of wear in the two fossil molars (Table 6.1), as wear can affect the overall relief of the occlusal area (M'Kirera and Ungar, 2003; Dennis et al., 2004; Pampush et al., 2016).

The comparisons of curvature/sharpness are more difficult to interpret. *Macaca majori* M^2s possess very low values of DNE and ARC which indicates blunter occlusal surfaces. This further suggests an increased reliance on mechanically challenging food resources instead of tough and/or softer ones. However, in the case of DNE there is high overlap even between species with

Ψηφιακή βιβλιοθήκη Θεόφραστος – Τμήμα Γεωλογίας – Αριστοτέλειο Πανεπιστήμιο Θεσσαλονίκης

Ψηφιακή συλλογή
Βιβλιοθήκη
"ΘΕΟΦΡΑΣΤΟΣ"

contrasting dietary habits, such as *Cercocebus torquatus* and *Colobus guereza* (Fig. 6.4A, B). Previous analyses using DNE have yielded contrasting results, with some providing meaningful interpretations regarding diet in some primate groups (Bunn et al., 2011; Godfrey et al., 2012), while others not (Berthaume and Schroer, 2017). In the analysis and sample considered here, area–relative curvature (ARC) discriminates better cercopithecids with contrasting dietary habits (e.g. *Cercocebus torquatus* vs *Colobus guereza*). Lastly, OPCR shows considerable overlap even between species with contrasting dietary habits (Fig. 2.6), supporting previous suggestions that dental complexity may be a poor indicator of diet in some primates (Guy et al., 2013; Winchester et al., 2014; Berthaume et al., 2018; Ungar et al., 2018).

The principal component analysis (PCA) clearly separates papionins from cercopithecins and colobines, with the latter two groups exhibiting some overlap. Moreover, the papionin sample is heterogeneous in terms of size, with the largest species (e.g. *Papio anubis*, *Papio cynocephalus*, *Papio hamadryas*, *Theropithecus gelada* and *Mandrillus leucophaeus*) being separated from the medium-sized ones (*Lophocebus albigena*, *Lophocebus aterrimus*, *Cercocebus torquatus*, *Cercocebus sp*), and *Macaca sylvanus* situated in an intermediate space between them (Fig. 6.5). Both fossil M^2s of *Macaca majori* fall outside of the area of the morphospace occupied by extant papionins. Moreover, *Macaca majori* is situated closer to *Lophocebus* species instead of the extant *Macaca sylvanus*. This implies a molar morphology slightly different from its presumed closest extant relative *Macaca sylvanus*, indicative of more durophagous dietary habits. Lastly, the pattern of variation between M^2 and M^3 is not the same in the two fossil specimens (Fig. 6.5). Both fossil M^2s fall outside of the space occupied by modern papionini, whereas only the M^3 of Ty5203 falls within the range of the modern sample of M^2s. Lastly, Ty5199 more closely resembles the pattern shown by *Macaca sylvanus* than Ty5203 (Fig. 6.5). The observed differences between the fossil M^3s are most likely related to the slightly different wear displayed by the two fossil specimens (Table 6.1).

6.5.2. Dental microwear texture analysis

The results of dental microwear texture analysis suggest that there are significant differences in dental microwear textures between populations of Japanese macaques and between extant and fossil *Macaca* species. The observed differences are possibly associated with the diversity of food resources in their habitat, as well as their availability throughout seasons.

Intraspecific variation

The Japanese macaque (*Macaca fuscata*) is one of the best studied macaque species (Nakagawa et al., 2010). The fact that it is the northernmost non-human primate species and athat is shows a wide distribution across latitudes and various habitats in Japan, makes it an interesting primate species to explore their dietary ecology.

Previous research has shown that there are significant differences in the dietary composition and the time spent feeding of Japanese macaque groups depending on latitude in Japan, which is probably related to the different vegetal resources available in each habitat (Agetsuma and Nakagawa, 1998; Tsuji et al., 2015). As the diversity of available vegetal resources decreases towards northern latitudes in Japan, macaque populations that inhabit mainland Japan (e.g. Honso Island), tend to range over larger areas compared to southern populations (Maruhashi, 1980; Takasaki, 1981). Home range expansion most likely reflects a behavioral/foraging strategy; securing a diverse diet, in terms of quality and quantity, by ranging over larger areas which include

Ψηφιακή βιβλιοθήκη Θεόφραστος – Τμήμα Γεωλογίας – Αριστοτέλειο Πανεπιστήμιο Θεσσαλονίκης

Ψηφιακή συλλογή
Βιβλιοθήκη
"ΘΕΟΦΡΑΣΤΟΣ"

several mosaic vegetation types (Maruhashi, 1980). Furthermore, there is altidudinal variation in the dietary diversity of the Japanese macaques, with populations from higher elevations exhibiting lower dietary diversity compared to populations found in lower elevations (Hanya et al., 2003; Tsuji et al., 2015). Lastly, the abundance of food resources and their quality seem to influence population density of macaque troops (Hanya et al., 2006), as habitat rich in food resources, such as the forests of Yakushima, are more densely populated compared to habitats found in mainland Japan (Maruhashi, 1980).

When focusing into the microwear sample of *Macaca fuscata*, differences are found in the values of heterogeneity ($Hasfc_{81}$) in Phase II, and complexity (Asfc) in Phase I dental facets between populations (Table 6.4). Results of previous analyses suggest differences in heterogeneity between primates with more durophagous dietary habits and tough foliage consumers, possibly as a result of more heterogeneous diet in terms of wear particle size and food composition in the former (Krueger et al., 2008; Ragni et al., 2017; Scott et al., 2012). Higher values of complexity (Asfc) are commonly associated with a diet composed mostly of hard food resources (Scott et al., 2012; Calandra and Merceron, 2016). Both central (Nagano) and southern (Yakushima) populations show higher heterogeneity and complexity compared to the northern one (Aomori) for both dental facet types (Table 6.3, Table S6 Appendix 6.7). This supports more frequent consumption of mechanically challenging food resources, such as some fruits and seeds, for the central and southern populations compared wth the northern. Alternatively it might indicate a less diverse diet in terms of food mechanical properties for the northern populations (Aomori). This in turn, suggests that the northern population displays a more constrained dietary spectrum, in terms of vegetal resources and food mechanical properties, in agreement with the previously suggested lower dietary diversity of Japanese macaques from northern latitudes (e.g. Rosenzweig, 1995; Zhou et al., 2011; Tsuji et al., 2015). Furthermore, the presumed lower dietary diversity of the northern population is also influenced by snowfall and its concomitant effect on the available food resources (e.g. Enari and Sakamaki-Enari, 2013; Tsuji et al., 2015). Nevertheless, the number of individuals from each population is not equal, as well as the number of facets, thus requiring more investigation in the future. However, previous dental microwear analyses on *Macaca fuscata* heavily worn molars using scanning electron microscopy (SEM) categorized the Japanese macaque as a hard object feeder, being more similar to the hard object feeders *Lophocebus albigena* and *Cebus apella* instead of the highly folivorous *Colobus guereza* (Hojo, 1991a,b). Nevertheless, this might have been an expected outcome given the marked dietary differences between macaque species and *Colobus guereza* (Rowe et al., 1996).

Interspecific variation

As Phase I and II dental facets contribute to the shearing and crushing/grinding of food items, respectively, it may be hypothesized that variation in textures on Phase I facets would reflect the abundance and availability of tough vegetal resources in each habitat, whereas texture differences on Phase II facets would reflect other food resources available such as fruits, nuts and seeds. Instead of graphically representing variations of each texture parameter for each dental facet type, a synthetic linear combination was computed to summarize the entire dental microwear texture into two components (e.g. Principal Components), making it easier to graphically represent texture differences between species, while also observing the interaction between variables (Fig. 6.6).

Macaca fuscata differs from *Macaca sylvanus* in the values of complexity (Asfc) and heterogeneity ($Hasfc_{81}$) for Phase II dental facets, while for Phase I they only differ in the latter

Ψηφιακή βιβλιοθήκη Θεόφραστος – Τμήμα Γεωλογίας – Αριστοτέλειο Πανεπιστήμιο Θεσσαλονίκης

Ψηφιακή συλλογή
Βιβλιοθήκη
"ΘΕΟΦΡΑΣΤΟΣ"

variable (Table 6.5). This suggests a lower consumption of hard food resources for *Macaca fuscata* compared with *Macaca sylvanus*. Both *Macaca sylvanus* and *Macaca fuscata* prefer fruits and/or seeds when available but their diets include significant amount of leaves (Hanya et al., 2011). *Macaca fuscata* is the most northerly distributed non-human primate, and it is found in overall cooler and more temperate habitats than, *Macaca sylvanus* which is restricted in northwestern Africa. Thus, it can be presumed that *Macaca fuscata* shows higher reliance on tough foliage compared with *Macaca sylvanus*. This also implies that the overall higher seasonality observed in cooler and more temperate habitats has a significant influence on the availability of preferred food resources, consequently affecting the dietary choices of *Macaca* (Hanya et al., 2013; Tsuji et al., 2013). Conversely, macaques found in tropical habitats tend to feed almost exclusively on fruits which are available most of the time throughout the year (Krishnamani, 1994; Albert et al., 2013a; Sengupta and Radhakrishna, 2016 and references therein). The observed texture differences between *Macaca nemestrina* (Table 6.5), which is mainly found in tropical habitats of the Malay Peninsula, and *Macaca fuscata–Macaca sylvanus* are consistent with this notion.

The fossil macaque from Sardinia differs in several respects for both dental facet types from *Macaca fuscata* (Table 6.5). These texture differences suggest a diet composed mainly of hard food resources and significantly lower amount of tough foliage for the fossil species from Sardinia compared with *Macaca fuscata*. However, when focusing in Phase I dental facets, it is noteworthy that *Macaca majori* is relatively closer to the sample of *Macaca fuscata* from the island of Yakushima (Fig. 6.6). Something similar is observed when observing the differences between *Macaca majori* with *Macaca sylvanus* and *Macaca nemestrina*. Texture differences between *Macaca majori* and *Macaca sylvanus–Macaca nemestrina* are subtler for both dental facet types compared with the observed differences between *Macaca majori* and *Macaca fuscata* (Table 6.5). However, such differences are suggestive of more durophagous dietary habits for the fossil species from Sardinia. *Macaca majori* differs from *Macaca sylvanus* in Phase II dental facets having higher values of textural fill volume (Tfv) (Table 6.5), which is the variable that explains most of the variance seen along PC1 in this dental facet type (Fig. 6.6). It is suggested that textural fill volume may be used as complementary to complexity (Scott et al., 2012). Similarly, *Macaca majori* exhibits significantly higher values of complexity (Asfc) than *Macaca sylvanus* for Phase I dental facets, which further suggests the more frequent consumption of mechanically challenging food resources for the fossil *Macaca* from Sardinia. Likewise, *Macaca majori* has lower values of anisotropy (epLsar) in Phase I dental facets compared to *Macaca nemestrina*. This variable explains most of the variance along PC1 in this dental facet type (Table 6.9; Fig. 6.6) and implies a lesser reliance on foliage for the Sardinian fossil macaque than for *Macaca nemestrina*.

The pairwise comparisons of *Macaca s. florentina* revealed several differences in texture variables relative to *Macaca majori*, *Macaca sylvanus* and *Macaca nemestrina*, whereas it exhibits no differences from *Macaca fuscata* (Table 6.5). This is more clearly evidenced by observing the dispersion of values shown by *Macaca s. florentina* individuals along PC1 and PC2, for both dental facet types (Fig. 6.6). On the one hand, in Phase II dental facets individuals from the latest Early Pleistocene faunas of Cal Guardiola and Vallparadís (IPS35016 and EVT24036 respectively in Alba et al., 2008), the Early Pleistocene of Upper Valdarno (Va1415 and Va2075), and the Late Pliocene of Villafranca d'Asti (Vj88) all fall within the range of *Macaca fuscata*, and more specifically closer to the northern population (Aomori). On the other hand, individuals from Upper Valdarno and Cal Guardiola (Va1088 and IPS14955 respectively) fall closer to *Macaca nemestrina*, *Macaca sylvanus* and *Macaca majori* (Fig. 6.6). Moreover, in Phase I dental facets, all available *Macaca s. florentina* individuals are distributed within the area of the morphospace occupied by *Macaca fuscata,* and closer to the sample from the northern (Aomori) population (Fig. 6.6). All the

Ψηφιακή βιβλιοθήκη Θεόφραστος – Τμήμα Γεωλογίας – Αριστοτέλειο Πανεπιστήμιο Θεσσαλονίκης

Ψηφιακή συλλογή
Βιβλιοθήκη
"ΘΕΟΦΡΑΣΤΟΣ"

above imply a diverse dietary behavior for *Macaca s. florentina*, more closely resembling *Macaca fuscata*. This might be indicative of a low abundance of preferred food resources in their respective habitats. However, dental microwear textures record the dietary behavior days or even weeks prior to death, thus indicating that it might have also been influenced by a seasonal bias in the fossil record, if specimens died more frequently at a given season. Even if the low fossil sample size restricts to some extent the interpretations that can be drawn, the fact that all individuals show the same pattern supports a low abundance of preffered food resources in their respective habitats.

6.5.3. The dietary niches of fossil Plio-Pleistocene European *Macaca* representatives

Fossil Plio-Pleistocene European macaques were by far the long-lasting and widely distributed European papionins, surviving the longest in the fossil record with an extensive distribution within the European realm. Their ability to survive even in the challenging environments of the Pleistocene of Europe was probably facilitated by their dietary flexibility.

The results in the analysis presented here indicate that the Ty5203 and Ty5199 fossil molars possessed some morphological features indicative of durophagous dietary habits (i.e. high $3DRET_{vol}$ and $3DRET_{geo}$, very low ARC, DNE, OPCR), but were also capable of processing more tough food resources, such as leaves, similar to most extant macaque species (see Rowe et al., 1996). Furthermore, some morphological differences are observed between *Macaca majori* and the extant *Macaca sylvanus* (i.e. $3DRET_{vol}$, $3DRET_{geo}$, ACS, LRFI), presumably related to a more durophagous diet for the Sardinian fossil macaque, while they reinforce its distinct species status. (e.g. Rook and O'Higgins, 2005). Nevertheless, the limited comparative sample of extant *Macaca sylvanus* does not allow further interpretation regarding this matter. Additional analyses, based on a larger sample of *Macaca sylvanus* and idealy additional extant *Macaca* species would be required to investigate these questions further.

The suggested dental capabilities of Ty5199 and Ty5203 are in accordance with the dental microwear textures of the *Macaca majori* sample, which indicate a high amount of mechanically challenging food resources in its diet. This is in contrast with its mainland close relative *Macaca s. florentina*. Hence, it is possible that the two fossil European Plio-Pleistocene macaque species (e.g. *Macaca majori* and *Macaca s. florentina*) occupied somewhat different dietary niches, resulting from the different paleoenvironmental conditions of their respective habitats.

Insular habitats/environments can potentially affect several aspects of the ecology of an organism, as isolation from mainland can promote evolutionary diversification and the production of mammal faunas with many ecological variants having convergent functional and anatomical features to varying degrees (Sondaar, 1977). The best known trait shift that characterizes insular mammals is body size change, a graded trend from gigantism in small species to dwarfism in large species (see Rozzi et al., 2020 and references therein). In addition to shifts in body size towards that of intermediate-sized taxa, insular mammals often undergo morphological changes in their skull, brain, teeth and appendicular skeleton (de Vos, 2000; Köhler and Moyà-Solà, 2004; Angelone et al., 2018; van der Geer et al., 2018; Rozzi et al., 2020). The magnitude and direction of such changes result from a combination of selective biotic and abiotic factors (Heaneyl, 1978; Palombo et al., 2013; Van der Geer et al., 2013; van der Geer et al., 2016), the most important probably the absence of predation pressures (Sondaar, 1977; Runemark et al., 2014). Indeed, usually in insular faunas there is absence of large terrestrial predators (Sondaar, 1977; van der Made, 1999). However, the Plio-Pleistocene fossil record of Sardinia records some terrestrial

Ψηφιακή βιβλιοθήκη Θεόφραστος – Τμήμα Γεωλογίας – Αριστοτέλειο Πανεπιστήμιο Θεσσαλονίκης

Ψηφιακή συλλογή
Βιβλιοθήκη
"ΘΕΟΦΡΑΣΤΟΣ"

predators that may have posed a threat to the existing population of the Sardinian *Macaca* (Azzaroli, 1983), and will be discussed next.

A potential predator most likely contemporary to *Macaca majori* in Sardinia is *Chasmaporthetes melei* found in a fissure opening in the Monte Tuttavista quarry area. This insular predator differs from all other *Chasmaporthetes species* in Europe by its smaller size (Rook et al., 2004). It possesses relatively larger canines and narrower fourth premolars, that could be associated with adaptations to the insular ecosystem (Rook et al., 2004). Furthermore, investigations of the enamel structure of *C. melei* suggest that it was not specialized in bone processing and consumption, and it probably relied more on hunting than on scavenging (Ferretti, 1999). Both were undoubtedly present in the late Pliocene to Early Pleistocene of Monte Tuttavista and it has been hypothesized that both entered Sardinia during the dessication of the Mediterranean (Palombo, 2006), even if a later dispersal cannot be excluded, perhaps during the Pliocene sea level standing (e.g. Haq et al., 1987). Be that as it may, it remains unknown if this predator would exert strong predation pressures to *Macaca majori* mainly because their interaction is not so frequent today, and there is no interaction between hyena and macaques in an insular environment. Interesting to note is that interaction between extant striped hyenas (*Hyaena hyaena*) and rhesus macaques (*Macaca mulatta*) has been observed in lowland Nepal, where rhesus macaques sometimes fall prey to hyena, yet it is suggested that they are not the most preferred prey (Bhandari et al., 2020). Thus, even if *Chasmaporthetes* sometimes preyed on *Macaca majori*, other species in the Sardinian environments, such as suids, bovids and other micromammals present (see Palombo, 2006 for more details) might have been more suitable for this predator.

Around Middle to Late Pleistocene, canids arrived into Sardinia, being mainly represented by *Cynotherium* (Palombo, 2006; Madurell-Malapeira et al., 2015). This fossil canine was a small-sized highly specialized hunter of small and swift prey (Lyras & Van Der Geer, 2006). It is noteworthy that the arrival time of canids roughly coincides with the disappearance of *Macaca* in Sardinia. However, at present there is no evidence supporting a causal relationship between the two events and previous research suggested that *Cynotherium* most likely targeted smaller prey (Lyras and Van Der Geer, 2006; Madurell-Malapeira et al., 2015). A unique characteristic worthy of further investigation in Capo Figari and Monte Tuttavista macaque sample is the high percentage of juvenile (and infantile) individuals. Zanaga (1998) who studied the *Macaca majori* sample from Capo Figari, suggested a selective accumulation by large birds of prey, based on some similarities between Capo Figari and the Taung cercopithecid sample as studied by Berger & Clarke (1995) (e.g. the raptor hypothesis). More recently, a study on fossil cercopithecids from the Humpata Plateau in Southern Angola concluded that raptor predation might have been a strong and perhaps underappreciated selective force during the course of primate evolution (Gilbert et al., 2009).

One important question that derives from the above is if predation pressures could be related to *Macaca majori* sudden disappearance around the Early/Middle Pleistocene boundary (i.e.~1.0–0.8 Ma); The abundancy of specimens for *Macaca majori*, suggests that the taxon probably thrived in its environment around Early to Middle Pleistocene. Its disappearance from an insular environment may suggest that predation pressures could have contributed to its extinction. On the other hand, the dietary habits of *Macaca s. florentina*, based on dental microwear textures, are suggestive of more eclectic dietary behavior. This might imply more challenging ecological conditions in European mainland habitats, starting probably as early as latest Pliocene. Hence, while it is plausible that predation pressures might have contributed to the extinction of *M. majori* from Sardinia, it is also plausible that its extinction might be related to vegetation changes related to global paleoenvironmental changes. However, all the above may suggest that several factors may

Ψηφιακή βιβλιοθήκη Θεόφραστος – Τμήμα Γεωλογίας – Αριστοτέλειο Πανεπιστήμιο Θεσσαλονίκης

Ψηφιακή συλλογή
Βιβλιοθήκη
"ΘΕΟΦΡΑΣΤΟΣ"

have contributed to the demise of the genus *Macaca* from European paleohabitats (e.g. Elton and O'Regan, 2014).

The ecological plasticity of macaques and their ability to survive in suboptimal environments is most likely due to their highly eclectic feeding behavior (Jablonski, 2002; O'Regan et al., 2008). Indeed, there are often marked differences in their diets determined by habitat (Hill, 1997; Hanya et al., 2003). Also, at times of lower productivity, such as winter, macaques may fallback to less nutritional resources, including underground storage organs (Iguchi and Izawa, 1990; Tsuji et al., 2013). Thus, fossil macaques can be considered as highly ecologically flexible as their extant relatives and probably were able to survive the more challenging environmental conditions of European habitats during Middle Pleistocene and later on. (e.g. Elton and O'Regan, 2014). Furthermore, there are several pieces of evidence suggesting the presence of refugial biomes in Southern Europe (Tzedakis et al., 2002; Dubey et al., 2006; Gómez and Lunt, 2007; Grill et al., 2007; Postigo Mijarra et al., 2007; Médail and Diadema, 2009; Bertini, 2013; Stümpel et al., 2016; Angelone et al., 2018; Martínez-Freiría et al., 2020). Refugial areas were possibly present in southern Europe from around latest late Pliocene and persisted throughout the climatic fluctuations of the Pleistocene. Such areas might have prolonged the survival of fossil macaques for a period of time, at least until the harsh climatic conditions of the Pleistocene became considerably more intense around the Mid Pleistocene Transition (MPT, 1.0–0.8 Ma, e.g. Willeit et al., 2019). Thus, it is possible that fossil Plio-Pleistocene European macaques exploited the suboptimal habitats of central and northern regions of Europe during warm interglacial phases, while during colder intervals they probably retreated to refugial areas of southern Europe (Delson, 1980). As a result, the harsh climatic events that took place throughout Pleistocene cannot adequately explain the extinction of the genus *Macaca* in Europe. Another possible factor that might have also contributed to the extinction of European macaques during Late Pleistocene is the interaction with early *Homo* (Meloro and Elton, 2013; Elton and O'Regan, 2014).

The fossil record of Europe suggests that the chronostratigraphic range of European macaques and early *Homo* species overlapped for over 1.0 million years, with macaques and hominins co-occuring at a number of Early and Middle Pleistocene faunas in the Iberian Peninsula (see Marigó et al., 2014). Furthermore, the absence of *Macaca majori* after Middle Pleistocene (1.0–0.8 Ma) roughly coincides with the oldest evidence of *Homo* in Sardinia (Sondaar & Van Der Geer, 2005), whose occurence would have had major implications for an unbalanced insular fauna (Sondaar, 1977). Taking in mind the associations between fossil macaques and *Homo* in the late Early, Middle and Late Pleistocene fossil record and the fact that anthropogenic disturbance significantly affects extant barbary macaque habitats and distribution (Fa, 1986; Ménard, 2002; but see Maibeche et al., 2015), it is plausible that macaques were preyed by *Homo,* especially in resource-limited environments (Meloro and Elton, 2013). Hence, it is more likely that the combined effects of harsh climatic fluctuations, which influenced vegetation composition and resource availability, along with predation pressures from carnivores, raptors and/or *Homo,* led to the demise of the genus *Macaca* from Europe, even though other factors occurring as a result of declining populations cannot be excluded (e.g Elton and O'Regan, 2014).

Ψηφιακή βιβλιοθήκη Θεόφραστος – Τμήμα Γεωλογίας – Αριστοτέλειο Πανεπιστήμιο Θεσσαλονίκης

Ψηφιακή συλλογή
Βιβλιοθήκη
"ΘΕΟΦΡΑΣΤΟΣ"
Τμήμα Γεωλογίας
Α.Π.Θ

6.6 Appendix

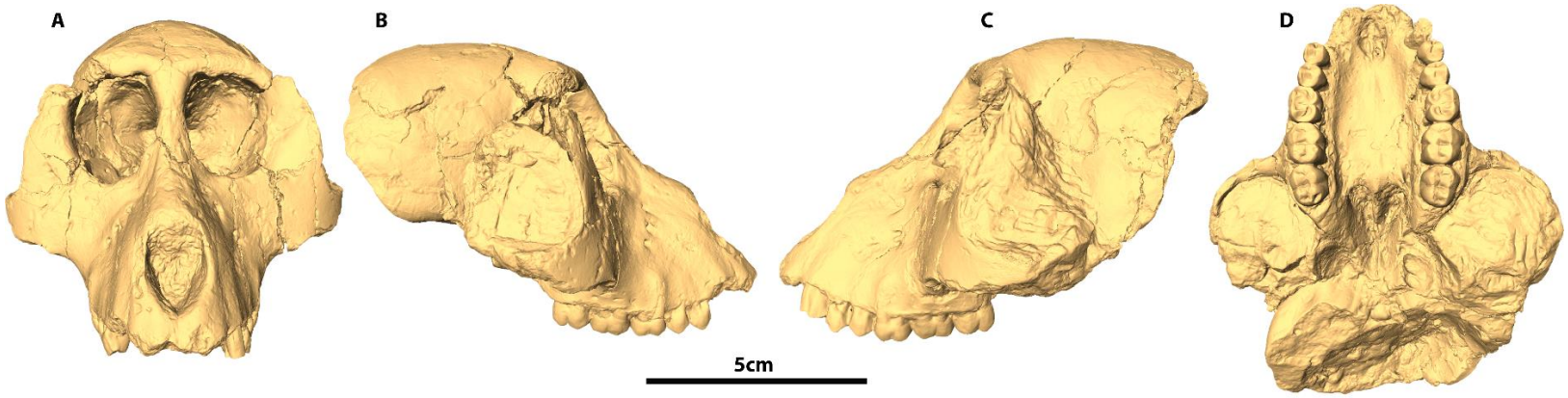

Fig. S1 Digital reconstruction of the fossil cranial specimen of *Macaca majori* (Ty5199) from Capo Figari in (A) facial, (B) lateral dex, (C) lateral sin, (D) occusal.

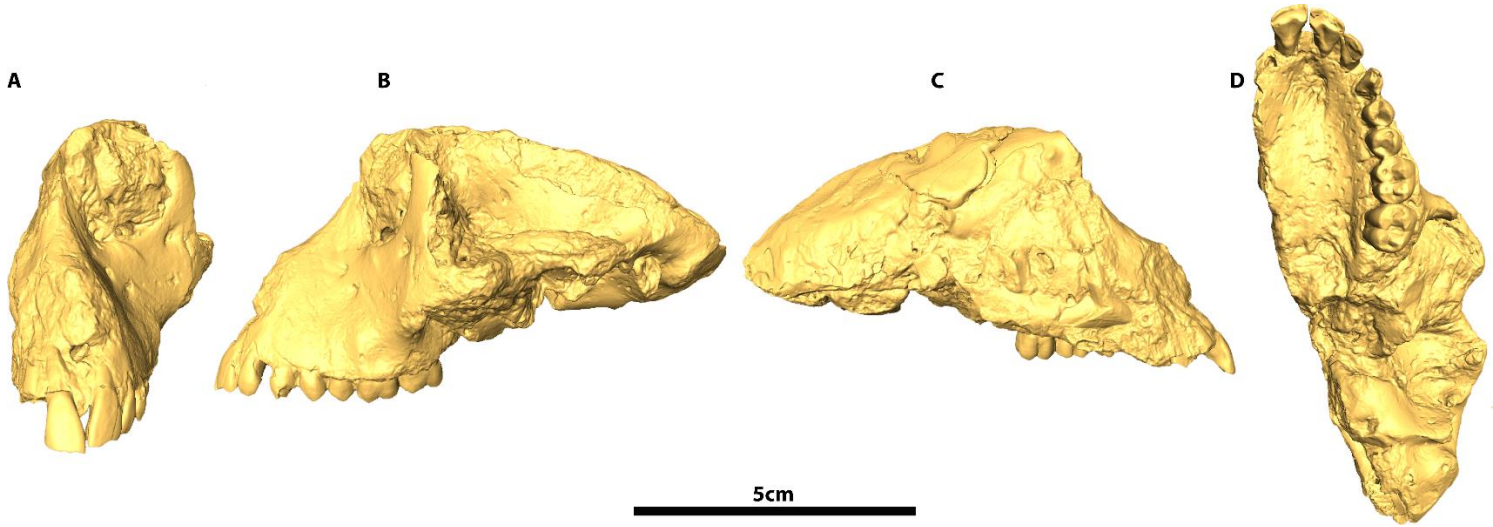

Fig. S2 Digital reconstruction of the fossil cranial specimen of *Macaca majori* (Ty5203) from Capo Figari in (A) facial, (B) lateral sin, (C) lateral dex, (D) occusal.

Ψηφιακή βιβλιοθήκη Θεόφραστος – Τμήμα Γεωλογίας – Αριστοτέλειο Πανεπιστήμιο Θεσσαλονίκης

Ψηφιακή συλλογή
Βιβλιοθήκη
"ΘΕΟΦΡΑΣΤΟΣ"
Τμήμα Γεωλογίας
Α.Π.Θ

Table S1 Enamel thickness and dental topographic variables raw data for fossil *Macaca* representatives and modern cercopithecid sample[a].

Taxon	ID	Institution	Tooth	Inclination	LRFI	ARC	DNE	OPCR	$3DRET_{vol}$	$3DRET_{geo}$	ACS
Ce. galeritus	14486	RMCA	M^2	122.564	0.302	1.552	474.249	159.250	0.336	0.308	1.466
Ce. torquatus	Cb2	PALEVOPRIM	M^2	123.232	0.291	1.417	46.573	141.875	0.295	0.283	1.677
Ce. sp	81–07–M–44	RMCA	M^2	127.353	0.250	1.385	294.715	121.625	0.336	0.301	1.444
Ch. aethiops	1972–302	MNHN	M^2	121.473	0.334	1.602	37.557	113.250	0.262	0.233	1.047
Ch. aethiops	1972–328	MNHN	M^2	119.975	0.353	1.606	474.058	114.500	0.284	0.241	1.140
Cer. campbelli	80–028–M–24	RMCA	M^2	119.841	0.338	1.703	343.609	91.125	0.167	0.179	1.218
Cer. campbelli	36280	RMCA	M^2	124.186	0.294	1.460	319.583	95.750	0.279	0.267	1.214
Cer. cephus	17507	RMCA	M^2	117.601	0.382	1.744	421.641	114.000	0.186	0.172	1.228
Cer. diana	Cc1	PALEVOPRIM	M^2	123.306	0.294	1.484	271.495	91.125	0.229	0.227	1.177
Cer. diana	Cc2	PALEVOPRIM	M^2	122.427	0.297	1.454	275.994	87.875	0.295	0.296	1.298
Cer. nictitans	15650	RMCA	M^2	125.737	0.267	1.451	321.576	93.250	0.232	0.231	1.076
Cer. pogonias	15595	RMCA	M^2	121.687	0.323	1.612	477.263	132.375	0.224	0.207	1.284
Cer. pogonias	18273	RMCA	M^2	128.787	0.233	1.401	295.574	108.500	0.314	0.304	1.289
Co. satanas	33512	SMF	M^2	118.648	0.351	1.798	377.846	9.375	0.206	0.186	1.246
Pi. badius	9201	RMCA	M^2	116.446	0.392	1.753	456.988	109.125	0.189	0.168	1.094
Pi. badius	91–060–M57	RMCA	M^2	116.188	0.403	1.857	519.659	141.625	0.184	0.171	1.228
Pi. badius	91–060–M76	RMCA	M^2	116.396	0.389	2.079	606.586	148.750	0.180	0.166	1.309
Pi. badius	83–042–M77	RMCA	M^2	118.836	0.351	1.813	456.921	124.125	0.215	0.200	1.322
Co. guereza	1216	RMCA	M^2	119.584	0.349	1.873	511.233	145.875	0.192	0.167	1.375
Co. guereza	3800	RMCA	M^2	12.654	0.321	1.804	368.015	12.750	0.208	0.195	1.368
Co. polykomos	10307	RMCA	M^2	126.014	0.264	1.637	34.975	123.375	0.265	0.244	1.287
Co. polykomos	10548	RMCA	M^2	121.873	0.319	1.819	421.911	128.125	0.206	0.194	1.291
Co. polykomos	10602	RMCA	M^2	119.803	0.342	1.673	441.497	120.375	0.157	0.150	1.248
Co. polykomos	8107–M174	RMCA	M^2	12.004	0.329	1.706	388.484	101.875	0.189	0.178	1.352
Co. polykomos	38158	RMCA	M^2	121.263	0.323	1.875	496.536	135.625	0.189	0.178	1.189

Ψηφιακή βιβλιοθήκη Θεόφραστος – Τμήμα Γεωλογίας – Αριστοτέλειο Πανεπιστήμιο Θεσσαλονίκης

Ψηφιακή συλλογή
Βιβλιοθήκη
"ΘΕΟΦΡΑΣΤΟΣ"
Τμήμα Γεωλογίας
Α.Π.Θ

E. patas	8629	RMCA	M^2	121.152	0.315	1.703	381.657	107.625	0.203	0.191	1.368
Lo. albigena	83006–M276	RMCA	M^2	127.332	0.230	1.525	359.662	104.125	0.327	0.318	1.404
Lo. albigena	90042–M–301	RMCA	M^2	124.923	0.270	1.552	461.065	114.625	0.338	0.318	1.633
Lo. albigena	90042–M–301	RMCA	M^2	125.815	0.260	1.553	393.931	107.375	0.333	0.314	1.634
Lo. albigena	Cb4	PALEVOPRIM	M^2	13.679	0.210	1.264	233.940	102.250	0.321	0.328	1.701
Lo. atterimus	14113	RMCA	M^2	125.357	0.259	1.628	451.067	134.500	0.362	0.343	1.403
M. leucophaeus	2002–105	RMCA	M^2	118.038	0.352	1.692	669.965	169.000	0.219	0.212	2.204
M. leucophaeus	1893–269	RMCA	M^2	123.855	0.278	1.599	526.326	16.875	0.185	0.241	2.055
N. larvatus	5042	SMF	M^2	117.571	0.378	1.885	557.442	162.750	0.185	0.174	1.453
P. anubis	80–44–M–101	RMCA	M^2	12.520	0.322	1.568	439.389	132.875	0.223	0.214	2.659
P. anubis	Pp4	PALEVOPRIM	M^2	121.559	0.312	1.664	473.599	163.250	0.267	0.252	2.394
P. anubis	90–042–M226	RMCA	M^2	131.650	0.201	1.567	376.859	165.250	0.199	0.215	2.285
P. cynocephalus	Pp3	PALEVOPRIM	M^2	123.383	0.279	1.570	43.042	134.000	0.328	0.297	2.616
P. hamadryas	97–020–M004	RMCA	M^2	123.688	0.280	1.614	489.983	158.625	0.226	0.241	2.704
P. anubis	C2	PALEVOPRIM	M^2	123.007	0.278	1.847	543.391	198.750	0.219	0.217	2.372
Pr. verus	86–002–M48	RMCA	M^2	117.408	0.382	1.942	539.493	148.750	0.165	0.149	.918
Pr. verus	86–002–M34	RMCA	M^2	115.602	0.410	1.801	414.207	109.250	0.133	0.125	.897
Pr. verus	86–002–M50	RMCA	M^2	121.642	0.313	1.736	295.388	88.750	0.151	0.148	.941
S. entellus	1964–1615	MNHN	M^2	121.695	0.317	1.685	351.854	113.125	0.200	0.202	1.317
T. cristatus	1085	SMF	M^2	12.159	0.328	1.741	408.080	118.875	0.191	0.199	1.259
Th. gelada	1969–449	MNHN	M^2	117.809	0.372	1.575	481.098	153.750	0.194	0.195	2.268
Th. gelada	1969–450	MNHN	M^2	116.726	0.376	1.660	439.736	125.375	0.186	0.188	2.232
Ma. sylvanus	T150kV	MNHN	M^2	124.733	0.274	1.463	257.836	97.375	0.266	0.266	2.006
Ma. sylvanus	T150kV	MNHN	M^2	127.022	0.249	1.406	259.168	103.750	0.246	0.265	2.007
Ma. sylvanus	T150kV	MNHN	M^3	122.533	0.298	1.451	313.061	100.375	0.290	0.307	2.030
Ma. majori	Ty5203	NHMB	M^2	125.156	0.286	1.260	196.770	73.000	0.383	0.340	1.718
Ma. majori	Ty5199	NHMB	M^2	134.320	0.199	1.361	273.333	107.625	0.333	0.332	1.750

Ψηφιακή βιβλιοθήκη Θεόφραστος – Τμήμα Γεωλογίας – Αριστοτέλειο Πανεπιστήμιο Θεσσαλονίκης

Ψηφιακή συλλογή
Βιβλιοθήκη
"ΘΕΟΦΡΑΣΤΟΣ"
Τμήμα Γεωλογίας
Α.Π.Θ

Ma. majori	Ty5203	NHMB	M^3	123.229	0.300	1.439	411.557	119.500	0.367	0.358	1.637
Ma. majori	Ty5199	NHMB	M^3	13.467	0.217	1.324	225.847	96.500	0.400	0.434	1.834

[a] 3DRETvol = 3D volumetric relative enamel thickness; 3DRETgeo = 3D geometric relative enamel thickness; ACS = absolute crown strength; LRFI = relief index; ARC = area–relative curvature; DNE = Dirichlet normal energy; OPCR = orientation patch–count rotated; OES 3D = 3D occlusal enamel surface; OES 2D = 2D occlusal enamel surface.

Table S2 Raw microwear data of fossil *Macaca* sample[a].

Filename	Taxon	Locality	Tooth	Phase	Facet	Asfc	epLsar ($x10^3$)	$HAsfc_{81}$	Tfv
CAPOFIGARI–Ty12456–UM2–sin–f3	*M. majori*	Capo Figari	M^2	1	shearing	3.604	0.759	1.055	42599.2
CAPOFIGARI–Ty12456–UM2–sin–f9	*M. majori*	Capo Figari	M^2	2	crushing	3.107	1.684	0.857	4005.9
CAPOFIGARI–Ty12457–UM2–dex–f3	*M. majori*	Capo Figari	M^2	1	shearing	3.027	3.053	0.533	45768.4
CAPOFIGARI–Ty12458–UM2–dex–f3	*M. majori*	Capo Figari	M^2	1	shearing	3.180	1.924	0.998	37587.2
CAPOFIGARI–Ty12458–UM2–dex–f9	*M. majori*	Capo Figari	M^2	2	crushing	3.150	1.303	0.702	50172.4
CAPOFIGARI–Ty12460–lm2–dex–f6	*M. majori*	Capo Figari	M_2	1	shearing	4.871	1.489	0.574	30903.2
CAPOFIGARI–Ty12460–lm2–dex–f9	*M. majori*	Capo Figari	M_2	2	crushing	4.385	2.313	0.833	37233.6
CAPOFIGARI–Ty12462–UM2–sin–f3	*M. majori*	Capo Figari	M^2	1	shearing	5.199	1.723	1.549	35216.7
CAPOFIGARI–Ty12462–UM2–sin–f9	*M. majori*	Capo Figari	M^2	2	crushing	3.040	0.760	1.002	42805.8
CAPOFIGARI–Ty12464–UM2–sin–f9	*M. majori*	Capo Figari	M^2	2	crushing	11.865	2.286	0.694	43647.7
CAPOFIGARI–Ty12469–lm3–sin–f6	*M. majori*	Capo Figari	M_3	1	shearing	4.181	1.365	1.453	43024.2
CAPOFIGARI–Ty12469–lm3–sin–f9	*M. majori*	Capo Figari	M_3	2	crushing	2.216	2.211	1.099	23349.7
CAPOFIGARI–Ty12470–lm3–sin–f6	*M. majori*	Capo Figari	M_3	1	shearing	1.577	4.657	0.644	39795.8
CAPOFIGARI–Ty12470–lm3–sin–f9	*M. majori*	Capo Figari	M_3	2	crushing	5.126	2.374	0.628	3519.1
CAPOFIGARI–Ty12472–UM2–dex–f4	*M. majori*	Capo Figari	M^2	1	shearing	6.632	1.795	0.593	45567.6
CAPOFIGARI–Ty12493–lm1–dex–f5	*M. majori*	Capo Figari	M_1	1	shearing	1.404	1.403	0.399	34603.0
CAPOFIGARI–Ty12499–lm2–sin–f9	*M. majori*	Capo Figari	M_2	2	crushing	6.555	2.519	0.577	49167.4
CAPOFIGARI–Ty12502–UM3–sin–f3	*M. majori*	Capo Figari	M^3	1	shearing	1.145	4.294	0.410	41987.0

Ψηφιακή βιβλιοθήκη Θεόφραστος – Τμήμα Γεωλογίας – Αριστοτέλειο Πανεπιστήμιο Θεσσαλονίκης

Ψηφιακή συλλογή
Βιβλιοθήκη
"ΘΕΟΦΡΑΣΤΟΣ"
Τμήμα Γεωλογίας
Α.Π.Θ

CAPOFIGARI–Ty12502–UM3–sin–f9	*M. majori*	Capo Figari	M^3	2	crushing	3.863	1.719	0.548	1812.0
CAPOFIGARI–Ty12514–lm3–dex–f5	*M. majori*	Capo Figari	M_3	1	shearing	1.985	1.499	0.704	1387.7
CAPOFIGARI–Ty12514–lm3–dex–f9	*M. majori*	Capo Figari	M_3	2	crushing	1.956	5.544	0.554	254809.9
CAPOFIGARI–Ty5203–UM2–dex–f4	*M. majori*	Capo Figari	M^2	1	shearing	4.531	0.703	1.651	36644.4
CAPOFIGARI–Ty5207–UM2–sin–f4	*M. majori*	Capo Figari	M^2	1	shearing	4.158	1.052	1.233	41671.9
CAPOFIGARI–Ty5209–lm2–dex–f6	*M. majori*	Capo Figari	M_2	1	shearing	1.250	3.759	0.414	39909.4
CAPOFIGARI–Ty5209–lm2–dex–f9	*M. majori*	Capo Figari	M_2	2	crushing	7.328	2.440	0.948	50773.1
CAPOFIGARI–Ty5210–lm2–dex–f6	*M. majori*	Capo Figari	M_2	1	shearing	3.307	3.591	0.794	35585.4
CAPOFIGARI–Ty5210–lm2–dex–f9	*M. majori*	Capo Figari	M_2	2	crushing	7.604	1.792	0.457	43386.4
CAPOFIGARI–Ty5211–lm3–dex–f6	*M. majori*	Capo Figari	M_3	1	shearing	3.684	1.320	0.784	53355.9
CAPOFIGARI–Ty5211–lm3–dex–f9	*M. majori*	Capo Figari	M_3	2	crushing	2.539	4.025	1.309	56952.9
CAPOFIGARI–Ty5213–lm3–dex–f6	*M. majori*	Capo Figari	M_3	1	shearing	3.528	0.045	0.529	51379.7
CAPOFIGARI–Ty5213–lm3–dex–f9	*M. majori*	Capo Figari	M_3	2	crushing	3.166	0.562	0.526	18555.1
CAPOFIGARI–Ty5214–lm3–sin–f5	*M. majori*	Capo Figari	M_3	1	shearing	1.702	2.375	0.769	30071.4
CAPOFIGARI–Ty5215–lm3–sin–f6	*M. majori*	Capo Figari	M_3	1	shearing	6.053	2.511	0.478	42891.5
CAPOFIGARI–Ty5215–lm3–sin–f9	*M. majori*	Capo Figari	M_3	2	crushing	5.350	3.177	0.446	34518.1
CAPOFIGARI–Ty5216–lm2–sin–f9	*M. majori*	Capo Figari	M_2	2	crushing	2.873	5.444	.935	36768.2
CAPOFIGARI–Ty5217–lm2–sin–f5	*M. majori*	Capo Figari	M_2	1	shearing	2.752	4.623	0.937	48613.7
CAPOFIGARI–Ty5217–lm2–sin–f9	*M. majori*	Capo Figari	M_2	2	crushing	3.543	1.133	0.610	4348.8
CAPOFIGARI–Ty5218–lm2–dex–f5	*M. majori*	Capo Figari	M_2	1	shearing	4.479	2.995	0.660	50127.5
CAPOFIGARI–Ty5218–lm2–dex–f9	*M. majori*	Capo Figari	M_2	2	crushing	6.599	1.301	0.629	33147.0
CAPOFIGARI–Ty5221–lm1–dex–f6	*M. majori*	Capo Figari	M_1	1	shearing	4.292	1.392	0.914	4271.8
CAPOFIGARI–Ty5221–lm1–dex–f9	*M. majori*	Capo Figari	M_1	2	crushing	8.272	1.972	0.827	5631.0
CAPOFIGARI–Ty5223–UM1–sin–f4	*M. majori*	Capo Figari	M^1	1	shearing	6.822	4.614	0.623	42351.1

Ψηφιακή βιβλιοθήκη Θεόφραστος – Τμήμα Γεωλογίας – Αριστοτέλειο Πανεπιστήμιο Θεσσαλονίκης

Ψηφιακή συλλογή
Βιβλιοθήκη
"ΘΕΟΦΡΑΣΤΟΣ"
Τμήμα Γεωλογίας
Α.Π.Θ

CAPOFIGARI–Ty5223–UM1–sin–f9	*M. majori*	Capo Figari	M^1	2	crushing	1.520	1.440	0.414	43031.0
CAPOFIGARI–Ty5226–UM1–dex–f9	*M. majori*	Capo Figari	M^1	2	crushing	1.937	1.425	0.537	39392.8
CAPOFIGARI–Ty5229–UM1–sin–f12	*M. majori*	Capo Figari	M^1	2	crushing	3.153	0.673	0.496	70381.0
CAPOFIGARI–Ty5229–UM1–sin–f4	*M. majori*	Capo Figari	M^1	1	shearing	2.614	2.600	0.918	37502.3
CAPOFIGARI–Ty5302–lm2–sin–f5	*M. majori*	Capo Figari	M_2	1	shearing	0.931	1.158	0.280	61133.8
CAPOFIGARI–Ty5302–lm2–sin–f9	*M. majori*	Capo Figari	M_2	2	crushing	3.012	2.054	0.539	232205.8
CAPOFIGARI–Ty5304–lm3–sin–f6	*M. majori*	Capo Figari	M_3	1	shearing	6.563	3.224	0.518	149495.3
CAPOFIGARI–Ty5304–lm3–sin–f9	*M. majori*	Capo Figari	M_3	2	crushing	5.327	2.489	0.574	81683.0
CALGUARDIOLA–IPS14955–UM2–dex–f12	*M.* cf. *sylvanus*	Cal Guardiola	M^2	2	crushing	2.468	0.886	0.557	58357.4
CALGUARDIOLA–IPS14955–UM2–dex–f3	*M.* cf. *sylvanus*	Cal Guardiola	M^2	1	shearing	1.052	3.996	0.510	26362.1
CALGUARDIOLA–IPS35016–lm1–dex–f11	*M.* cf. *sylvanus*	Cal Guardiola	M_1	2	crushing	1.734	4.772	0.575	33822.8
CALGUARDIOLA–IPS35016–lm1–dex–f5	*M.* cf. *sylvanus*	Cal Guardiola	M_1	1	shearing	1.261	3.526	0.682	40698.4
VALDARNO–VA1088–lm2–sin–f5	*M. s. florentina*	Upper Valdarno (Inferno)	M_2	1	shearing	0.606	4.208	0.362	31307.3
VALDARNO–VA1088–lm2–sin–f9	*M. s. florentina*	Upper Valdarno (Inferno)	M_2	2	crushing	4.877	3.507	0.689	40249.6
VALDARNO–VA1415–lm2–sin–f6	*M. s. florentina*	Upper Valdarno (Inferno)	M_2	1	shearing	0.923	1.772	0.524	92676.4
VALDARNO–VA1415–lm2–sin–f9	*M. s. florentina*	Upper Valdarno (Inferno)	M_2	2	crushing	0.912	5.189	0.309	39551.0
VALDARNO–VA2058–lm2–sin–f5	*M. s. florentina*	Upper Valdarno (Inferno di Sotto)	M_2	1	shearing	1.067	2.795	0.343	16841.0
VALDARNO–VA2075–lm1–dex–f6	*M. s. florentina*	Upper Valdarno (Tassinaia)	M_1	1	shearing	1.355	4.420	0.455	10125.9
VALDARNO–VA2075–lm1–dex–f9	*M. s. florentina*	Upper Valdarno (Tassinaia)	M_1	2	crushing	1.324	2.281	0.448	31852.9
VALDARNO–VA352–lm2–dex–f5	*M. s. florentina*	Upper Valdarno (Le Strette)	M_2	1	shearing	0.990	5.558	0.291	33349.8
VALLPARADIS–EVT24036–UM2–sin–f4	*M.* cf. *sylvanus*	Vallparadís	M^2	1	shearing	0.919	1.983	0.805	43137.1
VALLPARADIS–EVT24036–UM2–sin–f9a	*M.* cf. *sylvanus*	Vallparadís	M^2	2	crushing	1.628	3.196	0.553	33468.8
VILLAFRANCADASTI–Vj88–UM2–sin–f4	*M. s.* cf. *prisca*	Villafranca d'Asti (RDB)	M^2	1	shearing	0.679	3.767	0.405	20997.9

Ψηφιακή βιβλιοθήκη Θεόφραστος – Τμήμα Γεωλογίας – Αριστοτέλειο Πανεπιστήμιο Θεσσαλονίκης

Ψηφιακή συλλογή Βιβλιοθήκη "ΘΕΟΦΡΑΣΤΟΣ" Τμήμα Γεωλογίας Α.Π.Θ

VILLAFRANCADASTI–Vj88–UM2–sin–f12	*M. s.* cf. *prisca*	Villafranca d'Asti (RDB)	M^2	2	crushing	0.969	3.096	0.587	26065.2

[a] Asfc = area-scale fractal complexity; epLsar = exact proportion length-scale anisotropy of relief; Smc = scale of maximal complexity; $Hasfc_{9,36,81}$ = heterogeneity of area-scale fractal complexity on 9, 36 and 81 cell.

Table S3 Pearson's correlation on enamel thickness and dental topographic variables[a,b,c]. Pairs of variables that are significantly correlated are shown in bold.

		λ	LRFI	ARC	DNE	OPCR	$3DRET_{vol}$	$3DRET_{geo}$	ACS
λ	corr.		–0.984[b]	–0.728[b]	–0.567[b]	–0.135[a]	0.650[b]	0.739[b]	0.226[b]
	sig.		**< 0.05**	**< 0.05**	**< 0.05**	0.349	**< 0.05**	**< 0.05**	0.115
LRFI	corr.	–0.984[b]		0.714[b]	0.533[b]	0.107	–0.663[b]	–0.764[b]	–0.306[b]
	sig.	**< 0.05**		**< 0.05**	**< 0.05**	0.460	**< 0.05**	**< 0.05**	**< 0.05**
ARC	corr.	–0.728[b]	0.714[b]		0.651[b]	0.367[b]	–0.677[b]	–0.763[b]	–0.264[b]
	sig.	**< 0.05**	**< 0.05**		**< 0.05**	**< 0.05**	**< 0.05**	**< 0.05**	0.064
DNE	corr.	–0.567[b]	0.533[b]	0.651[b]		0.782[b]	–0.308[b]	–0.365[b]	0.186
	sig.	**< 0.05**	**< 0.05**	**< 0.05**		**< 0.05**	**< 0.05**	**< 0.05**	0.196
OPCR	corr.	–0.135	0.107	0.367[b]	0.782[b]		–0.121	–0.114	0.504[b]
	sig.	0.349	0.460	**< 0.05**	**< 0.05**		0.402	0.430	**< 0.05**
3DRETvol	corr.	0.650[b]	–0.663[b]	–0.677[b]	–0.308[b]	–0.121		0.962[b]	0.193[b]
	sig.	**< 0.05**	**< 0.05**	**< 0.05**	**< 0.05**	0.402		**< 0.05**	0.178
3DRETgeo	corr.	0.739[b]	–0.764[b]	–0.763[b]	–0.365[b]	–0.114	0.962[b]		0.302[b]
	sig.	**< 0.05**	**< 0.05**	**< 0.05**	**< 0.05**	0.430	**< 0.05**		0.033
ACS	corr.	0.226[b]	–0.306[b]	–0.264[b]	0.186	0.504[b]	0.193[b]	0.302[b]	
	sig.	0.115	**< 0.05**	0.064	0.196	**< 0.05**	0.178	**< 0.05**	

[a]Correlation is significant at the 0.05 level (2–tailed); [b]Correlation is significant at the 0.01 level (2–tailed); [c]3DRETvol = 3D volumetric relative enamel thickness; 3DRETgeo = 3D geometric relative enamel thickness; ACS = absolute crown strength; LRFI = relief index; λ = Inclination; ARC = area-relative curvature; DNE = Dirichlet normal energy; OPCR = orientation patch-count rotated.

Ψηφιακή βιβλιοθήκη Θεόφραστος – Τμήμα Γεωλογίας – Αριστοτέλειο Πανεπιστήμιο Θεσσαλονίκης

Ψηφιακή συλλογή
Βιβλιοθήκη
"ΘΕΟΦΡΑΣΤΟΣ"
Τμήμα Γεωλογίας
Α.Π.Θ

Table S4 Amount of explained variance for every principal component of the PCA including enamel thickness and dental topographic variables and its respective eigenvalues.

PC	Eigenvalue	Variance(%)
1	0.264612	71.113
2	0.0649843	17.464
3	0.0246364	6.6209
4	0.0128671	3.4579
5	0.00228306	0.61356
6	0.0017329	0.46571
7	0.000982401	0.26401
8	0.00000442	0.0011873

Table S5 Kruskal-Wallis test performed on different populations of *Macaca fuscata* using dental microwear texture variables and their dispersions with population as factor[a,b].

	Phase II			Phase I		
Variable	df	χ^2	*p*	df	χ	*p*
Asfc	2	1.921	0.384	2	8.632	**< 0.05**
epLsar	2	0.249	0.882	2	3.796	0.149
$Hasfc_{81}$	2	6.251	**< 0.05**	2	3.868	0.144
Tfv	2	5.570	0.061	2	1.716	0.424
Disp–Asfc	2	1.705	0.426	2	4.742	0.093
Disp–epLsar	2	0.727	0.694	2	0.101	0.950
Disp–$Hasfc_{81}$	2	0.235	0.889	2	1.383	0.500
Disp–Tfv	2	1.426	0.490	2	5.783	0.055

[a] df = degrees of freedom; χ^2 = Chi squared; F = F–statistic; *p* value = significance value; [b] Asfc = area-scale fractal complexity; epLsar = exact proportion length-scale anisotropy of relief; Smc = scale of maximal complexity, $Hasfc_{9,36,81}$ = heterogeneity of area-scale fractal complexity on 9, 36 and 81 cell.

Ψηφιακή βιβλιοθήκη Θεόφραστος – Τμήμα Γεωλογίας – Αριστοτέλειο Πανεπιστήμιο Θεσσαλονίκης

Ψηφιακή συλλογή
Βιβλιοθήκη
"ΘΕΟΦΡΑΣΤΟΣ"
Τμήμα Γεωλογίας
Α.Π.Θ

Table S6 Pairwise comparisons between populations of *Macaca fuscata*, variables in bold signify differences highlighted with Bonferroni adjustment[a].

Localities	Aomori (North)		Nagano (Central)		Yakushima (South)	
Facet	*Phase II*	*Phase I*	*Phase II*	*Phase I*	*Phase II*	*Phase I*
Aomori (North)			$Hasfc_{81}$(+)	Asfc(+)	$Hasfc_{81}$(+)	Asfc(+)
Nagano (Central)	$Hasfc_{81}$(–)	Asfc(–)				
Yakushima (South)	$Hasfc_{81}$(–)	Asfc(–)				

[a](–) and (+) indicate values that are either lower or higher respectively for species in column compared to the one in row.

Table S7 Single analysis of variance (ANOVA) on principal coordinates from PCA including dental microwear texture variables[a].

	Phase II						
Variable	Eig.	% Var.	df	SS	MS	F	*p*
PC1	0.198	53.558	4	777.521	194.380	5.617	< **0.05**
PC2	0.110	29.684	4	1715.528	428.882	5.449	< **0.05**
PC3	0.047	12.829	4	12.426	30.106	0.743	0.565
PC4	0.014	3.928	4	181.101	45.275	3.863	< **0.05**
	Phase I						
Variable	Eig.	% Var.	df	SS	MS	F	*p*
PC1	0.114	52.679	4	3976.101	994.025	13.949	< **0.05**
PC2	0.080	36.704	4	869.552	217.388	3.931	< **0.05**
PC3	0.022	1.504	4	384.770	96.192	5.094	< **0.05**
PC4	0.0002	0.113	4	1.774	0.444	2.255	0.070

[a]Eig = Eigenvalues; %Var = Percentage of variance; df = degrees of freedom; SS = sum of squares; MS = mean square; F = F–statistic; p value = significance value.

Ψηφιακή βιβλιοθήκη Θεόφραστος – Τμήμα Γεωλογίας – Αριστοτέλειο Πανεπιστήμιο Θεσσαλονίκης

Ψηφιακή συλλογή
Βιβλιοθήκη
"ΘΕΟΦΡΑΣΤΟΣ"
Τμήμα Γεωλογίας
Α.Π.Θ

Table S8 Pairwise comparisons on principal coordinates from PCA including all dental microwear texture variables, principal components in bold indicate differences highlighted by Tukey's HSD and Fisher's LSD post hoc tests[a].

LSD / HSD	*Macaca majori*		*Macaca s. florentina*		*Macaca. fuscata*		*Macaca sylvanus*		*Macaca nemestrina*	
Facet	*II*	*I*	*II*	*I*	*II*	*I*	*II*	*I*	*II*	*I*
Macaca majori			**PC2**(+)	**PC1**(−)	**PC1**(−) **PC4**(−) **PC2**(+)	**PC1**(−)				**PC1**(−)
Macaca s. florentina	PC1(−) **PC2**(−)	**PC1**(+) PC2(+)								**PC2**(+)
Macaca fuscata	**PC1**(+) **PC4**(+) **PC2**(−)	**PC1**(+)						**PC3**(+)		**PC2**(+) **PC3**(+)
Macaca sylvanus		PC1(+)		PC1(−)	PC1(−) PC4(−)	**PC3**(−)				
Macaca nemestrina		**PC1**(+) PC3(−)		**PC2**(−)	PC1(−) PC4(−)	**PC2**(−) **PC3**(−)				

[a](–) and (+) indicate values that are either lower or higher respectively for species in column compared to the one in row.

Ψηφιακή βιβλιοθήκη Θεόφραστος – Τμήμα Γεωλογίας – Αριστοτέλειο Πανεπιστήμιο Θεσσαλονίκης

Ψηφιακή συλλογή
Βιβλιοθήκη
"ΘΕΟΦΡΑΣΤΟΣ"
Τμήμα Γεωλογίας
Α.Π.Θ

Chapter 7. Discussion and concluding remarks

The ecological niche theory posts that co-occuring species should evolve adaptations for avoiding and/or reducing interspecific resource competition (Hutchinson, 1959). A plethora of studies have concluded that niche partitioning in sympatric species is mostly manifested in differential selection of habitat use and/or diet (Gautier-Hion, 1978; MacKinnon and MacKinnon, 1980; Rodman, 1991; Ungar, 1995; Tan, 1999; Schreier et al., 2009; Grueter et al., 2010; Singh et al., 2011; Hadi et al., 2012; Zhou et al., 2014, 2018; Oelze et al., 2014; Justa et al., 2019; Ruslin et al., 2019). Three main hypotheses have been proposed to explain the causes and consequences of coexistence: a) the competitive exclusion principle (e.g. "Gause's law", Gause, 1934), b) the theory of limiting similarity (MacArthur and Levins, 1967; Abrams, 1983), and c) ecological character displacement (Brown and Wilson, 1956).

The competitive exclusion principle first suggested by Gause (1934) later discussed by Hardin (1960), predicts that species occupying the same ecological niche cannot coexist at constant population values in long-term. This ultimately leads to the prevalence of one over the other, or to the progressive divergence of their respective niches. Some authors have also discussed the importance of this hypothesis, of shaping extant and fossil primate communities (Winterhalder, 1981; Reed and Bidner, 2004). However, competitive exlusion is difficult to demonstrate in the fossil record but requires, at minimum contemporaneity and adaptive similarity (Rossie et al., 2013). This also highlights the fact that very detailed investigations of densely sampled fossiliferous sequences are essential to better comprehend the complex interplay between biotic and abiotic factors that shaped past diversity (e.g. DeMiguel et al., 2021), as well as additional research on extant primate communities (Justa et al., 2019). The theory of limiting similarity is an outgrowth of the competitive exclusion principle (Abrams, 1983) and claims the existence of a theoretical limit to the resource use overlap between species for their stable coexistence (MacArthur and Levins, 1967). Previous research has uncovered the occurrence of limiting similarity in a wide array of organisms, yet this hypothesis has been controversial among ecologists and paleoecologists (see Huntley et al., 2008; Abrams and Rueffler, 2009 and references therein). Many studies that attempt to explore limiting similarity (e.g. Huntley et al., 2008) resort to examining character displacement as a morphological proxy for niche overlap. Ecological character displacement takes into account phylogenetic relationships, and predicts that competition for limited resources drives closely related species to diverge adaptively when in sympatry (see Stuart and Losos, 2013; Schroer and Wood, 2015). The concept of niche differentiation/separation has been widely used to explain how sympatric species limit competition over resources (Holt, 2009). In order to exploit efficiently different macro and microhabitats while minimizing conflict, sympatric primates often employ various foraging strategies: consumption of different resources and/or different parts of the available food resources (Ungar, 1995; Yamagiwa and Basabose, 2006; Ruslin et al., 2019), use of the same resource in different developmental stages, either their own (i.e. juvenile vs. adults) or that of the vegetal resource (i.e. ripe vs. unripe), and exploiting food resources from different canopy levels (Garber, 1987; Hadi et al., 2012 and references therein). Such behavioral divergences in food selection and dietary ecology can be followed by character displacement over evolutionary timescales (Macho, 2017), thus leading not only to body mass changes, but also to changes in the morphology in the masticatory apparatus and digestive physiology (Ganzhorn, 1989). Owing to inherent difficulties in paleontological studies, such as the limited sample size in most cases, and the fact that soft tissues cannot be preserved in the fossil record, it seems impossible to investigate changes in digestive physiology for infering diet in extinct species. However, the masticatory apparatus and most notably teeth are a useful focus of investigation.

Ψηφιακή βιβλιοθήκη Θεόφραστος – Τμήμα Γεωλογίας – Αριστοτέλειο Πανεπιστήμιο Θεσσαλονίκης

Ψηφιακή συλλογή
Βιβλιοθήκη
"ΘΕΟΦΡΑΣΤΟΣ"
Τμήμα Γεωλογίας

This study focused on fossil dental remains (specifically molars) to decipher the dietary ecology of fossil Cercopithecidae from Europe, provide additional paleoecological background to better comprehend the evolution and ecological diversity of this primate family. Cercopithecids are found in a wide array of habitats both in Africa and Asia and they are among the primates more widely studied at the field and have been subject to considerable research efforts from both genetic and anatomical viewpoints (Frost, 2017). Their evolutionary history is well known compared with that of other groups, mainly because their extensive and often well-dated fossil record, especially in Africa. Around the late Miocene (~8.0–6.0 Ma), cercopithecids became much more common faunal elements in both eastern and northern Africa, and roughly by the same time they also dispersed in Europe (Koufos, 2009a, 2016) and Asia (Gilbert et al., 2014).

The Pliocene and Pleistocene were characterized by major climatic changes and fluctuations, which affected ecosystems globally (Bobe and Behrensmeyer, 2004; Hernández Fernández and Vrba, 2006; Hernández Fernández et al., 2007; Wu et al., 2011; Hoyle et al., 2020 and references therein). The transition from latest Miocene to Pliocene marks a period of relatively warmer and humid conditions in southern Europe, which favored the expansion of forested habitats. On the other hand, the Pleistocene is characterized by overall colder and drier conditions, which promoted the expansion of more open and mosaic habitats. These ecological changes and their concomitant effects in floral composition, probably influenced significantly the way of life of European fossil cercopithecids, as well as the way they partitioned space and resources when in sympatry. This study provides a combined methodological approach to explore the ecological diversity from a dietary viewpoint of the Plio-Pleistocene cercopithecids from Europe.

Mesopithecus monspessulanus and *Dolichopithecus ruscinensis* were the last colobines from the Plio-Pleistocene of Europe, sometimes found in sympatry with the genus *Macaca* (Eronen and Rook, 2004). The results presented in this work suggest that these two fossil colobines occupied relatively different dietary niches (Chapter 3, 4). On one hand, the upper molars of *Dolichopithecus ruscinensis* possessed a series of morphological adaptations for processing and consuming a wide array of food resources, and its large size probably contributed further to its opportunistic dietary strategy. On the other hand, the analysis of a maxillary third molar (DKV 480) of *Mesopithecus monspessulanus* suggests that it was capable of sustaining high biting forces related to hard food consumption and/or to withstand and abrasive diet. The examination of lower molars indicate that *Mesopithecus monspessulanus* generally exhibited thicker enamel than *Dolichopithecus ruscinensis*. This may suggest a more durophagous (e.g. Kay, 1981; Dumont, 1995; Lambert et al., 2004; Lucas et al., 2008), and/or a more abrasive (e.g. Molnar and Gantt, 1977; King et al., 2005) diet for *Mesopithecus monspessulanus* compared with *Dolichopithecus ruscinensis*. Nevertheless, the analyzed fossil sample is too small to exclude alternative explanations and previous research has shown that enamel thickness shows a wide range of interspecific and intrageneric variation (Macho, 1994; Shellis et al., 1998; Schwartz, 2000; Kono, 2004; Smith et al., 2005, 2012; Olejniczak et al., 2008), even within the same tooth position. In addition, enamel thickness has also been demonstrated to be an evolutionary plastic trait, capable of rapid adaptation in response to functional dietary requirements (Hlusko et al., 2004; Kelley and Swanson, 2008; Pampush et al., 2013; Kato et al., 2014). Hence, further investigation based on additional extant and fossil unworn and/or minimally worn molar material would be required to test among several competing hypotheses, as wear can significantly alter enamel similarities. It would also be interesting to apply dental topographic analysis even on relatively worn lower molars of these fossil colobines to explore the type of tooth wear, as this methodology may be applied to variably worn molar teeth (Ungar and M'Kirera, 2003).

Notwithstanding the above, the results of dental microwear texture analysis indicate a more opportunistic and mixed diet for *Dolichopithecus ruscinensis* contrasting with the more folivorous

Ψηφιακή βιβλιοθήκη Θεόφραστος – Τμήμα Γεωλογίας – Αριστοτέλειο Πανεπιστήμιο Θεσσαλονίκης

Ψηφιακή συλλογή
Βιβλιοθήκη
"ΘΕΟΦΡΑΣΤΟΣ"

dietary behavior of *Mesopithecus monspessulanus*, similar to some extant African colobines such as *Colobus guereza* and *Piliocolobus badius*. The latter observation is consistent with previous suggestions on the locomotor adaptations of *Mesopithecus monspessulanus* and *Dolichopithecus ruscinensis* (Gabis, 1961; Jolly, 1967; Szalay and Delson, 1979; Koufos, 2009a). Both *Dolichopithecus ruscinensis* and *Mesopithecus monspessulanus* presumably appeared in Europe in the Early Pliocene, where Europe became more densely forested following the refilling of the desiccated Mediterranean Basin, and went extinct around the Early Pleistocene. Thus, it is possible that the appearance of both fossil species reflects the new environmental conditions of the European Pliocene, which would have probably been less favorable to *Mesopithecus pentelicus*. On the other hand, recent biochronological evidence supports previous suggestions that *Mesopithecus pentelicus* and *Mesopithecus monspessulanus* might have briefly coexisted (e.g. de Bonis et al., 1990; Delson et al., 2005; Koufos, 2019). This would be consistent with a higher diversity of available ecological niches, thereby promoting species diversity around 7.0–6.0 Ma (Ganzhorn, 1989; Fleagle and Reed, 1996), and/or a more gradual transition towards the new environmental conditions of the early Pliocene. On the other hand, the shift towards a more arboreal lifestyle in the genus *Mesopithecus* might simply reflect a "niche filling" (e.g. Rabosky and Lovette, 2008; Tran, 2014), as a strategy to withstand interspecific competition with *Dolichopithecus* and/or with cercopithecines (specifically the genus *Macaca*).

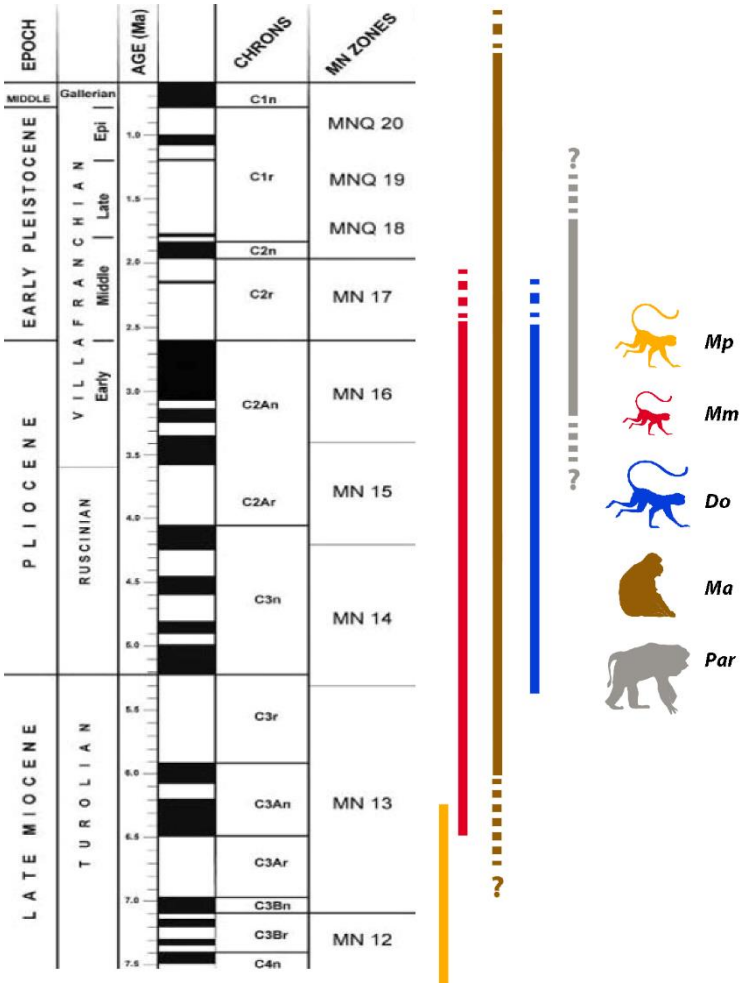

Fig. 7.1 Biostratigraphic distribution of fossil cercopithecids in Europe, *Mp*: *Mesopithecus pentelicus*, *Mm*: *Mesopithecus monspessulanus*, *Do*: *Dolichopithecus*, *Ma*: *Macaca*, *Par*: *Paradolichopithecus*, modified after Koufos, 2019.

Ψηφιακή βιβλιοθήκη Θεόφραστος – Τμήμα Γεωλογίας – Αριστοτέλειο Πανεπιστήμιο Θεσσαλονίκης

Ψηφιακή συλλογή
Βιβλιοθήκη
"ΘΕΟΦΡΑΣΤΟΣ"
Τμήμα Γεωλογίας

The appearance of *Mesopithecus monspessulanus* roughly post-dates the first appearance of the genus *Macaca* in Europe (Fig, 7.1, 7.2C), being recorded in two localities: Almenaraca-Casablanca M in Spain (Köhler et al., 2000) and Mocucco Torinese in Italy, where it co-occurred with *Mesopithecus pentelicus* (Alba et al., 2014). Even in the more open and dry and/or mixed habitats of the latest Miocene of Europe, the genus *Macaca* was probably quite capable of efficiently exploiting their surrounding environment. Macaques are semi- or even fully terrestrial cercopithecids, depending on species, and inhabit a wide range of habitats ranging from tropical to more temperate conditions, being very ecologically flexible (Tsuji et al., 2013). A key characteristic that enables *Macaca* to inhabit even ecologically sub-optimal environments is their highly eclectic and opportunistic diet (O'Regan et al., 2008 and references therein), although other factors such as rapid life history of cercopithecids in general might be important as well (Jablonski et al., 2000). However, at times where environmental conditions are sub-optimal and/or in resource-limited environments, competition for resources may be more intense. Hence, it is possible that by the time the genus *Macaca* entered Europe, habitats probably had sub-optimal ecological conditions for primates (e.g. Elton and O'Regan, 2014), most likely due to regional tectonic processes and its concomitant effects on the European flora (Jiménez-Moreno and Suc, 2007; Jiménez-Moreno et al., 2010). This may have promoted competition for space and resources with contemporaneous primates such as *Mesopithecus*, sometimes found in sympatry. When the semi-terrestrial colobine *Dolichopithecus* appeared later in Europe, competition for space and resources may have been more intense.

Thus, it is plausible that in resource limited habitats of Europe during the latest Late Miocene, members of the early European macaques competed for space and resources with *Mesopithecus*(Fig. 7.2B). The presumed folivorous dietary habits of *Mesopithecus monspessulanus* may reflect a strategy of the genus *Mesopithecus* to reduce/avoid competition with the genus *Macaca*, by shifting into a more arboreal niche, affecting also its overall size (Fig. 7.2C). By the time *Dolichopithecus ruscinensis* appeared in Europe during the early Pliocene (Fig. 7.2D), *Mesopithecus monspessulanus* probably had already shifted into a more arboreal niche. This strategy might have allowed the coexistence of these fossil cercopithecids at some sites (see Eronen and Rook, 2004; Alba et al., 2014), until the Early Pleistocene, when the fossil colobines of Europe went extinct. Their extinction from Europe reflects the colder and drier environmental conditions associated with the global cooling around 2.5 Ma, which probably led to local floristic extinction and a reduction in the extent of forests in southern Europe, making the majority of habitats relatively unsuited for colobine mokeys (Delson, 1994). Alternatively, some members of this fossil colobine lineage might have dispersed to more ecologically favorable habitats of southeastern Asia. To date, there is no evidence to support this notion, although, much remains to be investigated about the taxonomy and phylogenetic relationship of fossil European colobines in relation to contemporary species from Asia (Egi et al., 2007; Takai and Maschenko, 2009; Chang et al., 2012; Takai et al., 2015, 2016). In the future, it would be particularly interesting to explore the phylogenetic relationships of fossil European colobines (e.g. *Mesopithecus*, *Dolichopithecus*) among themselves and in relation to fossil colobines from Africa (e.g. *Libypithecus*, *Cercopithecoides*, *Paracolobus*, *Rhinocolobus*, *Kuseracolobus*) and Asia (e.g. *Parapresbytis*, *Kanagawapithecus*, *Myanmarcolobus*), with the help of non-destructive 3D techniques (e.g. Olejniczak et al., 2007; Skinner et al., 2008, 2010; Smith et al., 2009; Guy et al., 2015), while also exploring their dietary context. Lastly, it would be also interesting to investigate the morphological wear resistance of molar teeth of each fossil representative, as this dental aspect might provide useful dietary information (e.g. Berthaume, 2016a; 2019a; Stuhlträger et al., 2021).

These conclusions above derive from different types of analysis for each fossil species; for *Dolichopithecus ruscinensis*, the dental topographic and enamel thickness analysis was focused on an upper first molar and performed on subsampled part of the crown surface, whereas in the case

Ψηφιακή βιβλιοθήκη Θεόφραστος – Τμήμα Γεωλογίας – Αριστοτέλειο Πανεπιστήμιο Θεσσαλονίκης

Ψηφιακή συλλογή
Βιβλιοθήκη
"ΘΕΟΦΡΑΣΤΟΣ"
Τμήμα Γεω
Α.Π.

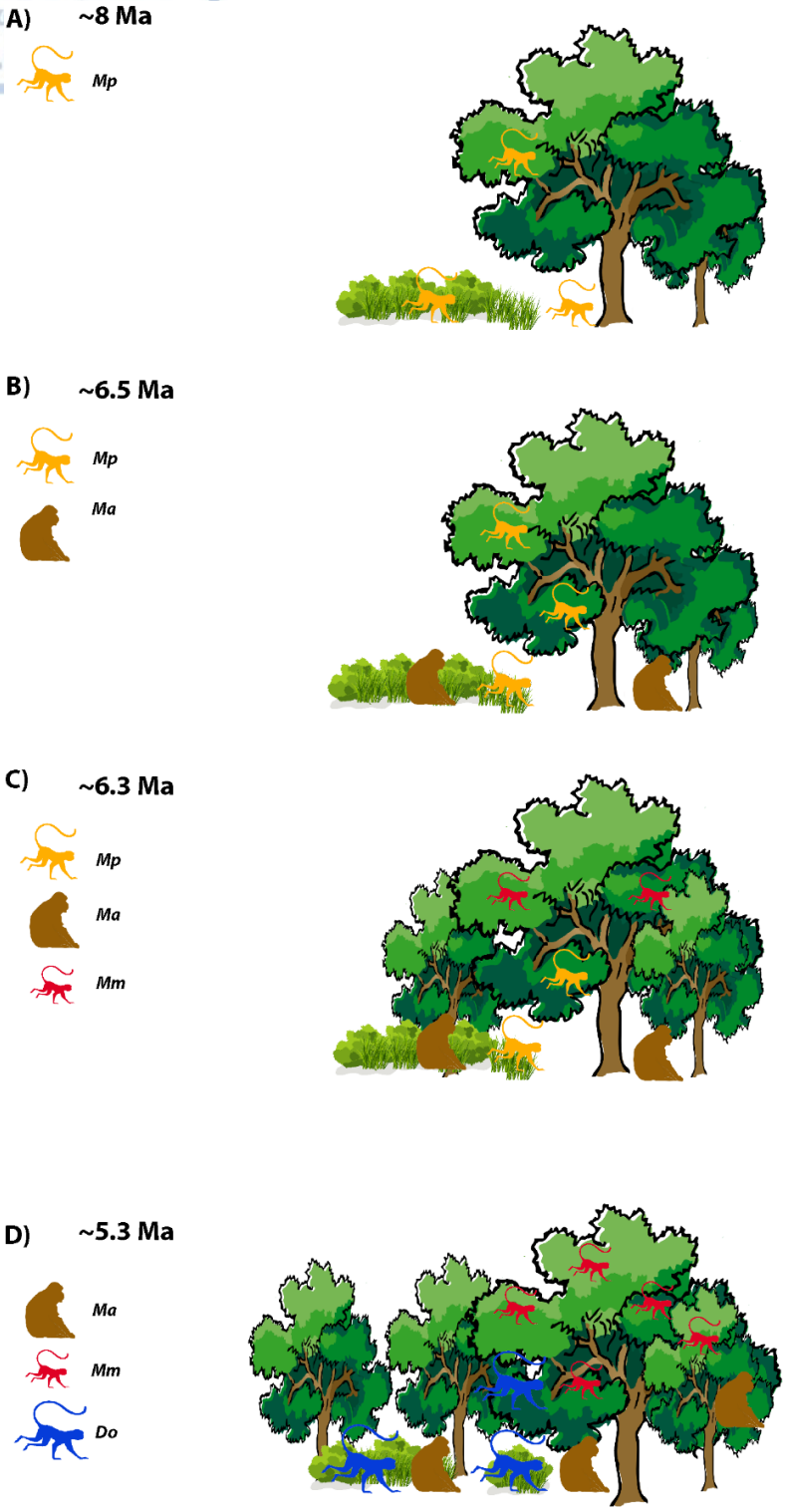

Fig. 7.2 Illustration of hypothetical niche partitioning between the fossil cercopithecids of Europe; (A) around 8 Ma in Europe only *Mesopithecus pentelicus* (*Mp*) was present, (B) hypothetical earlier dispersion of the genus *Macaca* (*Ma*) in Europe and partitioning of space and resources with *M. pentelicus*, (C) the appearance of *Mesopithecus monspessulanus* (*Mm*) may reflect an ecological shift towards a more arboreal niche to withstand interspecific competition with *Macaca*, (D) niche partitioning among *Macaca*, *Dolichopithecus* (*Do*) and *M. monspessulanus*.

Ψηφιακή βιβλιοθήκη Θεόφραστος – Τμήμα Γεωλογίας – Αριστοτέλειο Πανεπιστήμιο Θεσσαλονίκης

Ψηφιακή συλλογή
Βιβλιοθήκη
"ΘΕΟΦΡΑΣΤΟΣ"

of *Mesopithecus monspessulanus* only comparisons of enamel thickness analysis were performed focused on the whole crown surface of an upper third molar. Thus, until the same methodological protocols can be applied to both fossil species on the same molar positions, the possibility of alternative conclusions cannot be rejected. Moreover, the available fossil molar sample investigated is somewhat limited, although this is a common problem in studies on fossil primates due to their rarity in many sites. In addition, enamel thickness analyses are commonly performed on unworn and/or minimally worn molar material, which is not always the case in the fossil record and extant collections, where the majority of dental elements exhibits at least moderate wear. It is also important to note that the lower molars of *Mesopithecus monspessulanus* derive from a single individual from the fossil site of Montpellier (UM4043), whereas the lower molars of *Dolichopithecus ruscinensis* derive from two different individuals from the fossil sites of Perpignan-Serrat d'en Vaquer in France and Megalo Emvolon in Greece. As the fossil material from each site is too limited to characterize the variation of enamel thickness and dental topographic metrics within species and genera, intepretations should be taken with caution in the hope that future findings will provide a more robust baseline to investigate such matters.

With the extinction of colobines from Europe around the Late Pliocene to Early Pleistocene, fossil cercopithecines became the dominant primates (Fig. 7.3C). Setting the macaques aside which dispersed in Europe in late Miocene, the large papionin *Paradolichopithecus* appeared in of Europe around 3.2 Ma (Eronen and Rook, 2004; Kostopoulos et al., 2018). Currently, the four fossil species recognized (i.e. *P. arvernensis*, *P. sushkini*, *P. geticus* and *P. gasuensis*) are overall sparsely documented with few published specimens recorded in some sites in France, Greece, Spain, Romania and China (Depéret, 1929; Necrasov et al., 1961; Trofimov, 1977; Aguirre and Soto, 1978; Qiu et al., 2004; Sondaar, 2006; Kostopoulos et al., 2018). Previous studies on available postcranial material suggested a locomotor behavior similar to baboons, yet some cranio-dental features suggest closer similarities to macaques (e.g. Szalay and Delson, 1979; Delson, 2004; Ting et al., 2004). The dental topographic and enamel thickness analysis applied to a series of available M^2 specimens from different extant papionin genera including the M^2 from the *Paradolichopithecus* cranium (DFN3–150) from Dafnero-3 fossil site in Northern Greece (see Kostopoulos et al., 2018), evince some morphological differences among modern taxa. These differences are possibly associated with the distinct ecological niches occupied by the extant forms, which may be also linked with dietary specializations. Similarities in some aspects of molar morphology between DFN3–150 and large-sized papionins, such as *Papio* and *Mandrillus* (e.g. enamel thickness, tooth strength/bite force, relief), and the differences relative to commited durophagous papionins (e.g. relief, curvature/sharpness and enamel thickness), such as members of *Cercocebus* and *Lophocebus*, most likely suggest that *Paradolichopithecus* occupied a more opportunistic dietary niche being capable of inhabiting a wide array of habitats (from woodlands to more open, dry grasslands and prairies). However, dental morphology and diet may vary among species of the same genus, so that more detailed investigation at the species level would be advisable. Nevertheless, the results reported here for DN3-150 from Dafnero-3 are indicative of a versatile molar morphology (e.g. Saito et al., 2018) that would have enabled it to switch to various food resources (from hard food items to more tough food resources) when needed. This further implies that the inferred versatile molar morphology of DFN3-150 might have been an adaptive response to spatiotemporal variation and scarcity of food resources (Hemingway and Bynum, 2005; Tsuji et al., 2013).

The results of dental microwear texture analysis also suggest an opportunistic dietary behavior for *Paradolichopithecus*, although the overall similarities of some individuals with *Theropithecus*, especially in Phase I dental wear facets (Fig. 5.3), may suggest a tough herbaceous

Ψηφιακή βιβλιοθήκη Θεόφραστος – Τμήμα Γεωλογίας – Αριστοτέλειο Πανεπιστήμιο Θεσσαλονίκης

Ψηφιακή συλλογή
Βιβλιοθήκη
"ΘΕΟΦΡΑΣΤΟΣ"
Τμήμα

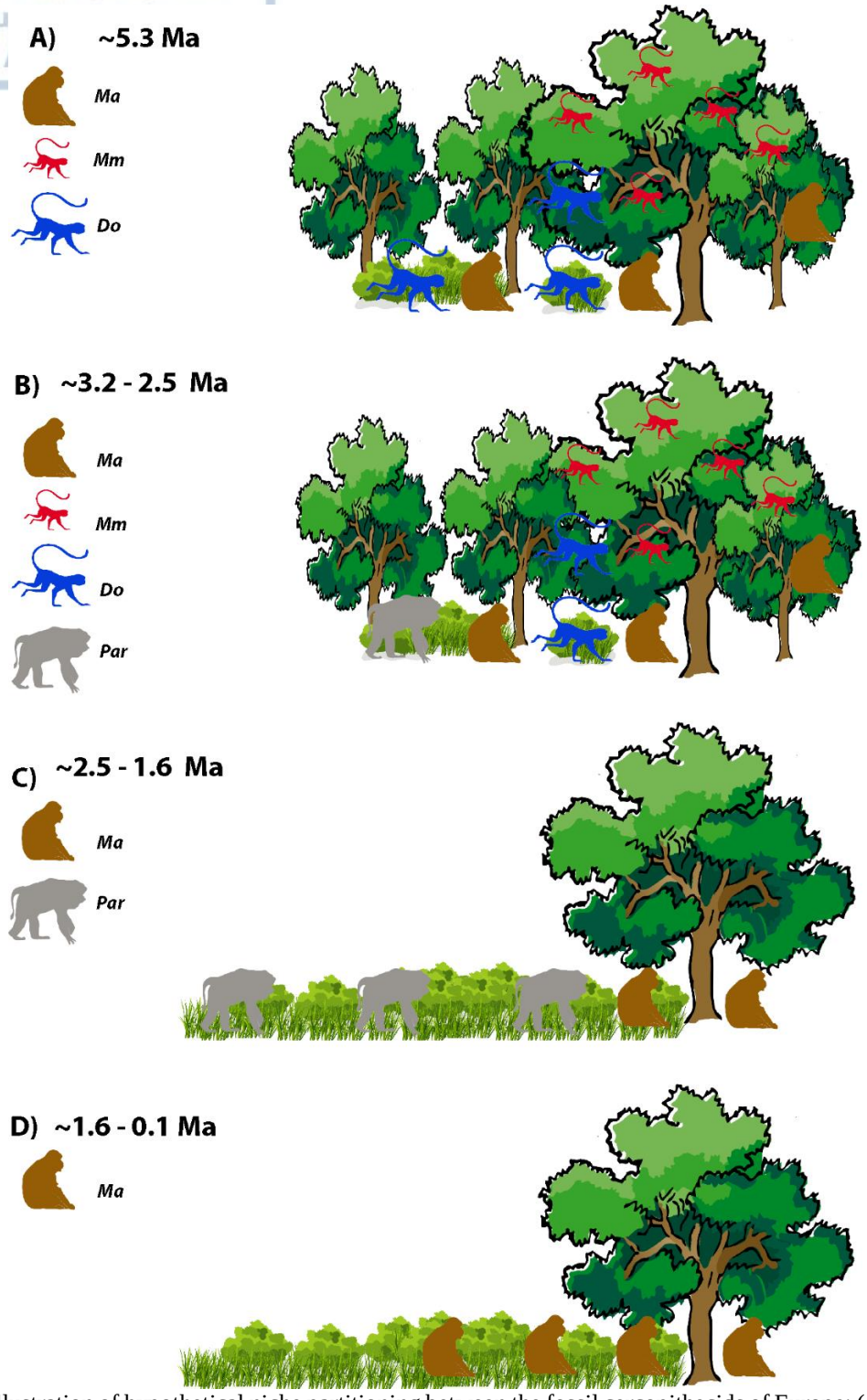

Fig. 7.3 Illustration of hypothetical niche partitioning between the fossil cercopithecids of Europe; (A) among *Mesopithecus monspessulanus* (Mm), *Dolichopithecus* (Do) and *Macaca* (Ma); (B) with the appearance of *Paradolichopithecus* (Par) for a brief point in time the fossil primate community of Europe reached its higher diversity; (C) in the beginning of Pleistocene colobines went extinct from Europe and only the papionins remained; (D) with the extinction of *Paradolichopithecus* from Europe, only the genus *Macaca* was present in Europe until 0.1 Ma.

Ψηφιακή βιβλιοθήκη Θεόφραστος – Τμήμα Γεωλογίας – Αριστοτέλειο Πανεπιστήμιο Θεσσαλονίκης

Ψηφιακή συλλογή
Βιβλιοθήκη
"ΘΕΟΦΡΑΣΤΟΣ"

vegetal component in its diet, in support of previous dietary investigations of *Paradolichopithecus* (see Williams and Holmes, 2011). These similarities between *Paradolichopithecus* and *Theropithecus* might be associated with the available resources in their respective paleohabitats, and could be indicative of changes in floral composition in Eurasian paleohabitats, likely reflecting the cooler and drier climatic conditions from the onset of the Plio-Pleistocene transition (Agusti and Antón, 2002; Kahlke et al., 2011). Nevertheless, diet may vary among different species even among different populations of the same primate species, thus caution is required when interpreting these results. Lastly, it would be of high interest to extract isotopic data information on this rare fossil papionin (Lee–Thorp et al., 1997; Crowley, 2012), but this is hindered by the scarcity of the fossil material.

The large size of *Paradolichopithecus* along with adaptations for semi-terrestrial locomotion (Delson and Nicolaescu-Plopsor, 1975b; Van der Geer and Sondaar, 2002; Frost et al., 2005; Delson et al., 2014), relatively fast life history traits (as evidenced by information regarding dental erruption sequence; e.g. van der Geer and Dermitzakis, 2008) and opportunistic dietary behavior were all likely key factors for its relatively rapid distribution around 2.4–2.0 Ma in the region of Europe. Coupled with previously available evidence, the results of the present work suggest that the genus *Paradolichopithecus* included ecologically flexible monkeys, which in turn creates questions regarding their absence from the fossil record beyond Early Pleistocene. Yet this could be a sampling bias. Nevertheless, its extinction was probably a combination of several biotic and abiotic factors that affected *Paradolichopithecus* populations in Europe. The overall large size of this fossil genus (most likely being the largest fossil Plio-Pleistocene cercopithecid representative in Eurasia along with *Procynocephalus*) and its opportunistic diet would have enabled the wide distribution of *Paradolicopithecus* in Europe. However, large body mass may also reflect an adaptive response to withstand potential pressures related to predation. Predation pressures aside, the increasingly fragmented habitats of Europe might have limited the distribution of this genus in Europe. Lastly, the rough coincidence in time between the extinction of large papionins of Eurasia (e.g. *Paradolichopithecus* and *Procynocephalus*) and the first direct and indirect evidence of *Homo* in Eurasia also suggests that antagonistic interactions between them could have contributed to the extinction of the former.

After the extinction of the large cercopithecines in Eurasia around the latest Early Pleistocene, the genus *Macaca* remained as the sole cercopithecid survivor (Fig. 7.3D). The earliest presence of this genus in Europe is sparsely documented only in the late Miocene fossil of Spain and Italy (Köhler et al., 2000; Alba et al., 2014). Based on these evidence and the lack of papionin remains from other fossil sites in Eurasia, it is suggested that macaques dispersed in Europe as early as the latest Miocene (Agustí et al., 2006; Alba et al., 2014; Alba et al., 2015a; Colombero et al., 2017). From the early Pliocene until the latest Middle Pleistocene, macaques maintained a wide distribution in Europe by exploiting a wide array of habitats, yet by the earliest Late Pleistocene they went extinct there. Currently, all European fossil representatives of this genus are considered to be closely related to *Macaca sylvanus*, with mainland fossil relatives being assigned to various extinct chronosubspecies whose distinctiveness is a bit uncertain (Alba et al., 2008). The only exception is the endemic *Macaca majori* from Sardinia, which is considered a distinct species, as it possesses a series of anatomical traits not observed in its mainland fossil representatives, potentially related to dietary adaptations (Rook and O'Higgins, 2005). Thus, the dietary niches of fossil European *Macaca* representatives are examined focusing on *Macaca majori* (e.g. Chapter 6).

The results of the dental topographic and enamel thickness analyses, based on fossil upper molars (M^2 and M^3) of *Macaca majori*, suggest that this species exhibited a combination of morphological molar features (low values of curvature/sharpness and relief, high relative enamel thickness) that most closely resemble those of commited hard object feeders such as species of

Ψηφιακή βιβλιοθήκη Θεόφραστος – Τμήμα Γεωλογίας – Αριστοτέλειο Πανεπιστήμιο Θεσσαλονίκης

Ψηφιακή συλλογή
Βιβλιοθήκη
"ΘΕΟΦΡΑΣΤΟΣ"

Lophocebus and *Cercocebus*. The extant sample of *Macaca* was limited and represented only by *Macaca sylvanus*, thus not being able to exclude the possibility that *Macaca majori* might fall within the variation of extant *Macaca* species from Asia. Nevertheless, the present results suggest the frequent consumption of mechanically challenging food resources. It is unknown if the dental morphology of *Macaca majori* reflects an adaptation for a more durophagous diet and/or a morphological tradeoff resulting from its overall smaller size, as no other upper molars of European fossil *Macaca* could be analyzed to explore such questions.

In turn, the results of the dental microwear texture analysis for *Macaca majori* show similarities with some modern species, such as *Macaca nemestrina* and *Macaca sylvanus*, aalthough the fossil species probably consumed mechanically challenging food resources more often (Fig. 6.6). In addition, the texture analysis revealed several microwear texture differences among extant *Macaca* species, which are suggestive of dietary variations in relation to the floristic composition of their respective habitats. *Macaca sylvanus* seems to differ from *Macaca nemestrina* in some texture characteristics, but both species appear to show differences in the dietary composition from *Macaca fuscata*. The diet of the latter includes significant amount of bark, leaves, buds and other tough terrestrial herbaceous vegetation compared to other extant species found in more tropical habitats (Bernstein, 1967; Caldecott, 1986; Ménard, 2002; Hanya, 2004; Hanya et al., 2011). Furthermore, the results revealed significant differences among *Macaca fuscata* populations from different latitudes in Japan. These observation reinforce the notion that macaque diets are mostly dependent on the available food resources of their occupying range and habitat. Even though these reaults need further investigation to be validated, they demonstrate the potential of DMTA to track seasonal and more subtle dietary variations, and more detailed investigation of *Macaca fuscata* is thus of high interest in this regard (e.g. Percher et al., 2018). The dental microwear textures of fossil Plio-Pleistocene *Macaca sylvanus* subspecies from mainland Europe (e.g. *M.* cf. *sylvanus*, *M. s. florentina*, *M. s*. cf. *prisca*) exhibit similarities with both *Macaca sylvanus* and *Macaca fuscata*, yet more closely resemble the latter species, suggesting that the diet of fossil Plio-Pleistocene macaques from mainland Europe included significant amounts of leaves and other less preferred food resources. It is possible that the diet of Plio-Pleistocene *Macaca* from mainland Europe (i.e. Cal Guardiola-Vallparadís, Upper Valdarno, Villafranca d'Asti Fornace RDB) were more diverse and showed higher variation compared to *Macaca majori* from Capo Figari. Thus, it is possible that the habitats of Sardinia during the Early to Middle Pleistocene had more favorable conditions for macaques (e.g. more abundant preferred food resources and/or absence of large predators) compared with most of the mainland habitats of Europe. However, the absence of *Macaca majori* from the fossil record of Sardinia beyond the Early/Middle Pleistocene boundary, suggests that major ecological changes by this time might have caused its extinction. Roughly by the same time that *Macaca majori* went extinct, canids arrived into Sardinia, with the presence of *Cynotherium sardous* (Palombo, 2006). Nevertheless, at present there is no evidence supporting a causal relationship between the two events.

In general, the high ecological flexibility of macaques would have allowed them to withstand the harsh paleoenvironmental conditions of Europe throughout the Pleistocene, even if they gradually became more ecologically challenging, especially after the Middle Pleistocene Transition (MPT, e.g. Willeit et al., 2019). Although their distribution was apparently affected by these changes, macaques managed to survive in Europe until the Late Pleistocene (e.g. Elton and O'Regan, 2014). Their survival was probably facilitated by retreating to refugial areas in southern Europe during cold interglacial intervals, whereas during interglacial phases macaques exploited habitats even in northern Europe (Delson, 1980; van den Hoek Ostende and de Vos, 2006; Reumer et al., 2018). The last record of *Macaca majori* roughly coincides with the first oldest evidence of the arrival of *Homo* in Sardinia, which would have significant implications for the local faunas (Sondaar, 2000; Sondaar and Van Der Geer, 2000, 2005; Palombo and Rozzi, 2014). Indeed, the

Ψηφιακή βιβλιοθήκη Θεόφραστος – Τμήμα Γεωλογίας – Αριστοτέλειο Πανεπιστήμιο Θεσσαλονίκης

Ψηφιακή συλλογή
Βιβλιοθήκη
"ΘΕΟΦΡΑΣΤΟΣ"

dispersal of early *Homo* throughout mainland Europe would have probably had a negative impact on the Middle to Late Pleistocene macaque populations as well, with evidence suggesting the coexistence of macaques alongside *Homo* for over 1.0 million years (Marigó et al., 2014). By the Late Pleistocene, *Homo* had considerably expanded its distribution across European habitats, and during times of food scarcity and/or in resource limited habitats may have preyed on fossil European macaques. It is possible that monkeys may have been used as an important supplementary protein resource (e.g. Fa et al., 2003).

All the above suggests that the ecological diversity of the Plio-Pleistocene cercopithecids from the western Palearctic (e.g. Europe), may have been triggered by climatic factors that profoundly affected the existing ecosystems. These climatic variations promoted changes in the structure of the existing fossil primate communities of Europe, inducing the competition for space and resources. These ecological interactions may have started around the latest Late Miocene, where the genus *Macaca* first dispersed to European habitats and co-existed with the genus *Mesopithecus*. Their coexistence, also with the large fossil colobine *Dolichopithecus*, was probably facilitated by changes in their locomotor and dietary behavior in order to reduce/avoid interspecific competition for space and resources, in a manner similar to modern primate communities (Fleagle and Reed, 1996; Reed and Bidner, 2004; Buzzard, 2010; Fleagle, 2013; Kane and McGraw, 2018 and references therein). The combination of these ecological pressures (e.g. climatic fluctuations and niche competition) might have promoted speciation and/or extinction, as suggested in the case of the genus *Mesopithecus*. This raises further questions regarding the significance of interspecific competition and niche partitioning in the evolution of Cercopithecinae and Colobinae, and in turn suggests that these ecological factors might have played an important role in the evolutionary success of Cercopithecidae.

The extinction of colobines from Europe around 2.5 Ma reflects major ecological changes in European habitats, promoted by the overall colder and drier climatic conditions of the Early Pleistocene and later on. Papionins were more adaptable to withstand the new environmental conditions, which further suggest that the disappearance of papionins from Europe by the Late Pleistocene may have been influenced by other factors as well. The disappearance of *Paradolichopithecus* along with *Procynocephalus* beyond the Early Pleistocene might have been influenced by the dispersal of the potential competitive *Theropithecus* from Africa, yet this seems unlikely. All known *Theropithecus* records outside of Africa so far significantly postdate the last occurrence datum of both *Paradolichopithecus* – *Procynocephalus* (Delson, 1993; Belmaker, 2010; Roberts et al., 2014; Gilbert et al., 2016), while its dispersal in Eurasia was relatively brief and with less extensive distribution to promote such ecological replacement. It is more likely that the increasingly fragmented habitats of Eurasia probably influenced the distribution of these large papionins, whereas the influence of predation pressures in their decline from Europe cannot be rejected. The genus *Macaca* was able to survive and exploit efficiently the resource-limited habitats of Europe until the Late Pleistocene. Thus, its extinction after that time may be suggestive that predation pressures were one of the contributing factors. Setting large carnivores aside (e.g. O'regan et al., 2002; Meloro and Elton, 2013), one potential predator that may have contributed to the extinction of papionins from Europe is the genus *Homo* (Elton and O'Regan, 2014). Indeed, the dispersal of *Homo* from Africa, would have negative implications on the existing European faunas, and may have also altered carnivore ecology more generally (see Meloro and Elton, 2013 for extended discussion). Hence, the extinction of papionins from Europe may have resulted from the cumulative effects of resource variations impacted by global climatic changes coupled with predation pressures, while other stochastic genetic factors resulting from small population sizes may have also contributed to their demise from Europe.

Ψηφιακή βιβλιοθήκη Θεόφραστος – Τμήμα Γεωλογίας – Αριστοτέλειο Πανεπιστήμιο Θεσσαλονίκης

Ψηφιακή συλλογή
Βιβλιοθήκη
"ΘΕΟΦΡΑΣΤΟΣ"
Τμήμα Γεωλογίας
Α.Π.Θ

References

Abbate, E., Sagri, M., 2012. Early to Middle Pleistocene *Homo* dispersals from Africa to Eurasia: Geological, climatic and environmental constraints. Quat. Int. 267, 3–19.

Abbazzi, L., Angelone, C., Arca, M., Barisone, G., Bedetti, C., Delfino, M., Kotsakis, T., Marcolini, F., Palombo, M.R., Pavia, M., Piras, P., Rook, L., Torre, D., Tuveri, C., Valli, A.M.F., Wilkens, B., 2004. Plio-Pleistocene fossil vertebrates of Monte Tuttavista (Orosei, Eastern Sardinia, Italy), an overview. Riv. Ital. di Paleontol. e Stratigr. 110, 681–706.

Abbazzi, L., Delfino, M., Gallai, G., Trebini, L., Rook, L., 2008. New data on the vertebrate assemblage of Fiume Santo (north-west Sardinia, Italy), and overview on the Late Miocene Tusco-Sardinian palaeobioprovince. Palaeontology. 51, 425–451.

Abrams, P., 1983. The Theory of Limiting Similarity. Annu. Rev. Ecol. Syst. 14, 359–376.

Abrams, P.A., Rueffler, C., 2009. Coexistence and limiting similarity of consumer species competing for a linear array of resources. Ecology. 90, 812–822.

Abu, K., 2018. Activity patterns and feeding ecology of the gelada baboon (*Theropithecus gelada arsi*) and human-gelada conflicts in Amigna, eastern Arsi, Ethiopia. Addis Ababa.

Abu, K., Mekonnen, A., Bekele, A., Fashing, P.J., 2018. Diet and activity patterns of Arsi geladas in low-elevation disturbed habitat south of the Rift Valley at Indetu, Ethiopia. Primates. 59, 153–161.

Ackermans, N.L., 2020. The history of mesowear: A review. PeerJ. 8.

Ackermans, N.L., Winkler, D.E., Martin, L.F., Kaiser, T.M., Clauss, M., Hatt, J.M., 2020. Dust and grit matter: Abrasives of different size lead to opposing dental microwear textures in experimentally fed sheep (*Ovis aries*). J. Exp. Biol. 223.

Agetsuma, N., 1995. Foraging strategies of yakushima macaques (*Macaca fuscata yakui*). Int. J. Primatol. 15, 595–609.

Agetsuma, N., Nakagawa, N., 1998. Effects of Habitat Differences on Feeding Behaviors of Japanese Monkeys: Comparison Between Yakushima and Kinkazan. Primates. 39, 275–289.

Aguirre, E., Soto, E., 1978. Paradolichopithecus in La Puebla de Valverde, Spain: Cercopithecoidea in European Neogene stratigraphy. J. Hum. Evol. 7, 559–565.

Agusti, J., Antón, M., 2002. Mammoths, sabertooths, and hominids: 65 million years of mammalian evolution in Europe. Columbia University Press.

Ψηφιακή βιβλιοθήκη Θεόφραστος – Τμήμα Γεωλογίας – Αριστοτέλειο Πανεπιστήμιο Θεσσαλονίκης

Ψηφιακή συλλογή
Βιβλιοθήκη
"ΘΕΟΦΡΑΣΤΟΣ"

Agustí, J., Garcés, M., Krijgsman, W., 2006. Evidence for African-Iberian exchanges during the Messinian in the Spanish mammalian record. Palaeogeogr. Palaeoclimatol. Palaeoecol. 238, 5–14.

Ahsan, M.F., Khan, M.R., 2006. Eco-ethology of the common langur *Semnopithecus entellus* (Dufresne) in Bangladesh. Univ. J. Zool. Rajshahi Univ. 25, 3–10.

Akosim, C., Joseph, J., Egwumah, P.O., 2010. Assessment of feeding behaviour of baboons (*Papio anubis*) in Hong Hills Adamawa State, Nigeria. J. Res. For. Wildl. Environ. 2, 60–72.

Alba, D.M., Carlos Calero, J.A., Mancheño, M.Á., Montoya, P., Morales, J., Rook, L., 2011. Fossil remains of *Macaca sylvanus florentina* (Cocchi, 1872) (Primates, Cercopithecidae) from the Early Pleistocene of Quibas (Murcia, Spain). J. Hum. Evol. 61, 703–718.

Alba, D. M., Colombero, S., Delfino, M., Martìnez-Navarro, B., Pavia, M., Rook, L., 2014a. A thorny question: The taxonomic identity of the Pirro Nord cervical vertebrae revisited. J. Hum. Evol. 76, 92–106.

Alba, David M., Delson, E., Carnevale, G., Colombero, S., Delfino, M., Giuntelli, P., Pavia, M., Pavia, G., 2014. First joint record of *Mesopithecus* and cf. *Macaca* in the Miocene of Europe. J. Hum. Evol. 67, 1–18.

Alba, D. M., Delson, E., Carnevale, G., Colombero, S., Delfino, M., Giuntelli, P., Pavia, M., Pavia, G., 2014b. New cercopithecid remains from Moncucco Torinese and the taxonomic identity of the earliest papionins from Europe [Abstract]. XII Annu. Meet. Eur. Assoc. Vertebr. Palaeontol. 4.

Alba, D.M., Delson, E., Morales, J., Montoya, P., Romero, G., 2018. Macaque remains from the early Pliocene of the Iberian Peninsula. J. Hum. Evol. 123, 141–147.

Alba, D.M., Fortuny, J., Moyà-Solà, S., 2010. Enamel thickness in the middle miocene great apes anoiapithecus, pierolapithecus and dryopithecus. Proc. R. Soc. B Biol. Sci. 277, 2237–2245.

Alba, D.M., Montoya, P., Pina, M., Rook, L., Abella, J., Morales, J., Delson, E., 2015a. First record of *Mesopithecus* (Cercopithecidae, Colobinae) from the Miocene of the Iberian Peninsula. J. Hum. Evol. 88, 1–14.

Alba, D.M., Moyà-Solà, S., Madurell, J., Aurell, P., 2008. Dentognathic remains of *Macaca* (Primates, Cercopithecidae) from the late early Pleistocene of Terrassa (Catalonia, Spain). J. Hum. Evol. 55, 1160–1163.

Albert, A., Hambuckers, A., Culot, L., Savini, T., Huynen, M.C., 2013a. Frugivory and Seed Dispersal by Northern Pigtailed Macaques (*Macaca leonina*), in Thailand. Int. J. Primatol. 34, 170–193.

Ψηφιακή βιβλιοθήκη Θεόφραστος – Τμήμα Γεωλογίας – Αριστοτέλειο Πανεπιστήμιο Θεσσαλονίκης

Ψηφιακή συλλογή
Βιβλιοθήκη
"ΘΕΟΦΡΑΣΤΟΣ"

Albert, A., Huynen, M.C., Savini, T., Hambuckers, A., 2013b. Influence of Food Resources on the Ranging Pattern of Northern Pig-tailed Macaques (*Macaca leonina*). Int. J. Primatol. 34, 696–713.

Allen, K.L., Cooke, S.B., Gonzales, L.A., Kay, R.F., 2015. Dietary inference from upper and lower molar morphology in platyrrhine primates. PLoS One. 10, 1–22.

Anderson, C.M., 1986. Predation and primate evolution. Primates. 27, 15–39.

Andrews, P., 1982. Ecological polarity in primate evolution. Zool. J. Linn. Soc. 74, 233–244.

Andrews, P., Harrison, T., Delson, E., Bernor, R.L., Martin, L.B., 1996. Distribution and Biochronology of European and Southwest Asian Miocene Catarrhines. In: The Evolution of Western Eurasian Neogene Mammal Faunas. pp. 168–207.

Angelone, C., Čermák, S., Moncunill-Solé, B., Quintana, J., Tuveri, C., Arca, M., Kotsakis, T., 2018. Systematics and paleobiogeography of *Sardolagus obscurus* n. gen. n. sp. (Leporidae, Lagomorpha) from the early Pleistocene of Sardinia. J. Paleontol. 92, 506–522.

Anthony, M.R.L., Kay, R.F., 1993. Tooth form and diet in ateline and alouattine primates: reflections on the comparative method. Am. J. Sci. 293 A, 356–382.

Ardito, G., Mottura, A., 1987. An overview of the geographic and chronologic distribution of west European cercopithecoids. Hum. Evol. 2, 29–45.

Arnold, C., Matthews, L.J., Nunn, C.L., 2010. The 10kTrees website: A new online resource for primate phylogeny. Evol. Anthropol. 19, 114–118.

Astaras, C., Krause, S., Mattner, L., Rehse, C., Waltert, M., 2011. Associations between the drill (*Mandrillus leucophaeus*) and sympatric monkeys in Korup National Park, Cameroon. Am. J. Primatol. 73, 127–134.

Astaras, C., Mühlenberg, M., Waltert, M., 2008. Note on drill (*Mandrillus leucophaeus*) ecology and conservation status in Korup National Park, Southwest Cameroon. Am. J. Primatol. 70, 306–310.

Astaras, C., Waltert, M., 2010. What does seed handling by the drill tell us about the ecological services of terrestrial cercopithecines in African forests? Anim. Conserv. 13, 568–578.

Ataabadi, M.M., Kaakinen, A., Kunimatsu, Y., Nakaya, H., Orak, Z., Paknia, M., Sakai, T., Salminen, J., Sawada, Y., Sen, S., Suwa, G., Watabe, M., Zaree, G., Zhaoqun, Z., Fortelius, M., 2016. The late Miocene hominoid-bearing site in the Maragheh Formation, Northwest Iran. Palaeobiodiversity and Palaeoenvironments. 96, 349–371.

Ψηφιακή βιβλιοθήκη Θεόφραστος – Τμήμα Γεωλογίας – Αριστοτέλειο Πανεπιστήμιο Θεσσαλονίκης

Ψηφιακή συλλογή
Βιβλιοθήκη
"ΘΕΟΦΡΑΣΤΟΣ"

Azzaroli, Augusto, 1983. Quaternary mammals and the "end-Villafranchian" dispersal event—a turning point in the history of Eurasia. Palaeogeogr. Palaeoclimatol. Palaeoecol. 44, 117–139.

Azzaroli, A., 1983. Biogeografia dei mammiferi della Sardegna. Biogeogr. – J. Integr. Biogeogr. 8.

Baines, D.C., Purnell, M.A., Hart, P.J.B., 2014. Tooth microwear formation rate in *Gasterosteus aculeatus*. J. Fish Biol. 84, 1582–1589.

Baker, W.E., Durand, H.M., 1836. Table of sub-Himalayan fossil genera in the Daduapur collection. J. Asiat. Soc. Bengal. 5, 291–293.

Barrett, A.S., 2005. Foraging ecology of the vervet monkey (*Chlorocebus aethiops*) in mixed lowveld bushveld and sour lowveld bushveld of the Blydeberg Conservancy, Northern Province, South Africa. University of South Africa.

Bartoli, G., Sarnthein, M., Weinelt, M., Erlenkeuser, H., Garbe-Schönberg, D., Lea, D.W., 2005. Final closure of Panama and the onset of northern hemisphere glaciation. Earth Planet. Sci. Lett. 237, 33–44.

Beaudet, A., Dumoncel, J., Thackeray, J.F., Bruxelles, L., Duployer, B., Tenailleau, C., Bam, L., Hoffman, J., de Beer, F., Braga, J., 2016. Upper third molar internal structural organization and semicircular canal morphology in Plio-Pleistocene South African cercopithecoids. J. Hum. Evol. 95, 104–120.

Belmaker, M., 2010. The presence of a large cercopithecine (cf. *Theropithecus* sp.) in the 'Ubeidiya formation (Early Pleistocene, Israel). J. Hum. Evol. 58, 79–89.

Benammi, M., Aidona, E., Merceron, G., Koufos, G.D., Kostopoulos, D.S., 2020. Magnetostratigraphy and Chronology of the Lower Pleistocene Primate Bearing Dafnero Fossil Site, N. Greece. Quaternary. 3, 22.

Benefit, B., 2008. The biostratigraphy and paleontology of fossil cercopithecoids from eastern Libya. Geol. East Libya. 3, 247–265.

Benefit, B.K., 1993. The permanent dentition and phylogenetic position of *Victoriapithecus* from Maboko Island, Kenya. J. Hum. Evol.

Benefit, B.R., 1994. Phylogenetic, paleodemographic, and taphonomic implications of *Victoriapithecus* deciduous teeth from Maboko, Kenva. Am. J. Phys. Anthropol. 95, 277–331.

Benefit, B.R., 1999. *Victoriapithecus*: The key to old world monkey and catarrhine origins. Evol. Anthropol. 7, 155–174.

Ψηφιακή βιβλιοθήκη Θεόφραστος – Τμήμα Γεωλογίας – Αριστοτέλειο Πανεπιστήμιο Θεσσαλονίκης

Ψηφιακή συλλογή
Βιβλιοθήκη
"ΘΕΟΦΡΑΣΤΟΣ"

Benefit, B.R., 2000. Old World monkey origins and diversification: an evolutionary study of diet and dentition. Old world monkeys. 133–179.

Benefit, B.R., McCrossin, M.L., 1997. Earliest known Old World monkey skull. Nature. 388, 368–371.

Benefit, B.R., Pickford, M., 1986. Miocene fossil cercopithecoids from Kenya. Am. J. Phys. Anthropol. 69, 441–464.

Bennett, E.L., 1994. The ecology of Asian colobines. In: Davies, G.E., Oates, J.F. (Eds.), Colobine Monkeys: Their Ecology, Behaviour and Evolution. Cambridge University Press, p. 129.

Bennett, E.L., Sebastian, A.C., 1988. Social organization and ecology of proboscis monkeys (*Nasalis larvatus*) in mixed coastal forest in Sarawak. Int. J. Primatol. 9, 233–255.

Bentley-Condit, Vicki K., 2009. Food choices and habitat use by the Tana river yellow baboons (*Papio cynocephalus*): A preliminary report on five years of data. Am. J. Primatol. 71, 432–436.

Berger, L.R., Clarke, R.J., 1995. Bird of prey involvement in the collection of the Taung child fauna. J. Hum. Evol. 29, 275–299.

Berlioz, É., Kostopoulos, D.S., Blondel, C., Merceron, G., 2018. Feeding ecology of *Eucladoceros ctenoides* as a proxy to track regional environmental variations in Europe during the early Pleistocene. Comptes Rendus - Palevol. 17, 320–332.

Bernstein, I.S., 1967. A field study of the pigtail monkey (*Macaca nemestrina*). Primates. 8, 217–228.

Berthaume, M.A., 2016a. On the Relationship Between Tooth Shape and Masticatory Efficiency: A Finite Element Study. Anat. Rec. 299, 679–687.

Berthaume, M.A., 2016b. Food mechanical properties and dietary ecology. Am. J. Phys. Anthropol. 159, S79–S104.

Berthaume, M.A., Delezene, L.K., Kupczik, K., 2018. Dental topography and the diet of Homo naledi. J. Hum. Evol. 118, 14–26.

Berthaume, M.A., Lazzari, V., Guy, F., 2020. The landscape of tooth shape: Over 20 years of dental topography in primates. Evol. Anthropol. 1–18.

Berthaume, M.A., Schroer, K., 2017. Extant ape dental topography and its implications for reconstructing the emergence of early Homo. J. Hum. Evol. 112, 15–29.

Ψηφιακή βιβλιοθήκη Θεόφραστος – Τμήμα Γεωλογίας – Αριστοτέλειο Πανεπιστήμιο Θεσσαλονίκης

Ψηφιακή συλλογή
Βιβλιοθήκη
"ΘΕΟΦΡΑΣΤΟΣ"

Berthaume, M.A., Winchester, J., Kupczik, K., 2019a. Ambient occlusion and PCV (portion de ciel visible): A new dental topographic metric and proxy of morphological wear resistance. PLoS One. 14.

Berthaume, M.A., Winchester, J., Kupczik, K., 2019b. Effects of cropping, smoothing, triangle count, and mesh resolution on 6 dental topographic metrics, PLoS ONE.

Bertini, A., 2013. Climate and vegetation in the Upper Valdarno Basin (central Italy) as a response to Northern Hemisphere insolation forcing and regional tectonics in the late Pliocene-early Pleistocene. Ital. J. Geosci. 132, 137–148.

Bhandari, S., Morley, C., Aryal, A., Shrestha, U.B., 2020. The diet of the striped hyena in Nepal's lowland regions. Ecol. Evol. 10, 7953–7962.

Bibi, F., Souron, A., Bocherens, H., Uno, K., Boisserie, J.R., 2013. Ecological change in the lower Omo Valley around 2.8 Ma. Biol. Lett. 9, 21–24.

Bobe, R., Behrensmeyer, A.K., 2004. The expansion of grassland ecosystems in Africa in relation to mammalian evolution and the origin of the genus *Homo*. Palaeogeogr. Palaeoclimatol. Palaeoecol. 207, 399–420.

Bobe, R., Behrensmeyer, A.K., Chapman, R.E., 2002. Faunal change, environmental variability and late Pliocene hominin evolution. J. Hum. Evol. 42, 475–497.

Böhme, M., Spassov, N., Ebner, M., Geraads, D., Hristova, L., Kirscher, U., Kötter, S., Linnemann, U., Prieto, J., Roussiakis, S., Theodorou, G., Uhlig, G., Winklhofer, M., 2017. Messinian age & savannah environment of the possible hominin *Graecopithecus* from Europe, PLoS ONE.

Bondioli, L., Bayle, P., Dean, C., Mazurier, A., Puymerail, L., Ruff, C., Stock, J.T., Volpato, V., Zanolli, C., Macchiarelli, R., 2010. Technical note: Morphometric maps of long bone shafts and dental roots for imaging topographic thickness variation. Am. J. Phys. Anthropol. 142, 328–334.

Boonratana, R., 1993. The ecology and behaviour of the Proboscis monkey (*Nasalis larvatus*) in the Lower Kinabatangan, Sabah.

Boyde, A., Fortelius, M., 1991. New confocal LM method for studying local relative microrelief with special reference to wear studies. Scanning. 13, 429–430.

Boyer, D.M., 2008. Relief index of second mandibular molars is a correlate of diet among prosimian primates and other euarchontan mammals. J. Hum. Evol. 55, 1118–1137.

Boyer, D.M., Costeur, L., Lipman, Y., 2012. Earliest record of Platychoerops (Primates, Plesiadapidae), a new species from Mouras Quarry, Mont de Berru, France. Am. J. Phys.

Ψηφιακή βιβλιοθήκη Θεόφραστος – Τμήμα Γεωλογίας – Αριστοτέλειο Πανεπιστήμιο Θεσσαλονίκης

Ψηφιακή συλλογή
Βιβλιοθήκη
"ΘΕΟΦΡΑΣΤΟΣ"
Α.Π.Θ

Anthropol. 149, 329–346.

Boyer, D.M., Evans, A.R., Jernvall, J., 2010. Evidence of dietary differentiation among late paleocene-early eocene plesiadapids (Mammalia, Primates). Am. J. Phys. Anthropol. 142, 194–210.

Boyer, D.M., Winchester, J., Kay, R.F., 2015. Technical note: The effect of differences in methodology among some recent applications of shearing quotients. Am. J. Phys. Anthropol. 156, 166–178.

Brown, C.A., Siegmann, S., 2001. Fundamental scales of adhesion and area-scale fractal analysis. Int. J. Mach. Tools Manuf. 41, 1927–1933.

Brown, W.L., Wilson, E.O., 1956. Character Displacement. Syst. Zool. 5, 49–64.

Brugiere, D., Gautier, J.P., Moungazi, A., Gautier-Hion, A., 2002. Primate diet and biomass in relation to vegetation composition and fruiting phenology in a rain forest in Gabon. Int. J. Primatol. 23, 999–1024.

Bunn, J.M., Boyer, D.M., Lipman, Y., St. Clair, E.M., Jernvall, J., Daubechies, I., 2011. Comparing Dirichlet normal surface energy of tooth crowns, a new technique of molar shape quantification for dietary inference, with previous methods in isolation and in combination. Am. J. Phys. Anthropol. 145, 247–261.

Bunn, J.M., Ungar, P.S., 2009. Dental topography and diets of four old world monkey species. Am. J. Primatol. 71, 466–477.

Butler, P.M., 1952. The milk-molars of Perissodactyla with remarks on molar occlusion. Proc. Zool. Soc. London. 121, 777–817.

Buzzard, P.J., 2006. Ecological partitioning of *Cercopithecus campbelli*, *C. petaurista*, and *C. diana* in the Taï Forest. Int. J. Primatol. 27, 529–558.

Buzzard, P.J., 2010. Polyspecific associations of *Cercopithecus campbelli* and *C. petaurista* with *C. diana*: What are the costs and benefits? Primates. 51, 307–314.

Byrne, R.W., Whiten, A., Henzi, S.P., McCulloch, F.M., 1993. Nutritional constraints on mountain baboons (*Papio ursinus*): Implications for baboon socioecology. Behav. Ecol. Sociobiol. 33, 233–246.

Cai, M., Fang, X., Wu, F., Miao, Y., Appel, E., 2012. Pliocene-Pleistocene stepwise drying of Central Asia: Evidence from paleomagnetism and sporopollen record of the deep borehole SG-3 in the western Qaidam Basin, NE Tibetan Plateau. Glob. Planet. Change. 94–95, 72–81.

Ψηφιακή βιβλιοθήκη Θεόφραστος – Τμήμα Γεωλογίας – Αριστοτέλειο Πανεπιστήμιο Θεσσαλονίκης

Ψηφιακή συλλογή
Βιβλιοθήκη
"ΘΕΟΦΡΑΣΤΟΣ"

Calandra, I., Merceron, G., 2016. Dental microwear texture analysis in mammalian ecology. Mamm. Rev. 46, 215–228.

Calandra, I., Schulz, E., Pinnow, M., Krohn, S., Kaiser, T.M., 2012. Teasing apart the contributions of hard dietary items on 3D dental microtextures in primates. J. Hum. Evol. 63, 85–98.

Calandra, I., Zub, K., Szafrańska, P.A., Zalewski, A., Merceron, G., 2016. Silicon-based plant defences, tooth wear and voles. J. Exp. Biol. 219, 501–507.

Caldecott, J.O., 1986. A summary of the ranging and activity patterns of the pig-tailed macaque (*Macaca n. nemestrina*) in relation to those of sympatric primates in Peninsular Malaysia.

Cashner, F.M., 1972. The ecology of Cercocebus albigena and C. torquatus in Rio Muni, Republic of Equatorial Guinea, West Africa. Tulane University.

Castaños, P., Murelaga, X., Arrizabalaga, A., Iriarte, M.J., 2011. First evidence of *Macaca sylvanus* (Primates, Cercopithecidae) from the Late Pleistocene of Lezetxiki II cave (Basque Country, Spain). J. Hum. Evol. 60, 816–820.

Caton, J.M., 1999. Digestive strategy of the Asian colobine genus *Trachypithecus*. Primates. 40, 311–325.

Cerling, T.E., Chritz, K.L., Jablonski, N.G., Leakey, M.G., Manthi, F.K., 2013. Diet of *Theropithecus* from 4 to 1 Ma in Kenya. Proc. Natl. Acad. Sci. U. S. A. 110, 10507–10512.

Cerling, T.E., Ehleringer, J.E., Harris, J.M., 1998. Carbon dioxide starvation, the development of C_4 ecosystems, and mammalian evolution. Philos. Trans. R. Soc. B Biol. Sci. 353, 159–171.

Cerling, T.E., Hart, J.A., Hart, T.B., 2004. Stable isotope ecology in the Ituri Forest. Oecologia. 138, 5–12.

Cerling, T.E., Wang, Y., Quade, J., 1993. Expansion of C_4 ecosystems as an indicator of global ecological change in the late Miocene. Nature. 361, 344–345.

Chang, C.H., Takai, M., Ogino, S., 2012. First discovery of colobine fossils from the early to middle Pleistocene of southern Taiwan. J. Hum. Evol. 63, 439–451.

Chapman, C.A., Chapman, L.J., 1990. Dietary variability in primate populations. Primates. 31, 121–128.

Chapman, C.A., Chapman, L.J., Cords, M., Gathua, J.M., Gautier-Hion, A., Lambert, J.E., Rode, K., Tutin, C.E.G., White, L.J.T., 2005. Variation in the Diets of *Cercopithecus* Species: Differences within Forests, among Forests, and across Species. Guenons Divers. Adapt. African Monkeys. 325–350.

Ψηφιακή βιβλιοθήκη Θεόφραστος – Τμήμα Γεωλογίας – Αριστοτέλειο Πανεπιστήμιο Θεσσαλονίκης

Ψηφιακή συλλογή
Βιβλιοθήκη
"ΘΕΟΦΡΑΣΤΟΣ"

Chapman, C.A., Chapman, L.J., Gillespie, T.R., 2002. Scale issues in the study of primate foraging: Red colobus of Kibale National Park. Am. J. Phys. Anthropol. 117, 349–363.

Chenery, C., O'Regan, H.J., Lamb, A.L., Rook, L., Elton, S., 2008. Modern stable isotope analogues for palaeo diet and environment studies in fossil macaques. In: Giornate Di Paleontologia VIII. Simposio Della Società Paleontologica Italiana. Workshop Sui Primati Fossili Europei. Riassunti Dei Lavori, Accademia Dei Fisiocritici, Siena 9-13 September.

Chivers, D.J., 1994. Functional anatomy of the gastrointestinal tract. In: Davies, G.E., Oates, J.F. (Eds.), Colobine Monkeys: Their Ecology, Behaviour and Evolution. Cambridge University Press, pp. 205–227.

Ciochon, R.L., 1993. Evolution of the cercopithecoid forelimb. Phylogenetic Funct. Implic. from Morphometric Anal. Univ. Calif. Press. Berkeley, CA.

Clavel, J., Merceron, G., Hristova, L., Spassov, N., Kovachev, D., Escarguel, G., 2012. On *Mesopithecus* habitat: Insights from late Miocene fossil vertebrate localities of Bulgaria. J. Hum. Evol. 63, 162–179.

Clutton-Brock, T.H., Harvey, P.H., 1979. Comparison and Adaptation. 205, 547–565.

Clutton-Brock, T.H., Harvey, P.H., 1977. Primate ecology and social organization. J. Zool. 183, 1–39.

Cnudde, V., Boone, M.N., 2013. High-resolution X-ray computed tomography in geosciences: A review of the current technology and applications. Earth-Science Rev. 123, 1–17.

Codron, D., Luyt, J., Lee-Thorp, J.A., Sponheimer, M., De Ruiter, D., Codron, J., 2005. Utilization of savanna-based resources by Plio-Pleistocene baboons. S. Afr. J. Sci. 101, 245–248.

Coiner-Collier, Susan, Scott, R.S., Chalk-Wilayto, J., Cheyne, S.M., Constantino, P., Dominy, N.J., Elgart, A.A., Glowacka, H., Loyola, L.C., Ossi-Lupo, K., Raguet-Schofield, M., Talebi, M.G., Sala, E.A., Sieradzy, P., Taylor, A.B., Vinyard, C.J., Wright, B.W., Yamashita, N., Lucas, P.W., Vogel, E.R., 2016. Primate dietary ecology in the context of food mechanical properties. J. Hum. Evol. 98, 103–118.

Coiner-Collier, S., Scott, R.S., Chalk-Wilayto, J., Cheyne, S.M., Constantino, P., Dominy, N.J., Elgart, A.A., Glowacka, H., Loyola, L.C., Ossi-Lupo, K., Raguet-Schofield, M., Talebi, M.G., Sala, E.A., Sieradzy, P., Taylor, A.B., Vinyard, C.J., Wright, B.W., Yamashita, N., Lucas, P.W., Vogel, E.R., 2016. Primate dietary ecology in the context of food mechanical properties. J. Hum. Evol. 98, 103–118.

Colombero, S., Alba, D.M., D'Amico, C., Delfino, M., Esu, D., Giuntelli, P., Harzhauser, M., Mazza, P.P.A., Mosca, M., Neubauer, T.A., Pavia, G., Pavia, M., Villa, A., Carnevale, G., 2017. Late messinian mollusks and vertebrates from moncucco torinese, north-western Italy.

Ψηφιακή βιβλιοθήκη Θεόφραστος – Τμήμα Γεωλογίας – Αριστοτέλειο Πανεπιστήμιο Θεσσαλονίκης

Ψηφιακή συλλογή
Βιβλιοθήκη
"ΘΕΟΦΡΑΣΤΟΣ"
Τμήμα Γεωλογίας
Α.Π.Θ

Paleoecological and paleoclimatological implications. Palaeontol. Electron. 20, 1–66.

Conover, W.J., Iman, R.L., 1981. Rank Transformations as a Bridge Between Parametric and Nonparametric Statistics. Am. Stat. 35, 124–129.

Constantino, P.J., Markham, K., Lucas, P.W., 2012. Tooth Chipping as a Tool to Reconstruct Diets of Great Apes (*Pongo*, *Gorilla*, *Pan*). Int. J. Primatol. 33, 661–672.

Constantino, P.J., Wright, B.W., 2009. The importance of fallback foods in primate ecology and evolution. Am. J. Phys. Anthropol. 140, 599–602.

Cooke, C., 2012. The Feeding, Ranging, and Positional Behaviors of *Cercocebus torquatus*, the Red- Capped Mangabey, in Sette Cama Gabon: A Phylogenetic Perspective. The Ohio University.

Corp., 2013. IBM SPSS statistics for Windows, Version 22.0.

Council, N.R., 2003. Nutrient Requirements of Nonhuman Primates: Second Revised Edition, Nutrient Requirements of Nonhuman Primates. Washington, DC.

Covert, H.H., Kay, R.F., 1981. Dental microwear and diet: Implications for determining the feeding behaviors of extinct primates, with a comment on the dietary pattern of *Sivapithecus*. Am. J. Phys. Anthropol. 55, 331–336.

Cowlishaw, G., 1997. Refuge use and predation risk in a desert baboon population. Anim. Behav. 54, 241–253.

Crowley, B.E., 2012. Stable Isotope Techniques and Applications for Primatologists. Int. J. Primatol. 33, 673–701.

Cui, Z., Shao, Q., Grueter, C.C., Wang, Z., Lu, J., Raubenheimer, D., 2019. Dietary diversity of an ecological and macronutritional generalist primate in a harsh high-latitude habitat, the Taihangshan macaque (*Macaca mulatta tcheliensis*). Am. J. Primatol. 81.

Cui, Z., Wang, Z., Zhang, S., Wang, B., Lu, J., Raubenheimer, D., 2020. Living near the limits: Effects of interannual variation in food availability on diet and reproduction in a temperate primate, the Taihangshan macaque (*Macaca mulatta tcheliensis*). Am. J. Primatol. 82, 1–11.

Cuozzo, F.P., Sauther, M.L., 2006. Severe wear and tooth loss in wild ring-tailed lemurs (*Lemur catta*): A function of feeding ecology, dental structure, and individual life history. J. Hum. Evol. 51, 490–505.

Curran, S., Terhune, C., Croitor, R., Drăguşin, V., Fox, D.L., Garrett, N., Ironside, L.B., Petculescu, A., Pobiner, B., Robinson, C., Robu, M., Tanţău, I., Ungar, P., 2021. Multiproxy

Ψηφιακή βιβλιοθήκη Θεόφραστος – Τμήμα Γεωλογίας – Αριστοτέλειο Πανεπιστήμιο Θεσσαλονίκης

Ψηφιακή συλλογή
Βιβλιοθήκη
"ΘΕΟΦΡΑΣΤΟΣ"
Τμήμα Γεωλογίας

paleoenvironmental reconstruction of Early Pleistocene sites from the Olteţ River Valley of Romania. Palaeogeogr. Palaeoclimatol. Palaeoecol. 574.

Curtin, S.H., 2004. Diet of the Roloway Monkey, *Cercopithecus diana roloway*, in Bia National Park, Ghana. In: Glenn, M.E., Cords, M. (Eds.), The Guenons: Diversity and Adaptation in African Monkeys. NY: Kluwert Academin Publishers, New York, pp. 351–371.

Daegling, D.J., Grine, F.E., 1999. Terrestrial foraging and dental microwear in *Papio ursinus*. Primates. 40, 559–572.

Daegling, D.J., Mcgraw, W.S., 2001. Feeding, diet, and jaw form in West African *Colobus* and *Procolobus*. Int. J. Primatol. 22, 1033–1055.

Daegling, D.J., McGraw, W.S., Ungar, P.S., Pampush, J.D., Vick, A.E., Bitty, E.A., 2011. Hard-object feeding in sooty mangabeys (*Cercocebus atys*) and interpretation of early hominin feeding ecology. PLoS One. 6.

Dasilva, G.L., 1994. Diet of *Colobus polykomos* on Tiwai Island: Selection of food in relation to its seasonal abundance and nutritional quality. Int. J. Primatol. 15, 655–680.

Davies, A.G., Bennett, E.L., Waterman, P.G., 1988. Food selection by two South-east Asian colobine monkeys (*Presbytis rubicunda* and *Presbytis melalophos*) in relation to plant chemistry. Biol. J. Linn. Soc. 34, 33–56.

Davies, A.G., Oates, J.F., Dasilva, G.L., 1999. Patterns of frugivory in three west African colobine monkeys. Int. J. Primatol. 20, 327–357.

Davies, G.E., 1994. Colobine monkeys: their ecology, behaviour and evolution. Cambridge University Press, Cambridge.

de Bonis, L., Bouvrain, G., Geraads, D., Koufos, G., 1990. New remains of *Mesopithecus* (Primates, Cercopithecoidea) from the late Miocene of Macedonia (Greece), with the description of a new species. J. Vertebr. Paleontol. 10, 473–483.

de Vos, J., 2000. Pleistocene Deer Fauna in Crete: Its Adaptive Radiation and Extinction. Tropics. 10, 125–134.

de Vos, J., Van der Made, J., Athanassiou, A., Lyras, G. a., Sondaar, P.Y., Dermitzakis, M.D., 2002. Preliminary note on the late Pliocene fauna from Vatera (Lesvos, Greece). Ann. Géologiques des Pays Helléniques. 39, 37–70.

Dean, M.C., Leakey, M.G., 2004. Enamel and dentine development and the life history profile of *Victoriapithecus macinnesi* from Maboko Island, Kenya. Ann. Anat. 186, 405–412.

Ψηφιακή βιβλιοθήκη Θεόφραστος – Τμήμα Γεωλογίας – Αριστοτέλειο Πανεπιστήμιο Θεσσαλονίκης

Ψηφιακή συλλογή
Βιβλιοθήκη
"ΘΕΟΦΡΑΣΤΟΣ"

Dela, J.D.S., 2007. Seasonal food use strategies of *Semnopithecus vetulus nestor*, at Panadura and Piliyandala, Sri Lanka. Int. J. Primatol. 28, 607–626.

Delson, 1973. Fossil Colobine Monkeys of the Circum-Mediterranean Region and the Evolutionary History of the Cercopithecidae (Primates, Mammalia).

Delson, 1975. Evolutionary history of the Cercopithecidae.

Delson, 1993. *Theropithecus* fossils from Africa and India and the taxonomy of the genus. In: Jablonski, N.G. (Ed.), *Theropithecus*: The Rise and Fall of a Primate Genus. Cambridge University Press, pp. 157–189.

Delson, E., 1974. Preliminary review of Cercopithecid distribution in the Circum Mediterranean Region. Mémoires du Bur. pour la Rech. Géologique Minière. 78, 131–135.

Delson, E., 1980. Fossil macaques, phyletic relationships and a scenario of deployment. Macaques Stud. Ecol. Behav. Evol.

Delson, E., 1994. Evolutionary history of the colobine monkeys in paleoenvironmental perspective. In: Davies, G.E., Oates, J.F. (Eds.), Colobine Monkeys: Their Ecology, Behaviour, and Evolution. Cambridge University Press, pp. 11–48.

Delson, E., 2004. Paradolichopithecus: A large-bodied terrestrial papionin (Cercopithecidae) from the Pliocene of western Eurasia. Am J Phys Anthr. Suppl. 38, 85.

Delson, E., Alba, D.M., Frost, S.R., Harcourt-Smith, W.E., Martín Suárez, E., Mazelis, E.J., Morales, J., Moyà-Solà, S., Shearer, B.M., 2014. *Paradolichopithecus*, a large terrestrial Pliocene cercopithecine from Europe: New remains and an update. Abstr. B. F. Trip Guid. XII Annu. Meet. Eur. Assoc. Vertebr. Palaeontol. 50.

Delson, E., Faure, M., Guérin, C., Aprile, L., Argant, J., Blackwell, B.A.B., Debard, E., Harcourt-Smith, W., Martin-Suarez, E., Monguillon, A., Parenti, F., Pastre, J.F., Sen, S., Skinner, A.R., Swisher, C.C., Valli, A.M.F., 2006. Franco-American renewed research at the Late Villafranchian locality of Senèze (Haute-Loire, France). In: Late Neogene and Quaternary Biodiversity and Evolution: Regional Developments and Interregional Correlations. Proceedings of the 18th International Senckenberg Conference (VI IPCW) Volume I. pp. 275–290.

Delson, E., Nicolaescu-Plopsor, D., 1975a. Paradolichopithecus, a large terrestrial monkey (Cercopithecidae, Primates) from the Plio-Pleistocene of Souther Europe and its importance for mammalian biochronology. In: VIth Session, Regional Committee on Mediterranean Neogene Stratigraphy, Bratislava (Slovak Academy Sciences). pp. 91–96.

Delson, E., Nicolaescu-Plopsor, D., 1975b. *Paradolichopithecus*, a large terrestrial monkey (Cercopithecidae, Primates) from the Plio-Pleistocene of Southern Europe and its importance

Ψηφιακή βιβλιοθήκη Θεόφραστος – Τμήμα Γεωλογίας – Αριστοτέλειο Πανεπιστήμιο Θεσσαλονίκης

Ψηφιακή συλλογή
Βιβλιοθήκη
"ΘΕΟΦΡΑΣΤΟΣ"
Τμήμα Γεωλογίας
Α.Π.Θ

for mammalian Biochronology.

Delson, E., Terranova, C.J., Jungers, W.L., Sargis, E.J., Jablonski, N.G., Dechow, P.C., 2000. Body mass in Cercopithecidae (Primates, Mammalia): estimation and scaling in extinct and extant taxa. Anthropol. Pap. Am. Mus. Nat. Hist. 83, 1–159.

Delson, E., Thomas, H., Spassov, N., 2005. Fossil Old World monkeys (Primates, Cercopithecidae) from the Pliocene of Dorkovo, Bulgaria. Geodiversitas. 27, 159–166.

deMenocal, P.B., 2004. African climate change and faunal evolution during the Pliocene-Pleistocene. Earth Planet. Sci. Lett. 220, 3–24.

DeMiguel, D., Domingo, L., Sánchez, I.M., Casanovas-Vilar, I., Robles, J.M., Alba, D.M., 2021. Palaeoecological differences underlie rare co-occurrence of Miocene European primates. BMC Biol. 19, 1–15.

Dennis, J.C., Ungar, P.S., Teaford, M.F., Glander, K.E., 2004. Dental topography and molar wear in Alouatta palliata from Costa Rica. Am. J. Phys. Anthropol. 125, 152–161.

Depéret, C., 1889. Sur le *Dolichopithecus ruscinensis*, nouveau singe fossile du Pliocène du Roussillon. Gauthier-Villars.

Depéret, C., 1890. Les animaux pliocènes du Roussillon. Baudry.

Depéret, C., 1929. *Dolichopithecus arvernesis* Depéret: nouveau singe du Pliocène supérieur de Senèze (Haute-Loire). Trav. du Lab. Géologie la Fac. des Sci. Lyon. 15, 5–12.

DeSantis, L.R.G., Schubert, B.W., Scott, J.R., Ungar, P.S., 2012. Implications of Diet for the Extinction of Saber-Toothed Cats and American Lions. PLoS One. 7.

Dominy, N.J., Vogel, E.R., Yeakel, J.D., Constantino, P., Lucas, P.W., 2008. Mechanical properties of plant underground storage organs and implications for dietary models of early hominins. Evol. Biol. 35, 159–175.

Donohue, S.L., 2013. Using dental microwear textures to assess feeding ecology of extinct and extant bears.

Drapier, M., Chauvin, C., Thierry, B., 2002. Tonkean macaques (*Macaca tonkeana*) find food sources from cues conveyed by group-mates. Anim. Cogn. 5, 159–165.

Dubey, S., Zaitsev, M., Cosson, J.F., Abdukadier, A., Vogel, P., 2006. Pliocene and Pleistocene diversification and multiple refugia in a Eurasian shrew (*Crocidura suaveolens* group). Mol. Phylogenet. Evol. 38, 635–647.

Ψηφιακή βιβλιοθήκη Θεόφραστος – Τμήμα Γεωλογίας – Αριστοτέλειο Πανεπιστήμιο Θεσσαλονίκης

Ψηφιακή συλλογή
Βιβλιοθήκη
"ΘΕΟΦΡΑΣΤΟΣ"

Dumont, E.R., 1995. Enamel thickness and dietary adaptation among extant primates and chiropterans. J. Mammal. 76, 1127–1136.

Dunham, N.T., Lambert, A.L., 2016. The role of leaf toughness on foraging efficiency in Angola black and white colobus monkeys (*Colobus angolensis palliatus*). Am. J. Phys. Anthropol. 161, 343–354.

Eaglen, R.H., 1984. Incisor size and diet revisited: The view from a platyrrhine perspective. Am. J. Phys. Anthropol. 64, 263–275.

Egi, N., Nakatsukasa, M., Kalmykov, N.P., Maschenko, E.N., Takai, M., 2007. Distal humerus and ulna of *Parapresbytis* (Colobinae) from the Pliocene of Russia and Mongolia: Phylogenetic and ecological implications based on elbow morphology. Anthropol. Sci. 115, 107–117.

El-Zaatari, S., Grine, F.E., Teaford, M.F., Smith, H.F., 2005. Molar microwear and dietary reconstructions of fossil Cercopithecoidea from the Plio-Pleistocene deposits of South Africa. J. Hum. Evol. 49, 180–205.

El Alami, A., Van Lavieren, E., Rachida, A., Chait, A., 2012. Differences in Activity Budgets and Diet Between Semiprovisioned and Wild-Feeding Groups of the Endangered Barbary Macaque (*Macaca sylvanus*) in the Central High Atlas Mountains, Morocco. Am. J. Primatol. 74, 210–216.

Elton, S., 2006. Forty years on and still going strong: The use of hominin–cercopithecid comparisons in palaeoanthropology. J. R. Anthropol. Inst. 12, 19–38.

Elton, S., 2007. Environmental correlates of the cercopithecoid radiations. Folia Primatol. 78, 344–364.

Elton, S., O'Regan, H.J., 2014. Macaques at the margins: The biogeography and extinction of Macaca sylvanus in Europe. Quat. Sci. Rev. 96, 117–130.

Enari, H., Sakamaki-Enari, H., 2013. Influence of Heavy Snow on the Feeding Behavior of Japanese Macaques (*Macaca fuscata*) in Northern Japan. Am. J. Primatol. 75, 534–544.

Eronen, J.T., Rook, L., 2004. The Mio-Pliocene European primate fossil record: Dynamics and habitat tracking. J. Hum. Evol. 47, 323–341.

Eronen, J.T., Zohdy, S., Evans, A.R., Tecot, S.R., Wright, P.C., Jernvall, J., 2017. Feeding Ecology and Morphology Make a Bamboo Specialist Vulnerable to Climate Change. Curr. Biol. 27, 3384-3389.e2.

Escarguel, G., 2005. Mathematics and the lifeway of *Mesopithecus*. Int. J. Primatol. 26, 801–823.

Ψηφιακή βιβλιοθήκη Θεόφραστος – Τμήμα Γεωλογίας – Αριστοτέλειο Πανεπιστήμιο Θεσσαλονίκης

Ψηφιακή συλλογή
Βιβλιοθήκη
"ΘΕΟΦΡΑΣΤΟΣ"

Estebaranz, F., Martínez, L.M., Galbany, J., Turbón, D., Pérez-Pérez, A., 2009. Testing hypotheses of dietary reconstruction from buccal dental microwear in *Australopithecus afarensis*. J. Hum. Evol. 57, 739–750.

Evans, A.R., Jernvall, J., 2009. Patterns and Constraints in Carnivoran and Rodent Dental Complexity and Tooth Size. J. Vertebr. Paleontol. 29, 24A.

Evans, A.R., Wilson, G.P., Fortelius, M., Jernvall, J., 2007. High-level similarity of dentitions in carnivorans and rodents. Nature. 445, 78–81.

Fa, J.E., 1986. On the ecological status of the Barbary macaque *Macaca sylvanus* L. in North Morocco: Habitat influences versus human impact. Biol. Conserv. 35, 215–258.

Fa, J.E., 1989. The genus Macaca: a review of taxonomy and evolution. Mamm. Rev. 19, 45–81.

Fa, J.E., Currie, D., Meeuwig, J., 2003. Bushmeat and food security in the Congo Basin: Linkages between wildlife and people's future. Environ. Conserv. 30, 71–78.

Falótico, T., Ottoni, E.B., 2016. The manifold use of pounding stone tools by wild capuchin monkeys of Serra da Capivara National Park, Brazil. Behaviour. 153, 421–442.

Fashing, P.J., 2001. Feeding ecology of guerezas in the Kakamega Forest, Kenya: The importance of *Moraceae* fruit in their diet. Int. J. Primatol. 22, 579–609.

Fashing, P.J., Nguyen, N., Venkataraman, V. V., Kerby, J.T., 2014. Gelada feeding ecology in an intact ecosystem at Guassa, Ethiopia: Variability over time and implications for theropith and hominin dietary evolution. Am. J. Phys. Anthropol. 155, 1–16.

Feeroz, M.M., 2012. Niche separation between sympatric pig-tailed macaque (*Macaca leonina*) and rhesus macaque (*M. mulatta*) in Bangladesh. J Primatol. 1.

Ferràndez-Cañadell, C., Ribot, F., Gibert, L., 2014. New fossil teeth of *Theropithecus oswaldi* (Cercopithecoidea) from the early Pleistocene at Cueva victoria (SE Spain). J. Hum. Evol. 74, 55–66.

Ferretti, M.P., 1999. Tooth Enamel Structure in the Hyaenid *Chasmaporthetes lunensis lunensis* from the Late Pliocene of Italy , with Implications for Feeding Behavior. J. Vertebr. Paleontol. 19, 767–770.

Fleagle, J. G., 2013a. Primate Adaptations. In: Primate Adaptation and Evolution. pp. 181–200.

Fleagle, J. G., 2013b. Primate adaptation and evolution. Academic press.

Ψηφιακή βιβλιοθήκη Θεόφραστος – Τμήμα Γεωλογίας – Αριστοτέλειο Πανεπιστήμιο Θεσσαλονίκης

Ψηφιακή συλλογή
Βιβλιοθήκη
"ΘΕΟΦΡΑΣΤΟΣ"
Α.Π.Θ

Fleagle, John G., 2013. Primate Communities and Biogeography. Primate Adapt. Evol. 169–180.

Fleagle, J.G., Mcgraw, W.S., 1999. Skeletal and dental morphology supports diphyletic origin of baboons and mandrills. Proc. Natl. Acad. Sci. U. S. A. 96, 1157–1161.

Fleagle, J.G., McGraw, W.S., 2002. Skeletal and dental morphology of African papionins: Unmasking a cryptic clade. J. Hum. Evol. 42, 267–292.

Fleagle, J.G., Reed, K.E., 1996. Comparing primate communities: A multivariate approach. J. Hum. Evol. 30, 489–510.

Fooden, J., 2000. Systematic review of rhesus macaque, *Macaca mulatta* (Zimmermann, 1780). Fieldiana Zool. 96, 1–180.

Fooden, J., 2011. Systematic review of the Barbary macaque, *Macaca sylvanus* (Linnaeus, 1758) / Jack Fooden. Syst. Rev. Barbar. macaque, *Macaca sylvanus* (Linnaeus, 1758) / Jack Fooden. 1–60.

Forsyth Major, C.J., 1913. Observations sur la faune des mammifères quaternaires de la Corse et de la Sardaigne. Natura. 4, 594.

Fortuny, J., Zanolli, C., Bernardini, F., Tuniz, C., Alba, D.M., 2021. *Dryopithecine* palaeobiodiversity in the Iberian Miocene revisited on the basis of molar endostructural morphology. Palaeontology. 64, 531–554.

Fourie, N.H., Lee-Thorp, J.A., Ackermann, R.R., 2008. Biogeochemical and craniometric investigation of dietary ecology, niche separation, and taxonomy of plio-pleistocene cercopithecoids from the Makapansgat limeworks. Am. J. Phys. Anthropol. 135, 121–135.

Francisco, A., Blondel, C., Brunetiere, N., Ramdarshan, A., Merceron, G., 2018. Enamel surface topography analysis for diet discrimination. A methodology to enhance and select discriminative parameters. Surf. Topogr. Metrol. Prop. 6.

Frost, S., Ting, N., Harcourt-Smith, W., Delson, E., 2005. Positional and locomotor behavior of *Paradolichopithecus arvernensis* as inferred from the functional morphology of the postcrania. Am. J. Primatol. 66, 134–135.

Frost, S.R., 2001. Fossil Cercopithecidae of the Afar depression, Ethiopia: Species systematics and comparison to the Turkana basin.

Frost, S.R., 2002. East African cercopithecid fossil record and its relationship to global climatic change. Am. J. Phys. Anthropol.

Frost, S.R., 2017. Evolution of the Cercopithecidae. In: Fuentes, A. (Ed.), The International

Ψηφιακή βιβλιοθήκη Θεόφραστος – Τμήμα Γεωλογίας – Αριστοτέλειο Πανεπιστήμιο Θεσσαλονίκης

Ψηφιακή συλλογή
Βιβλιοθήκη
"ΘΕΟΦΡΑΣΤΟΣ"
Α.Π.Θ

Encyclopedia of Primatology. John Wiley and Sons, Inc, pp. 1–3.

Frost, S.R., Gilbert, C.C., Pugh, K.D., Guthrie, E.H., Delson, E., 2015. The hand of Cercopithecoides williamsi (mammalia, primates): Earliest evidence for thumb reduction among colobine monkeys. PLoS One. 10, 1–17.

Frost, S.R., Plummer, T., Bishop, L.C., Ditchfield, P., Ferraro, J., Hicks, J., 2003. Partial Cranium of Cercopithecoides kimeui Leakey, 1982 From Rawi Gully, Southwestern Kenya. Am. J. Phys. Anthropol. 122, 191–199.

Frost, S.R., Simpson, S.W., Levin, N.E., Quade, J., Rogers, M.J., Semaw, S., 2020. Fossil Cercopithecidae from the Early Pliocene Sagantole Formation at Gona, Ethiopia. J. Hum. Evol. 144, 102789.

Gabis, R. V., 1961. Bones of the extremities of *Dolichopithecus*, fossil monkey of the Pliocene period from Roussilon. C. R. Hebd. Seances Acad. Sci. 252, 1368–1370.

Gabis, R. V, 1960. Les os des membres des singes cynomorphes. Mammalia. 24, 577–607.

Ganas, J., Robbins, M.M., Nkurunungi, J.B., Kaplin, B.A., McNeilage, A., 2004. Dietary variability of mountain gorillas in Bwindi impenetrable National Park, Uganda. Int. J. Primatol. 25, 1043–1072.

Gantt, D.G., 1982. Neogene hominoid evolution: a tooth's inside view. Teeth form, Funct. Evol. 93–108.

Ganzhorn, J.U., 1989. Niche separation of seven lemur species in the eastern rainforest of Madagascar. Oecologia. 79, 279–286.

Garber, P.A., 1987. Foraging Strategies among Living Primates. Annu. Rev. Anthropol. 16, 339–364.

Gaulin, S.J.C., Konner, M., 1977. On the natural diet of primates, including humans. Nutr. Brain. 1, 1–86.

Gause, G.F., 1934. The struggle for existence. Baltimore: Williams and Wilkins. 163 p.

Gautier-Hion, A., 1978. Food-niches and co-existence in sympatric primates in Gabon. Behaviour.

Gautier-Hion, A., 1980. Seasonal Variations of Diet Related to Species and Sex in a Community of Cercopithecus Monkeys A. J. Anim. Ecol. 49, 237–269.

Geissler, E., 2013. Dental microwear analysis of *Cercopithecoides wiilliamsi*. Georgia State

Ψηφιακή βιβλιοθήκη Θεόφραστος – Τμήμα Γεωλογίας – Αριστοτέλειο Πανεπιστήμιο Θεσσαλονίκης

Ψηφιακή συλλογή
Βιβλιοθήκη
"ΘΕΟΦΡΑΣΤΟΣ"
Τμήμα Γεωλογίας
Α.Π.Θ

University.

Gentili, S., Mottura, A., Rook, L., 1998. The Italian fossil primate record: Recent finds and their geological context. Geobios. 31, 675–686.

Geraads, D., 1987. Dating the Northern African cercopithecid fossil record. Hum. Evol. 2, 19–27.

Geraads, D., de Bonis, L., 2020. First record of *Theropithecus* (Cercopithecidae) from the Republic of Djibouti. J. Hum. Evol. 138, 102686.

Gibert, J., Ribot, F., Gibert, L., Leakey, M., Arribas, A., Martinez, B., 1995a. Presence of the Cercopithecid genus *Theropithecus* in Cueva Victoria (Murcia, Spain). J. Hum. Evol.

Gibert, J., Ribot, F., Gibert, L., Leakey, M., Arribas, A., Martinez, B., 1995b. Presence of the Cercopithecid genus Theropithecus in Cueva Victoria (Murcia, Spain). J. Hum. Evol. 28, 487–493.

Gilbert, C.C., Bibi, F., Hill, A., Beech, M.J., 2014. Early guenon from the late Miocene Baynunah Formation, Abu Dhabi, with implications for cercopithecoid biogeography and evolution. Proc. Natl. Acad. Sci. U. S. A. 111, 10119–10124.

Gilbert, C.C., Frost, S.R., Delson, E., 2016. Reassessment of Olduvai Bed I cercopithecoids: A new biochronological and biogeographical link to the South African fossil record. J. Hum. Evol. 92, 50–59.

Gilbert, C.C., Goble, E.D., Hill, A., 2010. Miocene Cercopithecoidea from the Tugen Hills, Kenya. J. Hum. Evol. 59, 465–483.

Gilbert, C.C., McGraw, W.S., Delson, E., 2009. Brief communication: Plio-Pleistocene eagle predation on fossil cercopithecids from the Humpata Plateau, southern Angola. Am. J. Phys. Anthropol. 139, 421–429.

Gill, P.G., Purnell, M.A., Crumpton, N., Brown, K.R., Gostling, N.J., Stampanoni, M., Rayfield, E.J., 2014. Dietary specializations and diversity in feeding ecology of the earliest stem mammals. Nature. 512, 303–305.

Gingerich, P.D., 1977. Correlation of tooth size and body size in living hominoid primates, with a note on relative brain size in *Aegyptopithecus* and *Proconsul*. Am. J. Phys. Anthropol. 47, 395–398.

Gingerich, P.D., Smith, B.H., Rosenberg, K., 1982. Allometric scaling in the dentition of primates and prediction of body weight from tooth size in fossils. Am. J. Phys. Anthropol. 58, 81–100.

Godfrey, L.R., Winchester, J.M., King, S.J., Boyer, D.M., Jernvall, J., 2012. Dental topography

Ψηφιακή βιβλιοθήκη Θεόφραστος – Τμήμα Γεωλογίας – Αριστοτέλειο Πανεπιστήμιο Θεσσαλονίκης

Ψηφιακή συλλογή
Βιβλιοθήκη
"ΘΕΟΦΡΑΣΤΟΣ"
Τμήμα Γεωλογίας
Α.Π.Θ

indicates ecological contraction of lemur communities. Am. J. Phys. Anthropol. 148, 215–227.

Goldstein, S., Post, D., Melnick, D.O.N., 1978. An Analysis of Cercopithecoid Odontometrics. Am. J. Phys. Anthropol. 49, 517–532.

Goldstein, S.J., Richard, A.F., 1989. Ecology of rhesus macaques (*Macaca mulatta*) in northwest Pakistan. Int. J. Primatol. 10, 531–567.

Gómez, A., Lunt, D.H., 2007. Refugia within Refugia: Patterns of Phylogeographic Concordance in the Iberian Peninsula. In: Phylogeography of Southern European Refugia: Evolutionary Perspectives on the Origins and Conservation of European Biodiversity. pp. 155–188.

Gordon, K.D., 1982. A study of microwear on chimpanzee molars: Implications for dental microwear analysis. Am. J. Phys. Anthropol. 59, 195–215.

Gordon, K.D., 1984. The assessment of jaw movement direction from dental microwear. Am. J. Phys. Anthropol. 63, 77–84.

Green, J.L., Croft, D.A., 2018. Using Dental Mesowear and Microwear for Dietary Inference: A Review of Current Techniques and Applications. In: Methods in Paleoecology. pp. 53–73.

Green, J.L., Kalthoff, D.C., 2015. Xenarthran dental microstructure and dental microwear analyses, with new data for *Megatherium americanum* (*Megatheriidae*). J. Mammal. 96, 645–657.

Green, J.L., Resar, N.A., 2012. The link between dental microwear and feeding ecology in tree sloths and armadillos (Mammalia: Xenarthra). Biol. J. Linn. Soc. 107, 277–294.

Gremiatskiy, M.A., 1958. Fossil primates from the territory of the Soviet Union (with relationships of the phylogenic question of the higher Primates). In: Treatises of the VI All Union Conference of Anatomists, Gistologysts and Embryologists, July 14-18, 1958, Kiev. pp. 576–579.

Grill, A., Casula, P., Lecis, R., Menken, S., 2007. Endemism in Sardinia. Phylogeography South. Eur. Refug. Evol. Perspect. Orig. Conserv. Eur. Biodivers. 273–296.

Grine, F.E., 1986. Dental evidence for dietary differences in *Australopithecus* and *Paranthropus*: a quantitative analysis of permanent molar microwear. J. Hum. Evol. 15, 783–822.

Grine, F.E., Spencer, M.A., Demes, B., Smith, H.F., Strait, D.S., Constant, D.A., 2005. Molar enamel thickness in the chacma baboon, *Papio ursinus* (Kerr 1792). Am. J. Phys. Anthropol. 128, 812–822.

Grine, F.E., Ungar, P.S., Teaford, M.F., 2002. Error rates in buccal-dental microwear quantification

Ψηφιακή βιβλιοθήκη Θεόφραστος – Τμήμα Γεωλογίας – Αριστοτέλειο Πανεπιστήμιο Θεσσαλονίκης

Ψηφιακή συλλογή
Βιβλιοθήκη
"ΘΕΟΦΡΑΣΤΟΣ"
Τμήμα Γεωλογίας
Α.Π.Θ

using scanning electron microscopy. Scanning. 24, 144–153.

Grueter, C.C., Li, D.Y., Feng, S.K., Ren, B.P., 2010. Niche partitioning between sympatric rhesus macaques and Yunnan snub-nosed monkeys at Baimaxueshan Nature Reserve, China. Zool. Res. 31, 516–522.

Gupta, V.J., Sahni, A., 1981. *Theropithecus delsoni*, a new cercopithecine species from the Upper Siwaliks of India.

Guy, F., Gouvard, F., Boistel, R., Euriat, A., Lazzari, V., 2013. Prospective in (Primate) Dental Analysis through Tooth 3D Topographical Quantification. PLoS One. 8.

Guy, F., Lazzari, V., Gilissen, E., Thiery, G., 2015. To what extent is primate second molar enamel occlusal morphology shaped by the enamel-dentine junction? PLoS One. 10, 1–15.

Guy, F., Thiery, G., Lazzari, V., 2017. 3D quantification of the occlusal enamel curvature: a decisive feature in dental function analysis and diet in Primates. In: 17th International Symposium on Dental Morphology 2nd Congress of International Association for Paleodontology. p. 104.

Hadi, S., 2012. Niche differentiation of two sympatric colobines, Simias concolor and Presbytis potentiani on the Mnetaway Island of Siberut, Indonesia.

Hadi, S., Ziegler, T., Waltert, M., Syamsuri, F., Mühlenberg, M., Hodges, J.K., 2012. Habitat Use and Trophic Niche Overlap of Two Sympatric Colobines, Presbytis potenziani and Simias concolor, on Siberut Island, Indonesia. Int. J. Primatol. 33, 218–232.

Hall, K.R.L., 1966. Behaviour and ecology of the wild Patas monkey, *Erythrocebus patas*, in Uganda. J. Zool. 148, 15–87.

Ham, R.M., 1994. Behaviour and ecology of grey-cheeked mangabeys (*Cercocebus albigena*) in the Lope Reserve, Gabon. University of Stirling.

Hammer, Ø., Harper, D.A., Ryan, P.D., 2001. PAST: Paleontological statistics software package for education and data analysis. Palaeontol. Electron. 4, 9.

Hanya, G., 2004. Diet of a Japanese Macaque Troop in the Coniferous Forest of Yakushima. Int. J. Primatol. 25, 55–71.

Hanya, G., Kiyono, M., Yamada, A., Suzuki, K., Furukawa, M., Yoshida, Y., Chijiiwa, A., 2006. Not only annual food abundance but also fallback food quality determines the japanese macaque density: Evidence from seasonal variations in home range size. Primates. 47, 275–278.

Ψηφιακή βιβλιοθήκη Θεόφραστος – Τμήμα Γεωλογίας – Αριστοτέλειο Πανεπιστήμιο Θεσσαλονίκης

Ψηφιακή συλλογή
Βιβλιοθήκη
"ΘΕΟΦΡΑΣΤΟΣ"

Hanya, G., Ménard, N., Qarro, M., Tattou, M.I., Fuse, M., Vallet, D., Yamada, A., Go, M., Takafumi, H., Tsujino, R., Agetsuma, N., Wada, K., 2011. Dietary adaptations of temperate primates: Comparisons of Japanese and Barbary macaques. Primates. 52, 187–198.

Hanya, G., Noma, N., Agetsuma, N., 2003. Altitudinal and seasonal variations in the diet of Japanese macaques in Yakushima. Primates. 44, 51–59.

Hanya, G., Tsuji, Y., Grueter, C.C., 2013. Fruiting and flushing phenology in Asian tropical and temperate forests: implications for primate ecology. Primates. 54, 101–110.

Hanya, G., Yoshihiro, S., Zamma, K., Matsubara, H., Ohtake, M., Kubo, R., Noma, N., Agetsuma, N., Takahata, Y., 2004. Environmental determinants of the altitudinal variations in relative group densities of Japanese macaques on Yakushima. Ecol. Res. 19, 485–493.

Happel, R., 1988. Seed-eating by West African cercopithecines, with reference to the possible evolution of bilophodont molars. Am. J. Phys. Anthropol. 75, 303–327.

Haq, B.U., Hardenbol, J., Vail, P.R., 1987. Chronology of fluctuating sea levels since the Triassic. Science (80-.). 235, 1156–1167.

Hardin, G., 1960. The Competitive Exclusion Principle. Am. Assoc. Adv. Sci. 131, 1292–1297.

Harding, R.S.O., 1981. An Order of Omnivores: Nonhuman Primate Diets in the Wild. In: Omnivorous Primates. Gathering and Hunting in Human Evolution. pp. 191–214.

Harris, T.R., 2010. Multiple resource values and fighting ability measures influence intergroup conflict in guerezas (*Colobus guereza*). Anim. Behav. 79, 89–98.

Harris, T.R., Chapman, C.A., 2007. Variation in diet and ranging of black and white colobus monkeys in Kibale National Park, Uganda. Primates. 48, 208–221.

Harrison, T., 1989. New postcranial remains of *Victoriapithecus* from the middle Miocene of Kenya. J. Hum. Evol. 18, 3–54.

Heaneyl, L.R., 1978. Island area and body size of insular mammals: Evidence from the tri-colored squirrel (*Callosciurus prevosti*) of Southeast Asia. Evolution (N. Y). 29–44.

Heintz, Emile, Brunet, M., Battail, B., 1981. A Cercopithecid Primate from the Late with Remarks on Mesopithecus. Int. J. Primatol. 2, 273–284.

Heintz, E., Brunet, M., Battait, B., 1981. A cercopithecid primate from the late miocene of Molayan, Afghanistan, with remarks on *Mesopithecus*. Int. J. Primatol. 2, 273–284.

Ψηφιακή βιβλιοθήκη Θεόφραστος – Τμήμα Γεωλογίας – Αριστοτέλειο Πανεπιστήμιο Θεσσαλονίκης

Ψηφιακή συλλογή
Βιβλιοθήκη
"ΘΕΟΦΡΑΣΤΟΣ"

Hemingway, C.A., Bynum, N., 2005. The influence of seasonality on primate diet and ranging. In: Brockman, D., Van Schaik, C.P. (Eds.), Seasonality in Primates. Cambridge University Press, p. 57104.

Henzi, S.P., Brown, L.R., Barrett, L., Marais, A.J., 2011. Troop Size, Habitat Use, and Diet of Chacma Baboons (*Papio hamadryas ursinus*) in Commercial Pine Plantations: Implications for Management. Int. J. Primatol. 32, 1020–1032.

Hermier, R., Merceron, G., Kostopoulos, D.S., 2020. The emblematic Eurasian Villafranchian antelope *Gazellospira* (Mammalia: Bovidae): New insights from the Lower Pleistocene Dafnero fossil sites (Northern Greece). Geobios. 61, 11–29.

Hernandez-Aguilar, R.A., Moore, J., Pickering, T.R., 2007. Savanna chimpanzees use tools to harvest the underground storage organs of plants. Proc. Natl. Acad. Sci. U. S. A. 104, 19210–19213.

Hernández Fernández, M., Álvarez Sierra, M.Á., Peláez-Campomanes, P., 2007. Bioclimatic analysis of rodent palaeofaunas reveals severe climatic changes in Southwestern Europe during the Plio-Pleistocene. Palaeogeogr. Palaeoclimatol. Palaeoecol. 251, 500–526.

Hernández Fernández, M., Vrba, E.S., 2006. Plio-Pleistocene climatic change in the Turkana Basin (East Africa): Evidence from large mammal faunas. J. Hum. Evol. 50, 595–626.

Hill, A., Leakey, M., Kingston, J.D., Ward, S., 2002. New cercopithecoids and a hominoid from 12·5 Ma in the Tugen Hills succession, Kenya. J. Hum. Evol. 42, 75–93.

Hill, D.A., 1997. Seasonal variation in the feeding behavior and diet of Japanese macaques (*Macaca fuscata yakui*) in lowland forest of Yakushima. Am. J. Primatol. 43, 305–320.

Hill, R.A., Barrett, L., Gaynor, D., Weingrill, T., Dixon, P., Payne, H., Henzi, S.P., 2003. Day length, latitude and behavioural (in)flexibility in baboons (*Papio cynocephalus ursinus*). Behav. Ecol. Sociobiol. 53, 278–286.

Hill, R.A., Dunbar, R.I.M., 1998. An evaluation of the roles of predation rate and predation risk as selective pressures on primate grouping behaviour. Behaviour. 135, 411–430.

Hill, R.A., Dunbar, R.I.M., 2002. Climatic determinants of diet and foraging behaviour in baboons. Evol. Ecol. 16, 579–593.

Hladik, C.M., 1977. Chimpanzees of Gabon and Chimpanzees of Gombe: some Comparative Data on the Diet. In: Clutton-Brock, T.H. (Ed.), Primate Ecology: Studies of Feeding and Ranging Behavior in Lemurs, Monkey and Apes. Academic Press, London, pp. 481–501.

Hladik, C.M., 1978. Adaptive strategies of primates in relation to leaf eating. Ecol. Arboreal

Ψηφιακή βιβλιοθήκη Θεόφραστος – Τμήμα Γεωλογίας – Αριστοτέλειο Πανεπιστήμιο Θεσσαλονίκης

Ψηφιακή συλλογή
Βιβλιοθήκη
"ΘΕΟΦΡΑΣΤΟΣ"
Τμήμα Γεωλογίας
Α.Π.Θ

Folivores. 373–395.

Hlusko, L.J., 2006. A new large Pliocene colobine species (Mammalia: Primates) from Asa Issie, Ethiopia. Geobios. 39, 57–69.

Hlusko, L.J., 2007. a New Late Miocene Species of Paracolobus and Other Cercopithecoidea (Mammalia: Primates) Fossils From Lemudong'O, Kenya. Kirtlandia. December, 72–85.

Hlusko, L.J., Suwa, G., Kono, R.T., Mahaney, M.C., 2004. Genetics and the evolution of primate enamel thickness: A baboon model. Am. J. Phys. Anthropol. 124, 223–233.

Hockings, K.J., Anderson, J.R., Matsuzawa, T., 2010. Flexible feeding on cultivated underground storage organs by rainforest-dwelling chimpanzees at Bossou, West Africa. J. Hum. Evol. 58, 227–233.

Hoffman, J.M., Fraser, D., Clementz, M.T., 2015. Controlled feeding trials with ungulates: a newapplication of in vivo dental molding to assess the abrasive factors of microwear. J. Exp. Biol. 218, 1538–1547.

Hojo, T., 1991a. Scanning electron microscopic analysis of dental wear on the heavily worn second molars of the wild Japanese monkey (*Macaca fuscata*). Scanning Microsc. 5, 505–508.

Hojo, T., 1991b. SEM study of microwear on the teeth of Japanese monkeys and Japanese people. Primatol. Today. Ehara, A.(ed.). Elsevier Sci. 1991a. 551–554.

Holt, R.D., 2009. Bringing the Hutchinsonian niche into the 21st century: Ecological and evolutionary perspectives. Proc. Natl. Acad. Sci. U. S. A. 106, 19659–19665.

Homewood, K.M., 1978. Feeding strategy of the Tana mangabey (*Cercocebus galeritus galeritus*) (Mammalia: Primates). J. Zool. 186, 375–391.

Hopley, P.J., Latham, A.G., Marshall, J.D., 2006. Palaeoenvironments and palaeodiets of mid-Pliocene micromammals from Makapansgat Limeworks, South Africa: A stable isotope and dental microwear approach. Palaeogeogr. Palaeoclimatol. Palaeoecol. 233, 235–251.

Horn, A.D., 1987. The socioecology of the Black Mangabey (*Cercocebus aterrimus*) Near Lake Tumba, Zaire. Am. J. Primatol. 12, 165–180.

Hoshino, J., 1985. Feeding ecology of mandrills (*Mandrillus sphinx*) in campo animal reserve, Cameroon. Primates. 26, 248–273.

Hoyle, T.M., Leroy, S.A.G., López-Merino, L., Miggins, D.P., Koppers, A.A.P., 2020. Vegetation succession and climate change across the Plio-Pleistocene transition in eastern Azerbaijan, central Eurasia (2.77–2.45 Ma). Palaeogeogr. Palaeoclimatol. Palaeoecol. 538.

Ψηφιακή βιβλιοθήκη Θεόφραστος – Τμήμα Γεωλογίας – Αριστοτέλειο Πανεπιστήμιο Θεσσαλονίκης

Ψηφιακή συλλογή
Βιβλιοθήκη
"ΘΕΟΦΡΑΣΤΟΣ"

Hrdy, S.B., 1974. Male-male competition and infanticide among the langurs (*Presbytis entellus*) of Abu, Rajasthan. Folia Primatol. 22, 19–58.

Hsü, K.J., Ryan, W.B.F., Cita, M.B., 1973. Late miocene desiccation of the mediterranean. Nature. 242, 240–244.

Hughes, J.K., Elton, S., O'Regan, H.J., 2008. Theropithecus and "Out of Africa" dispersal in the Plio-Pleistocene. J. Hum. Evol. 54, 43–77.

Huntley, J.W., Yanes, Y., Kowalewski, M., Castillo, C., Delgado-Huertas, A., Ibáñez, M., Alonso, M.R., Ortiz, J.E., de Torres, T., 2008. Testing limiting similarity in Quaternary terrestrial gastropods. Paleobiology. 34, 378–388.

Hutchinson, G.E., 1959. Homage to Santa Rosalia or Why Are There So Many Kinds of Animals? Am. Nat. 93, 145–159.

Hylander, W.L., 1975. Incisor size and diet in anthropoids with special reference to cercopithecidae. Science (80-.). 189, 1095–1098.

Iguchi, M., Izawa, K., 1990. Digging and eating of underground plant-parts by wild Japanese monkeys (*Macaca fuscata*). Primates. 31, 621–624.

Ingicco, T., 2008. Analyse morphofonctionnelle des os longs de deux colobes fossiles: *Mesopithecus* et *Dolichopithecus*. Sez. di Museol. Sci. e Nat. 3, 1–7.

Isbell, L.A., 1990. Sudden short-term increase in mortality of vervet monkeys (*Cercopithecus aethiops*) due to leopard predation in Amboseli National Park, Kenya. Am. J. Primatol. 21, 41–52.

Isbell, L.A., 1998a. Diet for a small primate: insectivory and gummivory in the (large) patas monkey (*Erythrocebus patas pyrrhonotus*). Am. J. Primatol. 45, 381–398.

Isbell, L.A., Young, T.P., 2007. Interspecific and Temporal Variation of Ant Species Within Acacia drepanolobium Ant Domatia, a Staple Food of Patas Monkeys (*Erythrocebus patas*) in Laikipia, Kenya. Am. J. Primatol. 69, 1387–1398.

Iwamoto, M., Hasegawa, Y., Koizumi, A., 2005. A Pliocene colobine from the Nakatsu Group, Kanagawa, Japan. Anthropol. Sci. 113, 123–137.

Iwamoto, T., 1979. Ecological and sociological studies of gelada baboons. Feeding ecology.

Iwamoto, T., 1993. The ecology of *Theropithecus gelada*. In: Jablonsky N., (Eds.). *Theropithecus*: The rise and fall of a primate genus. Cambridge University Press.

Ψηφιακή βιβλιοθήκη Θεόφραστος – Τμήμα Γεωλογίας – Αριστοτέλειο Πανεπιστήμιο Θεσσαλονίκης

Ψηφιακή συλλογή
Βιβλιοθήκη
"ΘΕΟΦΡΑΣΤΟΣ"

Jablonski, N.G., 1993. Quaternary environments and the evolution of primates in East Asia, with notes on two new specimens of fossil Cercopithecidae from China. folia. +0, 118–132.

Jablonski, Nina G., 1998. The response of catarrhine primates to Pleistocene environmental fluctuations in East Asia. Primates. 39, 29–37.

Jablonski, N. G., 1998. The Evolution of the Doucs and Snub-nosed Monkeys and the Question of the Phyletic Unity of the Odd-nosed Colobines. In: Jablonski, N.G. (Ed.), The Natural History of the Doucs and Snub-Nosed Monkeys. World Scientific Publishing, Singapore, pp. 13–52.

Jablonski, N.G., 2002. Fossil Old World monkeys: the late Neogene radiation. In: Hartwig, E.C. (Ed.), The Primate Fossil Record. Cambridge University Press, pp. 255–299.

Jablonski, N.G., 2005. *Theropithecus*: the rise and fall of a primate genus. Cambridge University Press.

Jablonski, N.G., Frost, S.R., 2010. Cercopithecoidea. In: Werdelin, L., Sanders, W.J. (Eds.), Cenozoic Mammals of Africa. University of California Press, pp. 393–428.

Jablonski, N.G., Ji, X., Kelley, J., Flynn, L.J., Deng, C., Su, D.F., 2020. *Mesopithecus pentelicus* from Zhaotong, China, the easternmost representative of a widespread Miocene cercopithecoid species. J. Hum. Evol. 146, 102851.

Jablonski, N.G., Leakey, M.G., Kiarie, C., Antón, M., 2002. A new skeleton of *Theropithecus brumpti* (Primates: Cercopithecidae) from Lomekwi, West Turkana, Kenya. J. Hum. Evol. 43, 887–923.

Jablonski, N.G., Whitfort, M.J., Roberts-Smith, N., Qinqi, X., 2000. The influence of life history and diet on the distribution of catarrhine primates during the Pleistocene in eastern Asia. J. Hum. Evol. 39, 131–157.

Jarvey, J.C., 2016. The importance of underground foods in female gelada (*Theropithecus gelada*) socioecology. J. Chem. Inf. Model.

Jarvey, J.C., Low, B.S., Pappano, D.J., Bergman, T.J., Beehner, J.C., 2018. Graminivory and Fallback Foods: Annual Diet Profile of Geladas (*Theropithecus gelada*) Living in the Simien Mountains National Park, Ethiopia. Int. J. Primatol. 39, 105–126.

Jernvall, J., Selänne, L., 1999. Laser confocal microscopy and geographic information systems in the study of dental morphology. Palaeontol. Electron. 1–17.

Ji, X., Youlatos, D., Jablonski, N.G., Pan, R., Zhang, C., Li, P., Tang, M., Yu, T., Li, W., Deng, C., Li, S., 2020. Oldest colobine calcaneus from East Asia (Zhaotong, Yunnan, China). J. Hum. Evol. 147, 102866.

Ψηφιακή βιβλιοθήκη Θεόφραστος – Τμήμα Γεωλογίας – Αριστοτέλειο Πανεπιστήμιο Θεσσαλονίκης

Ψηφιακή συλλογή
Βιβλιοθήκη
"ΘΕΟΦΡΑΣΤΟΣ"

Jiménez-Moreno, G., Burjachs, F., Expósito, I., Oms, O., Carrancho, Á., Villalaín, J.J., Agustí, J., Campeny, G., Gómez de Soler, B., van der Made, J., 2013. Late Pliocene vegetation and orbital-scale climate changes from the western Mediterranean area. Glob. Planet. Change. 108, 15–28.

Jiménez-Moreno, G., Fauquette, S., Suc, J.P., 2010. Miocene to Pliocene vegetation reconstruction and climate estimates in the Iberian Peninsula from pollen data. Rev. Palaeobot. Palynol. 162, 403–415.

Jiménez-Moreno, G., Suc, J.P., 2007. Middle Miocene latitudinal climatic gradient in Western Europe: Evidence from pollen records. Palaeogeogr. Palaeoclimatol. Palaeoecol. 253, 208–225.

Johnson, C., Swedell, L., Rothman, J., 2012. Feeding ecology of olive baboons (*Papio anubis*) in Kibale National Park, Uganda: preliminary results on diet and food selection. Afr. J. Ecol. 50, 367–370.

Jolly, C.J., 1967. The evolution of baboons. In: Vagtborg, H. (Ed.), The Baboon in Medical Research. Univ Texas Press, pp. 23–50.

Jolly, C.J., 1970. The large African monkeys as an adaptive array. In: Napier, J.R., Napier, P.H. (Eds.), Old World Monkeys. Academic Press, New York, pp. 139–174.

Justa, P., Kumar, R.S., Talukdar, G., Sinha, A., 2019. Sharing from the Same Bowl: Resource Partitioning between Sympatric Macaque Species in the Western Himalaya, India. Int. J. Primatol. 40, 356–373.

Kahlke, R.D., García, N., Kostopoulos, D.S., Lacombat, F., Lister, A.M., Mazza, P.P.A., Spassov, N., Titov, V. V., 2011. Western Palaearctic palaeoenvironmental conditions during the Early and early Middle Pleistocene inferred from large mammal communities, and implications for hominin dispersal in Europe. Quat. Sci. Rev. 30, 1368–1395.

Kalmykov, N.P., 1992. Biostratigraphy and fauna of the Transbaikalian Pliocene mammals.

Kane, E.E., McGraw, W.S., 2018. Dietary Variation in Diana Monkeys (*Cercopithecus diana*): The Effects of Polyspecific Associations. Folia Primatol. 88, 455–482.

Kato, A., Tang, N., Borries, C., Papakyrikos, A.M., Hinde, K., Miller, E., Kunimatsu, Y., Hirasaki, E., Shimizu, D., Smith, T.M., 2014. Intra- and interspecific variation in Macaque molar enamel thickness. Am. J. Phys. Anthropol. 155, 447–459.

Katsvanga, C.A.T., Jimu, L., Zinner, D., Mupangwa, J.F., 2009. Diet of pine plantation and non-plantation ranging baboon (*Papio ursinus*) groups with reference to bark consumption in the eastern highlands of Zimbabwe. J. Hortic. For. 1, 168–175.

Ψηφιακή βιβλιοθήκη Θεόφραστος – Τμήμα Γεωλογίας – Αριστοτέλειο Πανεπιστήμιο Θεσσαλονίκης

Ψηφιακή συλλογή
Βιβλιοθήκη
"ΘΕΟΦΡΑΣΤΟΣ"

Kavanagh, M., 1978. The Diet and Feeding Behaviour of *Cercopithecus aethiops tantalus*. Folia Primatol. 30, 30–63.

Kay, R.., Covert, H.H., 1984. Anatomy and behaviour of extinct primates. In: Chivers, D.J., Wood, B.A., Bilsborough, A. (Eds.), Food Acquisition and Processing in Primates. Plenum Press, New York, pp. 467–508.

Kay, R.F., 1975. The functional adaptations of primate molar teeth. Am. J. Phys. Anthropol. 43, 195–215.

Kay, R.F., 1977. The evolution of molar occlusion in the Cercopithecidae and early catarrhines. Am. J. Phys. Anthropol. 46, 327–352.

Kay, R.F., 1978. Molar structure and diet in extant cercopithecidae. In: Butler, P.M., Joysey, K.A. (Eds.), Development, Function and Evolution of Teeth. Academic Press, London, pp. 309–340.

Kay, R.F., 1981. The Nut-crackers- a new theory of the adaptations of the ramapithecinae. Am. J. Phys. Anthropol. 55, 141–151.

Kay, R.F., Hiiemae, K.M., 1974. Jaw movement and tooth use in recent and fossil primates. Am. J. Phys. Anthropol. 40, 227–256.

Kay, R.F., Sheine, W.S., 1979. On the relationship between chitin particle size and digestibility in the primate Galago senegalensis. Am. J. Phys. Anthropol. 50, 301–308.

Kelley, J., 1990. Incisor Microwear and diet in Three species of *Colobus*. J. Vis. Lang. Comput. 73–84.

Kelley, J.L., Swanson, W.J., 2008. Dietary change and adaptive evolution of enamelin in humans and among primates. Genetics. 178, 1595–1603.

Kennedy, F.E., Brown, C.A., Kolodny, J., Sheldon, B.M., 1999. Fractal analysis of hard disk surface roughness and correlation with static and low-speed friction.

Khan, M.A., Kelley, J., Flynn, L.J., Babar, M.A., Jablonski, N.G., 2020. New fossils of Mesopithecus from Hasnot, Pakistan. J. Hum. Evol. 145, 102818.

Kibaja, M., 2014. Diet of the ashy red colobus (*Piliocolobus tephrosceles*) and crop-raiding in a Forest-Farm Mosaic, Mbuzi, Rukwa Region, Tanzania. Primate Conserv. 28, 109–116.

Kilgore, L., 1989. Dental pathologies in ten free-ranging chimpanzees from Gombe National Park, Tanzania. Am. J. Phys. Anthropol. 80, 219–227.

Ψηφιακή βιβλιοθήκη Θεόφραστος – Τμήμα Γεωλογίας – Αριστοτέλειο Πανεπιστήμιο Θεσσαλονίκης

Ψηφιακή συλλογή
Βιβλιοθήκη
"ΘΕΟΦΡΑΣΤΟΣ"

King, S.J., Arrigo-Nelson, S.J., Pochron, S.T., Semprebon, G.M., Godfrey, L.R., Wright, P.C., Jernvall, J., 2005. Dental senescence in a long-lived primate links infant survival to rainfall. Proc. Natl. Acad. Sci. U. S. A. 102, 16579–16583.

King, T., Aiello, L.C., Andrews, P., 1999. Dental microwear of *Griphopithecus alpani*. J. Hum. Evol. 36, 3–31.

Kirk, E.C., Simons, E.L., 2001. Diets fo fossil primates from the fayum depression of Egypt: A quantitative analysis of molar shearing. J. Hum. Evol. 40, 203–229.

Klette, R., Rosenfeld, A., 2004. Digital Geometry: Geometric Methods for Digital Picture Analysis. Digit. Geom. Geom. Methods Digit. Pict. Anal. 1–656.

Klukkert, Z.S., Dennis, J.C., M'Kirera, F., Ungar, P.S., 2012a. Dental topographic analysis of the molar teeth of primates. In: Methods in Molecular Biology (Clifton, N.J.). pp. 145–152.

Klukkert, Z.S., Teaford, M.F., Ungar, P.S., 2012b. A dental topographic analysis of chimpanzees. Am. J. Phys. Anthropol. 148, 276–284.

Köhler, M., Moyà-Solà, S., 2004. Reduction of Brain and Sense Organs in the Fossil Insular Bovid Myotragus. Brain. Behav. Evol. 63, 125–140.

Köhler, M., Moyà-Solà, S., Alba, D.M., 2000. *Macaca* (Primates, Cercopithecidae) from the late miocene of Spain. J. Hum. Evol. 38, 447–452.

Kono, R.T., 2004. Molar enamel thickness and distribution patterns in extant great apes and humans: New insights based on a 3-dimensional whole crown perspective. Anthropol. Sci. 112, 121–146.

Kono, R.T., Suwa, G., 2008. Enamel distribution patterns of extant human and hominoid molars: Occlusal versus lateral enamel thickness. Bull Natl Mus Nat Sci D. 34, 1–9.

Kool, K.M., 1992. Food selection by the silver leaf monkey, *Trachypithecus auratus sondaicus*, in relation to plant chemistry. Oecologia. 90, 527–533.

Kool, K.M., 1993. The diet and feeding behavior of the silver leaf monkey (*Trachypithecus auratus sondaicus*) in Indonesia. Int. J. Primatol. 14, 667–700.

Kopp, G.H., Roos, C., Butynski, T.M., Wildman, D.E., Alagaili, A.N., Groeneveld, L.F., Zinner, D., 2014. Out of Africa, but how and when? The case of hamadryas baboons (*Papio hamadryas*). J. Hum. Evol. 76, 154–164.

Kortlandt, A., Holzhaus, E., 1987. New data on the use of stone tools by chimpanzees in Guinea and Liberia. Primates. 28, 473–496.

Ψηφιακή βιβλιοθήκη Θεόφραστος – Τμήμα Γεωλογίας – Αριστοτέλειο Πανεπιστήμιο Θεσσαλονίκης

Ψηφιακή συλλογή
Βιβλιοθήκη
"ΘΕΟΦΡΑΣΤΟΣ"

Kostopoulos, D.S., 2009. The Pikermian Event: Temporal and spatial resolution of the Turolian large mammal fauna in SE Europe. Palaeogeogr. Palaeoclimatol. Palaeoecol. 274, 82–95.

Kostopoulos, D.S., Guy, F., Kynigopoulou, Z., Koufos, G.D., Valentin, X., Merceron, G., 2018. A 2Ma old baboon-like monkey from Northern Greece and new evidence to support the Paradolichopithecus – Procynocephalus synonymy (Primates: Cercopithecidae). J. Hum. Evol. 121, 178–192.

Kostopoulos, D.S., Palombo, M.R., Alberdi, M.T., Valli, A.M.F., 2007. Pliocene to Pleistocene large mammal diversity and turnover in North Mediterranean region: The Greek Peninsula with respect to the Iberian and Italian ones. Geodiversitas. 29, 401–419.

Koufos, George D., 2009a. The genus *Mesopithecus* (Primates, Cercopithecidae) in the late Miocene of Greece. Boll. della Soc. Paleontol. Ital. 48, 157–166.

Koufos, G. D., 2009. The Neogene cercopithecids (Mammalia, Primates) of Greece. Geodiversitas. 31, 817–850.

Koufos, George D., 2009b. The Neogene cercopithecids (Mammalia, Primates) of Greece. Geodiversitas. 31, 817–850.

Koufos, G.D., 2016. Primates. Geobios. 49, 45–51.

Koufos, G.D., 2019a. Late Turolian Mesopithecus (Mammalia: Cercopithecidae) from Axios Valley (Macedonia, Greece): earliest presence of M. monspessulanus in Europe. Comptes Rendus - Palevol. 18, 1057–1072.

Koufos, G.D., 2019b. First evidence of *Mesopithecus monspessulanus* (Mammalia : Cercopithecidae) in the Late Miocene of Macedonia , Greece.

Koufos, G.D., Spassov, N., Kovatchev, D., 2003. Study of *Mesopithecus* (Primates, Cercopithecidae) from the late Miocene of Bulgaria. In: Palaeontographica Abteilunga. pp. 39–91.

Koufos, G.D., Syrides, G.E., Kalliopi, K., 1991. A Pliocene primate from Macedonia (Greece). J. Hum. Evol. 21, 283–294.

Koufos, G.D., Vasileiadou, K., 2015. Miocene/Pliocene mammal faunas of southern Balkans: implications for biostratigraphy and palaeoecology. Palaeobiodiversity and Palaeoenvironments. 95, 285–303.

Kovar-Eder, J., Kvaček, Z., Martinetto, E., Roiron, P., 2006. Late Miocene to Early Pliocene vegetation of southern Europe (7-4 Ma) as reflected in the megafossil plant record. Palaeogeogr. Palaeoclimatol. Palaeoecol. 238, 321–339.

Ψηφιακή βιβλιοθήκη Θεόφραστος – Τμήμα Γεωλογίας – Αριστοτέλειο Πανεπιστήμιο Θεσσαλονίκης

Ψηφιακή συλλογή
Βιβλιοθήκη
"ΘΕΟΦΡΑΣΤΟΣ"
Α.Π.Θ

Krebs, J.R., Davies, N.B., 2009. An Introduction to Behavioural Ecology.

Krishnamani, R., 1994. Diet composition of the bonnet macaque (*Macaca radiata*) in a tropical dry evergreen forest of southern India. Trop. Biodivers. 2, 285–302.

Krueger, K.L., Scott, J.R., Kay, R.F., Ungar, P.S., 2008. Technical note: Dental microwear textures of "Phase I" and "Phase II" facets. Am. J. Phys. Anthropol. 137, 485–490.

Kumar, S., Hedges, S.B., 1998. A molecular timescale for vertebrate evolution. Nature. 392, 917–920.

Kunz, B.K., Linsenmair, K.E., 2007. Changes in baboon feeding behavior: Maturity-dependent fruit and seed size selection within a food plant species. Int. J. Primatol. 28, 819–835.

Kunz, B.K., Linsenmair, K.E., 2010. Fruit Traits in Baboon Diet: A Comparison with Plant Species Characteristics in West Africa. Biotropica. 42, 363–371.

Kupczik, K., Chattah, N.L.T., 2014. The adaptive significance of enamel loss in the mandibular incisors of cercopithecine primates (Mammalia: Cercopithecidae): A finite element modelling study. PLoS One. 9, 1–8.

Lahm, S.A., 1986. Diet and Habitat Preference of Mandrillus sphinx in Gabon: Implications for foraging strategy. Am. J. Primatol. 26, 9–26.

Laird, M.F., Kozma, E.E., Kwekason, A., Harrison, T., 2018. A new fossil cercopithecid tibia from Laetoli and its implications for positional behavior and paleoecology. J. Hum. Evol. 118, 27–42.

Lambert, J.E., 1998. Primate digestion: Interactions among anatomy, physiology, and feeding ecology. Evol. Anthropol. 7, 8–20.

Lambert, J.E., 2009. Summary to the symposium issue: Primate fallback strategies as adaptive phenotypic plasticity-scale, pattern, and process. Am. J. Phys. Anthropol. 140, 759–766.

Lambert, J.E., Chapman, C.A., Wrangham, R.W., Conklin-Brittain, N. Lou, 2004. Hardness of cercopithecine foods: Implications for the critical function of enamel thickness in exploiting fallback foods. Am. J. Phys. Anthropol. 125, 363–368.

Landen, G., Wrangham, R., 2005. The rise of the hominids as an adaptive shift in fallback foods: Plant underground storage organs (USOs) and australopith origins. J. Hum. Evol. 49, 482–498.

Lanjouw, A., 2002. Behavioural adaptations to water scarcity in Tongo chimpanzees. In: Behavioural Diversity in Chimpanzees and Bonobos. Cambridge University Press., pp. 52–

Ψηφιακή βιβλιοθήκη Θεόφραστος – Τμήμα Γεωλογίας – Αριστοτέλειο Πανεπιστήμιο Θεσσαλονίκης

Ψηφιακή συλλογή
Βιβλιοθήκη
"ΘΕΟΦΡΑΣΤΟΣ"
Τμήμα Γεωλογίας
Α.Π.Θ

60.

Lawrence, K.T., Sosdian, S., White, H.E., Rosenthal, Y., 2010. North Atlantic climate evolution through the Plio-Pleistocene climate transitions. Earth Planet. Sci. Lett. 300, 329–342.

Lazagabaster, I.A., 2019. Dental microwear texture analysis of Pliocene Suidae from Hadar and Kanapoi in the context of early hominin dietary breadth expansion. J. Hum. Evol. 132, 80–100.

Lazzari, V., Charles, C., Tafforeau, P., Vianey-Liaud, M., Aguilar, J.P., Jaeger, J.J., Michaux, J., Viriot, L., 2008a. Mosaic convergence of rodent dentitions. PLoS One. 3.

Lazzari, V., Guy, F., 2014. Application quantitative de la topographie tridimensionnelle de la morphologie dentaire à la taxonomie des catarrhiniens. Bull. Mem. Soc. Anthropol. Paris. 26, 140–146.

Lazzari, V., Tafforeau, P., Aguilar, J.-P., Michaux, J., 2008b. Topographic maps applied to comparative molar morphology: the case of murine and cricetine dental plans (Rodentia, Muroidea). Paleobiology. 34, 46–64.

Leakey, M.G., 1982. Extinct large colobines from the Plio-Pleistocene of Africa. Am. J. Phys. Anthropol. 58, 153–172.

Leakey, M.G., Teaford, M.F., Ward, C.V., 2003. Cercopithecidae from lothagam. In: Leakey, M.G., Harris, J.M. (Eds.), Lothagam: The Dawn of Humanity in Eastern Africa. Columbia University Press, New York, pp. 201–235.

Ledogar, J.A., Winchester, J.M., St. Clair, E.M., Boyer, D.M., 2013. Diet and dental topography in pitheciine seed predators. Am. J. Phys. Anthropol. 150, 107–121.

Lee-Thorp, J.A., Manning, L., Sponheimer, M., 1997. Exploring Problems and Opportunities Offered By Down-Scaling Sample Sizes for Carbon Isotope Analyses of Fossils. Bull. la Soc. Geol. Fr. 168, 767–773.

Leonard, W.R., Robertson, M.L., 1994. Evolutionary perspectives on human nutrition: The influence of brain and body size on diet and metabolism. Am. J. Hum. Biol. 6, 77–88.

Levina, N.E., Haile-Selassieb, Y., Frostc, S.R., Saylord, B.Z., 2015. Dietary change among hominins and cercopithecids in Ethiopia during the early Pliocene. Proc. Natl. Acad. Sci. U. S. A. 112, 12304–12309.

Lucas, P., Constantino, P., Wood, B., Lawn, B., 2008. Dental enamel as a dietary indicator in mammals. BioEssays. 30, 374–385.

Ψηφιακή βιβλιοθήκη Θεόφραστος – Τμήμα Γεωλογίας – Αριστοτέλειο Πανεπιστήμιο Θεσσαλονίκης

Ψηφιακή συλλογή
Βιβλιοθήκη
"ΘΕΟΦΡΑΣΤΟΣ"

Lucas, P.W., Omar, R., Al-Fadhalah, K., Almusallam, A.S., Henry, A.G., Michael, S., Thai, L.A., Watzke, J., Strait, D.S., Atkins, A.G., 2013. Mechanisms and causes of wear in tooth enamel: Implications for hominin diets. J. R. Soc. Interface. 10.

Lussi, A., Jaeggi, T., 2006. Chemical factors., Monographs in oral science.

Lyras, G., Van Der Geer, A.A.E., 2006. Adaptations of the Pleistocene island canid Cynotherium sardous (Sardinia, Italy) for hunting small prey. Cranium. 23, 51–60.

Lyras, G.A., Van Der Geer, A.A.E., 2007. The Late Pliocene vertebrate fauna of Vatera (Lesvos Island, Greece). Cranium. 24, 11–24.

M'Kirera, F., Ungar, P.S., 2003. Occlusal relief changes with molar wear in Pan troglodytes troglodytes and *Gorilla gorilla gorilla*. Am. J. Primatol. 60, 31–41.

Maas, M.C., 1991. Enamel structure and microwear: An experimental study of the response of enamel to shearing force. Am. J. Phys. Anthropol. 85, 31–49.

MacArthur, R., Levins, R., 1967. The limiting similarity hypothesis. Am. Nat. 101, 377–385.

Macharia, A.N., Cerling, T.E., Jorgensen, M.J., Kaplan, J.R., 2014. The hair-diet 13C and 15N fractionation in *Chlorocebus aethiops sabaeus* based on a control diet study. Ann. Zool. Fennici. 51, 66–72.

Macho, G.A., 1994. Variation in enamel thickness and cusp area within human maxillary molars and its bearing on scaling techniques used for studies of enamel thickness between species. Arch. Oral Biol. 39, 783–792.

Macho, G.A., 2016. Niche Partitioning. In: Fuentes, A. (Eds.), The International Encyclopedia of Primatology. John Wiley and Sons, Inc, pp. 1–4.

MacKinnon, J.R., MacKinnon, K.S., 1980. Niche Differentiation in a Primate Community. Malayan For. Primates. 167–190.

Madden, R.H., 2014. Hypsodonty in mammals: Evolution, Geomorphology, and the Role of Earth Surface Processes. Cambridge University Press, New York.

Madurell-Malapeira, J., Minwer-Barakat, R., Alba, D.M., Garcés, M., Gómez, M., Aurell-Garrido, J., Ros-Montoya, S., Moyà-Solà, S., Berástegui, X., 2010. The Vallparadís section (Terrassa, Iberian Peninsula) and the latest Villafranchian faunas of Europe. Quat. Sci. Rev. 29, 3972–3982.

Madurell-Malapeira, J., Palombo, M.R., Sotnikova, M., 2015. *Cynotherium malatestai*, sp. Nov. (Carnivora, Canidae) from the early middle Pleistocene deposits of Grotta dei Fiori (Sardinia,

Ψηφιακή βιβλιοθήκη Θεόφραστος – Τμήμα Γεωλογίας – Αριστοτέλειο Πανεπιστήμιο Θεσσαλονίκης

Ψηφιακή συλλογή
Βιβλιοθήκη
"ΘΕΟΦΡΑΣΤΟΣ"
Τμήμα Γεωλογίας
Α.Π.Θ

Western Mediterranean). J. Vertebr. Paleontol. 35.

Madurell-Malapeira, J., Ros-Montoya, S., Espigares, M.P., Alba, D.M., Aurell-Garrido, J.A., 2014. Villafranchian large mammals from the Iberian Peninsula: paleobiogeography, paleoecology and dispersal events. J. Iber. Geol. 40, 167–178.

Maibeche, Y., Moali, A., Yahi, N., Menard, N., 2015. Is diet flexibility an adaptive life trait for relictual and peri-urban populations of the endangered primate Macaca sylvanus? PLoS One. 10, 1–22.

Maier, W., 1977. Die evolution der bilophodonten molaren der Cercopithecoidea: eine funktionsmorphologische untersuchung. Z. Morphol. Anthropol. 26–56.

Marigó, J., Susanna, I., Minwer-Barakat, R., Madurell-Malapeira, J., Moyà-Solà, S., Casanovas-Vilar, I., Robles, J.M., Alba, D.M., 2014. The primate fossil record in the Iberian Peninsula. J. Iber. Geol. 40, 179–211.

Marsh, C.W., 1981. Diet Choice among Red *Colobus* (*Colobus badius rufomitratus*) on Tanariver, Kenya. Folia Primatol. 35, 147–178.

Marshall, A.J., Wrangham, R.W., 2007. Evolutionary consequences of fallback foods. Int. J. Primatol. 28, 1219–1235.

Martin, F., Plastiras, C.-A., Merceron, G., Souron, A., Boisserie, J.-R., 2018. Dietary niches of terrestrial cercopithecines from the Plio-Pleistocene Shungura Formation, Ethiopia: evidence from Dental Microwear Texture Analysis. Sci. Rep. 8.

Martin, L., 1985. Significance of enamel thickness in hominoid evolution. Nature. 314, 260–263.

Martin, L.B., 1983. The relationships of the later Miocene Hominoidea. University College London.

Martin, L.B., 1985. Significance of enamel thickness in hominoid evolution. Nature. 314, 260–263.

Martin, L.B., Olejniczak, A.J., Maas, M.C., 2003. Enamel thickness and microstructure in pitheciin primates, with comments on dietary adaptations of the middle Miocene hominoid Kenyapithecus. J. Hum. Evol. 45, 351–367.

Martínez-Freiría, F., Freitas, I., Zuffi, M.A.L., Golay, P., Ursenbacher, S., Velo-Antón, G., 2020. Climatic refugia boosted allopatric diversification in Western Mediterranean vipers. J. Biogeogr. 47, 1698–1713.

Martínez-Navarro, B., 2010. Early Pleistocene Faunas of Eurasia and Hominin Dispersals. Vertebr. Paleobiol. Paleoanthropology. 207–224.

Ψηφιακή βιβλιοθήκη Θεόφραστος – Τμήμα Γεωλογίας – Αριστοτέλειο Πανεπιστήμιο Θεσσαλονίκης

Ψηφιακή συλλογή
Βιβλιοθήκη
"ΘΕΟΦΡΑΣΤΟΣ"

Martínez, L.M., Estebaranz-Sánchez, F., Ferràndez-Cañadell, C., Romero, A., Ribot, F., Galbany, J., Gibert, L., Pérez-Pérez, A., 2020. Buccal dental-microwear and feeding ecology of Early Pleistocene *Theropithecus oswaldi* from Cueva Victoria (Spain). J. Hum. Evol. 142.

Martínez, L.M., Estebaranz-Sánchez, F., Galbany, J., Pérez-Pérez, A., 2016. Testing dietary hypotheses of east African hominines using buccal dental microwear data. PLoS One. 11, 1–26.

Maruhashi, T., 1980. Feeding behavior and diet of the Japanese monkey (*Macaca fuscata yakui*) on Yakushima Island, Japan. Primates. 21, 141–160.

Maschenko, E.N., 1991. Tooth system and taxonomic status of early Pliocene cercopithecid monkey *Dolichopithecus hipsulophus* (Primates, Cercopithecidae). Biol. Moscow Ov. Ist. Prir. Geol. 66, 61–74.

Maschenko, E.N., 2005. Cenozoic Primates of eastern Eurasia (Russia and adjacent areas). Anthropol. Sci. 113, 103–115.

Maschenko, E.N., Baryshnikov, G.F., 2002. The taxonomic status of a macaque (Primates, Cercopithecidae) from the Middle Pleistocene of Georgia. Paleontol. J. 36, 403–413.

Matsuda, I., Chapman, C.A., Clauss, M., 2019. Colobine forestomach anatomy and diet. J. Morphol. 280, 1608–1616.

Matsuda, I., Clauss, M., Tuuga, A., Sugau, J., Hanya, G., Yumoto, T., Bernard, H., Hummel, J., 2017. Factors Affecting Leaf Selection by Foregut-fermenting Proboscis Monkeys: New Insight from in vitro Digestibility and Toughness of Leaves. Sci. Rep. 7, 1–10.

Matsuda, I., Tuuga, A., Higashi, S., 2009. The feeding ecology and activity budget of proboscis monkeys. Am. J. Primatol. 71, 478–492.

Matthews, J.K., Ridley, A., Niyigaba, P., Kaplin, B.A., Grueter, C.C., 2019. Chimpanzee feeding ecology and fallback food use in the montane forest of Nyungwe National Park, Rwanda. Am. J. Primatol. 81, 1–15.

McGraw, W.S., 2017. Mangabeys (*Cercocebus* and *Lophocebus*) . Int. Encycl. Primatol. 1–3.

McGraw, W.S., Pampush, J.D., Daegling, D.J., 2012. Brief communication: Enamel thickness and durophagy in mangabeys revisited. Am. J. Phys. Anthropol. 147, 326–333.

McGraw, W.S., van Casteren, A., Kane, E., Geissler, E., Burrows, B., Daegling, D.J., 2016. Feeding and oral processing behaviors of two colobine monkeys in Tai Forest, Ivory Coast. J. Hum. Evol. 98, 90–102.

Ψηφιακή βιβλιοθήκη Θεόφραστος – Τμήμα Γεωλογίας – Αριστοτέλειο Πανεπιστήμιο Θεσσαλονίκης

Ψηφιακή συλλογή
Βιβλιοθήκη
"ΘΕΟΦΡΑΣΤΟΣ"

McGraw, W.S., Vick, A.E., Daegling, D.J., 2011. Sex and age differences in the diet and ingestive behaviors of sooty mangabeys (*Cercocebus atys*) in the Tai forest, Ivory coast. Am. J. Phys. Anthropol. 144, 140–153.

McGraw, W.S., Vick, A.E., Daegling, D.J., 2014. Dietary variation and food hardness in sooty mangabeys (Cercocebus atys): Implications for fallback foods and dental adaptation. Am. J. Phys. Anthropol. 154, 413–423.

McGrew, W.C., 1983. Animal foods in the diets of wild chimpanzees (*Pan troglodytes*): Why cross-cultural variation? J. Ethol. 46–61.

McGrew, W.C., 2007. Savanna chimpanzees dig for food. Proc. Natl. Acad. Sci. U. S. A. 104, 19167–19168.

McKey, D., Gartlan, J.S., Waterman, P.G., F.L.S., Choo, G.M., 1981. Food selection by black colobus monkeys (*Colobus satanas*) in relation to plant chemistry. Biol. J. Linn. Soc. 16, 115–146.

McLaren, S., Wallace, M.W., 2010. Plio-Pleistocene climate change and the onset of aridity in southeastern Australia. Glob. Planet. Change. 71, 55–72.

Médail, F., Diadema, K., 2009. Glacial refugia influence plant diversity patterns in the Mediterranean Basin. J. Biogeogr. 36, 1333–1345.

Meikle, W.E., 1977. Molar Wear Stages in Theropithecus gelada. Kroeber Anthropol. Soc. Pap. 50, 21–25.

Meikle, W.E., 1987. Fossil cercopithecidae from the Sahabi Formation. Neogene Paleontol. Geol. Sahabi.

Meloro, C., Elton, S., 2013. The evolutionary history and palaeo-ecology of primate predation: Macaca sylvanus from plio-pleistocene europe as a case study. Folia Primatol. 83, 216–235.

Ménard, N., 2002. Ecological Plasticity of Barbary Macaques (*Macaca sylvanus*). Evol. Anthropol. 11, 95–100.

Ménard, N., Vallet, D., 1997. Behavioral responses of Barbary macaques (*Macaca sylvanus*) to variations in environmental conditions in Algeria. Am. J. Primatol. 43, 285–304.

Merceron, G., Berlioz, E., Vonhof, H., Green, D., Garel, M., Tütken, T., 2020. Tooth tales told by dental diet proxies: An alpine community of sympatric ruminants as a model to decipher the ecology of fossil fauna. Palaeogeogr. Palaeoclimatol. Palaeoecol.

Merceron, G., Blondel, C., Brunetiere, N., Francisco, A., Gautier, D., Ramdarshan, A., 2017.

Ψηφιακή βιβλιοθήκη Θεόφραστος – Τμήμα Γεωλογίας – Αριστοτέλειο Πανεπιστήμιο Θεσσαλονίκης

Ψηφιακή συλλογή
Βιβλιοθήκη
"ΘΕΟΦΡΑΣΤΟΣ"

Dental microwear and controlled food testing on sheep: The TRIDENT project. Biosurface and Biotribology. 3, 174–183.

Merceron, G., Escarguel, G., Angibault, J.M., Verheyden-Tixier, H., 2010a. Can dental microwear textures record inter-individual dietary variations? PLoS One. 5.

Merceron, G., Kaiser, T.M., Kostopoulos, D.S., Schulz, E., 2010b. Ruminant diets and the Miocene extinction of European great apes. Proc. R. Soc. B Biol. Sci. 277, 3105–3112.

Merceron, G., Kallend, A., Francisco, A., Louail, M., Martin, F., Plastiras, C.-A., Thiery, G., Noûs, C., Boisserie, J.-R., 2021. Further away with dental microwear analysis: food resource partitioning among Plio-Pleistocene monkeys from the Shungura Formation, Ethiopia. Palaeogeogr. Palaeoclimatol. Palaeoecol. 572, 110414.

Merceron, G., Koufos, G.D., Valentin, X., 2009a. Habitudes alimentaires du premier colobiné européen, Mesopithecus : Apports de l'analyse comparative des micro-usures dentaires avec des cercopithecidés actuels. Geodiversitas. 31, 865–878.

Merceron, G., Ramdarshan, A., Blondel, C., Boisserie, J.R., Brunetiere, N., Francisco, A., Gautier, D., Milhet, X., Novello, A., Pret, D., 2016. Untangling the environmental from the dietary: Dust does not matter. Proc. R. Soc. B Biol. Sci. 283.

Merceron, G., Scott, J., Scott, R.S., Geraads, D., Spassov, N., Ungar, P.S., 2009b. Folivory or fruit/seed predation for *Mesopithecus*, an earliest colobine from the late Miocene of Eurasia? J. Hum. Evol. 57, 732–738.

Merceron, G., Taylor, S., Scott, R., Chaimanee, Y., Jaeger, J.J., 2006. Dietary characterization of the hominoid *Khoratpithecus* (Miocene of Thailand): Evidence from dental topographic and microwear texture analyses. Naturwissenschaften. 93, 329–333.

Mihlbachler, M.C., Beatty, B.L., 2012. Magnification and resolution in dental microwear analysis using light microscopy. Palaeontol. Electron. 15.

Mihlbachler, M.C., Beatty, B.L., Caldera-Siu, A., Chan, D., Lee, R., 2012. Error rates and observer bias in dental microwear analysis using light microscopy. Palaeontol. Electron. 15.

Mihlbachler, M.C., Rivals, F., Solounias, N., Semprebon, G.M., 2011. Dietary Change and Evolution of Horses in North America. Am. Assoc. Adv. Sci. 331, 1178–1181.

Miller, E.R., Benefit, B.R., McCrossin, M.L., Plavcan, J.M., Leakey, M.G., El-Barkooky, A.N., Hamdan, M.A., Abdel Gawad, M.K., Hassan, S.M., Simons, E.L., 2009. Systematics of early and middle Miocene Old World monkeys. J. Hum. Evol. 57, 195–211.

Mills, J.R.E., 1963. Occlusion and Malocclusion of the Teeth of Primates. Dent. Anthropol. 29–51.

Ψηφιακή βιβλιοθήκη Θεόφραστος – Τμήμα Γεωλογίας – Αριστοτέλειο Πανεπιστήμιο Θεσσαλονίκης

Ψηφιακή συλλογή
Βιβλιοθήκη
"ΘΕΟΦΡΑΣΤΟΣ"

Mills, J.R.E., 1967. A comparison of lateral jaw movements in some mammals from wear facets on the teeth. Arch. Oral Biol. 12, 645–661.

Milton, K., 1993. Diet and primate evolution. Sci. Am. 269, 70–77.

Mitani, M., 1989. *Cercocebus torquatus*: Adaptive feeding and ranging behaviors related to seasonal fluctuations of food resources in the tropical rain forest of south-western Cameroon. Primates. 30, 307–323.

Modolo, L., Salzburger, W., Martin, R.D., 2005. Phylogeography of Barbary macaques (*Macaca sylvanus*) and the origin of the Gibraltar colony. Proc. Natl. Acad. Sci. U. S. A. 102, 7392–7397.

Molnar, S., Gantt, D.G., 1977. Functional implications of primate enamel thickness. Am. J. Phys. Anthropol. 46, 447–454.

Monteiro, L.R., 2013. Shape descriptors as ecometrics in dental ecology. Hystrix, Ital. J. Mammal. 24, 25–32.

Moura, A.C.D.A., Lee, P.C., 2004. Capuchin stone tool use in Caatinga dry forest. Science (80-.). 306, 1909.

Mowry, C.B., Decker, B.S., Shure, D.J., 1996. The role of phytochemistry in dietary choices of Tana river red *Colobus* monkeys (*Procolobus badius rufomitratus*). Int. J. Primatol. 17, 63–84.

Nakagawa, N., 2000a. Seasonal, sex, and interspecific differences in activity time budgets and diets of patas monkeys (Erythrocebus patas) and tantalus monkeys (Cercopithecus aethiops tantalus), living sympatrically in Northern Cameroon. Primates. 41, 161–174.

Nakagawa, N., 2000b. Foraging energetics in patas monkeys (*Erythrocebus patas*) and tantalus monkeys (*Cercopithecus aethiops tantalus*): implications for reproductive seasonality. Am. J. Primatol. Off. J. Am. Soc. Primatol. 52, 169–185.

Nakagawa, N., 2003a. Difference in food selection between patas monkeys (*Erythrocebus patas*) and tantalus monkeys (*Cercopithecus aethiops tantalus*) in Kala Maloue National Park, Cameroon, in relation to nutrient content. Primates. 44, 3–11.

Nakagawa, N., Nakamichi, M., Sugiura, H., 2010. The Japanese macaques. Springer Science & Business Media.

Nakatsukasa, M., Mbua, E., Sawada, Y., Sakai, T., Nakaya, H., Yano, W., Kunimatsu, Y., 2010. Earliest colobine skeletons from Nakali, Kenya. Am. J. Phys. Anthropol. 143, 365–382.

Ψηφιακή βιβλιοθήκη Θεόφραστος – Τμήμα Γεωλογίας – Αριστοτέλειο Πανεπιστήμιο Θεσσαλονίκης

Ψηφιακή συλλογή
Βιβλιοθήκη
"ΘΕΟΦΡΑΣΤΟΣ"

Nash, L.T., 1986. Dietary, behavioral, and morphological aspects of gummivory in primates. Am. J. Phys. Anthropol. 29, 113–137.

Necrasov, O., Samson, P., Radulesco, C., 1961. Sur un nouveau singe catarhinien fossile, decouvert dans un nid fossilifere d' Oltenie (R.P.R). J. Vis. Lang. Comput. 7, 55.

Newbery, D.M., Songwe, N.C., Chuyong, G.B., others, 1998. Phenology and dynamics of an African rainforest at Korup, Cameroon. Blackwell Science Ltd.

Newton-Fisher, N.E., Okecha, A.A., 2006. The diet of olive baboons (*Papio anubis*) in the Budongo Forest Reserve, Uganda. In: Newton-Fisher, N.E., Notman, H., Paterson, J.D., Reynolds, V. (Eds.), Primates of Western Uganda. Springer, pp. 61–73.

Newton, P., 1992. Feeding and ranging patterns of forest hanuman langurs (*Presbytis entellus*). Int. J. Primatol. 13, 245–285.

Nishida, T., 1976. The bark-eating habits in primates, with special reference to their status in the diet of wild chimpanzees. Folia Primatol. 25, 277–287.

Nishimura, T.D., Ito, T., Yano, W., Ebbestad, J.O.R., Takai, M., 2014. Nasal architecture in *Procynocephalus wimani* (Early Pleistocene, China) and implications for its phyletic relationship with *Paradolichopithecus*. Anthropol. Sci. 122, 101–113.

Nishimura, T.D., Takai, M., Maschenko, E.N., 2007. The maxillary sinus of *Paradolichopithecus sushkini* (late Pliocene, southern Tajikistan) and its phyletic implications. J. Hum. Evol. 52, 637–646.

Nishimura, T.D., Takai, M., Senut, B., Taru, H., Maschenko, E.N., Prieur, A., 2012. Reassessment of *Dolichopithecus* (*Kanagawapithecus*) *leptopostorbitalis*, a colobine monkey from the Late Pliocene of Japan. J. Hum. Evol. 62, 548–561.

Nishimura, T.D., Zhang, Y., Takai, M., 2010. Nasal anatomy of *Paradolichopithecus gansuensis* (early Pleistocene, Longdan, China) with comments on phyletic relationships among the species of this genus. Folia Primatol. 81, 53–62.

Norris, J., 1988. Diet and feeding behavior of semi-free ranging mandrills in an enclosed gabonais forest. Primates. 29, 449–463.

Norton, G.W., Rhine, R.J., Wynn, G.M., Wynn, R.D., 1987. Baboon Diet: Afive-year study of stability and variability in the plant feeding and habitat of the yellow baboons (*Papio cynocephalus*) of Mikumi National Park, Tanzania. Folia Primatol. 48, 78–120.

Nsi Akoue, G., Mbading-Mbading, W., Willaume, E., Souza, A., Mbatchi, B., Charpentier, M.J.E., 2017. Seasonal and individual predictors of diet in a free-ranging population of mandrills.

Ψηφιακή βιβλιοθήκη Θεόφραστος – Τμήμα Γεωλογίας – Αριστοτέλειο Πανεπιστήμιο Θεσσαλονίκης

Ψηφιακή συλλογή
Βιβλιοθήκη
"ΘΕΟΦΡΑΣΤΟΣ"
Α.Π.Θ

Ethology. 123, 600–613.

O'Brien, T.G., Kinnaird, M.F., 1997. Behavior, diet, and movements of the Sulawesi crested black macaque (*Macaca nigra*). Int. J. Primatol. 18, 321–351.

O'Regan, H.J., Chenery, C., Lamb, A.L., Stevens, R.E., Rook, L., Elton, S., 2008. Modern macaque dietary heterogeneity assessed using stable isotope analysis of hair and bone. J. Hum. Evol. 55, 617–626.

O'regan, H.J., Turner, A., Wilkinson, D.M., 2002. European Quaternary refugia: A factor in large carnivore extinction? J. Quat. Sci. 17, 789–795.

Oates, J.F., 1978. Water-Plant and Soil Consumption by Guereza Monkeys (*Colobus guereza*): A Relationship with Minerals and Toxins in the Diet? Biotropica. 10, 241.

Oates, J.F., Swain, T., Zantovska, J., 1977. Secondary compounds and food selection by colobus monkeys. Biochem. Syst. Ecol. 5, 317–321.

Oates, J.F., Whitesides, G.H., 1990. Association between olive colobus (*Procolobus verus*), Diana guenons (*Cercopithecus diana*), and other forest monkeys in Sierra Leone. Am. J. Primatol. 21, 129–146.

Oelze, V.M., Head, J.S., Robbins, M.M., Richards, M., Boesch, C., 2014. Niche differentiation and dietary seasonality among sympatric gorillas and chimpanzees in Loango National Park (Gabon) revealed by stable isotope analysis. J. Hum. Evol. 66, 95–106.

Olejniczak, A.J., Gilbert, C.C., Martin, L.B., Smith, T.M., Ulhaas, L., Grine, F.E., 2007. Morphology of the enamel-dentine junction in sections of anthropoid primate maxillary molars. J. Hum. Evol. 53, 292–301.

Olejniczak, A. J., Smith, T.M., Skinner, M.M., Grine, F.E., Feeney, R.N.M., Thackeray, J.F., Hublin, J.J., 2008. Three-dimensional molar enamel distribution and thickness in Australopithecus and Paranthropus. Biol. Lett. 4, 406–410.

Olejniczak, Anthony J., Tafforeau, P., Feeney, R.N.M., Martin, L.B., 2008. Three-dimensional primate molar enamel thickness. J. Hum. Evol. 54, 187–195.

Olupot, W., 1988. Long-term variation in mangabey (*Cercocebus albigena johnstoni* Lydekker) feeding in Kibale National Park, Uganda. Afr. J. Ecol. 36, 96–101.

Owens, J.R., Honarvar, S., Nessel, M., Hearn, G.W., 2015. From frugivore to folivore: Altitudinal variations in the diet and feeding ecology of the Bioko Island drill (*Mandrillus leucophaeus poensis*). Am. J. Primatol. 77, 1263–1275.

Ψηφιακή βιβλιοθήκη Θεόφραστος – Τμήμα Γεωλογίας – Αριστοτέλειο Πανεπιστήμιο Θεσσαλονίκης

Ψηφιακή συλλογή
Βιβλιοθήκη
"ΘΕΟΦΡΑΣΤΟΣ"

Page, S.L., Chiu, C.H., Goodman, M., 1999. Molecular Phylogeny of Old World Monkeys (Cercopithecidae) as Inferred from γ-Globin DNA Sequences. Mol. Phylogenet. Evol. 13, 348–359.

Pal, A., Kumara, H.N., Mishra, P.S., Velankar, A.D., Singh, M., 2018. Extractive foraging and tool-aided behaviors in the wild Nicobar long-tailed macaque (*Macaca fascicularis umbrosus*). Primates. 59, 173–183.

Pallas, L., Daver, G., Mackaye, H.T., Likius, A., Vignaud, P., Guy, F., 2019. A window into the early evolutionary history of Cercopithecidae: Late Miocene evidence from Chad, Central Africa. J. Hum. Evol. 132, 61–79.

Palombo, M.R., 2006. Biochronology of the Plio-Pleistocene Terrestrial mammals of Sardinia : The state of the art. Hell. J. Geosci. 41, 47–66.

Palombo, M.R., Rozzi, R., 2014. How correct is any chronological ordering of the Quaternary Sardinian mammalian assemblages? Quat. Int. 328–329, 136–155.

Palombo, M.R., Rozzi, R., Bover, P., 2013. The endemic bovids from Sardinia and the Balearic Islands: State of the art. Geobios. 46, 127–142.

Pampush, J.D., Duque, A.C., Burrows, B.R., Daegling, D.J., Kenney, W.F., McGraw, W.S., 2013. Homoplasy and thick enamel in primates. J. Hum. Evol. 64, 216–224.

Pampush, J.D., Spradley, J.P., Morse, P.E., Harrington, A.R., Allen, K.L., Boyer, D.M., Kay, R.F., 2016. Wear and its effects on dental topography measures in howling monkeys (Alouatta palliata). Am. J. Phys. Anthropol. 161, 705–721.

Pan, R., Groves, C., Oxnard, C., 2004. Relationships between the Fossil Colobine Mesopithecus pentelicus and Extant Cercopithecoids, Based on Dental Metrics. Am. J. Primatol. 62, 287–299.

Pastre, J.F., Debard, E., Nomade, S., Guillou, H., Faure, M., Guérin, C., Delson, E., 2015. Nouvelles données géologiques et téphrochronologiques sur le gisement paléontologique du maar de Senèze (Pléistocène inférieur, Massif Central, France). Quat. Rev. l'Association française pour l'étude du Quat. 26, 225–244.

Pedreschi, F., Aguilera, J.M., Brown, C.A., 2000. Characterization of food surfaces using scale-sensitive fractal analysis. J. Food Process Eng. 23, 127–143.

Peigné, S., Merceron, G., 2019. Palaeoecology of cave bears as evidenced by dental wear analysis: a review of methods and recent findings. Hist. Biol. 31, 448–460.

Peignot, P., Charpentier, M.J.E., Bout, N., Bourry, O., Massima, U., Dosimont, O., Terramorsi, R.,

Ψηφιακή βιβλιοθήκη Θεόφραστος – Τμήμα Γεωλογίας – Αριστοτέλειο Πανεπιστήμιο Θεσσαλονίκης

Ψηφιακή συλλογή
Βιβλιοθήκη
"ΘΕΟΦΡΑΣΤΟΣ"

Wickings, E.J., 2008. Learning from the first release project of captive-bred mandrills Mandrillus sphinx in Gabon. Oryx. 42, 122–131.

Percher, A.M., Merceron, G., Nsi Akoue, G., Galbany, J., Romero, A., Charpentier, M.J.E., 2018. Dental microwear textural analysis as an analytical tool to depict individual traits and reconstruct the diet of a primate. Am. J. Phys. Anthropol. 165, 123–138.

Percher, A.M., Romero, A., Galbany, J., Akoue, G.N., Pérez-Pérez, A., Charpentier, M.J.E., 2017. Buccal dental-microwear and dietary ecology in a free-ranging population of mandrills (*Mandrillus sphinx*) from southern Gabon. PLoS One. 12, 1–18.

Petculescu, A., Stiucã, E., Radulescu, C., Samson, P.-M., 2003. Pliocene large mammals of Romania. Coloquios Paleontol. 549–558.

Philippe, M., Bourgat, R., 1985. La collection de vertébrés pliocènes du Muséum de Perpignan. Bull. Mens. la Société linnéenne Lyon. 54, 146–160.

Pilbeam, D., Walker, A., 1968. Fossil monkeys from the Miocene of Napak, north-east Uganda. Nature. 220, 657–660.

Pinkall, U., Polthier, K., 1993. Computing Discrete Minimal Surfacesand Their Conjugates. Exp. Math. 2.

Plastiras, Ch, Kostopoulos, D.S., Merceron, G., 2017. Tooth morphology, molar enamel thickness and dental microwear textural analysis with application on European *Paradolichopithecus*/*Procynocephalus* and comparisons with Pleistocene papionins. In: 2nd International Meeting of early-stage researchers in Paleontology 2017, pp. 160e171 abstract. http://www.imerp2.upatras.gr/index. php.

Plavcan, J.M., Cope, D.A., 2001. Metric variation and species recognition in the fossil record. Evol. Anthropol. 10, 204–222.

Plavcan, J.M., Ward, C. V., Kay, R.F., Manthi, F.K., 2019. A diminutive Pliocene guenon from Kanapoi, West Turkana, Kenya. J. Hum. Evol. 135, 102623.

Pochron, S.T., 2000. The core dry-season diet of yellow baboons (*Papio hamadryas cynocephalus*) in Ruaha National Park, Tanzania. Folia Primatol. 71, 346–349.

Popescu, S.M., 2002. Repetitive changes in Early Pliocene vegetation revealed by high-resolution pollen analysis: Revised cyclostratigraphy of southwestern Romania. Rev. Palaeobot. Palynol. 120, 181–202.

Post, D.G., 1982. Feeding behavior of yellow baboons (*Papio cynocephalus*) in the Amboseli National Park, Kenya. Int. J. Primatol. 3, 403–430.

Ψηφιακή βιβλιοθήκη Θεόφραστος – Τμήμα Γεωλογίας – Αριστοτέλειο Πανεπιστήμιο Θεσσαλονίκης

Ψηφιακή συλλογή
Βιβλιοθήκη
"ΘΕΟΦΡΑΣΤΟΣ"

Postigo Mijarra, J.M., Burjachs, F., Gómez Manzaneque, F., Morla, C., 2007. A palaeoecological interpretation of the lower-middle Pleistocene Cal Guardiola site (Terrassa, Barcelona, NE Spain) from the comparative study of wood and pollen samples. Rev. Palaeobot. Palynol. 146, 247–264.

Poulsen, J.R., Clark, C.J., Smith, T.B., 2001. Seasonal variation in the feeding ecology of the grey-cheeked mangabey (*Lophocebus albigena*) in Cameroon. Am. J. Primatol. 54, 91–105.

Pradella, C., Rook, L., 2007. *Mesopithecus* (Primates: Cercopithecoidea) from Villafranca d'Asti (Early Villafranchian; NW Italy) and palaeoecological context of its extinction. Swiss J. Geosci. 100, 145–152.

Prideaux, G.J., Ayliffe, L.K., DeSantis, L.R.G., Schubert, B.W., Murray, P.F., Gagan, M.K., Cerling, T.E., 2009. Extinction implications of a chenopod browse diet for a giant Pleistocene kangaroo. Proc. Natl. Acad. Sci. U. S. A. 106, 11646–11650.

Pruetz, J.D., Isbell, L.A., 2000. Correlations of food distribution and patch size with agonistic interactions in female vervets (*Chlorocebus aethiops*) and patas monkeys (*Erythrocebus patas*) living in simple habitats. Behav. Ecol. Sociobiol. 38–47.

Prufrock, K.A., López-Torres, S., Silcox, M.T., Boyer, D.M., 2016. Surfaces and spaces: Troubleshooting the study of dietary niche space overlap between North American stem primates and rodents. Surf. Topogr. Metrol. Prop. 4, 24005.

Pugh, K.D., Gilbert, C.C., 2018. Phylogenetic relationships of living and fossil African papionins: Combined evidence from morphology and molecules. J. Hum. Evol. 123, 35–51.

Punekar, S.A., 2002. Some food plants of Hanuman langur *Semnopithecus entellus* (Dufresne) in the Western Ghats of Maharashtra, India. Zoos' Print J. 17, 797–801.

Purnell, M., Seehausen, O., Galis, F., 2012. Quantitative three-dimensional microtextural analyses of tooth wear as a tool for dietary discrimination in fishes. J. R. Soc. Interface. 9, 2225–2233.

Purnell, M.A., Crumpton, N., Gill, P.G., Jones, G., Rayfield, E.J., 2013. Within-guild dietary discrimination from 3-D textural analysis of tooth microwear in insectivorous mammals. J. Zool. 291, 249–257.

Raaum, R.L., Sterner, K.N., Noviello, C.M., Disotell, T.R., 2005. Catarrhine primate divergence dates estimated from complete mitochondrial genomes: Concordance with fossil and nuclear DNA evidence. J. Hum. Evol. 48, 237–257.

Rabenold, D., Pearson, O.M., 2011. Abrasive, silica phytoliths and the evolution of thick molar enamel in primates, with implications for the diet of *Paranthropus boisei*. PLoS One. 6.

Ψηφιακή βιβλιοθήκη Θεόφραστος – Τμήμα Γεωλογίας – Αριστοτέλειο Πανεπιστήμιο Θεσσαλονίκης

Ψηφιακή συλλογή
Βιβλιοθήκη
"ΘΕΟΦΡΑΣΤΟΣ"

Rabosky, D.L., Lovette, I.J., 2008. Density-dependent diversification in North American wood warblers. Proc. R. Soc. B Biol. Sci. 275, 2363–2371.

Radović, P., Lindal, J., Marković, Z., Alaburić, S., Roksandic, M., 2019. First record of a fossil monkey (Primates, Cercopithecidae) from the Late Pliocene of Serbia. J. Hum. Evol. 137.

Radulescu, C., Samson, P.M., Petculescu, A., Stiucã, E., 2003. Grandes Mamíferos del Plioceno de Rumania. Coloquios Paleontol. 549–558.

Rae, T.C., 2008. Paranasal pneumatization in extant and fossil Cercopithecoidea. J. Hum. Evol. 54, 279–286.

Ragni, A.J., Teaford, M.F., Ungar, P.S., 2017. A molar microwear texture analysis of pitheciid primates. Am. J. Primatol. 79, 1–12.

Ramdarshan, A., Blondel, C., Gautier, D., Surault, J., Merceron, G., 2017. Overcoming sampling issues in dental tribology: Insights from an experimentation on sheep. Palaeontol. Electron.

Randimbiharinirina, D.R., Raharivololona, B.M., Hawkins, M.T.R., Frasier, C.L., Culligan, R.R., Sefczek, T.M., Randriamampionona, R., Louis, E.E., 2018. Behaviour and ecology of male aye-Ayes (*Daubentonia madagascariensis*) in the kianjavato classified forest, South-Eastern Madagascar. Folia Primatol. 89, 123–137.

Rasmussen, D.T., Friscia, A.R., Gutierrez, M., Kappelman, J., Miller, E.R., Muteti, S., Reynoso, D., Rossie, J.B., Spell, T.L., Tabor, N.J., Gierlowski-Kordesch, E., Jacobs, B.F., Kyongo, B., Macharwas, M., Muchemi, F., 2019. Primitive old world monkey from the earliest miocene of kenya and the evolution of cercopithecoid bilophodonty. Proc. Natl. Acad. Sci. U. S. A. 116, 6051–6056.

Ravosa, M.J., 1996. Jaw morphology and function in living and fossil Old World monkeys. Int. J. Primatol. 17, 909–932.

Reed, K.E., 1997. Early hominid evolution and ecological change through the African Plio-Pleistocene. J. Hum. Evol. 32, 289–322.

Reed, K.E., Bidner, L.R., 2004. Primate communities: Past, present, and possible future. Yearb. Phys. Anthropol. 47, 2–39.

Reumer, J.W.F., Mol, D., Kahlke, R.D., 2018. First finds of pleistocene macaca sylvanus (cercopithecidae, primates) from the North Sea. Rev. Paleobiol. 37, 555–560.

Rhine, R.J., Norton, G.W., Wynn, G.M., Wynn, R.D., 1989. Plant feeding of yellow baboons (*Papio cynocephalus*) in Mikumi national park, Tanzania, and the relationship between seasonal feeding and immature survival. Int. J. Primatol. 10, 319–342.

Ψηφιακή βιβλιοθήκη Θεόφραστος – Τμήμα Γεωλογίας – Αριστοτέλειο Πανεπιστήμιο Θεσσαλονίκης

Ψηφιακή συλλογή
Βιβλιοθήκη
"ΘΕΟΦΡΑΣΤΟΣ"

Rhine, R.J., Norton, G.W., Wynn, G.M., Wynn, R.D., Rhine, H.B., 1986. Insect and meat eating among infant and adult baboons (*Papio cynocephalus*) of Mikumi National Park, Tanzania. Am. J. Phys. Anthropol. 70, 105–118.

Richard, A.F., Goldstein, S.J., Dewar, R.E., 1989. Weed macaques: The evolutionary implications of macaque feeding ecology. Int. J. Primatol. 10, 569–594.

Riley, E.P., 2008. Ranging patterns and habitat use of Sulawesi Tonkean macaques (*Macaca tonkeana*) in a human-modified habitat. Am. J. Primatol. 70, 670–679.

Riley, E.P., Tolbert, B., Farida, W.R., 2013. Nutritional content explains the attractiveness of cacao to crop raiding Tonkean macaques. Curr. Zool. 59, 160–169.

Riptianingsih, F.D., Farajallah, D.P., Astuti, D.A., 2015. Feeding Behavior of Tonkean Macaques (*Macaca tonkeana*) in Schmutzer Primates Center and Ragunan Zoo, Jakarta. Makara J. Sci. 19, 55–63.

Rivals, F., Prignano, L., Semprebon, G.M., Lozano, S., 2015. A tool for determining duration of mortality events in archaeological assemblages using extant ungulate microwear. Sci. Rep. 5, 1–12.

Rivals, F., Semprebon, G.M., 2010. What can incisor microwear reveal about the diet of ungulates? Mammalia. 74, 401–406.

Roberts, P., Delson, E., Miracle, P., Ditchfield, P., Roberts, R.G., Jacobs, Z., Blinkhorn, J., Ciochon, R.L., Fleagle, J.G., Frost, S.R., Gilbert, C.C., Gunnell, G.F., Harrison, T., Korisettar, R., Petraglia, M.D., 2014. Erratum: Continuity of mammalian fauna over the last 200,000 y in the Indian subcontinent (Proceedings of the National Academy of Sciences of the United States of America (2014) 111 (5848-5853) DOI 10.1073/pnas.1323465111). Proc. Natl. Acad. Sci. U. S. A. 113.

Roberts, P., Delson, E., Miracle, P., Ditchfield, P., Roberts, R.G., Jacobs, Z., Blinkhorn, J., Ciochon, R.L., Fleagle, J.G., Frost, S.R., Gilbert, C.C., Gunnell, G.F., Harrison, T., Korisettar, R., Petraglia, M.D., 2016. Continuity of mammalian fauna over the last 200,000 y in the Indian subcontinent. Proc. Natl. Acad. Sci. U. S. A. 113.

Rodman, P.S., 1991. Structural differentiation of microhabitats of sympatric *Macaca fascicularis* and *M. nemestrina* in East Kalimantan, Indonesia. Int. J. Primatol. 12, 357–375.

Rogers, M.E., Abernethy, K., Bermejo, M., Cipolletta, C., Doran, D., Mcfarland, K., Nishihara, T., Remis, M., Tutin, C.E.G., 2004. Western gorilla diet: A synthesis from six sites. Am. J. Primatol. 64, 173–192.

Rook, L., 1999. Late Turolian *Mesopithecus* (mammalia, primates, colobinae) from Italy. J. Hum. Evol. 36, 535–547.

Ψηφιακή βιβλιοθήκη Θεόφραστος – Τμήμα Γεωλογίας – Αριστοτέλειο Πανεπιστήμιο Θεσσαλονίκης

Ψηφιακή συλλογή
Βιβλιοθήκη
"ΘΕΟΦΡΑΣΤΟΣ"

Rook, L., Alba, D.M., 2012. Charles Immanuel Forsyth Major (1843-1923), pioniere della paleoprimatologia, e un dente di Mesopithecus proveniente da una località ignota (probabilmente il bacino del Casino, Siena) nelle collezioni del Museo di Storia Naturale di Basilea. Boll. della Soc. Paleontol. Ital. 51, 1–6.

Rook, L., Croitor, R., Delfino, M., Ferretti, M.P., Gallai, G., Pavia, M., 2013. The Upper Valdarno Plio-Pleistocene vertebrate record: An historical overview, with notes on palaeobiology and stratigraphic significance of some important taxa. Ital. J. Geosci. 132, 104–125.

Rook, L., Ferretti, M.P., Arca, M., Tuveri, C., 2004. Chasmaporthetes melei n. sp. an endemic hyaenid (Carnivora, Mammalia) from the Monte Tuttavista fissure fillings (Late Pliocene to early Pleistocene; Sardinia, Italy. Riv. Ital. di Paleontol. e Stratigr. 110, 707–714.

Rook, L., Martínez-Navarro, B., 2013. The large sized cercopithecoid from Pirro Nord and the importance of Theropithecus in the Early Pleistocene of Europe: Faunal marker for hominins dispersal outside Africa. Palaeontogr. Abteilung A Palaozoologie - Stratigr. 298, 107–112.

Rook, Lorenzo, Martínez-Navarro, B., Howell, F.C., 2004. Occurrence of *Theropithecus* sp. in the Late Villafranchian of Southern Italy and implication for Early Pleistocene “out of Africa” dispersals. J. Hum. Evol. 47, 267–277.

Rook, L., Mottura, A., Gentili, S., 2001. Fossil *Macaca* remains from RDB quarry (villafranca d’asti, Italy): New data and overview. J. Hum. Evol. 40, 187–202.

Rook, L., O’Higgins, P., 2005. A comparative study of adult facial morphology and its ontogeny in the fossil macaque Macaca majori from Capo Figari, Sardinia, Italy. Folia Primatol. 76, 151–171.

Roos, Christian, Kothe, M., Alba, D.M., Delson, E., Zinner, D., 2019. The radiation of macaques out of Africa: Evidence from mitogenome divergence times and the fossil record. J. Hum. Evol. 133, 114–132.

Roos, C., Kothe, M., Alba, D.M., Delson, E., Zinner, D., 2019. The radiation of macaques out of Africa: Evidence from mitogenome divergence times and the fossil record. J. Hum. Evol. 133, 114–132.

Rosenberger, A.L., 2013. Fallback foods, preferred foods, adaptive zones, and primate origins. Am. J. Primatol. 75, 883–890.

Rosenberger, A.L., Kinzey, W.G., 1976. Functional patterns of molar occlusion in platyrrhine primates. Am. J. Phys. Anthropol. 45, 281–297.

Rosenzweig, M.L., 1995. Patterns: In space & time, Species diversity in space and time.

Ψηφιακή βιβλιοθήκη Θεόφραστος – Τμήμα Γεωλογίας – Αριστοτέλειο Πανεπιστήμιο Θεσσαλονίκης

Ψηφιακή συλλογή
Βιβλιοθήκη
"ΘΕΟΦΡΑΣΤΟΣ"

Rossie, J.B., Gilbert, C.C., Hill, A., 2013. Early Cercopithecid Monkeys from the Tugen hills, Kenya. Proc. Natl. Acad. Sci. U. S. A. 110, 5818–5822.

Rowe, N., Goodall, J., Mittermeier, R., 1996. The pictorial guide to the living primates. Pogonias Press East Hampton New York.

Rowell, T.E., 1966. Hierarchy in the organization of a captive baboon group. Anim. Behav. 14, 430–443.

Rozzi, R., Varela, S., Bover, P., Martin, J.M., 2020. Causal explanations for the evolution of 'low gear' locomotion in insular ruminants. J. Biogeogr. 47, 2274–2285.

Rugis, J., Klette, R., 2006. A scale invariant surface curvature estimator. Lect. Notes Comput. Sci. (including Subser. Lect. Notes Artif. Intell. Lect. Notes Bioinformatics). 4319 LNCS, 138–147.

Runemark, A., Brydegaard, M., Svensson, E.I., 2014. Does relaxed predation drive phenotypic divergence among insular populations? J. Evol. Biol. 27, 1676–1690.

Ruppert, N., Holzner, A., See, K.W., Gisbrecht, A., Beck, A., 2018. Activity Budgets and Habitat Use of Wild Southern Pig-Tailed Macaques (*Macaca nemestrina*) in Oil Palm Plantation and Forest. Int. J. Primatol. 39, 237–251.

Ruslin, F., Matsuda, I., Md-Zain, B.M., 2019. The feeding ecology and dietary overlap in two sympatric primate species, the long-tailed macaque (*Macaca fascicularis*) and dusky langur (*Trachypithecus obscurus obscurus*), in Malaysia. Primates. 60, 41–50.

Ryan, A.S., 1979. A Preliminary Scanning Electron Microscope Examination of Wear Striation Direction on Primate Teeth. J. Dent. Res. 58, 525–530.

Saito, V.S., Laroche, F., Siqueira, T., Pavoine, S., 2018. Ecological versatility and the assembly of multiple competitors: cautionary notes for assembly inferences. Ecology. 99, 1173–1183.

Salter, R.E., MacKenzie, N.A., Nightingale, N., Aken, K.M., Chai, P., 1985. Habitat use, ranging behaviour, and food habits of the proboscis monkey, *Nasalis larvatus* (van Wurmb), in Sarawak. Primates. 26, 436–451.

Sanson, G.D., Kerr, S., Read, J., 2017. Dietary exogenous and endogenous abrasives and tooth wear in African buffalo. Biosurface and Biotribology. 3, 211–223.

Sayers, K., Norconk, M.A., 2008. Himalayan *Semnopithecus entellus* at Langtang National Park, Nepal: Diet, activity patterns, and resources. Int. J. Primatol. 29, 509–530.

Schreiber, H.D., 2020. Fossil remains of *Macaca sylvanus* (Mammalia , Cercopithecidae) from the

Ψηφιακή βιβλιοθήκη Θεόφραστος – Τμήμα Γεωλογίας – Αριστοτέλειο Πανεπιστήμιο Θεσσαλονίκης

Ψηφιακή συλλογή
Βιβλιοθήκη
"ΘΕΟΦΡΑΣΤΟΣ"
Α.Π.Θ

early Middle Pleistocene locality of Mauer (SW Germany). Carolinea. 78, 5–13.

Schreiber, H.D., Löscher, M., 2011. The second find of a primate from the early Middle Pleistocene locality of Mauer (SW Germany): A molar of *Macaca* (Mammalia, Cercopithecidae). Neues Jahrb. fur Geol. und Palaontologie - Abhandlungen. 260, 297–304.

Schreier, B.M., Harcourt, A.H., Coppeto, S.A., Somi, M.F., 2009. Interspecific competition and niche separation in primates: A global analysis. Biotropica. 41, 283–291.

Schroer, K., Wood, B., 2015. The role of character displacement in the molarization of hominin mandibular premolars. Evolution (N. Y). 69, 1630–1642.

Schubert, B.W., Ungar, P.S., DeSantis, L.R.G., 2010. Carnassial microwear and dietary behaviour in large carnivorans. J. Zool. 280, 257–263.

Schulz-Kornas, E., Winkler, D.E., Clauss, M., Carlsson, J., Ackermans, N.L., Martin, L.F., Hummel, J., Müller, D.W.H., Hatt, J.M., Kaiser, T.M., 2020. Everything matters: Molar microwear texture in goats (*Capra aegagrus hircus*) fed diets of different abrasiveness. Palaeogeogr. Palaeoclimatol. Palaeoecol. 552, 109783.

Schwartz, G.T., 1997. Taxonomic \& functional aspects of enamel cap structure in South African Plio-Pleistocene hominids: a high-resolution computed tomographic study. Ph. D. Diss. Washingt. Univ. Washington University.

Schwartz, G.T., 2000. Taxonomic and functional aspects of the patterning of enamel thickness distribution in extant large-bodied hominoids. Am. J. Phys. Anthropol. 111, 221–244.

Schwartz, G.T., McGrosky, A., Strait, D.S., 2020. Fracture mechanics, enamel thickness and the evolution of molar form in hominins. Biol. Lett. 16, 3–8.

Schwartz, G.T., Thackeray, J.F., Reid, C., Van Reenan, J.F., 1998. Enamel thickness and the topography of the enamel-dentine junction in South African Plio-Pleistocene hominids with special reference to the Carabelli trait. J. Hum. Evol. 35, 523–542.

Scott, J.E., Campbell, R.M., Baj, L.M., Burns, M.C., Price, M.S., Sykes, J.D., Vinyard, C.J., 2018. Dietary signals in the premolar dentition of primates. J. Hum. Evol. 121, 221–234.

Scott, J.R., 2012. Dental microwear texture analysis of extant African Bovidae. Mammalia. 76, 157–174.

Scott, R.S., Teaford, M.F., Ungar, P.S., 2012. Dental microwear texture and anthropoid diets. Am. J. Phys. Anthropol. 147, 551–579.

Scott, R.S., Ungar, P.S., Bergstrom, T.S., Brown, C.A., Childs, B.E., Teaford, M.F., Walker, A.,

Ψηφιακή βιβλιοθήκη Θεόφραστος – Τμήμα Γεωλογίας – Αριστοτέλειο Πανεπιστήμιο Θεσσαλονίκης

Ψηφιακή συλλογή
Βιβλιοθήκη
"ΘΕΟΦΡΑΣΤΟΣ"
Τμήμα Γεωλογίας
Α.Π.Θ

2006. Dental microwear texture analysis: technical considerations. J. Hum. Evol. 51, 339–349.

Scott, R.S., Ungar, P.S., Bergstrom, T.S., Brown, C.A., Grine, F.E., Teaford, M.F., Walker, A., 2005. Dental microwear texture analysis shows within-species diet variability in fossil hominins. Nature. 436, 693–695.

Semprebon, G.M., Godfrey, L.R., Solounias, N., Sutherland, M.R., Jungers, W.L., 2004. Can low-magnification stereomicroscopy reveal diet? J. Hum. Evol. 47, 115–144.

Sengupta, A., Radhakrishna, S., 2016. Influence of Fruit Availability on Fruit Consumption in a Generalist Primate, the Rhesus Macaque *Macaca mulatta*. Int. J. Primatol. 37, 703–717.

Shan, S., Kovalsky, S.Z., Winchester, J.M., Boyer, D.M., Daubechies, I., 2019. ariaDNE: A robustly implemented algorithm for Dirichlet energy of the normal. Methods Ecol. Evol. 10, 541–552.

Sheine, W.S., Kay, R.F., 1977. An analysis of chewed food particle size and its relationship to molar structure in the primates *Cheirogaleus medius* and *Galago senegalensis* and the insectivoranTupaia glis. Am. J. Phys. Anthropol. 47, 15–20.

Sheine, W.S., Kay, R.F., 1982. A model for comparison of masticatory effectiveness in primates. J. Morphol. 172, 139–149.

Shellis, R.P., Beynon, A.D., Reid, D.J., Hiiemae, K.M., 1998. Variations in molar enamel thickness among primates. J. Hum. Evol. 35, 507–522.

Shen, G., Gao, X., Gao, B., Granger, D.E., 2009. Age of Zhoukoudian Homo erectus determined with 26Al/ 10Be burial dating. Nature. 458, 198–200.

Shimizu, D., 2002. Functional implications of enamel thickness in the lower molars of red colobus (*Procolobus badius*) and Japanese macaque (*Macaca fuscata*). J. Hum. Evol. 43, 605–620.

Simionescu, I., 1930. Vertebratele Pliocene dela Malusteni (Covurlui). Publ. Adamachi. 9, 1689–1699.

Singels, E., 2013. Underground storage organs of plants as a food source for Pleistocene hunter-gatherers in the southern Cape.

Singer, R., Wolff, R.G., Gladfelter, B.G., J.J., W., 1982. Pleistocene *Macaca* from Hoxne, Sufforlk, England. Folia Primatol. 141–152.

Singh, M., Roy, K., Singh, M., 2011. Resource partitioning in sympatric langurs and macaques in tropical rainforests of the central Western Ghats, south India. Am. J. Primatol. 73, 335–346.

Ψηφιακή βιβλιοθήκη Θεόφραστος – Τμήμα Γεωλογίας – Αριστοτέλειο Πανεπιστήμιο Θεσσαλονίκης

Ψηφιακή συλλογή
Βιβλιοθήκη
"ΘΕΟΦΡΑΣΤΟΣ"

Singleton, M., 2003. Functional and phylogenetic implications of molar flare variation in Miocene hominoids. J. Hum. Evol. 45, 57–79.

Skinner, M.M., Evans, A., Smith, T., Jernvall, J., Tafforeau, P., Kupczik, K., Olejniczak, A.J., Rosas, A., Radovčić, J., Thackeray, J.F., Toussaint, M., Hublin, J.J., 2010. Brief communication: Contributions of enamel-dentine junction shape and enamel deposition to primate molar crown complexity. Am. J. Phys. Anthropol. 142, 157–163.

Skinner, M.M., Gunz, P., Wood, B.A., Hublin, J.J., 2008. Enamel-dentine junction (EDJ) morphology distinguishes the lower molars of *Australopithecus africanus* and *Paranthropus robustus*. J. Hum. Evol. 55, 979–988.

Smith, T., Olejniczak, A., Kupczik, K., Lazzari, V., Vos, J., Kullmer, O., Schrenk, F., Hublin, J.J., Jacob, T., Tafforeau, P., 2009. Taxonomic assessment of the Trinil molars using non-destructive 3D structural and developmental analysis. PaleoAnthropology. 118, 117–129.

Smith, T.M., Olejniczak, A.J., Martin, L.B., Reid, D.J., 2005. Variation in hominoid molar enamel thickness. J. Hum. Evol. 48, 575–592.

Smith, T.M., Olejniczak, A.J., Zermeno, J.P., Tafforeau, P., Skinner, M.M., Hoffmann, A., Radovčić, J., Toussaint, M., Kruszynski, R., Menter, C., Moggi-Cecchi, J., Glasmacher, U.A., Kullmer, O., Schrenk, F., Stringer, C., Hublin, J.J., 2012. Variation in enamel thickness within the genus Homo. J. Hum. Evol. 62, 395–411.

Smith, T.M., Tafforeau, P., Pouech, J., Begun, D.R., 2019. Enamel thickness and dental development in Rudapithecus hungaricus. J. Hum. Evol. 136, 102649.

Solounias, N., Semprebon, G., 2002. Advances in the Reconstruction of Ungulate Ecomorphology with Application to Early Fossil Equids. Am. Museum Novit. 3366, 1–49.

Sondaar, P., 1987. Pleistocene mammals and extinctions of islands endemics. Mem. Soc. Geol. Fr. NS. 150, 159–165.

Sondaar, P., 2000. Early human exploration and exploitation of islands. Tropics. 10, 203–229.

Sondaar, P., 2006. The unique Postcranial of the Old World Monkey *Paradolichopithecus*: more similar to *Australopithecus* than to Baboons*. Hell. J. Geo. 19–28.

Sondaar, P.Y., 1977. Insularity and its effect on mammal evolution. 671–707.

Sondaar, P.Y., Van Der Geer, A.A.E., 2000. Mesolithic environment and animal exploitation on Cyprus and Sardinia-Corsica. In: Archaeozoology of the Near East IV B: Proceedings of the IVth ASWA Symposium. pp. 67–73.

Ψηφιακή βιβλιοθήκη Θεόφραστος – Τμήμα Γεωλογίας – Αριστοτέλειο Πανεπιστήμιο Θεσσαλονίκης

Ψηφιακή συλλογή
Βιβλιοθήκη
"ΘΕΟΦΡΑΣΤΟΣ"

Sondaar, P.Y., Van Der Geer, A.A.E., 2005. Evolution and extinction of Plio-Pleistocene Islands Ungulates. Quat. Suppl. 241–256.

Souron, A., 2018. Morphology, diet, and stable carbon isotopes: On the diet of *Theropithecus* and some limits of uniformitarianism in paleoecology. Am. J. Phys. Anthropol. 166, 261–267.

Souron, A., Merceron, G., Blondel, C., Brunetière, N., Colyn, M., Hofman-Kamińska, E., Boisserie, J.R., 2015. Three-dimensional dental microwear texture analysis and diet in extant Suidae (Mammalia: Cetartiodactyla). Mammalia. 79, 279–291.

Spassov, N., 2000. Biochronology and zoogeographic affinities of the Villafranchian faunas of Bulgaria and South Europe.

Spassov, N., Geraads, D., 2007. Dolichopithecus balcanicus sp. nov., a new Colobinae (Primates, Cercopithecidae) from the early Pliocene of southeastern Europe, with a discussion on the taxonomy of the genus. J. Hum. Evol. 52, 434–442.

Spassov, Nikolai, Geraads, D., 2007. Dolichopithecus balcanicus sp. nov., a new Colobinae (Primates, Cercopithecidae) from the early Pliocene of southeastern Europe, with a discussion on the taxonomy of the genus. J. Hum. Evol. 52, 434–442.

Spassov, N., Geraads, D., Hristova, L., Markov, G.N., Merceron, G., Tzankov, T., Stoyanov, K., Böhme, M., Dimitrova, A., 2012. A hominid tooth from Bulgaria: The last pre-human hominid of continental Europe. J. Hum. Evol. 62, 138–145.

Spradley, J.P., Pampush, J.D., Morse, P.E., Kay, R.F., 2017. Smooth operator: The effects of different 3D mesh retriangulation protocols on the computation of Dirichlet normal energy. Am. J. Phys. Anthropol. 163, 94–109.

Stanford, C.B., 2002. Avoiding Predators: Expectations and evidence in primate antipredator behavior. 23, 741–757.

Steiper, M.E., Young, N.M., Sukarna, T.Y., 2004. Genomic data support the hominoid slowdown and an Early Oligocene estimate for the hominoid-cercopithecoid divergence. Proc. Natl. Acad. Sci. U. S. A. 101, 17021–17026.

Sterck, E.H.M., Steenbeek, R., 2012. Female Dominance Relationships and Food Competition in the Sympatric Thomas Langur and Long-Tailed Macaque A. Behaviour. 134, 749–774.

Stevens, N.J., Seiffert, E.R., O'Connor, P.M., Roberts, E.M., Schmitz, M.D., Krause, C., Gorscak, E., Ngasala, S., Hieronymus, T.L., Temu, J., 2013. Palaeontological evidence for an Oligocene divergence between Old World monkeys and apes. Nature. 497, 611–614.

Stewart, A.M.E., Gordon, C.H., Wich, S.A., Schroor, P., Meijaard, E., 2008. Fishing in Macaca

Ψηφιακή βιβλιοθήκη Θεόφραστος – Τμήμα Γεωλογίας – Αριστοτέλειο Πανεπιστήμιο Θεσσαλονίκης

Ψηφιακή συλλογή
Βιβλιοθήκη
"ΘΕΟΦΡΑΣΤΟΣ"
Τμήμα Γεωλογίας
Α.Π.Θ

fascicularis: A rarely observed innovative behavior. Int. J. Primatol. 29, 543–548.

Strani, F., DeMiguel, D., Alba, D.M., Moyà-Solà, S., Bellucci, L., Sardella, R., Madurell-Malapeira, J., 2019. The effects of the "0.9 Ma event" on the Mediterranean ecosystems during the Early-Middle Pleistocene transition as revealed by dental wear patterns of fossil ungulates. Quat. Sci. Rev. 210, 80–89.

Strasser, E., 1988. Pedal evidence for the origin and diversification of cercopithecid clades. J. Hum. Evol. 17, 225–245.

Strasser, E., Delson, E., 1987. Cladistic analysis of cercopithecid relationships. J. Hum. Evol. 16, 81–99.

Stromer, E., 1913. Mitteilungen über Wirbeltierreste aus dem Mittelpliocän des Natrontales (Ägypten).-1. Affen. Zeitschrift der Dtsch. Geol. Gesellschaft. 350–372.

Stuart, Y.E., Losos, J.B., 2013. Ecological character displacement: Glass half full or half empty? Trends Ecol. Evol. 28, 402–408.

Stuhlträger, J., Schulz-Kornas, E., Kullmer, O., Janocha, M.M., Wittig, R.M., Kupczik, K., 2021. Dental wear patterns reveal dietary ecology and season of death in a historical chimpanzee population. PLoS One. 16, 1–18.

Stümpel, N., Rajabizadeh, M., Avci, A., Wüster, W., Joger, U., 2016. Phylogeny and diversification of mountain vipers (Montivipera, Nilson et al., 2001) triggered by multiple Plio-Pleistocene refugia and high-mountain topography in the Near and Middle East. Mol. Phylogenet. Evol. 101, 336–351.

Sukselainen, L., Fortelius, M., Harrison, T., 2015. Co-occurrence of pliopithecoid and hominoid primates in the fossil record: An ecometric analysis. J. Hum. Evol. 84, 25–41.

Surbeck, M., Fowler, A., Deimel, C., Hohmann, G., 2009. Evidence for the consumption of arboreal, diurnal primates by bonobos (*Pan paniscus*). Am. J. Primatol. 71, 171–174.

Sutton, M., Rahman, I., Garwood, R., 2016. Virtual Paleontology—an Overview. Paleontol. Soc. Pap. 22, 1–20.

Suwa, G., Kono, R.T., 2005. A micro-CT based study of linear enamel thickness in the mesial cusp section of human molars: Reevaluation of methodology and assessment of within-tooth, serial, and individual variation. Anthropol. Sci. 113, 273–289.

Suwa, G., Kunimatsu, Y., Mirzaie Ataabadi, M., Orak, Z., Sasaki, T., Fortelius, M., 2016. The first hominoid from the Maragheh Formation, Iran. Palaeobiodiversity and Palaeoenvironments. 96, 373–381.

Ψηφιακή βιβλιοθήκη Θεόφραστος – Τμήμα Γεωλογίας – Αριστοτέλειο Πανεπιστήμιο Θεσσαλονίκης

Ψηφιακή συλλογή
Βιβλιοθήκη
"ΘΕΟΦΡΑΣΤΟΣ"

Swedell, L., Hailemeskel, G., Schreier, A., 2008. Composition and seasonality of diet in wild hamadryas baboons: Preliminary findings from filoha. Folia Primatol. 79, 476–490.

Swindler, D.R., 2002. Primate Dentition: An Introduction to the Teeth of Non-human Primates. Cambridge University Press.

Symonds, M.R.E., Blomberg, S.P., 2014. Modern phylogenetic comparative methods and their application in evolutionary biology. In: Garamszegi, L.Z. (Ed.), Modern Phylogenetic Comparative Methods and Their Application in Evolutionary Biology. Springer Berlin Heidelberg, pp. 105–130.

Szalay, F.S., Delson, E., 1979. Evolutionary History of the Primates. Academic Press.

Tafforeau, P., Boistel, R., Boller, E., Bravin, A., Brunet, M., Chaimanee, Y., Cloetens, P., Feist, M., Hoszowska, J., Jaeger, J.J., Kay, R.F., Lazzari, V., Marivaux, L., Nel, A., Nemoz, C., Thibault, X., Vignaud, P., Zabler, S., 2006. Applications of X-ray synchrotron microtomography for non-destructive 3D studies of paleontological specimens. Appl. Phys. A Mater. Sci. Process. 83, 195–202.

Takai, M., Maschenko, E.N., 2009. Parapresbytis eohanuman: the northernmost colobine monkey from the Pliocene of Transbaikalia. Asian Paleoprimatology. 5, 1–14.

Takai, M., Maschenko, E.N., Nishimura, T.D., Anezaki, T., Suzuki, T., 2008. Phylogenetic relationships and biogeographic history of *Paradolichopithecus sushkini* Trofimov 1977, a large-bodied cercopithecine monkey from the Pliocene of Eurasia. Quat. Int. 179, 108–119.

Takai, M., Nishioka, Y., Thaung-Htike, Maung, M., Khaing, K., Zin-Maung-Maung-Thein, Tsubamoto, T., Egi, N., 2016. Late Pliocene *Semnopithecus* fossils from central Myanmar: rethinking of the evolutionary history of cercopithecid monkeys in Southeast Asia. Hist. Biol. 28, 172–188.

Takai, M., Thaung-Htike, Zin-Maung-Maung-Thein, Soe, A.N., Maung, M., Tsubamoto, T., Egi, N., Nishimura, T.D., Nishioka, Y., 2015. First discovery of colobine fossils from the Late Miocene/Early Pliocene in central Myanmar. J. Hum. Evol. 84, 1–15.

Takai, M., Zhang, Y., Kono, R.T., Jin, C., 2014. Changes in the composition of the Pleistocene primate fauna in southern China. Quat. Int. 354, 75–85.

Takasaki, H., 1981. Troop size, habitat quality, and home range area in Japanese macaques. Behav. Ecol. Sociobiol. 9, 277–281.

Tan, C.L., 1999. Group composition, home range size, and diet of three sympatric bamboo lemur species (*Genus hapalemur*) in Ranomafana National Park, Madagascar. Int. J. Primatol. 20, 547–566.

Ψηφιακή βιβλιοθήκη Θεόφραστος – Τμήμα Γεωλογίας – Αριστοτέλειο Πανεπιστήμιο Θεσσαλονίκης

Ψηφιακή συλλογή
Βιβλιοθήκη
"ΘΕΟΦΡΑΣΤΟΣ"

Teaford, M.F., 2007. Dental microwear and Paleoanthropology: Cautions and possibilities. Vertebr. Paleobiol. Paleoanthropology. 345–368.

Teaford, M.F., Glander, K.E., 1991. Dental Microwear in Live, Wild-Trapped. Am. J. Phys. Anthropol. 319, 313–319.

Teaford, M.F., Maas, M.C., Simons, E.L., 1996. Dental microwear and microstructure in early oligocene primates from the Fayum, Egypt: Implications for diet. Am. J. Phys. Anthropol. 101, 527–543.

Teaford, M.F., Oyen, O.J., 1989. In vivo and in vitro turnover in dental microwear. Am. J. Phys. Anthropol. 80, 447–460.

Teaford, M.F., Walker, A., 1984. Quantitative differences in dental microwear between primate species with different diets and a comment on the presumed diet of Sivapithecus. Am. J. Phys. Anthropol. 64, 191–200.

Team, R.C., 2013. R: A language and environment for statistical computing.

Teelen, S., 2007. Primate adundance along five transect lines at Ngogo, Kibale national park, Uganda. Am. J. Primatol. 69, 1030–1044.

Terhune, C.E., Curran, S., Croitor, R., Drăguşin, V., Gaudin, T., Petculescu, A., Robinson, C., Robu, M., Werdelin, L., 2020. Early Pleistocene fauna of the Olteţ River Valley of Romania: Biochronological and biogeographic implications. Quat. Int. 553, 14–33.

Terhune, C.E., Curran, S., Fox, D.L., Garrett, N., Hubbard, J., Petculescu, A., Robinson, C.A., Robu, M., Stiucã, E., Tantu, I., 2013. Paleoenvironmental conditions in early Pleistocene Romania: implications for hominin dispersals 2004.

Thiery, G., 2016. Analyse morpho-fonctionnelle de la topographie dentaire 3d chez les primates actuels et fossiles.

Thiery, G., Gibert, C., Guy, F., Lazzari, V., Geraads, D., Spassov, N., Merceron, G., 2021. From leaves to seeds? The dietary shift in late Miocene colobine monkeys of southeastern Europe. Evol. - Int. J. Org. Evol. 1–15.

Thiery, G., Gillet, G., Lazzari, V., Merceron, G., Guy, F., 2017a. Was *Mesopithecus* a seed eating colobine? Assessment of cracking, grinding and shearing ability using dental topography. J. Hum. Evol. 112, 79–92.

Thiery, G., Guy, F., Lazzari, V., 2017b. Investigating the dental toolkit of primates based on food mechanical properties: Feeding action does matter. Am. J. Primatol. 79, 1–15.

Ψηφιακή βιβλιοθήκη Θεόφραστος – Τμήμα Γεωλογίας – Αριστοτέλειο Πανεπιστήμιο Θεσσαλονίκης

Ψηφιακή συλλογή
Βιβλιοθήκη
"ΘΕΟΦΡΑΣΤΟΣ"

Thiery, Ghislain, Guy, F., Lazzari, V., 2019. A comparison of relief estimates used in three-dimensional dental topography. Am. J. Phys. Anthropol. 170, 260–274.

Thiery, G., Guy, F., Lazzari, V., 2019. Enamel distribution in 3D: Is enamel thickness more uneven in the upper second molars of durophagous hominoids? Bull. Mem. Soc. Anthropol. Paris. 31, 52–59.

Thiery, G., Lazzari, V., Ramdarshan, A., Guy, F., 2017c. Beyond the map: Enamel distribution characterized from 3D dental topography. Front. Physiol. 8.

Thiery, G., Sha, J.C.M., 2020. Low occurrence of molar use in black-tufted capuchin monkeys: Should adaptation to seed ingestion be inferred from molars in primates? Palaeogeogr. Palaeoclimatol. Palaeoecol. 555, 109853.

Ting, N., Harcourt-Smith, W.E.H., Frost, S.R., Delson, E., 2004. Description and analysis of postcranial elements of *Paradolichopithecus arvernensis*: A large-bodied papionin from the Pliocene of Eurasia. In: American Journal of Physical Anthropology. p. 195.

Tobien, H., 1970. Biostratigraphy of the mammalian faunas at the Pliocene-Pleistocene boundary in Middle and Western Europe. Palaeogeogr. Palaeoclimatol. Palaeoecol. 8, 77–93.

Tosi, A.J., Detwiler, K.M., Disotell, T.R., 2005. X-chromosomal window into the evolutionary history of the guenons (Primates: Cercopithecini). Mol. Phylogenet. Evol. 36, 58–66.

Tran, L.A.P., 2014. The role of ecological opportunity in shaping disparate diversification trajectories in a bicontinental primate radiation. Proc. R. Soc. B Biol. Sci. 281.

Trofimov, B.A., 1977. Primate *Paradolichopithecus sushkini* sp. nov. from upper Pliocene of the Pamirs piedmont. J. Paleontol. Soc. India.

Truppa, V., Marino, L.A., Izar, P., Fragaszy, D.M., Visalberghi, E., 2019. Manual skills for processing plant underground storage organs by wild bearded capuchins. Am. J. Phys. Anthropol. 170, 48–64.

Tsuji, Y., Hanya, G., Grueter, C.C., 2013. Feeding strategies of primates in temperate and alpine forests: Comparison of Asian macaques and colobines. Primates. 54, 201–215.

Tsuji, Y., Ito, T., Wada, K., Watanabe, K., 2015. Spatial patterns in diet of the Japanese macaque Macaca fuscata and their environmental determinants. Mamm. Rev. 45, 227–238.

Tutin, C.E.G., Fernandez, M., Rogers, M.E., Williamson, E.A., McGrew, W.C., 1991. Foraging profiles of sympatric lowland gorillas and chimpanzees in the Lope Reserve, Gabon. Philos. Trans. - R. Soc. London, B. 334, 179–186.

Ψηφιακή βιβλιοθήκη Θεόφραστος – Τμήμα Γεωλογίας – Αριστοτέλειο Πανεπιστήμιο Θεσσαλονίκης

Ψηφιακή συλλογή
Βιβλιοθήκη
"ΘΕΟΦΡΑΣΤΟΣ"

Tutin, C.E.G., Ham, R.M., White, L.J.T., Harrison, M.J.S., 1997a. The primate community of the Lope Reserve, Gabon: Diets, responses to fruit scarcity, and effects on biomass. Am. J. Primatol. 42, 1–24.

Tutin, C.E.G., Ham, R.M., White, L.J.T., Harrison, M.J.S., 1997b. The primate community of the Lope Reserve, Gabon: Diets, responses to fruit scarcity, and effects on biomass. Am. J. Primatol. 42, 1–24.

Tzedakis, P.C., Lawson, I.T., Frogley, M.R., Hewitt, G.M., Preece, R.C., 2002. Buffered tree population changes in a Quaternary refugium: Evolutionary implications. Science (80-.). 297, 2044–2047.

Ulhaas, L., Kullmer, O., Schrenk, F., Henke, W., 2004. A new 3-d approach to determine functional morphology of cercopithecoid molars. Ann. Anat. 186, 487–493.

Ungar, P., Williamson, M., 2000. Exploring the effects of tooth wear on functional morphology: A preliminary study using dental topographic analysis. Palaeontol. Electron. 3.

Ungar, P.S., 1994. Incisor microwear of Sumatran anthropoid primates. Am. J. Phys. Anthropol. 94, 339–363.

Ungar, P.S., 1995. Fruit preferences of four sympatric primate species at Ketambe, northern Sumatra, Indonesia. Int. J. Primatol. 16, 221–245.

Ungar, P.S., 2015. Mammalian dental function and wear: A review. Biosurface and Biotribology. 1, 25–41.

Ungar, P.S., 2019. Inference of Diets of Early Hominins from Primate Molar Form and Microwear. J. Dent. Res. 98, 398–405.

Ungar, P.S., Abella, E.F., Burgman, J.H.E., Lazagabaster, I.A., Scott, J.R., Delezene, L.K., Manthi, F.K., Plavcan, J.M., Ward, C. V., 2020. Dental microwear and Pliocene paleocommunity ecology of bovids, primates, rodents, and suids at Kanapoi. J. Hum. Evol. 140, 102315.

Ungar, P.S., Brown, C.A., Bergstrom, T.S., Walker, A., 2003. Quantification of dental microwear by tandem scanning confocal microscopy and scale-sensitive fractal analyses. Scanning. 25, 185–193.

Ungar, P.S., Hartgrove, C.L., Wimberly, A.N., Teaford, M.F., 2017. Dental topography and microwear texture in Sapajus apella. Biosurface and Biotribology. 3, 124–134.

Ungar, P.S., Healy, C., Karme, A., Teaford, M., Fortelius, M., 2018. Dental topography and diets of platyrrhine primates. Hist. Biol. 30, 64–75.

Ψηφιακή βιβλιοθήκη Θεόφραστος – Τμήμα Γεωλογίας – Αριστοτέλειο Πανεπιστήμιο Θεσσαλονίκης

Ψηφιακή συλλογή
Βιβλιοθήκη
"ΘΕΟΦΡΑΣΤΟΣ"

Ungar, P.S., Kay, R.F., 1995. The dietary adaptations of European miocene catarrhines. Proc. Natl. Acad. Sci. U. S. A. 92, 5479–5481.

Ungar, P.S., Livengood, S. V., Crittenden, A.N., 2019. Dental microwear of living Hadza foragers. Am. J. Phys. Anthropol. 169, 356–367.

Ungar, P.S., M'Kirera, F., 2003. A solution to the worn tooth conundrum in primate functional anatomy. In: Proceedings of the National Academy of Sciences of the United States of America. pp. 3874–3877.

Ungar, P.S., Merceron, G., Scott, R.S., 2007. Dental microwear texture analysis of Varswater bovids and early Pliocene paleoenvironments of Langebaanweg, Western Cape Province, South Africa. J. Mamm. Evol. 14, 163–181.

Ungar, P.S., Scott, R.S., Scott, J.R., Teaford, M.F., 2008. Dental microwear analys: historical perspectives and new approaches. In: Irish, J.D., Nelso, G.C. (Eds.), Technique and Application in Dental Anthropology. Cambridge University Press, Cambridge, pp. 389–425.

Ungar, P.S., Spencer, M.A., 1999. Incisor microwear, diet, and tooth use in three Amerindian populations. Am. J. Phys. Anthropol. 109, 387–396.

van Casteren, A., Strait, D.S., Swain, M. V., Michael, S., Thai, L.A., Philip, S.M., Saji, S., Al-Fadhalah, K., Almusallam, A.S., Shekeban, A., McGraw, W.S., Kane, E.E., Wright, B.W., Lucas, P.W., 2020. Hard plant tissues do not contribute meaningfully to dental microwear: evolutionary implications. Sci. Rep. 10, 1–9.

van Casteren, A., Wright, E., Kupczik, K., Robbins, M.M., 2019. Unexpected hard-object feeding in Western lowland gorillas. Am. J. Phys. Anthropol. 170, 433–438.

van den Hoek Ostende, L.W., de Vos, J., 2006. A century of research on the classical locality of Tegelen (Province of Limburg, The Netherlands). CFS Cour. Forschungsinstitut Senckenb. 291–304.

Van der Geer, A.A., Lyras, G.A., Lomolino, M. V., Palombo, M.R., Sax, D.F., 2013. Body size evolution of palaeo-insular mammals: Temporal variations and interspecific interactions. J. Biogeogr. 40, 1440–1450.

van der Geer, A.A.E., Dermitzakis, M.D., 2008. Dental eruption sequence in the Pliocene papionin *Paradolichopithecus arvernensis* (Mammalia: Primates) from Greece. J. Vertebr. Paleontol. 28, 1238–1244.

van der Geer, A.A.E., Lyras, G.A., Mitteroecker, P., MacPhee, R.D.E., 2018. From Jumbo to Dumbo: Cranial Shape Changes in Elephants and Hippos During Phyletic Dwarfing. Evol. Biol. 45, 303–317.

Ψηφιακή βιβλιοθήκη Θεόφραστος – Τμήμα Γεωλογίας – Αριστοτέλειο Πανεπιστήμιο Θεσσαλονίκης

Ψηφιακή συλλογή
Βιβλιοθήκη
"ΘΕΟΦΡΑΣΤΟΣ"

Van der Geer, A.A.E., Sondaar, P.Y., 2002. The postcranial elements of Paradolichopithecus arvernensis (Primates, Cercopithecidae, Papionini) from Lesvos, Greece. . Ann. Géologiques des Pays Helléniques. 1e Série. 39 A, 71–86.

van der Geer, A.A.E., van den Bergh, G.D., Lyras, G.A., Prasetyo, U.W., Due, R.A., Setiyabudi, E., Drinia, H., 2016. The effect of area and isolation on insular dwarf proboscideans. J. Biogeogr. 43, 1656–1666.

van der Made, J., 1999. Biogeography and stratigraphy of the Mio-Pleistocene mammals of Sardinia and the. Deinsea - Annu. Nat. Hist. MUSEUM ROTTERDAM. 337–360.

van Doorn, A.C., O'Riain, M.J., Swedell, L., 2010. The effects of extreme seasonality of climate and day length on the activity budget and diet of semi-commensal chacma baboons (papio ursinus) in the Cape Peninsula of South Africa. Am. J. Primatol. 72, 104–112.

Vandercone, R., 2011. Dietary Shifts , Niche Relationships and Interspecific Competition in Sympatric Grey Langur (*Semnopithecus entellus*) and Purple-faced Langur (*Trachypithecus vetulus*) in Sri Lanka.

Vandercone, R.P., Dinadh, C., Wijethunga, G., Ranawana, K., Rasmussen, D.T., 2012. Dietary Diversity and Food Selection in Hanuman Langurs (*Semnopithecus entellus*) and Purple-Faced Langurs (*Trachypithecus vetulus*) in the Kaludiyapokuna Forest Reserve in the Dry Zone of Sri Lanka. Int. J. Primatol. 33, 1382–1405.

Verma, B.C., 1969. Procynocephalus pinjorii, sp. nov. a new fossil primate from Pinjor Beds (lower Pleistocene), East of Chandigarh. J. Palaeontol. Soc. India.

Vogel, E.R., Haag, L., Mitra-Setia, T., Van Schaik, C.P., Dominy, N.J., 2009. Foraging and ranging behavior during a fallback episode: Hylobates albibarbis and *Pongo pygmaeus wurmbii* compared. Am. J. Phys. Anthropol. 140, 716–726.

Vogel, E.R., van Woerden, J.T., Lucas, P.W., Utami Atmoko, S.S., van Schaik, C.P., Dominy, N.J., 2008. Functional ecology and evolution of hominoid molar enamel thickness: *Pan troglodytes schweinfurthii* and *Pongo pygmaeus wurmbii*. J. Hum. Evol. 55, 60–74.

Vrba, E.S., 1993. Turnover pulses, the Red Queen and related topics. Am. J. Sci. 293, 418–452.

Wahungu, G.M., 1998. Diet and habitat overlap in two sympatric primate species, the tana crested mangabey *Cercocebus galeritus* and yellow baboon *Papio cynocephalus*. Afr. J. Ecol. 36, 159–173.

Walker, P., Murray, P., 2011. An Assessment of Masticatory Efficiency in a Series of Anthropoid Primates with Special Reference to the Colobinae and Cercopithecinae. In: Tuttle, R.H. (Ed.), Primate Functional Morphology and Evolution. Walter de Gruyter, p. 135.

Ψηφιακή βιβλιοθήκη Θεόφραστος – Τμήμα Γεωλογίας – Αριστοτέλειο Πανεπιστήμιο Θεσσαλονίκης

Ψηφιακή συλλογή
Βιβλιοθήκη
"ΘΕΟΦΡΑΣΤΟΣ"

Watts, D.P., 2020. Meat eating by nonhuman primates: A review and synthesis. J. Hum. Evol. 149, 102882.

Werdelin, L., 2010. Chronology of Neogene mammal localities. In: Werdelin, L., Sanders, W.J. (Eds.), Cenozoic Mammals of Africa. University of California Press, pp. 27–43.

White, L.J.T., 1994. Patterns of fruit-fall phenology in the Lopé Reserve, Gabon. J. Trop. Ecol. 289–312.

Whiten, A., Byrne, R.W., Barton, R.A., Waterman, P.G., Henzi, S.P., 1991. Dietary and foraging strategies of baboons. Philos. Trans. - R. Soc. London, B. 334, 187–197.

Whitten, P.L., 1983. Diet and dominance among female vervet monkeys (*Cercopithecus aethiops*). Am. J. Primatol. 5, 139–159.

Wieczkowski, J., 2004. Ecological correlates of abundance in the Tana mangabey (*Cercocebus galeritus*). Am. J. Primatol. 63, 125–138.

Wieczkowski, J., 2009. Brief communication: Puncture and crushing resistance scores of Tana River mangabey (*Cercocebus galeritus*) diet items. Am. J. Phys. Anthropol. 140, 572–577.

Willeit, M., Ganopolski, A., Calov, R., Brovkin, V., 2019. Mid-Pleistocene transition in glacial cycles explained by declining CO2 and regolith removal. Sci. Adv. 5, 1–9.

Williams, F. L. E., Geissler, E., 2014. Reconstructing the diet and paleoecology of Plio-Pleistocene Cercopithecoides Williamsi from Sterkfontein, South Africa. Palaios. 29, 483–494.

Williams, F. L E., Geissler, E., 2014. Reconstructing the diet and paleoecology of Plio-Pleistocene Cercopithecoides williamsi from Sterkfontein, South Africa. Palaios. 29, 483–494.

Williams, F.L.E., Holmes, N.A., 2011. Evidence of terrestrial diets in pliocene Eurasian papionins (Mammalia: Primates) inferred from low-magnification stereomicroscopy of molar enamel use-wear scars. Palaios. 26, 720–729.

Williams, F.L.E., Holmes, N.A., 2012. Dental microwear texture analysis of late Pliocene *Procynocephalus subhimalayanus* (Primates: Cercopithecidae) of the upper siwaliks, India. Cent. Eur. J. Geosci. 4, 425–438.

Winchester, J.M., 2016. MorphoTester: An Open Source Application for Morphological Topographic Analysis. PLoS One. 11, 1–18.

Winchester, J.M., Boyer, D.M., St. Clair, E.M., Gosselin-Ildari, A.D., Cooke, S.B., Ledogar, J.A., 2014. Dental topography of platyrrhines and prosimians: Convergence and contrasts. Am. J. Phys. Anthropol. 153, 29–44.

Ψηφιακή βιβλιοθήκη Θεόφραστος – Τμήμα Γεωλογίας – Αριστοτέλειο Πανεπιστήμιο Θεσσαλονίκης

Ψηφιακή συλλογή
Βιβλιοθήκη
"ΘΕΟΦΡΑΣΤΟΣ"

Winkler, D.E., Schulz-Kornas, E., Kaiser, T.M., Codron, D., Leichliter, J., Hummel, J., Martin, L.F., Clauss, M., Tütken, T., 2020. The turnover of dental microwear texture: Testing the" last supper" effect in small mammals in a controlled feeding experiment. Palaeogeogr. Palaeoclimatol. Palaeoecol. 557, 109930.

Winterhalder, B., 1981. Hominid paleoecology and competitive exclusion: Limits to similarity, niche differentiation, and the effects of cultural behavior. Am. J. Phys. Anthropol. 24, 101–121.

Wood, B.A., 1979. An Analysis of Tooth and Body Size Relationships in Five Primate Taxa. Folia Primatol. 31, 187–211.

Wrangham, R., Cheney, D., Seyfarth, R., Sarmiento, E., 2009. Shallow-water habitats as sources of fallback foods for hominins. Am. J. Phys. Anthropol. 140, 630–642.

Wright, B.W., Ulibarri, L., O'Brien, J., Sadler, B., Prodhan, R., Covert, H.H., Nadler, T., 2008. It's tough out there: Variation in the toughness of ingested leaves and feeding behavior among four colobinae in Vietnam. Int. J. Primatol. 29, 1455–1466.

Wright, B.W., Willis, M.S., 2012. Relationships between the diet and dentition of Asian leaf monkeys. Am. J. Phys. Anthropol. 148, 262–275.

Wu, F., Fang, X., Herrmann, M., Mosbrugger, V., Miao, Y., 2011. Extended drought in the interior of Central Asia since the Pliocene reconstructed from sporopollen records. Glob. Planet. Change. 76, 16–21.

Wu, F., Fang, X., Ma, Y., Herrmann, M., Mosbrugger, V., An, Z., Miao, Y., 2007. Plio-Quaternary stepwise drying of Asia: Evidence from a 3-Ma pollen record from the Chinese Loess Plateau. Earth Planet. Sci. Lett. 257, 160–169.

Xia, J., Zhou, Z., Qian, L., Ungar, P.S., 2018. Comment on Van Casteren et al. (2018): Softer metallic spheres do abrade harder enamel. R. Soc. Open Sci. 5.

Yamagiwa, J., Basabose, A.K., 2006. Diet and seasonal changes in sympatric gorillas and chimpanzees at Kahuzi-Biega National Park. Primates. 47, 74–90.

Yamashita, N., 1998. Functional dental correlates of food properties in five Malagasy lemur species. Am. J. Phys. Anthropol. 106, 169–188.

Yamashita, N., Cuozzo, F.P., Sauther, M.L., 2012. Interpreting food processing through dietary mechanical properties: A Lemur catta case study. Am. J. Phys. Anthropol. 148, 205–214.

Yamashita, N., Cuozzo, F.P., Sauther, M.L., Fitzgerald, E., Riemenschneider, A., Ungar, P.S., 2016. Mechanical food properties and dental topography differentiate three populations of

Ψηφιακή βιβλιοθήκη Θεόφραστος – Τμήμα Γεωλογίας – Αριστοτέλειο Πανεπιστήμιο Θεσσαλονίκης

Ψηφιακή συλλογή
Βιβλιοθήκη
"ΘΕΟΦΡΑΣΤΟΣ"
Τμήμα Γεωλογίας
Α.Π.Θ

Lemur catta in southwest Madagascar. J. Hum. Evol. 98, 66–75.

Yeager, C.P., 1989. Feeding ecology of the proboscis monkey (*Nasalis larvatus*). Int. J. Primatol. 10, 497–530.

Yeager, C.P., Kool, K., 1994. The behavioral ecology of Asian colobines. In: Colobine Monkeys: Their Ecology, Behaviour, and Evolution. pp. 496–521.

Youlatos, D., 2003. Caractères calcanéens du primate du Miocène de Grèce *Mesopithecus* pentelicus (Cercopithecoidea : Colobinae). Geobios. 36, 229–239.

Youlatos, D., Couette, S., Koufos, G.D., 2012. A functional multivariate analysis of *Mesopithecus* (Primates: Colobinae) humeri from the Turolian of Greece. J. Hum. Evol. 63, 219–230.

Youlatos, D., Koufos, G.D., 2010. Locomotor evolution of *Mesopithecus* (Primates: Colobinae) from Greece: Evidence from selected astragalar characters. Primates. 51, 23–35.

Young, C.C., 1934. On the Insectivora, Chiroptera, Rodentia and Primates other than Sinanthropus from locality 1 at Choukoutien. Palaeontol. Sin. Ser. C. 8, 1–161.

Zanaga, M., 1998. Macaca majori Azzaroli 1946, primate endemico del Pleistocene della Sardegna. Unpubl. Thesis, Univ. degli Stud. di Firenze.

Zanolli, C., Bayle, P., Macchiarelli, R., 2010. Proportions des tissus et distribution de l'épaisseur de l'émail des molaires déciduales humaines du début du Pléistocène moyen de Tighenif, Algérie. Comptes Rendus - Palevol. 9, 341–348.

Zanolli, C., Bondioli, L., Coppa, A., Dean, C.M., Bayle, P., Candilio, F., Capuani, S., Dreossi, D., Fiore, I., Frayer, D.W., Libsekal, Y., Mancini, L., Rook, L., Medin Tekle, T., Tuniz, C., Macchiarelli, R., 2014. The late early pleistocene human dental remains from uadi aalad and mulhuli-amo (buia), eritrean danakil: Macromorphology and microstructure. J. Hum. Evol. 74, 96–113.

Zanolli, C., Cantaloube, M., Bayle, P., Beer, F. De, Jakata, K., Martín-francés, L., Ortiz, A., Skinner, M., Tawane, M., Zanolli, C., Cantaloube, M., Bayle, P., Beer, F. De, Hoffman, J., 2020. Molar enamel thickness distribution and hominid taxonomy. In: Proceeding of European Society for Human Evolution.

Zapfe, H., 1991. Mesopithecus pentelicus Wagner aus dem Turolien von Pikermi bei Athen, Odontologie und Osteologie:(eine Dokumentation).

Zhang, B., Liu, X., Brown, C.A., Bergstrom, T.S., 2002. Microgrinding of nanostructured material coatings. CIRP Ann. 51, 251–254.

Ψηφιακή βιβλιοθήκη Θεόφραστος – Τμήμα Γεωλογίας – Αριστοτέλειο Πανεπιστήμιο Θεσσαλονίκης

Ψηφιακή συλλογή
Βιβλιοθήκη
"ΘΕΟΦΡΑΣΤΟΣ"

Zhang, H., Wang, Y., Janis, C.M., Goodall, R.H., Purnell, M.A., 2017. An examination of feeding ecology in Pleistocene proboscideans from southern China (*Sinomastodon*, *Stegodon*, *Elephas*), by means of dental microwear texture analysis. Quat. Int. 445, 60–70.

Zhou, Q., Wei, H., Huang, Z., Huang, C., 2011. Diet of the Assamese macaque *Macaca assamensis* in limestone habitats of Nonggang, China. Curr. Zool. 57, 18–25.

Zhou, Q., Wei, H., Tang, H., Huang, Z., Krzton, A., Huang, C., 2014. Niche separation of sympatric macaques, *Macaca assamensis* and M. mulatta, in limestone habitats of Nonggang, China. Primates. 55, 125–137.

Zhou, Q.H., Huang, Z.H., Wei, H., Huang, C.M., 2018. Variations in diet composition of sympatric Trachypithecus francoisi and Macaca assamensis in the limestone habitats of Nonggang, China. Zool. Res. 39, 284–290.

Zinner, D., Peláez, F., Torkler, F., 2001. Distribution and habitat associations of baboons (*Papio hamadryas*) in central Eritrea. Int. J. Primatol. 22, 397–413.

Zoboli, D., Pillola, G.L., Rook, L., 2016. New remains of *Macaca majori* azzaroli, 1946 (Primates, cercopithecidae) from is oreris (fluminimaggiore, Southwestern Sardinia). Boll. della Soc. Paleontol. Ital. 55, 227–230.

Zuccotti, L.F., Williamson, M.D., Limp, W.F., Ungar, P.S., 1998. Technical note: Modeling primate occlusal topography using geographic information systems technology. Am. J. Phys. Anthropol. 107, 137–142.

Ψηφιακή βιβλιοθήκη Θεόφραστος – Τμήμα Γεωλογίας – Αριστοτέλειο Πανεπιστήμιο Θεσσαλονίκης